DISSERTATION

A PRACTICAL CATALYST SYSTEM FOR THE ASYMMETRIC EPOXIDATION OF OLEFINS

Submitted by

David Lee Goeddel

Department of Chemistry

In partial fulfillment of the requirements

For the Degree of Doctor of Philosophy

Colorado State University

Fort Collins, Colorado

Fall 2006

COLORADO STATE UNIVERSITY

August 21, 2006

WE HEREBY RECOMMEND THAT THE DISSERTATION PREPARED UNDER OUR SUPERVISION BY DAVID LEE GOEDDEL ENTITLED A PRACTICAL CATALYST SYSTEM FOR THE ASYMMETRIC EPOXIDATION OF OLEFINS BE ACCEPTED AS FULFILLING IN PART REQUIREMENTS FOR THE DEGREE OF DOCTOR OF PHILOSOPHY

Committee on Graduate Work

Prof. Louis S. Hegédus

Prof. Michael R. McNeil

Prof. Matthew Paul Shores

Prof. Robert M. Williams

Prof. Yian Shi/**Advisor**

Prof. Anthony K. Rappé/**Department Head**

ABSTRACT OF **DISSERTATION**

A PRACTICAL CATALYST SYSTEM FOR THE ASYMMETRIC EPOXIDATION OF OLEFINS

A complementary ketone to a fructose-derived asymmetric epoxidation catalyst has been developed in the following manner. The synthesis of a previously-reported oxazolidinone catalyst was improved to prepare quantities suitable for use on small scale. Substrate scope was extended to styrenes with a carbocyclic analog of the original oxazolidinone ketone catalyst made in 15 steps from quinic acid. During the course of the studies of the carbocyclic catalysts, we discovered an electronic effect responsible for enhancing secondary orbital interactions and ultimately, enantioselectivity. The origin of the electronic attraction was studied by synthesizing new ketones with varying functionality where the oxazolidinone previously was found. Having obtained information about the nature of the attraction, we prepared a series of aniline substituted oxazolidinone ketones bearing structural and electronic features the aforementioned work found to be beneficial. We observed 86-92% ee for the epoxidation of *meta*- and *para*-substituted styrenes with the optimized 4-ethylaniline-derived ketone, and coworkers have observed high ee for a variety of conjugated *cis*-olefins with this ketone catalyst. Considering the potential usefulness of this catalyst, we optimized the synthesis of the

ethyl aniline oxazolidinone ketone as well as the epoxidation conditions themselves so the catalyst preparation and olefin epoxidation can be performed on large scale.

David Lee Goeddel
Chemistry Department
Colorado State University
Fort Collins, CO 80523
Fall 2006

ACKNOWLEDGEMENTS

The author wishes to thank the people whose support and efforts have made this work possible. Professor Yian Shi has been instrumental in the completion of this project, not only for creating and directing the work, but also allowing the author to develop by allowing him a great deal of freedom while pursue the overall objectives of the research. During the second half of 2005, Professor Albert I. Meyers led this project and greatly assisted in securing future opportunities for the author. Professor Debra L. Mohler aided in the completion of this dissertation by providing the author with a solid scientific background and continually supporting him throughout his career. Furthermore, every member of the Shi Research Group has made contributions to this dissertation ranging from personal support to scientific discussion. Due to the collaborative nature of this research, Dr. Lianhe Shu, Mr. Zackary D. Crane, Mr. Matthew R. Hickey, Ms. O. Andrea Wong, Dr. Mei-Xin Zhao, Mr. Christopher P. Burke, Dr. Yi Yuan, Dr. Yu-Mei Shen, and Mr. Bin Wang all merit recognition for their experimental efforts. Finally, Ms. Lori J. Placek, Mr. David L. Goeddel, and Mrs. Patricia J. Goeddel all deserve special thanks for all of their support through the years. The author is forever indebted to all these people for their assistance in this endeavor.

TABLE OF CONTENTS

CHAPTER ONE

EPOXIDATION OF OLEFINS WITH ORGANIC OXIDANTS

1.A. INTRODUCTION

Epoxides are very useful intermediates in the synthesis of organic compounds. Consequently, a great deal of effort has been dedicated to their synthesis. One class of epoxidizing agent that has received a tremendous amount of interest is organic oxidants. Generally speaking, organic epoxidizing agents consist of peroxy-containing compounds, oxaziridines, and dioxiranes. Depending on the situation, the active oxidizing agents can either be isolated/purchased and used directly, or they can be generated *in situ.* In many cases, the epoxidation of olefins with organic oxidants proceeds with high efficiency, yield, chemoselectivty, regioselectivity, diastereoselectivity, and/or enantioselectivity.

1.B. SYNTHESIS OF EPOXIDES BY ORGANIC PEROXY-CONTAINING COMPOUNDS

Organic peroxy-containing compounds are a large class of very powerful reagents for oxidation, including the epoxidation of olefins. One feature common to the many variations of organic-peroxy containing compounds is that hydrogen bonding activates the peroxide to concerted nucleophilic attack by an alkene. Hydrogen bonding is also possible to substrates with preexisting stereochemistry, often resulting in directed olefin epoxidation with high diastereoselectivty. For olefins without directing groups, the oxidant generally approaches from the least hindered face. Peracids (**1-1**) with varying degrees of reactivity, in particular *meta*-chloroperoxybenzoic acid (MCPBA), are some of the most widely used organic peroxy-containing oxidants. Many other variations exist for the generation of organic peroxy-containing compounds, usually by activating H_2O_2. Some successful oxidants of this type include peroxyimidic acids (**1-2**), peroxyisourea (**1-3**), peroxycarbonic acids (**1-4**), peroxycarbamic acids (**1-5**), α-hydroperoxy compounds (**1-6**), peroxyphosphates (**1-7**), and peroxides (**1-8**) activated in an intermolecular manner (Figure 1.1).

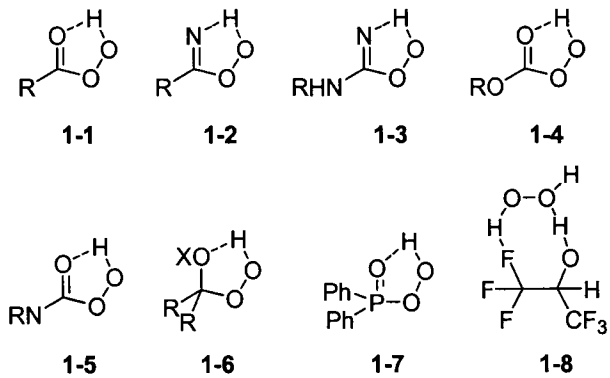

Figure 1.1 Organic peroxy-containing epoxidizing agents

1.B.1. *m*-Chloroperoxybenzoic Acid (MCPBA)

Of all the peroxy-containing compounds, MCPBA[1] is one of the most widely used, not only because of its commercial availability, but also because different sets of conditions can be used to arrive at different epoxides in a predictable manner. The earliest report of MCPBA epoxidation did not contain any yields,[2] but subsequent studies have shown a wide variety of substrate classes can be epoxidized in good yield, including silyl enol ethers and acetals, which rearrange under reaction conditions to give α-hydroxy ketones and acids (Table 1.1, Entries 5, 6).[3] Since MCPBA is an electrophilic oxidant, electron-rich olefins are epoxidized faster than electron-poor olefins, quite often resulting in excellent regioselectivity (Table 1.2, Entries 1, 2, 5). Furthermore, MCPBA can also act as a nucleophilic oxidant in the presence of base (Table 1.1, Entry 7).[3f] Good levels of diastereoselectivity can also be achieved in many instances with MCPBA epoxidation.[4] For substrates without the potential for hydrogen bonding to the oxidizing agent, epoxidation usually occurs on the less hindered face of the alkene

---

[1] For reviews, see: (a) Rao, A.S. In *Comprehensive Organic Synthesis, Vol. 7*; Trost, B.M.; Fleming, I.; Ley, S.V.; Eds.; Permagon: Elmsford, **1991**, 357. (b) Swern, D. In *Organic Peroxides, Vol. 2*; Swern, D.; Ed.; Wiley: New York, **1971**, 355. (c) Rao, A.S.; Mohan, H.R. In *Encyclopedia of Reagents for Organic Synthesis, Vol. 2;* Paquette, L.A.; Ed.; Wiley: New York, **1995**, 1192.

[2] Lynch, B.M.; Pausacker, K.H. *J. Chem. Soc.* **1955**, 1525.

[3] For examples of MCPBA epoxidation, see: (a) Schwartz, N.N.; Blumbergs, J.H. *J. Org. Chem.* **1964**, *29*, 1976. (b) Bissing, D.E.; Speziale, A.J. *J. Am. Chem. Soc.* **1965**, *87*, 2683. (c) Chai, K.-B.; Sampson, P. *Tetrahedron Lett.* **1992**, *33*, 585. (d) Rubottom, G.M.; Gruber, J.M. *J. Org. Chem.*, **1978**, *43*, 1599. (e) Rubottom, G.M.; Marrero, R. *J. Org. Chem.* **1975**, *40*, 3783. (f) Ruano, J.L.G.; Fajardo, C.; Fraile, A.; Martín, M.R. *J. Org. Chem.* **2005**, *70*, 4300.

[4] For examples of regio- or diastereoselective MCPBA epoxidation, see: (a) Camps, F.; Messeguer, A.; Sánchez, F.-J. *Tetrahedron* **1988**, *44*, 5161. (b) Bowles, S.; Campbell, M.M.; Sainsbury, M.; Davies, G.M. *Tetrahedron Lett.* **1989**, *30*, 3711. (c) Brown, H.C.; Kawakami, J.H.; Ikegami, S.; *J. Am. Chem. Soc.* **1970**, *92*, 6914. (d) Henbest, H.B.; Wilson, R.A.L. *J. Chem. Soc.* **1957**, 1958. (e) McKittrick, B.A.; Ganem, B. *Tetrahedron Lett.* **1985**, *26*, 4895. (f) Itoh, T.; Jitsukawa, K.; Kaneda, K.; Teranishi, S. *J. Am. Chem. Soc.* **1979**, *101*, 159. (g) Kočovský, P.; Starý, I. *J. Org. Chem.* **1990**, *55*, 3236.

(Table 1.2, Entries 2-4,8).[4b,c] For many cases where hydrogen bonding to the substrate is possible, directed epoxidation is possible, resulting in good diastereoselectivity (Table 1.2, Entries 7, 9).[4d-g]

Table 1.1. Select Examples of Epoxidation with MCPBA

Entry	Substrate	Product	Yield (%)	Ref
1	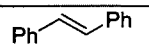	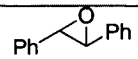	90	3b
2	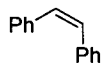	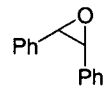	55	3b
4	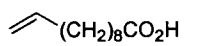	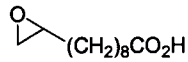	75	3c
5	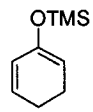	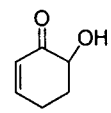	70[a]	3d
6	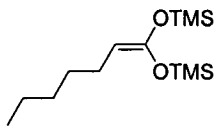	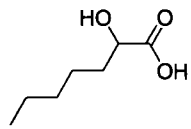	80[a]	3e
7[b]	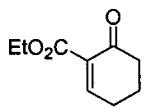	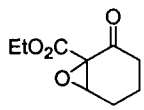	89	3f

[a] After treatment with fluoride source
[b] KOH added to reaction mixture

Table 1.2. Regio- or Diastereoselective Epoxidations with MCPBA

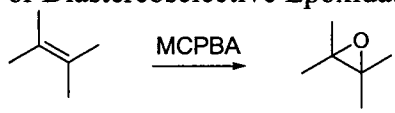

Entry	Substrate	Epoxide A	Epoxide B	Ratio (A:B)
1[4a]	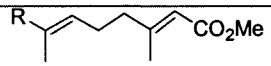	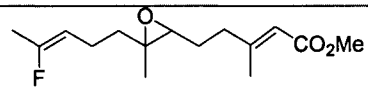	None	1:0
2[4b]	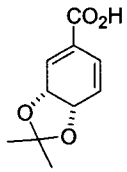	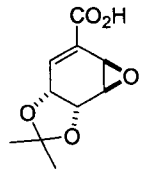	None	1:0
3[4c]		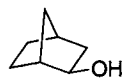	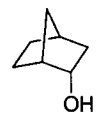	99:1[a]
4[4c]	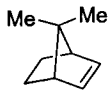	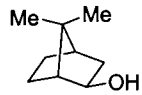	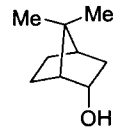	6:94[a]
5[3f]	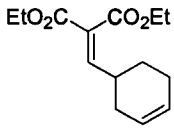	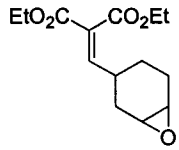	None	1:0
6[b,3f]	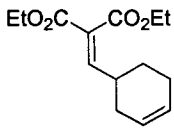	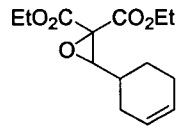	None	1:0
7[4e]	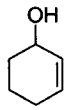	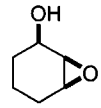	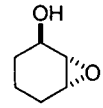	24:1
8[4e]	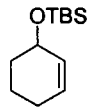	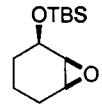	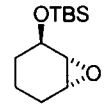	1:7
9[4f]	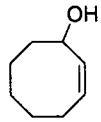	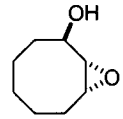	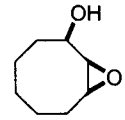	>99:1

[a] Product after MCPBA epoxidation followed by treatment with [H]
[b] KOH added to reaction mixture

Since many substrates aren't amenable to the acidic epoxidation conditions of MCPBA, neutral biphasic epoxidation conditions have been developed.[5,6] Aqueous biphasic mixtures buffered with bicarbonate efficiently epoxidize acid sensitive olefins (Table 1.3).[5] Furthermore, a similar procedure using a phosphate buffer system provides good results for acid sensitive alkenes as well (Table 1.4).[6]

Table 1.3. Select Examples of Epoxidation with MCPBA/$NaHCO_3$[5]

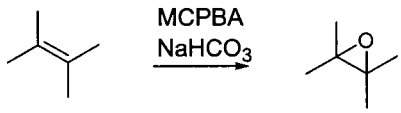

Entry	Substrate	Product	Time (h)	Yield[a] (%)
1	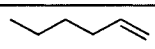	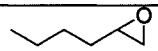	9	56
2			4	71
3	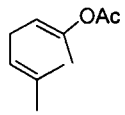	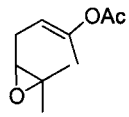	2	86
4	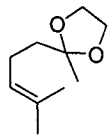	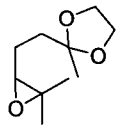	NR	80-85

[a] Calculated by glc

[5] Anderson, W.K.; Veysoglu, T. *J. Org. Chem.* **1973**, *38*, 2267.
[6] Imuta, M.; Ziffer, H. *J. Org. Chem.* **1979**, *44*, 1351.

Table 1.4. Select Examples of Epoxidation with MCPBA/NaH_2PO_4[6]

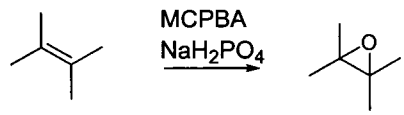

Entry	Substrate	Product	Time (h)	Yield (%)
1	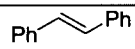	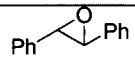	10	90[a]
2			7	95[a]
3	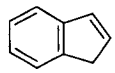	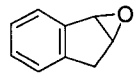	10	91
4	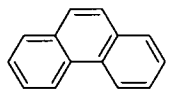	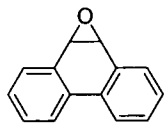	8	100[a]

[a] Determined by NMR

1.B.2. Additional Peracids

In addition to MCPBA, numerous other peracids, either isolated and used directly or generated *in situ*, have been reported to epoxidize olefins. Since peracids have been reviewed in great detail,[1b] the remainder of this section will focus on historical and especially useful examples. An early example is peroxybenzoic acid, which is easily prepared and can epoxidize a wide variety of substrates in good yield.[1b,7] Peroxybenzoic acid has very similar reactivity and selectivity to MCPBA, but unlike MCPBA, isn't commercially available.

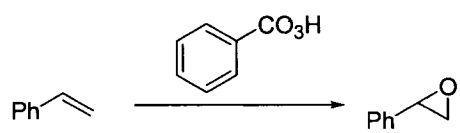

Scheme 1.1[8]

[7] Swern, D. In *Organic Reactions, Vol. 7*; Wiley: New York, **1953**.
[8] Hibbert, H.; Burt, P. *Org. Syn. Coll. Vol. 1*, 102.

Another successful peroxy-containing acid for the epoxidation of olefins is peracetic acid.[1b,9] Commercially available as a 40% solution in acetic acid, peracetic acid epoxidizes olefins in good yield (Table 1.5, Entries 1-2).[10] Epoxidation with freshly prepared peracetic acid in organic solvent (EtOAc or acetone) gives sensitive epoxides in good yield (Table 1.5, Entries 3-4).[11]

Table 1.5. Epoxidations with Peracetic Acid

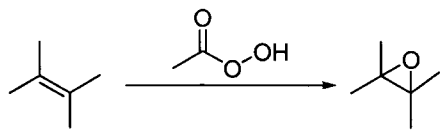

Entry	Substrate	Product	Time (h)	Yield (%)	Ref
1	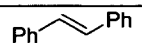	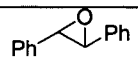	15	70-75	10a
2		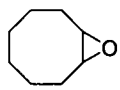	0.75	86	10b
3	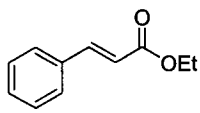	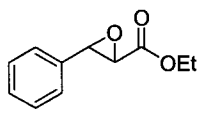	8	58	11a
4	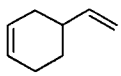	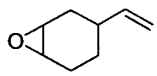	1/60	82	11b

Although the aforementioned peracids are effective for the epoxidation of a number of substrates, researchers continued to search for more active oxidants.

---

[9] Rao, A.S.; Mohan, H.R. In *Encyclopedia of Reagents for Organic Synthesis, Vol. 6*; Paquette, L.A.; Ed.; Wiley: New York, **1995**, 3933.

[10] For examples of epoxidation with 40% peracetic acid solution, see: (a) Reif, D.J.; House, H.O. *Org. Syn. Coll. Vol. 4,* 83. (b) Cope, A.C.; Fenton, S.W.; Spencer, C.F. *J. Am. Chem. Soc.* **1952**, *74*, 5884.

[11] For examples of epoxidation with peracetic acid in organic solvent, see: (a) MacPeek, D.L.; Starcher, P.S.; Phillips, B. *J. Am. Chem. Soc.* **1959**, *81*, 680. (b) Frostick, Jr., F. C.; Phillips, B.; Starcher, P.S. *J. Am. Chem. Soc.* **1959**, *81*, 3350.

It was found that peracids containing electron-withdrawing groups are more active for epoxidation than those lacking them. Of those reagents tested, nitro-substituted peroxybenzoic acids and trifluoroperacetic acid[1b,12] are particularly effective (Figure 1.2).

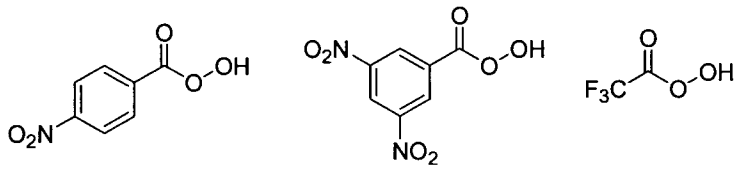

Figure 1.2 Activated peracids

p-Nitroperoxybenzoic acid[1b,13] is an efficient oxidizing reagent for a number of compounds, including stilbene (Table 1.6, Entry 1).[14] However, for a number of other substrates, including **1-9** (Table 1.6, Entry 2), reactions with *p*-nitroperoxybenzoic acid are still low yielding. To circumvent this problem, the more active 3,5-dinitroperoxybenzoic acid (DNPBA) is used to obtain epoxides in good yield (Table 1.6, Entry 2).[15] α,β-Unsaturated compounds as well as terminal olefins were found to efficiently yield oxiranes (Table 1.6, Entries 3-4). Solid DNPBA can be stored in the freezer for one year without much loss in reactivity.

---

[12] Caster, K.C. In *Encyclopedia of Reagents for Organic Synthesis Vol. 8*; Paquette, L.A.; Ed.; Wiley: New York, **1995**, 5167.
[13] Rao, A.S.; Mohan, H.R. In *Encyclopedia of Reagents for Organic Synthesis, Vol. 6*; Paquette, L.A.; Ed.; Wiley: New York, **1995**, 3750.
[14] Berti, G.; Bottari, F.; Ferrarini, P.L.; Macchia, B. *J. Org. Chem.* **1965**, *30*, 4091.
[15] Rastetter, W.H.; Richard, T.J.; Lewis, M.D. *J. Org. Chem.* **1978**, *43*, 3163.

Table 1.6. Epoxidations with Nitroperoxybenzoic Acids

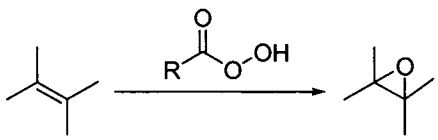

Entry	Oxidizer	Substrate	Product	Time (h)	Yield (%)	Ref
1	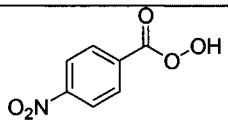	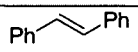	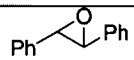	24	93	14
2	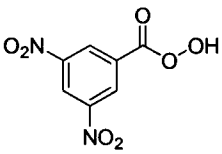	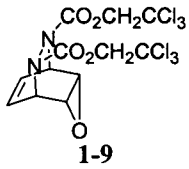 **1-9**	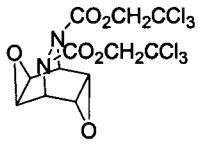	1	52	15
3	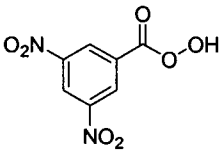	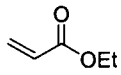	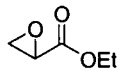	8	79	15
4	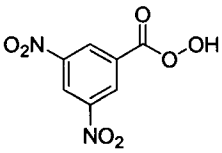	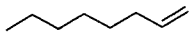	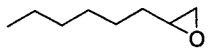	2	87	15

An even more powerful epoxidizing agent than DNPBA is trifluoroperacetic acid. Both reactive and unreactive olefins can be epoxidized in short reaction times in the presence of either Na_2HPO_4 or Na_2CO_3.[16] Excellent selectivities can also be observed for some diastereoselective epoxidations. For cyclohexenol, excellent selectivity (50:1) can be seen with the *syn*- product being favored (Table 1.7, Entry 4).[4e] Furthermore, *syn*- products are also obtained for

[16] Emmons, W.D.; Pagano, A.S. *J. Am. Chem. Soc.*, **1955**, *77*, 89.

epoxidation with TBS-protected cyclohexenol, the opposite product obtained with MCPBA (Table 1.7, Entry 5). A number of chiral, nonracemic peroxyacids have been used to epoxidize olefins with modest enantioselectivity (Figure 1.3).[1b,17,18]

Table 1.7. Select Epoxidations with Trifluoroperacetic Acid

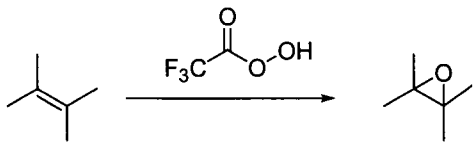

Entry	Base	Substrate	Major Product	Minor Product	Ratio	Yield (%)	Ref
1	Na_2CO_3	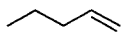	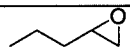	None	1:0	81	16
2	Na_2CO_3			None	1:0	74	16
3	Na_2HPO_4	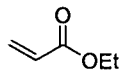	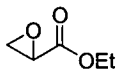	None	1:0	54	16
4	Na_2HPO_4	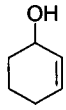	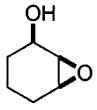	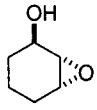	50:1	76	4e
5	Na_2HPO_4	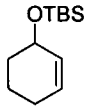	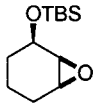	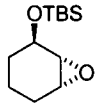	4.5:1	82	4e

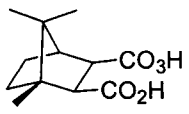

Figure 1.3 Monopercamphoric acid

[17] Morrison, J.D.; Mosher, H.S. *Asymmetric Organic Reactions*; Prentice-Hall: Englewood Cliffs, **1971**, 258.
[18] Ewins, R.C; Henbest, H.B.; McKervey, M.A. *J. Chem. Soc., Chem. Comm.*, **1967**, 1085.

1.B.3. Peroxyimidic Acids

In addition to peracids, other types of peroxy-containing reagents have been developed for epoxidation, including peroxyimidic acids.[19,20] Reaction of hydrogen peroxide with a nitrile generates a peroxyimidic acid *in situ*, which can then transfer oxygen to a double bond yielding an epoxide (Scheme 1.2). A handful of nitriles are effective for peroxyimidic acid oxidation, and a number of substrates have been successfully epoxidized, including electron-rich, electron-poor, and compounds susceptible to Bayer-Villager oxidation by other methods (Table 1.8).[21] Furthermore, high diastereoselectivity can also be observed for cases with preexisting stereochemistry. Both free and protected cyclohexenols give *syn*-products predominantly with exceptionally good *syn*-selectivity for benzyl protected ethers (Table 1.8, Entries 9-11).[21e] Asymmetric Payne epoxidation is also possible with chiral nitriles and a very structurally similar chiral cyanate (Figure 1.4).[22,23]

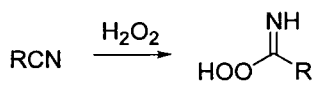

Scheme 1.2

---

[19] Bach, R.D. In *Encyclopedia of Reagents for Organic Synthesis, Vol. 6*; Paquette, L.A.; Ed.; Wiley: New York, **1995**, 3944.
[20] Payne, G.B.; Williams, P.H. *J. Org. Chem.* **1961**, *26*, 651.
[21] For examples of Payne oxidation, see: (a) Payne, G.B.; Deming, P.H.; Williams, P.H. *J. Org. Chem.* **1961**, *26*, 659. (b) Arias, L.A.; Adkins, S.; Nagel, C.J.; Bach, R.D. *J. Org. Chem.* **1983**, *48*, 888. (c) Bach, R.D.; Knight, J.W. *Org. Syn. Coll. Vol. 7,* 63. (d) Payne, G.B. *Tetrahedron* **1962**, *18*, 763. (e) Bachmann, C.; Gesson, J.-P.; Renoux, B.; Tranoy, I. *Tetrahedron Lett.* **1998**, *39*, 379.
[22] Hassine, B.B.; Gorsane, M.; Geerts-Evrard, F.; Pecher, J.; Martin, R.H.; Castelet, D. *Bull. Chem. Soc. Belg.* **1986**, *95*, 547.
[23] Rebek, J. *Heterocycles* **1981**, *15*, 517.

Table 1.8. Select Payne Oxidations

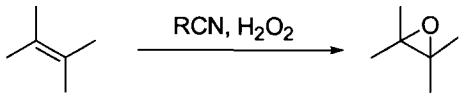

Entry	Nitrile	Substrate	Major Product	Minor Product	Ratio	Yield (%)	Ref
1	MeCN		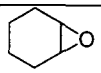			70	21a
2	PhCN					73	21a
3	Cl_3CCN					52, 60	21a,b
4	MeCN					70	21a
5	MeCN	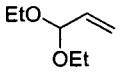	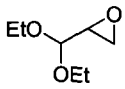			62	21a
6	MeCN		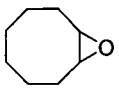			60	21c
7	PhCN	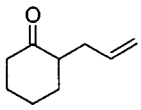	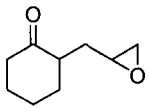			54	21d
8	PhCN					73	21d
9	MeCN	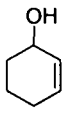	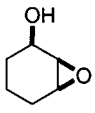	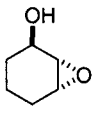	24:1	65	21e
10	MeCN	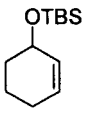	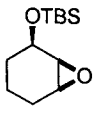	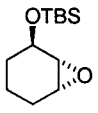	3.7:1	56	21e
11	MeCN	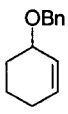	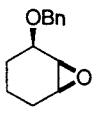	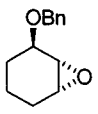	8:1	83	21e

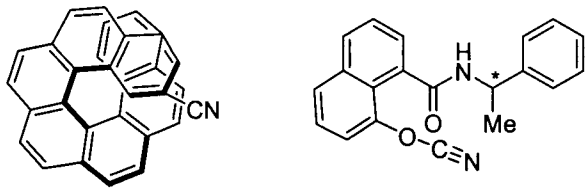

Figure 1.4 Chiral oxidizing agents[22,23]

Even though the peroxyimidic acid intermediate is most commonly generated through activation of a nitrile group, the cationic version of it can be prepared by oxidation of a Vilsmeier reagent (Scheme 1.3).[24,25] High levels of regioselectivity can be observed for cases with multiple olefins (Table 1.9).

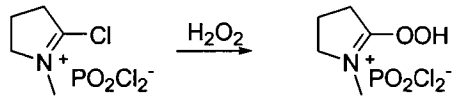

Scheme 1.3

Table 1.9. Epoxidation with an Activated Vilsmeier Reagent[25]

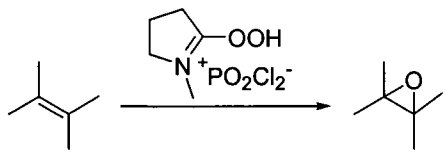

Entry	Substrate	Product	Yield (%)
1		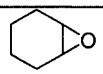	46
2			90
3	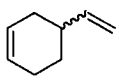	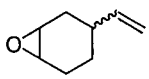	63

[24] Dulcere, J.-P.; Rodriguez, J. *Tetrahedron Lett.* **1982**, *23*, 1887.
[25] Rodriguez, J.; Dulcere, J.-P. *J. Org. Chem.* **1991**, *56*, 469.

1.B.4. Peroxyisourea

Another reagent that activates H_2O_2 is DCC, which epoxidizes olefins by way of a peroxyisourea (Scheme 1.4)[26] A number of unactivated olefins can be epoxidized in good yield with the DCC/H_2O_2 system, including some that give poor yields with other peroxy-containing compounds (Table 1.10). Alternatively, UHP can be used as an efficient H_2O_2 source.[26e,f] Much like the peracid and Payne oxidation cases, chiral carbodiimides have been reported to epoxidize olefins in modest ee (Figure 1.5).[23,27]

Table 1.10. DCC-Mediated Epoxidations

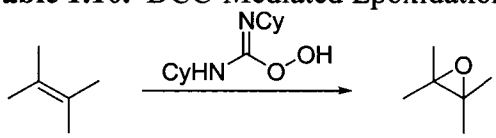

Entry	Oxidant	Substrate	Product	Yield (%)	Ref
1	H_2O_2		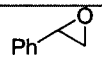	75	26d
2	UHP			81	26e
3	H_2O_2	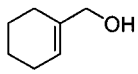	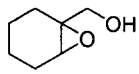	68	26c
4	H_2O_2		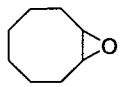	58	26d
5	H_2O_2		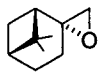	91	26d
6	H_2O_2	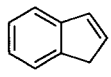	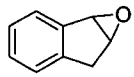	98	26d

[26] For examples of peroxyisourea epoxidation, see: (a) Mitsunobu, O.; Tomari, M.; Morimoto, H.; Sato, T.; Sudo, M. *Bull. Chem. Soc. Jpn.* **1972**, *45*, 3607. (b) Krishnan, S.; Kuhn, D.G.; Hamilton, G.A. *Tetrahedron Lett.* **1977**, 1369. (c) Majetich, G.; Hicks, R. *Synlett* **1996**, 649. (d) Majetich, G.; Hicks, R.; Sun, G.-r.; McGill, P. *J. Org. Chem.* **1998**, *63*, 2564. (e) Murray, R.W.; Iyanar, K. *J. Org. Chem.* **1998**, *63*, 1730. (f) Patil, G.S.; Nagendrappa, G. *Syn. Comm.* **2002**, *32*, 2677.
[27] Rebek, J.; Wolf, S.; Mossman, A. *J. Org. Chem.* **1978**, *43*, 180.

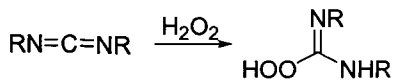

Scheme 1.4

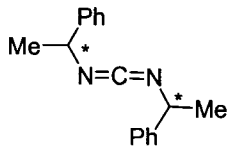

Figure 1.5 Chiral carbodiimide

1.B.5. Peroxycarbonic Acids

Either isolated or generated *in situ* from chloroformates (Scheme 1.5) or imidazoles (Scheme 1.6), peroxycarbonic acids can also epoxidize olefins in good yield.[28] Initial studies found O-benzylmonoperoxycarbonic acid to be less active than MCPBA but more active than perbenzoic acid (Table 1.11, Entry 1). Since then, O-ethyl- and O-*t*-butylperoxycarbonic acids were also found to be effective agents for epoxidation of olefins, and in some cases, excellent diastereoselectivity can be observed for olefins with preexisting stereochemistry (Table 1.11, Entries 2-6).

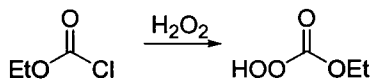

Scheme 1.5

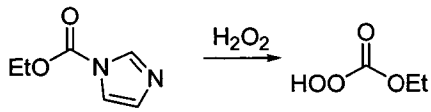

Scheme 1.6

[28] For examples of epoxidation with peroxycarbonic acids, see: (a) Coates, R.M.; Williams, J.W. *J. Org. Chem.* **1974**, *39*, 3054. (b) Bach, R.D.; Klein, M.W.; Ryntz, R.A.; Holubka, J.W. *J. Org. Chem.* **1979**, *44*, 2569. (c) Tsunokawa, Y.; Iwasaki, S.; Okuda, S. *Tetrahedron Lett.* **1982**, *23*, 2113.

Table 1.11. Epoxidation with O-Alkylperoxycarbonic Acids

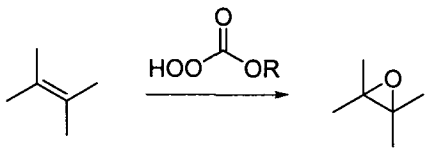

Entry	Oxidizing Agent	Substrate	Product	Yield (%)	Ref
1		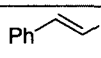	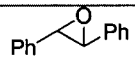	75	28a
2			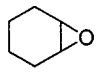	55	28b
3			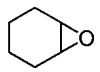	95[a]	28c
4		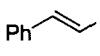	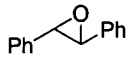	71[a]	28c
5		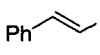	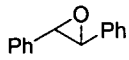	84[a]	28c
6		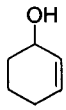	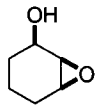	NR	28c

[a] GLC yield

1.B.6. Peroxycarbamic Acids

Peroxycarbamic acids are another class of reagents that have been shown to epoxidize olefins. They can be prepared from reaction of H_2O_2 with isocyantes[29] or carbonyldiheterocycles (Schemes 1.7, 1.8).[30] Upon treatment with olefins, they give epoxides in good yield (Table 1.12).

[29] Matsumura, N.; Sonoda, N.; Tsutsumi, S. *Tetrahedron Lett.* **1970**, 2029.
[30] Rebek, J.; McCready, R.; Wolf, S.; Mossman, A. *J. Org. Chem.* **1979**, *44*, 1485.

Chiral peroxycarbamic acids have also been reported to epoxidize olefins (Figure 1.6).[23,27]

Table 1.12. Epoxidation with Peroxycarbamic Acid

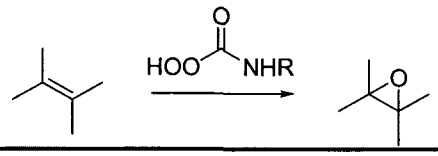

Entry	Oxidizing Agent	Substrate	Product	Yield (%)	Ref
1	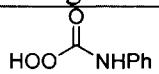		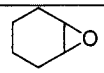	69	29
2	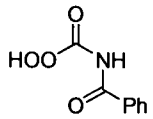			99	30
3	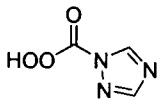			99[a]	30
4	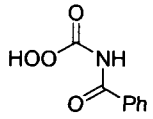	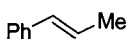	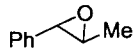	92	30
5	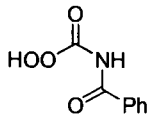	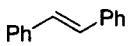	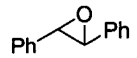	59	30
6	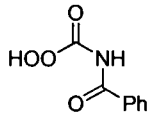	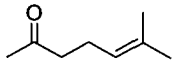	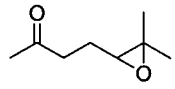	>90	30

[a] GLC yield

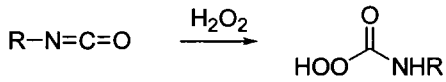

Scheme 1.7

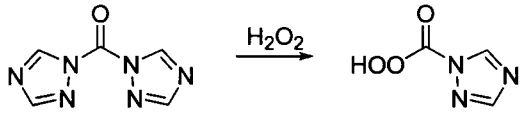

Scheme 1.8

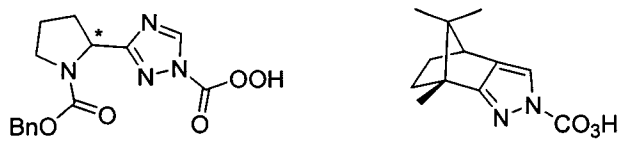

Figure 1.6 Chiral peroxycarbamic acids

1.B.7. Perhydrates[31]/ α-Hydroperoxy-Compounds

An alternative approach for generating peroxy-containing compounds capable of epoxidizing olefins is the reaction of H_2O_2 with either ketones or orthoesters to give either free or protected perhydrates (Schemes 1.9, 1.10). A number of activated ketones and orthoesters have been tested, both achiral and chiral, and hexafluoroacetone was found to be very efficient (Table 1.13).[23,32] In fact, this reaction can be catalytic in ketone, since regeneration of the ketone occurs after oxygen delivery (Table 1.14). α-Hydroperoxy- compounds capable of activation are also competent epoxidizing agents. For orthoester-derived hydroperoxides, intramolecular reactions are also possible (Table 1.13, Entry 9). Asymmetric epoxidation has been obtained with chiral hydroperoxides, and up to 31% ee was observed for the reaction of stilbene with **1-10** (Figure 1.7).

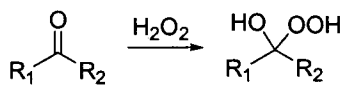

Scheme 1.9

[31] Ganeshpure, P.A.; Adam, W. *Synthesis* **1996**, 179.

[32] For examples of perhydrate epoxidation, see: (a) Stark, C.J. *Tetrahedron Lett.* **1981**, *22*, 2089. (b) Heggs, R.P.; Ganem, B. *J. Am. Chem. Soc.* **1979**, *101*, 2484. (c) Van Vliet, M.C.A.; Arends, I.W.C.E.; Sheldon, R.A. *J. Chem. Soc., Chem. Comm.* **1999**, 263. (d) Rebek, J.; McCready, R. *Tetrahedron Lett.* **1979**, 1001. (e) Rebek, J.; McCready, R. *J. Am. Chem. Soc.* **1980**, *102*, 5602. (f) Legros, F.; Crousse, B.; Bonnet-Delpon, D.; Bégué, J.-P. *Eur. J. Org. Chem.* **2002**, 3290.

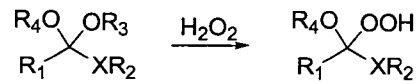

Scheme 1.10

Table 1.13. Epoxidation with Perhydrate

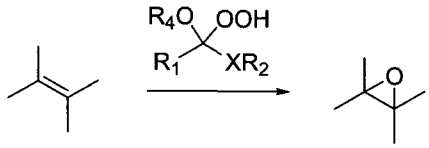

Entry	Oxidizing Agent	Substrate	Product	Time (h)	Yield (%)	Ref
1	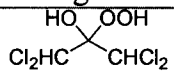		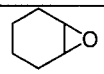	24	80	32a
2	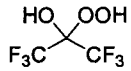			¼	90	32b
3	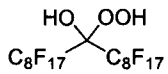			2	92[a]	32c
4	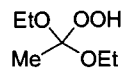			4	99[a]	32d
5	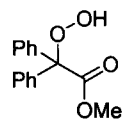			24	63[a]	32e
7	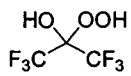	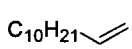	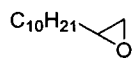	6	93	32b
8	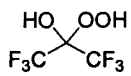	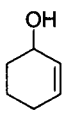	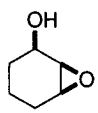	22	90	32b
9	H_2O_2	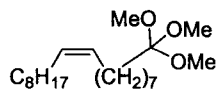	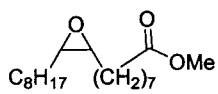	24	40	32e

[a] GLC/NMR yield

Table 1.14. Examples of Catalytic Perhydrate Epoxidation[a]

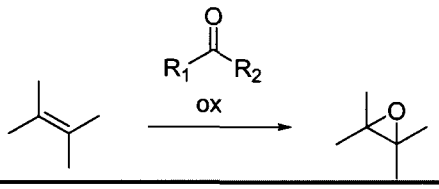

Entry	Equiv Ketone	Ketone	Substrate	Time (h)	Yield (%)	Ref
1	0.13	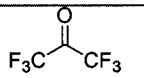	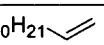	72	77	32b
2	0.05	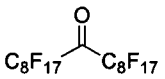		2	92[b]	32c
3	0.03	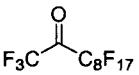		1	85	32f
4	0.05	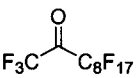	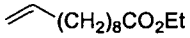	48	89	32f

[a] All perhydrates generated from H_2O_2 except entries 3-4, where the perhydrate was generated by UHP.
[b] GC Yield

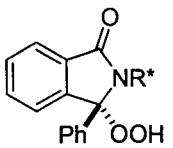

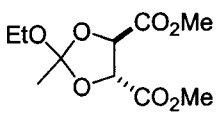

$HC(OCH_2CH(CH_3)CH_2CH_3)_3$

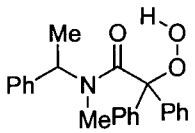

1-10

Figure 1.7 Chiral hydroperoxides

1.B.8. Selenium, Phosphorous, and Sulfur-Containing Oxidants

Although the discussion up to this point has focused on activated peroxides bound to carbon, organic peroxides bound to heteroatoms are also competent epoxidizing agents (Figure 1.8). Stoichiometric benzeneperoxyselenic acid was originally shown to epoxidize olefins, and since then, other selenium

reagents have been shown to catalyze the epoxidation of olefins (Table 1.15).[33] Organophosphorous compounds can also epoxidize olefins in good yield (Table 1.16).[34] Modest ee (22 %) is observed for asymmetric epoxidation of styrene with a binol-type phosphorous reagent (**1-11**) (Figure 1.9).[35] Furthermore, good yield and diastereoselectivity can be achieved with the peracid of *p*-toluenesulfonic acid when prepared with H_2O_2 (Table 1.17).[36] Use of superoxide to generate similar species results in poor diastereoselectivity for *cis*-olefins, presumably due to radical isomerization.[36c] Finally, cyclic peroxides bound to sulfur are also capable of epoxidizing olefins (Scheme 1.11).[36d]

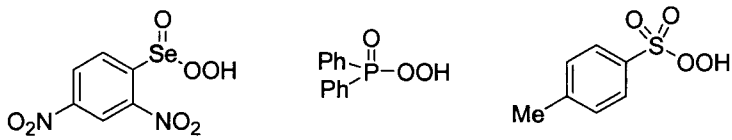

Figure 1.8 Examples of oxidants

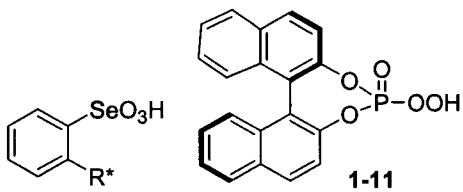

Figure 1.9 Chiral oxidizing agents

---

[33] For examples of epoxidation with organoselenium agents, see: (a) Grieco, P.A.; Yokoyama, Y.; Gilman, S.; Nishizawa, M. *J. Org. Chem.* **1977**, *42*, 2034. (b) Hori, T.; Sharpless, K.B. *J. Org. Chem.* **1978**, *43*, 1689.

[34] Kende, A.S.; Delair, P.; Blass, B.E. *Tetrahedron Lett.* **1994**, *35*, 8123.

[35] Berkessel, A.; Frauenkron, M. *Tetrahedron Asym.* **1996**, *7*, 671.

[36] For examples of epoxidation with organosulfur reagents, see: (a) Schulz, M.; Kluge, R.; Lipke, M. *Synlett* **1993**, 915. (b) Kluge, R.; Schulz, M.; Liebsch, S. *Tetrahedron* **1996**, *52*, 2957. (c) Kim, Y.H. In *Modern Methodology in Organic Synthesis*; Shono, T.; Ed.; VCH Publishers, **1992**, 303. (d) Martin, L.D.; Martin, J.C. *J. Am. Chem. Soc.* **1977**, *99*, 3511.

Table 1.15. Epoxidation with Organoselenium Reagents

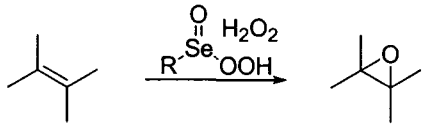

Entry	Equiv Se	Oxidizer	Product	Time (h)	Yield (%)	Ref
1	1.2	PhSe(O)OOH	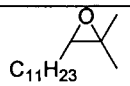	¾	85	33a
2	1.2	PhSe(O)OOH	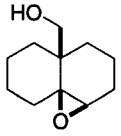	1/3	75	33a
3	0.05	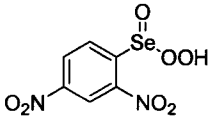	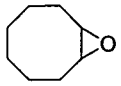	20	95	33b
4	0.1	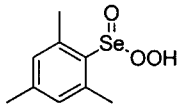	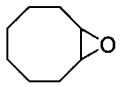	20	100[a]	33b

[a] Conversion (%)

Table 1.16. Oxidations with Organophosphorous Agents[34]

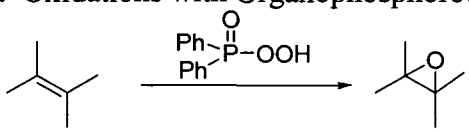

Entry	Olefin	Product	Yield (%)
1	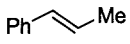	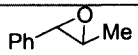	93
2	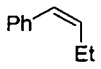	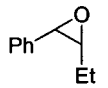	90
3		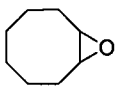	88
4	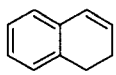	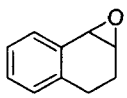	100

Table 1.17. Oxidations with Organosulfur Agents

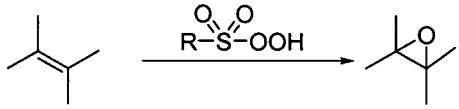

Entry	Acid	Substrate	Major Product	Ratio	Yield (%)	Ref
1	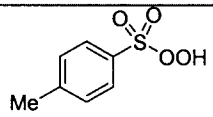	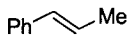	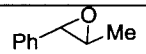	1:0	82	36b
2	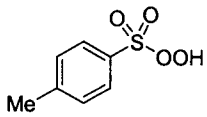	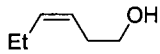	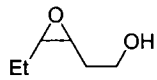	1:0	93	36b
3	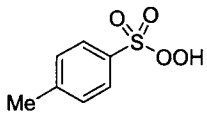	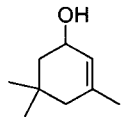	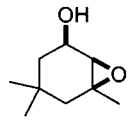	>>19:1	76	36b
4[a]	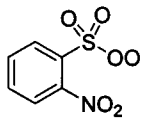	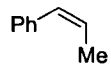	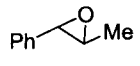	7:3	NR	36c
5[a]	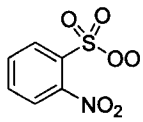	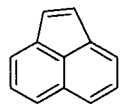	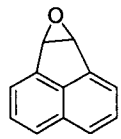	1:0	95	36c

[a] From superoxide

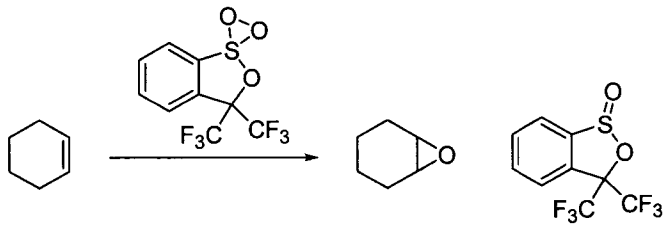

Scheme 1.11

1.B.9. Intermolecular H_2O_2 Activation

In almost all the aforementioned examples, activation of the peroxide occurs through intramolecular hydrogen bonding. However, it is possible for the oxidant to be activated by way of an intermolecular hydrogen bond from solvent molecules. Neumann found that 1,1,1,3,3,3-hexafluroisopropanol (HFIP) is an especially effective solvent for activation of H_2O_2, and good conversion can be obtained for reactive substrates (Figure 1.10, Table 1.18, Entries 1,2).[37] Further studies showed buffered trifluroethanol is also an effective solvent,[38] and UHP[32f] can be used as the oxidant for some olefins.

Table 1.18. Epoxidation of Olefins with H_2O_2 in Fluorinated Solvents

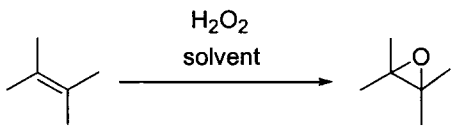

Entry	Oxidant	Solvent	Substrate	Yield (%)	Ref
1	H_2O_2	HFIP		100[a]	37
2	H_2O_2	HFIP		100[a]	37
3	H_2O_2	TFE		88	38
4	UHP	HFIP	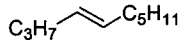	90	32f

[a] Conversion (%)

[37] Neimann, K.; Neumann, R. *Org. Lett.* **2000**, *2*, 2861.
[38] Van Vliet, M.C.A.; Arends, I.W.C.E.; Sheldon, R.A. *Synlett* **2001**, 298.

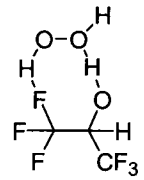

Figure 1.10 Intermolecular activation of H_2O_2 in HFIP

1.C. SYNTHESIS OF EPOXIDES BY OXAZIRIDINE

Oxaziridines, useful reagents for olefin epoxidation, are three membered rings containing oxygen, carbon, and nitrogen. Generally speaking, the oxygen transfers to the olefin in an oxidation reaction, leaving an imine as a byproduct (Scheme 1.12). Furthermore, there are two different variations of oxaziridines: the free oxaziridine containing a lone pair on the oxaziridine nitrogen and the oxaziridinium salt possessing a formal positive charge on the nitrogen (Figure 1.11). The majority of efforts has been focused on oxaziridinium salts, since they are the more active oxidizing reagents of the two. A number of catalysts[39] have been developed for racemic epoxidation of olefins (Figure 1.12), and a chiral dihydroisoquinolium salt catalyzes the asymmetric epoxidation of 6-substituted chromenes in high ee.

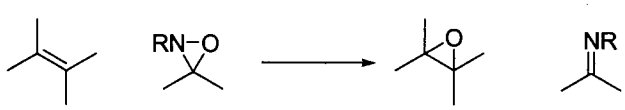

Scheme 1.12

[39] Adam, W.; Saha-Möller, C.R.; Ganeshpure, P.A. *Chem. Rev.* **2001**, *101*, 3499.

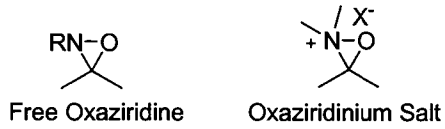

Figure 1.11 Free oxaziridines vs oxaziridinium salts

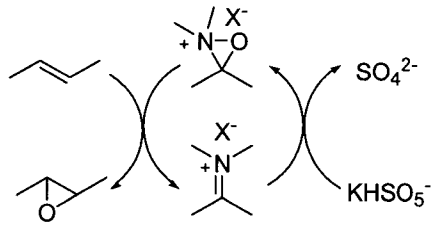

Figure 1.12 Catalytic epoxidation by oxaziridinium salt generated *in situ*

1.C.1. Free Oxaziridines

Free oxaziridines were first found to carry out a number of epoxidation reactions in good yield (Table 1.19).[40] Electron-withdrawing groups present on the oxaziridine increase the activity of the reagent toward epoxidation, and much like peracids, epoxidation with free oxaziridines proceeds with no *cis/trans* isomerization. Silyl enol ethers yield α-hydroxyketones after treatment with acid (Table 1.19, Entry 5). Additional oxaziridines have been found to epoxidize olefins in good yield (Table 1.20). Recently, a catalytic epoxidation via free oxaziridine has been developed using a selenium cooxidant (Table 1.21).[41]

---

[40] For examples of epoxidation with stoichiometirc oxaziridines, see: (a) Davis, F.A.; Chen, B.-C. *Chem. Rev.* **1992**, *92*, 919. (b) Davis, F.A.; Abdul-Malik, N.F.; Awad, S.B.; Harakal, M.E. *Tetrahedron Lett.* **1981**, *22*, 917. (c) Davis, F.A.; Sheppard, A.C. *J. Org. Chem.* **1987**, *52*, 955. (d) Arnone, A.; DesMarteau, D.D.; Novo, B.; Petrov, V.A.; Pregnolato, M.; Resnati, G. *J. Org. Chem.* **1996**, *61*, 8805.

[41] Brodsky, B.H.; Du Bois, J. *J. Am. Chem. Soc.* **2005**, *127*, 15391.

Table 1.19. First Epoxidation of Olefins by Oxaziridine

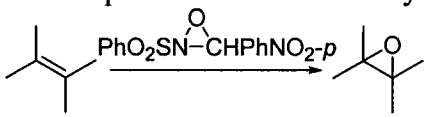

Entry	Substrate	Product	Time (h)	Yield (%)	Ref
1	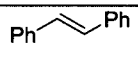	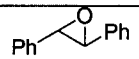	12	70	40b
2	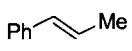	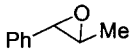	12	70	40b
3			3	50	40b
4[a]			3	81	40b
5[b]	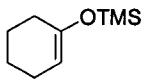	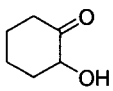	3	65	40c

[a] NMR yield using internal standard method
[b] After treatment with 5% HCl/THF

Table 1.20. Epoxidation of Olefins by Additional Oxaziridines

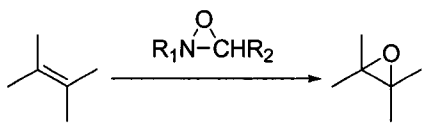

Entry	Substrate	Oxaziridine	Time (h)	Yield (%)	Ref
1		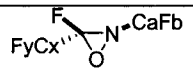	0.67	88	40d
2	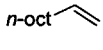	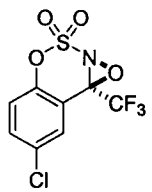	NR	85	41

Table 1.21. Catalytic Epoxidation of Olefins by Oxaziridine[41]

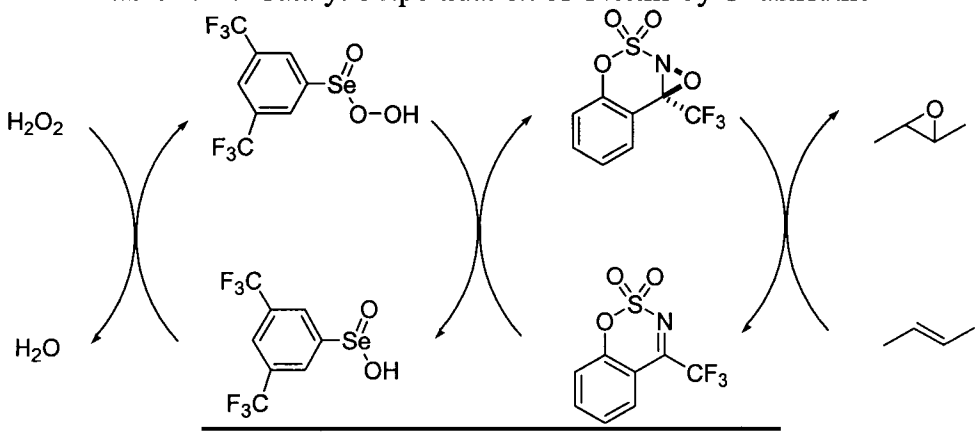

Entry	Substrate	Cat. Eq.	Time (h)	Yield (%)
1	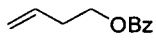	0.1	36	92
2	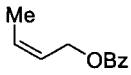	0.1	12	94
3	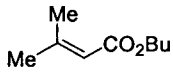	0.2	45	96

If stereogenic centers are located adjacent to the oxaziridine, an asymmetric epoxidation is possible. Chiral sulfamyloxaziridines epoxidize olefins in up to 65% ee (Table 1.22).[42]

[42] For examples of chiral oxaziridines, see: (a) Davis, F.A.; Chattopadhyay, S. *Tetrahedron Lett.* **1986**, *27*, 5079. (b) Davis, F.A.; Harakal, M.E.; Awad, S.B. *J. Am. Chem. Soc.* **1983**, *105*, 3123.

Table 1.22. Asymmetric Epoxidation of Olefins with Different Chiral Oxaziridines[42]

Oxaziridine	Ph⟋⟍Ph	Ph⟋⟍Me
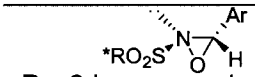 R = 3-bromocamphor Ar = 2-chloro-5-nitrophenyl	30% ee	27% ee
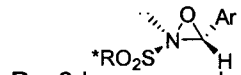 R = 3-bromocamphor Ar = 2-chloro-5-nitrophenyl	35% ee	28% ee
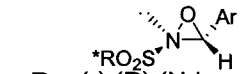 R = (-) (R) (N-benzyl)-1-phenylethylamine Ar = pentafluorophenyl	56% ee	65% ee
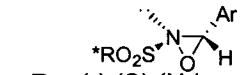 R = (-) (S) (N-benzyl)-1-phenylethylamine Ar = pentafluorophenyl	49% ee	53% ee

1.C.2. Oxaziridinium Salts

Even though success had been achieved with oxaziridines, the search continued for more robust oxidants. Oxaziridinium salts were found to efficiently transfer oxygen to a number of olefins, quite often with short reaction times.[43] Much like the free oxaziridine, oxaziridinium salts epoxidize olefins in a concerted manner (Table 1.23, entry 2), and good diastereoselectivity can be observed for some olefins with preexisting stereochemistry. In particular, oxaziridines yielded excellent selectivities for acetate protected alcohols, substrates that generally give lower selectivities with MCPBA and DMDO.

[43] For examples of epoxidations with stoichiometric oxaziridinium salts, see: (a) Hanquet, G.; Lusinchi, X.; Milliet, P. *Tetrahedron Lett.* **1988**, *29*, 3941. (b) Lusinchi, X.; Hanquet, G. *Tetrahedron* **1997**, *53*, 13727. (c) Poisson, D.; Cure, G.; Solladié, G.; Hanquet, G. *Tetrahedron Lett.* **2001**, *42*, 3745.

Furthermore, intramolecular epoxidation by a chiral oxaziridine yields an epoxyaldehyde in high ee after imine hydrolysis (Scheme 1.13).[44] Intramolecular oxygen transfer is also possible from achiral iminium salts to provide complementary products to MCPBA epoxidation (Scheme 1.14).[45]

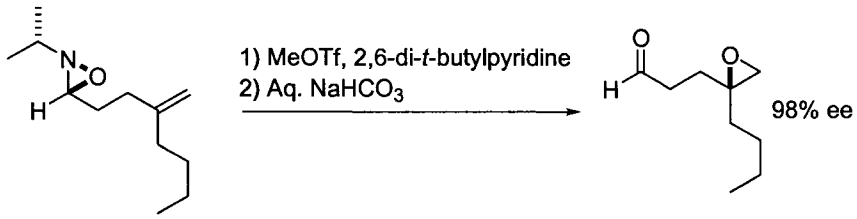

Scheme 1.13

Table 1.23. Epoxidation of Olefins by Oxaziridinium Salt[44b]

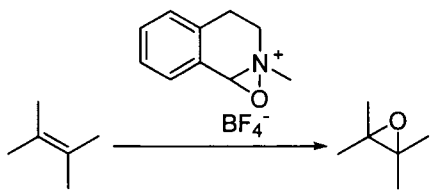

Entry	Substrate	Major Product	Time (min)	Yield (%) (Ratio)
1	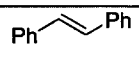	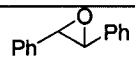	30	96
2	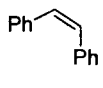	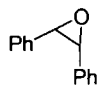	60	89
3	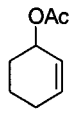	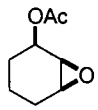	180	92 (19:1)
4			10	84

[44] Armstrong, A.; Draffin, A.G. *Tetrahedron Lett.* **1999**, *40*, 4453.
[45] Armstrong, A.; Draffin, A.G. *Synlett* **1998**, 646.

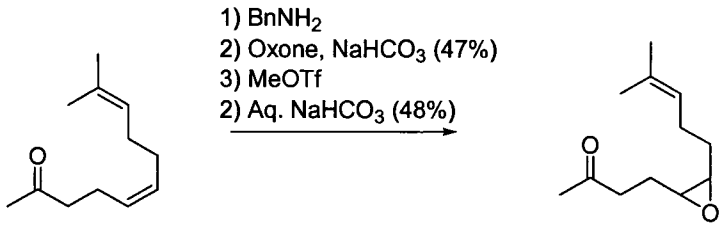

Scheme 1.14

Considering the activity of oxaziridinium salts, catalytic systems have been developed for olefin epoxidation. Aromatic and aliphatic iminium salts derived from pyrrolidine catalyze the epoxidation of olefins (Table 1.24).[46]

Table 1.24. Catalytic Epoxidation of Olefins by Iminium Salts

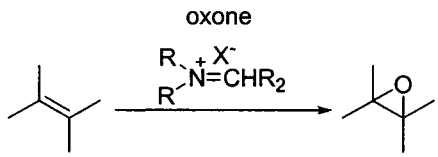

Entry	Substrate	Iminium Salt	Eq. Cat.	Time (h)	Conv (%)	Yield (%)	Ref
1	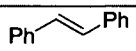	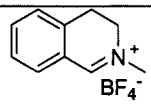	0.1	16	100	NR	46b
3	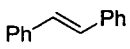	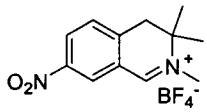	0.05	1.5	100	NR	46b
4	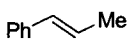	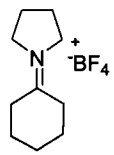	0.1	16	NR	81	46c
5	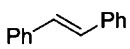	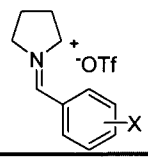	0.1	4	100	89	46d

[46] For examples of oxaziridinium salt catalyzed epoxidation, see: (a) Bohé, L.; Kammoun, M. *Tetrahedron Lett.* **2002**, *43*, 803. (b) Bohé, L.; Kammoun, M. *Tetrahedron Lett.* **2004**, *45*, 747. (c) Minakata, S.; Takemiya, A.; Nakamura, K.; Ryu, I.; Komatsu, M. *Synlett*, **2000**, 1810. (d) Armstrong, A.; Ahmed, G.; Garnett, I.; Goacolou, K. *Synlett*, **1997**, 1075. (e) Biscoe, M.R.; Breslow, R. *J. Am. Chem. Soc.* **2005**, *127*, 10812.

A number of iminium salt asymmetric epoxidation catalysts have also been developed.[47] Salts derived from **1-12**, binapthyl-based systems, proline derivatives, pyrrolidine-containing compounds, dihydroisoquinolium salts, and mixtures of the aforementioned functionalities with different counterions have been incorporated into chiral iminium salts with varying degrees of success (Table 1.25). Binapthyl-containing iminium salt **1-13** gives good ee for phenylclohexene (Table 1.25), while dihydroisoquinolium salt **1-14** yields 6-substituted chromene oxides in high ee using an organic persulfate compound as primary oxidant (Table 1.25).

Table 1.25. Asymmetric Epoxidation of Olefins with Different Iminium Catalysts

Ketone		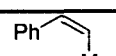		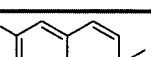	Ref
	ee (%)	ee (%)	ee (%)	ee (%)	
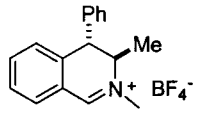 **1-12**	33				47a
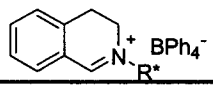	73		0-40		47c

[47] For examples of asymmetric epoxidation via oxaziridinium salts, see: (a) Bohé, L, Hanquet, G.; Lusinchi, M.; Lusinchi, X. *Tetrahedron Lett.* **1993**, *34*, 7271. (b) Gluszyńska, A.; Maćkowska, I.; Rozwadowska, M.D.; Sienniak, W. *Tetrahedron Asym.* **2004**, *15*, 2499. (c) Page, P.C.B.; Rassias, G.A.; Bethell, D.; Schilling, M.B. *J. Org. Chem.* **1998**, *63*, 2774. (d) Aggarwal, V.K.; Wang, M.F. *J. Chem. Soc., Chem. Comm.* **1996**, 191. (e) Armstrong, A.; Ahmed, G.; Garnett, I.; Goacolou, K.; Wailes, J.S. *Tetrahedron* **1999**, *55*, 2341. (f) Wong, M.-K.; Ho, L.-M.; Zheng, Y.-S.; Ho, C.-Y.; Yang, D. *Org. Lett.* **2001**, *3*, 2587. (g) Vachon, J.; Pérollier, C.; Monchaud, D.; Marsol, C.; Ditrich, K.; Lacour, J. *J. Org. Chem.* **2005**, *70*, 5903. (h) Lacour, J.; Monchaud, D.; Marsol, C. *Tetrahedron Lett.* **2002**, *43*, 8257. (i) Page, P.C.B.; Barros, D.; Buckley, B.R.; Ardakani, A.; Marples, B.A. *J. Org. Chem.* **2004**, *69*, 3595. (j) Page, P.C.B.; Buckley, B.R.; Blacker, A.J. *Org. Lett.* **2004**, *6*, 1543. (k) Page, P.C.B.; Buckley, B.R.; Heaney, H.; Blacker, A.J. *Org. Lett.* **2005**, *7*, 375.

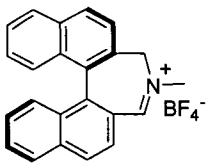	31	71	47d
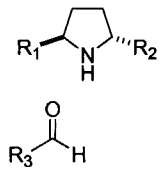	10-15	22	47e
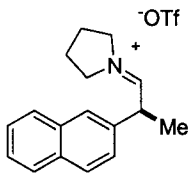	9		47e
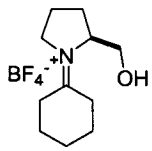 39% ee for cinnamyl alcohol			46c
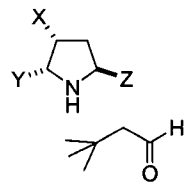	65	46	47f
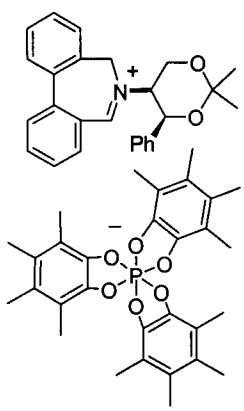	17	69	47g,h
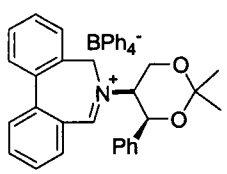	14	67	47i

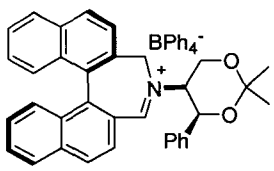 **1-13**	20	91		47j
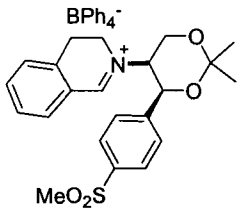 **1-14**	70		97	47k

1.D. SYNTHESIS OF EPOXIDES BY DIOXIRANE

Dioxiranes, three-membered cyclic peroxides, are useful oxidants for a wide variety of transformations, including the epoxidation of electron-rich and electron-poor olefins.[48] They can be isolated and used as reagents, or they can be generated *in situ* (Scheme 1.15). In many cases in which the dioxirane is generated *in situ*, only catalytic amounts of ketone are required, since the ketone is regenerated after oxygen delivery (Figure 1.13). For both catalytic and stoichiometric examples, high degrees of regioselectivity are often observed when multiple alkenes exist in a single substrate. Generally speaking, the observed selectivity is attributable to two factors. First, the electrophilic dioxirane reacts with more electron-rich olefins, as long as the dioxirane approach to the alkene is sterically feasible. Furthermore, steric factors also quite often lead to certain

[48] Adam, W.; Saha-Möller, C.R.; Zhao, C.-G. In *Organic Reactions, Vol. 61*; Overman, L. E.; Ed.; Wiley: Hoboken, **2002**, 219.

olefin classes being more reactive than others, such as *cis*-olefins being more reactive than their *trans*-counterparts. In addition to giving good regioselectivity for a number of olefins, dioxiranes can yield high levels of diastereoselectivty for olefins with preexisting stereochemistry. In addition to high regio- and diastereoselectivity, it is possible for stereogenic centers adjacent to the ketone to result in high ee for the epoxide product. A readily available chiral ketone can epoxidize *trans*- and trisubstituted olefins in high enantioselectivity.

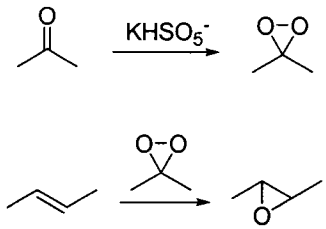

Scheme 1.15

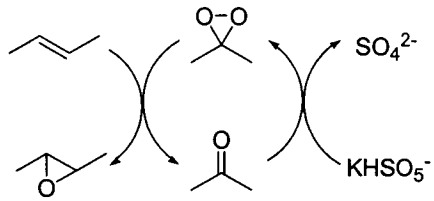

Figure 1.13 Catalytic epoxidation by dioxirane generated *in situ*

1.D.1. Dimethyldioxirane (DMDO)

Dimethyldioxirane (DMDO) can be generated *in situ* or isolated and used directly. The earliest reports were for *in situ* generated cases, where a biphasic solution was found to epoxidize a number of olefins in good yield at neutral pH (Table 1.26).[49] For acyclic *cis*-olefin epoxidation, no isomerization to *trans*-epoxides is observed, suggesting the reaction proceeds without the radical

[49] Curci, R.; Fiorentino, M.; Troisi, L. *J. Org. Chem.* **1980**, *45*, 4758.

intermediates often present during metal catalyzed epoxidations (Table 1.26, Entry 3). Recently, a procedure for efficient DMDO epoxidation in basic solution has been reported, providing an attractive alternative for base stable olefins and epoxides (Table 1.27).[50] For substrates unstable to the standard biphasic conditions at neutral or alkaline pH, DMDO can also be isolated and used directly (Table 1.28). [48,51] High levels of diastereoselectivity have been observed for olefins with preexistent, adjacent stereochemistry (Table 1.29).[52] Regioselectivity was also found to be excellent in many cases with multiple double bonds. The good diastereo- and regioselectivity observed in a number of cases with this reagent along with the numerous different procedures for its preparation make DMDO a very effective epoxidizing reagent.

Table 1.26. Epoxidation with DMDO Generated *in situ*[49]

Entry	Substrate	Time (h)	Conv. (%)	Yield (%)
1	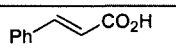	2.3	99	95
2	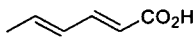	2	99	86
3	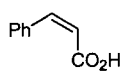	3.5	90	90
4	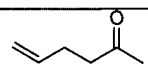	2	99	97

[50] Frohn, M.; Wang, Z.-X.; Shi, Y. *J. Org. Chem.* **1998**, *63*, 6425.
[51] For examples of epoxidation with isolated DMDO, see: (a) Murray, R.W.; Jeyaraman, R. *J. Org. Chem.* **1985**, *50*, 2847. (b) Murray, R.W.; Singh, M. *Org. Syn. Coll. Vol. 9*, 288. (c) Baumstark, A.L.; Harden, Jr., D.B. *J. Org. Chem.* **1993**, *58*, 7615.
[52] For examples of regio and diastereoselective epoxidations with DMDO, see: (a) Cicala, G.; Curci, R.; Fiorentino, M.; Laricchiuta, O. *J. Org. Chem.* **1982**, *47*, 2670. (b) Yang, D.; Jiao, G.-S.; Yip, Y.-C.; Wong, M.-K. *J. Org. Chem.* **1999**, *64*, 1635. (c) Lluch, A.-M.; Sánchez-Baeza, F.; Messeguer, A. *Tetrahedron* **1993**, *49*, 6299.

Table 1.27. Efficient Epoxidation with DMDO at High pH[50]

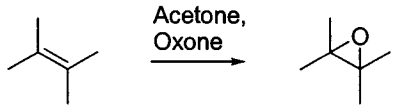

Entry	Substrate	Time (h)	Conv. (%)	Yield (%)
1	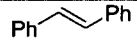	4	>95	87
2	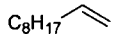	4	79	67
3	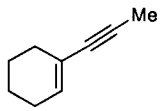	2	>95	84
4	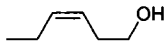	4	>95	90
5		4	>95	91

Table 1.28. Epoxidation with Isolated DMDO[48,51]

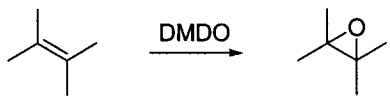

Entry	Substrate	Time (h)	Equiv. DMDO	Yield (%)
1	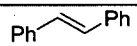	6	1	100
2		1/3	1	97
3		1	1	81
4	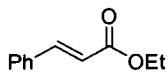	24	2	100

Table 1.29. Examples of Regio- or Diastereoselective Epoxidations with DMDO

Substrate	Major Product	Minor Product	Ratio
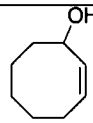	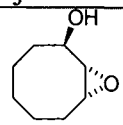	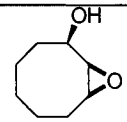	99:1[52a]
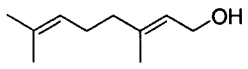	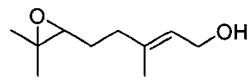	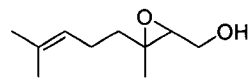	6.9:1[a,52a]
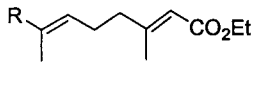	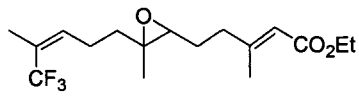	None	1:0[52c]
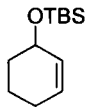	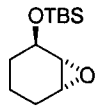	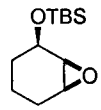	4.8:1[52b]

[a] 21% of bis-epoxide isolated

1.D.2. Methyl(trifluoromethyl)dioxirane (TFDO)

Although a great deal of success had been achieved, DMDO still wasn't reactive enough to epoxidize some substrates. Consequently, efforts were directed toward developing more robust ketones. In 1989, Mello and Curci first reported methyltrifluoromethyldioxirane (TFDO) to be an effective epoxidizing agent (Table 1.30).[53] First isolated, then used directly on the substrate, TFDO is more active than DMDO, increasing the substrate scope of dioxirane mediated epoxidations. Furthermore, the increased activity of TFDO substantially reduces the reaction times for a number of substrates. Given the potential usefulness of

[53] For early examples of TFDO epoxidation, see: (a) Mello, R.; Fiorentino, M.; Sciacovelli, M.F.O.; Curci, R. *J. Org. Chem.* **1988**, *53*, 3891. (b) Troisi, L.; Cassidei, L.; Lopez, L.; Mello, R.; Curci, R. *Tetrahedron Lett.* **1989**, *30*, 257.

TFDO, Yang developed an *in situ* generated dioxirane procedure for TFDO (Table 1.31).[54] Finally, an operationally simple, catalytic procedure using hydrogen peroxide as the primary oxidant by way of a peroxyimidic acid intermediate has also been developed (Table 1.32).[55]

Table 1.30. Epoxidation of Olefins with Isolated TFDO

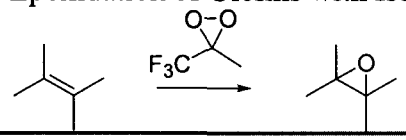

Substrate	Major Product	Time (min)	Yield (%)
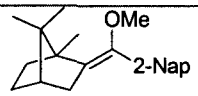	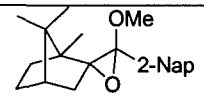	5	92[53b]
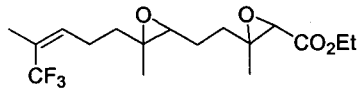	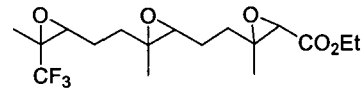	60	94[52c]

Table 1.31. Epoxidation with TFDO Generated *in situ*[54]

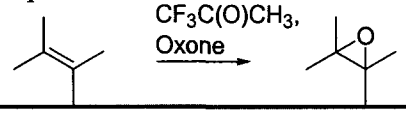

Entry	Substrate	Product	Time (h)	Yield (%)
1	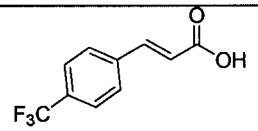	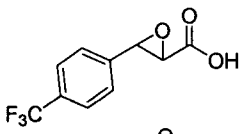	2	96
2	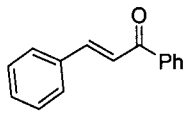	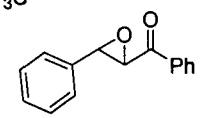	1.3 h	99
3			0.25	96
4	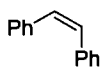	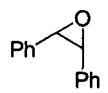	0.5	99

[54] Yang, D.; Wong, M.-K.; Yip, Y.-C. *J. Org. Chem.* **1995**, *60*, 3887.
[55] Shu, L.; Shi, Y. *J. Org. Chem.* **2000**, *65*, 8807.

Table 1.32. Catalytic Epoxidation with *in situ* Generated TFDO[55]

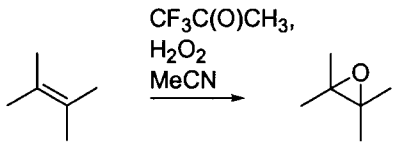

Entry	Substrate	Cat. (mol%)	Time (h)	Yield (%)
1		30	4	76
2		10	3	80
3	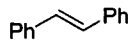	30	6	89
4	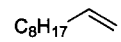	30	8	89

1.D.3. Additional Achiral Ketones

In addition to TFDO and DMDO, many additional ketones have been designed to be efficient epoxidation catalysts.[52b,56] As was the case with TFDO, the presence of electron-withdrawing groups makes the ketone more active for epoxidation. (Table 1.33). In particular, entry 3 contains a potentially useful catalyst because of its high reactivity and availability.

[56] For examples of ketones for catalytic racemic epoxidation, see: (a) Denmark, S.E.; Forbes, D.C.; Hays, D.S.; DePue, J.S.; Wilde, R.G. *J. Org. Chem.* **1995**, *60*, 1391. (b) Yang, D.; Yip, Y.-C.; Jiao, G.-S.; Wong, M.-K. *J. Org. Chem.* **1998**, *63*, 8952. (c) Yang, D.; Yip, Y.-C.; Tang, M.-W.; Wong, M.-K.; Cheung, K.-K. *J. Org. Chem.* **1998**, *63*, 9888. (d) Carnell, A.J.; Johnstone, R.A.W.; Parsy, C.C.; Sanderson, W.R. *Tetrahedron Lett.* **1999**, *40*, 8029. (e) Denmark, S.E.; Wu, Z. *J. Org. Chem.* **1998**, *63*, 2810.(f) Kan, J.T.W.; Toy, P.H. *Tetrahedron Lett.* **2004**, *45*, 6357.

Table 1.33. Epoxidation of *trans*-Stilbene or *trans*-β-Methylstyrene with Representative Catalysts

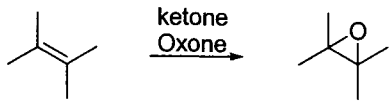

Entry	Ketone	Substrate	Time (h)	Ketone (mol%)	Conv (%)	Yield (%)
1[56a]	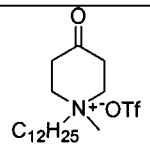	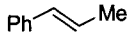	24	10	100	96
2[56b]	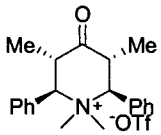	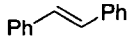	1.5	20	Nd	97
3[56b]	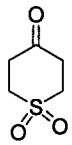	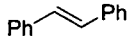	5	5	Nd	95
4[56c]	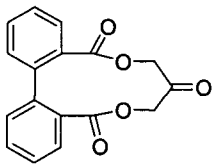	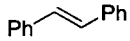	1.33	5	Nd	94
5[56d]	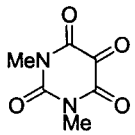	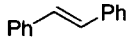	8	30	Nd	70
6[56e]	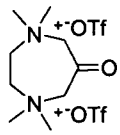	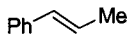	8	10	100	83

1.D.4. Noncarbohydrate-Derived Chiral Ketones

Dioxirane mediated epoxidations can give rise to enantioenriched epoxides if chiral ketones are used. The first asymmetric epoxidation by chiral dioxirane was demonstrated by Curci in 1984 (Table 1.34, Entries 3,4).[57a] Since that time, a number of different chiral ketones have been tested for asymmetric induction with varying degrees of success, including tetralone, indanone, binapthyl, biphenyl, tropinone, and dihydrocarvone derivatives (Table 1.34).[57] Notably, the first highly enantioselective epoxidation by chiral dioxirane was reported by Yang for substituted stilbenes with binapthyl derived ketone **1-15** (Table 1.34, Entry 15).

---

[57] For examples of chiral ketones not derived from sugars, see: (a) Curci, R.; Fiorentino, M.; Serio, M. *J. Chem. Soc., Chem. Comm.* **1984**, 755. (b) Brown, D.S.; Marples, B.A.; Smith, P.; Walton, L. *Tetrahedron* **1995**, *51*, 3587. (c) Curci, R.; D'Accolti, L.; Fiorentino, M.; Rosa, A. *Tetrahedron Lett.* **1995**, *36*, 5831. (d) Denmark, S.E.; Wu, Z.; Crudden, C.M.; Matsuhashi, H. *J. Org. Chem.* **1997**, *62*, 8288. (e) Denmark, S.E.; Matsuhashi, H. *J. Org. Chem.* **2002**, *67*, 3479. (f) Armstrong, A.; Ahmed, G.; Dominguez-Fernandez, B.; Hayter, B.R.; Wailes, J.S. *J. Org. Chem.* **2002**, *67*, 8610. (g) Armstrong, A.; Moss, W.O.; Reeves, J.R. *Tetrahedron Asym.* **2001**, *12*, 2779. (h) Armstrong, A.; Hayter, B.R.; Moss, W.O.; Reeves, J.R.; Wailes, J.S. *Tetrahedron Asym.* **2000**, *11*, 2057. (i) Sartori, G.; Armstrong, A.; Maggi, R.; Mazzacani, A.; Sartorio, R.; Bigi, F.; Dominguez-Fernandez, B. *J. Org. Chem.* **2003**, *68*, 3232. (j) Yang, D.; Yip, Y.-C.; Chen, J.; Cheung, K.-K. *J. Am. Chem. Soc.* **1998**, *120*, 7659. (k) Solladié-Cavallo, A.; Jierry, L.; Lupattelli, P.; Bovicelli, P.; Antonioletti, R. *Tetrahedron* **2004**, *60*, 11375. (l) Solladié-Cavallo, A.; Bouérat, L. *Org. Lett.* **2000**, *2*, 3531. (m) Solladié-Cavallo, A.; Bouérat, L.; Jierry, L. *Eur. J. Org. Chem.* **2001**, 4557. (n) Solladié-Cavallo, A.; Jierry, L.; Klein, A.; Schmitt, M.; Welter, R. *Tetrahedron Asym.* **2004**, *15*, 3891. (o) Bortolini, O.; Fantin, G.; Fogagnolo, M.; Forlani, R.; Maietti, S.; Pedrini, P. *J. Org. Chem.* **2002**, *67*, 5802. (p) Matsumoto, K.; Tomioka, K. *Tetrahedron Lett.* **2002**, *43*, 631. (q) Adam, W.; Zhao, C.-G. *Tetrahedron Asym.* **1997**, *8*, 3995. (r) Yang, D. *Acc. Chem. Res.* **2004**, *37*, 497. (s) Yang, D.; Yip, Y.-C.; Tang, M.-W.; Wong, M-K.; Zheng, J-H.; Cheung, K.-K. *J. Am. Chem. Soc.* **1996**, *118*, 491. (t) Yang, D.; Wang, X.-C.; Wong, M.-K.; Yip, Y.-C.; Tang, M.-W. *J. Am. Chem. Soc.* **1996**, *118*, 11311. (u) Yang, D.; Wong, M.-L.; Yip, Y.-C.; Wang, X.-C.; Tang, M.-W.; Zheng, J.-H.; Cheung, K.-K. *J. Am. Chem. Soc.* **1998**, *120*, 5943. (v) Stearman, C.J.; Behar, V. *Tetrahedron Lett.* **2002**, *43*, 1943. (w) Song, C.E.; Kim, Y.H.; Lee, K.C.; Lee, S.-g.; Jin, B.W. *Tetrahedron Asym.* **1997**, *8*, 2921.

Table 1.34. Asymmetric Epoxidation of Olefins with Representative Ketone Catalysts

Entry	Ketone	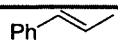	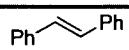	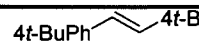	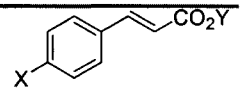
1[57b]	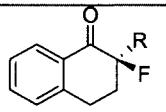	0% ee	0% ee		
2[57b]	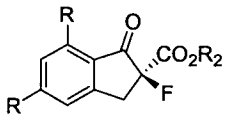	0% ee	0% ee		
3[57a]	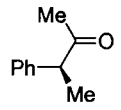	10% ee			
4[57a]	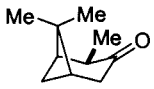	13% ee			
5[57c]	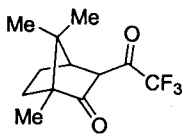	13% ee			
6[57c]	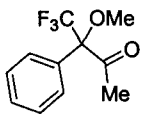	18% ee			
7[57d,e]	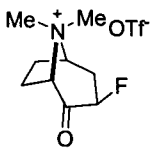	35% ee	58% ee		
8[57f-i]	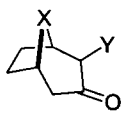	70% eemax 56% ee	46-95% eemax 41-81% ee		
9[57j-n]	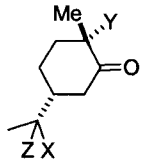		42-90% ee		22-68% ee X = OMe Y = Me

10[57o]	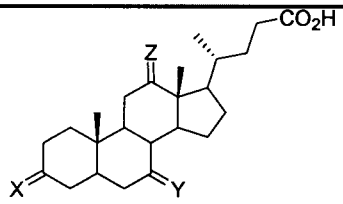				5-95% ee X = Me Y = H
11[57e]	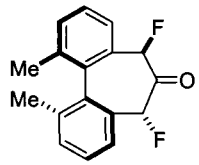	88% ee	94% ee		
12[57p]	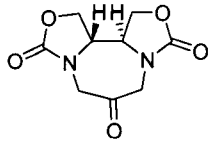	62% ee	64% ee		
13[57p]	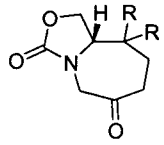	57% ee	6-57% ee		
14[57q]	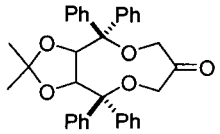		65% ee		
15[57r-u]	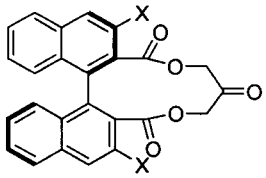 **1-15**		32-84% ee	76-95% ee	76-85% ee X = MeO Y = Me
16[57v]	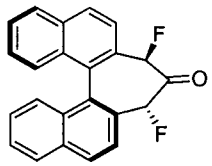		86%		
17[57w]	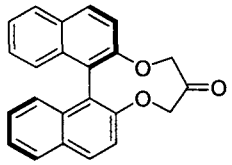	29% ee	26% ee		

1.D.5 Fructose-Derived Chiral Ketones

Although numerous ketones have been prepared for asymmetric epoxidation, catalysts derived from sugars have been demonstrated to have the broadest substrate scope. Fructose-derived ketone **1-16** gives high ee's for a number of *trans*- and trisubstituted olefins (Table 1.35).[58] Interestingly, high ee was found for trans-7-tetradecene, showing the catalyst's ability to epoxidize very simple *trans*-olefins in good enantioselectivity (Table 1.35, entry 4). 2,2-Vinyl silanes are also effective substrates, and when treated with TBAF, yield 1,1-disubstituted epoxides.[59] Allylic and homoallylic alcohols also found work well under the asymmetric epoxidation conditions (Table 1.36).[60] Enynes and conjugated dienes yield allyl and vinyl epoxides with both high regio- and enantioselectivity (Tables 1.37, 1.38).[61,62] Epoxidation of enol esters gives rise to the α-hydroxyketone of choice after treatment with the appropriate Lewis acid (Scheme 1.16).[63] The selected examples also show some of the functional groups that can be tolerated by the reaction conditions, including alkynes, esters, and silyl groups.

---

[58] For examples of *trans*- and trisubstituted olefin epoxidation with ketone **1-18**, see: (a) Shi, Y. *Acc. Chem. Res.* **2004**, *37*, 488. (b) Tu, Y.; Wang, Z.-X.; Shi, Y. *J. Am. Chem. Soc.* **1996**, *118*, 9806. (c) Wang, Z.-X.; Tu, Y.; Frohn, M.; Shi, Y. *J. Org. Chem.* **1997**, *62*, 2328. (d) Wang, Z.-X.; Tu, Y.; Frohn, M.; Zhang, J.-R.; Shi, Y. *J. Am. Chem. Soc.* **1997**, *119*, 11224.

[59] Warren, J.D.; Shi, Y. *J. Org. Chem.* **1999**, *64*, 7675.

[60] Wang, Z.-X.; Shi, Y. *J. Org. Chem.* **1998**, *63*, 3099.

[61] Frohn, M.; Dalkiewicz, M.; Tu, Y.; Wang, Z.-X.; Shi, Y. *J. Org. Chem.* **1998**, *63*, 2948.

[62] Wang, Z.-X.; Cao, G.-A.; Shi, Y. *J. Org. Chem.* **1999**, *64*, 7646.

[63] Zhu, Y.; Manske, K.J.; Shi, Y. *J. Am. Chem. Soc.* **1999**, *121*, 4080

Table 1.35. Catalytic Epoxidation of *trans*- and Trisubstituted Olefins by Ketone **1-16**

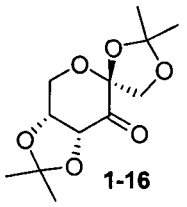

1-16

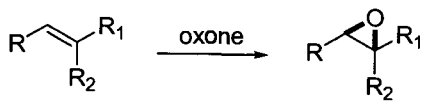

Entry	Epoxide	Yield (%)	ee (%)	Ref
1	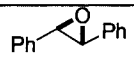	78	99	58d
2	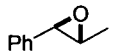	94	96	58d
3	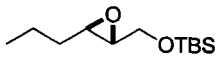	87	94	58d
4	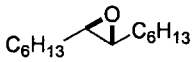	89	95	58d
5	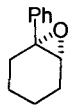	94	98	58d
6	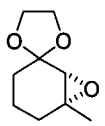	41	97	58d
7	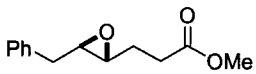	68	92	58d
8	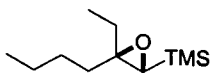	51	90	59
9	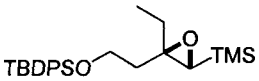	67	92	59
10	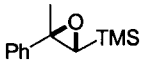	74	94	59

Table 1.36. Asymmetric Epoxidation of Alcohol-Containing Olefins by Ketone **1-16**[60]

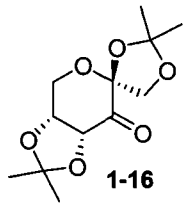

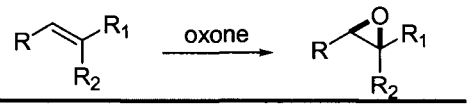

Entry	Epoxide	Yield (%)	Ee (%)
1	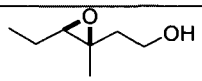	85	92
2	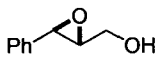	85	94
3	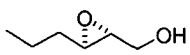	68	91
4	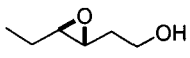	82	90
5	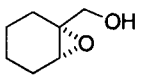	93	94

Table 1.37. Asymmetric Epoxidation of Dienes by Ketone **1-16**[61]

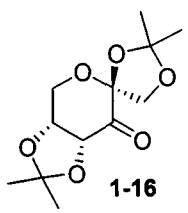

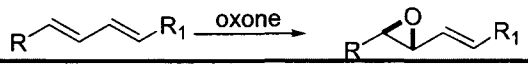

Entry	Major Epoxide	Minor Epoxide	Ratio	Yield (%)	ee (%)
1	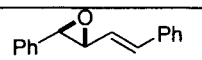	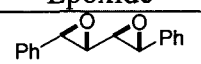	22:1	77	97
2	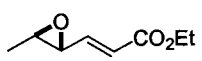	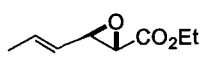	7:1	41	96
3	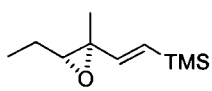			60	92
4	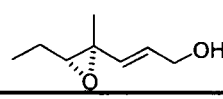			68	90

Table 1.38. Asymmetric Epoxidation of Enynes by Ketone **18**[62]

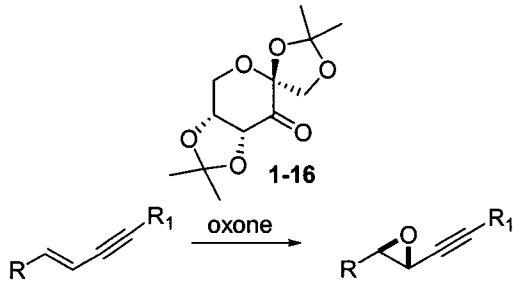

Entry	Epoxide	Yield (%)	Ee (%)
1	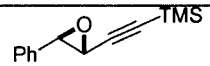	59	96
2	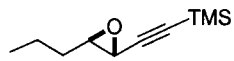	71	89
3	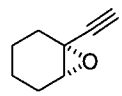	78	93
4	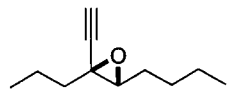	60	93

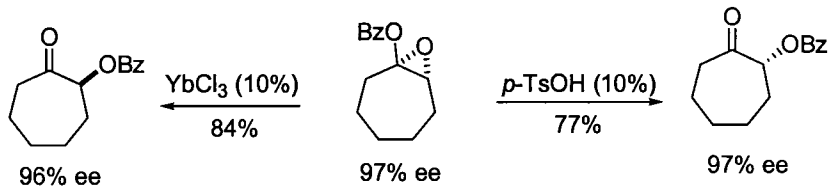

Scheme 1.16

A number of operational improvements have been made to facilitate the use of ketone **1-16** in synthesis. A protocol has been developed that utilizes H_2O_2 as primary oxidant instead of Oxone (Table 1.39).[64] Much like the aforementioned Payne oxidation, epoxidation proceeds through a peroxyimidic

[64] Shu, L.; Shi, Y. *Tetrahedron* **2001**, *57*, 5213.

acid intermediate that activates the chiral ketone. Advantages of this procedure include higher reaction concentration and milder conditions. Finally, while ketone **1-16** can be prepared from D-fructose quite easily in two steps, the unnatural sugar enantiomer was more difficult to obtain. Much effort has arrived at a convenient preparation of the L-Fructose from L-sorbose, which greatly improves the availability of chiral epoxides derived from **ent-1-16**.[65] Finally, an electronically modified ketone (**1-17**) analog is an effective catalyst for electron-poor olefins (Table 1.40).[66]

Table 1.39. Asymmetric Epoxidation with H_2O_2 as Primary Oxidant[64]

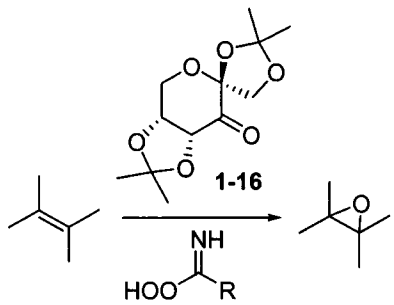

Entry	Epoxide	Yield (%)	Ee (%)
1	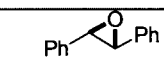	90	98
2	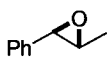	93	92
3	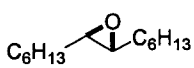	97	92
4	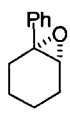	90	96

[65] Zhao, M.-X.; Shi, Y. *J. Org. Chem.* **2006**, *71*, 5377.
[66] Wu, X.-Y.; She, X.; Shi, Y. *J. Am. Chem. Soc.* **2002**, *124*, 8792.

Table 1.40. Asymmetric Epoxidation with an Electronically Modified Catalyst (**1-17**)[66]

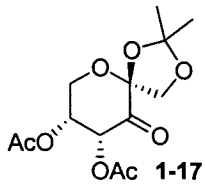

1-17

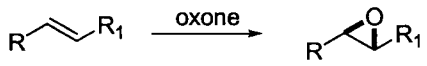

Entry	Epoxide	Yield (%)	ee (%)
1	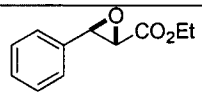	73	96
2	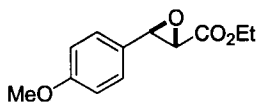	57	90
3	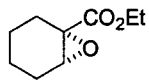	77	93
4	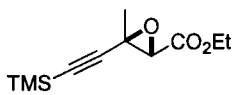	94	94

CHAPTER TWO

MECHANISTIC STUDIES AND AN IMPROVED SYNTHESIS OF A BOC-PROTECTED OXAZOLIDINONE CATALYST

2.A. INTRODUCTION

Even though a number of *trans*- and trisubstituted epoxides can be prepared in high ee with ketone **1-16**, some substrate classes still posed a challenge for dioxirane mediated epoxidations, including *cis*- and terminal olefins (Figure 2.1).[58-66] Consequently, efforts continued with the hope of developing catalysts capable of epoxidizing these important substrate classes in high ee. In 2000, a catalyst (**2-1**) containing a Boc-protected oxazolidinone in place of the spiro ketal in **1-16** was found to epoxidize conjugated *cis*-olefins in good ee and styrenes in encouragingly high ee with no *cis/trans* isomerization for the acyclic cases (Figure 2.2).[67]

[67] (a) Tian, H., She, X., Shu, L., Yu, H. & Shi, Y. *J. Am. Chem. Soc.* **2000**, *122*, 11551. (b) Tian, H.; She, X.; Xu, J.; Shi, Y. *Org. Lett.* **2001**, *3*, 1929. (c) Tian, H., She, X., Yu, H., Shu, L., Shi, Y. *J. Org. Chem.* **2002**, 67, 2435.

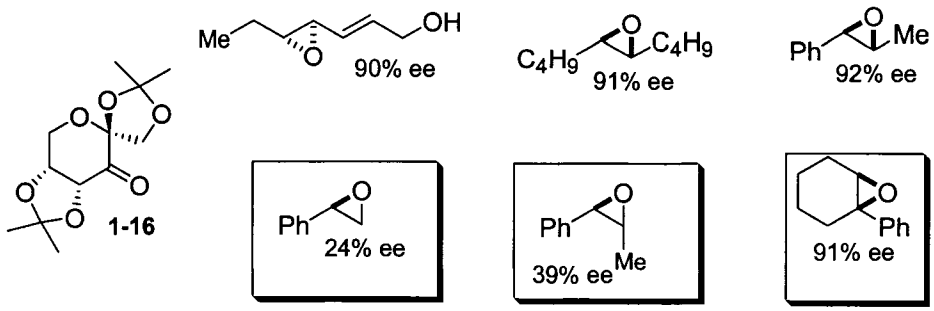

Figure 2.1 Select epoxidation examples with ketone **1-16**

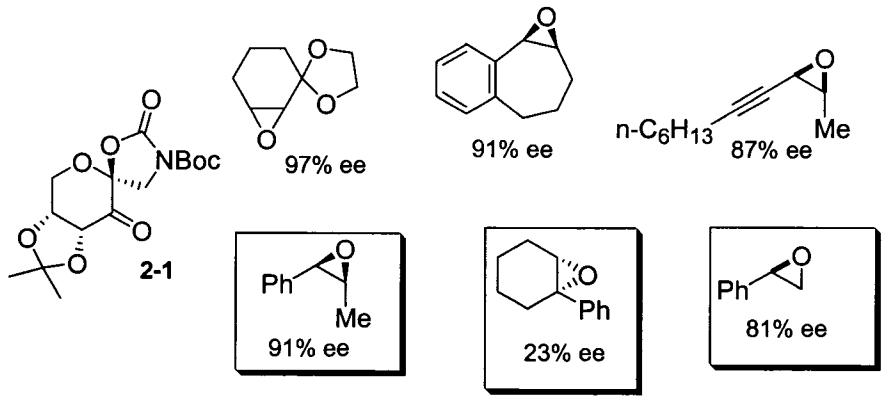

Figure 2.2 Select epoxidation examples with ketone **2-1**

The very large differences in enantioselectivity for these two structurally similar ketones can be explained by the spiro transition state model. In an epoxidation reaction, there are two extreme approaches of an olefin to a dioxirane, spiro and planar (Figure 2.3). Spiro approach is defined by dioxirane approaching orthogonal to the olefin, and planar is described as the olefin and dioxirane approaching in the same plane. For epoxidation of *trans*-olefins with ketone **1-16**, there are four geometrically feasible spiro and four geometrically feasible planar approaches of the olefin to the dioxirane (Figure 2.4).[58] Of those eight approaches, four are sterically disfavored: Spiro **E**, Spiro **F**, Planar **C**, and Planar **D**. For dioxirane mediated epoxidation, spiro transition states are generally

favored over planar ones[68] due to stabilizing secondary orbital interactions. Consequently, Spiro **A** and Spiro **B** are favored over Planar **G** and Planar **H**, and high ee is observed for *trans*-olefins.

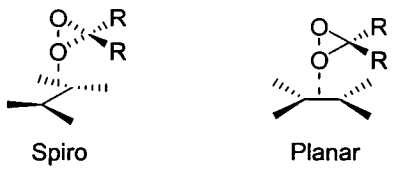

Figure 2.3 Sprio and planar approach

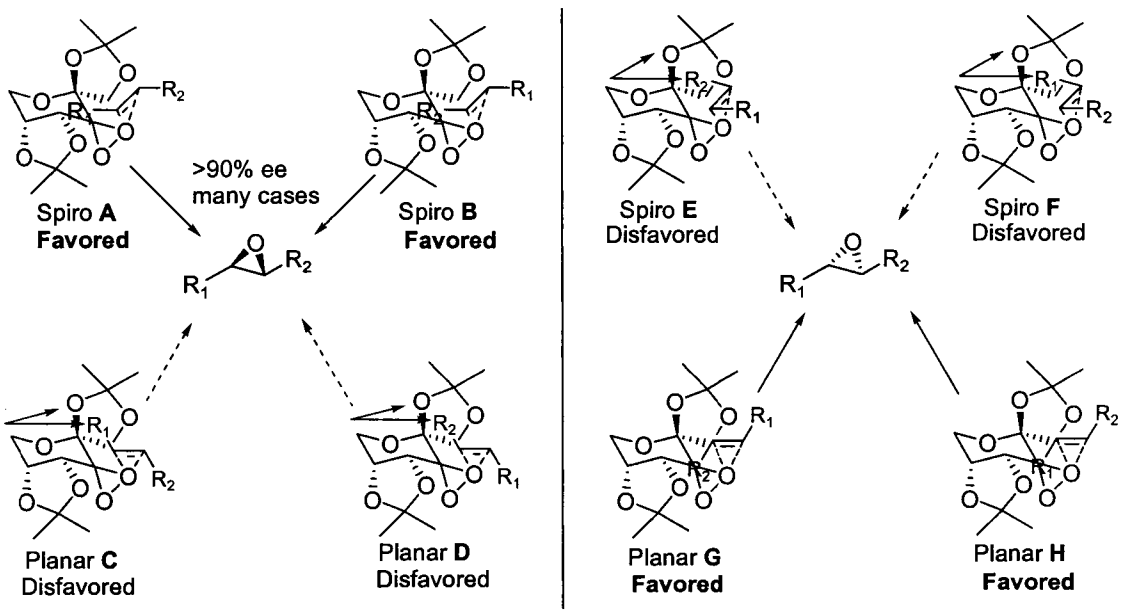

Figure 2.4 *trans*-Olefin transition state analysis for **1-16**

For *cis*-olefins, there are two geometrically feasible (Spiro **I** and Spiro **J**) approaches of the olefin to the dioxirane that yield opposite enantiomers (Figure 2.5). Consequently, modest ee (39% for cis-β-methylstyrene) is observed for *cis*-

[68] Baumstark, A.L.; Vasquez, P.C. *J. Org. Chem.* **1988**, *53*, 3437.

olefins with ketone **1-16**. However, for the very structurally similar ketone **2-1**, very high ee is observed for a number of (mostly conjugated) *cis*-olefins.[67] In these cases, the same two spiro approaches are possible (Spiro **K** and Spiro **L**), but there appears to be a strong attraction between the oxazolidinone region of the catalyst and the π-system of the olefin. Consequently, Spiro **K** is favored (> 20:1 in many cases), and high ee is observed for conjugated *cis*-olefins (Figure 2.6).

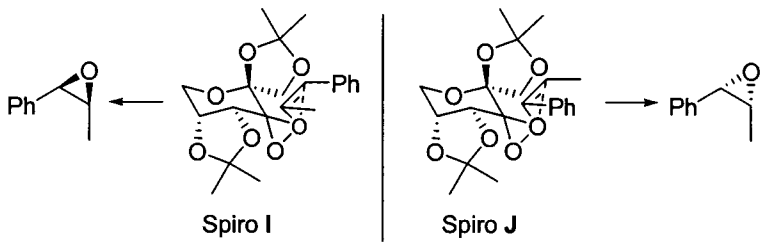

Figure 2.5 *cis*-Olefin transition state analysis for **1-16**

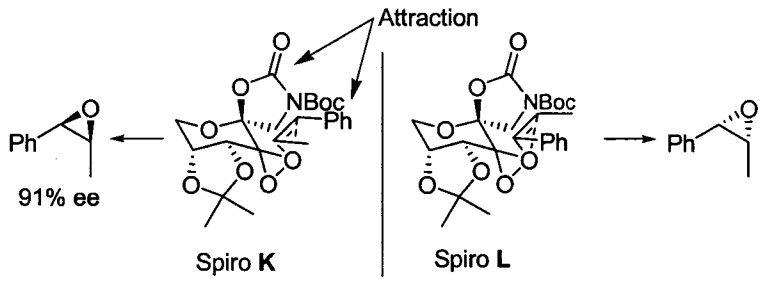

Figure 2.6 *cis*-Olefin transition state analysis for **2-1**

The slight erosion in ee from cis-β-methylstyrene to styrene for ketone **2-1** can also be explained by the spiro transition state model.[67] The same two transition states that were previously described for the *cis*-olefin case Spiro **M** and Spiro **N** are present. However, there is an additional planar transition state (**O**) that can now compete because of the presence of the attraction between the

aromatic ring of styrene and the oxazolidinone portion of the catalyst and the lack of steric repulsion due to the absence of the methyl group, resulting in slight loss in ee for styrene (Figure 2.7).

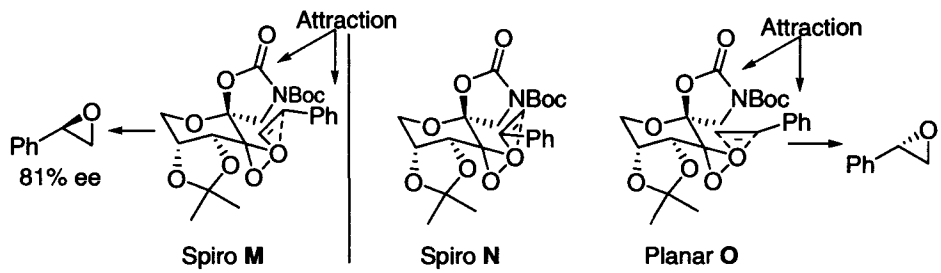

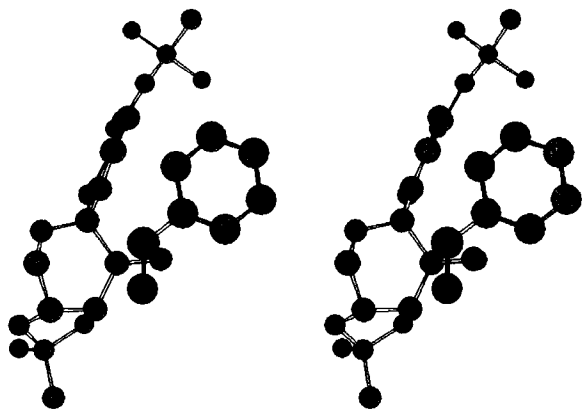

Spiro **M** (Crude stereoview in Chem 3D)

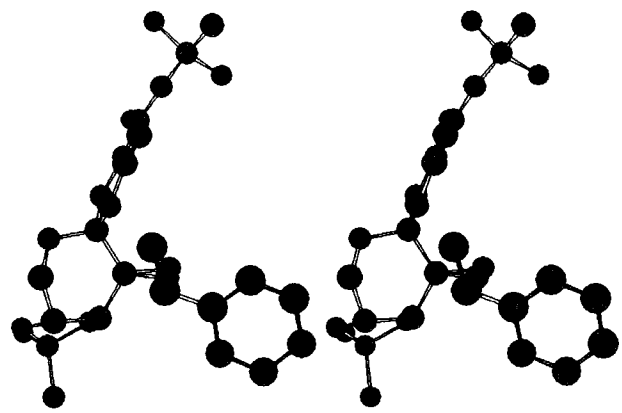

Spiro **N** (Crude stereoview in Chem 3D)

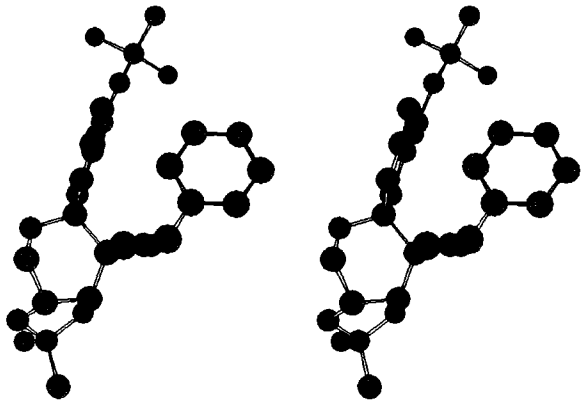

Planar **O** (Crude stereoview in Chem 3D)

Figure 2.7 Terminal olefin transition state analysis for **2-1**

The strength of the attraction can be illustrated well by the fact that epoxidation of phenylcyclohexene with ketones **1-16** and **2-1** yields opposite enantiomers of phenylcyclohexene oxide (Figure 2.8). For the epoxidation of phenylcyclohexene with ketone **1-16**, two approaches are sterically feasible, Spiro **P** and Planar **Q**. As a result of the same secondary orbital interactions that played a role in selectivity for *trans*-olefin epoxidation, Spiro **P** is favored over Planar **Q**, and high ee is observed.[58] For epoxidation with ketone **2-1**, the same two approaches are sterically feasible, Spiro **R** and Planar **S**. However, in this case, the attraction between the oxazolidinone portion of the catalyst and the aromatic ring is enough to overwhelm the inherent spiro bias of dioxirane mediated epoxidation, so the Planar **S** pathway is favored.[67]

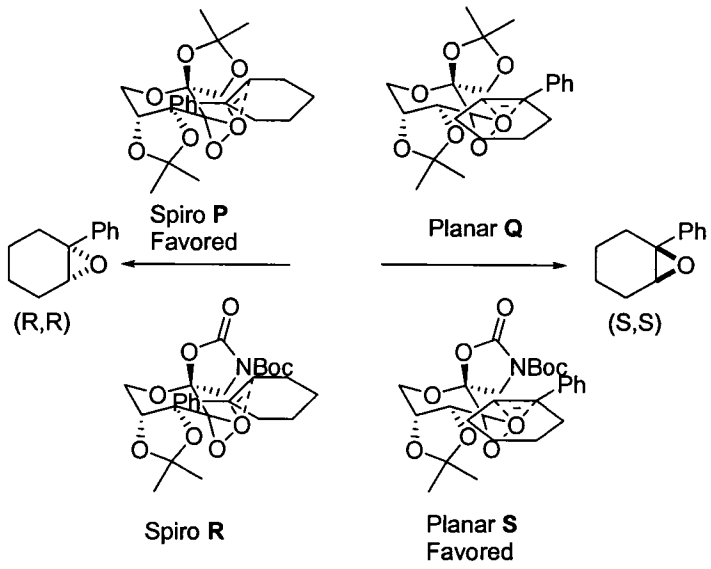

Figure 2.8 Epoxidation of phenylcyclohexene with ketones **1-16** and **2-1**

Although the differences in ee could now be attributed to an attraction between the π-systems of the olefins and the oxazolidinone portion of the ketone **(2-1)**, the exact nature of the interaction was not well understood. With the hope of gaining greater insight on the attraction responsible for giving high enantioselectivity, we targeted derivatives of the very sensitive phenylcyclohexene (**2-2**, **2-3**, **2-4**, and **2-5**) substituted with groups of varying electronic characteristics for epoxidation studies (Figure 2.9).

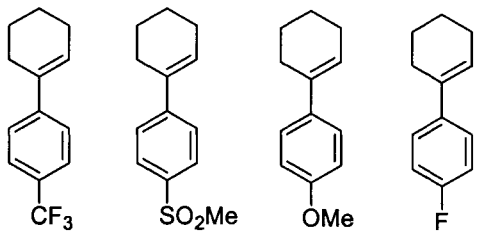

Figure 2.9 Targeted phenylclyclohexenes

2.B. RESULTS AND DISCUSSION

2.B.1. Synthesis of Phenylcyclohexenes

The four substrates have been synthesized by Grignard additions to cyclohexanone followed by simple E1 reactions (Scheme 2.1).[69] For the sulfone-containing olefin, a sulfide is carried through the first two steps and then oxidized to give the sulfone.[70] This pathway provided all of the desired substrates in adequate yield.

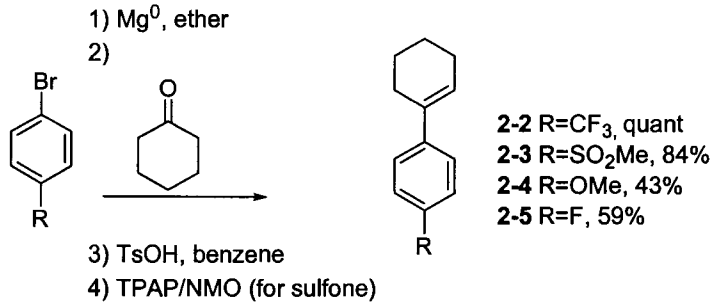

Scheme 2.1

2.B.2. Improved Catalyst Synthesis

With the desired substrates in hand, we turned our focus to catalyst (**2-1**) preparation. Unlike the fructose-derived ketone (**1-16**) that could be prepared in two steps, ketone **2-1** was originally made with a nine step synthesis,[67] which only allowed the catalyst to be made in small amounts (Scheme 2.2). In order to prepare the ketone on a scale suitable for substrate screening, not only for phenylcyclohexenes but other substrates as well, its synthesis was improved with

[69] Caldwell, R.A.; Cao, C.V. *J. Am. Chem. Soc.* **1982**, *104*, 6174.
[70] Guertin, K.R.; Kende, A.S. *Tetrahedron Lett.* **1993**, *34*, 5369.

the help of Lianhue Shu, Yu-Mei Shen, and Chris Burke. Use of $NaHCO_3$ as base with phosgene allowed carbonyl introduction to occur in a single step, and oxidation before BOC introduction avoided a protection/deprotection sequence (Scheme 2.3). These two major route improvements along with several minor changes allowed the ketone (**2-1**) to be prepared on a 3 gram scale in about a week.

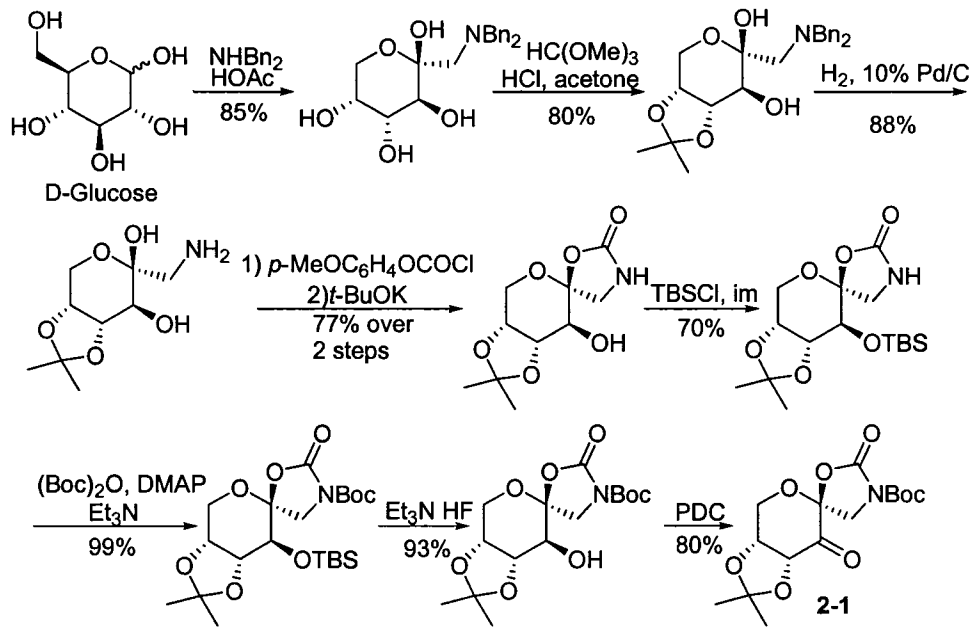

Scheme 2.2

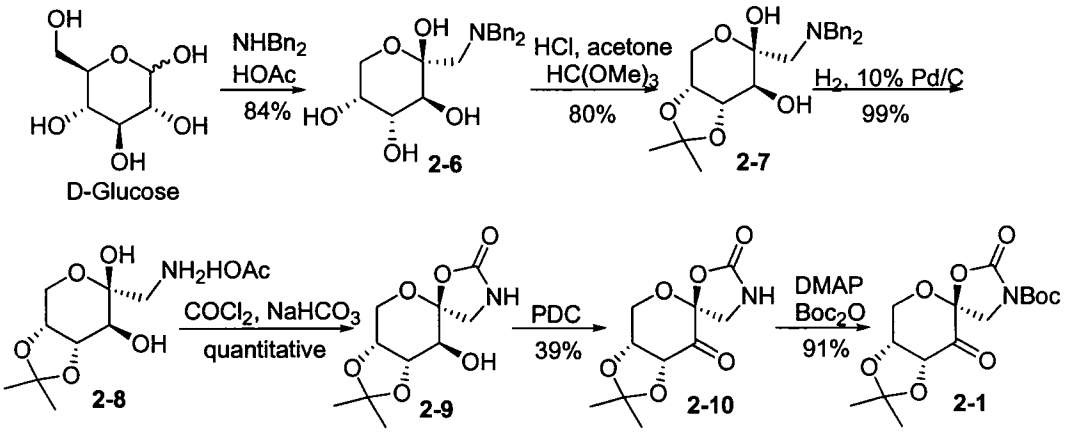

Scheme 2.3

2.B.3. Asymmetric Epoxidation of Phenylcyclohexenes

Asymmetric epoxidations were then performed on all the substrates with ketones **1-16** and **2-1** (Table 2.1). Not surprisingly, for epoxidation with ketone **1-16**, a compound that relies heavily on steric differentiation, little difference was observed for all of the substrates (88-94% ee), since the changes were made at locations far away from the chiral pocket (Figure 2.10).

Table 2.1. Asymmetric Epoxidation of Phenylcyclohexenes with Chiral Ketones[a]

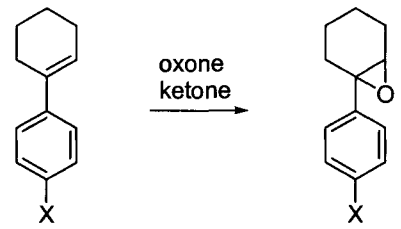

Conv. (ee) (Config)	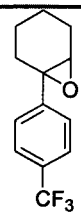 **2-11**	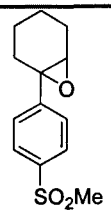 **2-12**	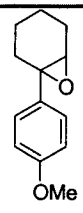 **2-13**	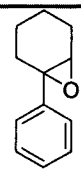	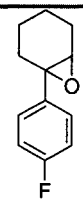 **2-14**
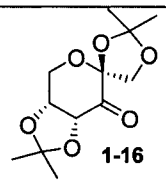 **1-16**	36% (94%) (R,R)	40% (91%) (R,R)	87% (88%) (R,R)	83% (91%) (R,R)	72% (93%) (R,R)
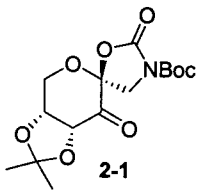 **2-1**	48% (17%) (R,R)	100% (13%) (S,S)	100% (17%) (S,S)	100% (26%) (S,S)	100% (27%) (S,S)

[a] Olefin 0.5 mmol, ketone 0.5 mmol, DME:DMM (3:1) 7.5 mL, 0.2 M K_2CO_3/AcOH, in aq EDTA (pH 8.0), 5 mL, Oxone (.212 M in aq. EDTA, 4.2 mL), K_2CO_3 (0.479 M in aq. EDTA, 4.2 mL), TBAHS (.02 mmol) Configuration was assigned based on comparison with **1-16**.

For epoxidations with ketone **2-1**, there were noticeable, but small, differences in ee between the different substrates, suggesting the ketone is effective for substrates with varying electronic differences (Table 2.1, Figure 2.10). Two major factors seem to influence the enantioselectivity. First, more electron-rich substrates generally favor planar transition states (Planar **W**) because of weaker secondary orbital interactions, leading the more electron rich substrates to generally follow epoxidation through planar pathways. Furthermore, substrates with hydrocarbon substitution generally have stronger interactions with the oxazolidinone portion of the catalyst than those with heteroatom substitution, presumably due to better hydrophobic interactions for the greasy substituents. Although the differences in ee are rather minor for these examples, these general trends will be regularly observed for epoxidation with oxazolidinone catalysts.

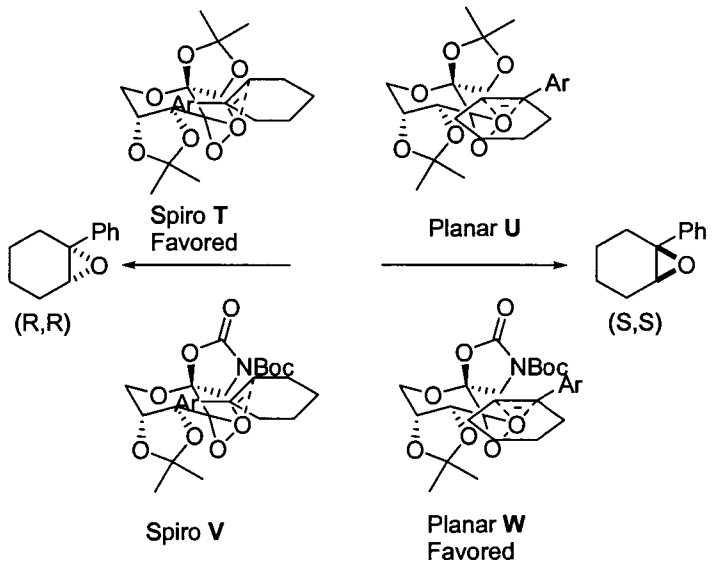

Figure 2.10 Epoxidation of phenylcyclohexene with ketones **2-1** and **1-16**

2.C. CONCLUSIONS

In short, phenylcyclohexene derivatives with varying electronic characteristics were used to probe the exact nature of the attraction in the transition state responsible for giving high ee with ketone **2-1**. The synthesis of ketone **2-1** was also reduced from nine to six steps, allowing for the catalyst to be prepared on 3 gram scale in about a week, yet many challenges still remain. Even though the synthesis of ketone **2-1** was much improved, it is still quite involved when compared to what one might expect of a useful catalyst. Furthermore, the epoxidation of terminal olefins with ketone **2-1** generally proceeds with lower enantioselectivity than their *cis*-counterparts. Efforts would focus on developing a useful catalyst system that could not only epoxidize the substrates already found to effective, but many additional useful substrates as well.

2.D. EXPERIMENTAL

Representative Olefin Synthesis

1-(4-fluorophenyl)-cyclohex-1-ene[71] (2-5) (DLG-I-22, DLG-I-23) A 1000 mL 3 necked flask was flame dried and then cooled under vacuum. Magnesium powder (0.72 g) was added and subjected to 15 min. of vigorous stirring under nitrogen without solvent. Ether (25 mL) was then added, and the suspension was allowed to stir for 5 min. 4-fluoro-1-bromobenzene (5.25 g, 30 mmol in 35 mL ether) was added dropwise while stirring at room temperature. Thirty min. after

[71] Balsamo, A. *Gaz. Chim. Ital.* **1976**, 77.

the cessation of bubbling, freshly distilled cyclohexanone (2.6 mL, 250 mmol in 25 mL of ether) was added dropwise, and the reaction mixture slowly darkened. After an additional h of stirring, satd. NH_4Cl (12 mL) was added dropwise, and the mixture was allowed to stir for 25 min. The organics were removed, the solid residue was washed with ether (5 x 10 mL), and the combined organics were concentrated. Reagent grade benzene (100 mL) was then added followed by *p*-TsOH (0.34 g, 1.68 mmol), and the mixture was subjected to an azeotropic distillation under nitrogen for 2 h. The mixture was cooled to rt, filtered through $NaHCO_3$, filtered through $MgSO_4$, concentrated, and purified by flash chromatograhy to give 1-(4-fluorophenyl)-cyclohex-1-ene as a clear oil (2.62 g, 59%). IR (film) 2929 cm^{-1}; ^1H NMR (300 MHz, $CDCl_3$) δ 7.37-7-30 (m, 2H), 7.04-6.94 (m, 2H), 6.10-6.05 (m, 1H), 2.42-2.34 (m, 2H), 2.25-2.16 (m, 2H), 1.84-1.73 (m, 2H), 1.71-1.63 (m, 2H); ^{13}C NMR (75 MHz, $CDCl_3$) δ 161.8 (d, J = 242.7 Hz), 138.8, 135.7, 126.5 (d, J = 7.0 Hz), 124.8, 115.0 (d, J = 20.9 Hz), 27.8, 26.1, 23.3, 22.4.

(DLG-I-34, DLG-I-35)

1-(4-Trifluoromethylphenyl)-cyclohex-1-ene (2-2)

Quant; clear oil; IR (film) 2935 cm^{-1}; ^1H NMR (300 MHz, $CDCl_3$) δ 7.56 (d, J = 8.4 Hz, 2H), 7.47 (d, J = 8.4 Hz, 2H), 6.25-6.20 (m, 1H), 2.51-2.37 (m, 2H), 2.29-2.20 (m, 2H), 1.87-1.76 (m, 2H), 1.74-1.64 (m, 2H) ^{13}C NMR (100 MHz, $CDCl_3$) δ 146.2, 135.8, 128.6 (q, J = 32.1 Hz), 127.2, 126.4, 125.2, 122.8, 27.6, 26.2, 23.2, 22.3.

(DLG-I-24, DLG-I-25)

1-(4-methoxyphenyl)-cyclohex-1-ene[72] (2-4)

(2.9 g, 43%); clear oil; IR (film) 2928 cm^{-1}; ^1H NMR (300 MHz, $CDCl_3$) δ 7.31 (d, J = 9.0 Hz, 2H), 6.84 (d, J = 9.0 Hz, 2H), 6.04-6.00 (m, 1H), 3.80 (s, 3H), 2.42-2.34 (m, 2H), 2.25-2.14 (m, 2H), 1.78-1.70 (m, 2H), 1.68-1.61 (m, 2H); ^{13}C NMR (75 MHz, $CDCl_3$) δ 158.4, 136.0, 135.4, 126.0, 123.2, 113.7, 55.5, 27.7, 26.1, 23.4, 22.5.

Sulfone (2-3) (DLG-II-33, DLG-II-34) To a solution of sulfide (0.204 g, 1 mmol) in MeCN (4.5 mL) was added NMO (0.352 g, 3 mmol), followed by 4A molecular sieves (100 mg), and after allowing to stir for 10 min., TPAP (18 mg, .05 mmol). After stirring under nitrogen for 8 h at 44 °C, the mixture was cooled to rt, filtered through a short plug of silica gel, and concentrated to give **2-3** as a white solid (0.198 g, 84%). mp 82-88 °C; IR ($CHCl_3$) 2928, 1309, 1151 cm^{-1}; ^1H NMR (300 MHz, $CDCl_3$) δ 7.86 (d, J = 8.7 Hz, 2H), 7.54 (d, J = 8.7 Hz, 2H), 6.29-6.24 (m, 1H), 3.04 (s, 3H), 2.45-2.37 (m, 2H), 2.29-2.21 (m, 2H), 1.85-1.75 (m, 2H), 1.72-1.64 (m, 2H); ^{13}C NMR (75 MHz, $CDCl_3$) δ 148.2, 138.1, 135.5, 128.7, 127.5, 125.8, 44.9, 27.5, 26.3, 23.1, 22.1.

[72] Gerteisen, T.J.; Kleinfelter, D.C.; Brophy, G.C.; Sternhell, S. *Tetrahedron* **1971**, *27*, 3013.

Improved Ketone Synthesis

Aminoalcohol (2-6)[67] (DLG-II-10) Absolute EtOH (300 mL) was added to a 1L round bottom flask containing D-glucose (59.8 g, 330 mmol). Following the subsequent addition of Bn_2NH (64 mL, 0.332 mol) and HOAc (57 mL), the mixture was heated to reflux while stirring for 3 h. Note: The reaction mixture became orange and viscous, so it was very important that stirring continue at all times. Also, in order to prevent decomposition, the temperature of the oil bath used to heat the mixture was never allowed to exceed 90 °C. The mixture was then cooled to 0 °C and filtered. The solid product was washed with EtOH until white and dried under vacuum overnight to give 1-dibenzylamino-1-deoxy-D-fructose (**2-6**) (97.2 g, 84%).

Ketal (2-7)[67] (DLG-II-13) In a 1L round bottom flask, acetone (700 mL) was added to a mixture of $HC(OMe)_3$ (35 mL, 320 mmol) and 1-dibenzylamino-1-deoxy-D-fructose (**2-6**) (26.9 g, 75 mmol), and the solution was cooled to 0 °C. Following addition of concentrated HCl (9 mL), the solution was stirred vigorously at 0 °C for 1.5 h under nitrogen. Regardless of whether or not any impurities are present, this reaction must not be allowed to stir for longer than 2 h. Immediately after the appearance of the impurity byproduct with Rf = 0.5 in 1:1 EtOAc: hexane (Note: the product shows a Rf of 0.6), the reaction mixture was quenched with NH_4OH (11 mL), filtered through a plug of silica gel, and the plug was washed with additional acetone. The filtrate was concentrated to

approximately 50 mL and then diluted with hexanes: EtOAc (3:2, 400 mL). The capped flask was then placed in the freezer for 3 h. The mixture was then filtered through a second plug of silica gel and washed with hexanes: EtOAc (3:2, 200 mL). The solvent was then removed and the product dried under vacuum overnight to give ketal (**2-7**) as a pale yellow oil (24.0 g, 80%).

Aminoalcohol (2-8)[67] (DLG-II-15) **2-7** (24.0 g, 60 mmol) was then dissolved in absolute EtOH (270 mL) and transferred to a 3-neck 2L flask. After degassing three times with nitrogen, HOAc (4 g, 67 mmol) and 10% Pd/C (4.35 g) were added. The mixture was then degassed three additional times and filled with hydrogen each time. Next, the reaction was stirred at rt for 4 h (Reaction can be followed by TLC using EtOAc as developing solution. The product does not move on the TLC plate, while the starting material will not only be UV active, but will also have an R_f value of 0.8. The intermediate monobenzylamine can also be followed with an R_f of 0.2). The mixture was then filtered through celite and concentrated without heating to give **2-8** as a a tan solid (16.7 g, 99%) that was used without further purification.

Oxazolidinone (2-9)[67] (DLG-II-16) To a mixture of **2-8** (16.7 g, 61 mmol) and $NaHCO_3$ (29.7 g) in DCM (290 mL) at 0 °C under nitrogen was added phosgene (20% in toluene, 44.3 mL) dropwise over 30 min. while stirring. The reaction mixture was then allowed to stir in the capped flask at rt for 4.5 h (The Rf of starting material is 0, while the product Rf is 0.5 in EtOAc) until no starting

material remains, always careful not to allow the $NaHCO_3$ to collect on the sides of the flask. After opening the flask to air, MeOH was then added to quench the reaction (10 mL over 30 min. *via* pipette followed by an additional 90 mL over another 30 min. with an addition funnel). The mixture, still open to air, was stirred for an additional 30 min. The reaction mixture was then flushed through a short column of silica gel (about 4 inches in height) and washed with additional MeOH until the brown liquid no longer came off the column. It was important not to wash with too much solvent in order to prevent excess $NaHCO_3$ from passing through the silica gel. The solvent was then removed and the brown solid (**2-9**) (16.4 g, quantitative) dried overnight on the high vacuum line and used without further purification.

Ketone (2-10)[67] (DLG-II-19) To a solution of alcohol **2-9** (3.5 g, 14.2 mmol) in DCM (64 mL) was added 3A molecular sieves (11.9 g) followed by PDC (7.47 g) and HOAc (1 drop). The mixture was stirred at room temperature in a capped flask for 6 h. In EtOAc, the Rf of the ketone is about 0.8, but the hydrate only appears slightly above the starting material at around 0.5. The two can be differentiated by color with *p*-anisaldehyde stain. The hydrate has a reddish tint, while the starting material appears darker. The reaction mixture was then filtered through a short plug of silica gel, washed with 500 mL of EtOAc: hexane (3:1), and concentrated. At that point in time, there was a mixture of ketone and hydrate, which can be seen with NMR (best seen by comparing the ketone peak at 3.38 with the hydrate peak at 3.47). The hydrate was removed over a 48-h period

on the high vacuum line. (If the solid has a pinkish tint to it, it should be passed through another short plug of silica gel and concentrated.) The ketone was then recrystallized with DCM: hexanes (1:3) to give **2-10** as a white solid (1.35 g, 39%) that was used without further purification.

Ketone (2-1)[67] (DLG-II-24) Before the reaction started, a 4-inch column was prepared, and all of the premeasured solvents were dried with Na_2SO_4. The time that the reaction is allowed to stir is critical for the success of this transformation. Too little time leads to a messy mixture of product and starting material, while too much time results in product decomposition. Therefore, the workup must immediately follow the reaction. To a solution of ketone **2-10** (1.22 g, 5.02 mmol) in THF (15 mL) was added Boc anhydride (1.43 g, 6.43 mmol) followed by DMAP (6.13 mg, 0.0502 mmol), and the mixture was allowed to stir at rt for 17 min. under nitrogen. The reaction was followed by TLC with a hexane: EtOAc (1:1) solvent system. The starting material stays near the baseline while the product has an Rf of about 0.6. There was also a highly UV-active impurity that appeared at around 0.8 near the end of the reaction. Immediately following consumption of the starting material, the reaction was stopped by addition of oxalic acid (7 mg). The mixture was then immediately filtered through the column and washed with hexanes:EtOAc (1:1, 50 mL) and concentrated to give a white solid. Hot hexane:ether (3:1, 15 mL) was added and stirred for 5 min. Then, the mixture was filtered and washed with additional cold hexane:ether (3:1, 15 mL) and concentrated to give **2-1** as a white solid (1.57 g, 91 %).

Representative Asymmetric Epoxidation Procedure

Epoxide (2-14)[71] (DLG-III-33). To a solution of 1-(4-fluorophenyl)-cyclohexene (0.088 g, 0.50 mmol) and ketone **1-16** (0.130 g, 0.5 mmol) in DME-DMM (3:1) (7.5 mL) were added buffer (0.2 M K_2CO_3-AcOH in 4 x 10^{-4} M aq. EDTA, pH = 8.0) (5.0 mL) and TBAHS (Bu_4NHSO_4) (0.0075 g, 0.02 mmol) with stirring. After the mixture was cooled to about 0 °C via an ice bath, a solution of Oxone (0.212 M in 4 x 10^{-4} M aq. EDTA, 4.2 mL) and a solution of K_2CO_3 (0.479 M in 4 x 10^{-4} M aq. EDTA, 4.2 mL) were added dropwise separately over a period of 3.5 h via syringe pump. The reaction mixture was quenched by addition of pentane, extracted with pentane, and analyzed directly by GC. The combined organics were dried, filtered, concentrated, and purified by flash chromatography hexane:ether (1:0 to 1:1 buffered with 1% NEt_3) to give **2-14** as a clear oil $[\alpha]^{20}_D$ = 9.3 (92% ee) (*c* 0.39, $CHCl_3$); IR (film) 2940 cm^{-1}; ^1H NMR (300 MHz, $CDCl_3$) δ 7.36-7.29 (m, 2H), 7.05-6.95 (m, 2H), 3.06-3.03 (m, 1H), 2.35-2.17 (m, 1H), 2.16-2.04 (m, 1H), 2.02-1.95 (m, 2H), 1.65-1.22 (m, 4H); ^{13}C NMR 162.1 (d, J = 244.1 Hz), 138.4, 127.1, (d, J = 7.0 Hz), 115.2 (d, J = 20.9 Hz), 62.2, 60.0, 29.2, 24.9, 20.4, 20.1.

(DLG-III-34)

1-(4-Trifluoromethylphenyl)-cyclohexene oxide (2-11) yellow oil; $[\alpha]^{20}_D$ = 22.0 (92% ee) (*c* 0.1, $CHCl_3$); IR (film) 2942 cm^{-1}; ^1H NMR (300 MHz, $CDCl_3$) δ

7.58 (d, J = 8.4 Hz, 2H), 7.48 (d, J = 8.4 Hz, 2H), 3.05-3.03 (m, 1H), 2.36-2.22 (m, 1H), 2.17-1.96 (m, 3H), 1.68-1.20 (m, 4H); ^{13}C NMR 146.6, 125.9, 125.4, 125.4, 125.3, 62.3, 60.1, 28.9, 24.9, 20.3, 19.9; HRMS Calcd for $C_{13}H_{13}OF_3$ (M+) 243.0952, found 243.0946.

(DLG-III-35)

Epoxide (2-12) white solid; mp 98-100 °C; $[\alpha]^{20}_D$ = 13.3 (92% ee) (*c* 0.18, $CHCl_3$); IR (film) 2938, 1313, 1153 cm^{-1}; ^1H NMR (300 MHz, $CDCl_3$) δ 7.90 (d, J = 8.4 Hz, 2H), 7.57 (d, J = 8.4 Hz, 2H), 3.05-3.03 (m, 4H), 2.35-2.23 (m, 1H), 2.17-1.97 (m, 3H), 1.69-1.44 (m, 3H), 1.43-1.24 (m, 1H); ^{13}C NMR (75 MHz, $CDCl_3$) 149.0, 139.4, 127.6, 126.5, 62.4, 60.1, 44.8, 28.8, 24.8, 20.2, 19.8; HRMS Calcd for $C_{13}H_{16}SO_3$ (M+) 252.0820, found 252.0818.

(DLG-III-36)

1-(4-methoxyphenyl)-cyclohexene oxide[72] (2-13) yellow oil; $[\alpha]^{20}_D$ = 6.4 (91% ee) (*c* 0.13, $CHCl_3$); IR (film) 2931 cm^{-1}; ^1H NMR (300 MHz, $CDCl_3$) δ 7.29 (d, J = 9.0 Hz, 2H), 6.86 (d, J = 9.0 Hz, 2H), 3.80 (s, 3H), 3.08-3.04 (m, 1H), 2.29-2.17 (m, 1H), 2.16-2.03 (m, 1H), 2.02-1.93 (m, 2H), 1.65-1.22 (m, 4H); ^{13}C NMR (75 MHz, $CDCl_3$) 134.8, 126.7, 113.8, 100.1, 62.2, 60.2, 55.5, 29.2, 25.1, 20.4, 20.2.

CHAPTER THREE

HIGHLY ENANTIOSELECTIVE EPOXIDATION OF STYRENES: IMPLICATION OF AN ELECTRONIC EFFECT ON THE COMPETITION BETWEEN SPIRO AND PLANAR TRANSITION STATES

3.A. INTRODUCTION

In order to develop a more general catalyst than oxazolidinone-containing ketone **2-1**, additional substrates, such as terminal olefins, would have to perform as well as their *cis*-counterparts. During our group's earlier studies, encouraging ee (81%) was obtained for the epoxidation of styrene with ketone **2-1,** a catalyst previously found to give high ee for conjugated *cis*-olefins (Figure 2.2).[67] The observed ee for ketone **2-1** can be explained by the transition state model in Figure 3.1. There are three geometrically feasible, electronically favored approaches, spiro **A**, spiro **B**, and planar **C**, in the transition state for the epoxidation of styrene with ketone **2-1** (Figure 3.1). As was discussed previously, it appears that an electronic attraction exists between the oxazolidinone and the aromatic ring of the substrate, resulting in the favoring of

spiro **A** over spiro **B** (Figure 3.1). Planar **C** can compete somewhat because it too benefits from the attraction without suffering from steric repulsions, but the inherent spiro bias of dioxirane mediated epoxidations due to secondary orbital interactions favors spiro **A** over planar **C**. Consequently, 81% ee is observed.

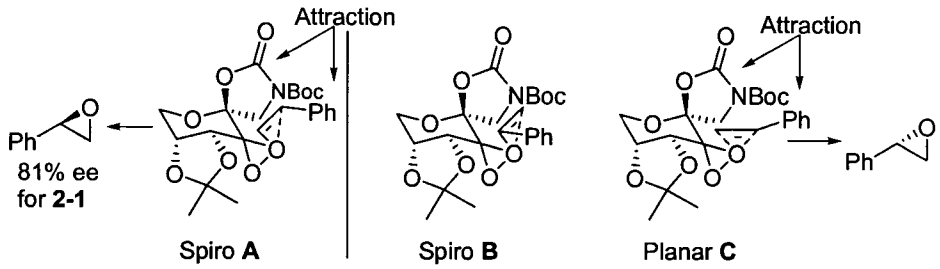

Figure 3.1 Transition state analysis for styrene and ketone **2-1**.

In order for a new catalyst to further enhance the enantioselectivity of terminal olefin epoxidation, spiro **A** would have to be amplified, planar **C** would have to be disfavored, or both. Since the aromatic group points away from the oxazolidinone group in spiro transition state **B**, it is unlikely that spiro **B** could be affected in any great manner by modifying the catalysts. With the hope of developing a better catalyst for terminal olefin epoxidation, we targeted three new carbocyclic ketones with very carefully designed structural features (Figure 3.2). First, the ketal functionality believed to successfully block the bottom approach to the dioxirane was to be left intact (Figure 3.3). Moreover, the Boc-protected oxazolidinone that provides the basis for the attraction between the styrene and the ketone catalyst was also left unmodified. One change was made, though; the oxygen present in the ring was removed in ketones **3-1**, **3-2**, and **3-3**. It was

hoped that the varying degrees of conformational freedom for the three new ketone catalysts would yield at least one catalyst that performed well with terminal olefin epoxidation.

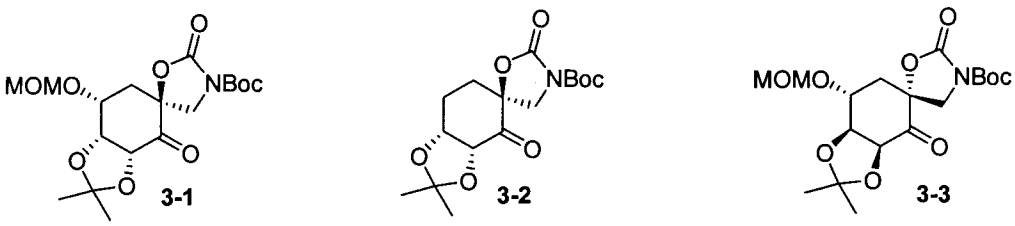

Figure 3.2 Carbocyclic ketones targeted for styrene epoxidation.

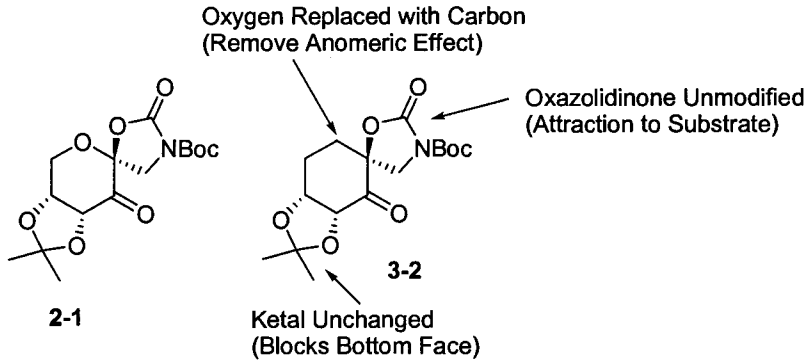

Figure 3.3 Structural features of ketone **3-2.**

3.B. RESULTS AND DISCUSSION

3.B.1. Synthesis of Carbocyclic Ketones

The three structurally similar ketones **3-1**, **3-2**, and **3-3** were chosen, not only because of their interesting structural features, but also because the potential existed to prepare them in an efficient manner from common intermediates (Scheme 3.1). Since Matthew Hickey had previously developed a route to ketone **3-1** from quinic acid,[73] we turned our focus to the preparation of ketone **3-2** with a similar strategy (Scheme 3.2). Alcohol **3-4**, prepared in several steps from quinic acid by Zackary Crane from a known literature procedure,[73] was deoxygenated by Barton's method of thiocarbonate formation followed by radical removal of oxygen. Recrystallization of the thiocarbonate is essential for the success of this transformation, suggesting that even trace impurities can impede the reaction. Ester **3-5** was reduced to alcohol **3-6** with DIBAL-H, then was converted to azide **3-7**. Flash dihydroxylation[74] and Swern oxidation yielded the acid-sensitive alcohol **3-8** and ketone **3-9**, which was subjected to aza-Wittig cyclization to afford oxazolidinone **3-10**. Boc introduction gave the desired deoxygenated ketone **3-2** in 13 steps and 1.1 % overall yield.

[73] Wang, Z.-X.; Miller, S.M.; Anderson, O.P.; Shi, Y. *J. Org. Chem.* **2001**, *66*, 521.
[74] Shing, T.K.M.; Tam, E.K.W.; Tai, v.W.-F.; Jiang, Q. *Chem. Eur. J.* **1996**, *2*, 50.

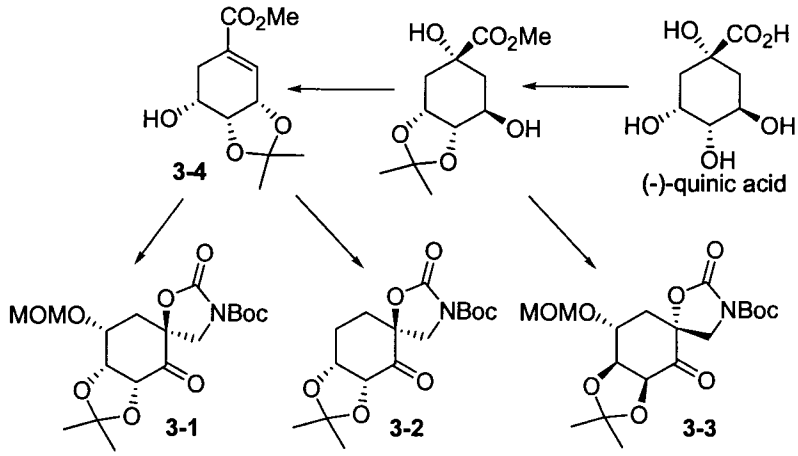

Scheme 3.1

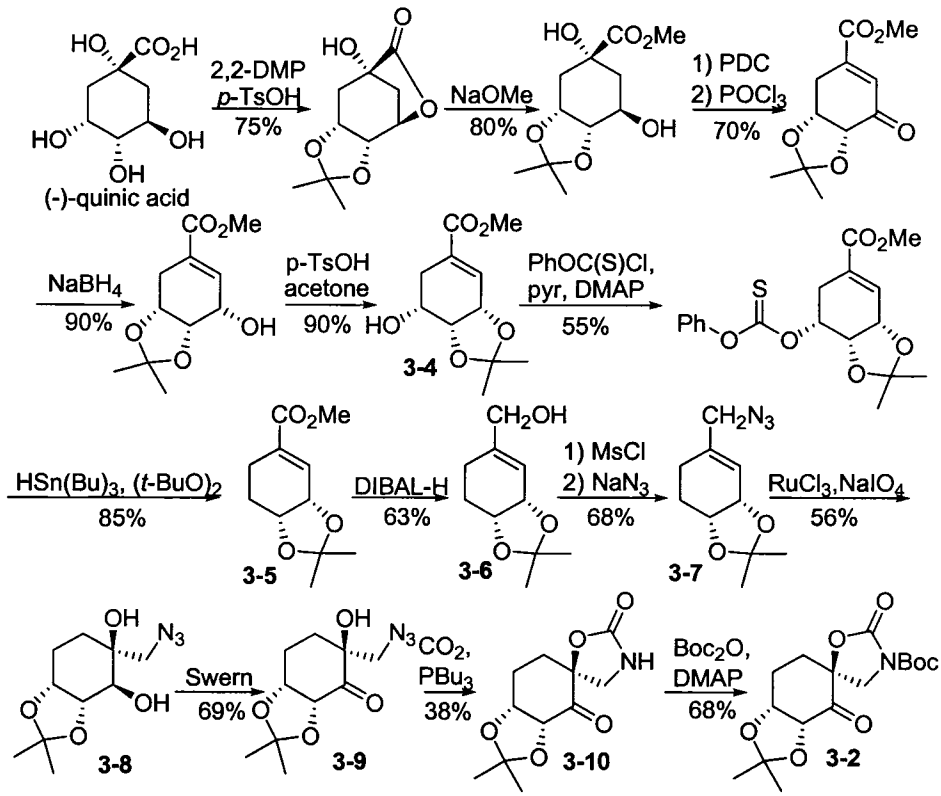

Scheme 3.2

The synthesis of ketone **3-3** was attempted in much the same way (Scheme 3.3). Alcohol **3-11**, prepared by Zackary Crane in several steps from quinic acid, was likely converted to to azide **3-12**, dihydroxylated to diol **3-13**, and oxidized to

ketone **3-14**. Unfortunately, attempts to cyclize this compound were ineffective, so the synthesis of ketone **3-3** was abandoned (Scheme 3.3).

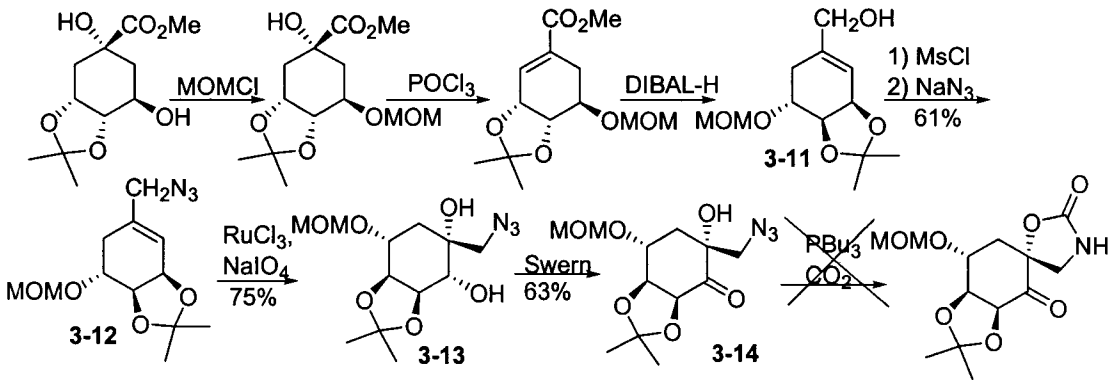

Scheme 3.3

3.B.2. Asymmetric Epoxidation Studies and Transition State Analysis

With two of the three ketones in hand, we began to turn our attention to asymmetric epoxidation studies. Styrene was used as a test substrate for the newly prepared carbocyclic ketone catalysts (Scheme 3.4). Ketones **3-1** and **3-2** gave 89 and 90% ee respectively for styrene, an increase of 8 and 9% respectively from glucose-derived ketone **2-1** (Figure 2.2).[67] Since ketone **3-2** gave the best ee for styrene, it was identified as the most promising candidate and tested on a number of other styrenes. High ee's were obtained for electron-deficient as well as electron-rich styrenes with varying substitution patterns (Table 3.1).

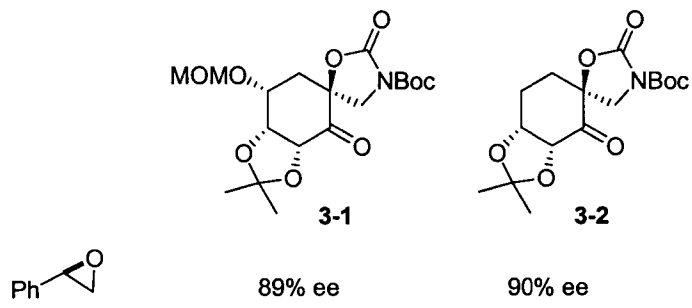

Scheme 3.4

Table 3.1. Asymmetric Epoxidation of Styrenes Catalyzed by Ketone **3-2**[a]

Entry	Substrate	yield[b](conv.[c])(%)	ee (%)	config.[f]
1	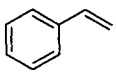	63 (100)	90[d]	(-)-(R)[75]
2	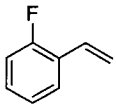	84 (100)	89[d]	(-)[76]
3	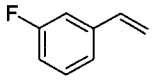	91	90[e]	(-)[77]
4	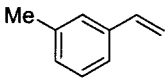	71 (98)	93[d]	(-)
5	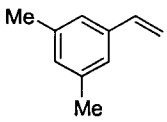	62 (100)	89[d]	(-)
6	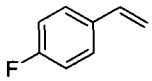	64 (94)	90[d]	(-)-(R)[78]
7	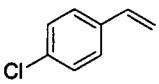	76 (99)	91[d]	(-)-(R)[75]
8	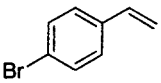	67 (90)	90[d]	(-)-(R)[78]
9	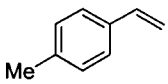	81	90[d]	(-)-(R)[78]
10	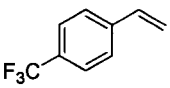	69 (77)	93[d]	(-)[79]
11	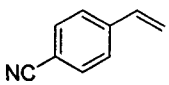	56 (69)	93[d]	(-)-(R)[78]

[a] All reactions were carried out with olefin (0.10 mmol), ketone **3-2** (0.02 mmol), Oxone (0.34 mmol), and K_2CO_3 (0.77 mmol), Bu_4NHSO_4 (0.02 mmol) in DME/DMM (5:1, v/v) (1.6 mL), and buffer (0.2 M K_2CO_3-AcOH, pH 8.0) (1.0 mL) at -10 °C (bath temperature). The reactions were stopped after 8 h except entries 10 & 11 where 0.03 mmol ketone was used and the reaction time was 12 h. [b] The epoxides were purified by flash chromatography and gave satisfactory spectroscopic characterization. [c] The conversion was determined by GC. [d] Enantioselectivity was determined by chiral GC

[75] Archelas, A., Furstoss, R. *J. Org. Chem.* **1999**, *64*, 6112.
[76] Doussot, J., Guy, A., Siaugue, J-M., Ferroud, C., Guieres, A.F. *Chirality* **1999**, *11*, 541.
[77] Pews, R.G. *J. Am. Chem. Soc.* **1967**, *89*, 5605.
[78] (a) Pedragosa-Moreau, S., Morisseau, C., Zylber, J., Archelas, A., Baratti, Furstoss, R. *J. Org. Chem.* **1996**, *61*, 7402. (b) Moussou, P., Archelas, A., Baratti, J., Furstoss, R. *J. Org. Chem.* **1998**, *63*, 3532.
[79] Zhang, R., Yu, W-Y., Sun, H-Z., Liu, W-S., Che, C-M. *Chem. Eur. J.* **2002**, *8*, 2495.

(Chiraldex B-DM). [e] Enantioselectivity was determined by chiral GC (Chiraldex G-TA). [f] The absolute configurations were determined by comparing the measured optical rotations with the reported ones.

The enantioselectivity observed for ketones **2-1** and **3-2** can be explained by the spiro transition state model. As was previously discussed for the epoxidation of *cis*-olefins with ketone **2-1**, an attractive interaction is possible between the aromatic group of the olefin and the oxazolidinone moiety of the ketone catalyst only for spiro transition state **D** (Figure 3.4). As a result, spiro transition state **D** is favored over spiro **E**, resulting in high ee's (90% for cis-β-methylstyrene).[67]

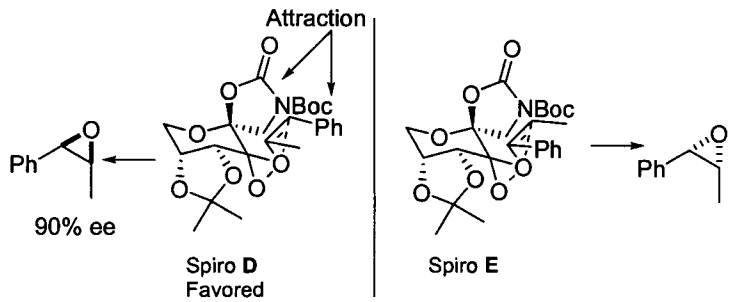

Figure 3.4 *cis*-Olefin transition state analysis.

For styrenes, in addition to spiro **G**, planar transition state **H** also competes with the favored transition state, spiro **F.** Consequently, 81% ee was observed for styrene with ketone **2-1**, a decrease of 9% from cis-β-methylstyrene (Figures 3.4-3.5).[67] The higher ee's obtained for styrene with ketone **3-2** (90%) suggest that the replacement of the pyranose oxygen with a carbon has a noticeable impact on the competition between the transition states, either by further favoring spiro **F** and/or disfavoring spiro **G** and planar **H**.

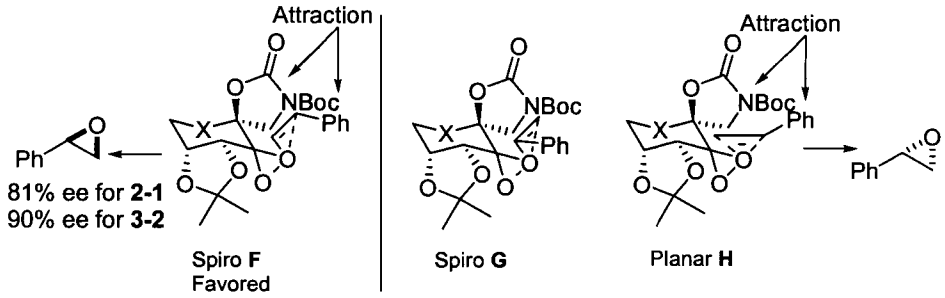

Figure 3.5 Styrene transition state analysis.

To explore the competition between spiro **F** and spiro **G** (Figure 3.5), the epoxidation of cis-β-methylstyrene using both ketones **2-1** and **3-2** was performed, since planar **K** is unlikely to compete substantially due to unfavorable steric interactions (Figure 3.6). Ketone **3-2** gave similar ee to ketone **2-1**, suggesting the replacement of the pyranose oxygen with a carbon has little effect on the competition between spiro **I** and spiro **J**. It was inferred from this result that higher ee obtained for styrene with ketone **3-2** is probably not due to the favoring of spiro **F** over spiro **G** (Figure 3.5).

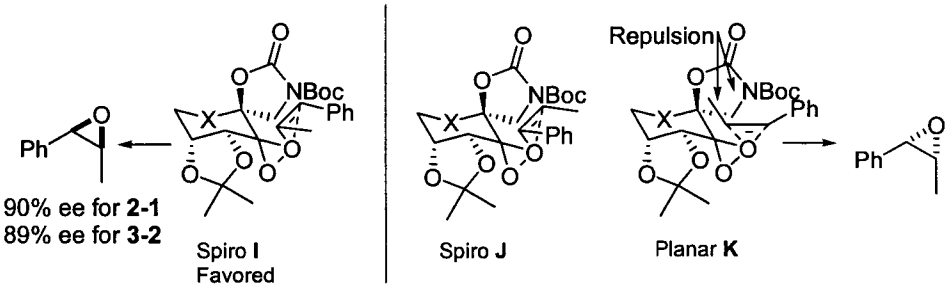

Figure 3.6 *cis*-Olefin epoxidation with ketones **2-1** and **3-2.**

To further explore the competition between spiro **F** and planar **H** (Figure 3.5), the epoxidation of phenylcyclohexene was investigated with ketones **2-1** and **3-2**. For ketone **2-1**, planar **M** is favored over spiro **L** due to the attractive

interaction between the phenyl group of the olefin and the oxazolidinone moiety of the ketone catalyst, and 39% ee of the (S,S) isomer was obtained (Figure 3.7). However, when ketone **3-2** was used, 40% ee of the (R,R) isomer of the epoxide was obtained, indicating spiro **N** is favored over planar **O**. This result indicates that replacement of the pyranose oxygen with a carbon leads to the favoring of spiro transition states over planar ones, suggesting that higher ee obtained for styrene with ketone **3-2** is due to the favoring of spiro **F** and **G** over planar **H** (Figure 3.5).

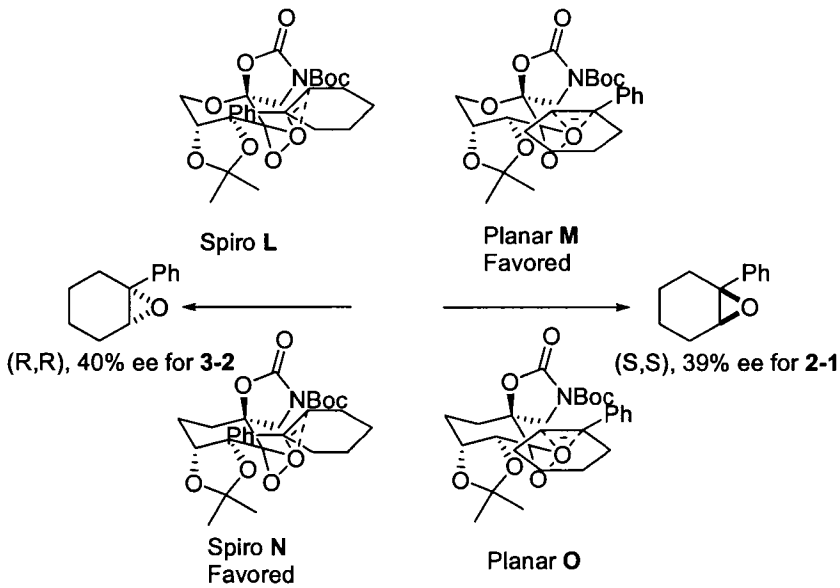

Figure 3.7 Epoxidation of phenylcyclohexene with ketones **2-1** and **3-2.**

The effect of the pyranose oxygen on the competition between spiro and planar transition states could be conformational and/or electronic in nature. Replacing the oxygen of the ring in ketone **2-1** with a carbon would allow the ketone to adopt a different conformation by eliminating the anomeric effect. However, an overlay of the X-ray structures of ketones **2-1** and **3-2** shows that the

two lie almost directly over each other (Figures 3.8,[67] 3.9,[80] 3.10[67,80]), suggesting these two ketones have similar conformations, at least in the solid state.

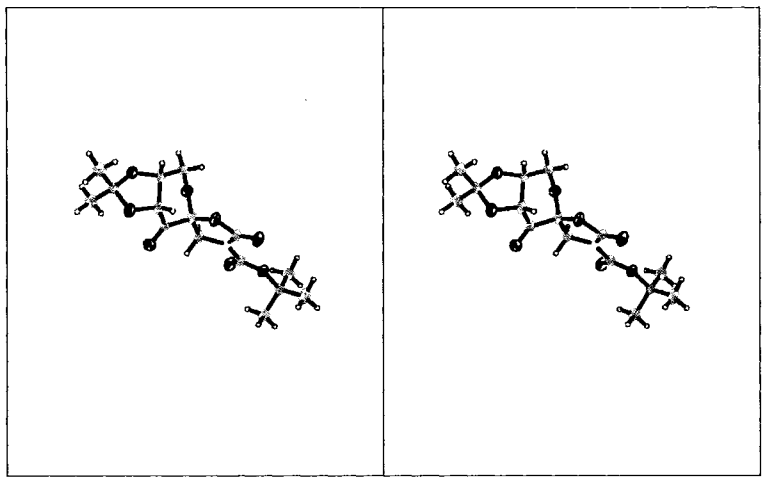

Figure 3.8 X-Ray structure of ketone **2-1** (stereoview).[67]

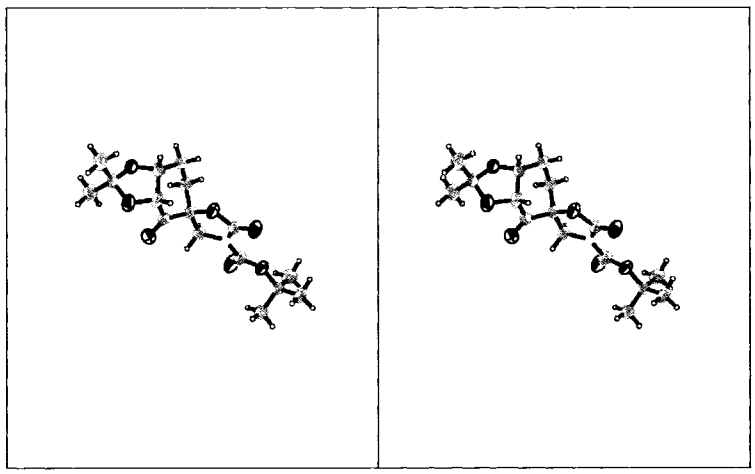

Figure 3.9 X-Ray structure of ketone **3-2** (stereoview).[80]

[80] The crystals used to obtain the X-ray structure of **3-2** were grown by Matthew Hickey, and Susie Miller obtained the X-ray structures.

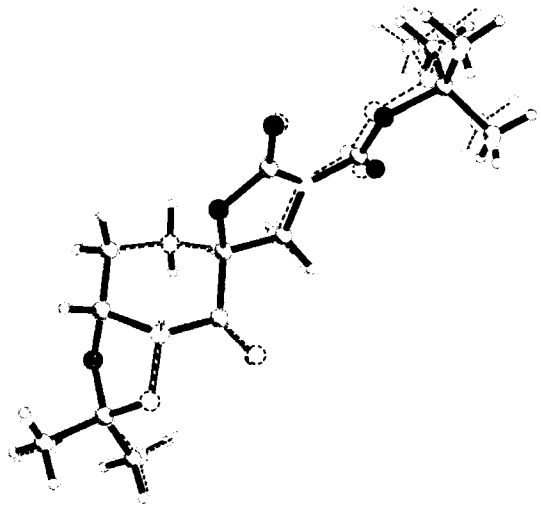

Figure 3.10 X-Ray overlay of ketones **2-1** and **3-2.**[67,80]

Since it seemed unlikely that conformational differences were causing this observed increase in enantioselectivity, we began to turn our attention to the frontier orbital interactions associated with this transformation. It is already known that the primary frontier orbital interaction for both spiro and planar approach is between the HOMO (π of C-C) of the olefin and the LUMO of the

dioxirane (σ^* of O-O), which accounts for the electrophilic nature of the dioxirane (Figure 3.11).[81]

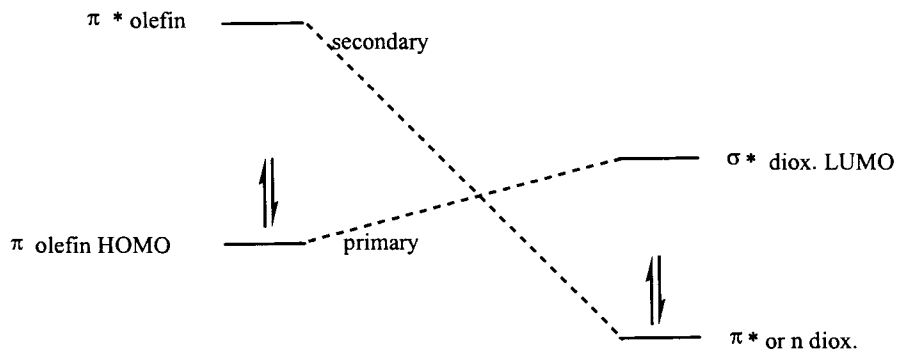

Figure 3.11 Frontier orbital interactions between dioxiranes and olefins.

In addition to this interaction, there is also an additional secondary interaction between the dioxirane (π^* of O-O) and the olefin (π^* of C-C) for a spiro approach (Figures 3.11-3.12). Achieving orbital overlap for the corresponding planar approach is not geometrically feasible, so planar transition states are generally disfavored relative to spiro ones. Since spiro and planar transition states usually lead to opposite enantiomers, factors influencing the competition between these two transition states could have a significant effect on enantioselectivity. Previously, it had been reported that groups that lower energy of the π^* orbital of the olefin, through conjugation or electron withdrawing, further favor spiro transition states due to better overlap.[58-66] Increased secondary orbital interactions could also be achieved by raising energy

[81] For leading mechanistic references of dioxirane epoxidations, see (a) Deubel, D.V. *J. Org. Chem.* **2001**, *66*, 3790. (b) Baukstark, A.L.; Vasquez, P.C. *J. Org. Chem.* **1988**, *53*, 3437. (c) Houk, K.N.; Liu, J.; DeMello, N.C.; Condroski, K.R. *J. Am. Chem. Soc.* **1997**, *119*, 10147.

of the π^* orbital of the dioxirane, which also could lead to an increase in spiro transition state composition and, ultimately, enantioselectivity. However, this potential approach to ee amplification has not been demonstrated experimentally. For ketone **3-2**, replacement of the pyranose oxygen with a carbon in ketone raises the π^* orbital of the dioxirane relative to ketone **2-1**, enabling even better secondary orbital overlap (Figure 3.13). Consequently, all spiro transition states are more favored over their corresponding planar ones. In the case of styrenes, spiro **F** and **G** are more favored over planar **H**, and a net increase in ee is observed for ketone **3-2** (Figure 3.5).

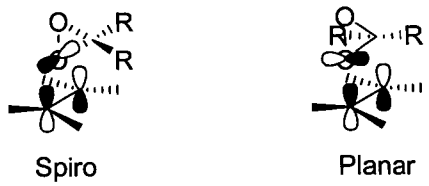

Figure 3.12 Secondary orbital interactions (general).

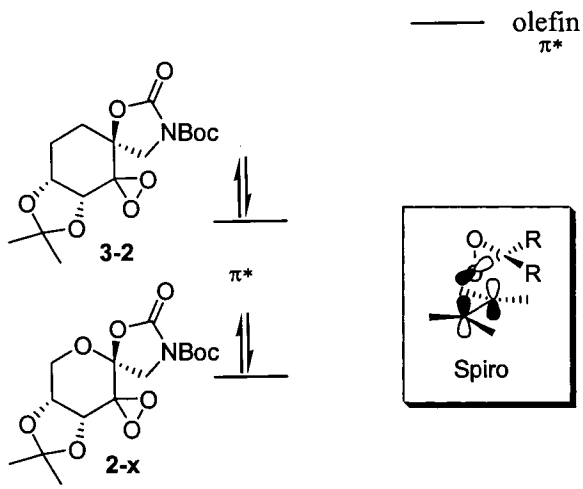

Figure 3.13 Secondary orbital interactions.

Not only does raising the π^* orbital of the dioxirane have an impact on the enantioselectivity of the epoxidation of terminal olefins with this system, but it also has broader implications for catalyst design in all of dioxirane chemistry. The results obtained for ketones **2-1** and **3-2** suggest that more the more electron-rich the groups are surrounding the dioxirane, the more spiro transition states will be favored over planar ones, often giving higher ee. This illustrates the delicate balance between reactivity and selectivity for successful future catalyst design.

3.C. CONCLUSIONS

In summary, the asymmetric epoxidation of styrenes using a carbocyclic oxazolidinone-containing ketone (**3-2**) as catalyst has been investigated. High enantioselectivity (89-93% ee) has been obtained for this challenging type of olefin. The results described herein reveal the potential of chiral dioxirane mediated asymmetric epoxidation as a viable entry into this important class of olefins. Ketone **3-2** provides a promising lead for further optimization of the ketone structure to enhance the enantioselectivity for terminal olefins. Mechanistic studies of the origin of high enantioselectivity of ketone **3-2** uncovered the electronic effects on secondary orbital interactions, which directly affect competition between spiro and planar transition states and, ultimately, enantioselectivity. Although the lengthy synthesis of ketone **3-2** precludes its practical use, the information obtained from these studies provides valuable insight for the design of new, more efficient catalysts.

3.D. EXPERIMENTAL

Representative Asymmetric Epoxidation Procedure

(Table 3.1, Entry 1) (DLG-V-39) To a solution of styrene (0.0104 g, 0.10 mmol) and ketone **3-2** (0.0060 g, 0.02 mmol) in DME-DMM (5:1) (1.6 mL) were added buffer (0.2 M K_2CO_3-AcOH in 4 x 10^{-4} M aq. EDTA, pH = 8.0) (1.0 mL) and TBAHS (0.0075 g, 0.02 mmol) with stirring. After the mixture was cooled to about -10 °C (bath temperature) via a NaCl-ice bath, a solution of Oxone (0.212 M in 4 x 10^{-4} M aq. EDTA, 1.6 mL) and a solution of K_2CO_3 (0.479 M in 4 x 10^{-4} M aq. EDTA, 1.6 mL) were added dropwise separately over a period of 8 h via syringe pump. The reaction mixture was quenched by addition of pentane and extracted with pentane. The combined organic layers were dried (Na_2SO_4), filtered, concentrated, and purified by flash chromatography [the silica gel was buffered by 1% Et_3N in pentane; pentane:ether (1:0 to 10:1) was used as the eluent] to give styrene oxide as a colorless oil (0.0076 g, 63% yield, 90% ee).

(Table 3.1, Entry 1) (DLG-V-39)

(-)-(R)-Styrene oxide[75] colorless oil; $[\alpha]^{20}_D$ = -47.5 (*c* 0.04, $CHCl_3$).

(Table 3.1, Entry 2) (DLG-V-29)

(-)-2-Fluorostyrene oxide[76] yellow oil; $[\alpha]^{20}_D$ = -5.30 (*c* 0.15, $CHCl_3$); IR (film) 3055 cm^{-1}; ^1H NMR (300 MHz, $CDCl_3$) δ 7.20-6.89 (m, 4H), 4.04-4.01 (m, 1H), 3.04 (dd, *J* = 5.7, 4.2 Hz, 1H), 2.66 (dd, *J* = 5.7, 2.7 Hz, 1H); ^{13}C NMR (75 MHz,

$CDCl_3$) δ 161.7 (d, J = 245.1 Hz), 129.5 (d, J = 7.3 Hz), 126.0 (d, J = 4.8 Hz), 125.1 (d, J = 13.4 Hz), 124.4 (d, J = 3.7 Hz), 115.3 (d, J = 20.6 Hz), 50.5, 47.1 (d, J = 6.1 Hz).

(Table 3.1, Entry 3) (DLG-V-46)

(-)-3-Fluorostyrene oxide[77] yellow oil; $[\alpha]^{20}_D$ = -4.87 (*c* 0.19, $CHCl_3$); IR (film) 2995 cm^{-1}; ^1H NMR (300 MHz, $CDCl_3$) δ 7.35-7.24 (m, 1H), 7.09 (d, J = 7.5 Hz, 1H), 7.10-6.92 (m, 2H), 3.87-3.81 (m, 1H), 3.15 (dd, J = 5.4, 4.2 Hz, 1H), 2.76 (dd, J = 5.4, 2.7 Hz, 1H); ^{13}C NMR (75 MHz, $CDCl_3$) δ 163.1 (d, J = 244.2 Hz), 140.5, 130.2 (d, J = 8.4 Hz), 121.4, 115.2 (d, J = 20.9 Hz), 112.3 (d, J = 22.4 Hz), 52.0, 51.5.

(Table 3.1, Entry 4) (DLG-V-28)

(-)-3-Methylstyrene oxide yellow oil; $[\alpha]^{20}_D$ = -6.02 (*c* 0.22, $CHCl_3$); IR (film) 2990 cm^{-1}; ^1H NMR (300 MHz, $CDCl_3$) δ 7.25-7.20 (m, 1H), 7.14-7.05 (m, 3H), 3.83 (dd, J = 3.9, 2.7 Hz, 1H), 3.13 (dd, J = 5.4, 3.9 Hz, 1H), 2.80 (dd, J = 5.4, 2.7 Hz, 1H), 2.35 (s, 3H); ^{13}C NMR (75 MHz, $CDCl_3$) δ 138.1, 137.5, 128.9, 128.4, 126.0, 122.7, 52.5, 51.2, 21.5; HRMS Calcd for $C_9H_{10}O$ (M+) 134.0732, found 134.0735.

(Table 3.1, Entry 5) (DLG-V-44)

(-)-3,5-Dimethystyrene oxide yellow oil; $[\alpha]^{20}_D$ = -17.1 (*c* 0.17, $CHCl_3$); IR (film) 2919 cm^{-1}; ^1H NMR (300 MHz, $CDCl_3$) δ 6.97 (s, 1H), 6.93 (s, 2H), 3.82

(dd, J = 3.9, 2.7 Hz, 1H), 3.14 (dd, J = 5.4, 3.9 Hz, 1H), 2.81 (dd, J = 5.4, 2.7 Hz, 1H), 2.34 (s, 6H); ^{13}C NMR (75 MHz, $CDCl_3$) δ 138.2, 137.5, 129.9, 123.3, 52.5, 51.2, 21.4; HRMS calcd for $C_{10}H_{13}O$ (M+1) 149.0966, found 148.0964.

(Table 3.1, Entry 6) (DLG-V-37)

(-)-(R)-4-Fluorostyrene oxide[78] yellow oil; $[\alpha]^{20}_D$ = -13.7 (*c* 0.08, $CHCl_3$); IR (film) 2993 cm^{-1}; ^{1}H NMR (300 MHz, $CDCl_3$) δ 7.28-7.20 (m, 2H), 7.08-6.99 (m, 2H), 3.88-3.83 (m, 1H), 3.16-3.11 (m, 2H), 2.79-2.75 (m, 1H); ^{13}C NMR (75 MHz, $CDCl_3$) δ 162.7 (d, J = 242.7 Hz), 133.4 (d, J = 2.8 Hz), 127.2 (d, J = 8.3 Hz), 115.6 (d, J = 20.9 Hz), 52.0, 51.4.

(Table 3.1, Entry 7) (DLG-V-36)

(-)-(R)-4-Chlorostyrene oxide[75] yellow oil; $[\alpha]^{20}_D$ = -10.8 (*c* 0.26, $CHCl_3$); IR (film) 2991 cm^{-1}; ^{1}H NMR (300 MHz, $CDCl_3$) δ 7.32 (d, J = 8.4 Hz, 2H), 7.21 (d, J = 8.4 Hz, 2H), 3.87-3.81 (m, 1H), 3.15 (dd, J = 5.4, 4.2 Hz, 1H), 2.75 (dd, J = 5.4, 2.7 Hz, 1H); ^{13}C NMR (75 MHz, $CDCl_3$) δ 136.3, 133.9, 128.8, 126.9, 51.8, 51.3.

(Table 3.1, Entry 8) (DLG-V-38)

(-)-(R)-4-Bromostyrene oxide[78] colorless oil; $[\alpha]^{20}_D$ = -13.8 (*c* 0.21, $CHCl_3$); IR (film) 2990 cm^{-1}; ^{1}H NMR (300 MHz, $CDCl_3$) δ 7.47 (d, J = 8.4 Hz, 2H), 7.15 (d, J = 8.4 Hz, 2H), 3.85-3.80 (m, 1H), 3.17-3.12 (m, 1H), 2.75 (dd, J = 5.4, 2.4 Hz, 1H); ^{13}C NMR (75 MHz, $CDCl_3$) δ 136.7, 131.6, 127.2, 122.0, 51.9, 51.4.

(Table 3.1, Entry 9) (DLG-V-22)

(-)-(R)-4-Methylstyrene oxide[78] yellow oil; $[\alpha]^{20}_{D}$ = -9.52 (*c* 0.11, $CHCl_3$); IR (film) 2987 cm^{-1}; ^1H NMR (300 MHz, $CDCl_3$) δ 7.19-7.12 (m, 4H), 3.83 (dd, *J* = 4.2, 2.4 Hz, 1H), 3.13 (dd, *J* = 5.4, 4.2 Hz, 1H), 2.80 (dd, *J* = 5.4, 2.4 Hz, 1H), 2.35 (s, 3H); ^{13}C NMR (75 MHz, $CDCl_3$) δ 137.9, 134.5, 129.2, 125.5, 52.5, 51.2, 21.4.

(Table 3.1, Entry 10) (DLG-V-47)

(-)-4-Trifluoromethylstyrene oxide[79] yellow oil; $[\alpha]^{20}_{D}$ = -12.2 (*c* 0.09, $CHCl_3$); IR (film) 2996 cm^{-1}; ^1H NMR (300 MHz, $CDCl_3$) δ 7.60 (d, *J* = 8.1 Hz, 2H), 7.39 (d, *J* = 8.1 Hz, 2H), 3.94-3.90 (m, 1H), 3.25-3.16 (m, 1H), 2.77 (dd, *J* = 5.7, 2.7 Hz, 1H); ^{13}C NMR (75 MHz, $CDCl_3$) δ 125.9, 125.6, 125.6, 52.0, 51.7.

(Table 3.1, Entry 11) (DLG-V-49)

(-)-(R)-4-Cyanostyrene oxide[78] white solid; $[\alpha]^{20}_{D}$ = -12.1 (*c* 0.24, $CHCl_3$); IR (film) 2228 cm^{-1}; ^1H NMR (300 MHz, $CDCl_3$) δ 7.63 (d, *J* = 8.4 Hz, 2H), 7.38 (d, *J* = 8.4 Hz, 2H), 3.92-3.88 (m, 1H), 3.22-3.18 (m, 1H), 2.75 (dd, *J* = 5.4, 2.4 Hz, 1H); ^{13}C NMR (75 MHz, $CDCl_3$) δ 143.3, 132.5, 126.2, 118.8, 112.1, 51.9.

Ester (3-5) (DLG-IV-36, 37, 38, 39, 41, 43)[73] To a solution of alcohol **3-4** (15 g, 65.7 mmol) in DCM (332 mL) was added pyridine (21.3 mL, 263 mmol), followed by DMAP (0.32 g), and finally PhOC(S)Cl (13.6 mL, 98.5 mmol)

slowly over a period of 20 min. After stirring overnight, the mixture was poured into satd NH_4Cl solution and then diluted with additional DCM. Next, the aqueous layer was washed 3 times with additional DCM, and the combined organics were then washed with brine, dried over $MgSO_4$, and finally concentrated to give a reddish sludge. The sludge was vacuum filtered through silica gel with a EtOAc:hexane (1:6), and the resulting filtrate was concentrated. This yellow solid was then recrystallized from EtOAc:hexane to give a white solid (16.75 g, 55%) which was used without further purification. The white solid (6.75 g, 18.5 mmol) and $HSnBu_3$ (8.5 mL, 31.5 mmol) were dissolved in freshly distilled toluene (300 mL). *t*-Butylperoxide (0.7 mL, 3.7 mmol) was added, and then the mixture was heated to reflux for 2 h under argon. After cooling to rt, the clear reaction mixture was concentrated and diluted with ether. The organics were washed with 1N NaOH, water, dried (Na_2SO_4), filtered, concentrated, and purified by flash chromatography (hexane:EtOAc 1:0 to 9:1) to give ester **3-5** as a clear oil (3.35 g, 85%) that was used without further purification.

Alcohol (3-6) (DLG-IV-40, 45) To a solution of ester **3-5** (5.05 g, 23.7 mmol) in freshly distilled THF (24 mL) was added DIBAL-H (39.7 mL, 1.5 M in toluene) dropwise under nitrogen at 0° C over a period of 20 min. After stirring for 2 h, satd aqueous NH_4Cl was added *extremely slowly* to the clear reaction mixture until a gelatin formed. The gelatin was stirred for several minutes, filtered, and

washed several times with ether. The filtrate was concentrated to give alcohol **3-6** as a clear oil (2.76 g, 63%) that was used without further purification.

Azide (3-7) (DLG-IV-42, 46) To a mixture of alcohol **3-6** (3.43 g, 18.6 mmol) in DCM (10 mL) at 0° C was added Et_3N (7.8 mL, 55.8 mmol) followed by MsCl (2.2 mL, 27.9 mmol), resulting in the mixture turning bright orange. After two hours of stirring, the solvent was removed on the rotory evaporator, and acetone (20 mL) followed by NaN_3 (1.57 g in 10.1 mL water) were then added to the flask, and the mixture was allowed to stir at rt for an additional 16 h. The acetone was removed on the rotory evaporator, and DCM was used to wash the aqueous layer 4 times. The combined organics were washed with brine, dried (Na_2SO_4), filtered, and concentrated to give azide **3-7** as an orange sludge (2.65 g, 68%). A small amount of the azide was chromatographed with EtOAc:hexane (1:1) for characterization purposes. The remainder of the material was used without further purification. IR (film) 2100 cm^{-1}; ^1H NMR (300 MHz, $CDCl_3$) δ 5.69 (brs, 1H), 4.49 (m, 1H), 4.29 (m, 1H), 3.70 (s, 2H), 2.15 (m, 1H), 2.00-1.76 (m, 3H), 1.37 (s, 3H), 1.35 (s, 3H); ^{13}C NMR (75 MHz, $CDCl_3$) δ 136.8, 124.1, 108.7, 72.5, 71.8, 56.9, 28.2, 26.6, 25.6, 22.3.

Diol (3-8) (DLG-IV-49) To a solution of azide **3-7** (2.0 g, 9.56 mmol) in MeCN (37 mL) and EtOAc (37 mL) at 0°C was added an aqueous solution (11.8 mL) of $RuCl_3$ (0.14 g, 0.67 mmol) and $NaIO_4$ (2.66 g, 12.4 mmol) dropwise over 5 min. After 15 additional min., satd. $Na_2S_2O_3$ (15 mL) was added. The layers were

separated, and the aqueous layer was washed 3 times with DCM. The combined organics were dried (Na_2SO_4), filtered, concentrated, and purified over silica gel (buffered with 1% Et_3N) with a 1:1 EtOAc:hexane to give diol **3-8** as a clear oil (1.30 g, 56%). Note: Ketone **3-9** (0.57 g, 25%) was also isolated in addition to the diol from the reaction mixture. Diol **3-8**: $[\alpha]^{20}_D$ = -44.2 (*c* 0.095, $CHCl_3$); IR (film) 3430, 2104 cm^{-1}; ^1H NMR (300 MHz, $CDCl_3$) δ 4.31 (m, 1H), 4.00 (dd, *J* = 7.2, 5.1 Hz, 1H), 3.57 (dd, *J* = 7.2, 3.0 Hz, 1H), 3.45 (d, *J* = 12.3, Hz, 1H), 3.36 (d, *J* = 12.3 Hz, 1H), 2.72 (brs, 1H), 2.37 (brs, 1H), 2.18-2.01 (m, 1H), 2.01-1.90 (m, 1H), 1.71-1.60 (m, 2H), 1.50 (s, 3H), 1.37 (s, 3H); ^{13}C NMR (75 MHz, $CDCl_3$) δ 109.1, 80.2, 74.3, 74.1, 74.0, 58.4, 28.7, 27.5, 26.6, 21.6; HRMS Calcd for $C_{10}H_{18}N_3O_4$ (M+1) 244.1297, found 244.1299.

Ketone (3-9) (DLG-XIV-50) To a solution of DMSO (0.10 mL, 1.44 mmol) in DCM (0.97 mL) at -78°C, oxalyl chloride (66.4 μL, 0.77 mmol) was added dropwise. The mixture was then allowed to stand at rt for exactly 3 min. and then cooled to -78°C again. Alcohol **3-8** (0.14 g, 0.58 mmol in 5.3 mL DCM) was then added dropwise, and the mixture was allowed to stir at -78°C for an additional 1.5 h. Et_3N (0.3 mL, 2.07 mmol) was added, and the mixture was allowed to warm to rt for 15 min. Satd. NH_4Cl was then added, followed by additional water. The layers were then separated, and the aqueous layer was washed 3 times with DCM. The combined organics were washed with brine, dried (Na_2SO_4), filtered, concentrated, and purified by flash chromatography (EtOAc:hexane 1:1 treated with 1% Et_3N) yielded **3-9** as a white solid (0.097 g, 69%). Note: It is

exceedingly important to not only buffer the column, but also the solvent used in the purification. Also, the column must be packed with the 1:1 mixture, not pure hexane. Failure to follow either of the two aforementioned procedures results in large amount of ketal removal catalyzed by silica gel. mp 73-75 °C; $[\alpha]^{20}_{D}$ = -18.2 (*c* 0.055, $CHCl_3$); IR (film) 3438, 2107, 1734 cm^{-1}; ^1H NMR (300 MHz, $CDCl_3$) δ 4.78 (d, *J* = 5.7 Hz, 1H), 4.60 (m, 1H), 3.74 (d, *J* = 12.6 Hz, 1H), 3.30 (d, *J* = 12.6 Hz, 1H), 3.23 (s, 1H), 2.21 (m, 1H), 2.00-1.85 (m, 3H), 1.44 (s, 3H), 1.35 (s, 3H); ^{13}C NMR (75 MHz, $CDCl_3$) δ 207.6, 110.3, 78.7, 78.0, 77.9, 56.4, 31.0, 27.0, 25.9, 21.8.

Oxazolidinone (3-10) (DLG-VI-32, MRH 1213)[82] A solution of **3-9** (0.091 g, 0.38 mmol) in anhydrous (NOTE: it is essential to use the driest MeCN available, as any incidental water in the reaction results in low yield) MeCN (29 mL) was sparged with CO_2 for ca. 2 h in a three necked round bottomed flask fitted with a reflux condenser. Bu_3P (0.097 g, 0.48 mmol) was then added dropwise at rt. The reaction progress was monitored by TLC (EtOAc: hexane, 2:1). When the reaction appeared complete, the clear yellow solution was concentrated to a red-orange oil. This oil was purified by flash chromatography on buffered silica gel (2% Et_3N) (EtOAc:hexanes 2:1), giving the product **3-10** as an off white solid (0.035 g, 38%) [NOTE: It is important to note that this compound is typically isolated containing some tributylphosphine oxide. The following reaction is tolerant of some (<5%) tributylphosphine oxide, however it is important to get

this material as clean as possible]: $[\alpha]^{20}_D$ = -32.8 (*c* 0.5, $CHCl_3$)[82]; IR (film) 3337, 1771, 1746 cm^{-1}; ^1H NMR (300 MHz, $CDCl_3$) δ 5.71 (brs, 1H), 4.85 (d, *J* = 5.1 Hz, 1H), 4.63 (m, 1H), 4.34 (d, *J* = 8.9 Hz, 1H), 3.16 (*J* = 8.9 Hz, 1H), 2.50 (m, 1H), 2.30-2.00 (m, 3H), 1.43 (s, 3H), 1.40 (s, 3H); ^{13}C NMR (75 MHz, $CDCl_3$) δ 201.4, 156.7, 110.0, 85.2, 78.8, 77.4, 44.4, 32.9, 27.1, 26.1, 21.1; HRMS calcd for $C_{11}H_{16}NO_5$ (M+1) 242.1028, found 242.1029.

Ketone (3-2) (DLG-VI-33, MRH 1223) To a solution of **3-10** (0.030 g, 0.12 mmol) in THF (1 mL) at rt was added $(Boc)_2O$ (0.035 g, 0.16 mmol) followed by 4 uL of a DMAP solution in THF (0.1 M, 0.001 mmol). The reaction was monitored by TLC (EtOAc:hexanes 2:1) until the starting material was consumed, ca. 30 minutes. The mixture was then filtered through a silica gel plug and washed with EtOAc:hexanes (1:1). The combined filtrate was concentrated and purified by flash chromatography (Et_2O:hexanes, 1:2) gave ketone **3-2** as a white solid (0.028 g, 68%): mp 130-132°C; $[\alpha]^{20}_D$ = -20 (*c* 0.10, $CHCl_3$); IR (film) 1824, 1747, 1728 cm^{-1}; ^1H NMR (300 MHz, $CDCl_3$) δ 4.82 (d, *J* = 5.1 Hz, 1H), 4.64 (d, *J* = 10.6 Hz, 1H), 4.62 (m, 1H), 3.48 (d, *J* = 10.6 Hz, 1H), 2.45 (m, 1H), 2.20 (m, 3H), 1.54 (s, 9H), 1.44 (s, 3H), 1.41 (s, 3H); ^{13}C NMR (75 MHz, $CDCl_3$) δ 201.1, 150.0, 148.9, 110.4, 84.7, 81.4, 78.9, 77.3, 47.5, 32.8, 28.0, 27.2, 26.1, 21.0; HRMS calcd for $C_{16}H_{24}NO_7$ (M+1) 342.1553, found 342.1545.

[82] The desired product is not completely pure, so optical rotation and melting point values should be viewed accordingly.

Azide (3-12) (DLG-V-5) To a solution of alcohol **3-11** (1.11 g, 4.6 mmol) in DCM (2.4 mL) at 0 °C was added Et_3N (1.9 mL, 13.7 mmol) followed by MsCl (0.5 mL, 6.8 mmol), and the mixture turned bright orange. After stirring for 2h., the solvent was removed on the rotory evaporator. Acetone (4.9 mL) and NaN_3 (0.4 g in 2.4 mL water) were then added to the flask, and the resulting mixture was allowed to stir at rt for 16 h. The acetone was removed on the rotory evaporator, and the aqueous layer was washed four times (DCM). The combined organics were washed with brine, dried (Na_2SO_4), and concentrated to give azide **3-12** as an orange sludge (0.74 g, 61%). A small amount of the azide was purified by chromatography with EtOAc:hexane (1:1) for characterization purposes. The remainder of the material was used without further purification. $[\alpha]^{20}_D$ = -48.4 (*c* 0.42, $CHCl_3$); IR (film) 2098 cm^{-1}; ^1H NMR (300 MHz, $CDCl_3$) δ 5.82 (m, 1H), 4.76 (d, *J* = 6.6 Hz, 1H), 4.71 (d, *J* = 6.6 Hz, 1H), 4.67-4.62 (m, 1H), 4.15-4.10 (m, 1H), 3.91-3.82 (m 1H), 3.75 (s, 2H), 3.38 (s, 3H), 2.39 (dd, *J* = 17.1, 4.5 Hz, 1H), 2.18-2.12 (m, 1H), 1.45 (s, 3H), 1.37 (s, 3H); ^{13}C NMR (75 MHz, $CDCl_3$) δ 134.8, 122.7, 109.4, 96.0, 76.8, 73.8, 72.6, 56.4, 55.6, 30.7, 28.3, 26.3.

Diol 3-13 (DLG-V-9) To a solution of azide **3-12** (0.46 g, 1.7 mmol) in MeCN (8.5 mL) and EtOAc (8.5 mL) at 0 °C was added an aqueous solution (2.7 mL) of $RuCl_3$ (0.03 g, 0.12 mmol) and $NaIO_4$ (0.48 g, 2.2 mmol) dropwise over 5 min. After 20 total min., the saturated $Na_2S_2O_3$ (5 mL) was added. The layers were separated, and the aqueous layer was washed 3 times (DCM). The combined organics were dried (Na_2SO_4), concentrated, and purified over silica gel (buffered

with 1% Et_3N 1:1 EtOAc:hexane) to give diol **3-13** as a clear oil (0.39 g, 75%). Note: Ketone **3-14** was also isolated in addition to the diol from the reaction mixture. $[\alpha]^{20}_D$ = 11.1 (*c* 0.40, $CHCl_3$); IR (film) 3445, 2105 cm^{-1}; ^1H NMR (300 MHz, $CDCl_3$) δ 4.74 (d, *J* = 6.9 Hz, 1H), 4.72 (d, *J* = 6.9 Hz, 1H), 4.29-4.22 (m, 2H), 4.18-4.12 (m, 1H), 3.57-3.40 (m, 6H), 3.29 (d, *J* = 12.3 Hz, 1H), 2.50 (d, *J* = 7.2 Hz, 1H), 2.00 (d, *J* = 5.4 Hz, 1H), 1.97 (d, *J* = 3.9 Hz, 1H), 1.50 (s, 3H), 1.37 (s, 3H); ^{13}C NMR (75 MHz, $CDCl_3$) δ 109.8, 96.1, 78.6, 76.8, 76.2, 74.4, 73.1, 57.5, 56.2, 33.5, 28.3, 26.1; HRMS Calcd for $C_{12}H_{22}N_3O_6$ (M+1) 304.1509, found 304.1516.

Ketone (3-14) (DLG-V-13)[82] To a solution of DMSO (0.67 mL, 8.6 mmol) in DCM (5.8 mL) at -78°C was added oxalyl chloride (0.33 mL, 3.8 mmol). The mixture was then allowed to stand at rt for exactly 3 min. and then cooled to -78°C again. Diol **3-13** (1.04 g, 3.4 mmol in 11.6 mL DCM) was added dropwise, and the mixture was allowed to stir at -78°C for an additional 1.5 h. Et_3N (1.7 mL, 12.2 mmol) was added to the mixture which was allowed to warm to rt for 15 min. Satd. NH_4Cl was then added followed by additional water. The layers were then separated, and the aqueous layer was washed 3 times (DCM). The combined organics were washed with brine, dried (Na_2SO_4), concentrated, and purified by flash chromatography (EtOAc:hexane 1:1) buffered with Et_3N) to yield the ketone **(3-14)** as a yellow oil (0.63 g, 63%). $[\alpha]^{20}_D$ = -29.5 (*c* 0.39, $CHCl_3$); IR (film) 3447, 2106, 1734 cm^{-1}; ^1H NMR (300 MHz, $CDCl_3$) δ 4.78-4.59 (m, 4H), 4.18-4.10 (m, 2H), 3.52 (d, *J* = 12.6 Hz, 1H), 3.43-3.32 (m, 4H), 2.40-2.26 (m,

2H), 1.50 (s, 3H), 1.37 (s, 3H); ^{13}C NMR (75 MHz, $CDCl_3$) δ 206.1, 111.7, 95.6, 79.9, 77.1, 77.0, 71.2, 57.8, 56.3, 34.6, 26.6, 25.0; HRMS calcd for $C_{12}H_{20}N_3O_6$ (M+1) 302.1352, found 302.1347.

CHAPTER FOUR

EXPLORING STRUCTURAL EFFECTS OF KETONE CATALYSTS ON ASYMMETRIC EPOXIDATION OF OLEFINS

4.A. INTRODUCTION

Previously, it was discussed that high ee's could be obtained for many *trans*- and trisubstituted olefins with ketone **1-16**.[58-66] Also, we have reported high ee's for conjugated *cis*-olefins and styrenes with ketones **2-1** and **3-2**, respectively (Figure 4.1).[67] The very different results for structurally similar ketones prompted us to explore the effects of different spiro ring substitution patterns on enantioselectivity for different olefin classes. Hopefully, with the information obtained, either catalysts capable of increasing substrate scope of asymmetric epoxidation or practical catalysts could be developed.

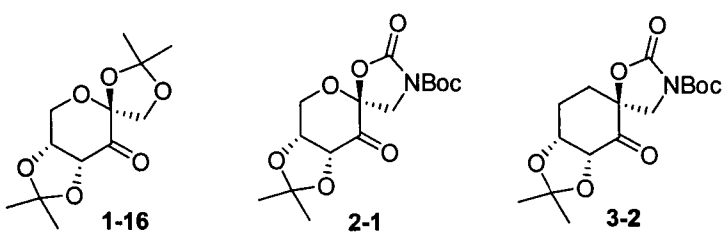

1-16 **2-1** **3-2**

Figure 4.1 Chiral ketone catalysts for asymmetric epoxidation

Considering the large differences in ee observed for *cis*- and terminal olefin epoxidation between catalysts **1-16** and **2-1, 3-2,** we began to turn our focus to the spiro ring structural requirements necessary to achieve the maximum attraction between the catalyst and substrate. With that in mind, several ketones bearing very different structural features were targeted for asymmetric epoxidation studies (Figure 4.2). Ketone **4-1** is very similar to **1-16** with the only difference being replacement of one of the oxygens in the spiro ring with a carbon atom. Ketone **4-2** has the same spiro ring as **4-1**, but lacks the methyl groups. Ketones **4-3** - **4-7** replace the oxazolidinone of **2-1** with a lactone. Ketones **4-4** and **4-5** contain alkyl groups α- to the lactone carbonyl, and ketones **4-6** and **4-7** possess halides α- to the lactone carbonyl. Halogenated ketones (**4-8**, **4-9**) not possessing the carbonyl of the lactone were also targeted, as was a similar ketone substituted with alkyl groups (**4-10**). A very hindered tetramethyl-substituted ketone (**4-11**) and a ketone with aromatic spiro ring substitution (**4-12**) were also targets of synthetic efforts.

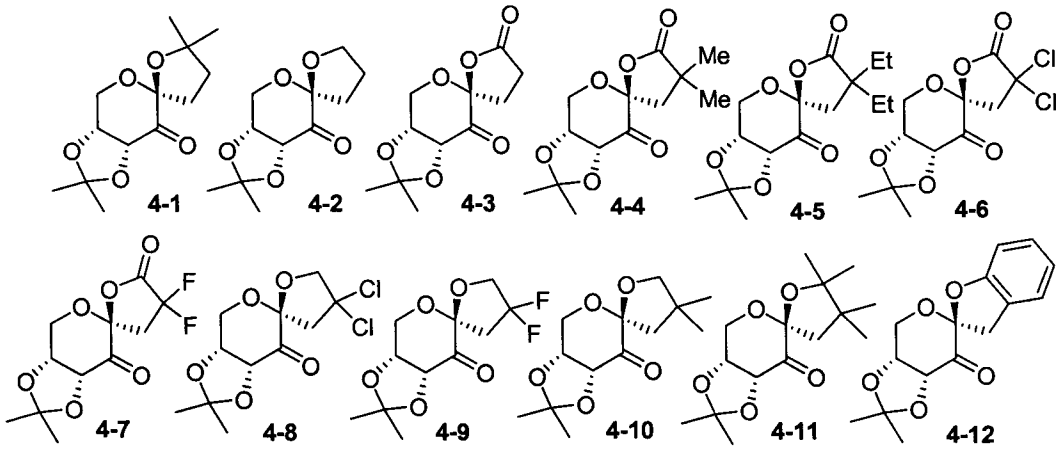

Figure 4.2 Chiral ketone synthetic targets

4.B. RESULTS AND DISCUSSION

4.B.1. Synthesis of Ketones

Since ketones **4-1**, **4-2**, **4-3**, **4-4**, and **4-5** were prepared by Zackary Crane and Yonghon Gan, their syntheses will not be decribed here. Using a very similar strategy to the one used to prepare ketones **4-1** - **4-5**, our efforts were focused on the preparation of ketones **4-6** - **4-11** (Scheme 4.1). For the synthesis of ketone **4-10**, ester **4-16** was prepared with a known literature procedure by thermodynamic ketalization of D-fructose,[83] oxidation, Wittig reaction,[84] and hydrogenation.[84] Dialkylation with LDA/MeI,[85] followed by reduction, TFA cyclization,[86] ketalization,[86] and oxidation yielded ketone **4-10** in 10 overall steps (Scheme 4.2). Ketone **4-11** was prepared in a very similar manner. Ester **4-17** was subjected to MeMgBr instead of LAH, which gave ketone **4-11** after the usual TFA cyclization, ketalization,[82] and oxidation[82] (Scheme 4.3).

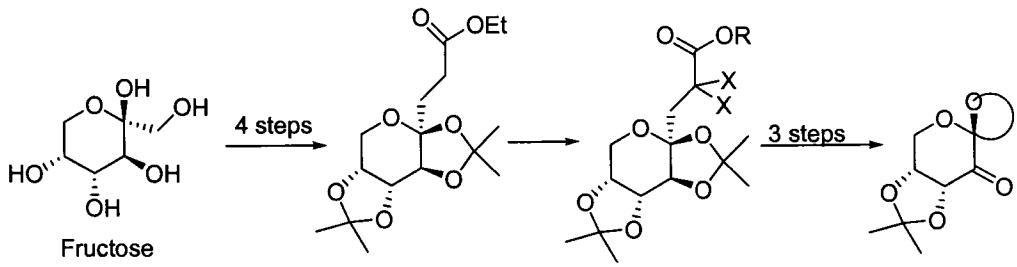

Scheme 4.1

[83] Brady, R.F. *Carbohyd. Res.* **1970**, *15*, 35.
[84] Aamlid, K.H.; Hough, L.; Richardson, A.C. *Carbohyd. Res.* **1990**, *202*, 117.
[85] Cregge, R.J.; Herrmann, J.L.; Lee, C.S.; Richman, J.E.; Schlessinger, R.H. *Tetrahedron Lett.* **1973**, *26*, 2425.
[86] Cubero, I.I.; Maria, P.; Lopez-Espinosa, M.T.; Richardson, A.C.; Kai, H.A. *Carbohyd. Res.* **1993**, *224*, 281.

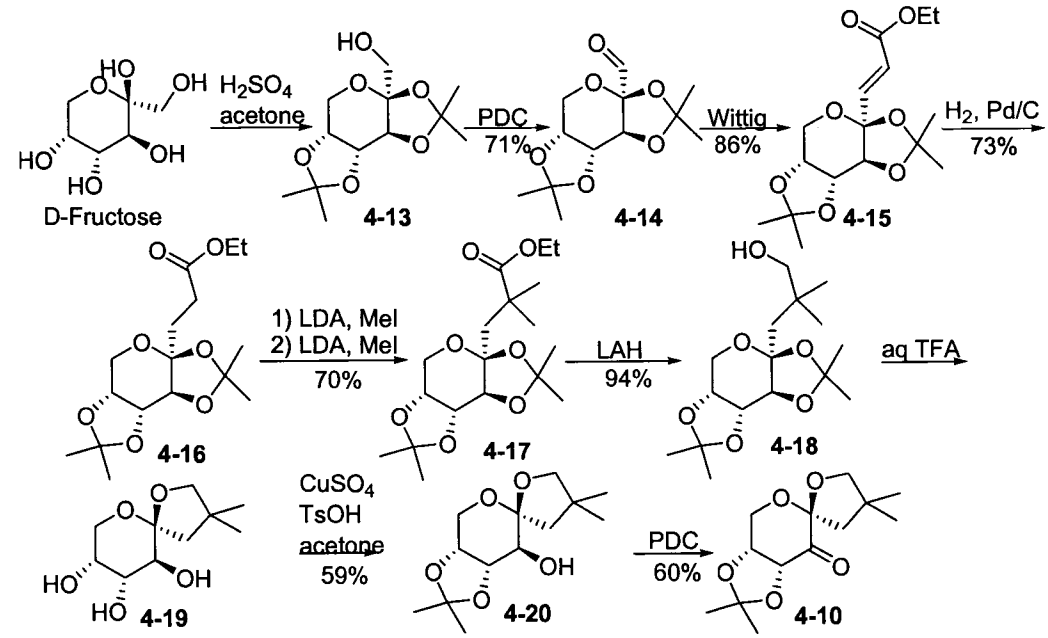

Scheme 4.2

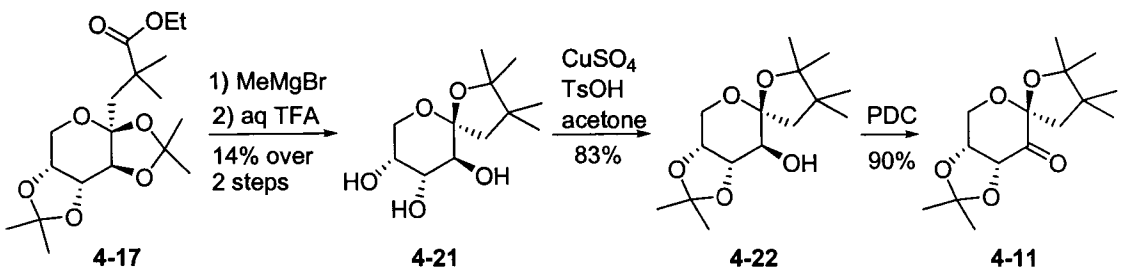

Scheme 4.3

With ketones **4-11** and **4-12** in hand, we began to turn our focus to the synthesis of halogenated ketones **4-6** - **4-9**. Unfortunately, both radical with CCl_4 and simple LDA chlorination using NCS were unsuccessful, suggesting that ester dichlorination was going to be difficult (Scheme 4.4). Poor results were also seen for the attempted fluorination of **4-16** with standard sources of F^+, including one previously found to be successful for difluorination. We thought the problem

might be able to be circumvented by adding a fluorinated zinc species directly into aldehyde **4-14**, but no addition was observed (Scheme 4.5)

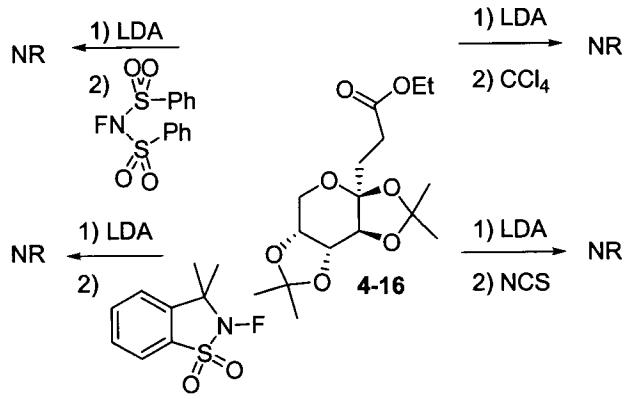

Scheme 4.4

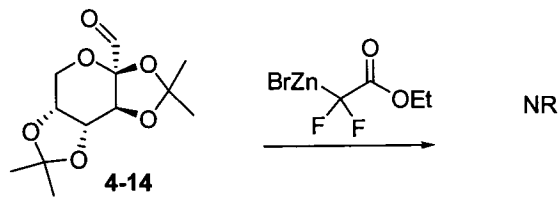

Scheme 4.5

Since the dihalogenation of ester **4-16** was unproductive, we began to turn our focus toward the dihalogenation of the aldehyde oxidation state. In particular, we were interested in doing a Wittig-type dichlorination with an aldehyde, tertiary amine, and NCS to give the dichlorinated compounds (Scheme 4.6). Reduction and oxidation gave the aldehyde,[82] which was subjected to standard Wittig chlorination conditions, and following hydrolysis, dichlorinated products were observed (Scheme 4.7).

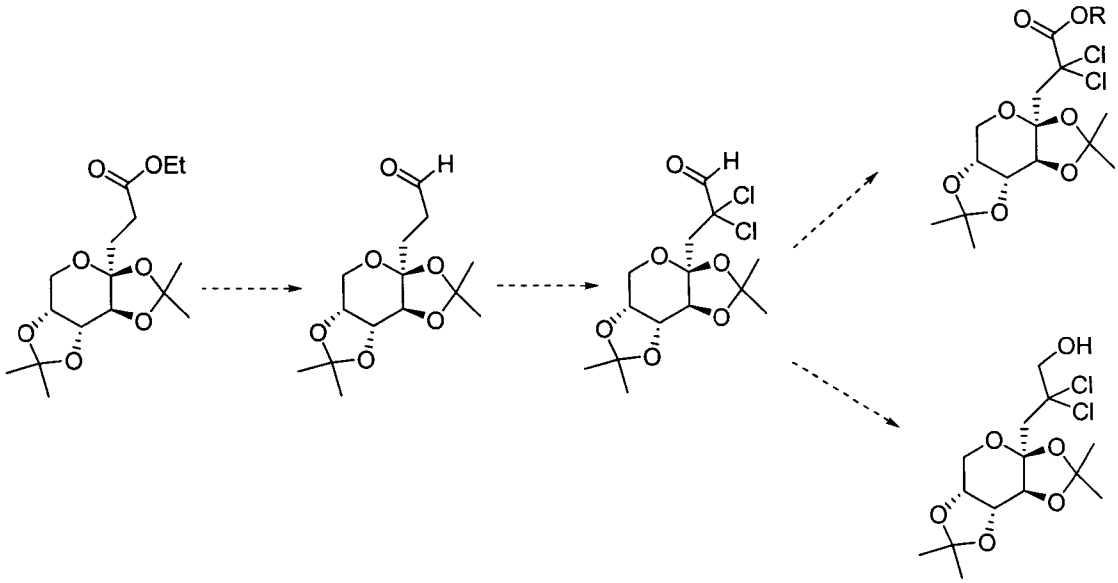

Scheme 4.6

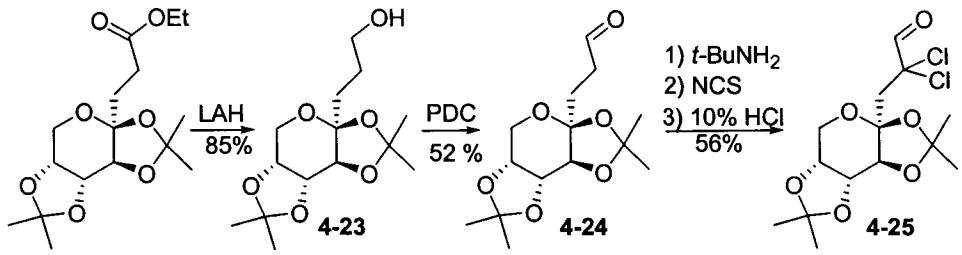

Scheme 4.7

Having seen the dihalogenation proceed smoothly, we turned our attention to the manipulation of oxidation states required for the two different ketones. The standard oxidation/reduction followed by TFA cyclization/$CuSO_4$ ketalization yielded no desired alcohol product (Scheme 4.8). Unfortunately, none of a myriad of reaction conditions attempted, from carefully following the TFA cyclization with the hope of stopping the reaction at the desired product to using different Lewis acids gave the desired product. Presumably, these failures were

due to the instability of the desired products, since we observed decomposition of intermediates including and after **4-25**. This product instability forced us to abandon the syntheses of halogenated ketones, since it was unlikely that they would be stable enough to withstand the standard epoxidation reaction conditions.

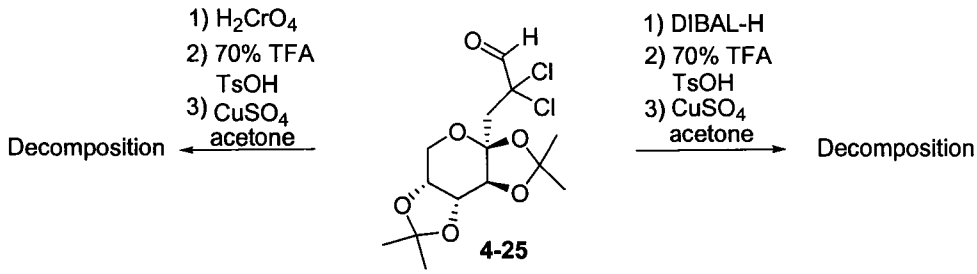

4-25

Scheme 4.8

With the synthesis of the halogenated ketones no longer being actively pursured, we began to investigate the synthesis of ketone **4-12**. The synthetic strategy for the preparation of ketone **4-12** was for aryl-M addition to fructose-derived aldehyde **4-14** followed by deoxygenation, cyclization, and oxidation to give the desired ketone product (Scheme 4.9). Initial efforts were directed at organolithium additions,[87] since it has been well documented that anisole can be deprotonated on the aromatic ring adjacent to the oxygen. Unfortunately, no reaction was observed under standard reaction conditions or at elevated temperature (Scheme 4.10).

[87] For examples of *ortho*-lithiation, see: Snieckus, V. *Chem. Rev,* **1990**, *90*, 879.

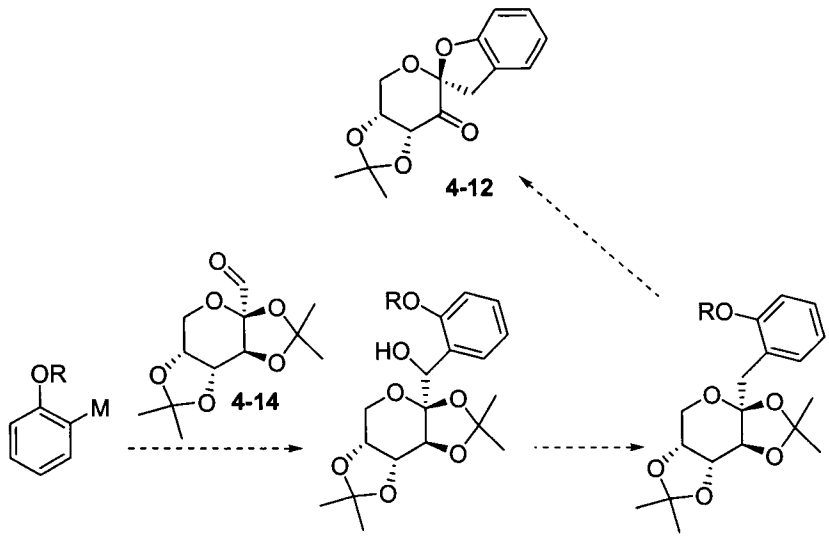

Scheme 4.9

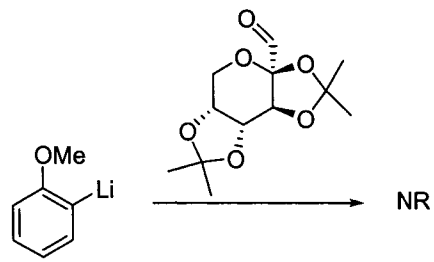

Scheme 4.10

Since organolithium additions to aldehydes did not appear to be promising, the focus of organometallic additions began to switch to Grignard reagents.[69] Subjecting aldehyde **4-14** to standard reaction conditions in ether from the Grignard reagent prepared from 2-bromoanisole and magnesium yielded no desired product (Scheme 4.11). It was thought that the activation barrier for the sterically crowded transition state could not be reached by heating in ether, so the solvent was switched to THF. The move proved fruitful, since excellent

conversion and yield of **4-26** was observed for the addition in the modified reaction conditions.

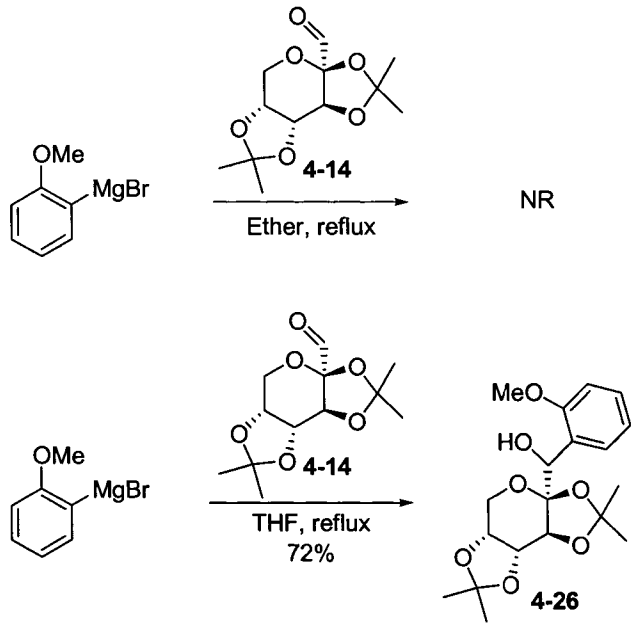

Scheme 4.11

Having finally enjoyed success with the Grignard addition, we began to turn our focus to deoxygenation. The Barton radical deoxygenation procedure was found to remove the oxygen very efficiently (Scheme 4.12).[82] Unfortunately, removal of the methyl group was found to be completely unselective.

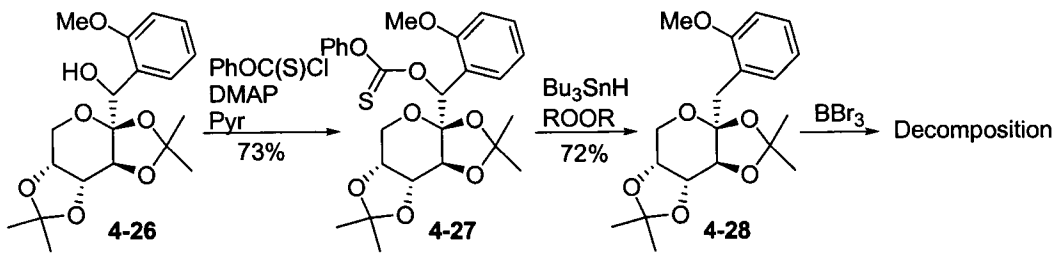

Scheme 4.12

Since the methyl group was difficult to remove, different protecting groups on the phenol that would be easier to remove were targeted (Scheme 4.13). Unfortunately, silyl-protected ethers, benzyl-protected ethers, and free phenols did not yield any addition products. Presumably, both the silyl and benzyl protected ethers are too sterically crowded for addition to aldehyde **4-14**. Given these setbacks, the synthesis of ketone **4-12** was suspended.

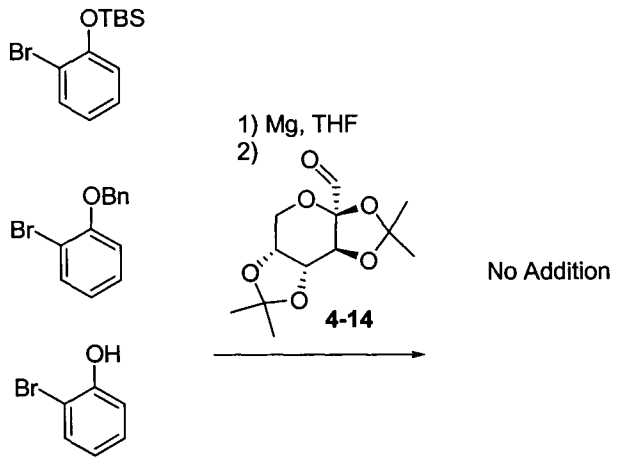

Scheme 4.13

4.B.2. Epoxidation Results and Transition State Analysis

The catalytic properties of the ketones were evaluated with *trans*-β-methylstyrene, *cis*-β-methylstyrene, phenylcyclohexene, and *trans*-stilbene. The epoxidation results are shown in Table 4.1. Method A uses MeCN-DMM (1:2) at pH 10.5-11.0, reaction conditions similar to those for ketone **1-16**.[58-66] Epoxidations with Methods B and C were carried out in DME-DMM (3:1), which is similar to the conditions for ketones **2-1** and **3-2**.[67] The reaction pH of Method

C is slightly lower than in Method B, since the different ketones have varying pH stability.

Table 4.1. Asymmetric Epoxidation of Olefins

Entry	Ketones	Method[a]	Conversion (ee)[e] (%) (config.)[f]			
			Ph–Me	Ph–Me	Ph	Ph–Ph
1	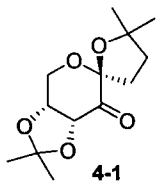 4-1	A	87 (93)[c]	88 (14)[c]	86 (96) (R,R)[c]	23 (97)[c]
2		B	69 (95)[g]	86 (33)[g]	92 (95) (R,R)[g]	
3	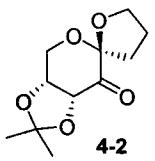 4-2	A	100 (74)[c]	100 (42)[c]	97 (33) (R,R)[c]	45 (96)[c]
4		B	98 (72)[g]	100 (61)	86 (29) (R,R)[g]	
5	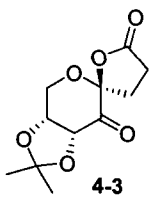 4-3	A	39 (65)[b]	58 (57)[b]	45 (17) (S,S)[b]	17(95)[b]
6		C	86 (67)[b]	100 (74)[b]	65 (16) (S,S)[b]	
7	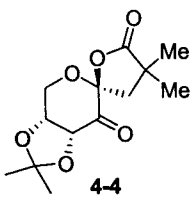 4-4	A	76 (83)	89 (70)[g]	89 (88) (R,R)	
8		C	52 (71)[g]	100 (80)[d]	85 (81) (R,R)[d]	
9	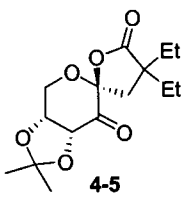 4-5	A	97 (78)	100 (67)	87 (84) (R,R)	
10		C	100 (77)	100 (81)	86 (86) (R,R)	

11 12	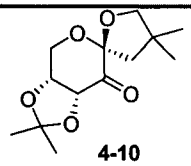 4-10	A B	76 (87) 94 (84)	100 (39) 100 (59)	100 (84) (R,R) 80 (92) (R,R)
13 14	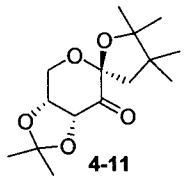 4-11	A B	21 (78) 41 (85)	32 (25) 59 (38)	39 (83) (R,R) 48 (92) (R,R)

[a] Method A: Reactions were carried out with olefin (0.10 mmol), ketone (0.03 mmol), Oxone (0.212 M, 0.65 mL), and K_2CO_3 (0.892 M, 0.65 mL), in CH_3CN/DMM (1:2 v/v) (1.5 mL) and buffer (0.1 M K_2CO_3-AcOH, pH 9.3) (1.0 mL) at 0 °C. The reactions were stopped after 1.5 h. Method B: Reactions were carried out with olefin (0.10 mmol), ketone (0.03 mmol), Oxone (0.212 M, 0.84 mL), and K_2CO_3 (0.892 M, 0.84 mL) in DME/DMM (3:1 v/v) (1.5 mL) and buffer (0.1 M K_2CO_3-AcOH, pH 9.3) (1.0 mL) at 0 °C. The reactions were stopped after 1.5 h. Method C: Reactions were carried out with olefin (0.10 mmol), ketone (0.015 mmol), Oxone (0.212 M, 0.84 mL), and K_2CO_3 (0.479 M, 0.84 mL) in DME/DMM (3:1 v/v) (1.5 mL) and buffer (0.1 M K_2CO_3-AcOH, pH 8) (1.0 mL) at 0 °C. The reactions were stopped after 3.5 h. [b] Reactions were carried out on 0.25 mmol (olefin) scale. [c] Reactions were carried out on 0.0625 mmol (olefin) scale. [d] Reactions carried out on a 0.125 mmol (olefin) scale [e] Enantioselectivity was determined by chiral GC (Chiraldex B-DM column). [f] The absolute configurations were determined by comparing the GC data with those observed for ketones **1** and **2**. For *trans*-β-methylstyrene, all epoxides have the (R,R) configuration. For *cis*-β-methylstyrene, all epoxides have the (1R,2S) configuration. For *trans*-stilbene, all epoxides have the (R,R) configuration. [g] Reaction carried out by Zackary Crane.

As shown in Table 4.1 (entries 1 and 2), the ee's obtained for *trans*-β-methylstyrene with ketone **4-1** were similar to those with ketone **1-16**,[58-66] suggesting that the simple replacement of the oxygen in ketone **1-16** with a carbon leads to no appreciable change in enantioselectivity (Figure 2.4, Figure 4.3). However, when the two methyl groups of ketone **4-1** were replaced by two hydrogens as in ketone **4-2** (Table 4.1, entries 3 and 4), the enantioselectivity decreased for *trans*-β-methylstyrene, indicating that transition state spiro **E**, became more competitive for ketone **4-2** (Figure 4.4). However, epoxidation of stilbene still proceeded with high ee. This is attributed to the fact that the phenyl substituent of stilbene is much larger than the corresponding methyl group of

trans-β-methylstyrene. The larger steric requirement of stilbene causes spiro transition state **E** to be disfavored due to steric repulsion. Consequently, ketone **4-2** gave comparable ee to ketone **4-1**.

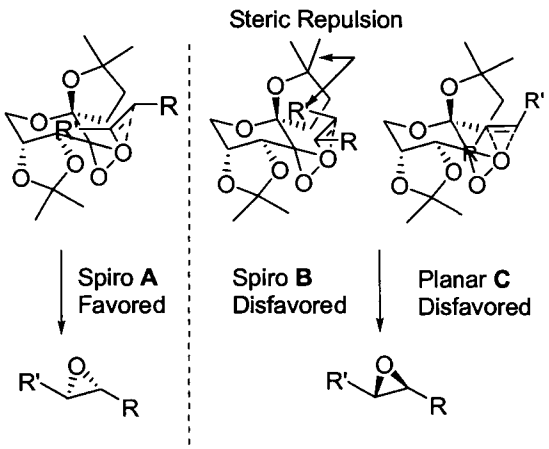

Figure 4.3 Transition state analysis for epoxidation of *trans*-olefins with **4-1**

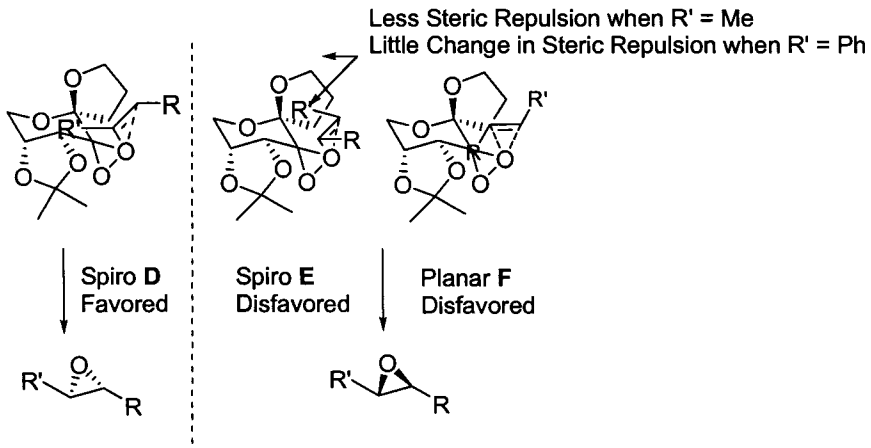

Figure 4.4 Transition state analysis for epoxidation of *trans*-olefins with **4-2**

Although the differing results of epoxidation of *trans*-olefins with ketones **4-1** and **4-2** are noteworthy, the interesting examples to check for this

type of ee erosion are those with a carbonyl present in the spiro ring of the catalyst, since the ketones (**2-1** and **3-2**) that give high ee for *cis*- and terminal olefins both contain this feature. Apparently, the carbonyl functionality in the spiro ring performs much like a methylene unit in terms of enantioselectivity (Table 4.1, entries 5,6). In other words, spiro transition state **H** can substantially compete with the major transition state spiro **G**, thus lowering the enantioselectivity (Figure 4.5). These results have large, but negative, implications for future catalyst design. One goal is to be able to prepare a single useful catalyst capable of epoxidizing a *trans*- and trisubstituted olefins by steric differentiation, while, at the same time, possessing the potential to epoxidize *cis*- and terminal olefins in high enantioselectivity by utilizing the aforementioned attraction. However, the carbonyl that is present on the best catalysts for attraction (**2-1**, **3-2**) doesn't possess the steric requirements necessary for obtaining high ee for a wide variety of *trans*- and trisubstituted olefins.

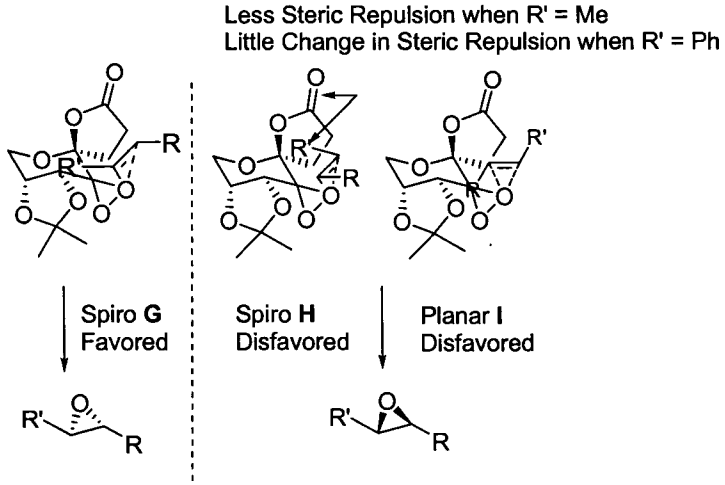

Figure 4.5 Transition state analysis for epoxidation of *trans*-olefins with **4-3**

Although the presence of a carbonyl in the spiro ring was found to lower ee for some *trans*-olefins, other findings created new hope for future catalyst design. Dialkyl substitution α- to the carbonyl, such as seen in ketones **4-4**, **4-5**, and **4-10,** actually causes the enantioselectivity of *trans*-β-methylstyrene to increase from the ketones bearing methylene substitution (**4-2**, **4-3**) α- to the carbonyl (Table 4.1, Entries 3-12). Apparently, substitution α- to the carbonyl causes planar transition state **L** to be relatively disfavored due to steric repulsion (Figure 4.6). This observation potentially has very large implications on future catalyst design. As was mentioned previously in great detail, planar transition states are quite often responsible for terminal olefins giving lower ee than their *cis*-counterparts. We have already demonstrated that electronic modification of the catalyst provides one way to reduce competition from planar transition states for terminal olefins, but this result suggests that steric interaction, namely disubstitution α- to the carbonyl, provides another potential avenue for planar transition state suppression that could be exploited in future catalyst design.

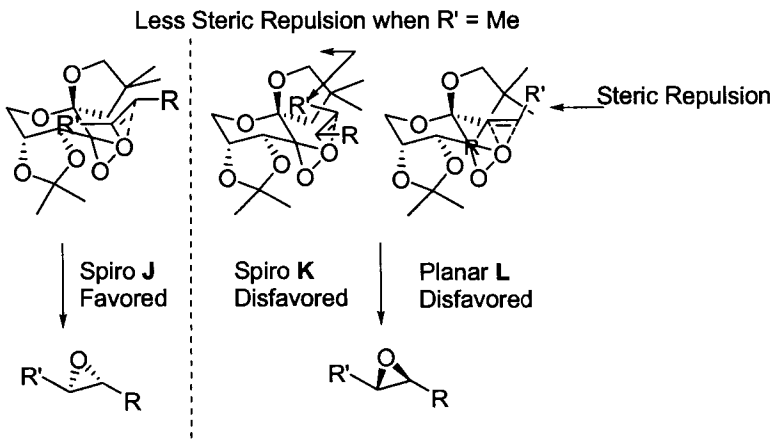

Figure 4.6 Transition state analysis for *trans*-olefin epoxidation with ketone **4-10**

Even though a fair amount of information was obtained during the epoxidation of *trans*-olefins, the most interesting results would involve testing the degree of attraction between the new catalysts and *cis*-olefins in the transition state. Ketone **4-3,** bearing the carbonyl functionality in the spiro ring, provides higher enantioselectivity for *cis*-β-methylstyrene when compared to the corresponding chiral ketone without a carbonyl group in its spiro ring (**4-2**) (Table 4.1). This suggests that the carbonyl group is at least partially responsible for the attraction between the phenyl group of the olefin and the spiro ring of the ketone catalysts (Figure 4.7). The reason for this observation is not well understood, but could be steric and/or electronic in nature. Furthermore, additional substitution α- to the carbonyl in ketones **4-4** and **4-5** resulted in an increase in enantioselectivity over a ketone (**4-3**) with a methylene group in the same location, presumably due to additional nonbonding interactions in the biphasic reaction mixture.

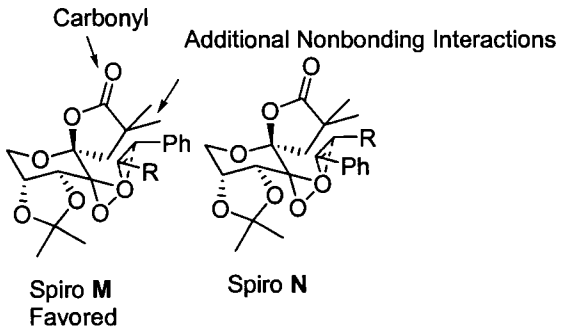

Figure 4.7 Epoxidation of *cis*-β-methylstyrene catalyzed with ketone **4-4**

The sensitivity of the electronic and steric effects on enantioselectivity can be well illustrated by the epoxidation results of phenylcyclohexene. Previously, it

was discussed that the attractive interaction between the phenyl group of phenylcyclohexene and the oxazolidinone moiety of ketones **2-1** and **3-2** could make a planar transition state compete with or even override the inherent bias of the spiro transition state (Figures 2.10, 3.7). The (S,S) epoxide obtained for 1-phenylcyclohexene (Table 4.1, entries 5,6) with ketone **4-3** shows the presence of an attraction between the phenyl group of the olefin and the spiro lactone of the ketone catalyst, thus enabling planar transition state **P** to overcome the inherent spiro bias of dioxirane mediated epoxidations. (Figure 4.8). However, the opposite enantiomer was obtained with ketones **4-4** and **4-5** (Table 1, entries 7-10). The reversal of the epoxide configuration could be due to the fact that the α-alkyl groups of the lactones of these two ketones sterically disfavor planar transition state **R** (Figure 4.9). Similar differences are also observed in ketones **4-2** and **4-10** which have different numbers of methyl groups, but no lactone in either case. These results along with the data obtained from *cis*- and *trans*-β-methylstyrene give an idea of the functionality requirements responsible for the good enantioselectivity for the different olefin classes.

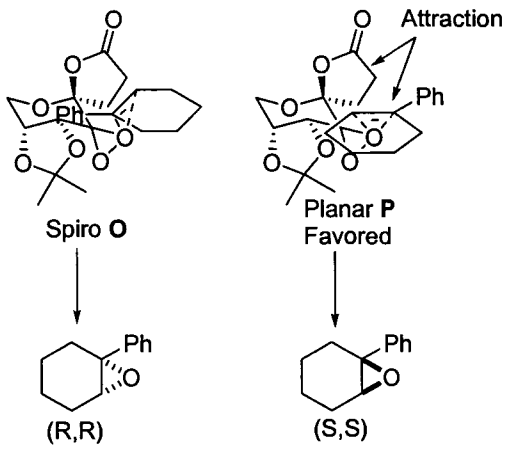

Figure 4.8 Epoxidation of phenylcyclohexene with ketone **4-3**

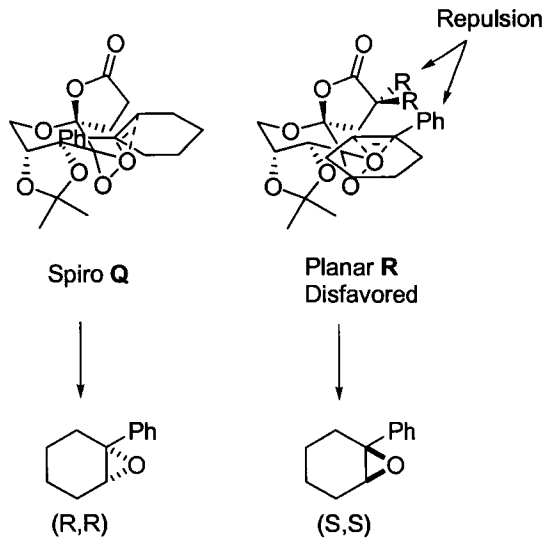

Figure 4.9 Epoxidation of phenylcyclohexene by ketones **4-4** and **4-5**

4.C. CONCLUSION

A number of chiral ketones with varying substitution patterns were targeted and prepared with the hope of probing the structural requirements for high enantioselectivity for different substrate classes. For *trans*-olefin epoxidation, lessening the steric bulk of the spiro ring leads to an erosion in enantioselectivity through undesired spiro transition states with ketones **4-2** and **4-3**. However, planar transition states can be suppressed by adding substitution to the ring in ketones **4-4**, **4-5**, and **4-10**, which could potentially play a role in the design of future catalysts for terminal olefin epoxidation. For the attraction to *cis*-olefins, a carbonyl present in the spiro ring (**4-3**, **4-4**, **4-5**, and **4-6**) was found to benefit the attraction. Additional substitution α- to the carbonyl also resulted in an ee increase, presumably due to the presence of nonbonding interactions. Phenylcyclohexene epoxidation with the different catalysts provided a nice

opportunity to see many of these factors present in the same substrate. Finally, despite all of the information obtained, no catalysts outperformed the original oxazolidinones (**2-1** and **3-2**) for any substrate classes, so the design of potentially useful catalysts for *cis*- and terminal olefin epoxidation would have to contain elements these studies found to be beneficial in the framework of the oxazolidinone.

4.D. EXPERIMENTAL

Aldehyde (4-14) (DLG-XIV-11) To a suspension of alcohol **4-13** (24 g, 92.2 mmol), PDC (38.2 g, 101.5 mmol) and 3A MS (82 g) in DCM (450 mL) was added HOAc (10 drops). Upon stirring at rt overnight, the reaction mixture was filtered through a pad of silica gel and washed with hexane:EtOAc (1:2). The filtrate was concentrated and dried on the high vacuum line to give the aldehyde as an off white solid which was used without further purification (16.8 g, 71%).

Olefin (4-15)[84] (ZDC-1-5-6, DLG-XIV-12) To a solution of aldehyde **4-14** (7.5 g, 29.0 mmol) in DCM (25 mL) at water bath temperature was added ethoxycarbonylmethylene phosphorane (13.1 g, 37.6 mmol) slowly. The reaction was allowed to stir at rt for 1 h. The solvent was then removed and the viscous oil was dissolved in ether, filtered and concentrated. The viscous oil was again dissolved in ether, filtered, and concentrated to remove Ph_3PO. The oil was then

dissolved in pentane: ether (5:1), allowed to stand for 1 h in the freezer, filtered, and concentrated to give the olefin (**4-15**) as a yellow oil (8.2 g, 86%).

Ester (4-16)[84] (ZDC-1-5-26, DLG-XIV-13) To a purged (3x, argon) solution of ester **4-15** (8.2 g, 25.0 mmol) in MeOH (20.0 mL) was added Pd / C (5%, 2.00 g), and the reaction was purged under argon (3x) followed by H_2 (3x) with a balloon. After stirring at rt for 40 h, the mixture was then filtered over a plug of celite, concentrated, and purified by flash chromatography (hexanes: ether, 3:2) to give **4-16** as a clear oil (6.0 g, 73%).

Ester (4-17) (ZDC-1-6-4, DLG-XIV-14) To a solution of N,N-diisopropylamine, (3.2 mL, 22.7 mmol) in THF (3.0 mL) at 0° C was added *n*-BuLi (13.3 mL, 21.3 mmol, 1.6 M in hexanes) slowly. This mixture was allowed to stir at 0°C for 45 min., and it was then cooled to -78°C. A solution of ester **4-16** (5.0 g, 15.1 mmol) in THF (8.0 mL) was added and the reaction was allowed to stir for 1 h at -78°C. A mixture of THF (3.3 mL), HMPA (2.3 mL, 12.7 mmol), and MeI (1.5 mL, 24.1 mmol) were added and was allowed to stir for 2 h at -78°C. The reaction was then warmed to rt and followed by GC. The reaction was then quenched with water, extracted (DCM) washed (brine), dried ($MgSO_4$), and concentrated. Repeating the entire process gave **4-17** as a white solid (3.8 g, 70%) after chromatography (2:3 ether : hexanes). mp 97-101°C; $[\alpha]^{25}_D$ = -7.19, (*c* 0.82, $CHCl_3$); IR (film) 1645 cm^{-1}; ^1H NMR (400 MHz, $CDCl_3$) δ 4.56 (dd, J = 6.1, 1.8 Hz, 1H), 4.18-4.08 (m, 3H), 3.99 (d, J = 2.1 Hz, 1H), 3.75 (dd, J = 9.7, 1.5 Hz, 1H), 3.61 (d, J =

9.7 Hz, 1H), 2.38 (d, J = 10.6 Hz, 1H), 1.84 (d, J = 10.6 Hz, 1H), 1.53 (s, 3H), 1.47 (s, 3H), 1.34 (s, 3H), 1.31 (s, 3H), 1.30 (s, 3H), 1.27 (s, 3H), 1.25 (t, J = 5.1 Hz, 3H); ^{13}C NMR (100 MHz, $CDCl_3$) δ 178.2, 109.2, 108.1, 103.8, 75.1, 70.9, 70.8, 60.9, 60.4, 51.0, 41.0, 27.6, 26.7, 26.5, 26.0, 25.1, 24.4, 14.4.

Alcohol (4-18) (DLG-XIV-15) To a solution of $LiAlH_4$ (0.8 g, 21.1 mmol) in THF (75 mL) at 0°C was slowly added a solution of ester **4-17** (3.8 g, 10.6 mmol) in THF (25 mL). The cold bath was removed and the reaction was allowed to stir at rt until complete as judged by TLC (hexanes: ether, 3:2). The reaction was then cooled to 0°C and diluted with ether (15 mL), quenched with water (3 mL), 15% NaOH (3 mL), and water (10 mL). The solution was vigorously stirred until the gray color gave way to an off-white color. The reaction was filtered over a glass frit and celite and concentrated to give **4-18** as a colorless oil (3.16 g, 94%) that was used without further purification. $[\alpha]^{25}_D$ = -4.9 (c .25, $CHCl_3$); IR (film) 3505 cm^{-1}; ^{1}H NMR (300 MHz, $CDCl_3$) δ 4.56 (dd, J = 8.0, 2.8 Hz, 1H), 4.19 (d, J = 8.0 Hz, 1H), 4.00 (d, J = 2.8 Hz, 1H), 3.79 (dd, J = 13.2, 1.8 Hz, 1H), 3.67 (d, J = 13.2 Hz, 1H), 3.46 (d, J = 11.2 Hz, 1H), 3.38 (d, J = 11.2 Hz, 1H), 3.12 (s, 1H), 2.04 (d, J = 14.8 Hz, 1H), 1.50-1.47 (m, 1H), 1.50 (s, 3H), 1.47 (s, 3H), 1.34 (s, 3H), 1.32 (s, 3H), 0.99 (s, 3H), 0.97 s, 3H); ^{13}C NMR (100 MHz, $CDCl_3$) δ 109.2, 108.4, 104.7, 75.6, 71.1, 70.9, 70.7, 61.0, 49.7, 36.4, 28.1, 27.0, 26.6, 26.1, 25.1, 24.4.

Alcohol (4-19) (DLG-XIV-22) Aqueous TFA (70%) (1.65 mL) was added to **4-18** (0.25 g, 0.79 mmol), and the mixture was allowed to stir overnight. The solvent was removed under vacuum at elevated temperatures. The viscous oil was loaded onto a column and flushed with EtOAc: MeOH (4:1). The column gave **4-19** as a red oil (0.27 g, quant). The product was taken on without further characterization or purification.

Alcohol (4-20) (DLG-XIV-23) To a solution of the above triol **4-19** (0.75 g, 3.4 mmol) in acetone (36 mL) at rt was added *p*-TsOH (0.06 g, 0.3 mmol) and $CuSO_4$ (1.2 g, 7.5 mmol). After stirring at rt for 50 h, solid K_2CO_3 (excess) was added until the pH of the reaction was made slightly basic. The reaction mixture was filtered over a plug of celite, concentrated, and purified by flash chromatography (hexanes:ether, 2:3) to give the alcohol (**4-20**) as a white solid (0.52 g, 59%). mp 110-115 °C; $[\alpha]^{25}_D$ = -110 (c 0.07, $CHCl_3$); IR (film) 3454 cm^{-1}; ^1H NMR (400 MHz, $CDCl_3$) δ 4.18 (dd, J = 6.0, 2.4 Hz, 1H), 4.11-4.06 (m, 1H), 4.01 (dd, J = 13.2, 2.4 Hz, 1H), 3.91 (d, J = 13.2 Hz, 1H), 3.67 (d, J = 8.4 Hz, 1H), 3.63-3.60 (m, 2H), 2.17-2.12 (m, 2H), 1.78 (d, J = 13.2 Hz, 1H), 1.53 (s, 3H), 1.36 (s, 3H), 1.16 (s, 3H), 1.10 (s, 3H); ^{13}C NMR (100 MHz, $CDCl_3$) δ 109.4, 108.7, 80.7, 78.1, 74.0, 72.3, 59.7, 48.7, 38.7, 28.5, 28.4, 27.1, 26.4.

Ketone (4-10) (DLG-XIV-28) To a suspension of alcohol **4-20** (0.52 g, 2.0 mmol), PDC (0.98 g, 2.6 mmol), and 3A MS (1.84 g) in DCM (17 mL) was added HOAc (2 drops). Upon stirring at rt overnight, the reaction mixture was filtered

through a pad of silica gel and washed with hexane: EtOAc (1/2). The filtrate was concentrated, dried, and purified by flash chromatography (hexanes:ether, 1:1) to give ketone **4-10** as a white solid (0.31 g, 60%). mp 124-127 °C; $[\alpha]^{25}_{D}$ = -102.7 (c 0.08, $CHCl_3$); IR (film) 1747 cm^{-1}; ^1H NMR (400 MHz,$CDCl_3$) δ 4.74 (d, J = 5.6 Hz, 1H), 4.51 (dd, J = 5.6, 0.8 Hz, 1H), 4.38 (dd, J = 13.6, 2.0 Hz, 1H), 4.02 (d, J = 13.6 Hz, 1H), 3.77 (d, J = 8.0 Hz, 1H), 3.64 (d, J = 8.0 Hz, 1H), 2.58 (d, J = 13.6 Hz, 1H), 1.69 (d, J = 13.6 Hz, 1H), 1.45 (s, 3H), 1.38 (s, 3H), 1.16 (s, 3H), 1.04 (s, 3H); ^{13}C NMR (100 MHz, $CDCl_3$) δ 198.3, 110.5, 108.9, 81.5, 78.5, 76.2, 59.5, 45.1, 39.1, 27.4, 27.1, 26.4, 26.1; HRMS calcd for $C_{13}H_{21}O_5$ (M+H) 257.1389, found 257.1387.

Alcohol (4-21) (DLG-XIV-38, DLG-XIV-39) To a solution of ester **4-17** (6.7 g, 18.7 mmol) in THF (100 mL) at 0 °C was added MeMgBr (26.2 mL, 3 M in ether) slowly. The reaction was stirred at rt overnight. The reaction was then cooled to 0°C and was slowly diluted with water. The mixture was extracted with EtOAc, washed (satd NH_4Cl), washed (brine), dried ($MgSO_4$), filtered, concentrated, and purified by flash chromatography (hexanes:EtOAc, 1:1). A solution of aqueous TFA (70%) (28 mL) was then added at rt and allowed to stir overnight. The solvent was removed under vacuum at elevated temperatures. The viscous oil was loaded onto a column and flushed with EtOAc:MeOH (1:0 to 4:1). The column gave **4-21** as an oil (0.65 g, 14%) that was taken on without further characterization or purification.

Alcohol (4-22) (DLG-XIV-40)[82] To a solution of the triol **4-21** (0.65 g, 2.6 mmol) in acetone (26 mL) at rt was added *p*-TsOH (0.03 g, 0.2 mmol) and $CuSO_4$ (0.81 g, 5.1 mmol). After stirring at rt for 50 h, solid K_2CO_3 (excess) was added until the pH of the reaction was made slightly basic. The reaction mixture was filtered over celite, concentrated, and purified by flash chromatography (hexanes: ether, 2:3) to give the alcohol (**4-22**) as a white solid (0.62 g, 83%). mp 62-64 °C; $[\alpha]^{25}_D$ = -57.1 (c 0.07, $CHCl_3$); IR (film) 3466 cm^{-1}; ^1H NMR (400 MHz, $CDCl_3$) δ 4.18-4.14 (m, 1H), 4.12-4.00 (m, 2H), 3.85 (d, J = 13.2 Hz, 1H), 3.62-3.55 (m, 1H), 2.27 (d, J = 13.6 Hz, 1H), 2.04 (s, 1H), 1.96 (d, J = 13.6 Hz, 1H), 1.52 (s, 3H), 1.35 (s, 3H), 1.25 (s, 3H), 1.13 (s, 3H), 1.06 (s, 3H), 0.97 (s, 3H); ^{13}C NMR (100 MHz, $CDCl_3$) δ 109.3, 105.0, 88.0, 77.6, 73.6, 72.5, 60.2, 50.0, 42.7, 28.1, 26.1, 25.4, 25.1, 25.1, 24.9.

Ketone (4-11) (DLG-XIV-45)[82] To a suspension of alcohol **4-22** (0.20 g, 20.7 mmol), PDC (0.34 g 0.91 mmol) and 3A MS (0.68 g) in DCM (6 mL) was added HOAc (1 drop). Upon stirring at rt overnight, the reaction mixture was filtered through a pad of silica gel and washed with hexane:EtOAc (1:2). The filtrate was concentrated, dried, purified by flash chromatography (hexane:ether, 1:1), and recrystallized (EtOAc:hexane) to give ketone **4-11** as an off-white solid (0.18 g, 90%). mp 45-47 °C; $[\alpha]^{25}_D$ = -126.2 (c 15, $CHCl_3$); IR (film) 1749 cm^{-1}; ^1H NMR (400 MHz, $CDCl_3$) δ 4.78 (d, J = 5.2 Hz, 1H), 4.50-4.46 (m, 2H), 4.44 (dd, J = 13.2, 2.4 Hz, 1H), 4.01 (d, J = 13.2 Hz, 1H), 2.76 (d, J = 14.0 Hz, 1H), 1.85 (d, J = 14.0 Hz, 1H), 1.45 (s, 3H), 1.38 (s, 3H), 1.26 (s, 3H), 1.07 (s, 3H), 1.03 (s, 3H),

0.89 (s, 3H); ^{13}C NMR (100 MHz, $CDCl_3$) δ 198.5, 110.3, 105.7, 89.8, 78.7, 76.2, 59.7, 44.9, 43.1, 27.5, 26.4, 24.7, 24.7, 24.0, 23.8; HRMS calcd for $C_{15}H_{25}O_5$ (M+H) 285.1702, found 285.1709.

Aldehyde (4-24) (DLG-XIV-15, DLG-XIV-16) To a solution of $LiAlH_4$ (3.7 g, 97 mmol) in THF (370 mL) at 0°C was slowly added a solution of ester **4-17** (16.1 g, 48.7 mmol) in THF (120 mL). The cold bath was removed and the reaction was allowed to stir at rt until complete as judged by TLC (hexane:ether, 3:2). The reaction was then cooled to 0°C and was diluted with ether (60 mL), quenched with water (12 mL), 15% NaOH (12 mL), and water (30 mL). The solution was vigorously stirred until the gray color gave way to an off-white color. The reaction was filtered over a glass frit and celite and concentrated. DCM (135 mL) was added, followed by PDC (17.1 g, 45.4 mmol), 3A MS (37 g), and finally HOAc (5 drops). Upon stirring at rt overnight, the reaction mixture was filtered through a pad of silica gel and washed with hexane:EtOAc (1:2). The filtrate was concentrated and dried on the high vacuum line to give aldehyde **4-24** (6.2 g, 44% over 2 steps) as a clear oil which was used without further purification.

Aldehyde (4-25) (DLG-XV-36)[82] To a solution of aldehyde **4-24** (2.0 g, 7.0 mmol) in DCM (10 mL) was added *t*-butylamine (1.10 mL, 10.5 mmol) and Na_2SO_4 (8.0 g). After stirring for 1 h, additional *t*-butylamine (0.2 mL, 1.9 mmol) was added. After stirriring for 3 h at rt, the mixture was filtered and washed with 10 mL of DCM. After cooling to 0°C, NCS (2.24 g, 16.8 mmol) was added, and

the mixture was allowed to warm to rt and stir overnight. The mixture was then filtered through celite, washed (DCM), and concentrated. The crude product was then taken up in DCM (10 mL) and 10% HCl (10 mL) and allowed to stir overnight. After separating the layers, the product was extracted with DCM (3X), washed (satd $Na_2S_2O_5$), dried (Na_2SO_4), concentrated, and purified by column chromatography to give **4-25** as a white solid (3.3 g, quant). mp 34-38°C; $[\alpha]^{25}_D$ = -17.3 (c .10, $CHCl_3$); IR (film) 2938, 1752 cm^{-1}; ^1H NMR (400 MHz, $CDCl_3$) δ 9.25 (s, 1H), 4.57 (dd, J = 8.0, 2.4 Hz, 1H), 4.16 (d, J = 8.0 Hz, 1H), 4.09 (d, J = 2.4 Hz, 1H), 3.76 (d, J = 12.8 Hz, 1H), 3.68 (d, J = 12.8 Hz, 1H), 3.21 (d, J = 14.8 Hz, 1H), 2.84 (d, J = 14.8 Hz, 1H), 1.50 (s, 3H), 1.48 (s, 3H), 1.37 (s, 3H), 1.32 (s, 3H); ^{13}C NMR (100 MHz, $CDCl_3$) δ 185.0, 109.6, 109.3, 101.3, 85.6, 73.8, 70.3, 70.2, 61.6, 54.4, 26.6, 26.1, 24.9, 24.1. HRMS calcd for $C_{14}H_{21}O_6Cl_2$ (M+H) 355.0715, found 355.0713.

Alcohol (4-26) (DLG-XV-17) To a flame dried flask equipped with a stir bar and a reflux condenser magnesium powder (3.6 g) was added and allowed to stir for 15 min. under argon. Following the addition of 75 mL of THF, 2-bromoanisole (27.5 g, 147.2 mmol in 44 mL THF) was added dropwise and allowed to stir at rt for 30 min. following cessation of bubbling. Aldehyde **4-14** (15.2 g, 58.9 mol in 66 mL of THF) was added dropwise, and the reaction mixture was heated to reflux while stirring for 3 h. After cooling to rt, satd. NH_4Cl was added dropwise and allowed to stir for 10 min. Then the organics were removed, and the solid residue was washed with ether (5x). Then the solvent was removed to afford

alcohol **4-26** as a yellow oil (15.5 g, 72 %) that was used without further purification.

Thiocarbonate (4-27) (DLG-XV-18) To a solution of alcohol **4-26** (15.5 g, 42.3 mmol) in DCM (250 mL) was added pyridine (14 mL, 169.2 mmol), then DMAP (0.15 g, 1.2 mmol), followed by PhOC(S)Cl (slowly over 20 min.) (9.5 g, 55.0 mmol), and the reaction mixture was allowed to stir overnight under argon until TLC showed the reaction was complete. The mixture was then poured into satd. NH_4Cl solution and then diluted with additional DCM. Next, the aqueous layer was washed with additional DCM (3x), and the combined organics were then washed (brine), dried ($MgSO_4$), and finally concentrated to give a reddish sludge. The sludge was vacuum filtered through silica gel with a EtOAc:hexane (1:6), and the resulting filtrate was concentrated to give a yellow solid. This yellow solid was then recrystallized in EtOAc: hexane to give the thiocarbonate (**4-27**) as a yellow solid (15.5 g, 30.9 mmol, 73%) that was used without further purification.

Ether (4-28) (DLG-XV-19)[82] To a solution of thiocarbonate **4-27** (15.5 g, 30.9 mmol) and $HSnBu_3$ (13.5 g, 46.4 mmol) in toluene (500 mL) was added *t*-butylperoxide (1.2 mL, 6.1 mmol), and the mixture was heated to reflux for 2 h under argon. After cooling to rt, the clear reaction mixture was concentrated and diluted with ether. The organics were washed with 1N NaOH, water, and brine. Filtration over Na_2SO_4 and concentration led to a crude product, which was then subjected to column chromatography (hexane: EtOAc, 0:1 to 1:1) to give **4-28** as

a clear oil (7.8 g, 72%). $[\alpha]^{25}_{D}$ = -24.5 (c .93, $CHCl_3$); IR (film) 1250 cm^{-1}; ^1H NMR (400 MHz, $CDCl_3$) δ 7.30 (dd, J = 7.2, 1.6 Hz, 1H), 7.25-7.17 (m, 1H), 6.95-6.83 (m, 2H), 4.57 (dd, J = 8.0, 2.4 Hz, 1H), 4.28 (d, J = 2.4 Hz, 1H), 4.21 (d, J = 8.0 Hz, 1H), 3.88 (dd, J = 13.2, 2.0 Hz, 1H), 3.81 (s, 3H), 3.73 (d, J = 13.2 Hz, 1H), 3.30 (d, J = 14.0 Hz, 1H), 3.12 (d, J = 14.0 Hz, 1H), 1.47 (s, 3H), 1.46 (s, 3H), 1.35 (s, 3H), 0.91 (s, 3H); ^{13}C NMR (100 MHz, $CDCl_3$) δ 158.5, 133.7, 128.2, 124.3, 120.3, 110.8, 109.1, 107.8, 104.3, 72.3, 71.1, 70.8, 61.4, 55.6, 38.6, 26.7, 26.0, 24.9, 24.3. HRMS calcd for $C_{19}H_{26}O_6$ (M+) 350.1729, found 350.1724.

Representative Asymmetric Epoxidation Procedure (Table 4.1, Entry 11, Method A). To a solution of *trans*-β-methylstyrene (0.012 g, 0.1 mmol) and ketone **4-10** (0.008 g, 0.03 mmol) in MeCN/DMM (1:2) (1.5 mL) were added buffer (0.1 M K_2CO_3-AcOH in 4 x 10^{-4} M aqueous EDTA, pH 9.3) (1.0 mL) and TBAHS (0.001 g, 0.003 mmol) with stirring. After the mixture was cooled to 0°C (bath temperature), a solution of oxone (0.212 M in 4 x 10^{-4} M aqueous EDTA) (0.65 mL) and a solution of K_2CO_3 (0.892 x 10^{-4} M aqueous EDTA) (0.65 mL) were added dropwise separately via syringe pump over a period of 1.5 h. The reaction mixture was quenched by addition of pentane and extracted with pentane. The combined organic layers were dried (Na_2SO_4), filtered, and concentrated. The resulting mixture was analyzed by GC to determine the conversion and enantiomeric excess.

Representative Asymmetric Epoxidation Procedure (Table 4.1, Entry 4, Method B). To a solution of *cis*-β-methylstyrene (0.012 g, 0.1 mmol) and ketone **4-2** (0.007 g, 0.03 mmol) in DME/DMM (3:1) (1.5 mL) were added buffer (0.2 M K_2CO_3-AcOH in 4 x 10^{-4} M aqueous EDTA, pH 9.3) (1.0 mL) and TBAHS(0.001 g, 0.003 mmol) with stirring. After the mixture was cooled to 0°C (bath temperature), a solution of oxone (0.212 M in 4 x 10^{-4} M aqueous EDTA) (0.84 mL) and a solution of K_2CO_3 (0.479 M x 10^{-4} M aqueous EDTA) (0.84 mL) were added dropwise separately over a period of 1.5 h via syringe pump. The reaction mixture was quenched by addition of pentane and extracted with pentane. The combined organic layers were dried (Na_2SO_4), filtered, and concentrated. The resulting mixture was analyzed by GC to determine the conversion and enantiomeric excess.

Representative Asymmetric Epoxidation Procedure (Table 1, Entry 10, Method C). To a solution of *cis*-β-methylstyrene (0.012 g, 0.1 mmol) and ketone **4-5** (0.0045 g, 0.015 mmol) in DME/DMM (3:1) (1.5 mL) were added buffer (0.2 M K_2CO_3-AcOH in 4 x 10^{-4} M aqueous EDTA, pH 8.0) (1.0 mL) and TBAHS (0.001 g, 0.003 mmol) with stirring. After the mixture was cooled to 0°C (bath temperature), a solution of oxone (0.212 M in 4 x 10^{-4} M aqueous EDTA) (0.84 mL) and a solution of K_2CO_3 (0.479 M x 10^{-4} M aqueous EDTA) (0.84 mL) were added dropwise separately over a period of 3.5 h via syringe pump. The reaction mixture was quenched by addition of pentane and extracted with pentane. The combined organic layers were dried (Na_2SO_4), filtered, and concentrated. The

resulting mixture was analyzed by GC to determine the conversion and enantiomeric excess.

CHAPTER FIVE

ANILINE-DERIVED OXAZOLIDINONE CATALYSTS

5.A. INTRODUCTION

Even though the previously discussed ketones **2-1** and **3-2** increased the substrate scope of asymmetric epoxidation, the synthesis of both ketones is nontrivial, which undoubtedly will limit their use in synthesis (Figure 5.1, Schemes 2.3, 3.2). However, results obtained with **2-1** and **3-2** suggest that if a readily available catalyst can be found to perform in a similar manner in terms of reactivity and selectivity, then a number of new oxirane classes could be easily prepared by asymmetric epoxidation. Consequently, spiro ring substitution patterns were varied for a number of ketones to better understand the structural and electronic requirements of the spiro ring to achieve high enantioselectivity for *cis*- and terminal olefins (Figure 4.2). Those studies showed that a carbonyl in the spiro ring of the catalyst as well as the presence of additional nonbonding interactions adjacent to the carbonyl are necessary to maximize the interaction between the catalyst and substrate, and most importantly, the attraction was the strongest for the oxazolidinone case (Figure 4.7). With this information in mind,

we began to think about designing new, practical ketone catalysts able to take advantage of information gained in earlier studies.

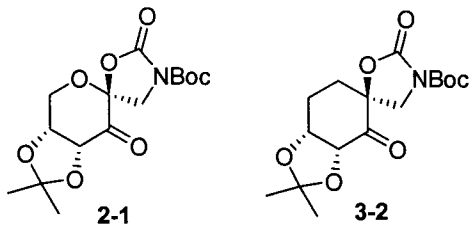

2-1 3-2

Figure 5.1 Chiral ketone catalysts

One catalyst class in particular that attracted our attention was aniline-containing oxazolidinones (Figure 5.2). These catalysts have all of the features that we thought would be necessary for a potentially useful catalyst. First and foremost, the potential to prepare them very quickly is possible, since anilines can be introduced directly into sugars, unlike the Boc protected amine. Moreover, the oxazolidinone found to give the best attraction is also present. Finally, the additional nonbonding interactions for aniline-containing oxazolidinones are particularly attractive, since not only can hydrophobic interactions be at work in these cases, but also additional π-π interactions.

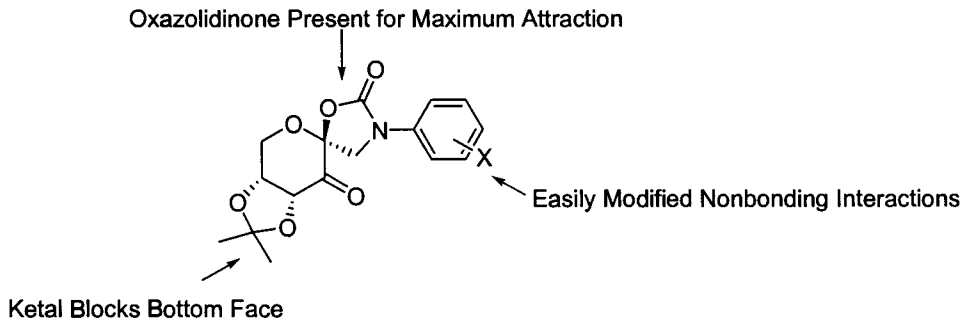

Figure 5.2 Structural features of aniline-containing oxazolidinones

Lianhue Shu prepared the *p*-toluidine-derived oxazolidinone catalyst (**5-1**), and encouraging ee was observed for *cis*-β-methylstyrene (Scheme 5.1).[88] Consequently, a number of other aniline-derived ketones with varying structural and electronic factors were targeted with the hope of maximizing the attraction between the substrate and the catalyst in the transition state (Figure 5.3).

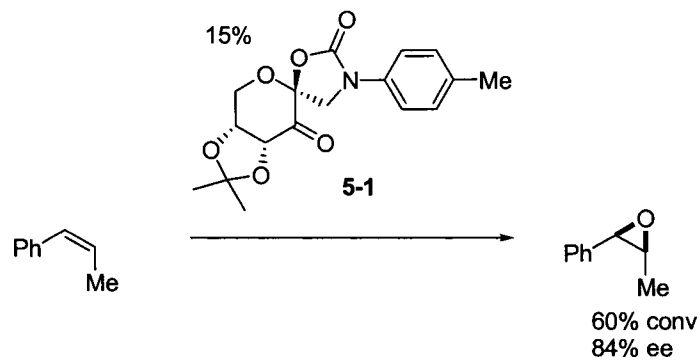

Scheme 5.1

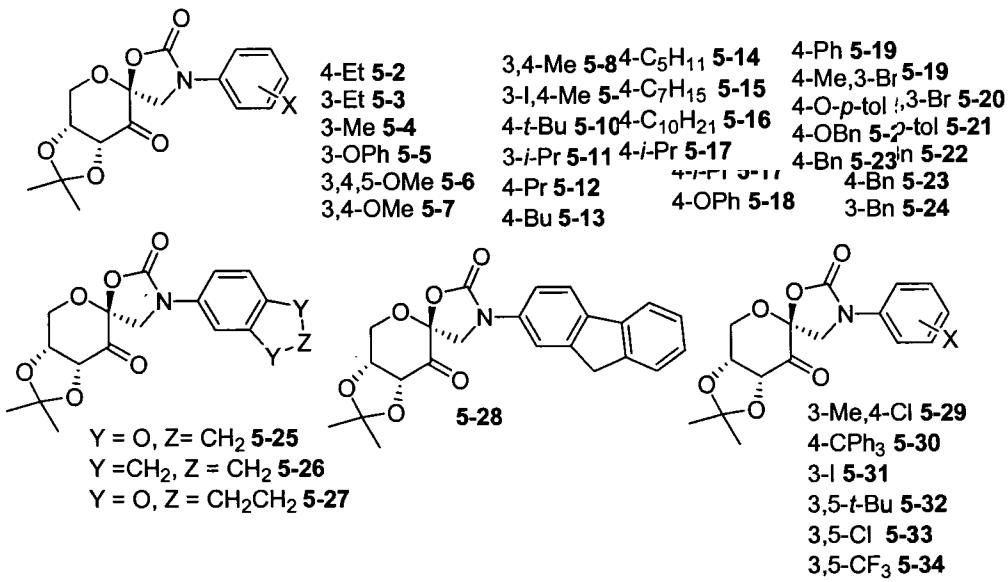

Figure 5.3 Targeted aniline-containing oxazolidinones

[88] Shu, L.; Wang, P.; Gan, Y.; Shi, Y. *Org. Lett.* **2003**, *5*, 293

5.B. RESULTS AND DISCUSSION

5.B.1. Ketone Synthesis

Since all of the targeted ketones are very similar, we decided to prepare them from a common route.[88] Working alongside Lianhue Shu, Yi Yuan and Bin Wang, Amadori rearrangement of the substituted anilines and D-glucose, followed by ketalization, phosgene cyclization, and PDC oxidation was found to efficiently give ketones **5-2** - **5-28** in good yield (Scheme 5.2).

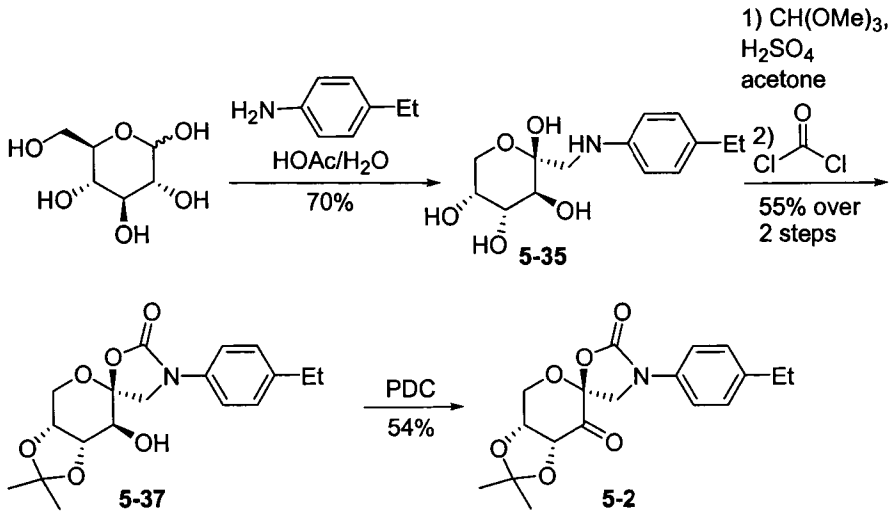

Scheme 5.2

Although this four step sequence was efficient for the synthesis of the vast majority of ketones, a handful of desired catalysts couldn't be prepared by this standard pathway. Amadori rearrangement of D-glucose and anilines **5-38** and **5-39** to give ketones **5-30** and **5-32** was unsuccessful, so the synthesis of those ketones was abandoned (Scheme 5.3).

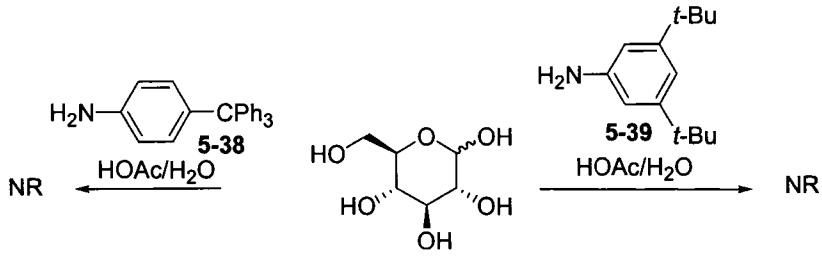

Scheme 5.3

The Amadori rearrangement of D-glucose and the electron-poor anilines, such as **5-40** and **5-41**, was found to proceed efficiently,[89] but the subsequent ketalization step only resulted in decomposition (Scheme 5.4). A few approaches can be envisioned that tackle this problem. One possible solution involves switching the order of operations in the sequence (Scheme 5.5). Treatment with phosgene first would then make the acid-catalyzed elimination more difficult, hopefully allowing us to synthesize ketones containing electron withdrawing groups on the aniline ring. Cyclization with phosgene itself, phosgene/$NaHCO_3$, as well as triphosgene gave no desired products, so it was decided that switching the order of operations might not be productive.

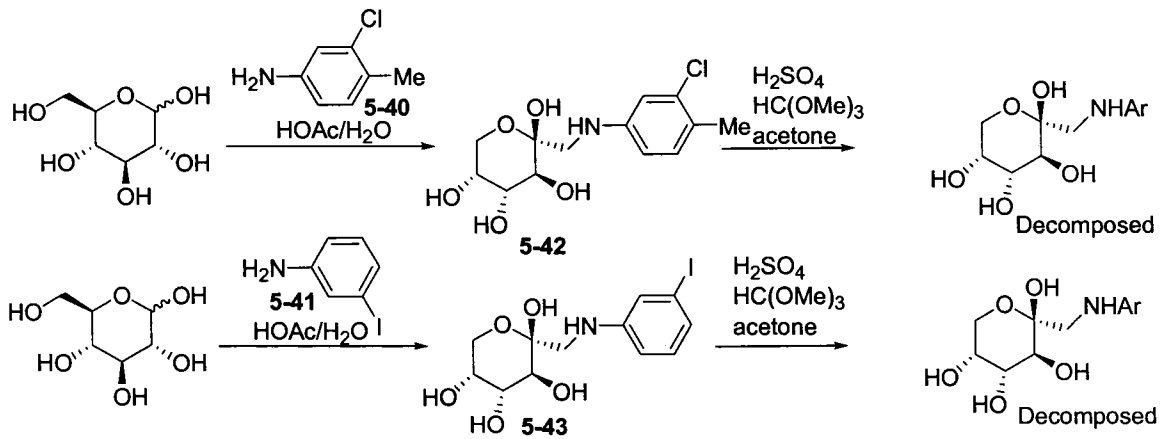

Scheme 5.4

[89] Amadori rearrangement products are taken on without characterization.

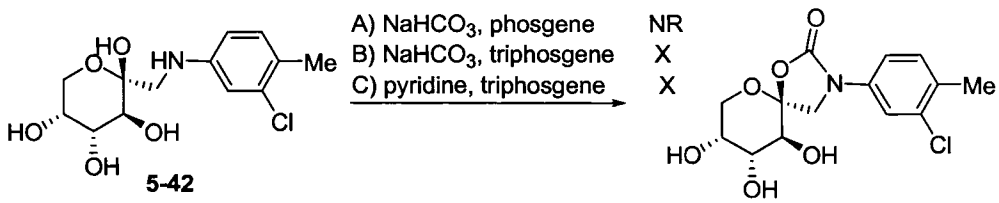

Scheme 5.5

Another approach to solving the elimination problem could be to lower the amount of acid present in solution. Varying the concentration of proton in solution had little effect on the reaction itself, since decomposition was observed in both cases (Scheme 5.6). Since varying the amount of H_2SO_4 was found to be unsuccessful, several protection conditions were attempted on three ketones that were susceptible to acid catalyzed decomposition (Table 5.1). Unfortunately, none of the conditions were able to successfully protect the diol. As a result, the syntheses of ketones that fell victim to this sort of elimination were abandoned.

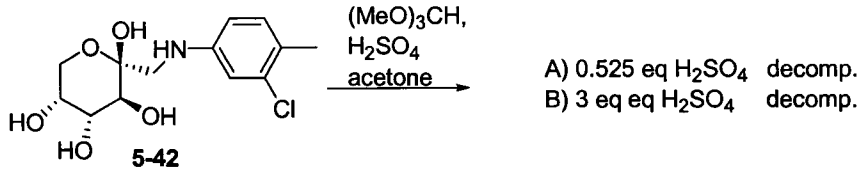

Scheme 5.6

Table 5.1. Attempted Ketalization of **5-4**[a]

5-43

Entry	Reaction Conditions	Result
1	1.2 eq. 2,2-DMP DMF	Decomposition
2	Excess $CuSO_4$ Cat. H_2SO_4 Acetone	Decomposition
3	1.7 eq. $CuSO_4$ Acetone	Decomposition
4	Cat. PTS Acetone	Decomposition
5	2,2-DMP Cat. PTS Acetone	Decomposition
6	2,2-DMP 1.2 Eq. PTS $HC(OMe)_3$	Decomposition
7	1.2 eq. 2,2-DMP Cat. PTS DMF	Decomposition
8	2,2-DMP 1.2 Eq. PTS Acetone	Decomposition
9	3 eq. 2,2-DMP Cat. PTS DMF	Decomposition

a All reactions carried out over 3 days with the conditions given. Reaction progress was monitored by TLC

5.B.2. Epoxidation of Styrenes

Since styrene oxides have been our main focal point of previous epoxidation studies, we first set out to probe the epoxidation of styrenes with these new ketone catalysts. In order to achieve the best results for styrene with the newly prepared ketones, solvent effects on enantioselectivity had to be explored (Table 5.2). For solutions made of DME:DMM mixtures, both conversion and enantioselectivity rapidly decreased as the ratio of DME:DMM decreased (Table 5.2). This suggests that the attraction between the substrate and the oxazolidinone portion of the catalyst is greatest when using DME as solvent (Table 5.2, Entry 1). Interestingly, dioxane was also found to perform quite well, providing another solvent alternative (Table 5.2, Entry 9).

After optimizing reaction conditions, asymmetric epoxidations were performed on styrene with the newly synthesized ketones (Table 5.3). Our studies showed that the *N*-substituents of the ketones have significant effects on the enantioselectivity of styrene epoxidation, with the ee varying from 55% to 87% using 15 mol% ketone catalyst in DME (Table 5.3). Generally speaking, aniline substitution with hydrocarbons consistently shows higher ee than substitution with ethers or halogens. Even though ketone **5-11** was found to give the absolute best enantioselectivity for styrene epoxidation, ketone **5-2** was deemed the most promising candidate, since the starting material used to prepare **5-2**, 4-ethylaniline, is relatively inexpensive ($ 0.21/ g). The low costs of glucose and the aniline precursor to ketone **5-2** as well as the catalyst's (**5-2**) good

performance for the epoxidation of styrene caused us to focus on **5-2** for the remaining epoxidation studies with styrene.

Table 5.2. Solvent Studies for Styrene Epoxidation

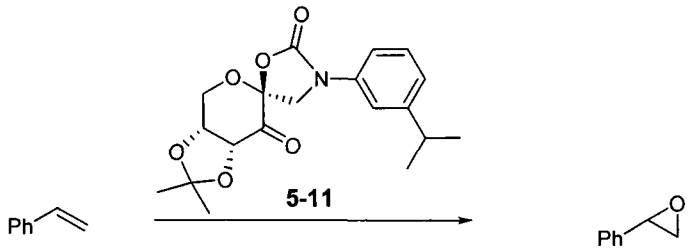

Entry	Solvent	Conv (%)	ee (%) [b]
1	DME	100	87
2	DMM:DME (1:5)	100	84
3	DMM:DME (1:3)	100	84
4	DMM:DME (1:1)	63	82
5	DMM:DME (3:1)	35	Nd
6	DMM	19	Nd
7	MeCN	5	Nd
8	EtCN	0	-
9	Dioxane	100	83
10	DMF	57	75
11	Water:DME (2:1)	20	Nd

[a] Reactions were carried out with olefin (0.10 mmol), ketone **5-11** (0.015 mmol), TBAHS (0.015 mmol), Oxone (0.212 M, 0.84 mL), and K_2CO_3 (0.479 M, 0.84 mL), in solvent (1.5 mL) and buffer (0.2 M K_2CO_3-AcOH, pH 8.0) (1.0 mL) at -10 °C (NaCl-ice bath). The reactions were stopped after 3.5 h. [b] The conversion and ee were determined by chiral GC (Chiraldex B-DM).

Table 5.3. Catalyst Screening on Styrene Epoxidation

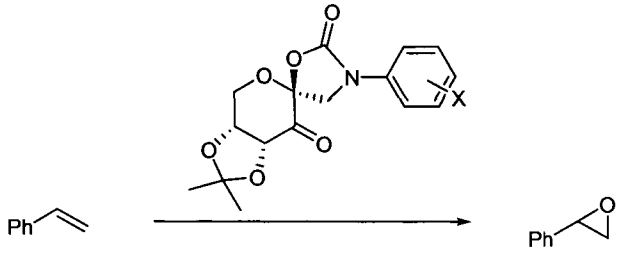

Entry	Ketone	Conv.,[b] (ee)(%)	Entry	Ketone	Conv.,[b] (ee)(%)
1	**5-1**	100 (84)	15	**5-15**	95 (85)
2	**5-2**	100 (87)	16	**5-16**	79 (83)
3	**5-3**	97 (84)	17	**5-17**	100 (84)
4	**5-4**	100 (83)	18	**5-18**	89 (85)
5	**5-5**	100 (79)	19	**5-19**	100 (86)
6	**5-6**	98 (69)	20	**5-20**	49 (78)
7	**5-7**	77 (70)	21	**5-21**	100 (81)
8	**5-8**	100 (81)	22	**5-22**	79 (75)
9	**5-9**	52 (55)	23	**5-23**	100 (78)
10	**5-10**	100 (86)	24	**5-24**	100 (80)
11	**5-11**	100 (87)	25	**5-25**	78 (78)
12	**5-12**	100 (84)	26	**5-26**	87 (84)
13	**5-13**	99 (84)	27	**5-27**	89 (79)
14	**5-14**	100 (82)	29	**5-28**	100 (86)

[a] All reactions were carried out with olefin (0.10 mmol), ketone (0.015 mmol), Oxone (0.212 M, 0.84 mL), and K_2CO_3 (0.48 M, 0.84 mL), TBAHS (0.015 mmol) in DME (1.5 mL), and buffer (0.1 M K_2CO_3-AcOH, pH 8.0) (1.0 mL) at -10 °C (bath temperature) (NaCl-ice bath) for 3.5 h. [b] The conversion and ee were determined by chiral GC (Chiraldex B-DM).

The ee obtained with ketone **5-2** for styrene encouraged us to extend the epoxidation to other styrenes. As shown in Table 5.4, up to 92% ee was obtained with the observed enantioselectivity being dependent on the phenyl group substituents of the olefins. Our earlier studies suggest that the asymmetric induction for ketone **5-2** is likely due to an attraction between the aryl group of the olefin and the oxazolidinone moiety of the ketone catalyst in the transition state. For styrenes, spiro **A** is likely to be the favored transition state with spiro **B** and planar **C** being competing transition states (Figure 5.4). For *ortho*-substituted styrenes (Table 5.4, entry 2), observed enantioselectivity is lower than styrene itself, presumably due to unfavorable steric interactions between the substituents on the styrene and the oxazolidinone moiety of the catalyst for spiro transition state **A**. For *meta*-substituted styrenes (Table 5.4, entries 8-11), certain substitutents on the phenyl group of the olefin appear to further favor spiro **A**, resulting in an increase in overall ee. For *para*-substituted styrenes (Table 5.4, entries 3-7), certain substituents do not significantly affect the competition of the transition states, thus giving ee similar to styrene itself. However, electron deficient olefins give higher ee than their more electron-rich counterparts, presumably due to enhanced secondary orbital interactions further favoring spiro transition states.[11] Styrenes bearing multiple substituents give ee's that are consistent with the various electronic and structural patterns of the simpler monosubstituted styrenes. For relatively insoluble or unreactive substrates, adding dioxane to the reaction mixture was found to substantially improve

conversion, which is an observation that has since been capitalized on many occasions (Table 5.4, Entry 13).

Table 5.4. Asymmetric Epoxidation of Styrenes with Ketone **5-2**[a]

Entry	Substrate	Yield[b] (Conv.[c]) (%)	ee (%)	Config.[h]
1[i,m]	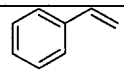	72 (100)	86[d]	(-)-(R)[75]
2[j,m]	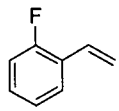	89 (95)	80[d]	(-)[76]
3[j,m]	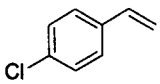	85 (100)	86[d]	(-)-(R)[75]
4[j,m]	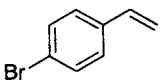	71 (99)	87[d]	(-)-(R)[78]
5[k,n]	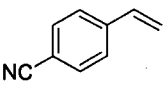	86 (100)	90[d]	(-)-(R)[78]
6[l,n]	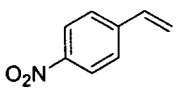	73 (99)	90[d]	(-)-(R)[78]
7[l,n]	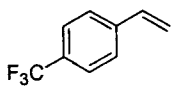	73 (100)	92[d]	(-)[79]
8[k,n,p]	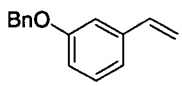	66 (79)	87[e]	(-)
9[i,m]	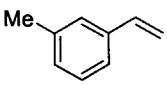	87 (100)	90[d]	(-)
10[k,n]	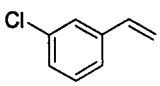	72 (100)	86[f]	(-)[75]
11[k,n]	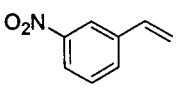	77 (100)	88[f]	(-)[90]
12[k,o]	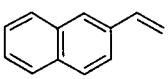	91 (100)	87[g]	(-)-(R)[91]
13[k,n]	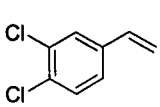	75 (95)	92[d]	(-)[91]

[90] Collman, J.P.; Wang, Z.; Straumanis, A.; Quelquejeu, M.; Rose, E. *J. Am. Chem. Soc.* **1999,** *121*, 460.
[91] Solladie-Cavallo, A.; Diep-Vohuule, A. *J. Org. Chem.* **1995,** *60*, 3494.

14[i,m]	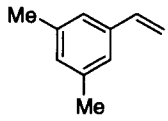	86 (99)	90[d]	(-)

[a] All reactions were carried out with olefin (0.40 mmol), ketone **5-2** (0.06-0.12 mmol), Oxone (1.07 mmol), and K_2CO_3 (4.23 mmol), TBAHS (0.04 mmol) in DME (6.0 mL), and buffer (0.1 M K_2CO_3-AcOH, pH 9.3) (4.0 mL) at -10 to -15 °C (bath temperature). For entry 12, the reaction was carried out at -5 °C. For entry 13, the reaction was carried out in DME (5.0 mL)-dioxane (1.0 mL) at 0 °C. [b] Isolated yield. [c] The conversion was determined by GC, except entries 8, 10, 11, and 12 which were determined by ^{1}H NMR. [d] The ee was determined by chiral GC (Chiraldex B-DM). [e] The ee was determined by chiral HPLC (Chiralcel AD). [f] The ee was determined by chiral HPLC (Chiralcel OD). [g] The ee was determined by chiral HPLC (Chiralcel OJ). [h] The absolute configurations were determined by comparing the measured optical rotations with the reported ones. [i] Reaction time 6 h. [j] Reaction time 8 h. [k] Reaction time 12 h. [l] Reaction time 16 h. [m] 0.06 mmol of ketone **5-2** used. [n] 0.12 mmol of ketone **5-2** used. [o] The reaction was carried out with 3.24 mmol of olefin and 0.98 mmol of ketone **5-2**. [p] The reaction was carried out by Andrea Wong.

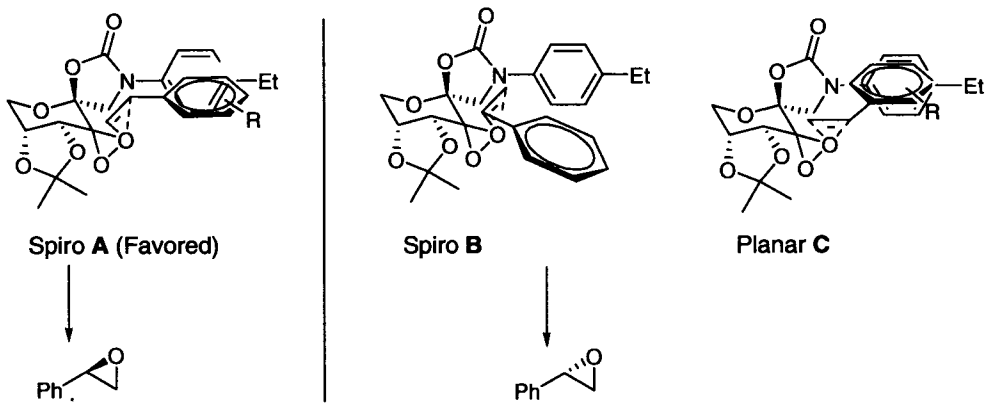

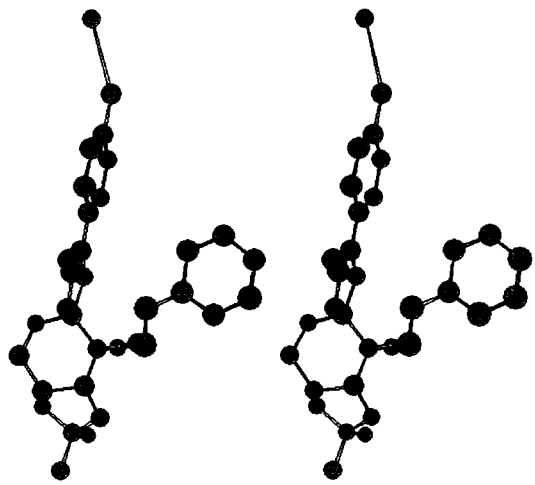

Spiro A (stereoview)

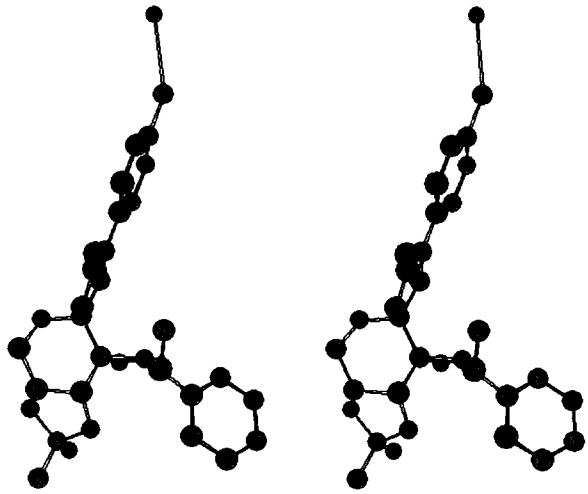

Spiro **B** (stereoview)

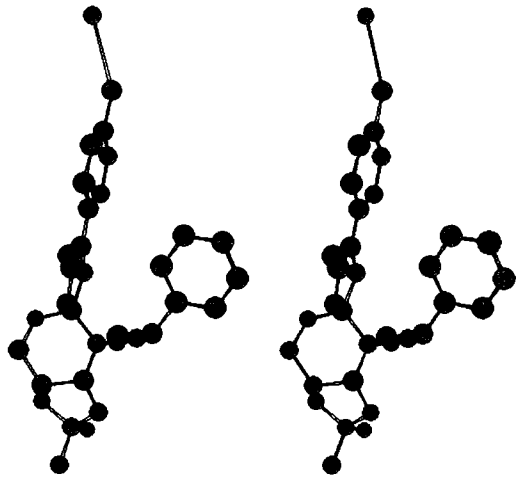

Planar **C** (stereoview)

Figure 5.4 Transition state analysis for styrene epoxidation with **5-2**

One potential application of styrene epoxidation with these new chiral ketones could be aromatic aminoalcohol synthesis. We decided to see if this

methodology could be utilized to rapidly synthesize one of these medicinally interesting compounds, β-adrenergic (-)-(R)-pronethalol.[91] Commercially available vinyl naphthalene was chosen as the starting point of the synthesis. Asymmetric epoxidation of 2-vinylnaphthalene proceeded with complete conversion and 87% ee (Scheme 5.7). Naphthalene oxide (87% ee) was then opened by gentle heating with isopropyl amine to give (-)-(R)-pronethalol. Simple recrystallization gave the desired target in >99% ee.

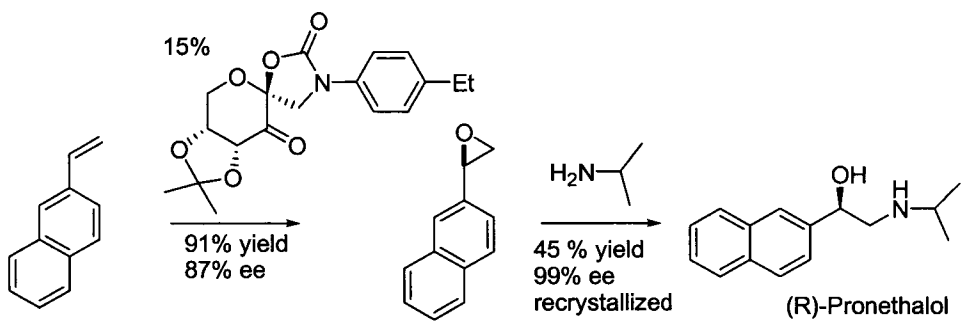

Scheme 5.7

5.B.3. Epoxidation of *cis*-olefins

Having shown that this efficiently-prepared ketone **5-2** could epoxidize a number of styrenes in good ee, we began to test whether or not additional substrate classes would be effective, such as conjugated *cis*-olefins. In order to optimize reaction conditions for *cis*-olefins, we chose to investigate the epoxidation of *cis*-β-methylstyrene (Figure 5.4). Much like the styrene case, a solvent system had to be found to best maximize the interaction between the substrate and catalyst in order to screen the catalysts. The best enantioselectivity was found with the DME:DMM (3:1) mixed solvent system (Table 5.5) previously found to be effective for epoxidation with **2-1**.

Table 5.5 Solvent Studies for *cis*-β-Methylstyrene

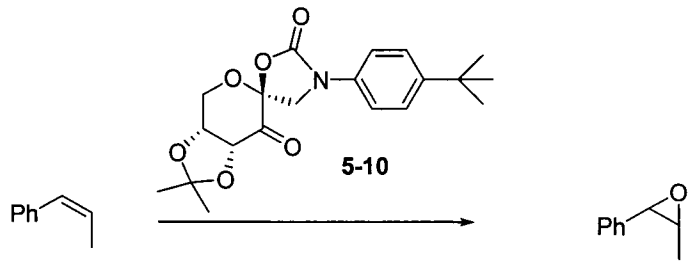

Entry	Solvent	Conv. (ee)
1	DME	100 (84)
2	DME:DMM (5:1)	93 (86)
3	DME:DMM (3:1)	100 (86)
4	Dioxane	100 (84)

[a] All reactions were carried out with olefin (0.10 mmol), ketone (0.015 mmol), Oxone (0.212 M, 0.84 mL), and K_2CO_3 (0.84 M, 0.84 mL), TBAHS (0.015 mmol) in solvent (1.5 mL), and buffer (0.1 M K_2CO_3-AcOH, pH 9.3) (1.0 mL) at -10 ^oC (bath temperature) (NaCl-ice bath) for 3.5 h. [b] The conversion and ee were determined by chiral GC (Chiraldex B-DM).

With the optimized solvent systems in hand, we set out to see if catalyst performance for some of aniline-derived catalysts (**5-2-5-28**) was different for *cis*-olefins than was previously observed for terminal olefins. *cis*-β-methylstyrene was used as the test case, and for the most part, the observed trends mirrored those that were seen for the epoxidation of styrene (Table 5.6). Once again, aniline substitution with hydrocarbons consistently shows higher ee than substitution with ethers or halogens. Furthermore, ketone **5-2** seemed the most promising candidate because of its performance and cost. Finally, and perhaps most importantly, bridging the enantioselectivity gap between *cis*- and terminal olefins was a major focus of our efforts with oxazolidinone ketones. With the

new sets of conditions, styrene can now be epoxidized in similar ee to *cis*-β-methylstyrene (Table 5.3, Entry 2, Table 5.6, Entry 2).

Table 5.6. Catalyst Screening on cis-β-Methylstyrene Epoxidation

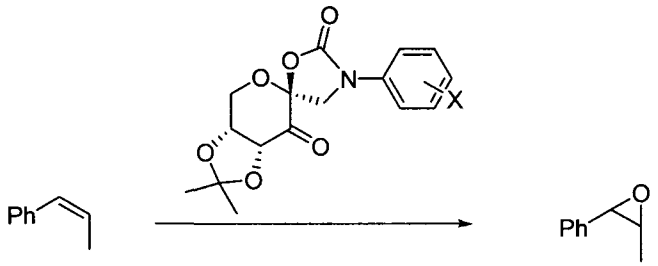

Entry	Ketone	Conv.(ee)(%)[b]	Entry	Ketone	conv.(ee)(%)[b]
1	**5-1**	60 (84)[88]	11	**5-11**	100 (86)
2	**5-2**	100 (86)	12	**5-12**	100 (85)
3	**5-3**	100 (86)	13	**5-15**	81 (82)
4	**5-4**	100 (85)	14	**5-18**	73 (81)
5	**5-5**	98 (85)	15	**5-19**	99 (85)
6	**5-6**	95 (82)	16	**5-25**	80 (82)
7	**5-7**	100 (76)	17	**5-26**	100 (86)
8	**5-8**	100 (82)	18	**5-27**	80 (82)
9	**5-9**	84 (53)	19	**5-28**	98 (87)
10	**5-10**	100 (86)			

[a] All reactions were carried out with olefin (0.10 mmol), ketone (0.015 mmol), Oxone (0.212 M, 0.84 mL), and K_2CO_3 (0.84 M, 0.84 mL), TBAHS (0.015 mmol) in DME (1.5 mL), and buffer (0.1 M K_2CO_3-AcOH, pH 9.3) (1.0 mL) at -10 °C (bath temperature) (NaCl-ice bath) for 3.5 h. [b] The conversion and ee were determined by chiral GC (Chiraldex B-DM).

Simultaneously, a number of people in our group have found that these aniline derived oxazolidinone ketones can epoxidize a number *cis*-, terminal, and trisubstituted olefins in high enantioselectivity. Chris Burke has reported that

cis-dienes can be epoxidized with good regio- and enantioselecitivty (Table 5.7).[92] Lianhe Shu and Andrea Wong have found that acyclic and cyclic *cis*-olefins, such as *cis*-β-methylstyrenes and chromenes, give epoxides in high enantioselectivity, and no *cis/trans* isomerization was observed for the acyclic cases under the standard reaction conditions (Table 5.8).[88,93,94] Finally, Yu Mei Shen and Bin Wang observed that tetra- and trisubstituted olefins can undergo epoxidation followed by rearrangement or rearrangement/oxidation to give chiral ketones or lactones (Scheme 5.8).[95]

Table 5.7. Asymmetric Epoxidation of Dienes by Chris Burke[92]

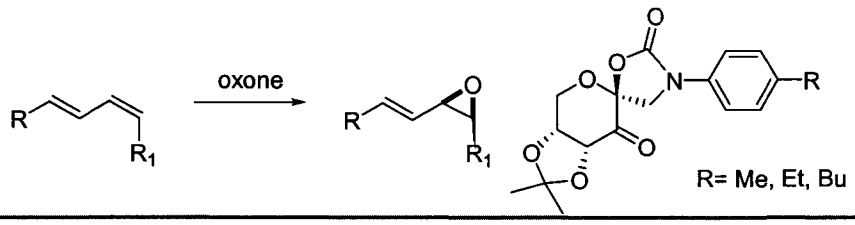

Entry	Major Epoxide	Minor Epoxide	Ratio	Yield (%)	ee (%) major
1	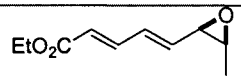			74	94
2	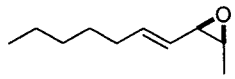			47	89
3	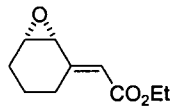	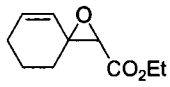	3.3:1	67	91
4	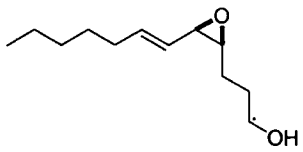			80	89

[92] Burke, C.P.; Shi, Y. *Angew. Chem. Intl. Ed.* **2006,** *45,* 4475.
[93] Wong, O.A.; Shi, Y. *J. Org. Chem.* **2006,** *71,* 3973.
[94] Shu, L.; Shi, Y. *Tetrahedron Lett.* **2004,** *45,* 8115.
[95] Shen, Y.-M.; Wang, B.; Shi, Y. *Angew. Chem. Intl. Ed.* **2006,** *45,* 1429.

Table 5.8. Asymmetric Epoxidation of Aromatic *cis*-Olefins by Andrea Wong and Lianhe Shu with an Aniline-Derived Oxazolidinone Catalyst[88,93-94]

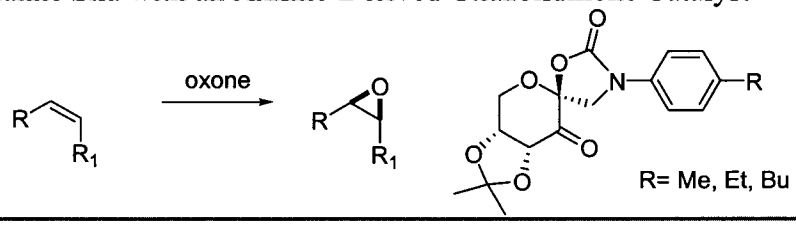

Entry	Epoxide	Yield (%)	Ee (%)	Ref
1	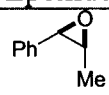	99[a]	84	88
2	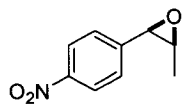	86[a]	98	94
3	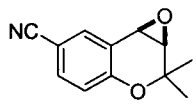	75	93	93
4	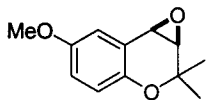	65	90	93

[a] Conversion (%)

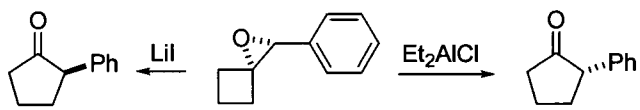

90% ee 90% ee 90% ee

Scheme 5.8

5.B.4. Improvement of Catalyst Synthesis

The aforementioned results with aniline-containing oxazolidinones are particularly encouraging, since they illustrate an effective way to prepare a number of synthetically useful epoxides in good enantioselectivity and diastereoselectivity. In order to facilitate the use of these aniline-derived

oxazolidinone ketones in synthesis, we targeted the improvement of catalyst synthesis.

The original synthetic route probably cannot be further improved in terms of total number of steps, since all four introduce essential functional groups into the catalyst structure (Scheme 5.9). Amadori rearrangement of D-glucose adds both the necessary nitrogen as well as the aromatic substituent on the nitrogen that have been found to enhance enantioselectivity. Ketalization blocks the olefin from approaching the bottom face of the catalyst structure, and phosgene cyclization provides the carbonyl that is essential for decent enantioselectivity. Finally oxidation of the final alcohol gives the ketone necessary for dioxirane formation. While the total number of chemical steps probably cannot be improved, the efficiency of those four steps was targeted. Multiple chromatographic steps, the removal of large amounts of water, and the use of oxidation reagents unsuitable for large scale reactions were previously required. Efforts were dedicated to improving these shortcomings.

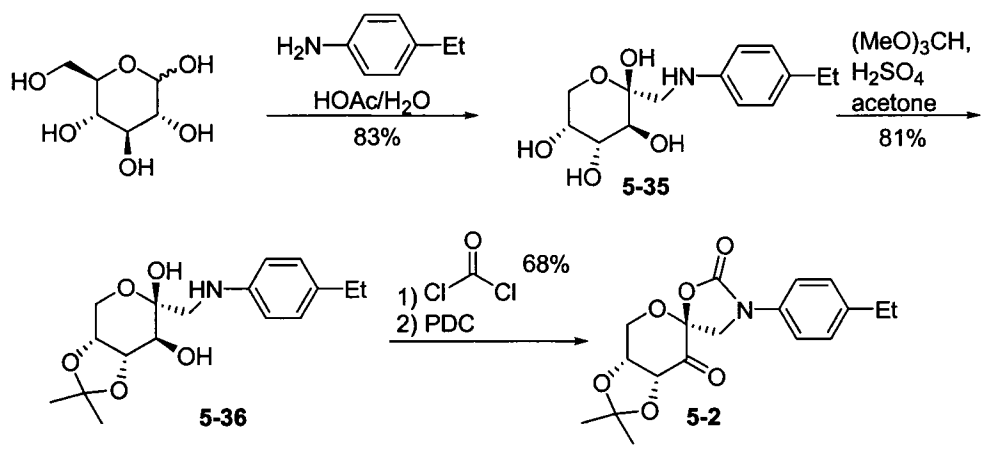

Scheme 5.9

The Amadori rearrangement step was the most efficient of the entire sequence. Heating while stirring gives a solid, which after cooling, washing with ether and ethanol, filtration, and drying under vacuum, gives the product as a white solid.

Although the Amadori rearrangement step was very efficient, the ketalization of the diol could be improved significantly. Following the 1.5 hour relatively simple reaction procedure, the mixture was quenched with NH_4OH, which required addition of a large amount of water, filtered through silica gel to remove unreacted starting material, concentrated somewhat, dried with additional Na_2SO_4, concentrated, and dried on high vacuum. In order to efficiently use this sequence in large scale synthesis, we targeted the elimination of the chromatography step. Another operation that hopefully could be avoided was quenching with NH_4OH, since a large amount of water is introduced. It was previously observed that as the reaction proceeds, the protonated form of the desired product, crystallizes in the reaction mixture. Mei-Xin Zhao found that use of the less expensive 2,2-DMP in place of $HC(OMe)_3$ causes a more efficient crystallization of the product in the reaction mixture. Simple filtration of the reaction mixture, washing with ether, and drying on the high vacuum gives the salt (**5-44**) as a pure white solid (Scheme 5.10).

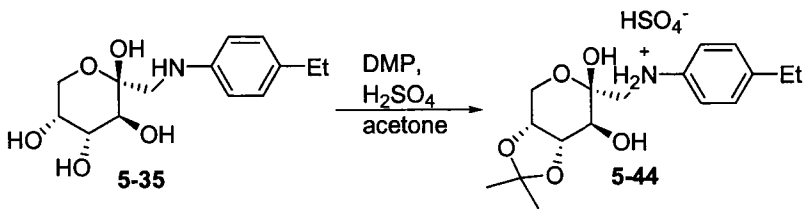

Scheme 5.10

The development of the amine salt procedure for the second step added the new challenges of overcoming any additional impurities as well as finding an efficient means for acid neutralization. Addition of NH_4OH, drying with Na_2SO_4 and concentration did give the neutralized product that could be cyclized by phosgene (Scheme 5.11). However, this approach was less desirable because of the addition of water as well as the increased time required for workup. Early efforts dedicated to neutralization of the protonated amine by $NaHCO_3$ in the DCM before addition of phosgene were unsuccessful, while treatment of the salt with other inorganic bases such as $NaHCO_3$ and K_2CO_3 did not give the desired product (Table 5.9). Mei-Xin Zhao found that a catalytic amount of diisopropylamine with $NaHCO_3$ enables the transfer of the proton from the salt to the inorganic, insoluble base, presumably due to the amine acting as a proton shuttle. Using this organic base circumvented the difficulty of water removal associated with using NH_4OH as a base to neutralize the salt. Furthermore, the increased purity of the ketalization step enabled us to obtain the pure phosgene cyclization product without the column chromatography that was previously required (Scheme 5.12).

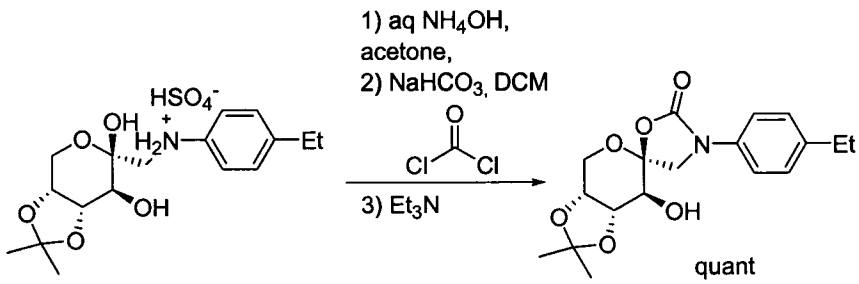

Scheme 5.11

Table 5.9. Attempted *in-situ* Neutralization/Phosgene Cyclization

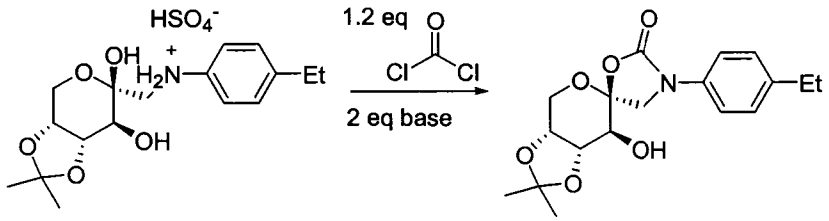

Base	Conv. (%)
$NaHCO_3$	0
K_2CO_3	0

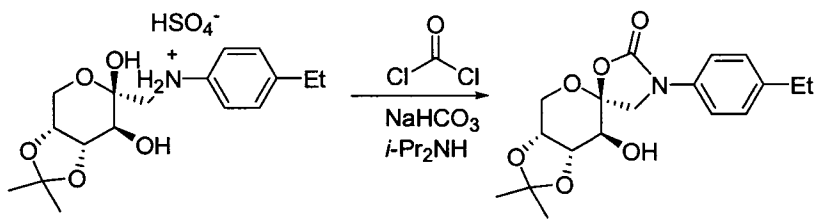

Scheme 5.12

Finally, we began to look at improving the oxidation step, since the oxidation procedure with PDC would not be amenable to larger scales. Several means of oxidation were considered, but two were deemed the most interesting. One was the TPAP/bleach procedure developed in part for the oxidation to give ketone **1-16**.[96] It gave fairly good conversion for this extremely unreactive alcohol (Scheme 5.13). While use of catalytic TPAP would mark a large improvement over PDC, catalyst cost encouraged us to explore other avenues. A TEMPO/bleach procedure using EtOAc as solvent has been developed and tested

[96] Gonsalvi, L.; Arends, I. W. C. E.; Sheldon, R. A. *Org. Lett.* **2002,** *4,* 1659.

on a number of substrates.[97] However, it was not clear this procedure would be successful for our unreactive alcohol. Performing the reaction under literature conditions did yield some product, albeit in low conversion (Table 5.10, Entry 1). Efforts were then dedicated to modifying the reaction conditions to give better yield. The pH of the reaction seemed to have little effect on conversion, with both buffered and non-buffered bleach solutions giving similar conversion (Table 5.10, Entries 7-8). Since excess bleach might be decomposing the active oxidant before the relatively unreactive alcohol can be oxidized, addition time but not volume of bleach was increased, and 100% conversion was obtained on the relatively small scale (Table 5.10, Entries 5-6). Unfortunately, Mei-Xin Zhao and Kai Li found conversion to be lower when the reaction was scaled up. They have since found that simply switching to DCM as solvent buffered to pH 9.3 gives the ketone product (**5-2**) in good yield following recrystallization (Scheme 5.14).

[97] Leanna, M.R.; Sowin, T.J.; Morton, H.E. *Tetrahedron Lett.* **1992,** *33,* 5029.

Table 5.10. TEMPO/Bleach Oxidation of **5-37**

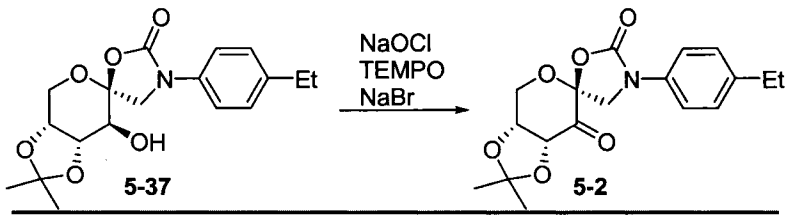

5-37 **5-2**

Entry	Addn time (h)	TEMPO (mol%)	NaOCl (wt %)	Temp(C)	Conv (%)
1	4	1	2.5	0	35
2	4	4	2.5	0	33
3	4	1	5.0	0	59
4	9	1	5.0	0	88
5	16	1	5.0	0	100
6	16	1	5.0	Rt	100
7	11	1	5.0	Rt	84
8	11[b]	1	5.0	Rt	65
9	13	1	5.0	Rt	61
10	0[b]	1	5.0	Rt	11
11	0	1	5.0	Rt	0

[a] All reactions carried out with alcohol (2.86 mmol), NaBr (2.95 mmol), EtOAc (9 mL), H_2O (1.5 mL), toluene (9 mL), and NaOCl (3.15 mmol) [b] No $NaHCO_3$ used

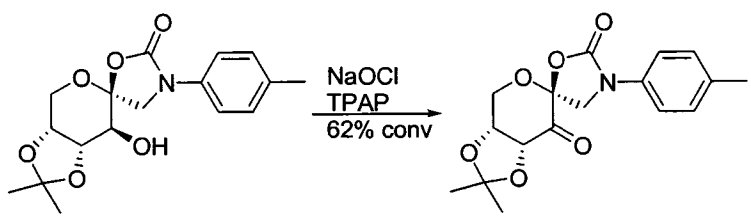

Scheme 5.13

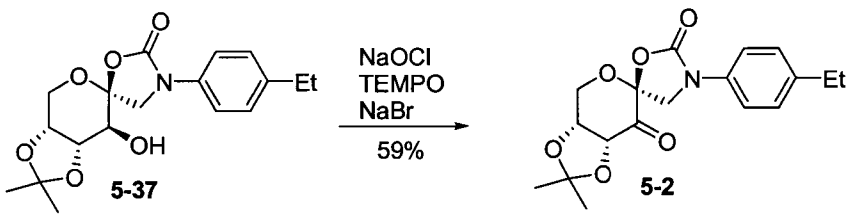

Scheme 5.14

The improved synthesis greatly facilitates the synthesis of aniline-derived ketone catalysts, including **5-2**. When an academic laboratory scale (<20 grams of ketone **5-2**) is desired, it is advantageous to use the improved sequence over the first three steps followed by the original PDC oxidation (Scheme 5.15), since TEMPO/bleach oxidation requires careful control of the reaction pH, and such control is difficult on small reaction scale. The original three step sequence followed by TEMPO/bleach oxidation are ideal for larger scale, since pH control is relatively easy and PDC removal is unnecessary (Scheme 5.15). With the new reaction sequences, substantial amounts of ketone catalysts can be prepared in short time with no column chromatography.

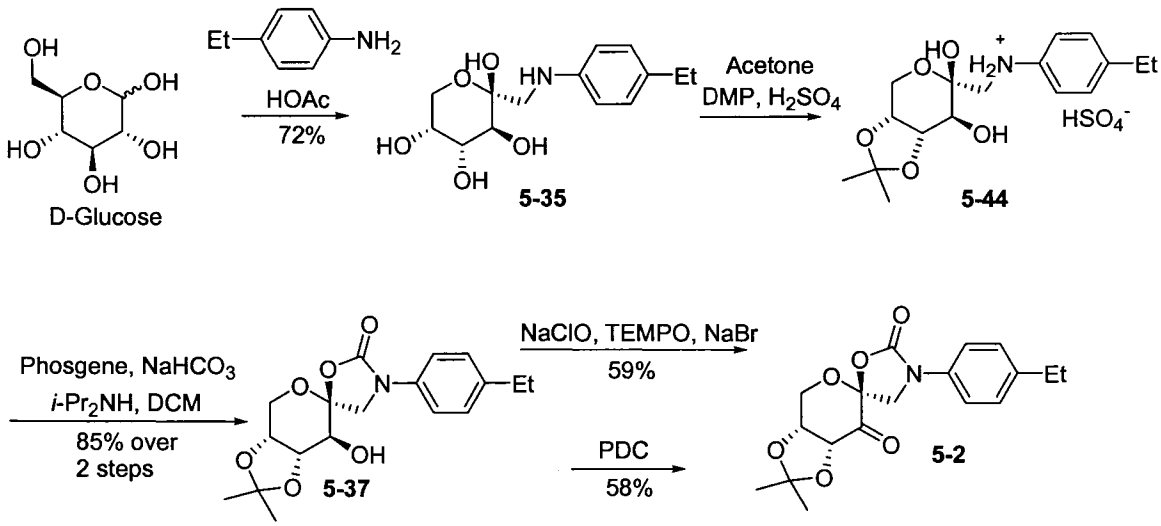

Scheme 5.15

5.B.5. Improvement of Epoxidation Procedure

Since the catalyst could now be synthesized rather quickly on large scale, we turned our focus to the optimization of the epoxidation reaction conditions. In the original procedure, the reaction was run at extremely dilute concentration (0.02 M). Consequently, the objective was to modify the reaction conditions in a manner that would hopefully enable reduction of the reaction concentration, while at the same time, still obtain similar yield and ee without greatly increasing reaction time.

Since we wanted to decrease the volume of the reaction, we chose to try to decrease both the amount of solvent originally in the flask as well as that added with the oxidant and base. Originally, conditions were chosen that were very similar to what was observed in unpublished results with ketone **1-16**. When the amount of solvent was decreased, conversion dropped to 70% when KOH was

added as the base over 6 hours in a 6:2 organic:water ratio (Table 5.11, entry 1). Addition of more catalyst, increasing the reaction time to 16 h, and modifying the aqueous to organic solvent ratio was able to increase the conversion to 92%, although complete conversion was never obtained with KOH as base (Table 5.11, Entries 1,2, 4-8). Use of the original base, K_2CO_3, resulted in complete conversion with a relatively short addition time (Table 5.11, Entry 3).

Table 5.11. Efforts to Decrease Solvent Volume for Styrene Epoxidation[a]

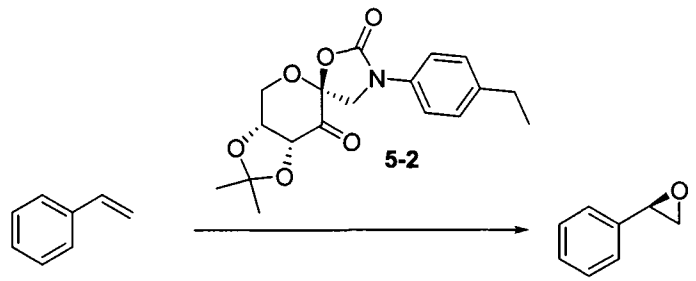

Entry	% cat	Time (h)	Base	Org:buffer (mL)	Solvent	Conv[b] (%)	ee[b] (%)
1	15	6	KOH	6:2	DME	70	76
2	30	6	KOH	6:2	DME	82	80
3	30	6	K_2CO_3	6:2	DME	100	81
4	30	8	KOH	6:2	DME	84	80
5	30	12	KOH	6:2	DME	88	80
6	30	16	KOH	6:2	DME	89	81
7	30	16	KOH	6:2	DME:dioxane (5:1)	88	81
8	30	16	KOH	5:3	DME	92	80

[a] Reactions performed with 1 mmol olefin, buffer (0.2 M K_2CO_3-AcOH, pH 9.3), Oxone (0.46 M, 3 mL), and KOH (1 M, 3 mL) or K_2CO_3 (1.93 M, 3 mL) at 0°C. [b] The conversion and ee were determined by chiral GC (Chiraldex B-DM).

With the conditions relatively optimized for styrene, we began to investigate whether or not these conditions would be amenable to other styrenes, so 3-methylstyrene was subjected to the aforementioned conditions (Table 5.11, entries, 3,8) for the two bases. Excellent conversion and ee were obtained in both cases (Table 5.12, entries 1 and 2).

Table 5.12. Epoxidation of 3-Methylstyrene at Higher Concentration[a]

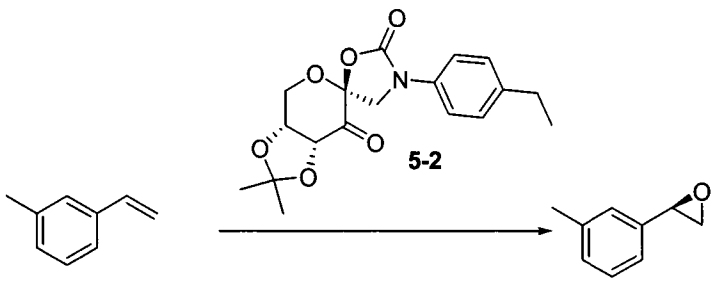

Entry	% cat	Time (h)	Base	Org:buffer (mL)	Conv.[b] (%)	ee[b] (%)
1	30	16	KOH	5:3	100	87
2	30	6	K_2CO_3	6:2	100	89

[a] Reactions performed with 1 mmol olefin, buffer (0.2 M K_2CO_3-AcOH, pH 9.3), Oxone (0.46 M, 3 mL), and KOH (1 M, 3 mL) or K_2CO_3 (1.93 M, 3 mL) at 0°C. [b] The conversion and ee were determined by chiral GC (Chiraldex B-DM).

With the hope of further increasing the concentration of the reaction, even less initial solvent was used for the two cases, one with concentrations of base and oxidant proportional to what was previously added and one with further concentrated base to decrease the reaction volume even more. Unfortunately, conversion was poor in both cases (Table 5.13, entries 1 and 2).

Table 5.13. Further Attempts at Solvent Reduction[a]

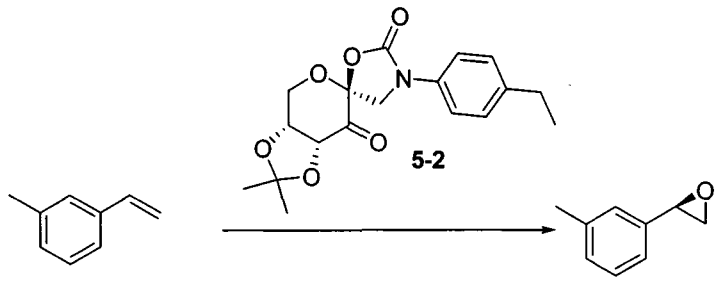

Entry	% cat	Time (h)	[KOH]	Org:buffer (mL)	Conv.[b] (%)	Ee[b] (%)
1	30	16	3M	8.3:5	1	Nd
2	30	16	1M	8.3:5	31	80

[a] Reactions performed with 5 mmol olefin, buffer (0.2 M K_2CO_3-AcOH, pH 9.3), Oxone (0.46 M, 15 mL), and KOH (1 M, 15 mL) or KOH (3 M, 5 mL). [b] The conversion and ee were determined by chiral GC (Chiraldex B-DM).

Additional 5 mmol scale reactions were then attempted both to make sure that reaction scale up was successful and also to see if the concentration of the added base could be increased under the more dilute initial concentration without hurting conversion or ee. Scaling up the reaction had little effect on the conversion or ee, and 8 hours addition time was found to give slightly better results than 6 hours (Table 5.14, entries 2 and 3). However, increasing the concentration of base still resulted in poor conversion (Table 5.14, entry 1), so efforts to further reduce the reaction volume were then abandoned.

With an optimized set of reaction conditions in hand, a moderate scale reaction (5 g) was attempted. 3-Methylstyrene oxide was obtained with 100% conversion, 91% yield, and 88% ee in a reaction that began at 0.13 M and finished at 0.08 M (Table 5.15, Entry 2).

Table 5.14. Epoxidation of 3-Methylstyrene

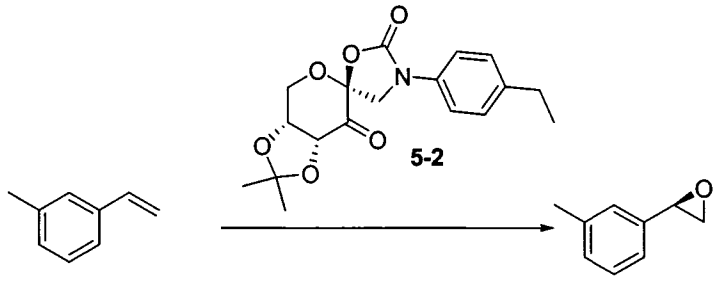

Entry	% cat	Time (h)	Base	Org:buffer (mL)	Conv.[b] (%)	Ee[b] (%)
1	30	16	KOH	25:15	43	84
2	30	6	K_2CO_3	30:10	91	88
3	30	8	K_2CO_3	30:10	98	87

[a] Reactions performed with 5 mmol olefin, buffer (0.2 M K_2CO_3-AcOH, pH 9.3), Oxone (0.46 M, 15 mL), and KOH (3 M, 5 mL) or K_2CO_3 (1.93 M, 15 mL) at 0° C. [b] The conversion and ee were determined by chiral GC (Chiraldex B-DM).

Table 5.15. Large Scale Epoxidation of 3-Methylstyrene

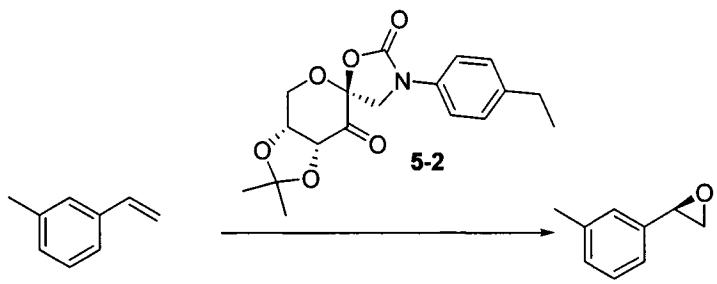

Entry	% cat	Time (h)	T (C)	Conv (%)	Yield (%)	Ee (%)
1	30	4	0	91	90	88
2	30	5	-10	100	93	89
3	15	5	-10	100	91	88

[a] Reactions performed with 3-methylstyrene (42.3 mmol), DME (250 mL), buffer (0.1 M K_2CO_3-AcOH, pH 9.3) (85 mL), TBAHS (0.15 mmol), Oxone (0.46 M, 127 mL), and K_2CO_3 (1.93 M, 127 mL) at -10° C (bath temperature) for 5 h.

5.C. CONCLUSIONS

With the goal of capitalizing on information obtained in previous studies, a number of oxazolidinone-containing catalysts were prepared from substituted anilines and D-glucose in 4 steps, and the ketone derived from 4-ethylaniline (**5-2**) was determined to be the most promising candidate. Styrenes and *cis*-olefins can be epoxidized in good ee, which could facilitate the synthesis of a number of compounds, including aminoalcohols derived from styrenes such as pronethalol. Considering the potential usefulness of this catalyst, the synthesis of ketone **5-2** was improved to allow catalyst preparation in 3 days. Finally, the epoxidation reaction conditions were optimized to allow the reaction to be carried out on large scale. As a result of these studies, a practical catalyst system for the asymmetric epoxidation of styrenes and conjugated *cis*-olefins has been developed.

5.D. EXPERIMENTAL

Representative Ketone Synthesis.

Aminoalcohol 5-35 (DLG-XII-36P) To a mixture of D-glucose (50.0 g, 279.0 mmol) and 4-ethylaniline (40.3 g, 333.0 mmol) was added water (13.7 mL), followed by AcOH (0.34 g, 5.66 mmol). After the mixture was stirred at 95°C (oil bath temperature) for 1 h (the mixture solidified), ether (200 mL) was added. Upon stirring at room temperature for 2 h and standing in the freezer overnight, the mixture was filtered. The filter cake was washed to white with additional

ether and dried to give a white solid that was used without further purification (55.5 g, 70 %).

Ketal 5-36 (DLG-XII-38) To a suspension of the above product (10.1 g, 35.6 mmol) in acetone (420 mL) was added $HC(OMe)_3$ (8.9 mL, 81.3 mmol), followed by H_2SO_4 (3.1 mL, 55.8 mmol) at 0°C. Upon stirring at 0°C for 1 h, the reaction mixture was quenched with concentrated NH_4OH (8.9 mL) and quickly filtered through a pad of silica gel. The filter cake was washed with additional acetone. The acetone solution was dried (Na_2SO_4), filtered, and concentrated to give a yellow oil (9.32 g) that was used without further purification.

Alcohol 5-37 (DLG-XII-39) A mixture of the above oil and $NaHCO_3$ (12.2 g) was suspended in DCM (142 mL). While stirring at 0°C, phosgene (20% solution in toluene, 21.3 mL) was added via a syringe pump under argon over 2 h. After the mixture was stirred at 0 °C for an additional 4 h, Et_3N (17.3 mL) was then added. Upon stirring at rt overnight, the mixture was filtered through a pad of silica gel, concentrated, and purified on silica gel with hexane:EtOAc (2:1 to 1:2) to give the alcohol product as a light brown solid (6.78 g, 55% yield over two steps).

Alcohol 5-2 (yy0908-3, DLG-XII-6) To a suspension of the alcohol (8.0 g, 22.9 mmol), PDC (12.9 g, 34.4 mmol) and 3A MS (14 g) in DCM (23 mL) was added acetic acid (5 drops). Upon stirring at rt overnight, the reaction mixture was

filtered through a pad of silica gel and washed with hexane:EtOAc (1:2). The filtrate was concentrated and dried on the high vacuum line. Recrystallization (ether:hexanes) gave the product (**5-2**) as a white solid (4.3 g, 54%). mp 135–136 °C; $[\alpha]^{20}_{D}$ = -40.6 (*c*, 0.32, $CHCl_3$); IR (film) 1774 cm^{-1}; ^1H NMR (300 MHz, $CDCl_3$) δ 7.42 (d, *J* = 8.4 Hz, 2H), 7.21 (d, *J* = 8.4 Hz, 2H), 4.87 (d, *J* = 5.1 Hz, 1H), 4.74 (d, *J* = 10.2 Hz, 1H), 4.66-4.59 (m, 2H), 4.26 (d, *J* = 13.5 Hz, 1H), 3.75 (d, *J* = 10.2 Hz, 1H), 2.63 (q, *J* = 7.5 Hz, 2H), 1.48 (s, 3H), 1.43 (s, 3H), 1.22 (t, *J* = 7.5 Hz, 3H); ^{13}C NMR (75 MHz, $CDCl_3$) δ 195.1, 151.4, 141.3, 134.7, 128.7, 119.0, 111.2, 99.3, 77.7, 75.7, 61.2, 50.1, 28.5, 27.4, 26.3, 15.9; HRMS calcd for $C_{18}H_{22}NO_6$ (M+1) 348.1447, found 348.1441.

Ketone (5-1)[88]

Ketone (5-3) (yy0809-4, DLG-XII-30M) white solid; mp 135-136 °C; $[\alpha]^{20}_{D}$ = -25.1 (*c*, 0.48, $CHCl_3$); IR (film) 1777 cm^{-1}; ^1H NMR (300 MHz, $CDCl_3$) δ 7.38-7.24 (m, 3H), 7.03 (m, 1H), 4.87 (d, *J* = 5.4 Hz, 1H), 4.77 (d, *J* = 10.5 Hz, 1H), 4.67-4.60 (m, 2H), 4.27 (d, *J* = 14.4 Hz, 1H), 3.77 (d, *J* = 10.5 Hz, 1H), 2.67 (q, *J* = 7.8 Hz, 2H), 1.49 (s, 3H), 1.44 (s, 3H), 1.24 (t, *J* = 7.8 Hz, 3H); ^{13}C NMR (100 MHz, $CDCl_3$) 195.3, 151.4, 145.8, 137.2, 129.3, 124.8, 118.5, 116.3, 111.2, 99.2, 77.7, 75.7, 61.1, 50.0, 29.2, 27.3, 26.2, 15.7; Anal. Calcd for $C_{18}H_{21}NO_6$: C, 62.24; H, 6.09; N, 4.03. Found: C, 62.50; H, 6.13; N, 3.86.

Ketone (5-4) (yy0622-3, DLG-XII-30F) white solid; mp 116-118 °C; $[\alpha]^{20}_{D}$ = -24.3 (*c*, 0.61, $CHCl_3$); IR (film) 1778, 1760 cm^{-1}; ^1H NMR (400 MHz, $CDCl_3$) δ

7.36-7.25 (m, 3H), 6.99 (d, J = 6.8 Hz, 1H), 4.87 (d, J = 4.8 Hz, 1H), 4.74 (d, J = 10.4 Hz, 1H), 4.67-4.59 (m, 2H), 4.26 (d, J = 13.6 Hz, 1H), 3.75 (d, J = 10.4 Hz, 1H), 2.37 (s, 3H), 1.48 (s, 3H), 1.43 (s, 3H); ^{13}C NMR (100 MHz, $CDCl_3$) δ 195.2, 151.2, 139.4, 137.1, 129.2, 125.9, 119.5, 115.9, 111.1, 99.2, 77.6, 75.6, 61.0, 49.9, 27.2, 26.1, 21.7; Anal. Calcd for $C_{17}H_{19}NO_6$: C, 61.25; H, 5.75; N, 4.20. Found: C, 61.02; H, 5.61; N, 4.10.

Ketone (5-5) (yy0908-1, DLG-XII-30W) yellow solid; mp 136–138 °C; $[\alpha]^{20}_D$ = -40.8 (*c*, 5.4, $CHCl_3$); IR (film) 1778 cm^{-1}; ^{1}H NMR (300 MHz, $CDCl_3$) δ 7.38-7.22 (m, 5H), 7.14-7.09 (m, 1H), 7.04-6.98 (m, 2H), 6.81-6.76 (m, 1H), 4.85 (d, J = 5.4 Hz, 1H), 4.70 (d, J = 10.5 Hz, 1H), 4.65-4.56 (m, 2H), 4.25 (d, J = 12.6 Hz, 1H), 3.73 (d, J = 10.5 Hz, 1H), 1.47 (s, 3H), 1.42 (s, 3H); ^{13}C NMR (75 MHz, $CDCl_3$) δ 195.0, 158.1, 156.6, 151.0, 138.5, 130.3, 129.9, 123.8, 119.1, 114.9, 113.1, 111.2, 109.4, 99.2, 77.7, 75.6, 61.2, 49.9, 27.3, 26.2; HRMS calcd for $C_{22}H_{21}NO_7$ (M+) 411.1318, found 411.1305.

Ketone (5-6) (yy-0715-2, DLG-XII-30N) yellow solid; mp 58-66 °C; $[\alpha]^{20}_D$ = -44.8 (*c*, 0.25, $CHCl_3$); IR (film) 3450, 1759 cm^{-1}; hydrate: ^{1}H NMR (400 MHz, $CDCl_3$) δ 6.75 (s, 2H), 4.62 (d, J = 10.0 Hz, 1H), 4.47 (d, J = 6.8 Hz, 1H), 4.42 (m, 1H), 4.32 (dd, J = 12.8, 2.4 Hz, 1H), 3.94 (d, J = 12.8 Hz, 1H), 3.82-3.78 (m, 10 H), 1.56 (s, 3H), 1.39 (s, 3H); ^{13}C NMR (100 MHz, $CDCl_3$) δ 153.3, 153.2, 135.0, 133.5, 110.1, 101.7, 97.1, 91.1, 76.0, 73.2, 63.3, 60.8, 56.1, 53.8, 26.2, 24.6; HRMS calcd for $C_{19}H_{23}NO_9$ (M+) 409.1373, found 409.1369.

Ketone (5-7) (yy0630-2, DLG-XII-30I) yellow solid; mp 108–110 °C; $[\alpha]^{20}_D$ = -21.2 (*c*, 0.34, $CHCl_3$); IR (film) 1772 cm^{-1}; ^1H NMR (400 MHz, $CDCl_3$) δ 7.35 (d, *J* = 2.2 Hz, 1H), 6.86 (d, *J* = 8.8 Hz, 1H), 6.79 (dd, *J* = 8.8, 2.2 Hz, 1H), 4.88 (d, *J* = 5.2 Hz, 1H), 4.74 (d, *J* = 10.4 Hz, 1H), 4.66-4.60 (m, 2H), 4.27 (d, *J* = 13.2 Hz, 1H), 3.91 (s, 3H), 3.88 (s, 3H), 3.74 (d, *J* = 10.4 Hz, 1H), 1.48 (s, 3H), 1.43 (s, 3H); ^{13}C NMR (100 MHz, $CDCl_3$) δ 195.3, 151.4, 149.4, 146.6, 130.6, 111.3, 111.1, 111.0, 104.0, 99.1, 77.6, 75.6, 61.0, 56.2, 56.1, 50.3, 27.2, 26.1; HRMS calcd for $C_{18}H_{21}NO_8$ (M+) 379.1267, found 379.1268.

Ketone (5-8) (yy0622-1, DLG-XII-30L) white solid; mp 191–193 °C; $[\alpha]^{20}_D$ = -37.4 (*c*, 0.50, $CHCl_3$); IR (film) 1773, 1756 cm^{-1}; ^1H NMR (300 MHz, $CDCl_3$) δ 7.30-7.12 (m, 3H), 4.87 (d, *J* = 5.1 Hz, 1H), 4.74 (d, *J* = 10.5 Hz, 1H), 4.67-4.60 (m, 2H), 4.26 (d, *J* = 13.5 Hz, 1H), 3.73 (d, *J* = 10.5 Hz, 1H), 2.27 (s, 3H), 2.24 (s, 3H), 1.48 (s, 3H), 1.43 (s, 3H); ^{13}C NMR (100 MHz, $CDCl_3$) δ 195.3, 151.4, 137.7, 134.8, 133.6, 130.3, 120.3, 116.5, 111.1, 99.2, 77.6, 75.6, 61.0, 50.0, 27.2, 26.1, 20.1, 19.3; Anal. Calcd for $C_{18}H_{21}NO_6$: C, 62.24; H, 6.09; N, 4.03. Found: C, 62.30; H, 5.85; N, 3.99.

Ketone (5-9) (yy-0908-4, DLG-XII-30E) white solid; mp 161-162 °C; $[\alpha]^{20}_D$ = -17.8 (*c*, 0.47, $CHCl_3$); IR (film) 1774 cm^{-1}; ^1H NMR (300 MHz, $CDCl_3$) δ 7.92 (d, *J* = 2.4 Hz, 1H), 7.46 (dd, *J* = 8.4, 2.4 Hz, 1H), 7.23, (d, *J* = 8.4 Hz, 1H), 4.86 (d, *J* = 5.7 Hz, 1H), 4.71 (d, *J* = 10.2 Hz, 1H), 4.66-4.58 (m, 2H), 4.27 (d, *J* = 13.8

Hz, 1H), 3.72 (d, J = 10.2 Hz, 1H), 2.41 (s, 3H), 1.48 (s, 3H), 1.43 (s, 3H); ^{13}C NMR (75 MHz, $CDCl_3$) δ 195.1, 151.1, 138.3, 135.7, 129.8, 128.7, 118.6, 111.2, 101.1, 99.3, 77.5, 75.6, 61.1, 49.8, 27.5, 27.2, 26.1; Anal. Calcd for $C_{17}H_{18}INO_6$: C, 44.46; H, 3.95; N, 3.05. Found: C, 44.26; H, 4.15; N, 2.76.

Ketone (5-10) (LS3115, DLG-XII-30S) white solid; mp 172-174 °C; $[\alpha]^{20}_D$ = -36.0 (*c*, 0.28, $CHCl_3$); IR (film) 1775 cm^{-1}; ^1H NMR (400 MHz, $CDCl_3$) δ 7.47-7.36 (m, 4H), 4.87 (d, J = 5.2 Hz, 1H), 4.75 (d, J = 10.4 Hz, 1H), 4.67-4.60 (m, 2H), 4.27 (d, J = 14.0 Hz, 1H), 3.75 (d, J = 10.4 Hz, 1H), 1.49 (s, 3H), 1.43 (s, 3H), 1.31 (s, 9H); ^{13}C NMR (100 MHz, $CDCl_3$) δ 195.3, 151.5, 148.3, 134.6, 126.3, 118.8, 111.3, 99.3, 77.7, 75.7, 61.1, 50.0, 34.6, 31.5, 27.3, 26.2; HRMS calcd for $C_{20}H_{26}NO_6$ (M+1) 376.1760, found 376.1764.

Ketone (5-11) (yy0809-1, DLG-XII-30B) white solid; mp 125–126 °C; $[\alpha]^{20}_D$ = -26.5 (*c*, 0.22, $CHCl_3$); IR (film) 1775 cm^{-1}; ^1H NMR (300 MHz, $CDCl_3$) δ 7.39 (s, 1H), 7.33-7.30 (m, 2H), 7.08-7.03 (m, 2H), 4.87 (d, J = 5.1 Hz, 1H), 4.77 (d, J = 10.5 Hz, 1H), 4.67-4.60 (m, 2H), 4.27 (d, J = 14.1 Hz, 1H), 3.77 (d, J = 10.5 Hz, 1H), 3.00-2.84 (m,1H), 1.49 (s, 3H), 1.43 (s, 3H), 1.25 (d, J = 6.9 Hz, 6H); ^{13}C NMR (100 MHz, $CDCl_3$) δ 195.3, 151.3, 150.4, 137.1, 129.3, 123.2, 117.1, 116.4, 111.2, 99.2, 77.6, 75.6, 61.0, 50.0, 34.4, 27.2, 26.1, 24.1, 24.0; Anal. Calcd for $C_{19}H_{23}NO_6$: C, 63.15; H, 6.41; N, 3.88. Found: C, 63.31; H, 6.48; N, 3.76.

Ketone (5-12) (yy0902-5, DLG-XII-30Q) white solid; mp 135-136 °C; $[\alpha]^{20}_D$ = -28.4 (*c*, 0.66, $CHCl_3$); IR (film) 1776 cm^{-1}; ^1H NMR (300 MHz, $CDCl_3$) δ 7.41 (d, *J* = 8.4 Hz, 2H), 7.19 (d, *J* = 8.4 Hz, 2H), 4.86 (d, *J* = 5.4 Hz, 1H), 4.73 (d, *J* = 10.2 Hz, 1H), 4.66-4.58 (m, 2H), 4.25 (d, *J* = 14.4 Hz, 1H), 3.74 (d, *J* = 10.2 Hz, 1H), 2.56 (t, *J* = 7.5 Hz, 2H), 1.68-1.54 (m, 2H), 1.48 (s, 3H), 1.42 (s, 3H), 0.92 (t, *J* = 7.5 Hz, 3H); ^{13}C NMR (75 MHz, $CDCl_3$) δ 195.1, 151.3, 139.7, 134.7, 129.3, 118.9, 111.2, 99.2, 77.7, 75.7, 61.1, 50.0, 37.5, 27.4, 26.2, 24.8, 14.0; Anal. Calcd for $C_{19}H_{23}NO_6$: C, 63.15; H, 6.41; N, 3.88. Found: C, 62.88; H, 6.41; N, 3.61.

Ketone (5-13) (LS3018, DLG-XII-30R) white solid; mp 164-166 °C; $[\alpha]^{20}_D$ = -32.9 (*c*, 0.28, $CHCl_3$); IR (film) 1776 cm^{-1}; ^1H NMR (300 MHz, $CDCl_3$) δ 7.45-7.39 (m, 2H), 7.22-7.14 (m, 2H), 4.87 (d, *J* = 5.4 Hz, 1H), 4.74 (d, *J* = 10.5 Hz, 1H), 4.66-4.60 (m, 2H), 4.26 (d, *J* = 13.8 Hz, 1H), 3.75 (d, *J* = 10.5 Hz, 1H), 2.59 (t, *J* = 7.5 Hz, 2H), 1.63-1.57 (m, 2H), 1.48 (s, 3H), 1.43 (s, 3H), 1.41-1.26 (m, 2H), 0.91 (t, *J* = 7.5 Hz, 3H); ^{13}C NMR (75 MHz, $CDCl_3$) δ 195.3, 151.5, 140.1, 134.8, 129.4, 119.0, 111.3, 99.3, 77.7, 75.7, 61.1, 50.0, 35.1, 33.8, 27.3, 26.2, 22.4, 14.1; Anal. Calcd for $C_{20}H_{25}NO_6$: C, 63.99; H, 6.71; N, 3.73. Found: C, 64.00; H, 6.77; N, 3.76.

Ketone (5-14) (yy0903-1, DLG-XII-30T) white solid; mp 93-94 °C; $[\alpha]^{20}_D$ = -26.9 (*c*, 0.36, $CHCl_3$); IR (film) 1776 cm^{-1}; ^1H NMR (300 MHz, $CDCl_3$) δ 7.42 (d, *J* = 7.8 Hz, 2H), 7.20 (d, J = 7.8 Hz, 2H), 4.87 (d, *J* = 5.4 Hz, 1H), 4.75 (d, *J* =

10.8 Hz, 1H), 4.67-4.60 (m, 2H), 4.26 (d, J = 14.4 Hz, 1H), 3.75 (d, J = 10.8 Hz, 1H), 2.59 (t, J = 7.2 Hz, 2H), 1.66-1.52 (m, 2H), 1.49 (s, 3H), 1.44 (s, 3H), 1.36-1.24 (m, 4H), 0.89 (t, J = 6.9 Hz, 3H); ^{13}C NMR (75 MHz, $CDCl_3$) δ 195.2, 151.3, 139.9, 134.7, 129.2, 118.8, 111.1, 99.2, 77.6, 75.6, 61.0, 49.9, 35.3, 31.4, 31.2, 27.2, 26.1, 22.6, 14.1; Anal. Calcd for $C_{21}H_{27}NO_6$: C, 64.77; H, 6.99; N, 3.60. Found: C, 64.90; H, 6.99; N, 3.49.

Ketone (5-15) (yy0903-2, DLG-XII-30U) yellow solid; mp 71-72 °C; $[\alpha]^{20}_D$ = -30.5 (*c*, 0.44, $CHCl_3$); IR (film) 1777 cm^{-1}; ^{1}H NMR (300 MHz, $CDCl_3$) δ 7.41 (d, J = 8.4 Hz, 2H), 7.19 (d, J = 8.4 Hz, 2H), 4.87 (d, J = 5.1 Hz, 1H), 4.74 (d, J = 10.5 Hz, 1H), 4.67-4.60 (m, 2H), 4.26 (d, J = 13.8 Hz, 1H), 3.75 (d, J = 10.5 Hz, 1H), 2.58 (t, J = 7.5 Hz, 2H), 1.66-1.52 (m, 2H), 1.49 (s, 3H), 1.43 (s, 3H), 1.36-1.22 (m, 8H), 0.88 (t, J = 7.2 Hz, 3H); ^{13}C NMR (75 MHz, $CDCl_3$) δ 195.3, 151.3, 139.9, 134.7, 129.2, 118.8, 111.1, 99.2, 77.6, 75.6, 61.0, 49.9, 35.3, 31.8, 31.5, 29.2, 27.2, 26.0, 22.7, 14.2; Anal. Calcd for $C_{23}H_{31}NO_6$: C, 66.17; H, 7.48; N, 3.35. Found: C, 66.10; H, 7.55; N, 3.18.

Ketone (5-16) (yy0809-3, DLG-XII-30O) white solid; mp 110-111 °C; $[\alpha]^{20}_D$ = -40.6 (*c*, 0.32, $CHCl_3$); IR (film) 3436, 1774 cm^{-1}; ketone: ^{1}H NMR (300 MHz, $CDCl_3$) δ 7.44-7.38 (m, 2H), 7.24-7.12 (m, 2H), 4.87 (d, J = 5.1 Hz, 1H), 4.74 (d, J = 10.5 Hz, 1H), 4.68-4.60 (m, 2H), 4.26 (d, J = 13.8 Hz, 1H), 3.75 (d, J = 10.5 Hz, 1H), 2.62-2.54 (m, 2H), 1.63-1.52 (m, 2H), 1.49 (s, 3H), 1.43 (s, 3H), 1.34-1.20 (m, 14H), 0.87 (t, J = 6.9 Hz, 3H); hydrate: ^{13}C NMR (100 MHz, $CDCl_3$) δ

153.3, 139.0, 135.1, 128.8, 118.8, 110.0, 101.9, 91.2, 76.0, 73.3, 63.3, 53.6, 35.2, 31.8, 31.4, 29.6, 29.5, 29.3, 29.2, 26.1, 24.6, 22.6, 14.0; Anal. Calcd for $C_{26}H_{37}NO_6$: C, 67.95, H, 8.11, N, 3.05. Found: C, 68.12, H, 7.94, N, 3.04.

Ketone (5-17) (yy0809-2, DLG-XII-30C) white solid; mp 180–182 °C; $[\alpha]^{20}_D$ = -33.1 (*c*, 0.51, $CHCl_3$); IR (film) 1775 cm^{-1}; ^1H NMR (300 MHz, $CDCl_3$) δ 7.43 (d, *J* = 8.4 Hz, 2H), 7.24 (d, *J* = 8.4 Hz, 2H), 4.87 (d, *J* = 5.1 Hz, 1H), 4.75 (d, *J* = 10.5 Hz, 1H), 4.67-4.60 (m, 2H), 4.26 (d, *J* = 14.4 Hz, 1H), 3.75 (d, *J* = 10.5 Hz, 1H), 2.96-2.84 (m,1H), 1.48 (s, 3H), 1.43 (s, 3H), 1.23 (d, *J* = 6.9 Hz, 6H); ^{13}C NMR (100 MHz, $CDCl_3$) δ 195.3, 151.4, 146.0, 134.8, 127.3, 119.1, 111.2, 99.2, 77.6, 75.6, 61.1, 50.0, 33.7, 27.3, 26.1, 24.1; Anal. Calcd for $C_{19}H_{23}NO_6$: C, 63.15; H, 6.41; N, 3.88. Found: C, 63.24; H, 6.39; N, 3.76.

Ketone (5-18) (yy0610-P, DLG-XII-30J) yellow solid; mp 136–138 °C; $[\alpha]^{20}_D$ = -5.9 (*c*, 1.75, $CHCl_3$); IR (film) 3385, 1752 cm^{-1}; hydrate: ^1H NMR (400 MHz, $CDCl_3$) δ 7.46-7.40 (m, 2H), 7.35-7.26 (m, 2H), 7.12-7.04 (m, 1H), 7.00-6.94 (m, 4H), 4.59 (d, *J* = 10.0 Hz, 1H), 4.46 (d, *J* = 7.2 Hz, 1H), 4.42 (m, 1H), 4.33 (d, *J* = 12.8, 2.4 Hz, 1H), 3.95 (d, *J* = 12.8 Hz, 1H), 3.80 (d, *J* = 10.0 Hz, 1H), 2.32 (brs, H), 1.56 (s, 3H), 1.38 (s, 3H); ^{13}C NMR (100 MHz, $CDCl_3$) δ 157.4, 154.1, 153.5, 132.9, 129.9, 123.5, 120.9, 119.6, 118.8, 110.4, 102.0, 91.2, 76.2, 73.4, 63.4, 53.8, 26.4, 24.8; HRMS calcd for $C_{22}H_{21}NO_7$ (M+) 411.1318, found 411.1326.

Ketone (5-19) (LS3038, DLG-XII-30V) white solid; mp 76-78 °C; $[\alpha]^{20}_D$ = -77.9 (*c*, 0.20, $CHCl_3$); IR (film) 1776 cm^{-1}; ^1H NMR (400 MHz, $CDCl_3$) δ 7.65-7.55 (m, 6H), 7.46-7.42 (m, 2H), 7.37-7.33 (m, 1H), 4.89 (d, *J* = 5.6 Hz, 1H), 4.80 (d, *J* = 10.4 Hz, 1H), 4.68-4.61 (m, 2H), 4.28 (d, *J* = 12.8 Hz, 1H), 3.81 (d, *J* = 10.4 Hz, 1H), 1.50 (s, 3H), 1.44 (s, 3H); ^{13}C NMR (100 MHz, $CDCl_3$) δ 195.2, 151.3, 140.2, 138.0, 136.4, 129.0, 128.0, 127.6, 127.1, 119.1, 111.3, 99.3, 77.7, 75.7, 61.2, 49.9, 27.3, 26.2; HRMS calcd for $C_{22}H_{22}NO_6$ (M+1) 396.1447, found 396.1440.

Ketone (5-20) (DLG-IX-43A) white solid; mp 146-148 °C; $[\alpha]^{20}_D$ = -44.4 (*c*, 0.135, $CHCl_3$); IR (film) 3404, 1774 cm^{-1}; ketone: ^1H NMR (300 MHz, $CDCl_3$) δ 7.70 (d, *J* = 2.4 Hz, 1H), 7.37 (dd, *J* = 8.4, 2.4 Hz, 1H), 7.21 (d, *J* = 8.4 Hz, 1H), 4.85 (d, *J* = 5.4 Hz, 1H), 4.69 (d, *J* = 10.2 Hz, 1H), 4.66-4.55 (m, 2H), 4.25 (d, *J* = 12.6 Hz, 1H), 3.71 (d, *J* = 10.2 Hz, 1H), 2.35 (s, 3H), 1.46 (s, 3H), 1.41 (s, 3H); hydrate: ^{13}C NMR (100 MHz, $CDCl_3$) δ 152.9, 136.4, 133.7, 130.7, 124.9, 122.1, 117.4, 110.1, 101.9, 91.1, 76.0, 73.3, 63.4, 53.3, 26.2, 24.7, 22.1; HRMS calcd for $C_{17}H_{18}BrNO_6$ (M+1) 412.0396, found 412.0395.

Ketone (5-21) (DLG-X-17A) yellow solid; mp 56-59 °C; $[\alpha]^{20}_D$ = -47.6 (*c*, 0.15, $CHCl_3$); IR (film) 3419, 1760 cm^{-1}; ^1H NMR (300 MHz, $CDCl_3$) δ 7.48-7.40 (m, 2H), 7.16-7.08 (m, 2H), 7.02-6.85 (m, 4H), 4.87 (d, *J* = 5.6 Hz, 1H), 4.74 (d, *J* = 10.4, Hz, 1H), 4.66-4.59 (m, 2H), 4.27 (d, *J* = 13.2 Hz, 1H), 3.74 (d, *J* = 10.4 Hz, 1H), 2.33 (s, 3H), 1.48 (s, 3H), 1.43 (s, 3H); ^{13}C NMR (100 MHz, $CDCl_3$) 195.3,

155.2, 154.7, 151.6, 133.3, 132.1, 130.5, 120.8, 119.2, 119.1, 111.2, 99.3, 77.6, 75.6, 61.1, 50.2, 27.3, 26.1, 20.9; HRMS calcd for $C_{23}H_{23}NO_7$ (M+) 425.1475, found 425.1465.

Ketone (5-22) (DLG-X-23) orange solid; mp 52-56 °C; $[\alpha]^{20}_D$ = -39.2 (*c*, 0.28, $CHCl_3$); IR (film) 1764 cm^{-1}; ^1H NMR (300 MHz, $CDCl_3$) δ 7.43-7.26 (m, 7H), 7.01-6.92 (m, 2H), 5.05 (s, 2H), 4.86 (d, *J* = 4.8 Hz, 1H), 4.71 (d, *J* = 10.8 Hz, 1H), 4.66-4.58 (m, 2H), 4.26 (d, *J* = 14.4 Hz, 1H), 3.72 (d, *J* = 10.8 Hz, 1H), 1.48 (s, 3H), 1.43 (s, 3H); ^{13}C NMR (100 MHz, $CDCl_3$) 195.3, 156.3, 151.6, 136.9, 130.4, 128.8, 128.3, 127.6, 121.0, 115.7, 111.2, 99.3, 77.7, 75.7, 70.5, 61.1, 50.3, 27.3, 26.2; HRMS calcd for $C_{23}H_{23}NO_7$ (M+) 425.1475, found 425.1469.

Ketone (5-23) (DLG-X-17B) yellow solid; mp 48-50 °C; $[\alpha]^{20}_D$ = -47.2 (*c*, 0.13, $CHCl_3$); IR (film) 3406, 1762 cm^{-1}; ^1H NMR (300 MHz, $CDCl_3$) δ 7.46-7.38 (m, 2H), 7.31-7.13 (m, 7H), 4.86 (d, *J* = 5.6 Hz, 1H), 4.72 (d, *J* = 10.4 Hz, 1H), 4.65-4.58 (m, 2H), 4.25 (d, *J* = 12.8 Hz, 1H), 3.96 (s, 2H), 3.73 (d, *J* = 10.4 Hz, 1H), 1.48 (s, 3H), 1.42 (s, 3H); ^{13}C NMR (100 MHz, $CDCl_3$) 195.3, 151.4, 140.9, 138.2, 135.3, 129.9, 129.0, 128.7, 126.4, 119.0, 111.2, 99.3, 77.6, 75.6, 61.1, 49.9, 41.4, 27.3, 26.1; HRMS calcd for $C_{23}H_{24}NO_6$ (M+1) 410.1604, found 410.1603.

Ketone (5-24) (DLG-IX-50) yellow solid; mp 58-60 °C; $[\alpha]^{20}_D$ = -46.0 (*c*, 0.15, $CHCl_3$); IR (film) 3411, 1759 cm^{-1}; ketone: ^1H NMR (400 MHz, $CDCl_3$) δ 7.38-7.16 (m, 8H), 7.01 (d, *J* = 7.6 Hz, 1H), 4.86 (d, *J* = 5.6 Hz, 1H), 4.71 (d, *J* = 10.4

Hz, 1H), 4.65-4.58 (m, 2H), 4.24 (d, J = 13.6 Hz, 1H), 3.99 (s, 2H), 3.72 (d, J = 10.4 Hz, 1H), 1.48 (s, 3H), 1.42 (s, 3H); hydrate: ^{13}C NMR (100 MHz, $CDCl_3$) 153.1, 142.4, 140.7, 137.8, 129.3, 129.0, 128.7, 126.4, 125.3, 119.3, 116.6, 110.3, 101.6, 91.0, 76.2, 73.3, 63.0, 53.2, 42.1, 27.3, 24.8; HRMS calcd for $C_{23}H_{24}NO_6$ (M+1) 410.1604, found 410.1616.

Ketone (5-25) (yy0630-1, DLG-XII-30K) white solid; mp 138-140 °C; $[\alpha]^{20}_D$ = -34.8 (*c*, 0.46, EtOH); IR (film) 3374, 1748 cm^{-1}; hydrate: ^{1}H NMR (300 MHz, $CDCl_3$) δ 7.22 (s, 1H), 6.76 (m, 2H), 5.96 (s, 2H), 4.48 (d, J = 9.9 Hz, 1H), 4.43 (m, 2H), 4.35-4.28 (m, 1H), 4.01 (d, J = 13.2 Hz, 1H), 3.81 (brs, 1H), 3.78 (d, J = 9.9 Hz, 1H), 3.56 (brs, 1H), 1.59 (s, 3H), 1.41 (s, 3H); ^{13}C NMR (100 MHz, $CO(CD_3)_2$) δ 153.4, 149.0, 145.0, 134.0, 112.1, 110.5, 108.8, 102.4, 101.7, 92.4, 77.4, 74.5, 64.8, 55.1, 26.7, 25.0; HRMS calcd for $C_{17}H_{17}NO_8$ (M+) 363.0954, found 363.0951.

Ketone (5-26) (yy0622-2, DLG-XII-30H) white solid; mp 78-80 °C; $[\alpha]^{20}_D$ = -45.7 (*c*, 0.07, $CHCl_3$); IR (film) 3450, 1774 cm^{-1}; ^{1}H NMR (300 MHz, $CDCl_3$) δ 7.43-7.38 (m, 1H), 7.23-7.16 (m, 2H), 4.87 (d, J = 5.4 Hz, 1H), 4.74 (d, J = 10.5 Hz, 1H), 4.67-4.60 (m, 2H), 4.26 (d, J = 13.8 Hz, 1H), 3.74 (d, J = 10.5 Hz, 1H), 2.94-2.82 (m, 4H), 2.13-2.02 (m, 2H), 1.48 (s, 3H), 1.43 (s, 3H); ^{13}C NMR (100 MHz, $CDCl_3$) δ 153.4, 145.6, 141.1, 135.7, 124.8, 117.4, 115.9, 110.4, 101.7, 91.1, 76.2, 73.4, 63.0, 53.8, 33.2, 32.5, 26.5, 25.8, 24.9; Anal. Calcd for $C_{19}H_{21}NO_6$: C, 63.50; H, 5.89; N, 3.90. Found: C, 63.39; H, 5.76; N, 3.79.

Ketone (5-27) (yy0706-f, DLG-XII-30G) white solid; mp 140-142 °C; $[\alpha]^{20}_D$ = -33.3 (*c*, 0.38, EtOH); IR (film) 3400, 1749 cm^{-1}; hydrate: ^1H NMR (300 MHz, $CDCl_3$) δ 7.06 (d, *J* = 2.4 Hz, 1H), 6.97 (dd, J = 8.7, 2.4 Hz, 1H), 6.83 (d, J = 8.7 Hz, 1H), 4.47 (d, *J* = 10.2 Hz, 1H), 4.42 (s, 2H), 4.32 (dd, *J* = 13.2, 1.8 Hz, 1H), 4.26-4.20 (m, 4H), 4.01 (d, *J* = 13.2 Hz, 1H), 3.77 (d, *J* = 10.2 Hz, 1H), 3.72 (brs, 1H), 3.46 (brs, 1H), 1.59 (s, 3H), 1.41 (s, 3H); ^{13}C NMR (100 MHz, $CO(CD_3)_2$) δ 153.3, 144.7, 141.2, 133.2, 118.0, 112.2, 110.4, 108.6, 102.4, 92.4, 77.4, 74.5, 65.4, 65.1, 64.7, 54.8, 26.7, 25.0; Anal. Calcd for $C_{18}H_{19}NO_8$: C, 57.29; H, 5.08; N, 3.71. Found: C, 57.15; H, 5.15; N, 3.53.

Ketone (5-28) (yy-0717-p, DLG-XII-30G) white solid; mp 195-197 °C; $[\alpha]^{20}_D$ = -82.6 (*c*, 0.12, $CHCl_3$); IR (film) 3400, 1757 cm^{-1}; hydrate: ^1H NMR (300 MHz, $CDCl_3$) δ 7.75-7.64 (m, 3H), 7.48-7.24 (m, 4H), 4.63 (d, *J* = 10.2 Hz, 1H), 4.46 (m, 2H), 4.35 (dd, *J* = 12.9, 2.1 Hz, 1H), 4.05 (brs, 1H), 4.02 (d, *J* = 12.9 Hz, 1H), 3.88 (d, *J* = 10.2 Hz, 1H), 3.88 (brs, 1H), 3.81 (s, 2H), 1.61 (s, 3H), 1.42 (s, 3H); ^{13}C NMR (100 MHz, $CDCl_3$) δ 153.3, 144.5, 143.3, 141.1, 138.6, 136.2, 127.0, 126.7, 125.2, 120.3, 119.9, 117.8, 116.2, 110.5, 101.9, 91.3, 76.2, 73.4, 63.2, 53.7, 37.2, 26.5, 24.9; HRMS calcd for $C_{23}H_{22}NO_6$ (M+1) 408.1447, found 408.1439.

Representative Asymmetric Epoxidation Procedure (Table 5.2, Entry 1) (DLG-VII-39). To a solution of styrene (0.010 g, 0.1 mmol) and ketone **5-11** (0.005 g, 0.015 mmol) in DME (1.5 mL) were added buffer (0.2 M K_2CO_3-AcOH

in 4 x 10^{-4} M aq. EDTA, pH 8.0) (1.0 mL) and TBAHS (0.005 g, 0.015 mmol) with stirring. After the mixture was cooled to about -10 °C (NaCl-ice bath temperature), a solution of Oxone (0.212 M in 4 x 10^{-4} M aq. EDTA, 0.84 mL) and a solution of K_2CO_3 (0.479 M in 4 x 10^{-4} M aq. EDTA, 0.84 mL) were added dropwise separately over 3.5 h via syringe pump. The reaction was quenched by addition of pentane and extracted with pentane. The crude extract was then analyzed directly by GC.

Representative Asymmetric Epoxidation Procedure (Table 5.3, Entry 2) (DLG-VII-50). To a solution of styrene (0.010 g, 0.1 mmol) and ketone **5-2** (0.005 g, 0.015 mmol) in DME (1.5 mL) were added buffer (0.2 M K_2CO_3-AcOH in 4 x 10^{-4} M aq. EDTA, pH 8.0) (1.0 mL) and TBAHS (0.005 g, 0.015 mmol) with stirring. After the mixture was cooled to about -10 °C (NaCl-ice bath temperature), a solution of Oxone (0.212 M in 4 x 10^{-4} M aq. EDTA, 0.84 mL) and a solution of K_2CO_3 (0.479 M in 4 x 10^{-4} M aq. EDTA, 0.84 mL) were added dropwise separately over 3.5 h via syringe pump. The reaction was quenched by addition of pentane and extracted with pentane. The crude extract was then analyzed directly by GC.

Representative Asymmetric Epoxidation Procedure (Table 5.4, Entry 3) (DLG-XI-7). To a solution of 4-chlorostyrene (0.055 g, 0.4 mmol) and ketone **5-2** (0.021 g, 0.06 mmol) in DME (6.0 mL) were added buffer (0.1 M K_2CO_3-AcOH in 4 x 10^{-4} M aq. EDTA, pH 9.3) (4.0 mL) and TBAHS (0.010 g, 0.03

mmol) with stirring. After the mixture was cooled to about -10 to -15 °C (bath temperature) via a NaCl-ice bath, a solution of Oxone (0.212 M in 4 x 10^{-4} M aq. EDTA, 5.04 mL) and a solution of K_2CO_3 (0.84 M in 4 x 10^{-4} M aq. EDTA, 5.04 mL) were added dropwise separately over 8 h via syringe pump. The reaction was quenched by addition of pentane and extracted with pentane. The combined organic layers were dried (Na_2SO_4), filtered, concentrated, and purified by flash chromatography [the silica gel was buffered by 1% Et_3N in pentane; pentane:ether (1:0 to 10:1) was used as the eluent] to give 4-chlorostyrene oxide as a colorless oil (0.0526 g, 85%, 86% ee).

(Table 5.4, Entry 1) (DLG-XI-10)

(-)-(R)-Styrene oxide[75] colorless oil; $[\alpha]^{20}_D$ = -5.74 (*c* 1.7, $CHCl_3$).

(Table 5.4, Entry 2) (DLG-XI-27)

(-)-2-Fluorostyrene oxide[76] yellow oil; $[\alpha]^{20}_D$ = -8.21 (*c* 2.2, $CHCl_3$); IR (film) 3055 cm^{-1}; ^1H NMR (300 MHz, $CDCl_3$) δ 7.20-6.89 (m, 4H), 4.04-4.01 (m, 1H), 3.04 (dd, *J* = 5.7, 4.2 Hz, 1H), 2.66 (dd, *J* = 5.7, 2.7 Hz, 1H); ^{13}C NMR (75 MHz, $CDCl_3$) δ 161.7 (d, *J* = 245.1 Hz), 129.5 (d, *J* = 7.3 Hz), 126.0 (d, *J* = 4.8 Hz), 125.1 (d, *J* = 13.4 Hz), 124.4 (d, *J* = 3.7 Hz), 115.3 (d, *J* = 20.6 Hz), 50.5, 47.1 (d, *J* = 6.1 Hz).

(Table 5.4, Entry 3) (DLG-XI-7)

(-)-(R)-4-Chlorostyrene oxide[75] yellow oil; $[\alpha]^{20}_D$ = -14.6 (*c* 1.63, $CHCl_3$); IR (film) 2991 cm^{-1}; ^1H NMR (300 MHz, $CDCl_3$) δ 7.32 (d, *J* = 8.4 Hz, 2H), 7.21 (d, *J* = 8.4 Hz, 2H), 3.87-3.81 (m, 1H), 3.15 (dd, *J* = 5.4, 4.2 Hz, 1H), 2.75 (dd, *J* = 5.4, 2.7 Hz, 1H); ^{13}C NMR (75 MHz, $CDCl_3$) δ 136.3, 133.9, 128.8, 126.9, 51.8, 51.3.

(Table 5.4, Entry 4) (DLG-XI-12)

(-)-(R)-4-Bromostyrene oxide[78] colorless oil; $[\alpha]^{20}_D$ = -13.0 (*c* 1.66, $CHCl_3$); IR (film) 2990 cm^{-1}; ^1H NMR (300 MHz, $CDCl_3$) δ 7.47 (d, *J* = 8.4 Hz, 2H), 7.15 (d, *J* = 8.4 Hz, 2H), 3.85-3.80 (m, 1H), 3.17-3.12 (m, 1H), 2.75 (dd, *J* = 5.4, 2.4 Hz, 1H); ^{13}C NMR (75 MHz, $CDCl_3$) δ 136.7, 131.6, 127.2, 122.0, 51.9, 51.4.

(Table 5.4, Entry 5) (DLG-XII-16)

(-)-(R)-4-Cyanostyrene oxide[78] white solid; $[\alpha]^{20}_D$ = -26.8 (*c* 2.05, $CHCl_3$); IR (film) 2228 cm^{-1}; ^1H NMR (300 MHz, $CDCl_3$) δ 7.63 (d, *J* = 8.4 Hz, 2H), 7.38 (d, *J* = 8.4 Hz, 2H), 3.92-3.88 (m, 1H), 3.22-3.18 (m, 1H), 2.75 (dd, *J* = 5.4, 2.4 Hz, 1H); ^{13}C NMR (75 MHz, $CDCl_3$) δ 143.3, 132.5, 126.2, 118.8, 112.1, 51.9.

(Table 5.4, Entry 6) (DLG-XI-28)

(-)-(R)-4-Nitrostyrene oxide[78] yellow solid; $[\alpha]^{20}_D$ = -27.6 (*c* 1.26, $CHCl_3$); ^1H NMR (400 MHz, $CDCl_3$) δ 8.22 (d, *J* = 8.4 Hz, 2H), 7.45 (d, *J* = 8.4 Hz, 2H),

3.96 (dd, J = 4.0, 2.4 Hz, 1H), 3.23 (dd, J = 5.6, 4.0 Hz, 1H), 2.78 (dd, J = 5.6, 2.4 Hz, 1H).

(Table 5.4, Entry 7) (DLG-XI-32)

(-)-(R)-4-Trifuloromethylstyrene oxide[79] yellow oil; $[\alpha]^{20}_D$ = -3.37 (*c* 1.75, $CHCl_3$); IR (film) 2996 cm^{-1}; ^1H NMR (300 MHz, $CDCl_3$) δ 7.60 (d, J = 8.1 Hz, 2H), 7.39 (d, J = 8.1 Hz, 2H), 3.94-3.90 (m, 1H), 3.25-3.16 (m, 1H), 2.77 (dd, J = 5.7, 2.7 Hz, 1H); ^{13}C NMR (75 MHz, $CDCl_3$) δ 125.9, 125.6, 125.6, 52.0, 51.7.

(Table 5.4, Entry 8) (OAW-0226)

(-)-3-Benzyloxystyrene oxide[98] white solid; $[\alpha]^{20}_D$ = -3.37 (*c* 1.75, $CHCl_3$); IR (film) 2980 m^{-1}; ^1H NMR (300 MHz, $CDCl_3$) δ 7.45-7.24 (m, 6H), 6.95-6.89 (m, 3H), 5.07 (s, 2H), 3.84 (dd, J = 4.0, 2.8 Hz, 1H), 3.13 (dd, J = 5.6, 4.0 Hz, 1H), 2.77 (dd, J = 5.6, 2.8 Hz, 1H); ^{13}C NMR (100 MHz, $CDCl_3$) δ 159.3, 139.5, 137.0, 129.8, 128.8, 128.2, 127.7, 118.4, 114.9, 111.7, 70.2, 52.5, 51.4.

(Table 5.4, Entry 9) (DLG-XI-11)

(-)-3-Methylstyrene oxide yellow oil; $[\alpha]^{20}_D$ = -7.67 (*c* 1.76, $CHCl_3$); IR (film) 2990 cm^{-1}; ^1H NMR (300 MHz, $CDCl_3$) δ 7.25-7.20 (m, 1H), 7.14-7.05 (m, 3H), 3.83 (dd, J = 3.9, 2.7 Hz, 1H), 3.13 (dd, J = 5.4, 3.9 Hz, 1H), 2.80 (dd, J = 5.4, 2.7 Hz, 1H), 2.35 (s, 3H); ^{13}C NMR (75 MHz, $CDCl_3$) δ 138.1, 137.5, 128.9, 128.4,

[98] Reaction carried out by O. Andrea Wong.

126.0, 122.7, 52.5, 51.2, 21.5; HRMS Calcd for $C_9H_{10}O$ (M+) 134.0732, found 134.0735.

(Table 5.4, Entry 10) (DLG-XIV-5b)

(-)-3-Chlorostyrene oxide[75] yellow oil; $[\alpha]^{20}_D$ = -5.96 (*c* 1.76, $CHCl_3$); IR (film) 2992 cm^{-1}; ^1H NMR (300 MHz, $CDCl_3$) δ 7.22-7.03 (m, 4H), 3.77 (dd, *J* = 3.9, 2.4 Hz, 1H), 3.08 (dd, *J* = 5.4, 3.9 Hz, 1H), 2.69 (dd, *J* = 5.4, 2.4 Hz, 1H); ^{13}C NMR (75 MHz, $CDCl_3$) δ 139.9, 134.6, 129.9, 128.3, 125.5, 123.8, 51.9, 51.4.

(Table 5.4, Entry 11) (DLG-XIV-5a)

(-)-3-Nitrostyrene oxide[90] yellow solid; $[\alpha]^{20}_D$ = -1.89 (*c* 2.01, $CHCl_3$); ^1H NMR (400 MHz, $CDCl_3$) δ 8.19-8.14 (m, 2H), 7.64-7.60 (m, 1H), 7.56-7.50 (m, 1H), 3.97 (dd, *J* = 4.0, 2.4 Hz, 1H), 3.22 (dd, *J* = 5.2, 4.0 Hz, 1H), 2.81 (dd, *J* = 5.2, 2.4 Hz, 1H).

(Table 5.4, Entry 12) (DLG-XIV-6)

(-)-2-Naphthalene oxide[91,99]

(Table 5.4, Entry 13) (DLG-XII-21)

(-)-3,4-Dichlorostyrene oxide[91] yellow oil; $[\alpha]^{20}_D$ = -9.95 (*c* 2.08, $CHCl_3$); IR (film) 2993 cm^{-1}; ^1H NMR (300 MHz, $CDCl_3$) δ 7.40 (d, *J* = 8.4 Hz, 1H), 7.36 (d, *J* = 2.1 Hz, 1H), 7.12 (dd, *J* = 8.4, 2.1 Hz, 1H), 3.81 (dd, *J* = 3.9, 2.4 Hz, 1H),

[99] The intermediate was used directly in the next step without further purification.

3.15 (dd, J = 5.4, 4.2 Hz, 1H), 2.73 (dd, J = 5.4, 2.4 Hz, 1H); ^{13}C NMR (100 MHz, $CDCl_3$) δ 138.3, 133.0, 132.3, 130.7, 127.6, 125.0, 51.5, 51.4.

(Table 5.4, Entry 14) (DLG-XI-24)

(-)-3,5-Dimethylstyrene oxide yellow oil; $[\alpha]^{20}_D$ = -12.2 (*c* 1.73, $CHCl_3$); IR (film) 2919 cm^{-1}; ^1H NMR (300 MHz, $CDCl_3$) δ 6.97 (s, 1H), 6.93 (s, 2H), 3.82 (dd, J = 3.9, 2.7 Hz, 1H), 3.14 (dd, J = 5.4, 3.9 Hz, 1H), 2.81 (dd, J = 5.4, 2.7 Hz, 1H), 2.34 (s, 6H); ^{13}C NMR (75 MHz, $CDCl_3$) δ 138.2, 137.5, 129.9, 123.3, 52.5, 51.2, 21.4; HRMS calcd for $C_{10}H_{13}O$ (M+1) 149.0966, found 148.0964.

(R)-Pronethalol[91] (DLG-XIV-6, DLG-XIV-8) To a solution of 2-vinylnaphthalene (0.5 g, 3.2 mmol) and ketone **5-2** (0.32 g, 0.92 mmol) in DME (49 mL) were added buffer (0.1 M K_2CO_3-AcOH in 4 x 10^{-4} M aq. EDTA, pH 9.3) (32 mL) and TBAHS (0.081 g, 0.24 mmol) with stirring. After the mixture was cooled to about -10 to -15 °C (bath temperature) via a NaCl-ice bath, a solution of Oxone (0.212 M in 4 x 10^{-4} M aq. EDTA, 40.3 mL) and a solution of K_2CO_3 (0.84 M in 4 x 10^{-4} M aq. EDTA, 40.3 mL) were added dropwise separately over 12 h via syringe pump. The reaction was quenched by addition of pentane and extracted with pentane. The combined organic layers were dried (Na_2SO_4), filtered, concentrated, and purified by flash chromatography [the silica gel was buffered by 1% Et_3N in pentane; pentane:ether (1:0 to 10:1) was used as the eluent] to give naphthalene oxide as a white solid 0.5 g, 91%, 87% ee). To a solution of 2-naphthalene oxide (0.5 g, 2.9 mmol, 87% ee) in 2.5 mL of MeOH

was added *i*-propylamine (5 mL). After stirring at 40° C for 24 h, the mixture was concentrated to give a yellow solid and recrystalized (isopropanol/hexane) to give (R)-pronethatol (0.30 g, 1.31 mmol, 45 %) as an off white solid. $[\alpha]^{20}_{D}$ = -26.0 (*c*, 0.62, EtOH) (99% ee); IR (film) 3134 cm^{-1}; ^{1}H NMR (400 MHz, $CDCl_3$) δ 7.84-7.80 (m, 4H), 4.48-7.46 (m, 3H). 4.85 (dd, *J* = 8.4, 3.6 Hz, 1H), 3.01 (dd, *J* = 12.0, 3.6 Hz, 1H), 2.85 (sept, *J* = 6.0 Hz, 1H), 2.75 (dd, *J* = 12.0, 8.4 Hz, 1H), 1.09 (d, *J* = 6.0 Hz, 6H); ^{13}C NMR (75 MHz, $CDCl_3$) δ 140.4, 133.5, 133.1, 128.3, 128.1, 127.9, 126.3, 125.9, 124.7, 124.2, 72.2, 54.7, 48.9, 23.4, 32.2; HRMS calcd for $C_{15}H_{20}NO$ (M+1) 230.1546, found 230.1544.

Representative Asymmetric Epoxidation Procedure (Table 5.5, Entry 1) (DLG-VIII-47). To a solution of cis-β-methylstyrene (0.012 g, 0.1 mmol) and ketone **5-10** (0.006 g, 0.015 mmol) in DME (1.5 mL) were added buffer (0.2 M K_2CO_3-AcOH in 4 x 10^{-4} M aq. EDTA, pH 9.3) (1.0 mL) and TBAHS (0.005 g, 0.015 mmol) with stirring. After the mixture was cooled to about -10 °C (NaCl-ice bath temperature), a solution of Oxone (0.212 M in 4 x 10^{-4} M aq. EDTA, 0.84 mL) and a solution of K_2CO_3 (0.84 M in 4 x 10^{-4} M aq. EDTA, 0.84 mL) were added dropwise separately over 3.5 h via syringe pump. The reaction was quenched by addition of pentane and extracted with pentane. The crude extract was then analyzed directly by GC.

Representative Asymmetric Epoxidation Procedure (Table 5.6, Entry 10) (DLG-VIII-47). To a solution of cis-β-methylstyrene (0.012 g, 0.1 mmol) and ketone **5-10** (0.006 g, 0.015 mmol) in DME:DMM (3:1, 1.5 mL) were added buffer (0.2 M K_2CO_3-AcOH in 4 x 10^{-4} M aq. EDTA, pH 9.3) (1.0 mL) and TBAHS (0.005 g, 0.015 mmol) with stirring. After the mixture was cooled to about -10 °C (NaCl-ice bath temperature), a solution of Oxone (0.212 M in 4 x 10^{-4} M aq. EDTA, 0.84 mL) and a solution of K_2CO_3 (0.84 M in 4 x 10^{-4} M aq. EDTA, 0.84 mL) were added dropwise separately over 3.5 h via syringe pump. The reaction was quenched by addition of pentane and extracted with pentane. The crude extract was then analyzed directly by GC.

Improved Synthesis of Ketone 5-2

Aminoalcohol 5-35 (DLG-XIII-43) Water (3.8 mL) and acetic acid (17.4 M, 0.12 mL) were added to a mixture of D-Glucose (20 g, 111 mmol) and 4-ethylaniline (16.6 mL, 134 mmol) in a 500 mL round bottom flask. This mixture was warmed to and stirred at 90°C (water bath temperature) by a rotory evaporator without vacuum but not open to air. A brown solid was observed after 30 min., and the mixture was stirred for an additional 60 min. at 90°C. The flask was then removed from the warm water bath and allowed to cool to rt. Ether (120 mL) and EtOH (30 mL) were then added, and the solid on the side of the flask was broken up with a spatula. The mixture was allowed to stir at room temperature for an additional hour. The mixture was then filtered, and the filter

cake was washed with ether, ether:EtOH (5:1), and ether. Drying overnight under vacuum gave the product (**5-35**) as a white solid (19.7 g, 63 %).

Alcohol 5-37 (DLG-XIII-44, DLG-XIII-45) H_2SO_4 (5.6 mL) was added to a suspension of diol (19.7 g, 69.5 mmol) and dimethoxypropane (25.6 mL) in acetone (162 mL) at 0°C. The mixture was then stirred at 0°C (ice water bath) for 90 min. in a rotory evaporator without vacuum but not open to air. Initially, the viscous reaction mixture became more fluid. After time, the white product began precipitating out of the reaction mixture, so the viscosity increased once again. Ether was added, and the mixture was filtered. After washing with acetone:ether (1:4, 3x) and ether, the filter cake was dried under vacuum for 30 min. to give **5-44** as a white solid that was used without further purification. A suspension of aminoalcohol (**5-44**) and $NaHCO_3$ (46.7 g, 556 mmol) in freshly distilled DCM (166 mL) was stirred for 1 h at 0°C (ice water bath) in a rotory evaporator without vacuum but not open to air. Diisopropylamine (4.8 mL, 34.2 mmol) was then added at 0°C, and the reaction mixture became more fluid as it was allowed to stir for 15 min. at 0°C. Phosgene (20% in toluene, 43 mL) was then added over 5 h via syringe pump at 0°C. After stirring overnight while warming to room temperature, the mixture became more fluid. The mixture was then filtered through a pad of silica gel, and washed with additional EtOAc. After removing the solvent with the rotory evaporator, the white solid product (**5-37**) (20.7 g, 85% over 2 steps) was dried for an additional hour under high vacuum.

PDC Oxidation

Ketone 5-2 (DLG-XIII-46) Acetic acid (5 drops) was added to a mixture of PDC (33.2 g, 88.3 mmol), 3A MS (53.2 g), and alcohol **5-37** (20.7 g, 59.2 mmol) in DCM (285 mL) at rt, and the capped reaction mixture was allowed to stir for 14 h. The reaction mixture was then filtered through a plug of silica gel and washed with additional EtOAc : hexane (3:1) until the yellow color finished coming off the plug. Concentration on the rotory evaporator give a yellow oil that turned to a yellow solid after drying on a high vacuum for 4 h to remove pyridine. EtOAc (100 mL) was then added to dissolve the product. After addition of hexane (100 mL), the solution was concentrated on a rotory evaporator (no water bath) until crystals began forming on the side of the flask. The mixture was then cooled in the freezer for 4 h and filtered to give some product, and the mother liquor was concentrated on the rotory evaporator (bath temperature 70 °C) until crystals began forming again. After cooling in the freezer overnight, the mixture was filtered again and washed with 100 mL of hexane to give **5-2** (12.0 g, 58%) as a white solid.

TEMPO Oxidation

Ketone 5-2 (MX-4-41) To a solution of alcohol **5-37** (31.4 g, 90 mmol) in DCM-toluene (5:1, 360 mL), was added NaBr (9.26 g, 90 mmol). After cooling to 0°C, TEMPO (143 mg, 0.9 mmol) was added. NaOCl at pH 9.3 (0.67 M prepared with $NaHCO_3$ solution, 23.4 mg/mL, 270 mL, 180 mmol) was then added over 2.5 h with vigorous stirring (the reaction was monitored by GC). The

reaction layers were separated and the aqueous phase was extracted with MeCN (2x). The combined organics were washed with satd $Na_2S_2O_3$ (2x), water (6x) until the organic phase became clear, and dried (Na_2SO_4). The organics were then filtered through a pad of silica gel, washed with EtOAc, and concentrated to 20 mL. Following addition of hexane (500 mL), the mixture was shaken until the product precipitated. Filtration and recrystallization (EtOAc: hexane) (1:1, 30 mL: 30 mL) gave the catalyst (**5-2**) as an off white solid (18.4 g, 59%).

Representative Asymmetric Epoxidation Procedure (Table 5.11, Entry 1) (DLG-XIV-18). To a solution of styrene (0.105 g, 1.0 mmol) and ketone **5-2** (0.052 g, 0.15 mmol) in DME (6.0 mL) were added buffer (0.2 M K_2CO_3-AcOH in 4 x 10^{-4} M aq. EDTA, pH 9.3) (2.0 mL) and TBAHS (0.014 g, 0.04 mmol) with stirring. After the mixture was cooled to about 0 °C (ice bath temperature), a solution of Oxone (0.46 M in 4 x 10^{-4} M aq. EDTA, 3.0 mL) and a solution of KOH (1 M in 4 x 10^{-4} M aq. EDTA, 3.0 mL) were added dropwise separately over 6 h via syringe pump. The reaction was quenched by addition of pentane and extracted with pentane. The crude extract was then analyzed directly by GC.

Representative Asymmetric Epoxidation Procedure (Table 5.12, Entry 1) (DLG-XIV-19). To a solution of 3-methylstyrene (0.118 g, 1.0 mmol) and ketone **5-2** (0.104 g, 0.30 mmol) in DME (5.0 mL) were added buffer (0.2 M K_2CO_3-AcOH in 4 x 10^{-4} M aq. EDTA, pH 9.3) (3.0 mL) and TBAHS (0.014 g, 0.04 mmol) with stirring. After the mixture was cooled to about 0 °C (ice bath

temperature), a solution of Oxone (0.46 M in 4 x 10^{-4} M aq. EDTA, 3.0 mL) and a solution of KOH (1 M in 4 x 10^{-4} M aq. EDTA, 3.0 mL) were added dropwise separately over 16 h via syringe pump. The reaction was quenched by addition of pentane and extracted with pentane. The crude extract was then analyzed directly by GC.

Representative Asymmetric Epoxidation Procedure (Table 5.13, Entry 1) (DLG-XIV-19). To a solution of 3-methylstyrene (0.59 g, 5.0 mmol) and ketone **5-2** (0.521 g, 1.5 mmol) in DME (8.3 mL) were added buffer (0.2 M K_2CO_3-AcOH in 4 x 10^{-4} M aq. EDTA, pH 9.3) (5.0 mL) and TBAHS (0.014 g, 0.04 mmol) with stirring. After the mixture was cooled to about 0 °C (ice bath temperature), a solution of Oxone (0.46 M in 4 x 10^{-4} M aq. EDTA, 15 mL) and a solution of KOH (3 M in 4 x 10^{-4} M aq. EDTA, 5.0 mL) were added dropwise separately over 16 h via syringe pump. The reaction was quenched by addition of pentane and extracted with pentane. The crude extract was then analyzed directly by GC.

Representative Asymmetric Epoxidation Procedure (Table 5.14, Entry 1) (DLG-XIV-19). To a solution of 3-methylstyrene (0.59 g, 5.0 mmol) and ketone **5-2** (0.521 g, 1.5 mmol) in DME (25 mL) were added buffer (0.2 M K_2CO_3-AcOH in 4 x 10^{-4} M aq. EDTA, pH 9.3) (15 mL) and TBAHS (0.014 g, 0.04 mmol) with stirring. After the mixture was cooled to about 0 °C (ice bath temperature), a solution of Oxone (0.46 M in 4 x 10^{-4} M aq. EDTA, 15 mL) and a

solution of KOH (3 M in 4 x 10^{-4} M aq. EDTA, 5.0 mL) were added dropwise separately over 16 h via syringe pump. The reaction was quenched by addition of pentane and extracted with pentane. The crude extract was then analyzed directly by GC

Optimized Large Scale Epoxidation Procedure

3-Methylstyrene Oxide[99] (Table 5.15, Entry 3) (DLG-XIV-20) To a solution of 3-methylstyrene (5.0 g, 42.3 mmol) and ketone **5-2** (2.2 g, 6.3 mmol) in DME (250 mL) were added buffer (0.2 M K_2CO_3-AcOH in 4 x 10^{-4} M aqueous EDTA, pH 9.3) (85 mL) and TBAHS (0.050 g, 0.15 mmol) with stirring. After the mixture was cooled to -10°C (bath temperature), a solution of Oxone (0.46 M in 4 x 10^{-4} M aqueous EDTA, 127 mL) and a solution of K_2CO_3 (1.93 M x 10^{-4} M aqueous EDTA, 127 mL) were added dropwise separately over a period of 5 h via addition funnels. After stirring for an additional 10 min., the reaction mixture was quenched by addition of pentane and extracted with pentane. The combined organic layers were dried (Na_2SO_4), filtered, and concentrated. Silica gel chromatography (pentane:ether (1:0 to 2:1) gave 3-methylstyrene oxide (5.15 g, 91%, 88% ee) as a yellow oil.

SUPPLEMENTARY MATERIAL

CHROMATOGRAPHS FOR EPOXIDE EE DETERMINATION

Table 2.1 Entry 1; 2-11
Column : B-DM
Oven temp: 105 °C
Pressure: 30 psi

Racemate

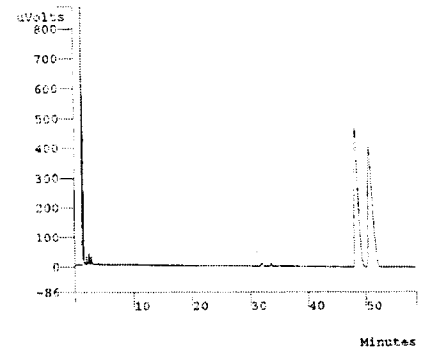

Peak No	Peak Name	Result ()	Ret. Time (min)	Time Offset (min)
1		50.2594	48.088	0.000
2		49.7406	50.537	0.000
	Totals	100.0000		0.000

Epoxidation with Ketone 1-16

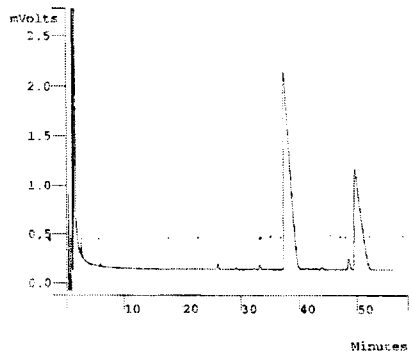

Peak No	Peak Name	Result ()	Ret. Time (min)	Time Offset (min)
1		64.0392	37.411	0.000
2		1.1530	48.516	0.000
3		34.8078	49.583	0.000
	Totals	100.0000		0.000

Epoxidation with Ketone 2-1

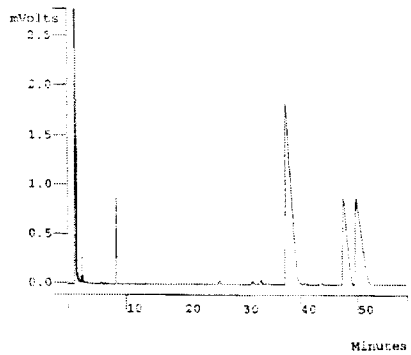

Peak No	Peak Name	Result ()	Ret. Time (min)	Time Offset (min)
1		52.2434	37.498	0.000
2		19.7387	47.516	0.000
3		28.0179	49.708	0.000
	Totals	100.0000		0.000

Table 2.1, 2-12
Column : Chiracel AD
Solvent: 98% Heptanes, 2% IPA
Flow: 1.0 mL/min
Detector: 220 nm

Racemate

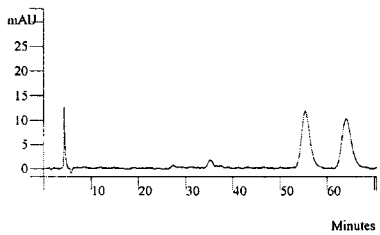

Peak No	Ret Time (min)	Result ()	Peak Area (counts)
1	55.246	50.3694	753578
2	64.044	49.6306	742525
		100.0000	**1496103**

Epoxidation with Ketone 2-1

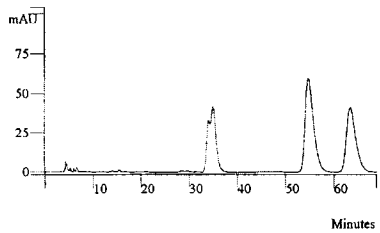

Peak No	Ret Time (min)	Result ()	Peak Area (counts)
1	54.749	56.4898	3780172
2	63.416	43.5102	2911605
		100.0000	**6691777**

Epoxidation with Ketone 1-16

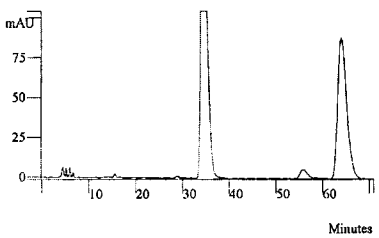

Peak No	Ret Time (min)	Result ()	Peak Area (counts)
1	55.917	4.3693	289110
2	64.004	95.6307	6327755
		100.0000	**6616865**

Table 2.1, 2-13
Column : Chiracel OB
Solvent: 99% Hexanes, 1% IPA
Flow: 0.5 mL/min
Detector: 220 nm

Racemate

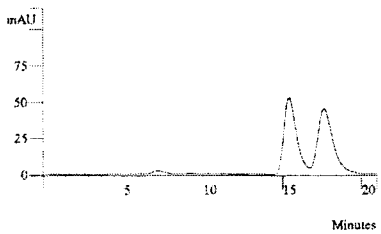

Peak No	Ret Time (min)	Result ()	Peak Area (counts)
1	15.416	49.2601	1556501
2	17.619	50.7399	1603260
		100.0000	**3159761**

Epoxidation with Ketone 2-1

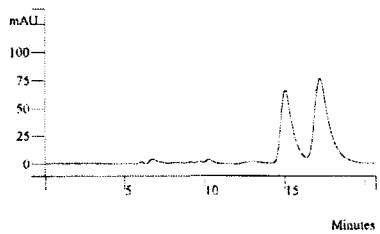

Peak No	Ret Time (min)	Result ()	Peak Area (counts)
1	15.006	41.3137	1581098
2	17.167	58.6863	2245962
		100.0000	**3827060**

Epoxidation with Ketone 1-16

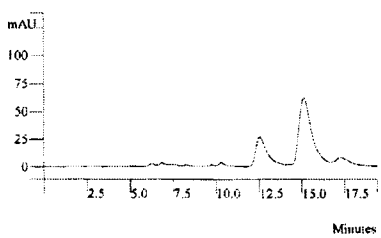

Peak No	Ret Time (min)	Result ()	Peak Area (counts)
1	15.101	93.9094	1553648
2	17.274	6.0906	100764
		100.0000	**1654412**

Table 2.1, Phenylcyclohexene oxide
Column : B-DM
Oven temp: 105 °C
Pressure: 30 psi

Racemate

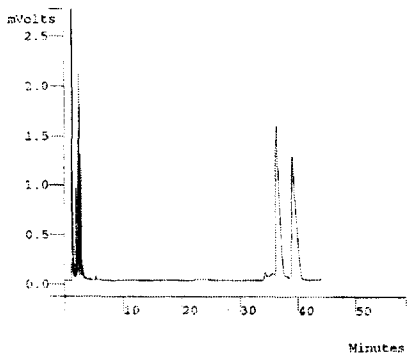

Peak No	Peak Name	Result ()	Ret. Time (min)	Time Offset (min)
1		49.6349	36.294	0.000
2		50.3651	39.054	0.000
	Totals	100.0000		0.000

Epoxidation with Ketone 2-1

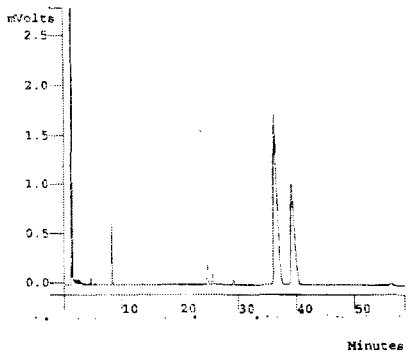

Peak No	Peak Name	Result ()	Ret. Time (min)	Time Offset (min)
1		62.8276	36.109	0.000
2		37.1724	39.121	0.000
	Totals	100.0000		0.000

Epoxidation with Ketone 1-16

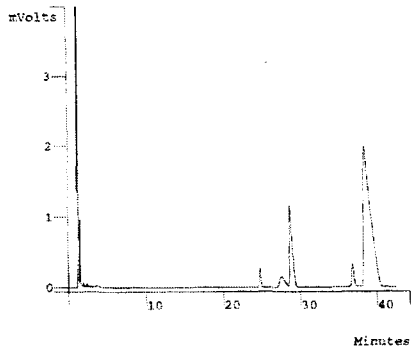

Peak No	Peak Name	Result ()	Ret. Time (min)	Time Offset (min)
1		17.1047	28.653	0.000
2		3.8076	36.776	0.000
3		79.0877	38.396	0.000
	Totals	100.0000		0.000

Table 2.1, 2-14
Column : B-DM
Oven temp: 95 °C
Pressure: 30 psi

Racemate

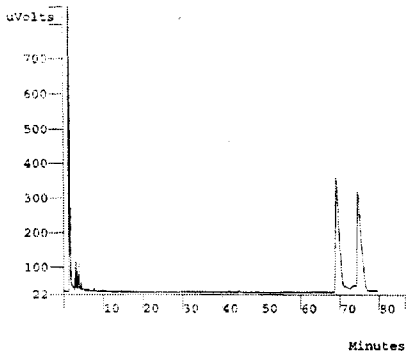

Peak No	Peak Name	Result ()	Ret. Time (min)	Time Offset (min)
1		51.7626	69.071	0.000
2		48.2374	74.604	0.000
	Totals	100.0000		0.000

Epoxidation with Ketone 2-1

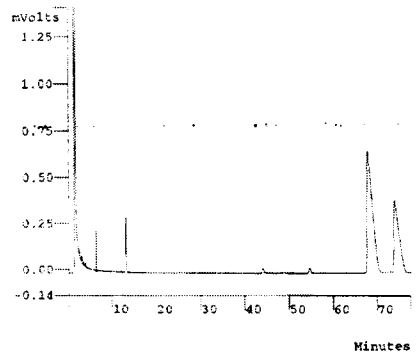

Peak No	Peak Name	Result ()	Ret. Time (min)	Time Offset (min)
1		63.4789	67.809	0.000
2		36.5211	73.984	0.000
	Totals	100.0000		0.000

Epoxidation with Ketone 1-16

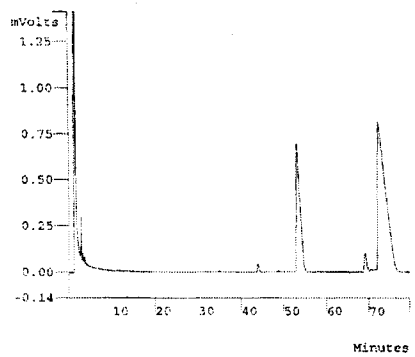

Peak No	Peak Name	Result ()	Ret. Time (min)	Time Offset (min)
1		28.4960	53.126	0.000
2		2.4183	69.216	0.000
3		69.0856	72.384	0.000
	Totals	99.9999		0.000

Styrene Oxide
Column : B-DM
Oven temp: 80 °C
Pressure: 25 psi

Racemate

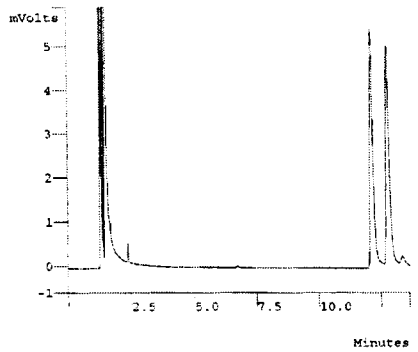

Peak No	Peak Name	Result ()	Ret. Time (min)	Time Offset (min)
1		50.0995	12.099	0.000
2		49.9005	12.743	0.000
	Totals	100.0000		0.000

Scheme 3.4, Entry 1

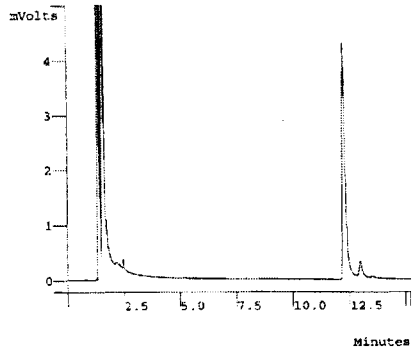

Peak No	Peak Name	Result ()	Ret. Time (min)	Time Offset (min)
1		94.2548	12.236	0.000
2		5.7452	12.977	0.000
	Totals	100.0000		0.000

Table 3.1, Entry 1

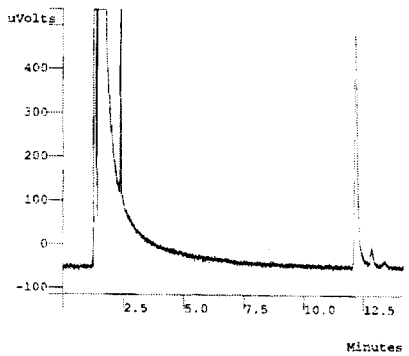

Peak No	Peak Name	Result ()	Ret. Time (min)	Time Offset (min)
1		95.0540	12.182	0.000
2		4.9460	12.849	0.000
	Totals	100.0000		0.000

Table 3.1, Entry 2
2-Fluorostyrene Oxide
Column : B-DM
Oven temp: 80 °C
Pressure: 25 psi

Racemate

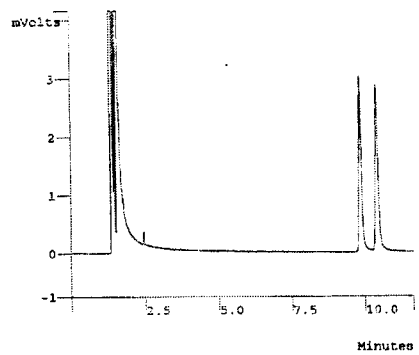

Peak No	Peak Name	Result ()	Ret. Time (min)	Time Offset (min)
1		50.3680	9.824	0.000
2		49.6320	10.394	0.000
	Totals	100.0000		0.000

Chiral Epoxide

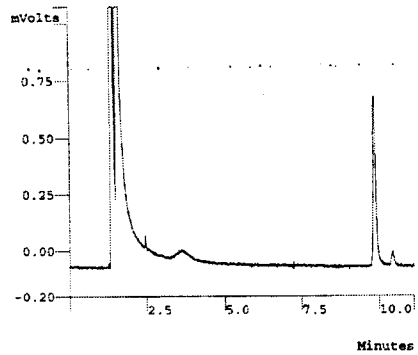

Peak No	Peak Name	Result ()	Ret. Time (min)	Time Offset (min)
1		94.3897	9.849	0.000
2		5.6103	10.441	0.000
	Totals	100.0000		0.000

Table 3.1, Entry 3
3-Fluorostyrene Oxide
Column : B-DM
Oven temp: 100 °C
Pressure: 25 psi

Racemate

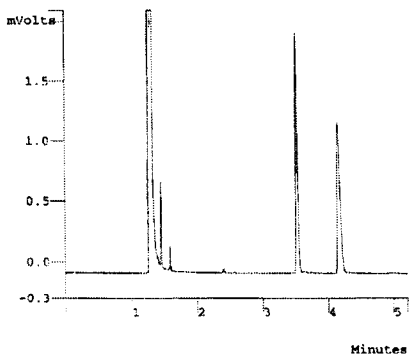

Peak No	Peak Name	Result ()	Ret. Time (min)	Time Offset (min)
1		50.4681	3.516	0.000
2		49.5319	4.151	0.000
	Totals	100.0000		0.000

Chiral Epoxide

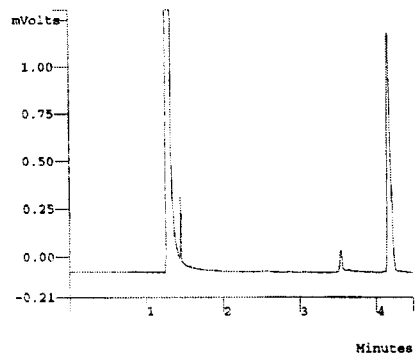

Peak No	Peak Name	Result ()	Ret. Time (min)	Time Offset (min)
1		5.1969	3.531	0.000
2		94.8031	4.154	0.000
	Totals	100.0000		0.000

Table 3.1, Entry 4
3-Methylstyrene Oxide
Column : B-DM
Oven temp: 60 °C
Pressure: 20 psi

Racemate

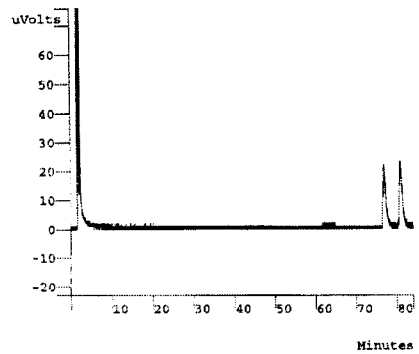

Peak No	Peak Name	Result ()	Ret. Time (min)	Time Offset (min)
1		50.1996	76.842	0.000
2		49.8004	80.891	0.000
	Totals	100.0000		0.000

Chiral Epoxide

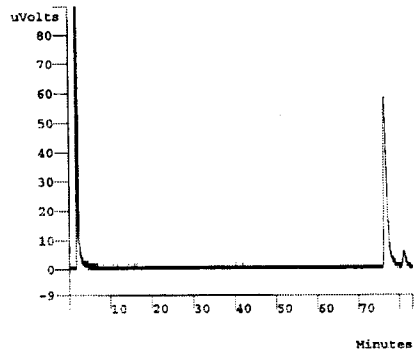

Peak No	Peak Name	Result ()	Ret. Time (min)	Time Offset (min)
1		96.2861	76.427	0.000
2		3.7139	81.033	0.000
	Totals	100.0000		0.000

Table 3.1, Entry 5
3,5-Dimethylstyrene Oxide
Column : B-DM
Oven temp: 70 °C
Pressure: 20 psi

Racemate

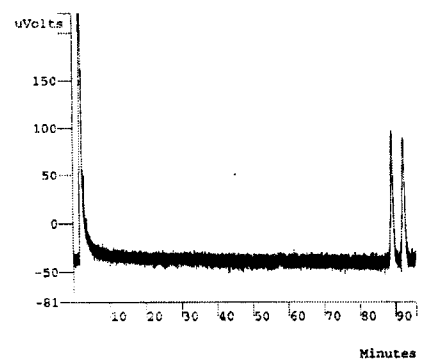

Peak No	Peak Name	Result ()	Ret. Time (min)	Time Offset (min)
1		49.2782	89.007	0.000
2		50.7218	92.313	0.000
	Totals	100.0000		0.000

Chiral Epoxide

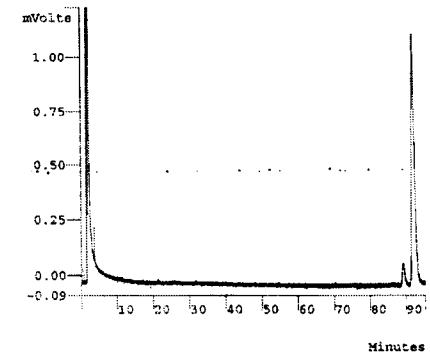

Peak No	Peak Name	Result ()	Ret. Time (min)	Time Offset (min)
1		5.2812	89.283	0.000
2		94.7188	91.923	0.000
	Totals	100.0000		0.000

Table 3.1, Entry 6
4-Fluorostyrene Oxide
Column : B-DM
Oven temp: 80 °C
Pressure: 25 psi

Racemate

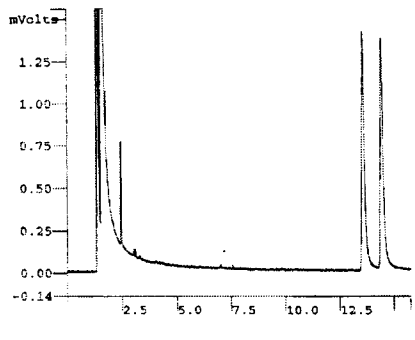

Peak No	Peak Name	Result ()	Ret. Time (min)	Time Offset (min)
1		49.6178	13.568	0.000
2		50.3822	14.424	0.000
	Totals	100.0000		0.000

Chiral Epoxide

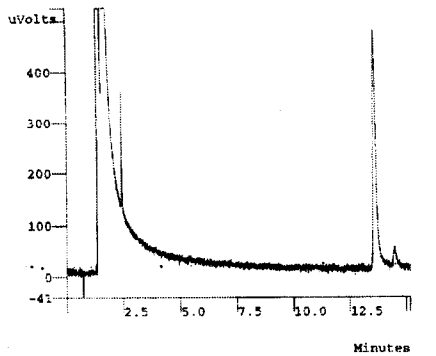

Peak No	Peak Name	Result ()	Ret. Time (min)	Time Offset (min)
1		95.1250	13.601	0.000
2		4.8750	14.481	0.000
	Totals	100.0000		0.000

Table 3.1, Entry 7
4-Chlorostyrene Oxide
Column : B-DM
Oven temp: 100 °C
Pressure: 25 psi

Racemate

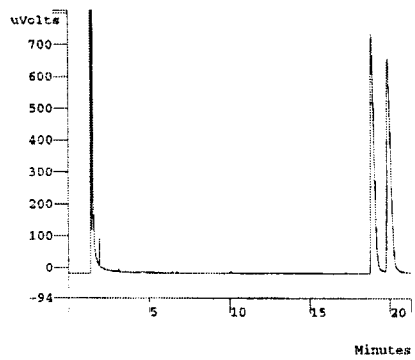

Peak No	Peak Name	Result ()	Ret. Time (min)	Time Offset (min)
1		49.4743	18.849	0.000
2		50.5257	19.868	0.000
	Totals	100.0000		0.000

Chiral Epoxide

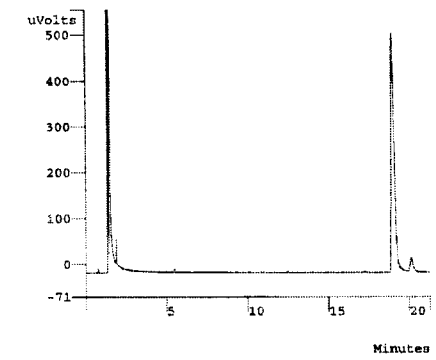

Peak No	Peak Name	Result ()	Ret. Time (min)	Time Offset (min)
1		95.3065	18.954	0.000
2		4.6935	20.134	0.000
	Totals	100.0000		0.000

Table 3.1, Entry 8
4-Bromostyrene Oxide
Column : B-DM
Oven temp: 110 °C
Pressure: 25 psi

Racemate

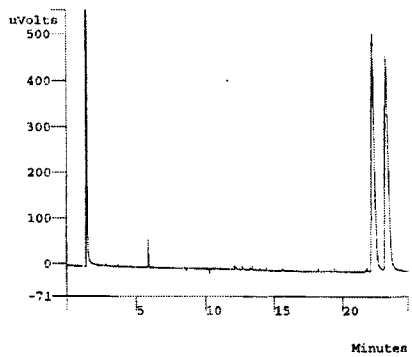

Peak No	Peak Name	Result ()	Ret. Time (min)	Time Offset (min)
1		49.4556	22.192	0.000
2		50.5444	23.179	0.000
Totals		100.0000		0.000

Chiral Epoxide

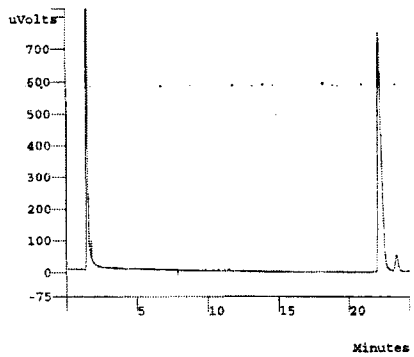

Peak No	Peak Name	Result ()	Ret. Time (min)	Time Offset (min)
1		95.2081	22.126	0.000
2		4.7919	23.397	0.000
Totals		100.0000		0.000

Table 3.1, Entry 9
4-Methylstyrene Oxide
Column : B-DM
Oven temp: 70 °C
Pressure: 20 psi

Racemate

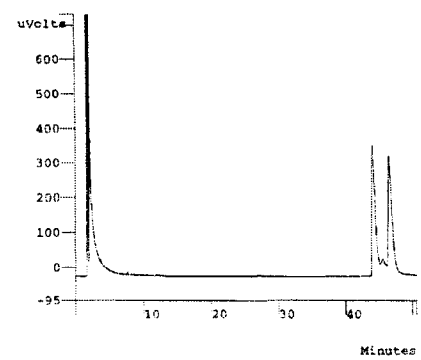

Peak No	Peak Name	Result ()	Ret. Time (min)	Time Offset (min)
1		49.7335	44.049	0.000
2		50.2665	46.476	0.000
Totals		100.0000		0.000

Chiral Epoxide

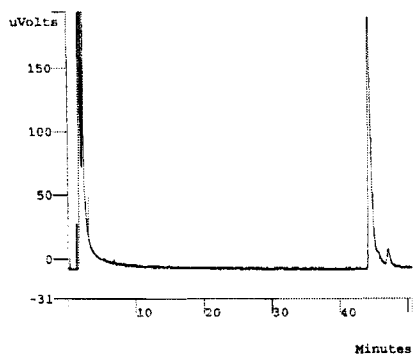

Peak No	Peak Name	Result ()	Ret. Time (min)	Time Offset (min)
1		94.8427	44.322	0.000
2		5.1573	47.112	0.000
Totals		100.0000		0.000

Table 3.1, Entry 10
4-Trifluoromethylstyrene Oxide
Column : B-DM
Oven temp: 80 °C
Pressure: 20 psi

Racemate

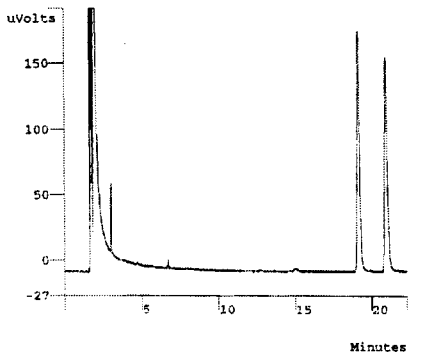

Peak No	Peak Name	Result ()	Ret. Time (min)	Time Offset (min)
1		50.3194	19.104	0.000
2		49.6806	20.927	0.000
	Totals	100.0000		0.000

Chiral Epoxide

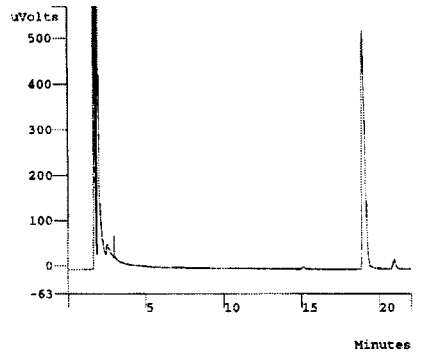

Peak No	Peak Name	Result ()	Ret. Time (min)	Time Offset (min)
1		96.6186	18.981	0.000
2		3.3814	21.014	0.000
	Totals	100.0000		0.000

Table 3.1, Entry 11
4-Cyanostyrene Oxide
Column : B-DM
Oven temp: 115 °C
Pressure: 25 psi

Racemate

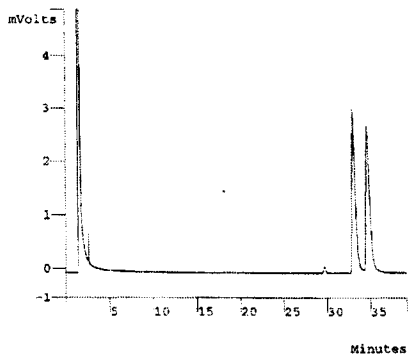

Peak No	Peak Name	Result ()	Ret. Time (min)	Time Offset (min)
1		49.7992	32.951	0.000
2		50.2008	34.572	0.000
	Totals	100.0000		0.000

Chiral Epoxide

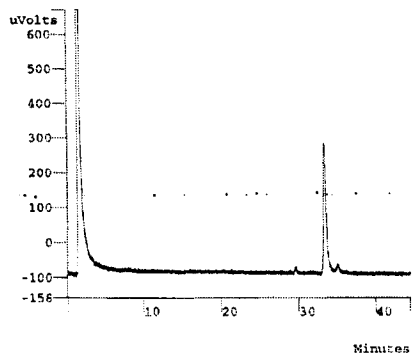

Peak No	Peak Name	Result ()	Ret. Time (min)	Time Offset (min)
1		96.2704	33.316	0.000
2		3.7296	35.026	0.000
	Totals	100.0000		0.000

cis-β-Methylstyrene Oxide
Column : B-DM
Oven temp: 100 °C
Pressure: 25 psi

Racemate

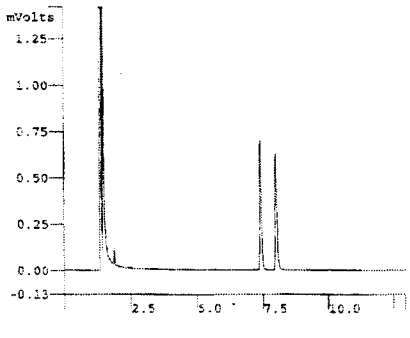

Peak No	Peak Name	Result ()	Ret. Time (min)	Time Offset (min)
1		49.7834	7.409	0.000
2		50.2166	7.997	0.000
	Totals	100.0000		0.000

Figure 3.6, Ketone 2-1

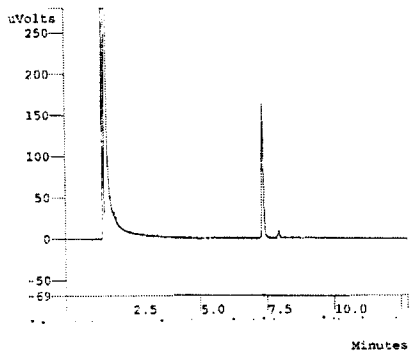

Peak No	Peak Name	Result ()	Ret. Time (min)	Time Offset (min)
1		95.2083	7.341	0.000
2		4.7917	7.938	0.000
	Totals	100.0000		0.000

Figure 3.6, Ketone 3-2

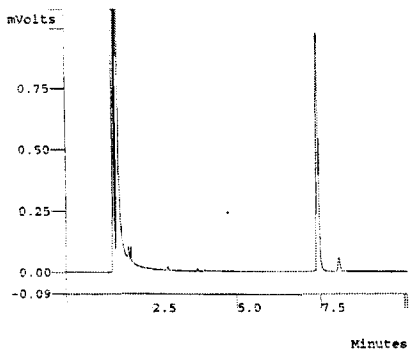

Peak No	Peak Name	Result ()	Ret. Time (min)	Time Offset (min)
1		94.6148	7.404	0.000
2		5.3852	8.036	0.000
	Totals	100.0000		0.000

Phenylcyclohexene Oxide
Column : B-DM
Oven temp: 105 °C
Pressure: 30 psi

Racemate

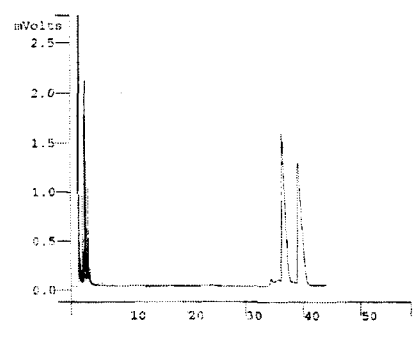

Peak No	Peak Name	Result ()	Ret. Time (min)	Time Offset (min)
1		49.6349	36.294	0.000
2		50.3651	39.054	0.000
	Totals	100.0000		0.000

Figure 3.6, Ketone 2-1

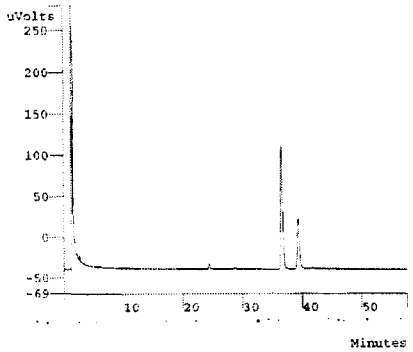

Peak No	Peak Name	Result ()	Ret. Time (min)	Time Offset (min)
1		69.4990	36.499	0.000
2		30.5009	39.313	0.000
	Totals	*99.9999*		*0.000*

Figure 3.7, Ketone 3-2

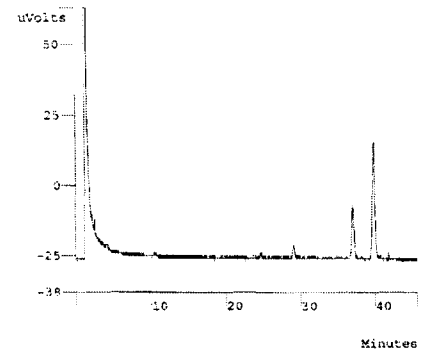

Peak No	Peak Name	Result ()	Ret. Time (min)	Time Offset (min)
1		29.8030	37.026	0.000
2		70.1970	39.806	0.000
	Totals	100.0000		0.000

trans-β-Methylstyrene Oxide
Column : B-DM
Oven temp: 100 °C
Pressure: 20 psi

Racemate

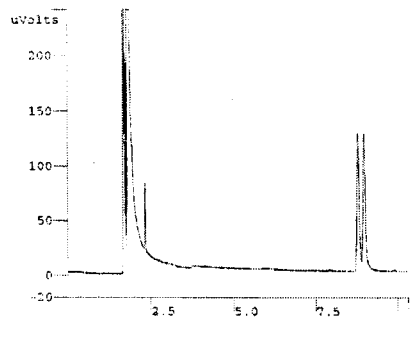

Peak No	Peak Name	Result ()	Ret. Time (min)	Time Offset (min)
1		49.7519	8.773	0.000
2		50.2481	8.961	0.000
	Totals	100.0000		0.000

Table 4.1, Entry 1

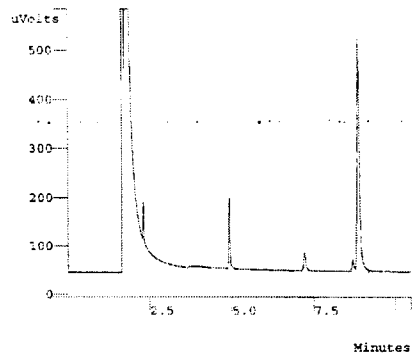

Peak No	Peak Name	Result ()	Ret. Time (min)	Time Offset (min)
1		12.9652	4.924	0.000
2		2.8428	8.693	0.000
3		84.1920	8.864	0.000
	Totals	100.0000		0.000

Table 4.1, Entry 3

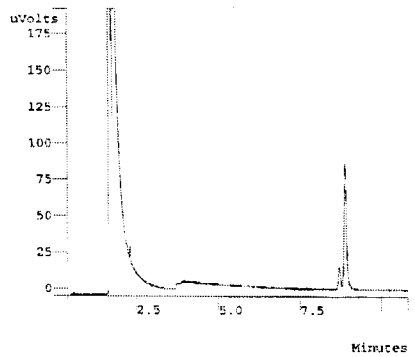

Peak No	Peak Name	Result ()	Ret. Time (min)	Time Offset (min)
1		12.9092	8.696	0.000
2		87.0908	8.887	0.000
	Totals	100.0000		0.000

Table 4.1, Entry 5

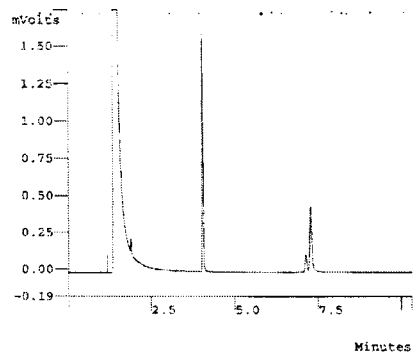

Peak No	Peak Name	Result ()	Ret. Time (min)	Time Offset (min)
1		61.1581	4.029	0.000
2		6.7326	7.122	0.000
3		32.1093	7.269	0.000
	Totals	100.0000		0.000

Table 4.1, Entry 6

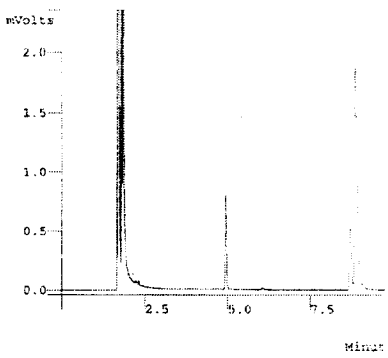

Peak No	Peak Name	Result ()	Ret. Time (min)
1		14.4116	4.946
2		14.1049	8.711
3		71.4835	8.858
	Totals	100.0000	

Table 4.1, Entry 7

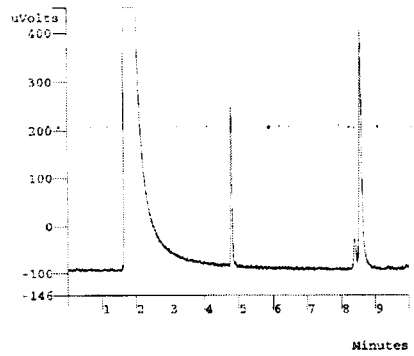

Peak No	Peak Name	Result ()	Ret. Time (min)	Time Offset (min)
1		24.4836	4.794	0.000
2		6.2779	8.394	0.000
3		69.2385	8.566	0.000
	Totals	100.0000		0.000

Table 4.1, Entry 9

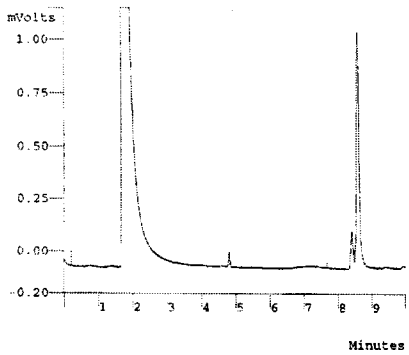

Peak No	Peak Name	Result ()	Ret. Time (min)	Time Offset (min)
1		2.9249	4.793	0.000
2		10.6783	8.398	0.000
3		86.3968	8.559	0.000
	Totals	100.0000		0.000

Table 4.1, Entry 10

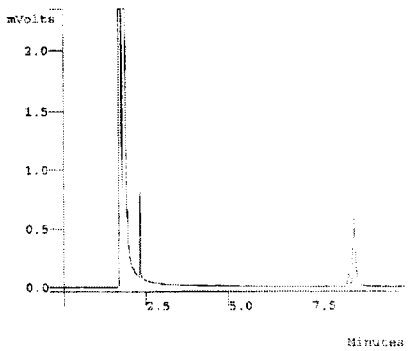

Peak No	Peak Name	Result ()	Ret. Time (min)	Time Offset (min)
1		11.5587	8.604	0.000
2		88.4413	8.766	0.000
	Totals	100.0000		0.000

Table 4.1, Entry 11

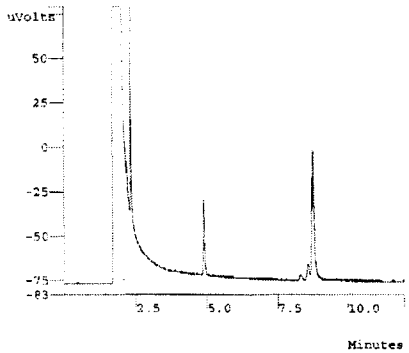

Peak No	Peak Name	Result ()	Ret. Time (min)	Time Offset (min)
1		23.9968	4.892	0.000
2		4.8426	8.579	0.000
3		71.1606	8.754	0.000
	Totals	**100.0000**		**0.000**

Table 4.1, Entry 12

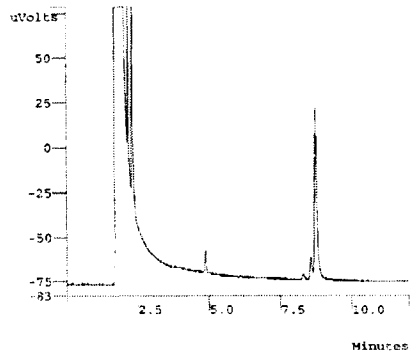

Peak No	Peak Name	Result ()	Ret. Time (min)	Time Offset (min)
1		5.7781	4.881	0.000
2		7.4998	8.566	0.000
3		86.7221	8.738	0.000
	Totals	**100.0000**		**0.000**

Table 4.1, Entry 13

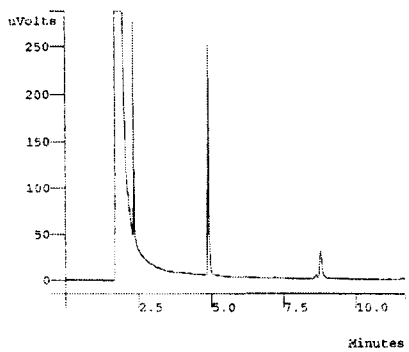

Peak No	Peak Name	Result ()	Ret. Time (min)	Time Offset (min)
1		79.3881	4.892	0.000
2		2.2811	8.583	0.000
3		18.3308	8.761	0.000
	Totals	**100.0000**		**0.000**

Table 4.1, Entry 14

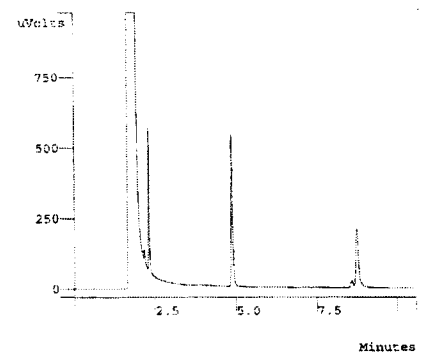

Peak No	Peak Name	Result ()	Ret. Time (min)	Time Offset (min)
1		58.9049	4.881	0.000
2		3.0894	8.571	0.000
3		38.0057	8.741	0.000
	Totals	**100.0000**		**0.000**

cis-β-Methylstyrene Oxide
Column : B-DM
Oven temp: 100 °C
Pressure: 25 psi

Racemate

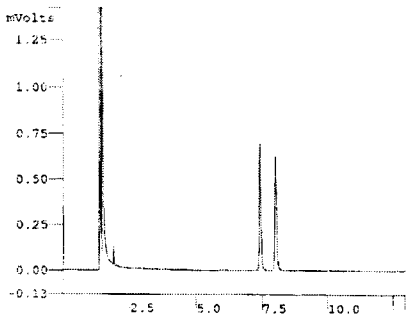

Peak No	Peak Name	Result ()	Ret. Time (min)	Time Offset (min)
1		49.7834	7.409	0.000
2		50.2166	7.997	0.000
Totals		100.0000		0.000

Table 4.1, Entry 1

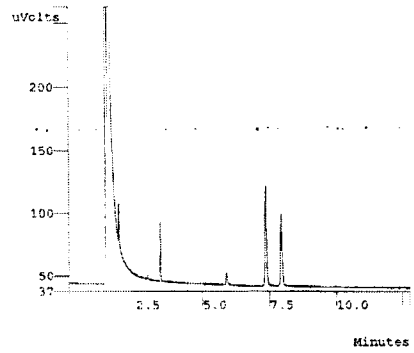

Peak No	Peak Name	Result ()	Ret. Time (min)	Time Offset (min)
1		11.8521	3.431	0.000
2		49.6863	7.354	0.000
3		38.4615	7.936	0.000
Totals		99.9999		0.000

Table 4.1, Entry 3

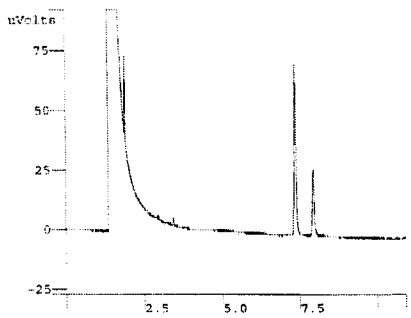

Peak No	Peak Name	Result ()	Ret. Time (min)	Time Offset (min)
1		70.8002	7.349	0.000
2		29.1998	7.931	0.000
Totals		100.0000		0.000

Table 4.1, Entry 5

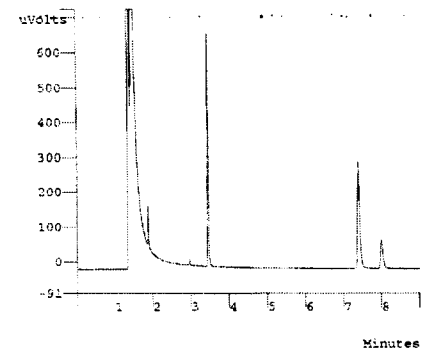

Peak No	Peak Name	Result ()	Ret. Time (min)	Time Offset (min)
1		41.7840	3.449	0.000
2		45.7583	7.406	0.000
3		12.4577	8.012	0.000
Totals		100.0000		0.000

Table 4.1, Entry 6

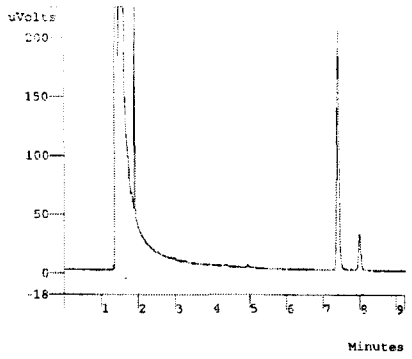

Peak No	Peak Name	Result ()	Ret. Time (min)	Time Offset (min)
1		87.2125	7.386	0.000
2		12.7875	7.986	0.000
	Totals	100.0000		0.000

Table 4.1, Entry 8

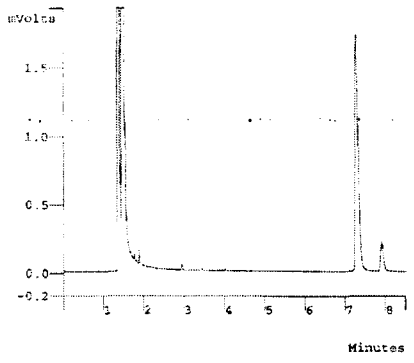

Peak No	Peak Name	Result ()	Ret. Time (min)	Time Offset (min)
1		90.0653	7.261	0.000
2		9.9347	7.899	0.000
	Totals	100.0000		0.000

Table 4.1, Entry 9

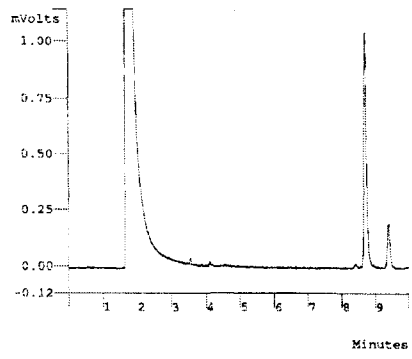

Peak No	Peak Name	Result ()	Ret. Time (min)	Time Offset (min)
1		83.6494	8.699	0.000
2		16.3506	9.381	0.000
	Totals	100.0000		0.000

Table 4.1, Entry 10

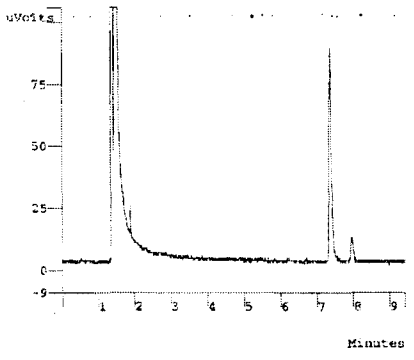

Peak No	Peak Name	Result ()	Ret. Time (min)	Time Offset (min)
1		90.6778	7.359	0.000
2		9.3222	7.951	0.000
	Totals	100.0000		0.000

Table 4.1, Entry 11

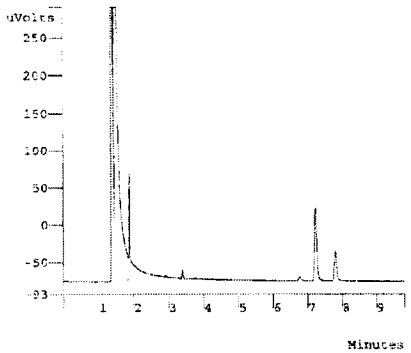

Peak No	Peak Name	Result ()	Ret. Time (min)	Time Offset (min)
1		69.7222	7.226	0.000
2		30.2778	7.799	0.000
	Totals	**100.0000**		**0.000**

Table 4.1, Entry 12

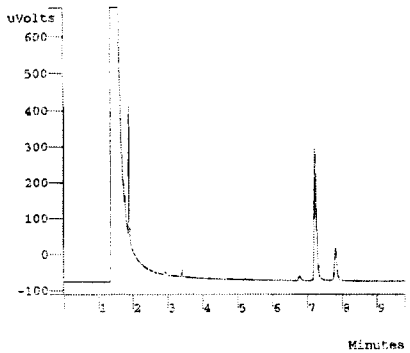

Peak No	Peak Name	Result ()	Ret. Time (min)	Time Offset (min)
1		79.6488	7.219	0.000
2		20.3512	7.802	0.000
	Totals	**100.0000**		**0.000**

Table 4.1, Entry 13

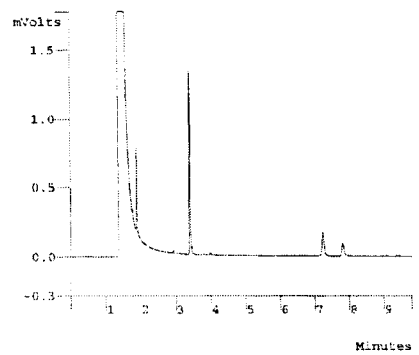

Peak No	Peak Name	Result ()	Ret. Time (min)	Time Offset (min)
1		67.7949	3.396	0.000
2		20.1328	7.226	0.000
3		12.0722	7.799	0.000
	Totals	**99.9999**		**0.000**

Table 4.1, Entry 14

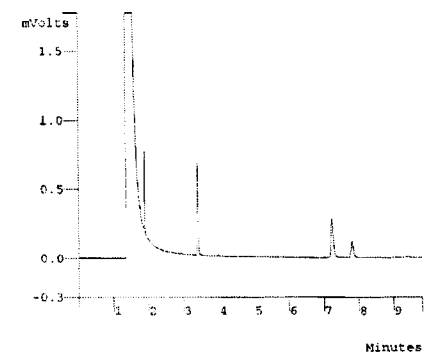

Peak No	Peak Name	Result ()	Ret. Time (min)	Time Offset (min)
1		40.9581	3.398	0.000
2		40.6660	7.219	0.000
3		18.3759	7.798	0.000
	Totals	**100.0000**		**0.000**

cis-β-Methylstyrene Oxide
Column : B-DM
Oven temp: 100 °C
Pressure: 20 psi

Racemate

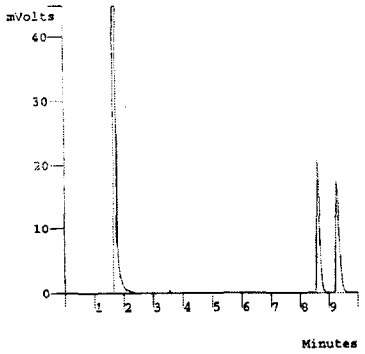

Peak No	Peak Name	Result 0	Ret. Time (min)	Time Offset (min)
1		50.1654	8.597	0.000
2		49.8346	9.254	0.000
	Totals	100.0000		0.000

Phenylcyclohexene Oxide
Column : B-DM
Oven temp: 105 °C
Pressure: 30 psi

Racemate

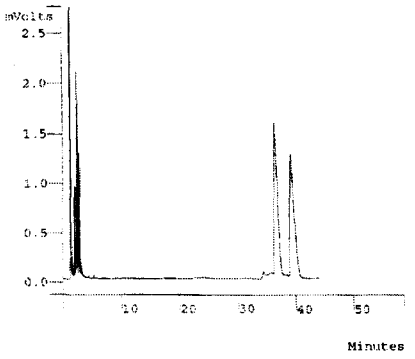

Peak No	Peak Name	Result ()	Ret. Time (min)	Time Offset (min)
1		49.6349	36.294	0.000
2		50.3651	39.054	0.000
	Totals	100.0000		0.000

Table 4.1, Entry 1

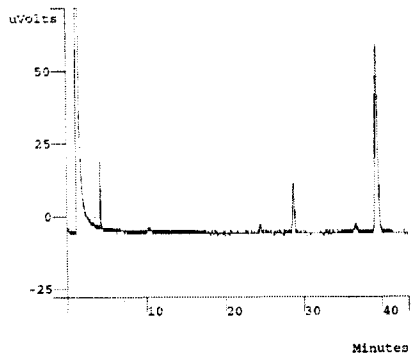

Peak No	Peak Name	Result ()	Ret. Time (min)	Time Offset (min)
1		14.0760	28.692	0.000
2		1.6220	36.619	0.000
3		84.3020	39.379	0.000
	Totals	100.0000		0.000

Table 4.1, Entry 3

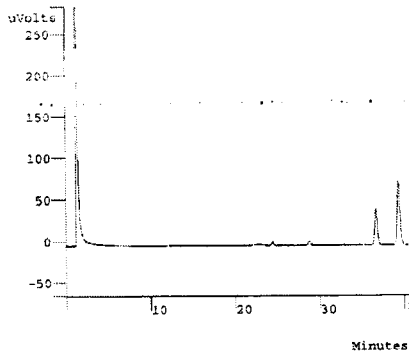

Peak No	Peak Name	Result ()	Ret. Time (min)	Time Offset (min)
1		3.0993	28.639	0.000
2		32.5916	36.664	0.000
3		64.3090	39.351	0.000
	Totals	99.9999		0.000

Table 4.1, Entry 5

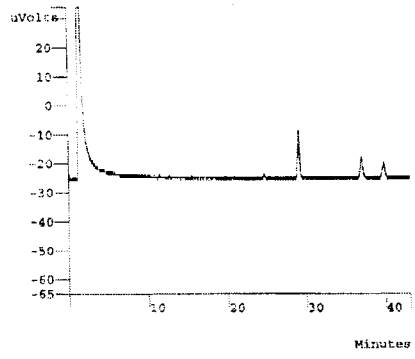

Peak No	Peak Name	Result ()	Ret. Time (min)	Time Offset (min)
1		54.6514	29.034	0.000
2		26.5181	37.063	0.000
3		18.8305	39.864	0.000
	Totals	100.0000		0.000

Table 4.1, Entry 6

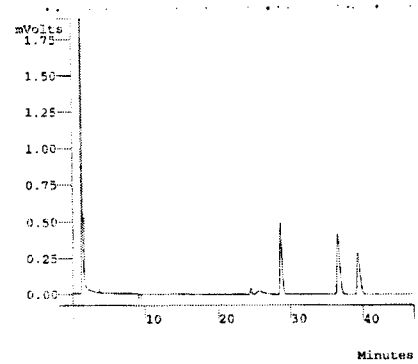

Peak No	Peak Name	Result ()	Ret. Time (min)	Time Offset (min)
1		35.1581	28.604	0.000
2		37.7002	36.513	0.000
3		27.1417	39.347	0.000
	Totals	100.0000		0.000

Table 4.1, Entry 7

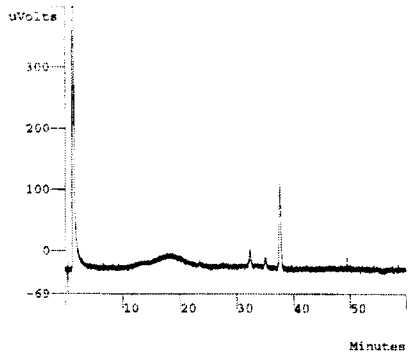

Peak No	Peak Name	Result ()	Ret. Time (min)	Time Offset (min)
1		10.5827	32.263	0.000
2		5.5407	34.961	0.000
3		83.8766	37.551	0.000
	Totals	100.0000		0.000

Table 4.1, Entry 8

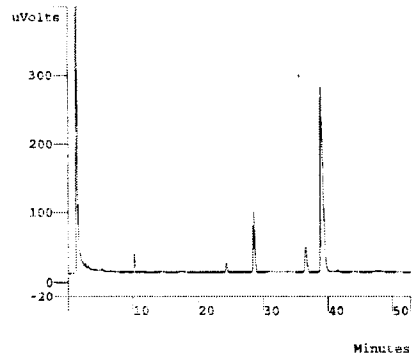

Peak No	Peak Name	Result ()	Ret. Time (min)	Time Offset (min)
1		15.2917	28.563	0.000
2		7.9234	36.549	0.000
3		76.7849	38.972	0.000
	Totals	100.0000		0.000

Table 4.1, Entry 9

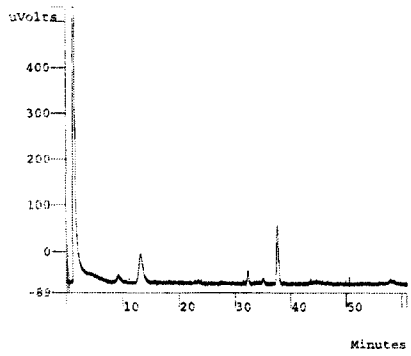

Peak No	Peak Name	Result ()	Ret. Time (min)	Time Offset (min)
1		12.6761	32.272	0.000
2		6.1514	34.966	0.000
3		81.1725	37.571	0.000
	Totals	100.0000		0.000

Table 4.1, Entry 10

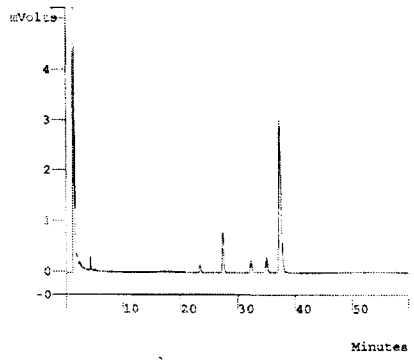

Peak No	Peak Name	Result ()	Ret. Time (min)	Time Offset (min)
1		13.5575	27.376	0.000
2		6.2670	34.966	0.000
3		80.1755	37.287	0.000
	Totals	100.0000		0.000

Table 4.1, Entry 11

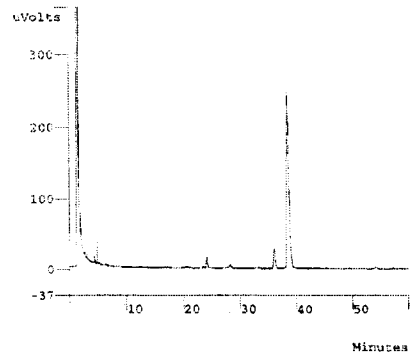

Peak No	Peak Name	Result ()	Ret. Time (min)	Time Offset (min)
1		7.9610	35.974	0.000
2		92.0390	38.362	0.000
	Totals	100.0000		0.000

Table 4.1, Entry 12

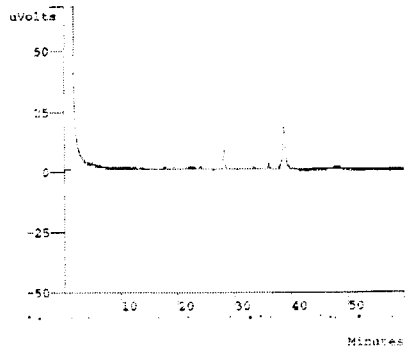

Peak No	Peak Name	Result ()	Ret. Time (min)	Time Offset (min)
1		20.1013	28.163	0.000
2		3.3662	36.014	0.000
3		76.5326	38.686	0.000
	Totals	100.0001		0.000

Table 4.1, Entry 13

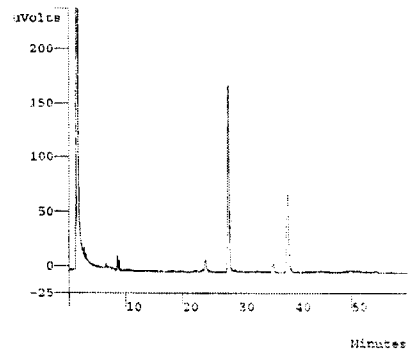

Peak No	Peak Name	Result ()	Ret. Time (min)	Time Offset (min)
1		60.7952	28.087	0.000
2		3.4119	36.029	0.000
3		35.7930	38.638	0.000
	Totals	100.0001		0.000

Table 4.1, Entry 14

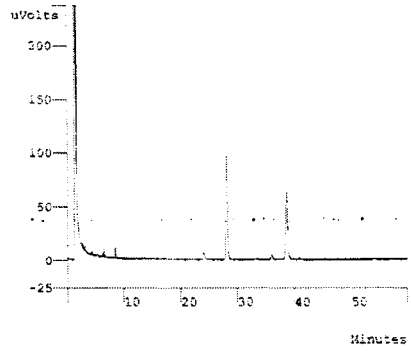

Peak No	Peak Name	Result ()	Ret. Time (min)	Time Offset (min)
1		52.0866	28.126	0.000
2		2.0173	36.014	0.000
3		45.8961	38.621	0.000
	Totals	100.0000		0.000

trans-Stilbene Oxide
Column : Chiracel OD
Solvent: 80% Hexanes, 20% IPA
Flow: 1.0 mL/min
Detector: 254 nm

Racemate

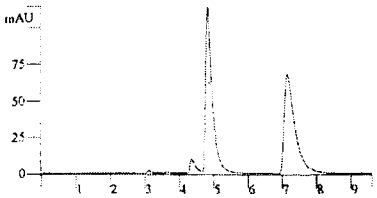

Peak No	Ret Time (min)	Result ()	Peak Area (counts)
1	4.806	49.8005	779720
2	7.129	50.1995	785966
		100.0000	**1565686**

Table 4.1, Entry 1

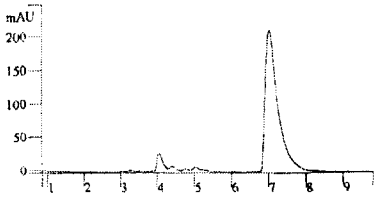

Peak No	Ret Time (min)	Result ()	Peak Area (counts)
1	5.009	1.3195	35565
2	7.008	98.6805	2659875
		100.0000	**2695440**

Table 4.1, Entry 3

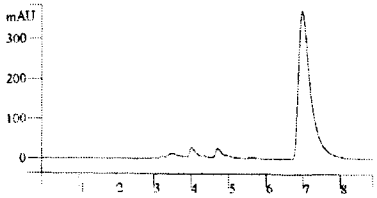

Peak No	Ret Time (min)	Result ()	Peak Area (counts)
1	4.701	1.9909	89761
2	6.956	98.0091	4418886
		100.0000	**4508647**

Table 4.1, Entry 5

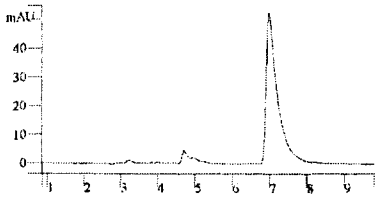

Peak No	Ret Time (min)	Result ()	Peak Area (counts)
1	4.701	2.4061	14349
2	6.986	97.5939	582008
		100.0000	**596357**

Styrene Oxide
Column : B-DM
Oven temp: 80 °C
Pressure: 25 psi

Racemate

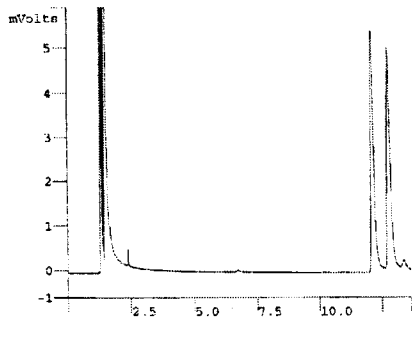

Peak No	Peak Name	Result ()	Ret. Time (min)	Time Offset (min)
1		50.0995	12.099	0.000
2		49.9005	12.743	0.000
	Totals	100.0000		0.000

Table 5.2, Entry 1

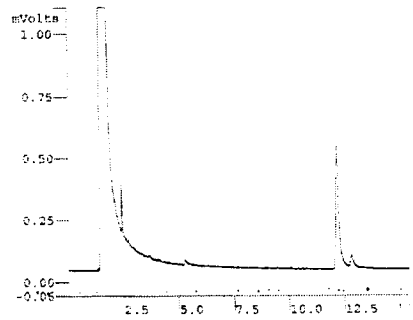

Peak No	Peak Name	Result ()	Ret. Time (min)	Time Offset (min)
1		91.9668	12.156	0.000
2		8.0332	12.819	0.000
	Totals	100.0000		0.000

Table 5.2, Entry 2

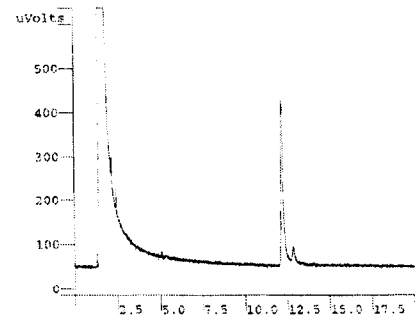

Peak No	Peak Name	Result ()	Ret. Time (min)	Time Offset (min)
1		91.7967	12.161	0.000
2		8.2033	12.829	0.000
	Totals	100.0000		0.000

Table 5.2, Entry 3

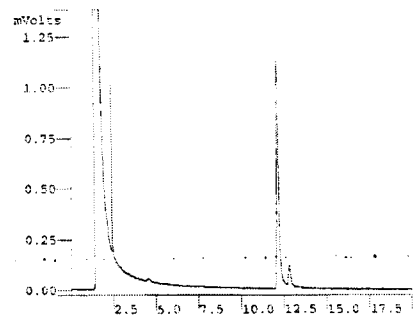

Peak No	Peak Name	Result ()	Ret. Time (min)	Time Offset (min)
1		91.9941	12.126	0.000
2		8.0059	12.804	0.000
	Totals	100.0000		0.000

Table 5.2, Entry 4

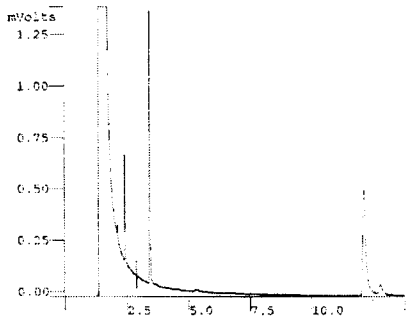

Peak No	Peak Name	Result ()	Ret. Time (min)	Time Offset (min)
			Minutes	
1		36.7546	3.424	0.000
2		57.5636	12.139	0.000
3		5.6817	12.813	0.000
	Totals	99.9999		0.000

Table 5.2, Entry 5

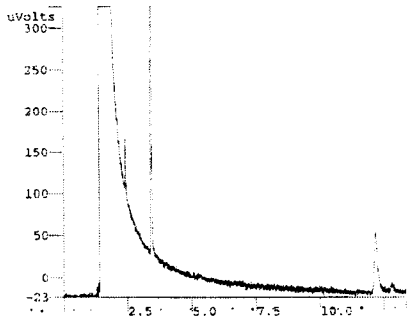

Peak No	Peak Name	Result ()	Ret. Time (min)	Time Offset (min)
			Minutes	
1		64.6267	3.428	0.000
2		32.5954	12.177	0.000
3		2.7780	12.783	0.000
	Totals	100.0001		0.000

Table 5.2, Entry 6

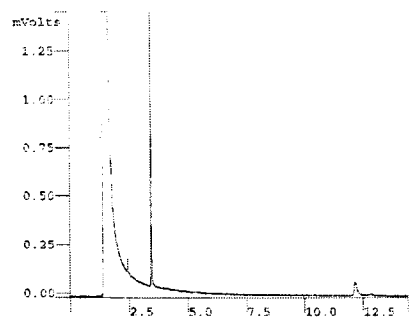

Peak No	Peak Name	Result ()	Ret. Time (min)	Time Offset (min)
			Minutes	
1		81.3336	3.428	0.000
2		16.4988	12.167	0.000
3		2.1676	12.834	0.000
	Totals	100.0000		0.000

Table 5.2, Entry 7

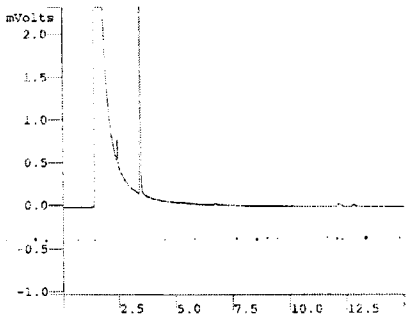

Peak No	Peak Name	Result ()	Ret. Time (min)	Time Offset (min)
			Minutes	
1		94.5750	3.426	0.000
2		3.0621	12.171	0.000
3		2.3629	12.818	0.000
	Totals	100.0000		0.000

Table 5.2, Entry 8

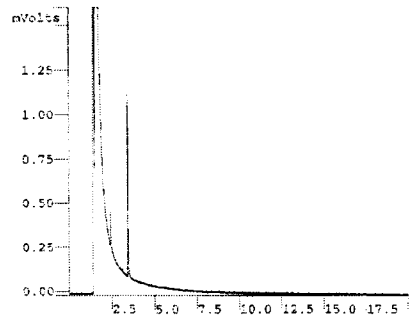

Peak No	Peak Name	Result ()	Ret. Time (min)	Time Offset (min)
			Minutes	
Totals		0.0000		0.000

Table 5.2, Entry 9

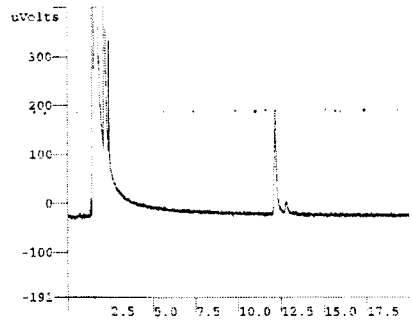

Peak No	Peak Name	Result ()	Ret. Time (min)	Time Offset (min)
			Minutes	
1		91.7035	12.158	0.000
2		8.2965	12.804	0.000
Totals		100.0000		0.000

Table 5.2, Entry 10

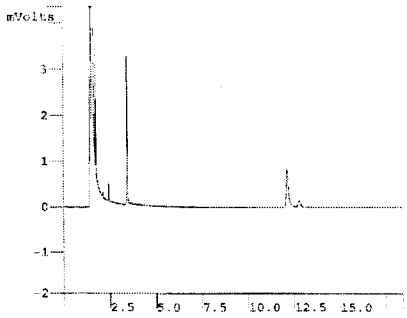

Peak No	Peak Name	Result ()	Ret. Time (min)	Time Offset (min)
			Minutes	
1		43.3458	3.419	0.000
2		49.6052	12.102	0.000
3		7.0490	12.764	0.000
Totals		100.0000		0.000

Table 5.2, Entry 11

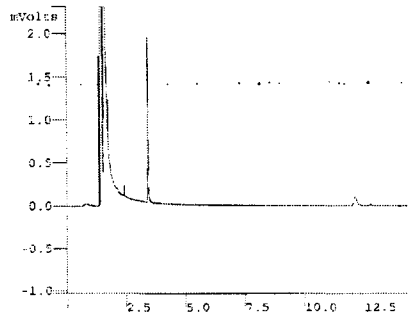

Peak No	Peak Name	Result ()	Ret. Time (min)	Time Offset (min)
			Minutes	
1		80.3374	3.422	0.000
2		17.6326	12.137	0.000
3		2.0300	12.778	0.000
Totals		100.0000		0.000

Table 5.3, Entry 1

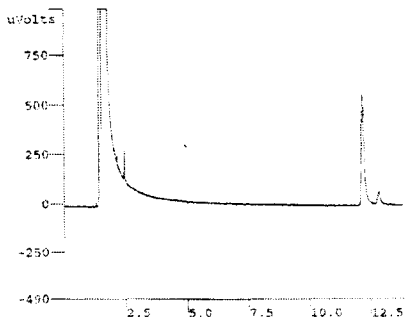

Peak No	Peak Name	Result ()	Ret. Time (min)	Time Offset (min)
1		91.8446	12.149	0.000
2		8.1554	12.799	0.000
	Totals	100.0000		0.000

Table 5.3, Entry 2

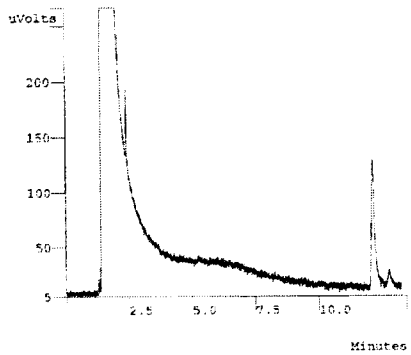

Peak No	Peak Name	Result ()	Ret. Time (min)	Time Offset (min)
1		93.2991	12.153	0.000
2		6.7009	12.819	0.000
	Totals	100.0000		0.000

Table 5.3, Entry 3

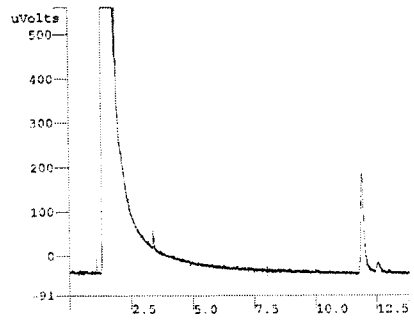

Peak No	Peak Name	Result ()	Ret. Time (min)	Time Offset (min)
1		3.0827	3.378	0.000
2		88.9909	11.901	0.000
3		7.9264	12.546	0.000
	Totals	100.0000		0.000

Table 5.3, Entry 4

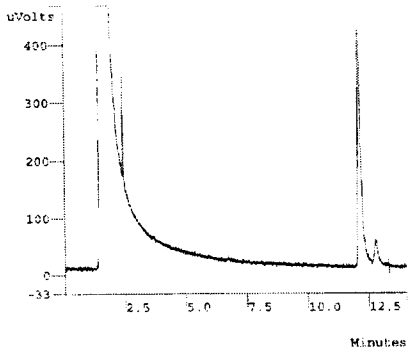

Peak No	Peak Name	Result ()	Ret. Time (min)	Time Offset (min)
1		91.3511	12.142	0.000
2		8.6489	12.784	0.000
	Totals	100.0000		0.000

Table 5.3, Entry 5

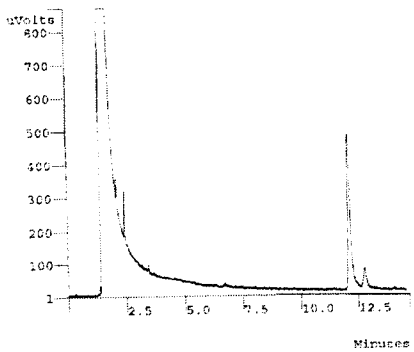

Peak No	Peak Name	Result ()	Ret. Time (min)	Time Offset (min)
1		89.6731	12.111	0.000
2		10.3269	12.756	0.000
	Totals	100.0000		0.000

Table 5.3, Entry 6

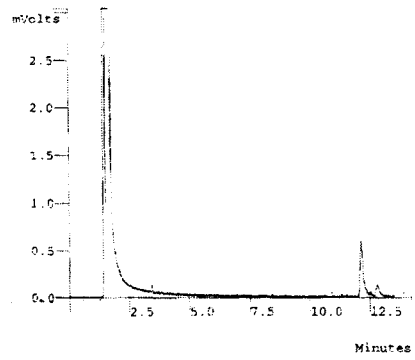

Peak No	Peak Name	Result ()	Ret. Time (min)	Time Offset (min)
1		1.6362	3.429	0.000
2		83.9280	12.132	0.000
3		14.4359	12.806	0.000
	Totals	100.0001		0.000

Table 5.3, Entry 7

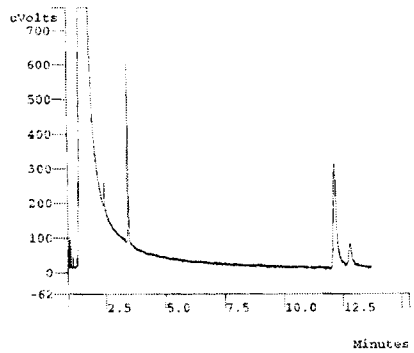

Peak No	Peak Name	Result ()	Ret. Time (min)	Time Offset (min)
1		23.3657	3.426	0.000
2		65.0734	12.144	0.000
3		11.5609	12.797	0.000
	Totals	100.0000		0.000

Table 5.3, Entry 8

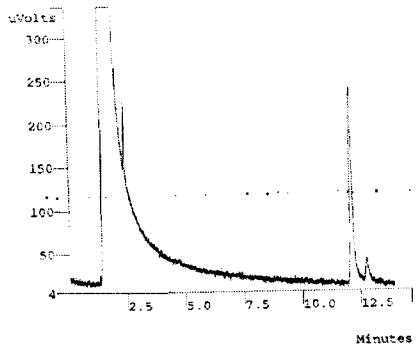

Peak No	Peak Name	Result ()	Ret. Time (min)	Time Offset (min)
1		90.7088	12.124	0.000
2		9.2912	12.762	0.000
	Totals	100.0000		0.000

Table 5.3, Entry 9

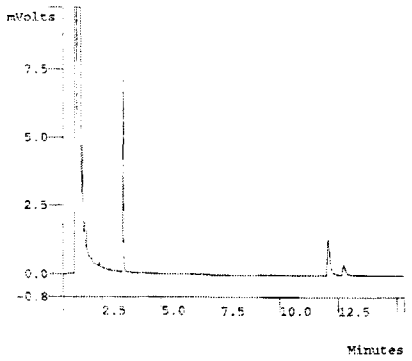

Peak No	Peak Name	Result ()	Ret. Time (min)	Time Offset (min)
1		48.3700	3.416	0.000
2		40.0796	12.086	0.000
3		11.5505	12.751	0.000
	Totals	100.0001		0.000

Table 5.3, Entry 10

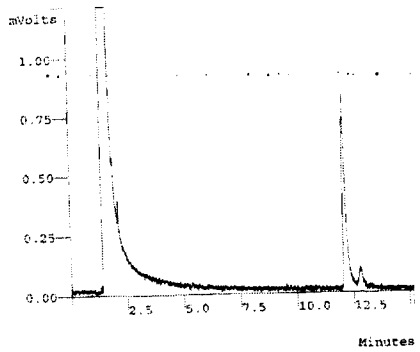

Peak No	Peak Name	Result ()	Ret. Time (min)	Time Offset (min)
1		93.1377	12.132	0.000
2		6.8623	12.786	0.000
	Totals	100.0000		0.000

Table 5.3, Entry 11

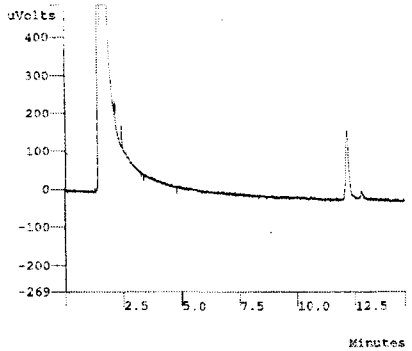

Peak No	Peak Name	Result ()	Ret. Time (min)	Time Offset (min)
1		93.3084	12.163	0.000
2		6.6916	12.799	0.000
	Totals	100.0000		0.000

Table 5.3, Entry 12

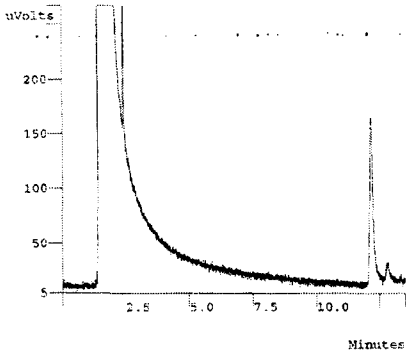

Peak No	Peak Name	Result ()	Ret. Time (min)	Time Offset (min)
1		91.7974	12.144	0.000
2		8.2026	12.784	0.000
	Totals	100.0000		0.000

Table 5.3, Entry 13

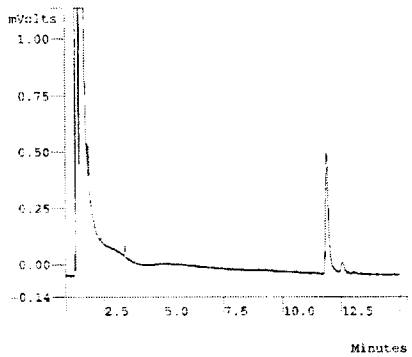

Peak No	Peak Name	Result ()	Ret. Time (min)	Time Offset (min)
1		1.4548	3.371	0.000
2		90.8880	11.889	0.000
3		7.6572	12.547	0.000
	Totals	100.0000		0.000

Table 5.3, Entry 14

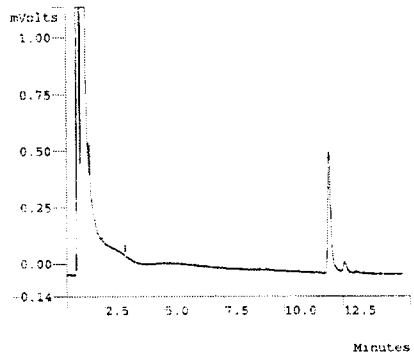

Peak No	Peak Name	Result ()	Ret. Time (min)	Time Offset (min)
1		1.4548	3.371	0.000
2		90.8880	11.889	0.000
3		7.6572	12.547	0.000
	Totals	100.0000		0.000

Table 5.3, Entry 15

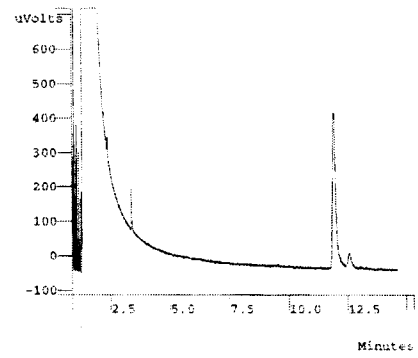

Peak No	Peak Name	Result ()	Ret. Time (min)	Time Offset (min)
1		4.6944	3.371	0.000
2		88.0536	11.901	0.000
3		7.2521	12.561	0.000
	Totals	100.0001		0.000

Table 5.3, Entry 16

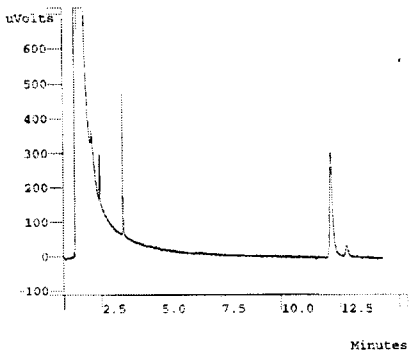

Peak No	Peak Name	Result ()	Ret. Time (min)	Time Offset (min)
1		21.4652	3.422	0.000
2		71.8093	12.111	0.000
3		6.7255	12.767	0.000
	Totals	100.0000		0.000

Table 5.3, Entry 17

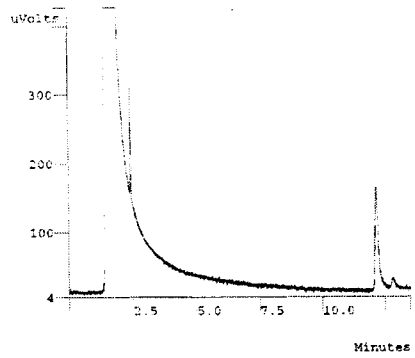

Peak No	Peak Name	Result ()	Ret. Time (min)	Time Offset (min)
1		91.7974	12.144	0.000
2		8.2026	12.784	0.000
Totals		100.0000		0.000

Table 5.3, Entry 18

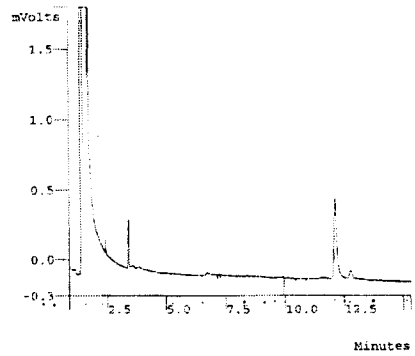

Peak No	Peak Name	Result ()	Ret. Time (min)	Time Offset (min)
1		10.7804	3.419	0.000
2		82.3396	12.096	0.000
3		6.8800	12.756	0.000
Totals		100.0000		0.000

Table 5.3, Entry 19

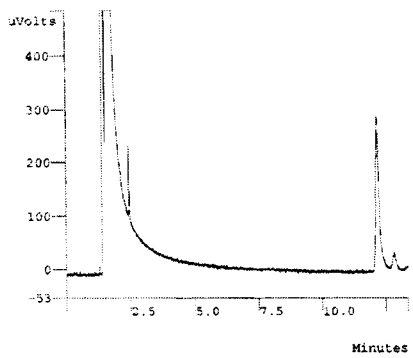

Peak No	Peak Name	Result ()	Ret. Time (min)	Time Offset (min)
1		92.9366	12.166	0.000
2		7.0634	12.836	0.000
Totals		100.0000		0.000

Table 5.3, Entry 20

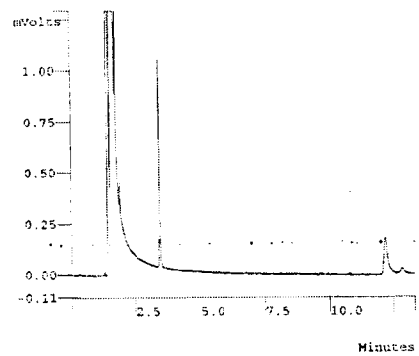

Peak No	Peak Name	Result ()	Ret. Time (min)	Time Offset (min)
1		51.1709	3.431	0.000
2		43.4254	12.171	0.000
3		5.4037	12.831	0.000
Totals		100.0000		0.000

Table 5.3, Entry 21

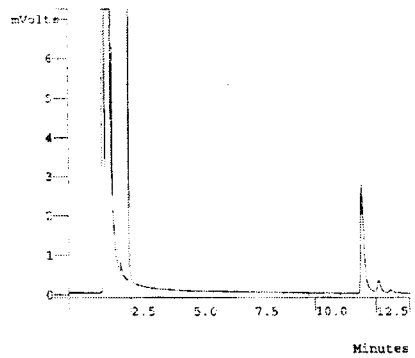

Peak No	Peak Name	Result ()	Ret. Time (min)	Time Offset (min)
1		90.6189	11.914	0.000
2		9.3811	12.609	0.000
	Totals	100.0000		0.000

Table 5.3, Entry 22

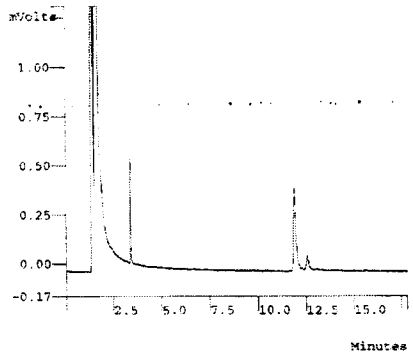

Peak No	Peak Name	Result ()	Ret. Time (min)	Time Offset (min)
1		20.5002	3.372	0.000
2		69.0425	11.894	0.000
3		10.4573	12.542	0.000
	Totals	100.0000		0.000

Table 5.3, Entry 23

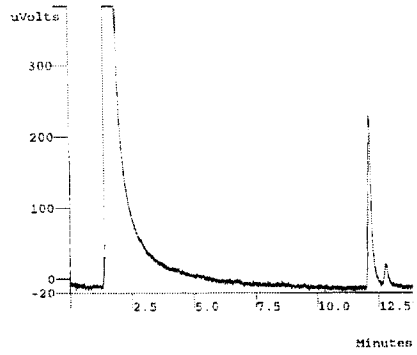

Peak No	Peak Name	Result ()	Ret. Time (min)	Time Offset (min)
1		89.2123	12.131	0.000
2		10.7877	12.774	0.000
	Totals	100.0000		0.000

Table 5.3, Entry 24

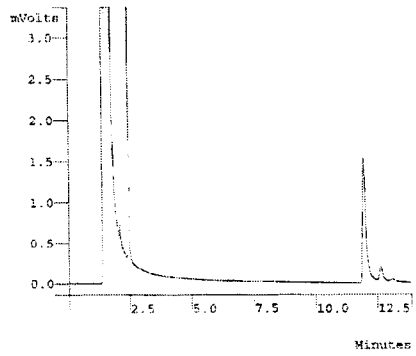

Peak No	Peak Name	Result ()	Ret. Time (min)	Time Offset (min)
1		90.1553	11.941	0.000
2		9.8447	12.618	0.000
	Totals	100.0000		0.000

Table 5.3, Entry 25

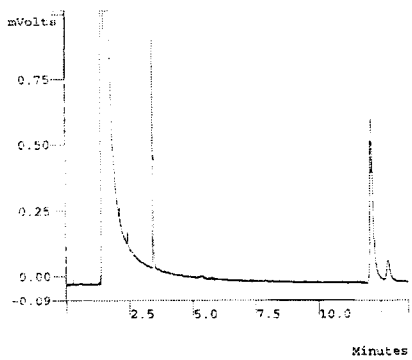

Peak No	Peak Name	Result ()	Ret. Time (min)	Time Offset (min)
1		22.2808	3.424	0.000
2		69.2881	12.119	0.000
3		8.4311	12.784	0.000
	Totals	**100.0000**		**0.000**

Table 5.3, Entry 26

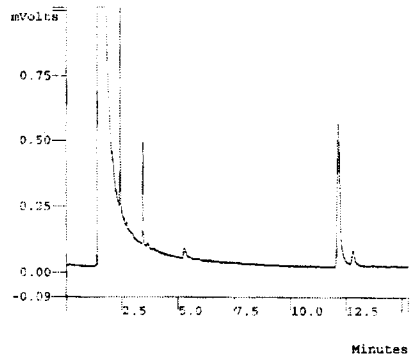

Peak No	Peak Name	Result ()	Ret. Time (min)	Time Offset (min)
1		12.9945	3.426	0.000
2		80.0869	12.139	0.000
3		6.9186	12.804	0.000
	Totals	**100.0000**		**0.000**

Table 5.3, Entry 27

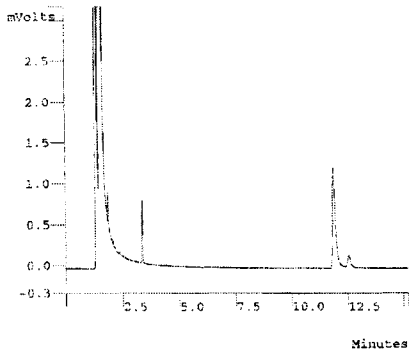

Peak No	Peak Name	Result ()	Ret. Time (min)	Time Offset (min)
1		10.9510	3.369	0.000
2		79.8610	11.874	0.000
3		9.1880	12.552	0.000
	Totals	**100.0000**		**0.000**

Table 5.3, Entry 28

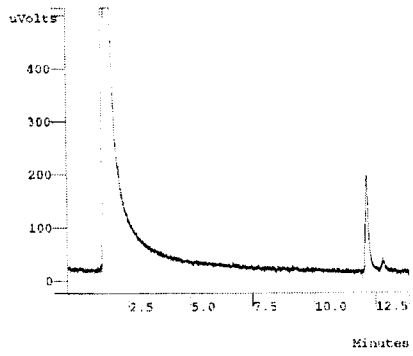

Peak No	Peak Name	Result ()	Ret. Time (min)	Time Offset (min)
1		93.0517	12.156	0.000
2		6.9483	12.801	0.000
	Totals	**100.0000**		**0.000**

Table 5.4, Entry 2
2-Fluorostyrene Oxide
Column : B-DM
Oven temp: 80 °C
Pressure: 25 psi

Racemate

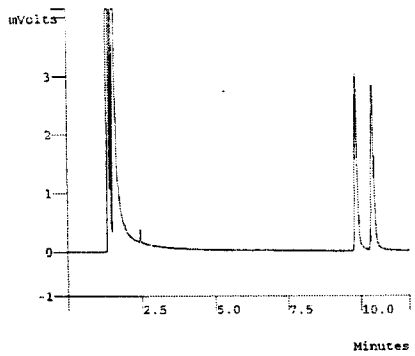

Peak No	Peak Name	Result ()	Ret. Time (min)	Time Offset (min)
1		50.3680	9.824	0.000
2		49.6320	10.394	0.000
	Totals	100.0000		0.000

Chiral Epoxide

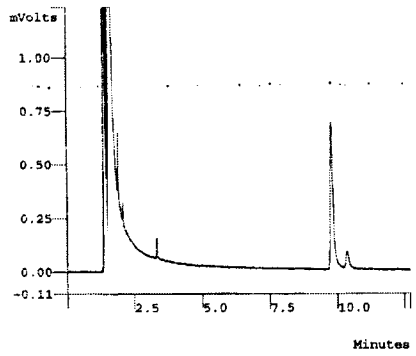

Peak No	Peak Name	Result ()	Ret. Time (min)	Time Offset (min)
1		89.8063	9.786	0.000
2		10.1937	10.359	0.000
	Totals	100.0000		0.000

Table 5.4, Entry 3
4-Chlorostyrene Oxide
Column : B-DM
Oven temp: 100 °C
Pressure: 25 psi

Racemate

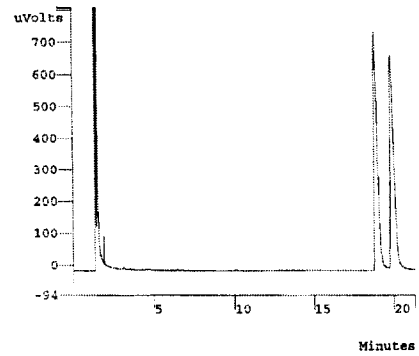

Peak No	Peak Name	Result ()	Ret. Time (min)	Time Offset (min)
1		49.4743	18.849	0.000
2		50.5257	19.868	0.000
	Totals	100.0000		0.000

Chiral Epoxide

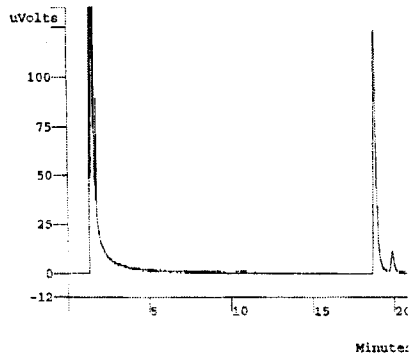

Peak No	Peak Name	Result ()	Ret. Time (min)
1		92.8989	18.791
2		7.1011	19.853
	Totals	100.0000	

Table 5.4, Entry 4
4-Bromostyrene Oxide
Column : B-DM
Oven temp: 110 °C
Pressure: 25 psi

Racemate

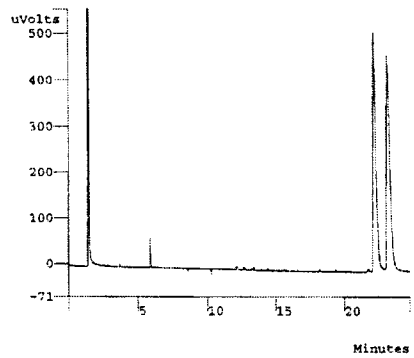

Peak No	Peak Name	Result ()	Ret. Time (min)	Time Offset (min)
1		49.4556	22.192	0.000
2		50.5444	23.179	0.000
	Totals	100.0000		0.000

Chiral Epoxide

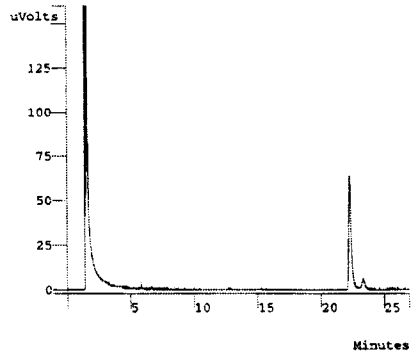

Peak No	Peak Name	Result ()	Ret. Time (min)	Time Offset (min)
1		93.4894	22.286	0.000
2		6.5106	23.301	0.000
	Totals	100.0000		0.000

Table 5.4, Entry 5
4-Cyanostyrene Oxide
Column : B-DM
Oven temp: 115 °C
Pressure: 25 psi

Racemate

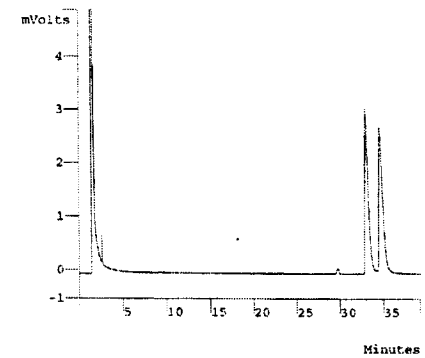

Peak No	Peak Name	Result ()	Ret. Time (min)	Time Offset (min)
1		49.7992	32.951	0.000
2		50.2008	34.572	0.000
	Totals	100.0000		0.000

Chiral Epoxide

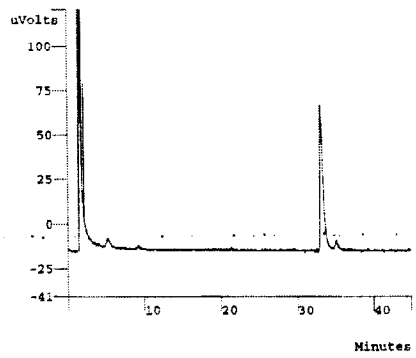

Peak No	Peak Name	Result ()	Ret. Time (min)	Time Offset (min)
1		95.1693	33.018	0.000
2		4.8307	35.004	0.000
	Totals	100.0000		0.000

Table 5.4, Entry 6
4-Nitrostyrene Oxide
Column : B-DM
Oven temp: 125 °C
Pressure: 30 psi

Racemate

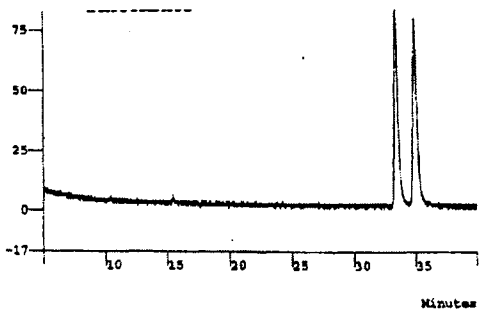

Peak No	Peak Name	Result ()	Ret. Time (min)
1		49.6084	33.397
2		50.3916	34.909
	Totals	100.0000	

Chiral Epoxide

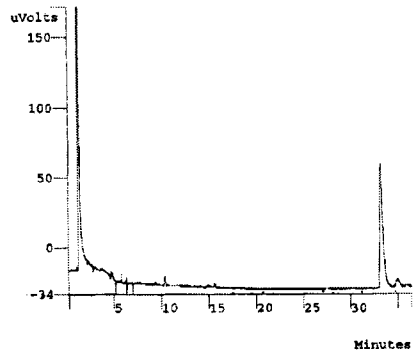

Peak No	Peak Name	Result ()	Ret. Time (min)	Time Offset (min)
1		95.0826	33.224	0.000
2		4.9174	34.899	0.000
	Totals	100.0000		0.000

Table 5.4, Entry 7
4-Trifluoromethylstyrene Oxide
Column : B-DM
Oven temp: 80 °C
Pressure: 20 psi

Racemate

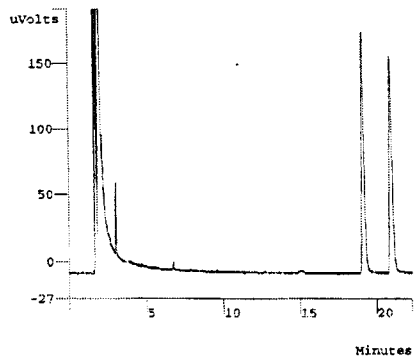

Peak No	Peak Name	Result ()	Ret. Time (min)	Time Offset (min)
1		50.3194	19.104	0.000
2		49.6806	20.927	0.000
	Totals	100.0000		0.000

Chiral Epoxide

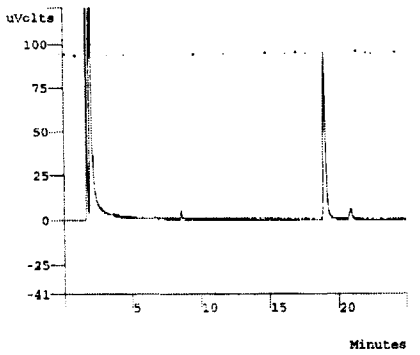

Peak No	Peak Name	Result ()	Ret. Time (min)	Time Offset (min)
1		95.8819	18.983	0.000
2		4.1181	20.897	0.000
	Totals	100.0000		0.000

Table 5.4, Entry 8
3-Benzyloxystyrene oxide
Column : Chiracel AD
Solvent: 95% Heptanes, 5% IPA
Flow: 1.0 mL/min
Detector: 270 nm

Racemate

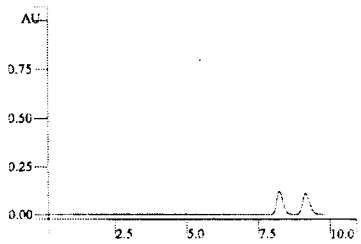

Peak No	Peak Name	Result ()	Ret. Time (min)	Time Offset (min)	Area (counts)
1		50.4842	8.216	0.000	980813
2		49.5158	9.137	0.000	961997
	Totals	00.0000		0.000	1942810

Chiral Epoxide

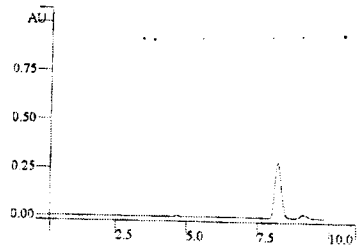

Peak No	Peak Name	Result ()	Ret. Time (min)	Time Offset (min)	Area (counts)
1		93.7436	8.179	0.000	2334929
2		6.2564	9.094	0.000	155832
	Totals	00.0000		0.000	2490761

Table 5.4, Entry 9
3-Methylstyrene Oxide
Column : B-DM
Oven temp: 60 °C
Pressure: 20 psi

Racemate

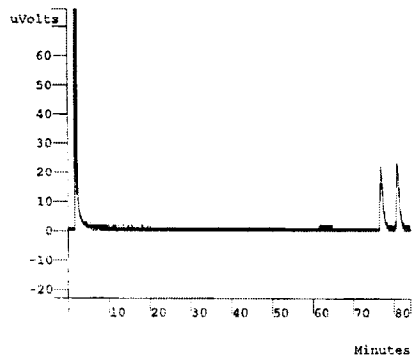

Peak No	Peak Name	Result ()	Ret. Time (min)	Time Offset (min)
1		50.1996	76.842	0.000
2		49.8004	80.891	0.000
	Totals	100.0000		0.000

Chiral Epoxide

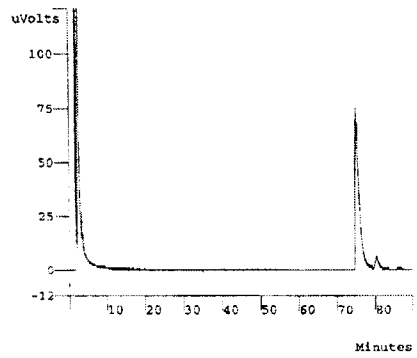

Peak No	Peak Name	Result ()	Ret. Time (min)	Time Offset (min)
1		95.0948	75.116	0.000
2		4.9052	80.199	0.000
	Totals	100.0000		0.000

Table 5.4, Entry 10
3-Chlorostyrene oxide
Column : Chiracel OD
Solvent: 99% Heptanes, 1% IPA
Flow: 1.0 mL/min
Detector: 220 nm

Racemate

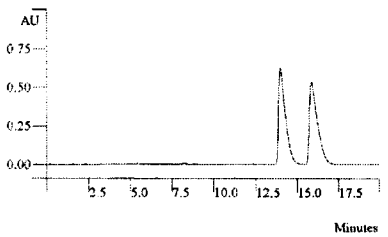

Peak No	Peak Name	Ret Time (min)	Result ()
1		13.979	50.0626
2		15.858	49.9374
Totals			100.0000

Chiral Epoxide

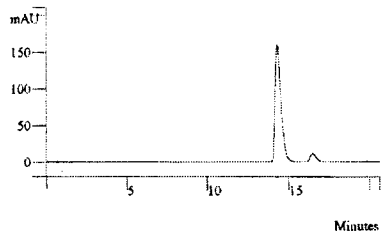

Peak No	Peak Name	Ret Time (min)	Result ()
1		14.283	92.9896
2		16.456	7.0104
Totals			100.0000

Table 5.4, Entry 11
3-Nitrostyrene oxide
Column : Chiracel OD
Solvent: 95% Heptanes, 5% IPA
Flow: 1.0 mL/min
Detector: 254 nm

Racemate

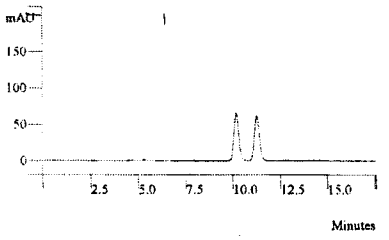

Peak No	Peak Name	Ret Time (min)	Result ()
1		10.151	49.6400
2		11.231	50.3600
Totals			100.0000

Chiral Epoxide

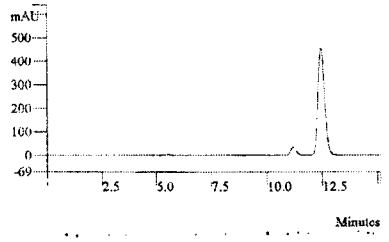

Peak No	Peak Name	Ret Time (min)	Result ()
1		11.182	6.2420
2		12.449	93.7580
Totals			100.0000

Table 5.4, Entry 12
Napthalene oxide
Column : Chiracel OJ
Solvent: 100% Hexanes
Flow: 1.0 mL/min
Detector: 210 nm

Racemate

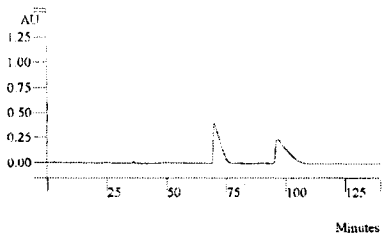

Peak No	Peak Name	Ret Time (min)	Result ()
1		69.844	49.6956
2		96.201	50.3044
	Totals		100.0000

Chiral Epoxide

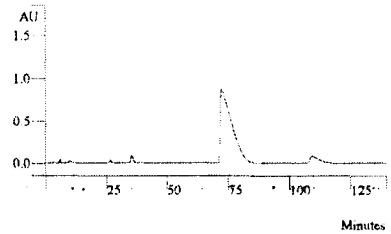

Peak No	Peak Name	Ret Time (min)	Result ()
1		72.253	93.6696
2		109.171	6.3304
	Totals		100.0000

Table 5.4, Entry 13
3,4-Dichlorostyrene Oxide
Column : B-DM
Oven temp: 80 °C
Pressure: 25 psi

Racemate

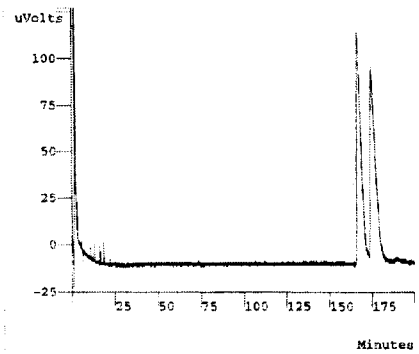

Peak No	Peak Name	Result ()	Ret. Time (min)	Time Offset (min)
1		50.1752	66.447	0.000
2		49.8248	74.494	0.000
	Totals	100.0000		0.000

Chiral Epoxide

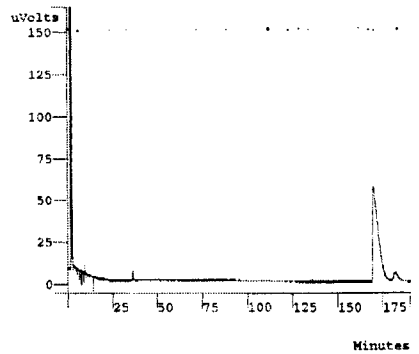

Peak No	Peak Name	Result ()	Ret. Time (min)	Time Offset (min)
1		95.8728	69.946	0.000
2		4.1272	81.523	0.000
	Totals	100.0000		0.000

Table 5.4, Entry 14
3,5-Dimethylstyrene Oxide
Column : B-DM
Oven temp: 70 °C
Pressure: 20 psi

Racemate

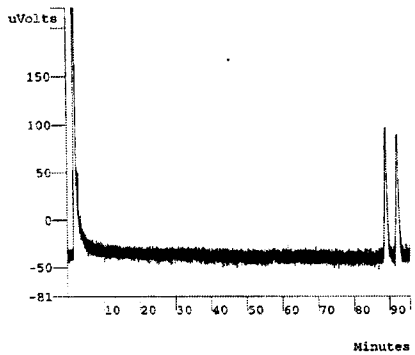

Peak No	Peak Name	Result ()	Ret. Time (min)	Time Offset (min)
1		49.2782	89.007	0.000
2		50.7218	92.313	0.000
	Totals	100.0000		0.000

Chiral Epoxide

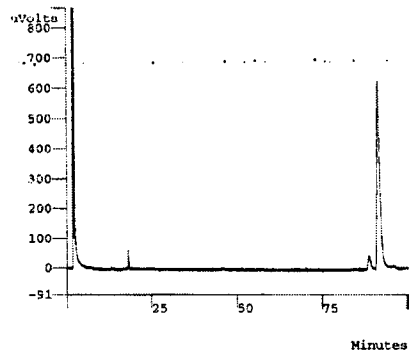

Peak No	Peak Name	Result ()	Ret. Time (min)	Time Offset (min)
1		5.1846	88.952	0.000
2		94.8154	91.556	0.000
	Totals	100.0000		0.000

Pronethalol
Column : Chiracel OD
Solvent: 95% Heptanes, 4.9% IPA, 0.1% Diethylamine
Flow: 1.0 mL/min
Detector: 270 nm

Racemate

Peak No	Peak Name	Ret Time (min)	Result ()
1		25.882	49.3563
2		27.894	50.6437
	Totals		100.0000

Chiral Epoxide

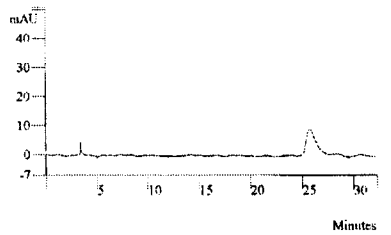

Peak No	Peak Name	Ret Time (min)	Result ()
1		25.746	100.0000
	Totals		100.0000

cis-β-Methylstyrene Oxide
Column : B-DM
Oven temp: 100 °C
Pressure: 25 psi

Racemate

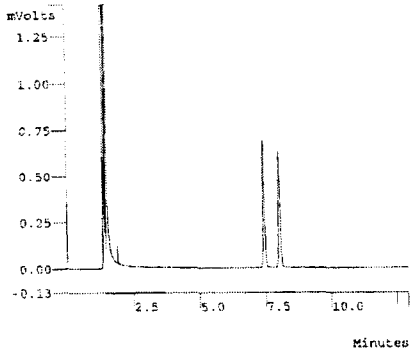

Peak No	Peak Name	Result ()	Ret. Time (min)	Time Offset (min)
1		49.7834	7.409	0.000
2		50.2166	7.997	0.000
	Totals	100.0000		0.000

Table 5.5, Entry 1

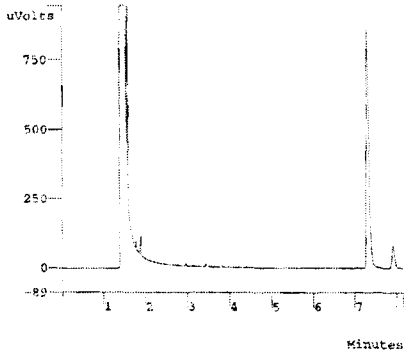

Peak No	Peak Name	Result ()	Ret. Time (min)	Time Offset (min)
1		91.8109	7.299	0.000
2		8.1891	7.914	0.000
	Totals	100.0000		0.000

Table 5.5, Entry 2

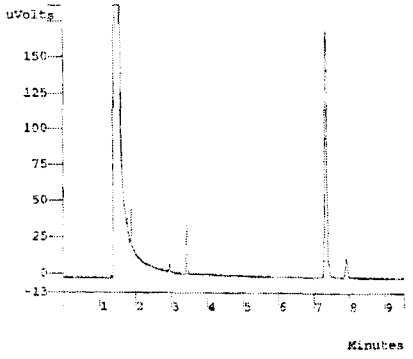

Peak No	Peak Name	Result ()	Ret. Time (min)	Time Offset (min)
1		6.9098	3.428	0.000
2		86.5043	7.334	0.000
3		6.5859	7.921	0.000
	Totals	100.0000		0.000

Table 5.5, Entry 3

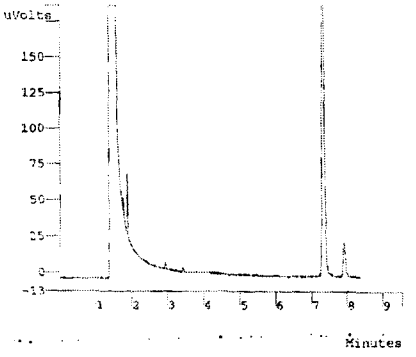

Peak No	Peak Name	Result ()	Ret. Time (min)	Time Offset (min)
1		92.9805	7.332	0.000
2		7.0195	7.929	0.000
	Totals	100.0000		0.000

Table 5.5, Entry 4

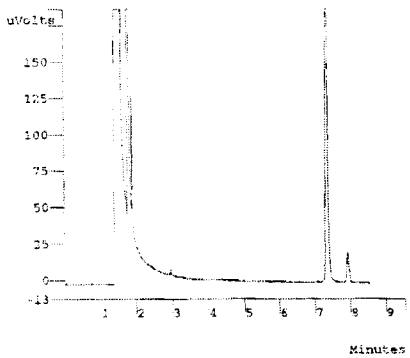

Peak No	Peak Name	Result ()	Ret. Time (min)	Time Offset (min)
1		92.1733	7.331	0.000
2		7.8267	7.919	0.000
	Totals	100.0000		0.000

Table 5.6, Entry 3

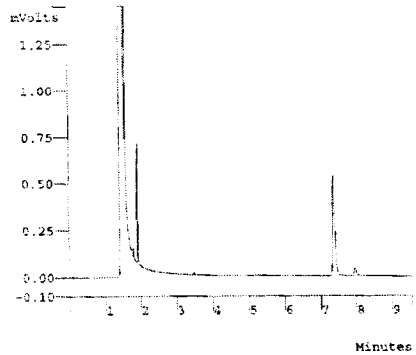

Peak No	Peak Name	Result ()	Ret. Time (min)	Time Offset (min)
1		92.9288	7.359	0.000
2		7.0712	7.964	0.000
	Totals	100.0000		0.000

Table 5.6, Entry 4

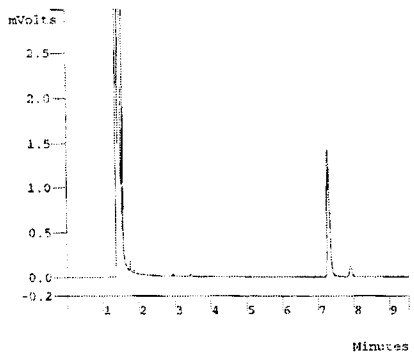

Peak No	Peak Name	Result ()	Ret. Time (min)	Time Offset (min)
1		92.7433	7.278	0.000
2		7.2567	7.909	0.000
	Totals	100.0000		0.000

Table 5.6, Entry 5

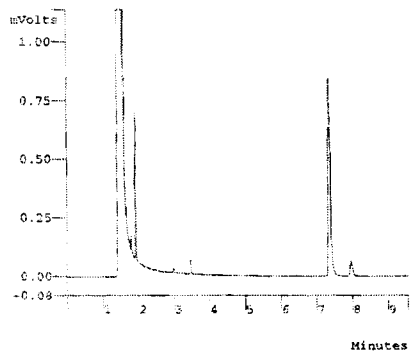

Peak No	Peak Name	Result ()	Ret. Time (min)	Time Offset (min)
1		2.3501	3.461	0.000
2		90.3572	7.344	0.000
3		7.2927	7.959	0.000
	Totals	100.0000		0.000

Table 5.6, Entry 6

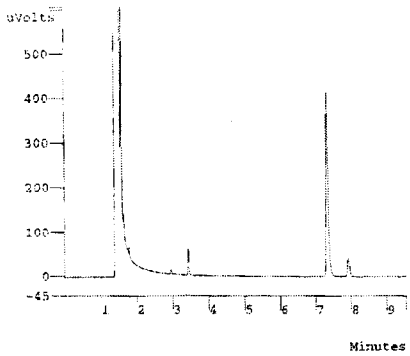

Peak No	Peak Name	Result ()	Ret. Time (min)	Time Offset (min)
1		5.3449	3.429	0.000
2		86.2552	7.323	0.000
3		8.3999	7.924	0.000
	Totals	100.0000		0.000

Table 5.6, Entry 7

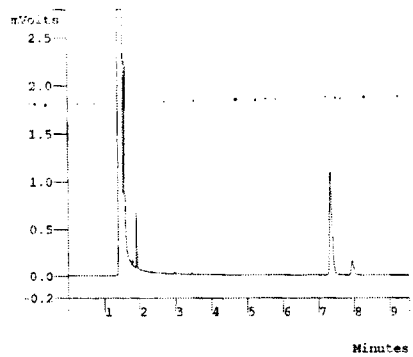

Peak No	Peak Name	Result ()	Ret. Time (min)	Time Offset (min)
1		87.7576	7.327	0.000
2		12.2424	7.946	0.000
	Totals	100.0000		0.000

Table 5.6, Entry 8

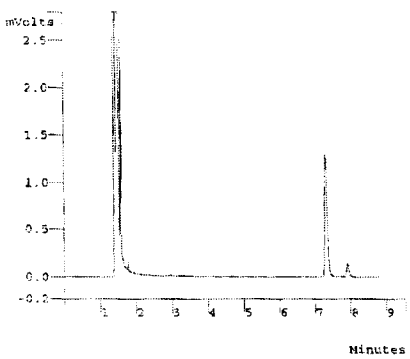

Peak No	Peak Name	Result ()	Ret. Time (min)	Time Offset (min)
1		91.1359	7.287	0.000
2		8.8641	7.914	0.000
	Totals	100.0000		0.000

Table 5.6, Entry 9

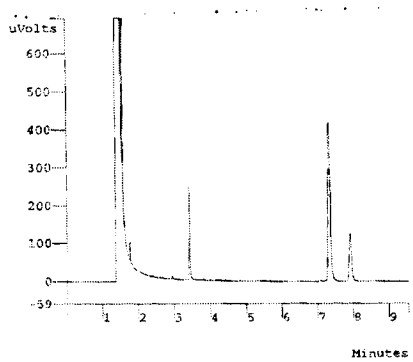

Peak No	Peak Name	Result ()	Ret. Time (min)	Time Offset (min)
1		15.5152	3.426	0.000
2		64.6735	7.326	0.000
3		19.8113	7.918	0.000
	Totals	100.0000		0.000

Table 5.6, Entry 10

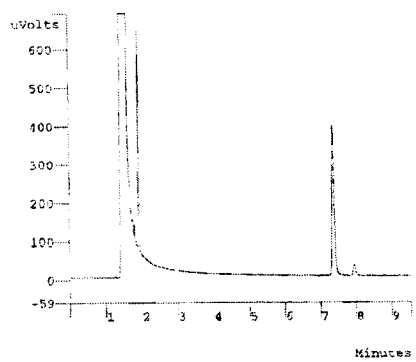

Peak No	Peak Name.	Result ()	Ret. Time (min)	Time Offset (min)
1		93.1533	7.358	0.000
2		6.8467	7.951	0.000
	Totals	100.0000		0.000

Table 5.6, Entry 11

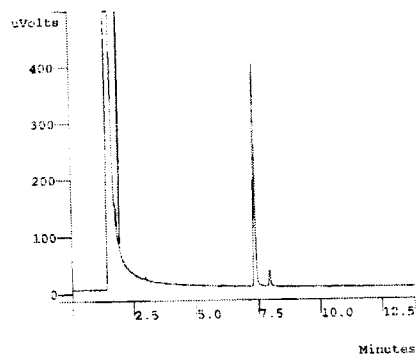

Peak No	Peak Name	Result ()	Ret. Time (min)	Time Offset (min)
1		93.1533	7.358	0.000
2		6.8467	7.951	0.000
	Totals	100.0000		0.000

Table 5.6, Entry 12

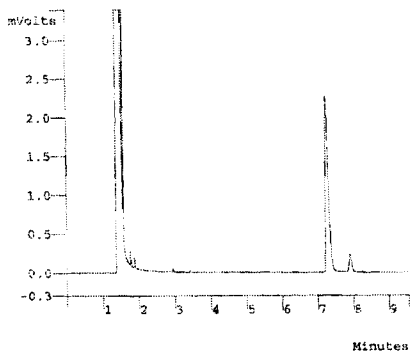

Peak No	Peak Name	Result ()	Ret. Time (min)	Time Offset (min)
1		92.5867	7.242	0.000
2		7.4133	7.899	0.000
	Totals	100.0000		0.000

Table 5.6, Entry 13

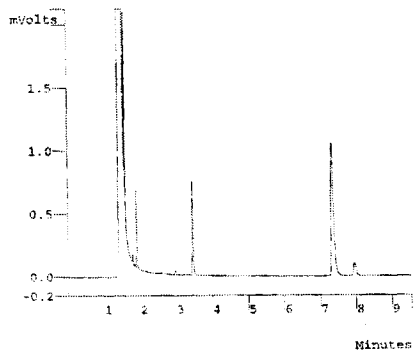

Peak No	Peak Name	Result ()	Ret. Time (min)	Time Offset (min)
1		19.4700	3.459	0.000
2		73.1947	7.336	0.000
3		7.3354	7.956	0.000
	Totals	100.0001		0.000

Table 5.6, Entry 14

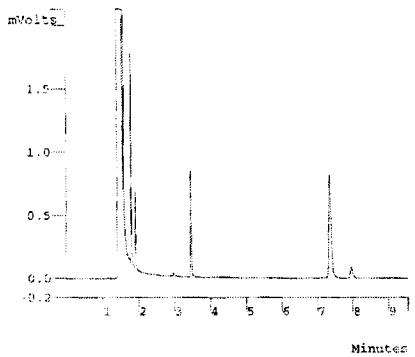

Peak No	Peak Name	Result ()	Ret. Time (min)	Time Offset (min)
1		26.9565	3.457	0.000
2		66.0034	7.347	0.000
3		7.0401	7.957	0.000
	Totals	100.0000		0.000

Table 5.6, Entry 15

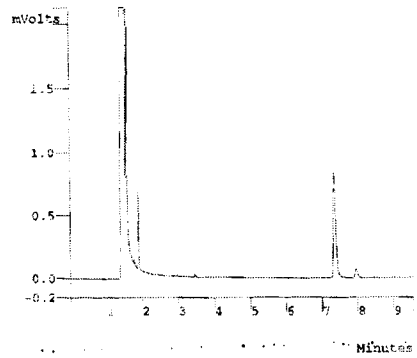

Peak No	Peak Name	Result ()	Ret. Time (min)	Time Offset (min)
1		0.6732	3.451	0.000
2		92.1055	7.336	0.000
3		7.2212	7.948	0.000
	Totals	99.9999		0.000

Table 5.6, Entry 16

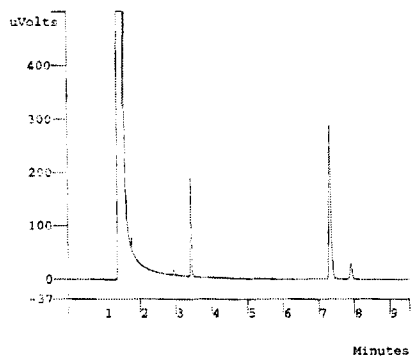

Peak No	Peak Name	Result ()	Ret. Time (min)	Time Offset (min)
1		19.8417	3.424	0.000
2		73.0296	7.323	0.000
3		7.1287	7.911	0.000
	Totals	100.0000		0.000

Table 5.6, Entry 17

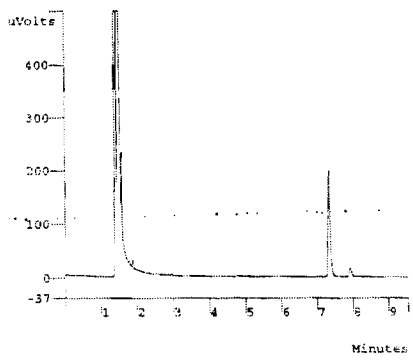

Peak No	Peak Name	Result ()	Ret. Time (min)	Time Offset (min)
1		92.8283	7.334	0.000
2		7.1718	7.921	0.000
	Totals	100.0001		0.000

Table 5.6, Entry 18

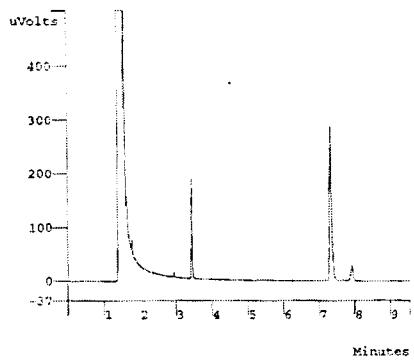

Peak No	Peak Name	Result ()	Ret. Time (min)	Time Offset (min)
1		19.8963	3.424	0.000
2		72.9799	7.323	0.000
3		7.1238	7.911	0.000
	Totals	**100.0000**		**0.000**

Table 5.6, Entry 19

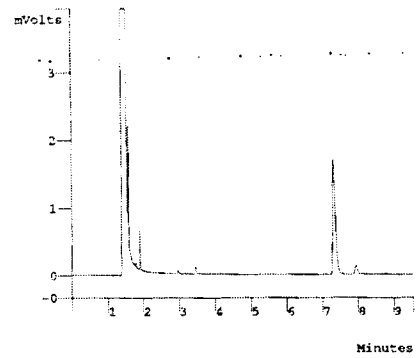

Peak No	Peak Name	Result ()	Ret. Time (min)	Time Offset (min)
1		2.2302	3.456	0.000
2		91.2532	7.304	0.000
3		6.5166	7.944	0.000
	Totals	**100.0000**		**0.000**

Styrene Oxide
Column : B-DM
Oven temp: 80 °C
Pressure: 25 psi

Racemate

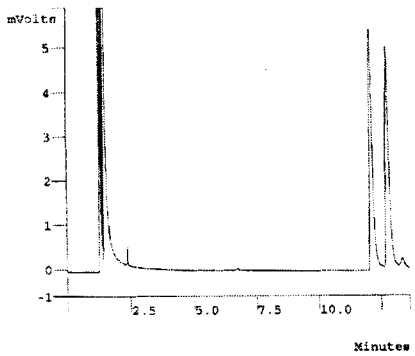

Peak No	Peak Name	Result ()	Ret. Time (min)	Time Offset (min)
1		50.0995	12.099	0.000
2		49.9005	12.743	0.000
	Totals	100.0000		0.000

Table 5.11, Entry 1

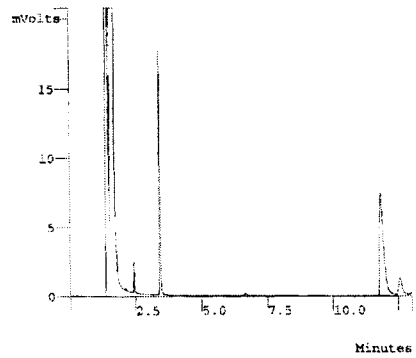

Peak No	Peak Name	Result ()	Ret. Time (min)	Time Offset (min)
1		30.1261	3.424	0.000
2		61.5822	11.819	0.000
3		8.2918	12.564	0.000
	Totals	100.0001		0.000

Table 5.11, Entry 2

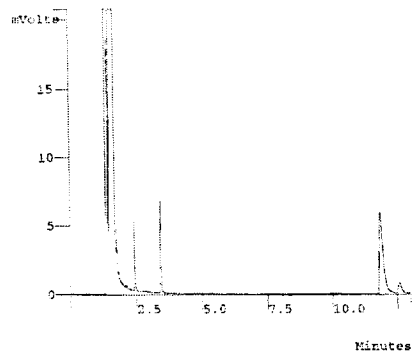

Peak No	Peak Name	Result ()	Ret. Time (min)	Time Offset (min)
1		17.5911	3.422	0.000
2		74.1399	11.841	0.000
3		8.2690	12.573	0.000
	Totals	100.0000		0.000

Table 5.11, Entry 3

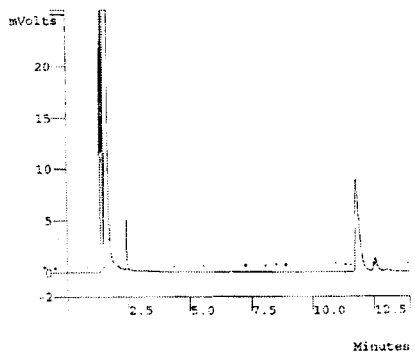

Peak No	Peak Name	Result ()	Ret. Time (min)	Time Offset (min)
1		90.3412	11.783	0.000
2		9.6588	12.551	0.000
	Totals	100.0000		0.000

Table 5.11, Entry 4

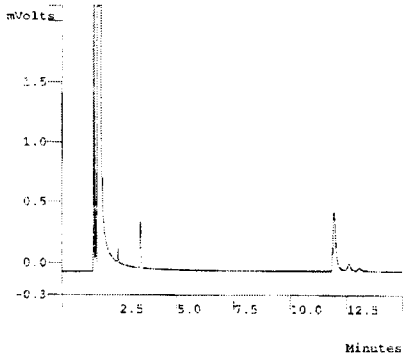

Peak No	Peak Name	Result ()	Ret. Time (min)	Time Offset (min)
1		15.6721	3.418	0.000
2		75.8714	11.934	0.000
3		8.4565	12.584	0.000
	Totals	100.0000		0.000

Table 5.11, Entry 5

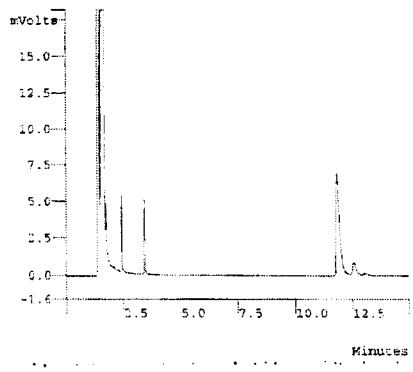

Peak No	Peak Name	Result ()	Ret. Time (min)	Time Offset (min)
1		11.5084	3.421	0.000
2		79.6944	11.818	0.000
3		8.7972	12.561	0.000
	Totals	100.0000		0.000

Table 5.11, Entry 6

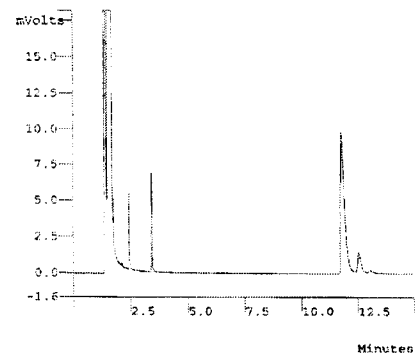

Peak No	Peak Name	Result ()	Ret. Time (min)	Time Offset (min)
1		10.6993	3.419	0.000
2		80.8629	11.757	0.000
3		8.4378	12.534	0.000
	Totals	100.0000		0.000

Table 5.11, Entry 7

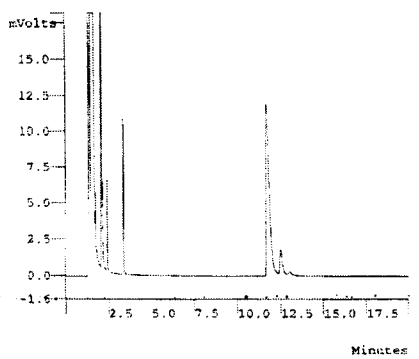

Peak No	Peak Name	Result ()	Ret. Time (min)	Time Offset (min)
1		11.9295	3.412	0.000
2		79.5526	11.712	0.000
3		8.5180	12.502	0.000
	Totals	100.0001		0.000

Table 5.11, Entry 8

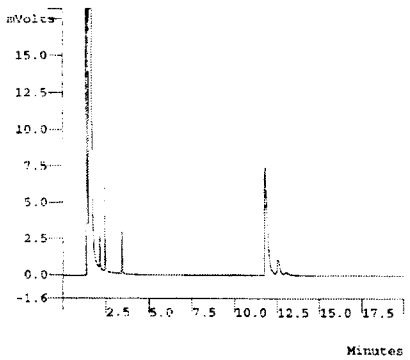

Peak No	Peak Name	Result ()	Ret. Time (min)	Time Offset (min)
1		7.6506	3.419	0.000
2		83.1680	11.796	0.000
3		9.1814	12.549	0.000
	Totals	**100.0000**		**0.000**

3-Methylstyrene Oxide

Column : B-DM
Oven temp: 60 °C
Pressure: 20 psi

Racemate

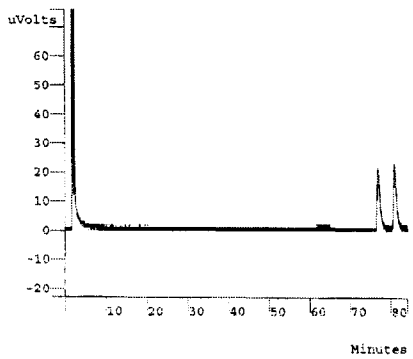

Peak No	Peak Name	Result ()	Ret. Time (min)	Time Offset (min)
1		50.1996	76.842	0.000
2		49.8004	80.891	0.000
	Totals	**100.0000**		**0.000**

Table 5.12, Entry 1

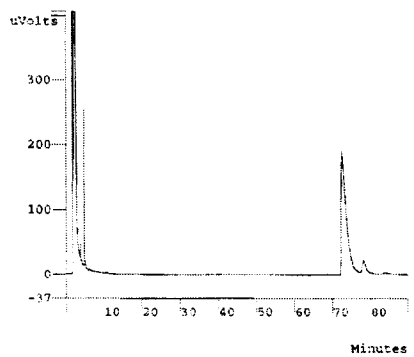

Peak No	Peak Name	Result ()	Ret. Time (min)	Time Offset (min)
1		93.4834	72.539	0.000
2		6.5166	78.077	0.000
	Totals	**100.0000**		**0.000**

Table 5.12, Entry 2

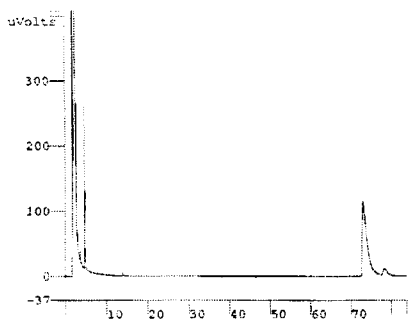

Peak No	Peak Name	Result ()	Ret. Time (min)	Time Offset (min)
1		94.7200	73.152	0.000
2		5.2800	78.384	0.000
	Totals	100.0000		0.000

Table 5.13, Entry 1

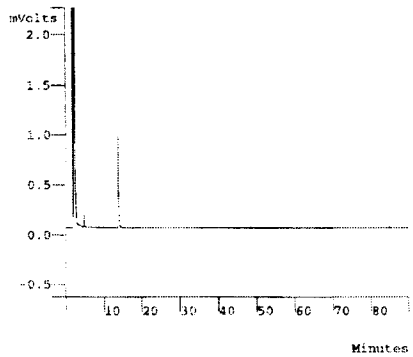

Peak No	Peak Name	Result ()	Ret. Time (min)	Time Offset (min)
1		99.4907	13.799	0.000
2		0.4109	71.791	0.000
3		0.0984	77.839	0.000
	Totals	100.0000		0.000

Table 5.13, Entry 2

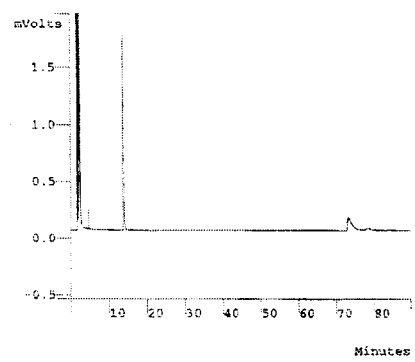

Peak No	Peak Name	Result ()	Ret. Time (min)	Time Offset (min)
1		69.3417	13.716	0.000
2		27.5712	73.199	0.000
3		3.0872	78.364	0.000
	Totals	100.0001		0.000

Table 5.14, Entry 1

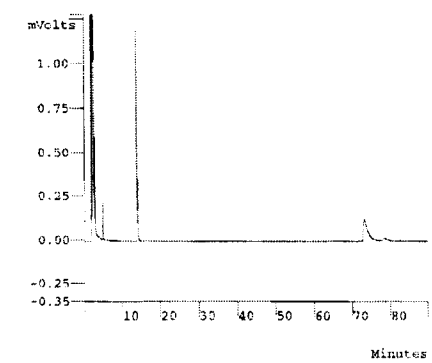

Peak No	Peak Name	Result ()	Ret. Time (min)	Time Offset (min)
1		57.0285	13.757	0.000
2		39.1697	73.121	0.000
3		3.8018	78.308	0.000
	Totals	100.0000		0.000

Table 5.14, Entry 2

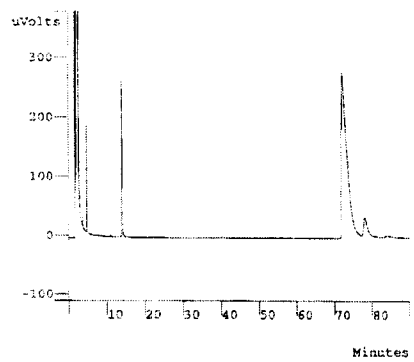

Peak No	Peak Name	Result ()	Ret. Time (min)	Time Offset (min)
1		8.7058	13.861	0.000
2		85.6705	72.081	0.000
3		5.6237	77.956	0.000
	Totals	100.0000		0.000

Table 5.14, Entry 3

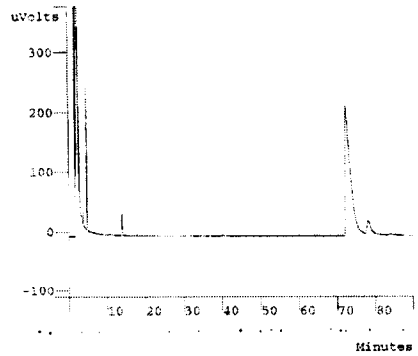

Peak No	Peak Name	Result ()	Ret. Time (min)	Time Offset (min)
1		1.8205	13.917	0.000
2		91.8085	72.454	0.000
3		6.3710	78.067	0.000
	Totals	100.0000		0.000

Table 5.15, Entry 1

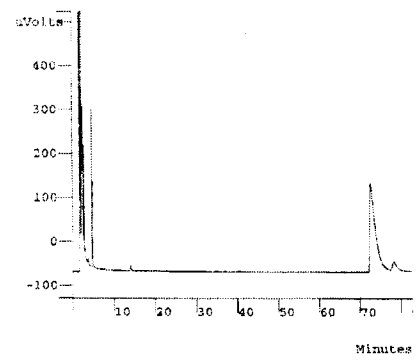

Peak No	Peak Name	Result ()	Ret. Time (min)	Time Offset (min)
1		93.9023	72.564	0.000
2		6.0977	78.301	0.000
	Totals	100.0000		0.000

Table 5.15, Entry 2

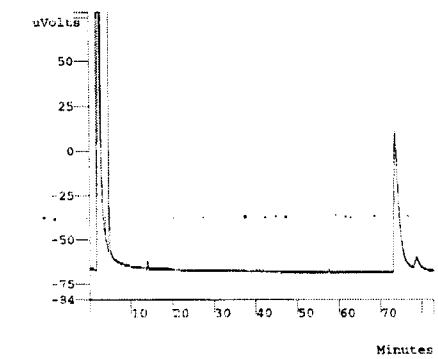

Peak No	Peak Name	Result ()	Ret. Time (min)	Time Offset (min)
1		94.5525	73.558	0.000
2		5.4475	78.634	0.000
	Totals	100.0000		0.000

Table 5.15, Entry 3

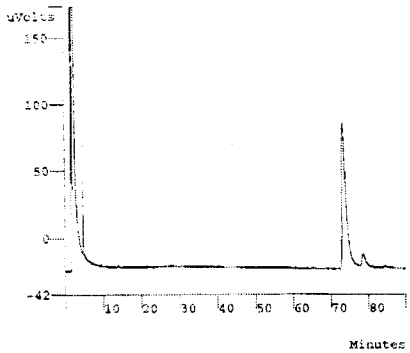

Peak No	Peak Name	Result ()	Ret. Time (min)	Time Offset (min)
1		93.9055	73.223	0.000
2		6.0945	78.473	0.000
	Totals	**100.0000**		**0.000**

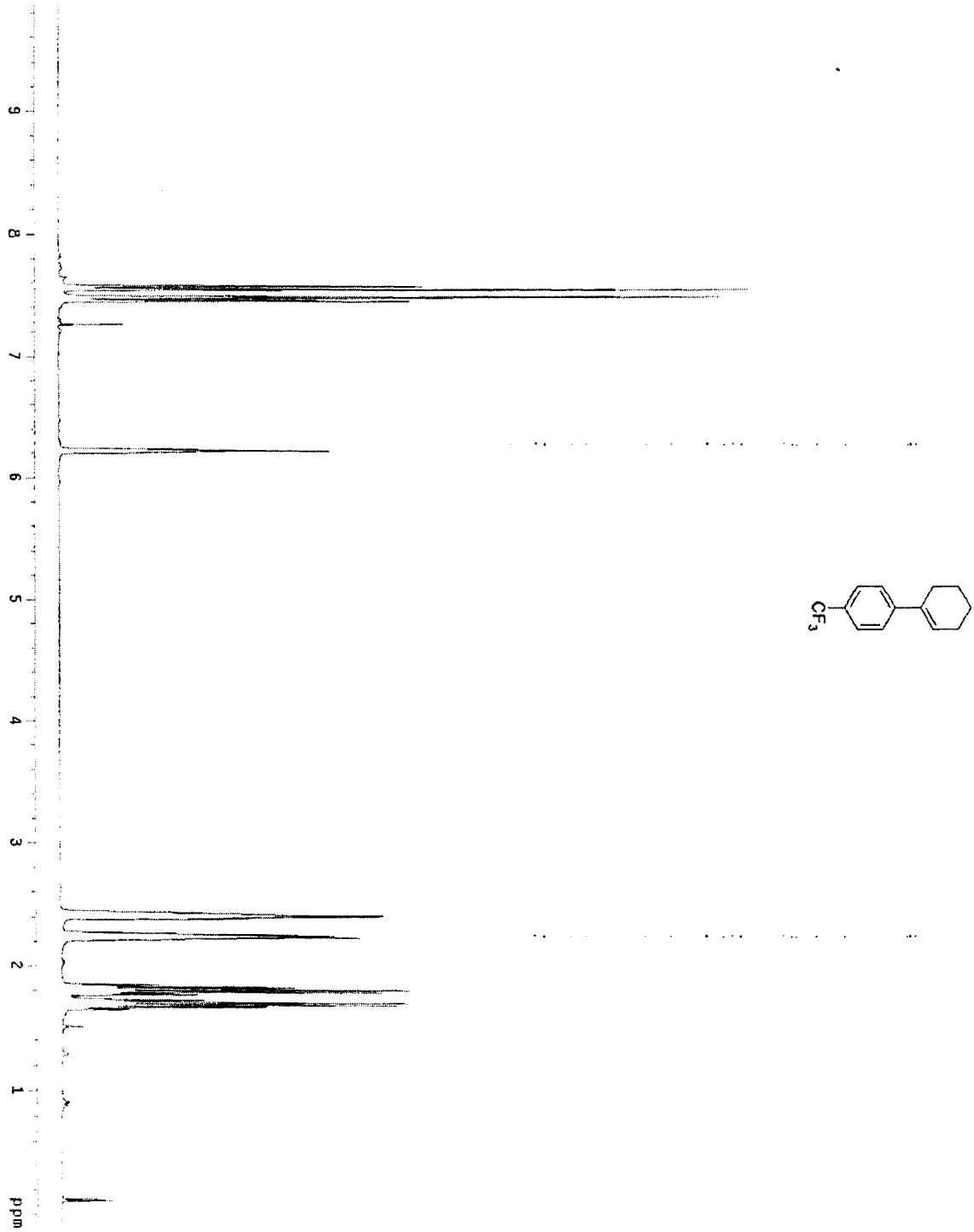

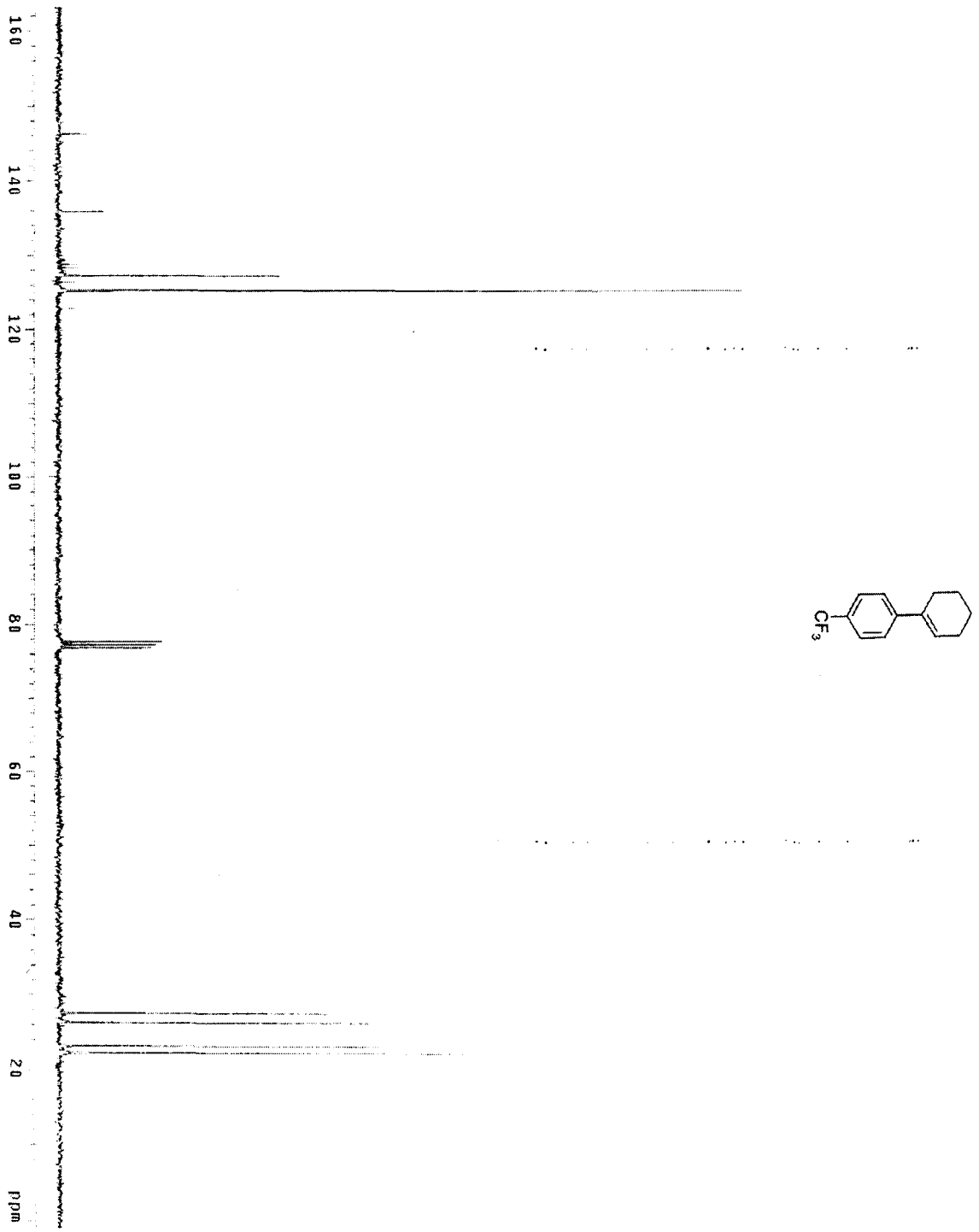

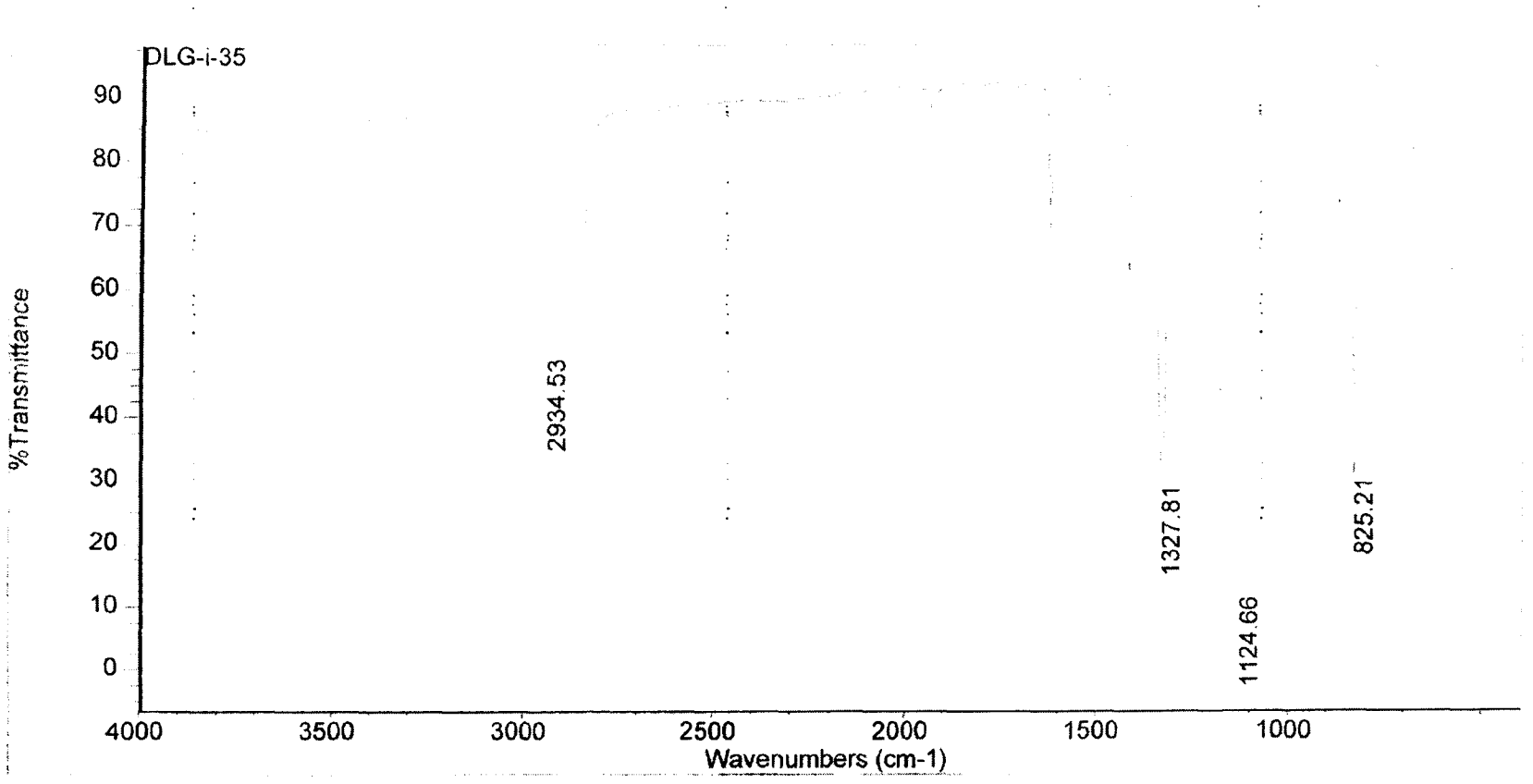

Sun Oct 20 21:18:36 2002
FIND PEAKS:

Spectrum:	DLG-i-35			
Region:	4000.00	400.00		
Absolute threshold:	53.297			
Sensitivity:	3			
Peak list:				
	Position:	1124.66	Intensity:	11.435
	Position:	1327.81	Intensity:	29.031
	Position:	825.21	Intensity:	30.208
	Position:	2934.53	Intensity:	49.251

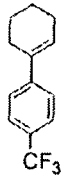

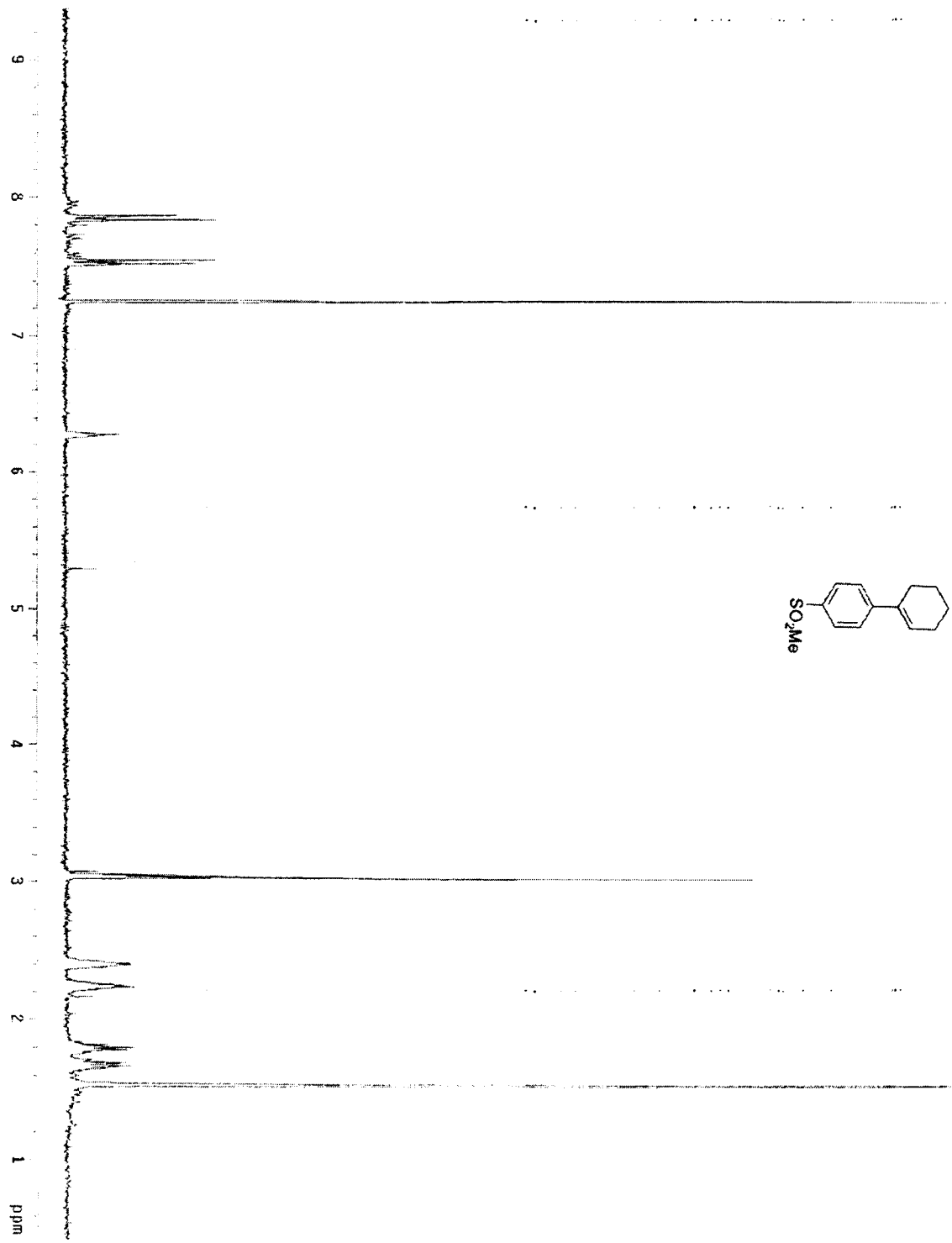

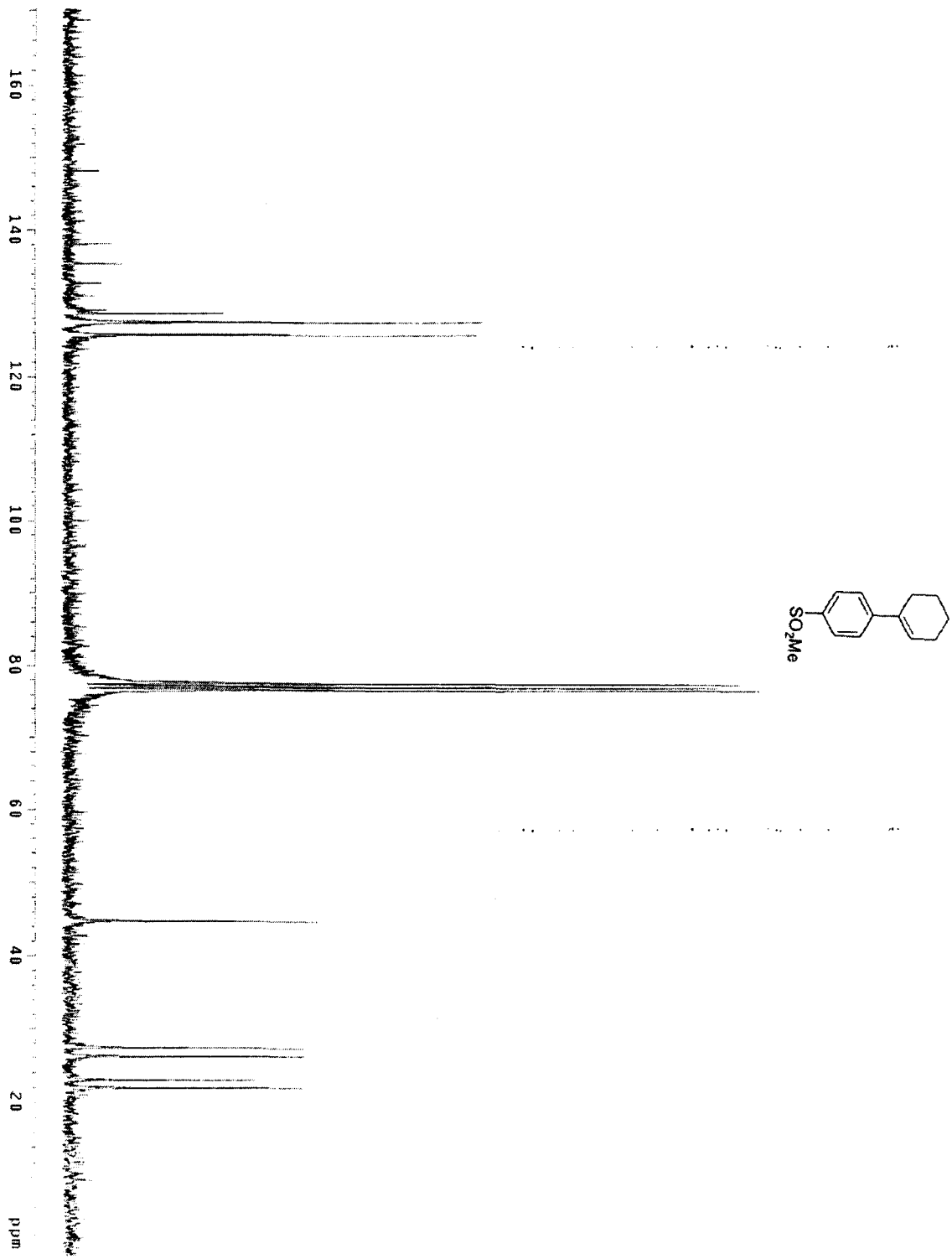

Wed Aug 21 10:14:06 2002
FIND PEAKS:
Spectrum: dlg-ii-33
Region: 4000.00 400.00
Absolute threshold: 80.942
Sensitivity: 50
Peak list:

Position:	1151.30	Intensity:	51.001
Position:	1309.14	Intensity:	59.336
Position:	777.33	Intensity:	65.947
Position:	1091.49	Intensity:	72.564
Position:	2927.89	Intensity:	73.670
Position:	956.95	Intensity:	74.681
Position:	748.09	Intensity:	75.689
Position:	823.89	Intensity:	77.348

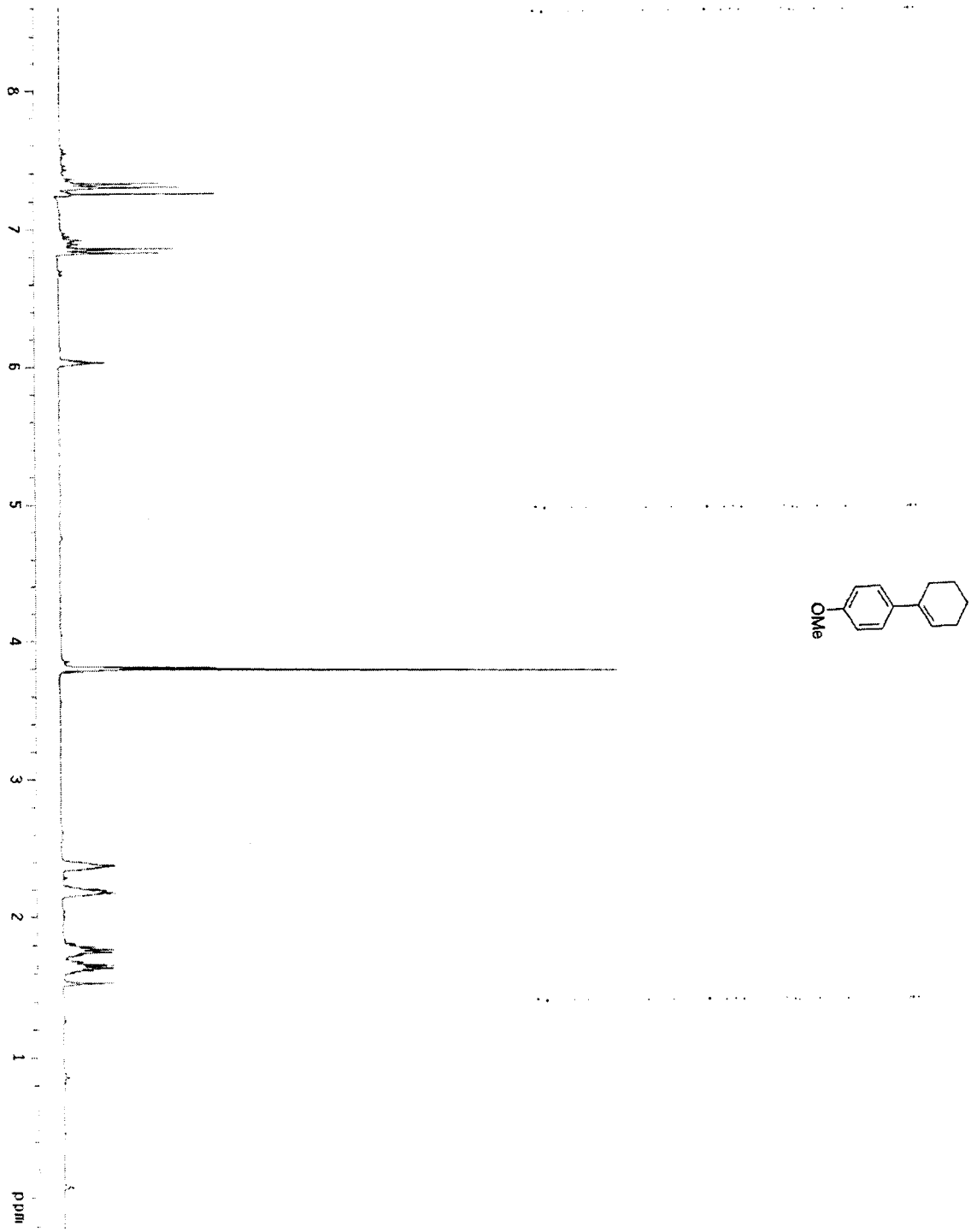

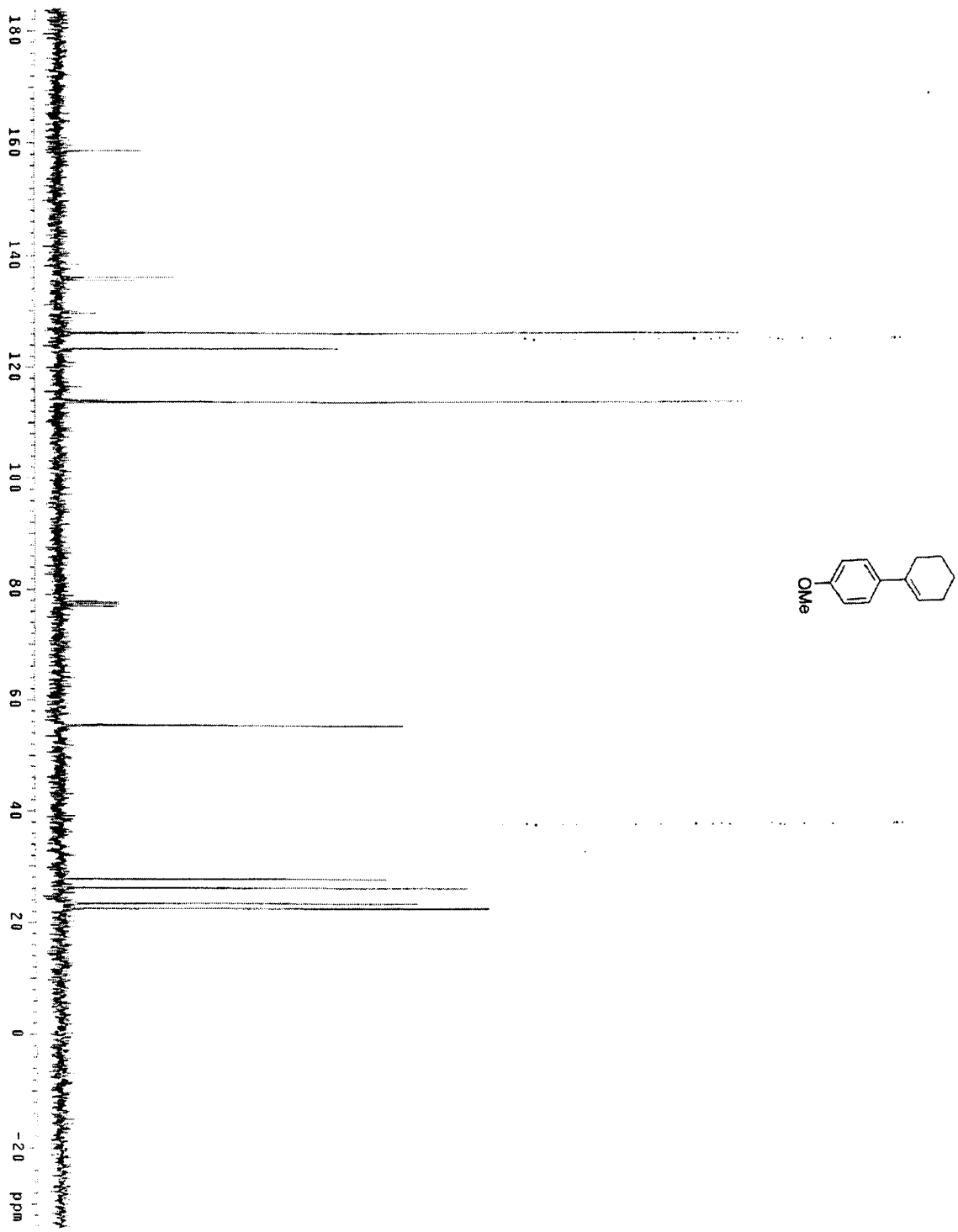

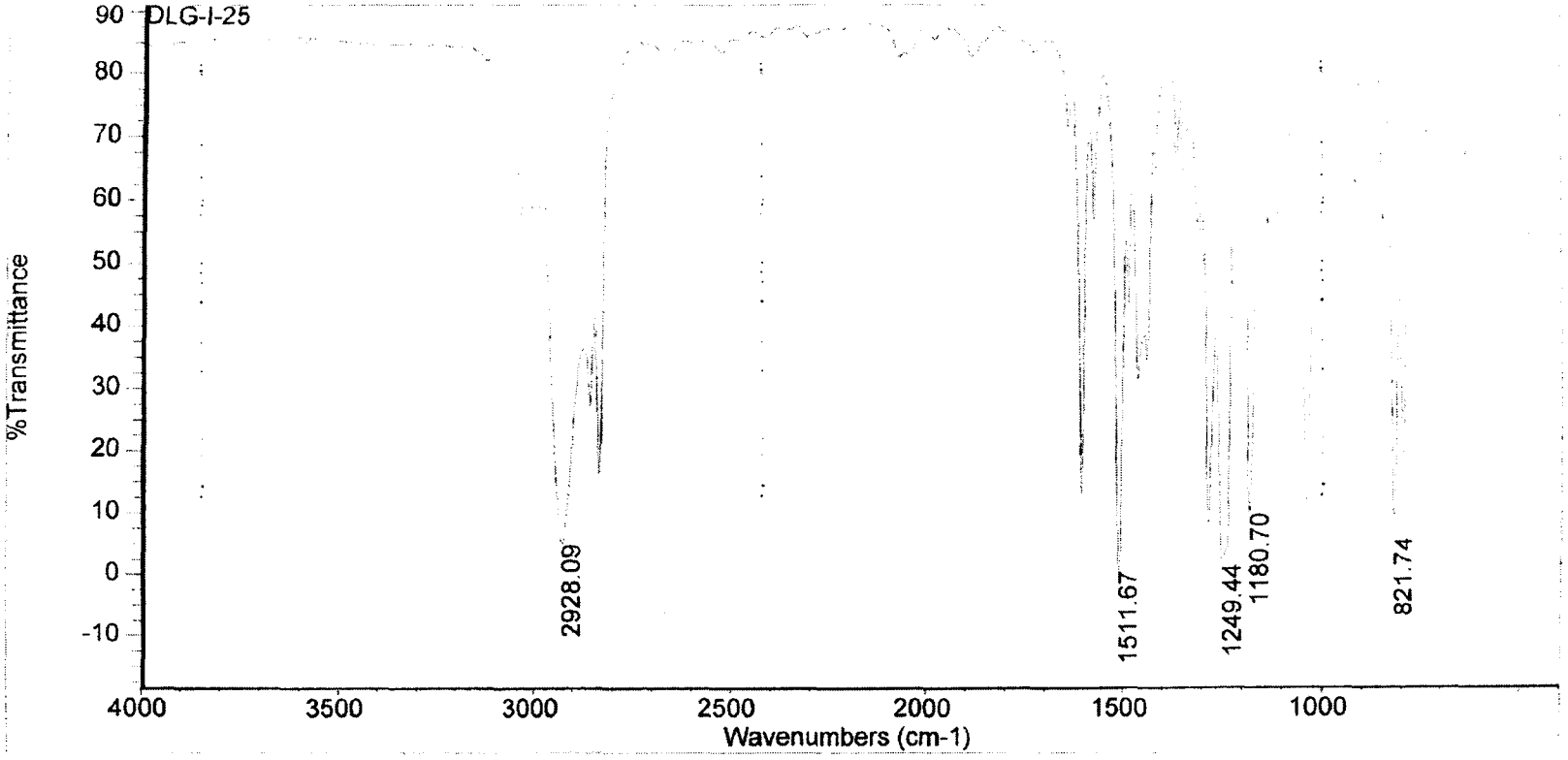

Sun Oct 13 16:34:27 2002
FIND PEAKS:

Spectrum:	DLG-I-25	
Region:	4000.00	400.00
Absolute threshold:	9.980	
Sensitivity:	4	
Peak list:		

Position:	1511.67	Intensity:	0.500
Position:	1249.44	Intensity:	1.563
Position:	2928.09	Intensity:	4.981
Position:	821.74	Intensity:	5.772
Position:	1180.70	Intensity:	9.877

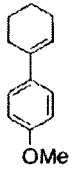

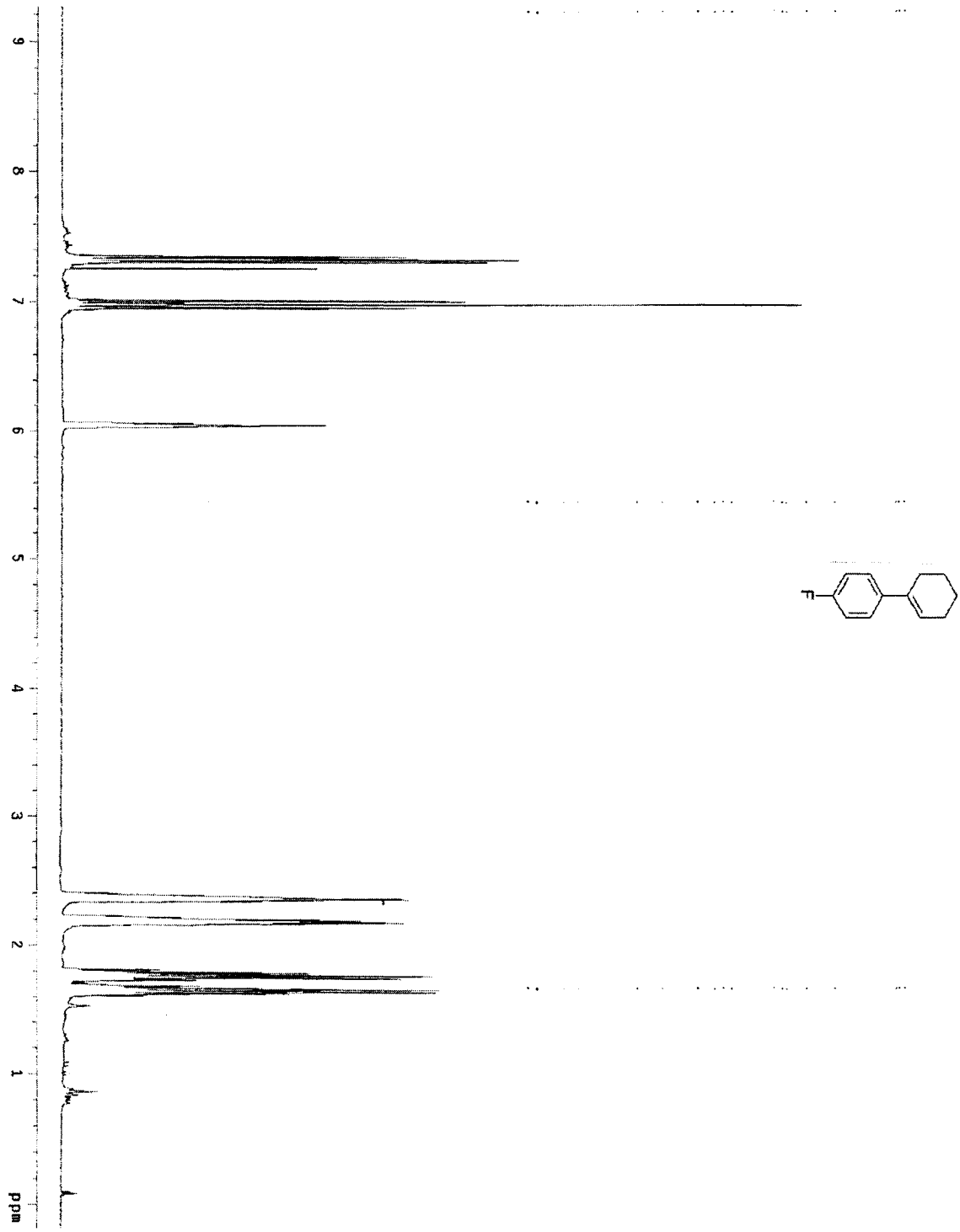

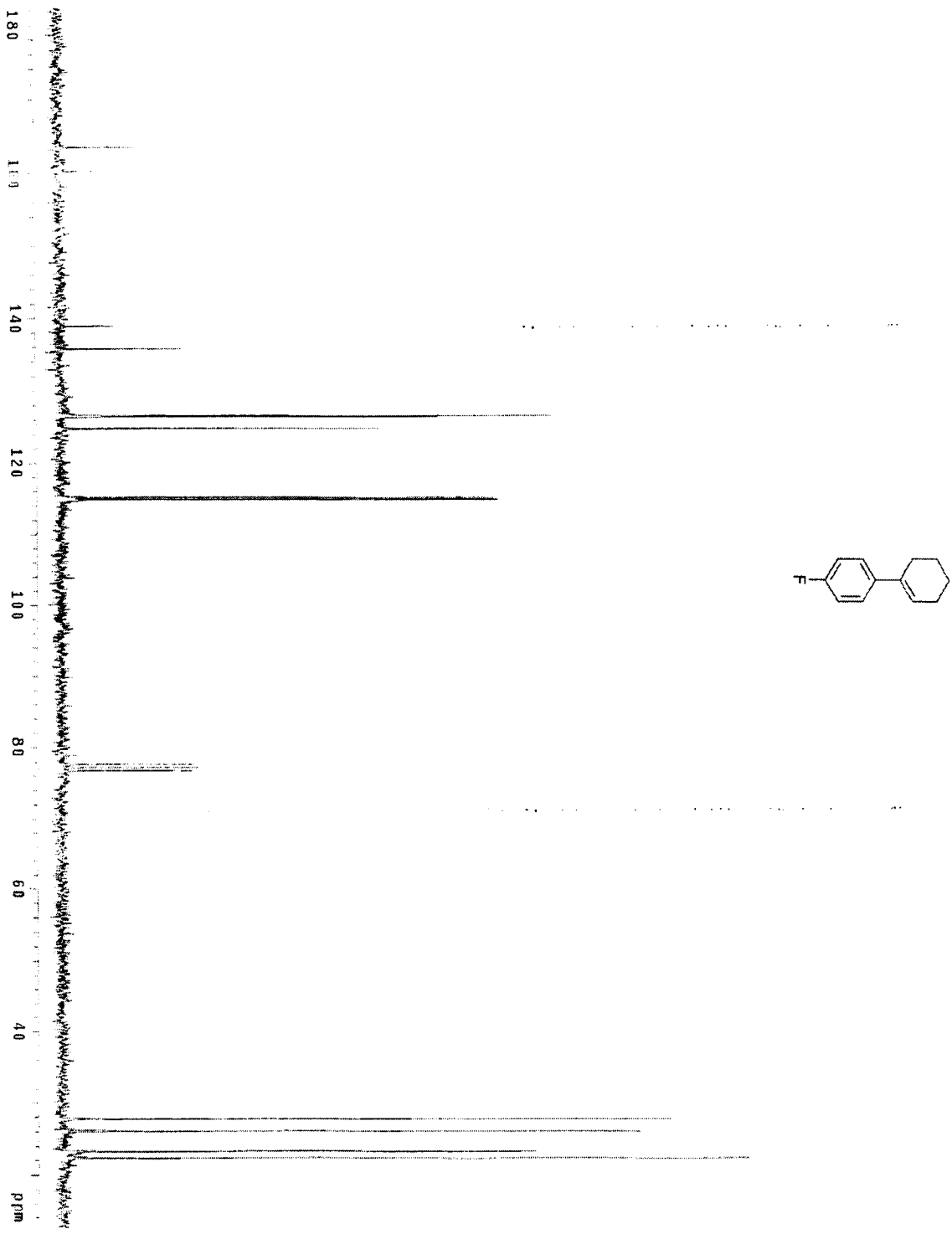

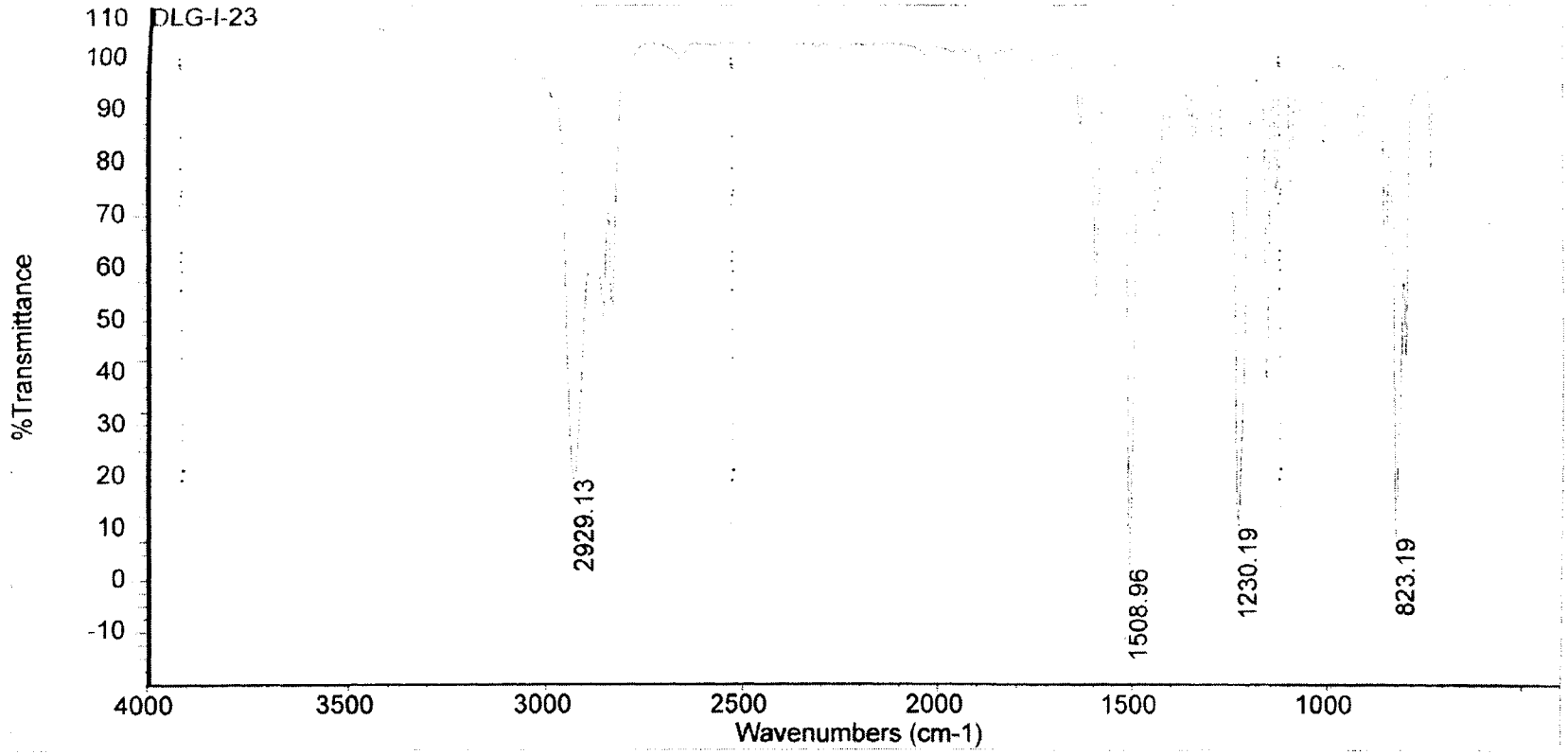

Sun Oct 20 21:32:36 2002
FIND PEAKS:

Spectrum: DLG-I-23
Region: 4000.00 400.00
Absolute threshold: 27.068
Sensitivity: 50
Peak list:

Position:	1508.96	Intensity:	2.315
Position:	823.19	Intensity:	8.286
Position:	1230.19	Intensity:	10.238
Position:	2929.13	Intensity:	19.641

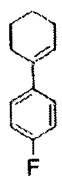

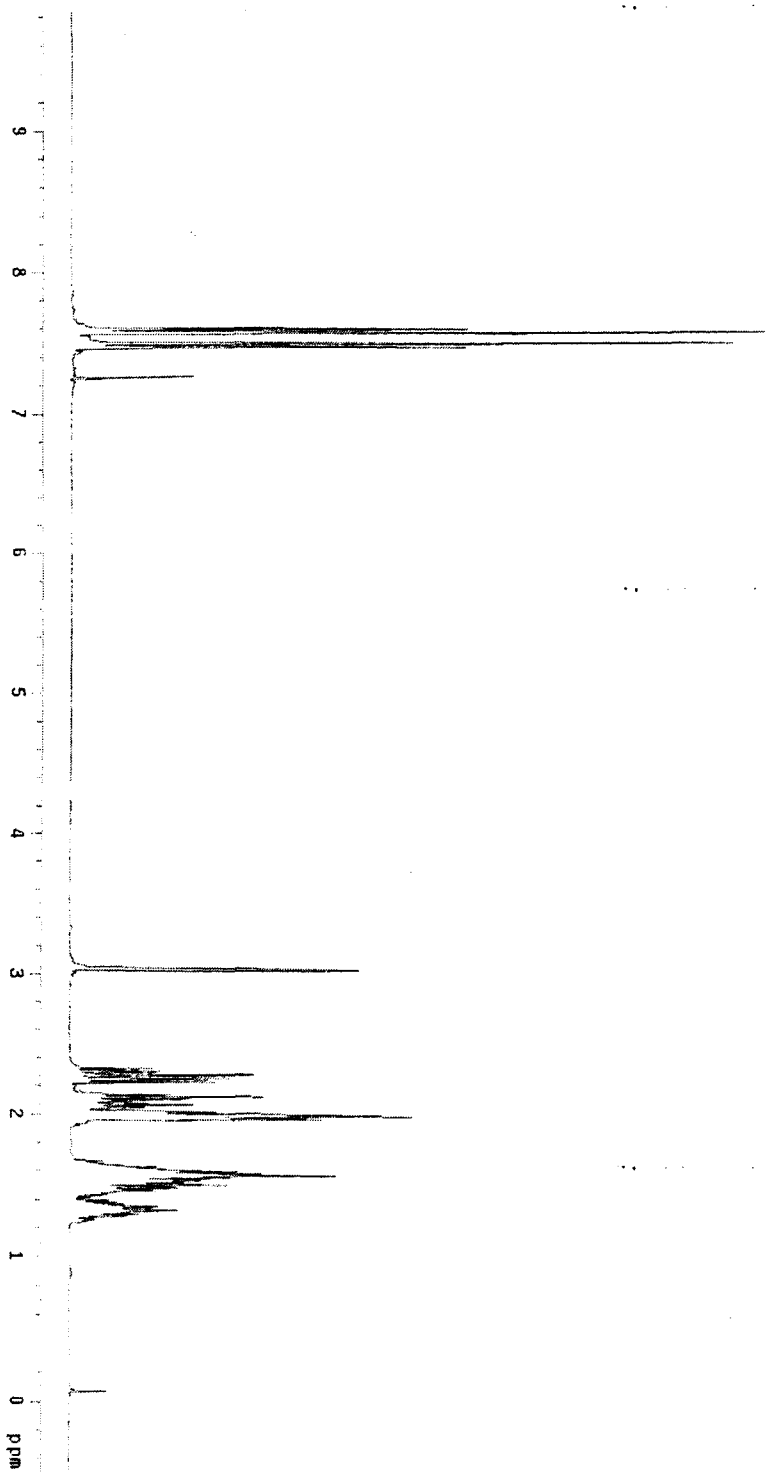

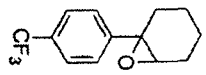

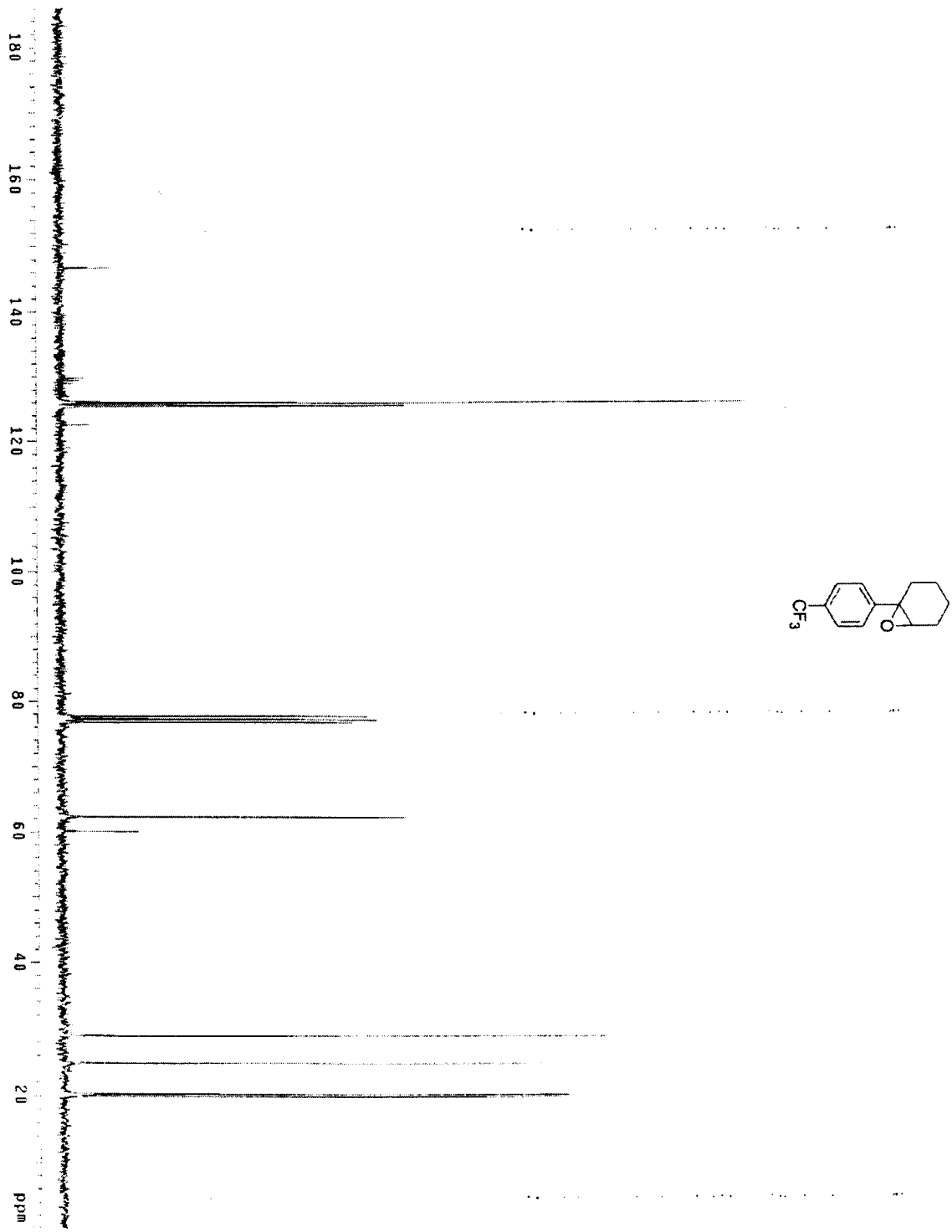

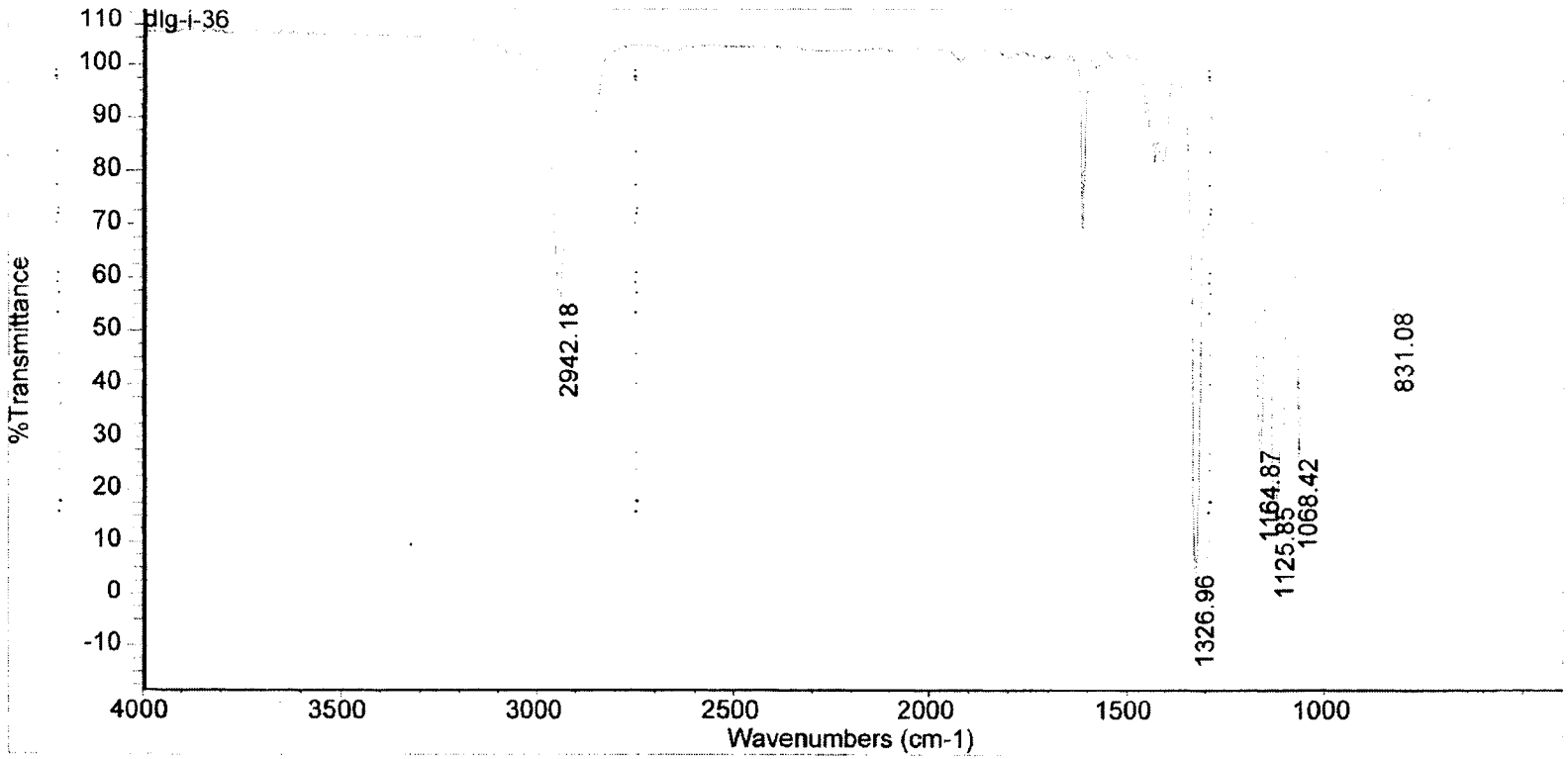

Tue Oct 08 17:55:20 2002
FIND PEAKS:

Spectrum:	dlg-i-36	
Region:	4000.00	400.00
Absolute threshold:	56.829	
Sensitivity:	50	
Peak list:		

Position:	1326.96	Intensity:	3.758
Position:	1125.85	Intensity:	16.734
Position:	1068.42	Intensity:	26.144
Position:	1164.87	Intensity:	27.738
Position:	831.08	Intensity:	53.688
Position:	2942.18	Intensity:	55.340

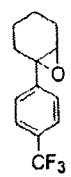

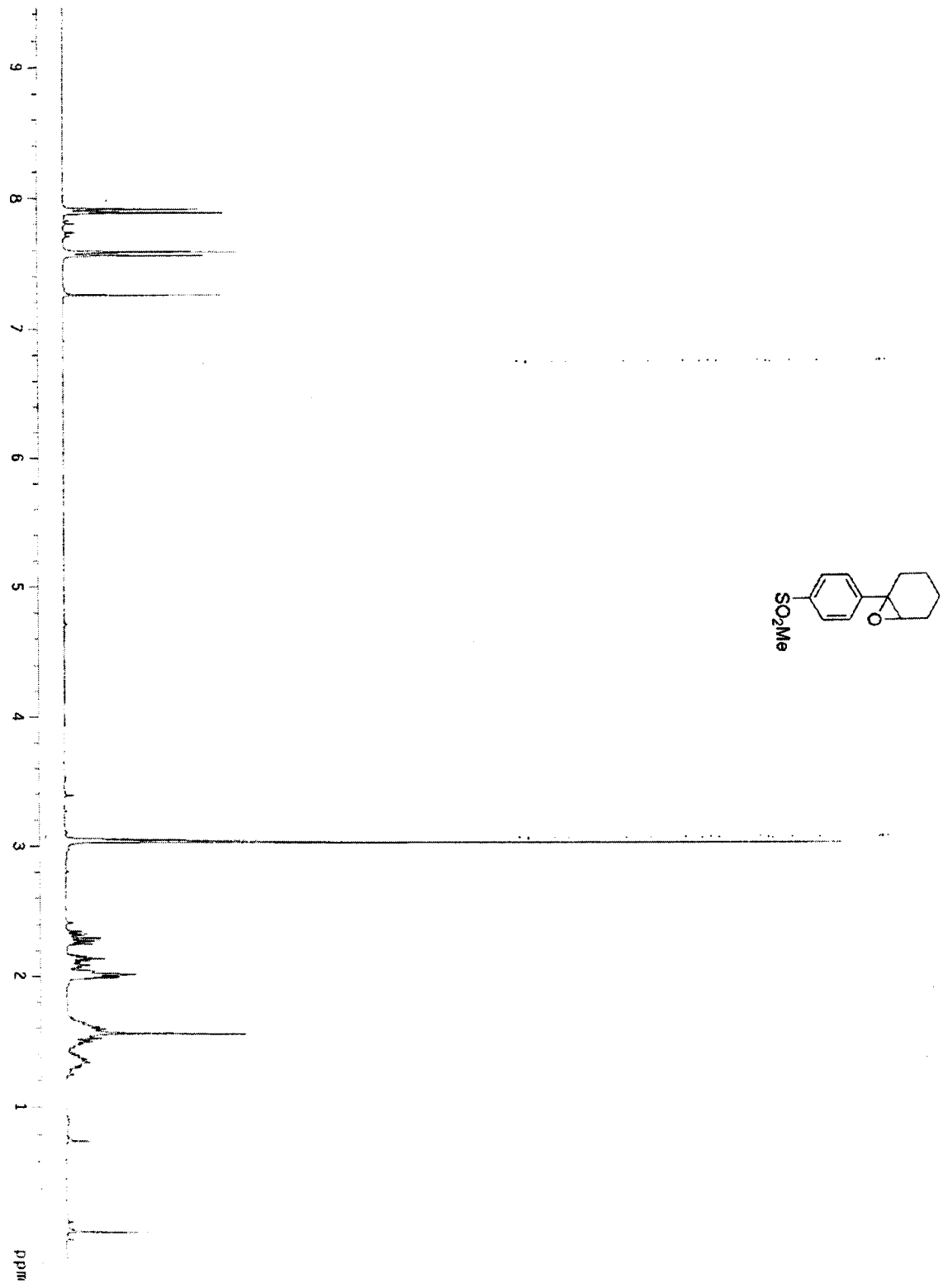

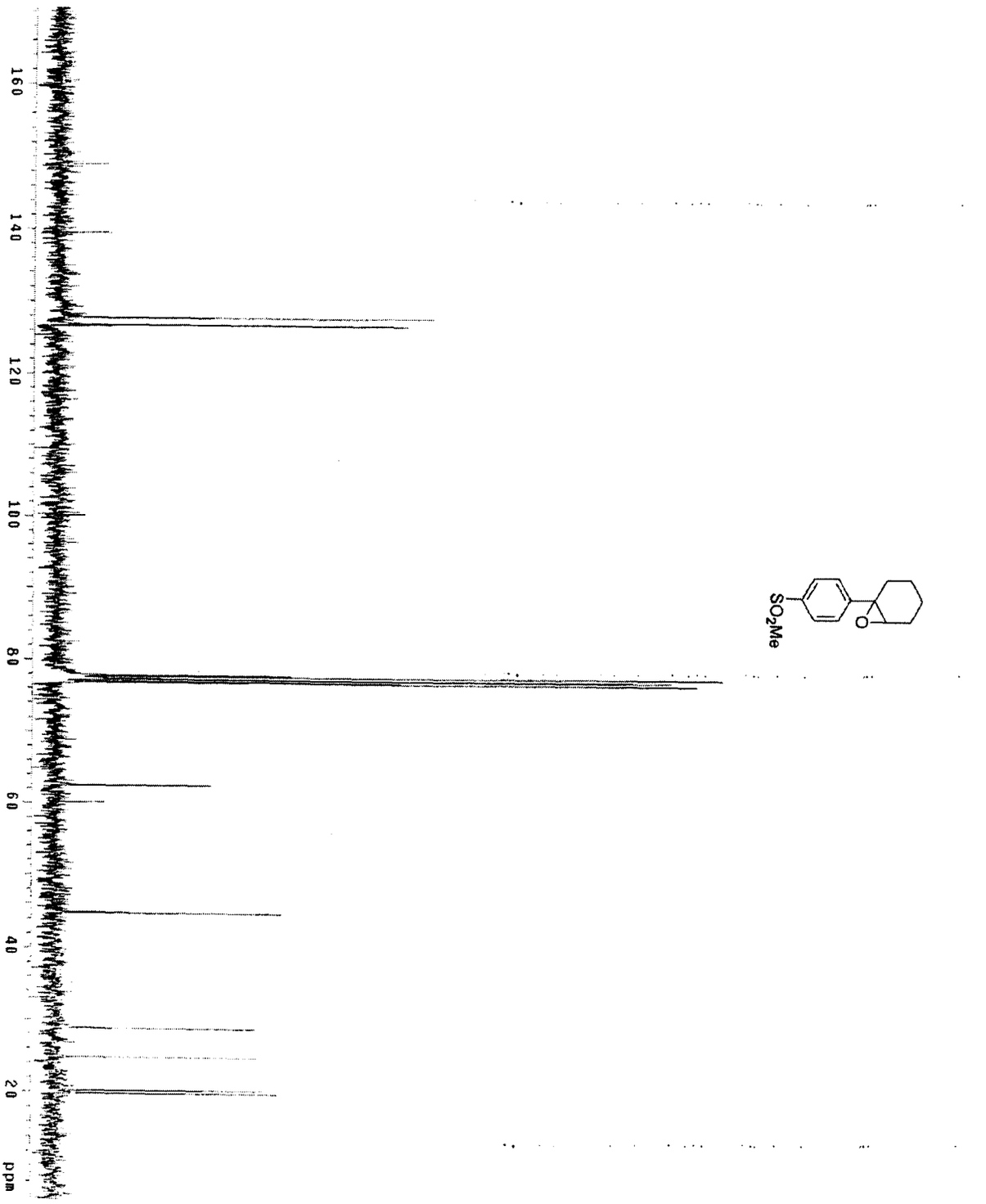

Mon Oct 14 13:05:21 2002
FIND PEAKS:

Spectrum:	DLG-III-35	
Region:	4000.00	400.00
Absolute threshold:	62.707	
Sensitivity:	58	
Peak list:		

Position:	1152.96	Intensity:	25.636
Position:	1312.73	Intensity:	36.432
Position:	767.74	Intensity:	52.873
Position:	2937.59	Intensity:	59.447
Position:	1089.60	Intensity:	61.010
Position:	958.52	Intensity:	62.467

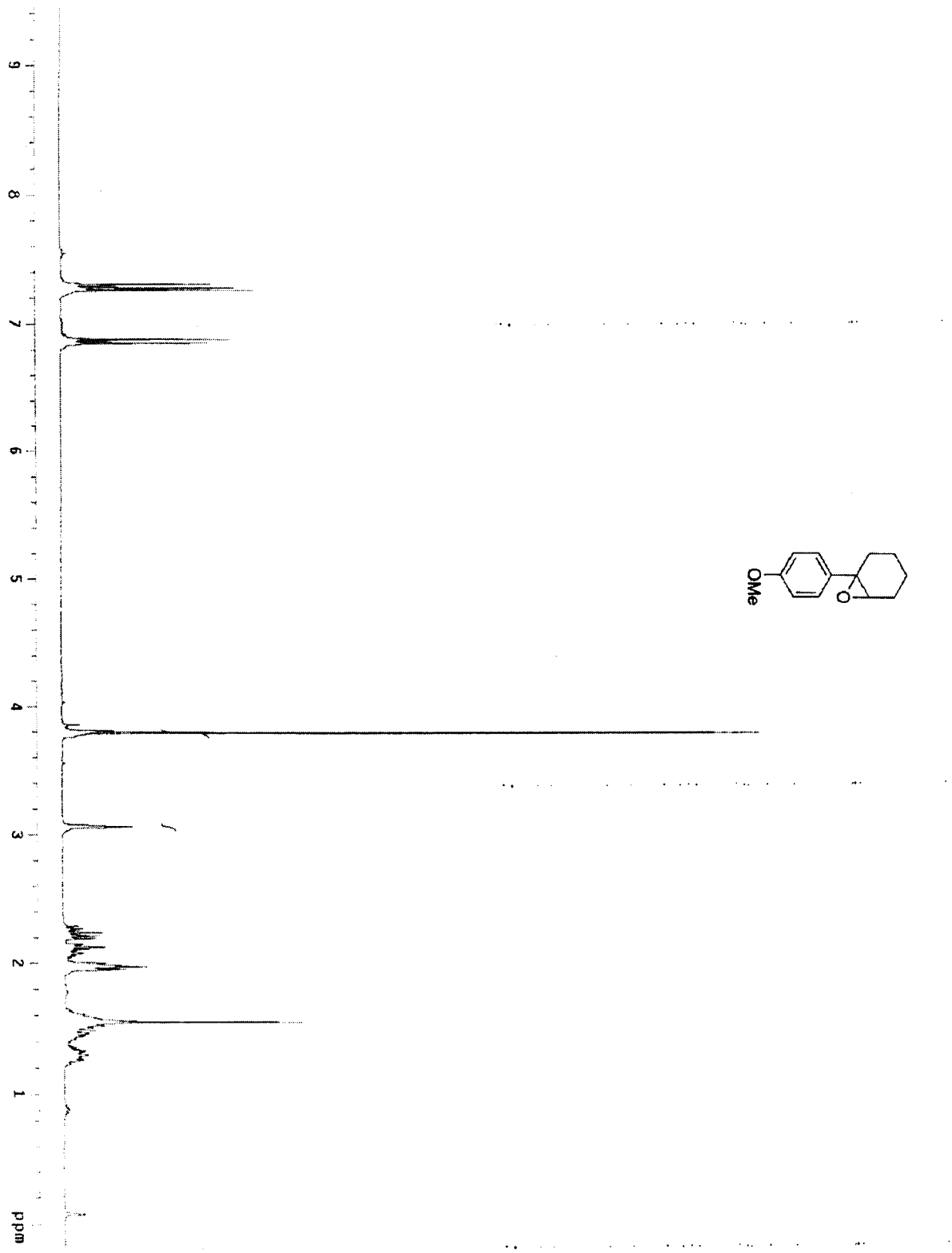

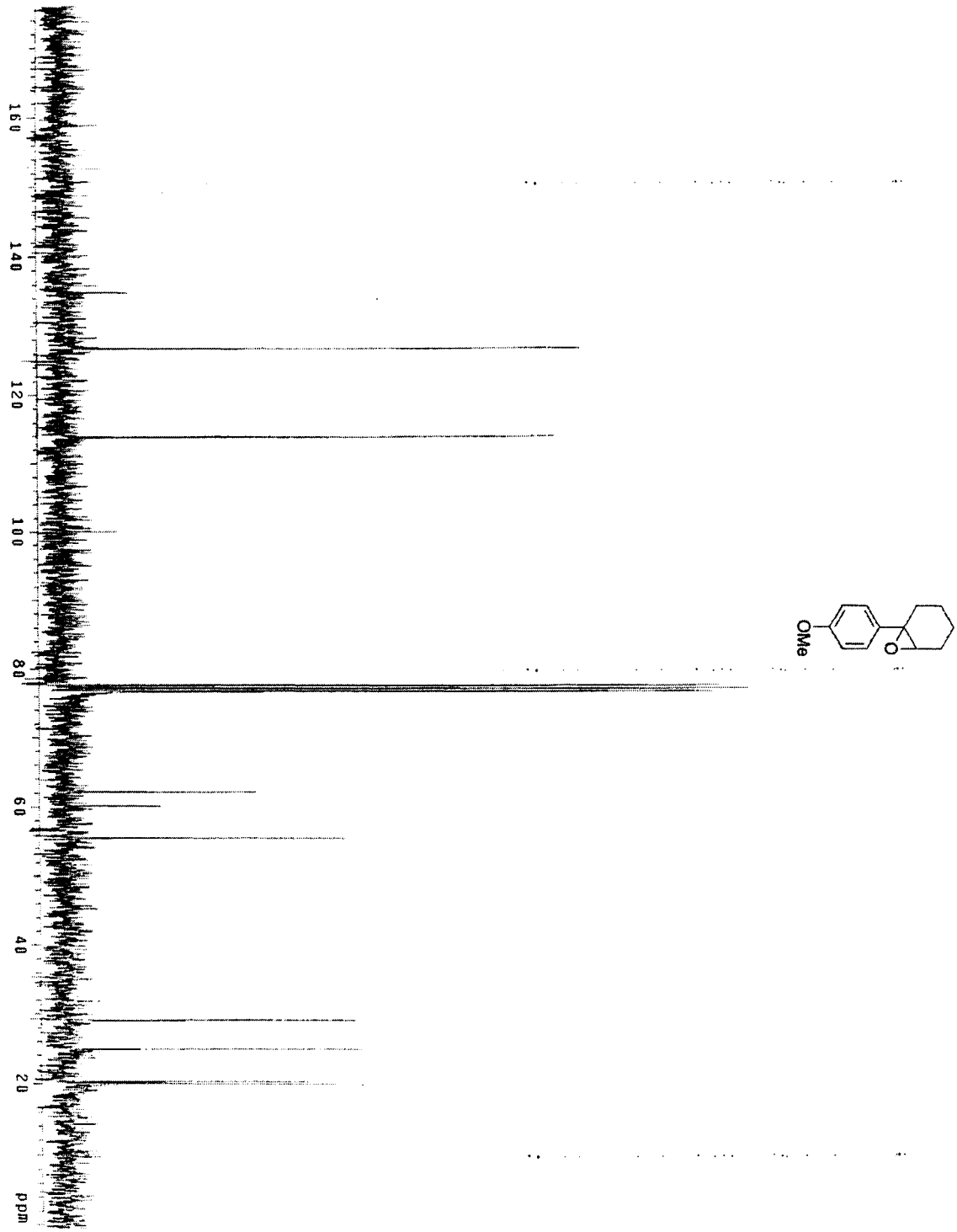

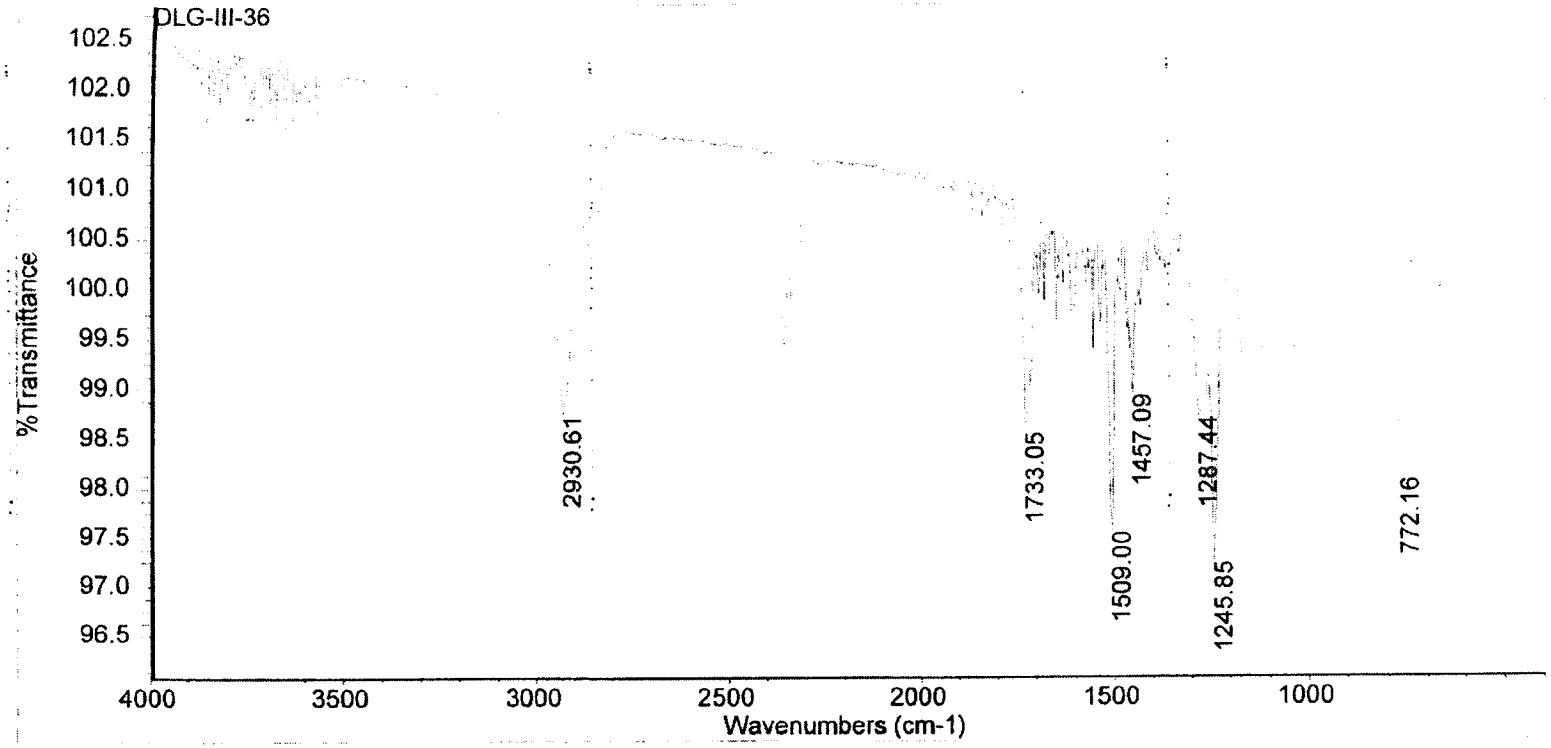

Wed Oct 16 13:26:49 2002
FIND PEAKS:

Spectrum:	DLG-III-36	
Region:	4000.00	400.00
Absolute threshold:	99.210	
Sensitivity:	50	
Peak list:		

Position:	1245.85	Intensity:	97.242
Position:	1509.00	Intensity:	97.553
Position:	772.16	Intensity:	98.082
Position:	1733.05	Intensity:	98.568
Position:	1287.44	Intensity:	98.717
Position:	2930.61	Intensity:	98.748
Position:	1457.09	Intensity:	98.937

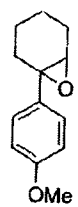

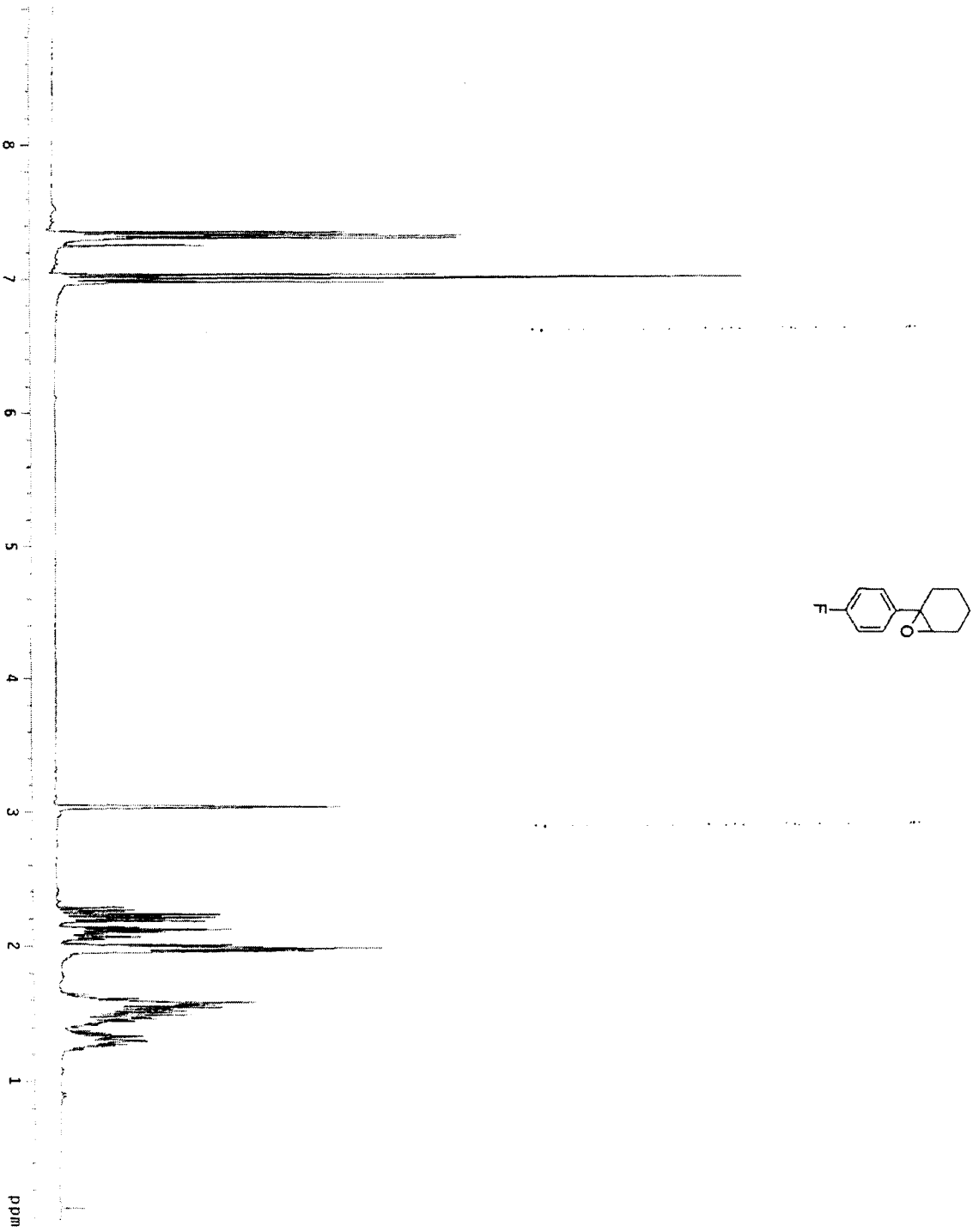

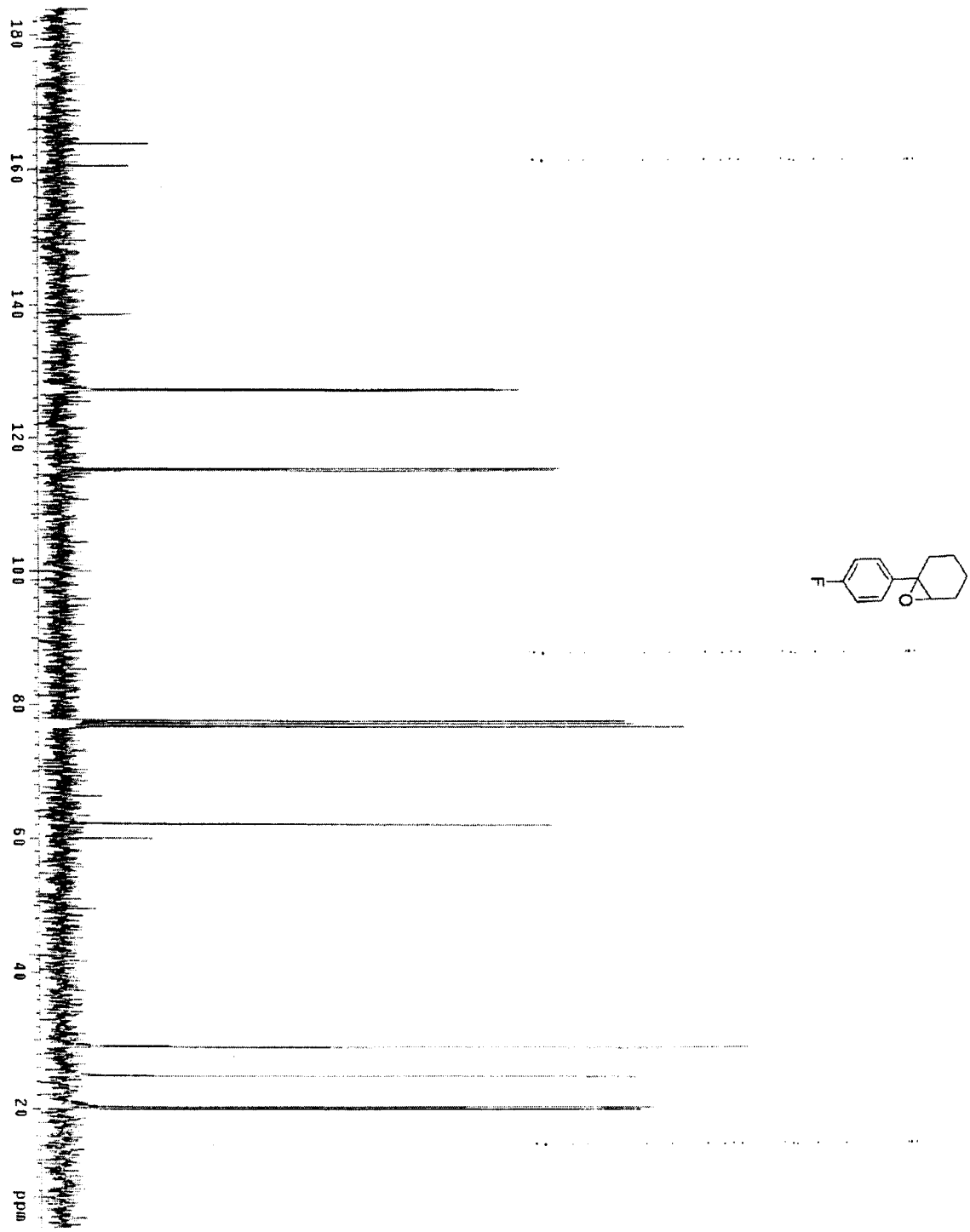

Thu Oct 10 12:17:03 2002
FIND PEAKS:

Spectrum:	DLG-III-33			
Region:	4000.00	400.00		
Absolute threshold:	91.227			
Sensitivity:	50			
Peak list:				
	Position:	1510.95	Intensity:	73.664
	Position:	831.72	Intensity:	80.058
	Position:	808.38	Intensity:	84.873
	Position:	1229.56	Intensity:	85.022
	Position:	2939.57	Intensity:	87.494
	Position:	1157.55	Intensity:	90.208
	Position:	854.65	Intensity:	90.586

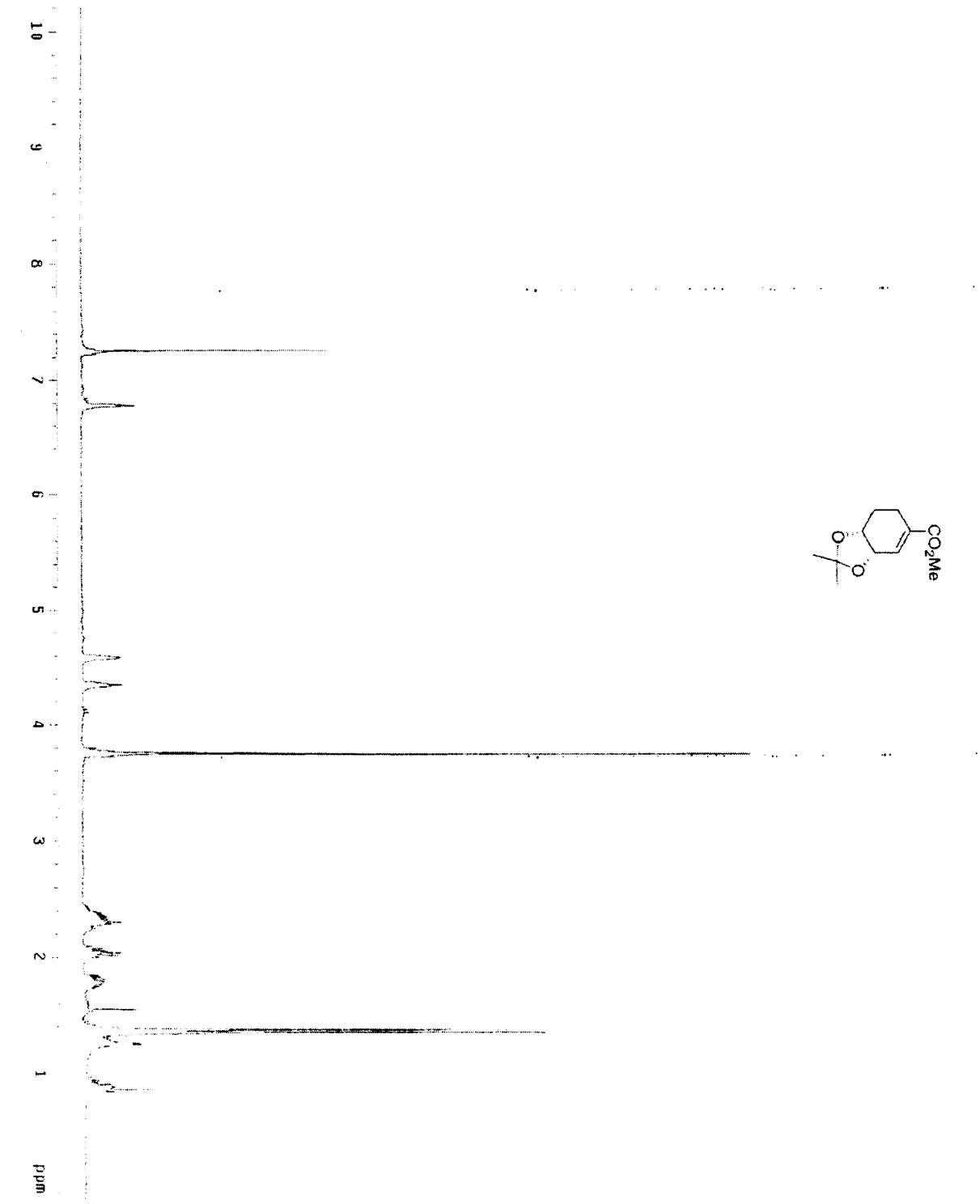

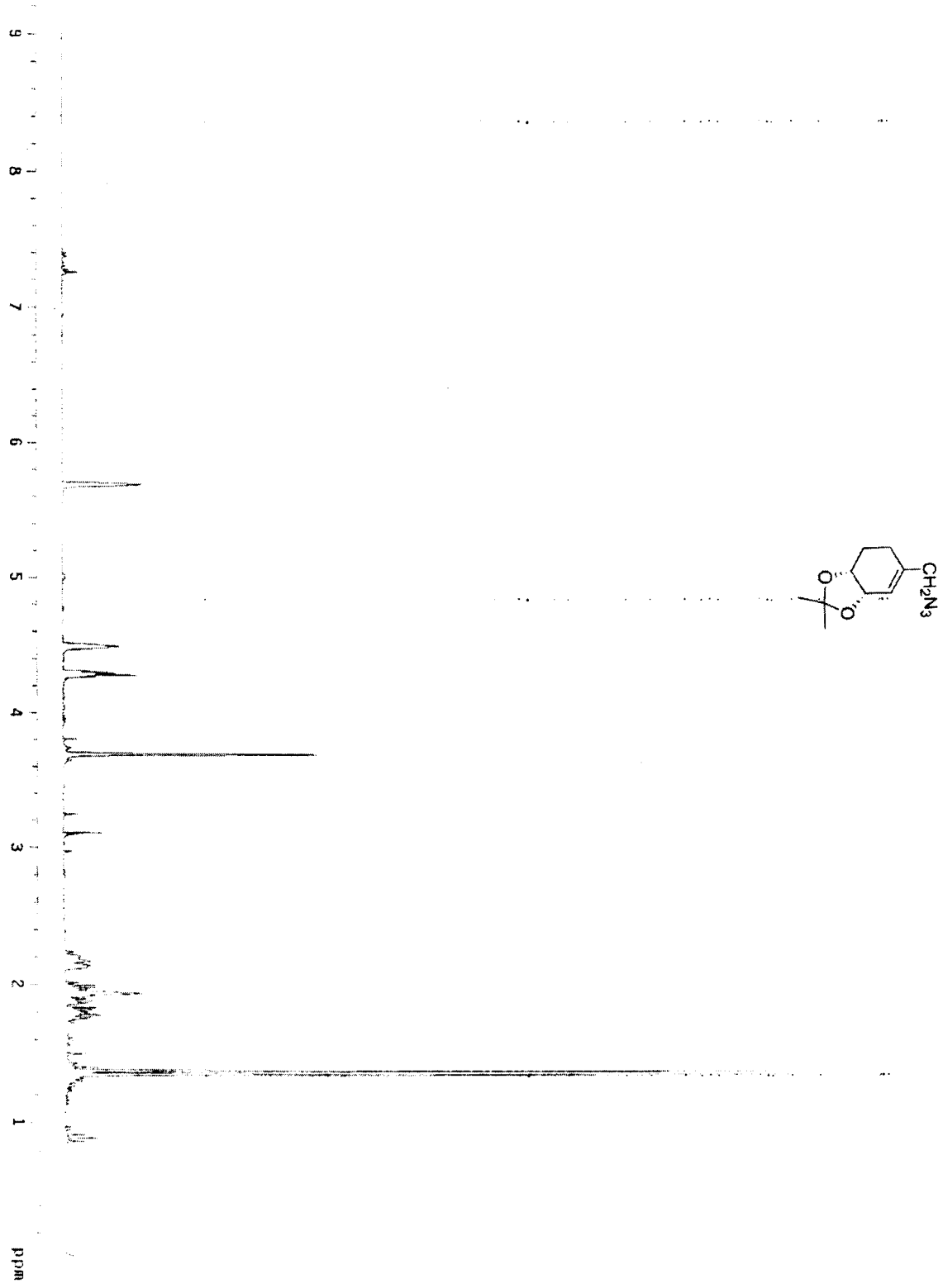

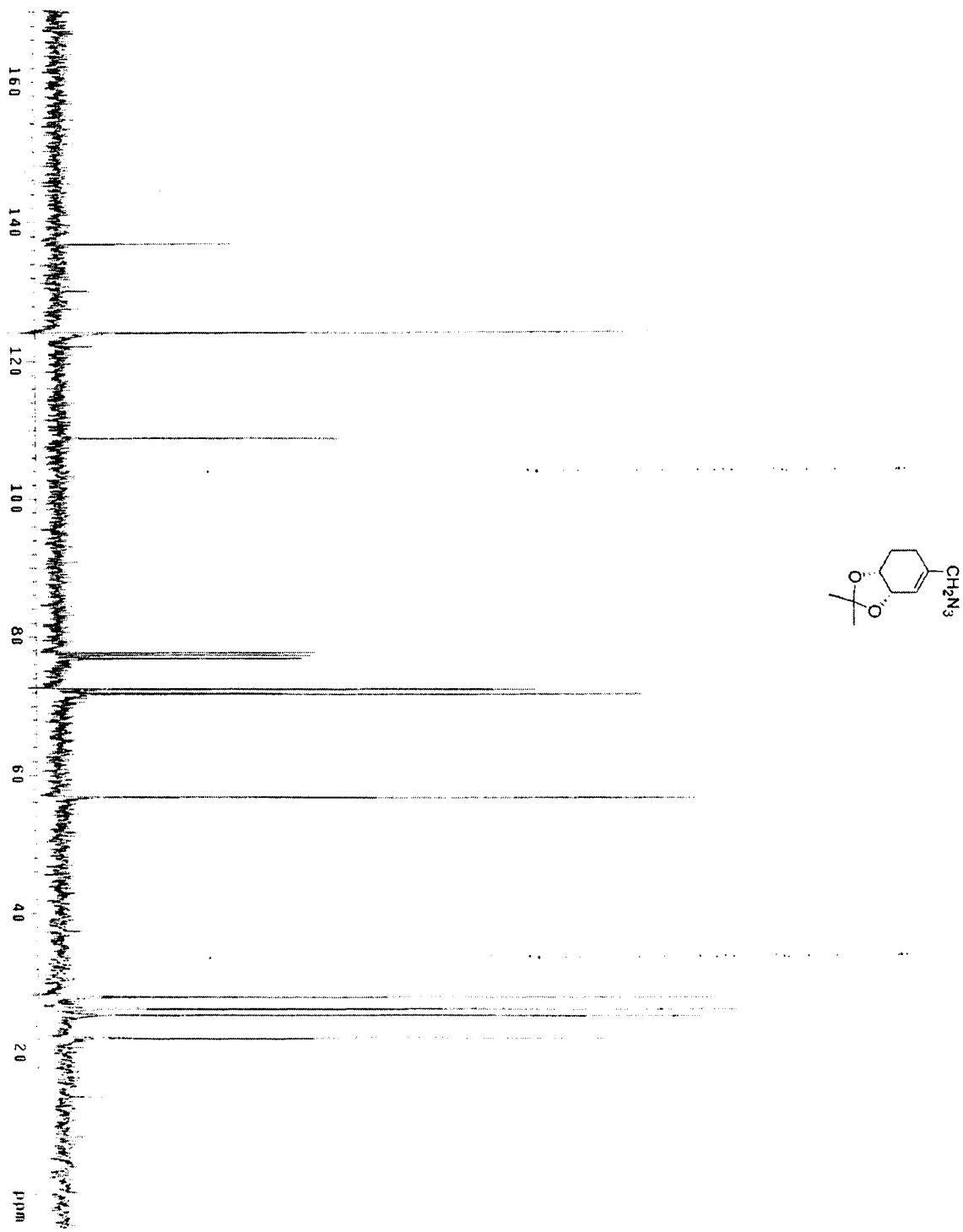

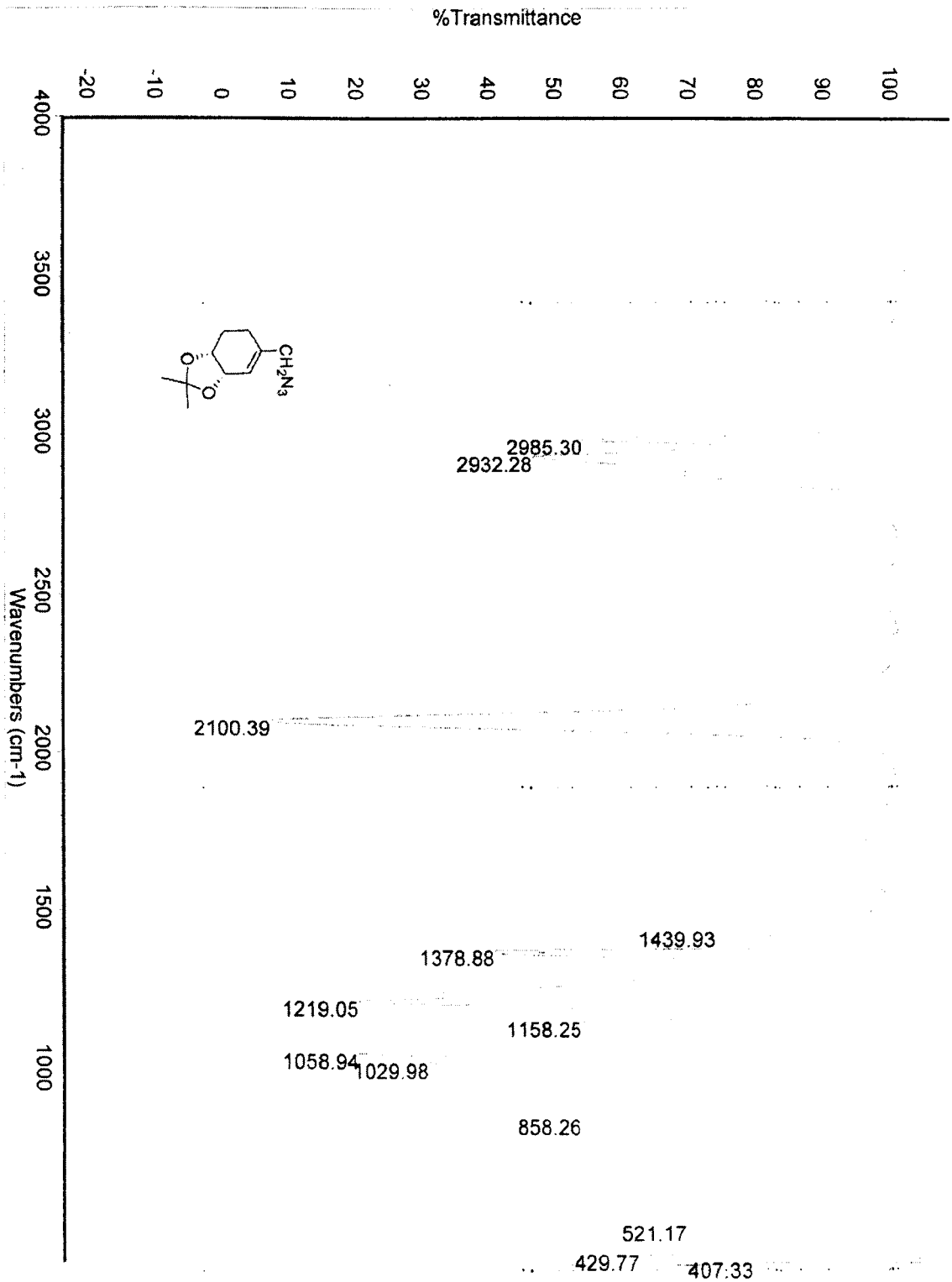

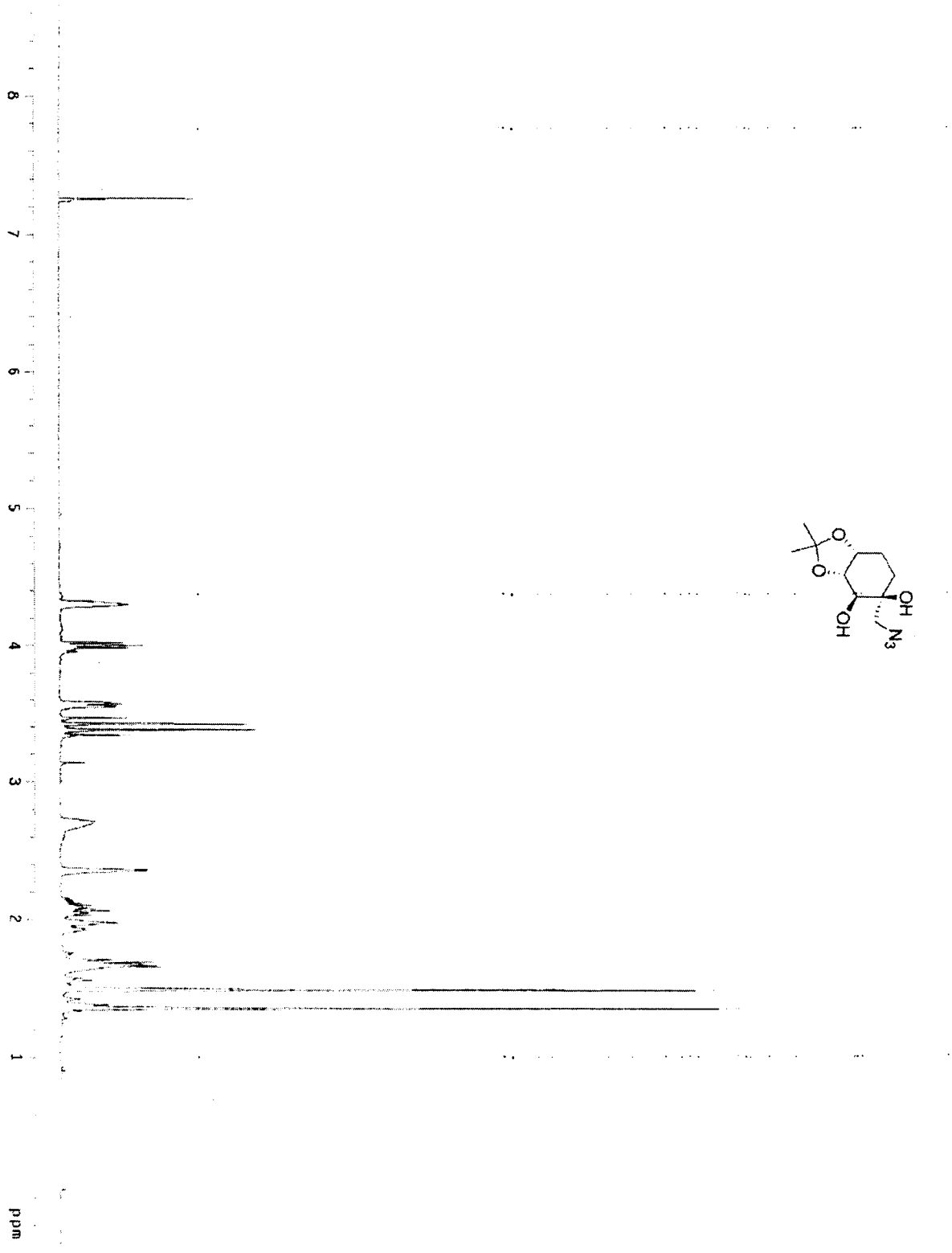

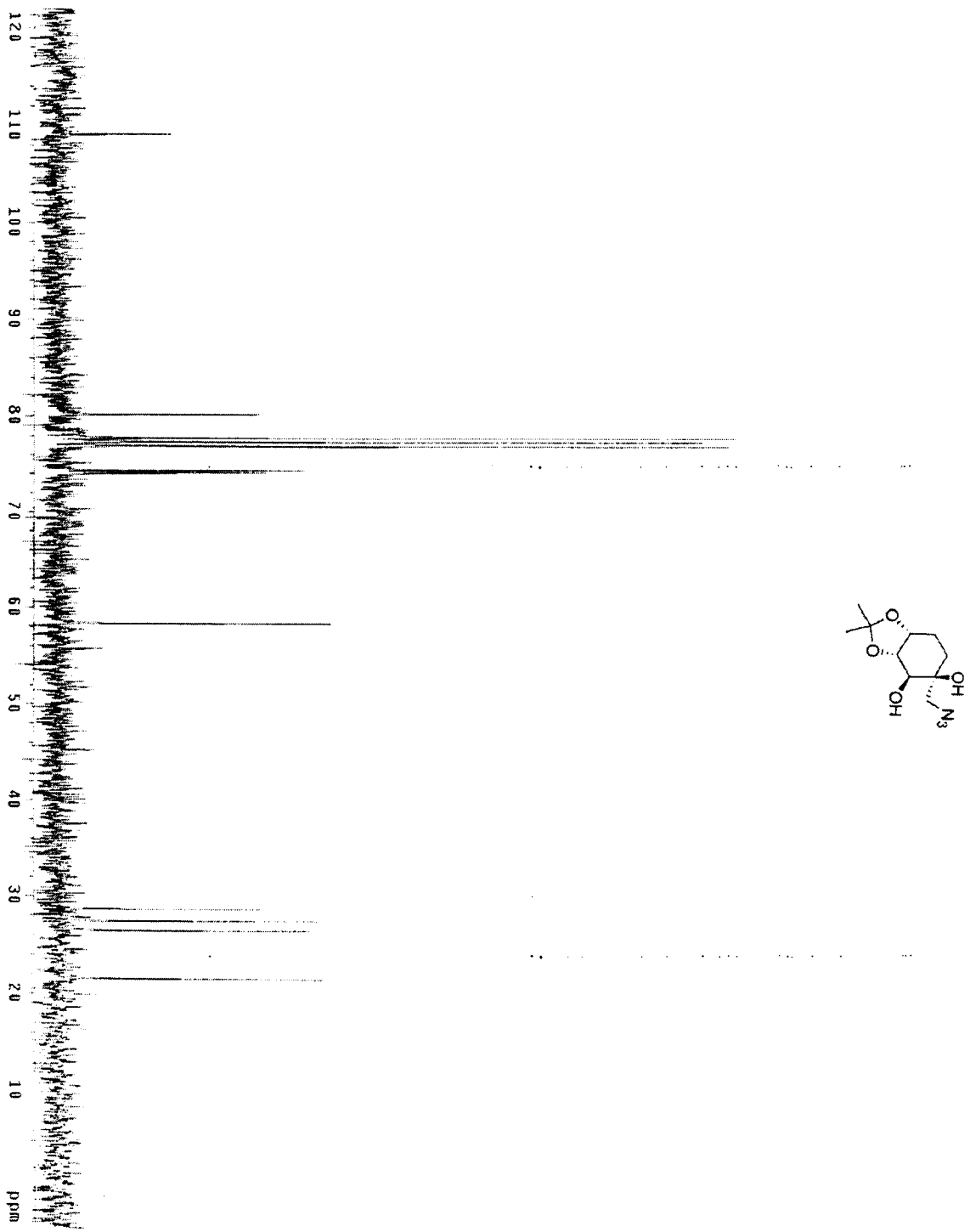

Thu Jan 16 21:00:50 2003
FIND PEAKS:

Spectrum:	DLG-IV-49	
Region:	4000.00	400.00
Absolute threshold:	83.235	
Sensitivity:	19	
Peak list:		

Position:	401.14	Intensity:	4.652
Position:	2104.38	Intensity:	49.107
Position:	1048.71	Intensity:	56.199
Position:	1219.67	Intensity:	64.171
Position:	426.01	Intensity:	67.848
Position:	3430.40	Intensity:	70.906
Position:	446.78	Intensity:	72.415
Position:	2935.58	Intensity:	76.520

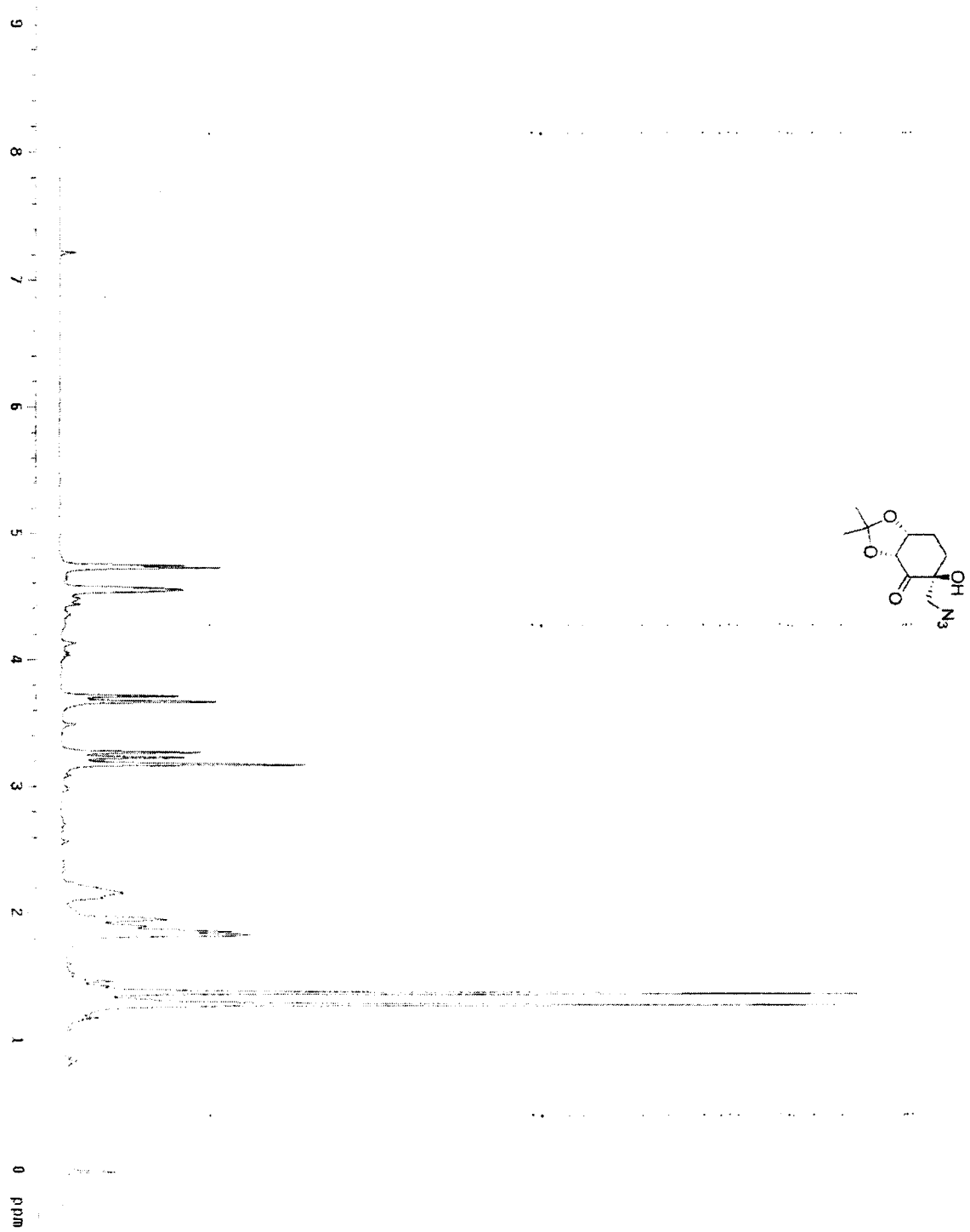

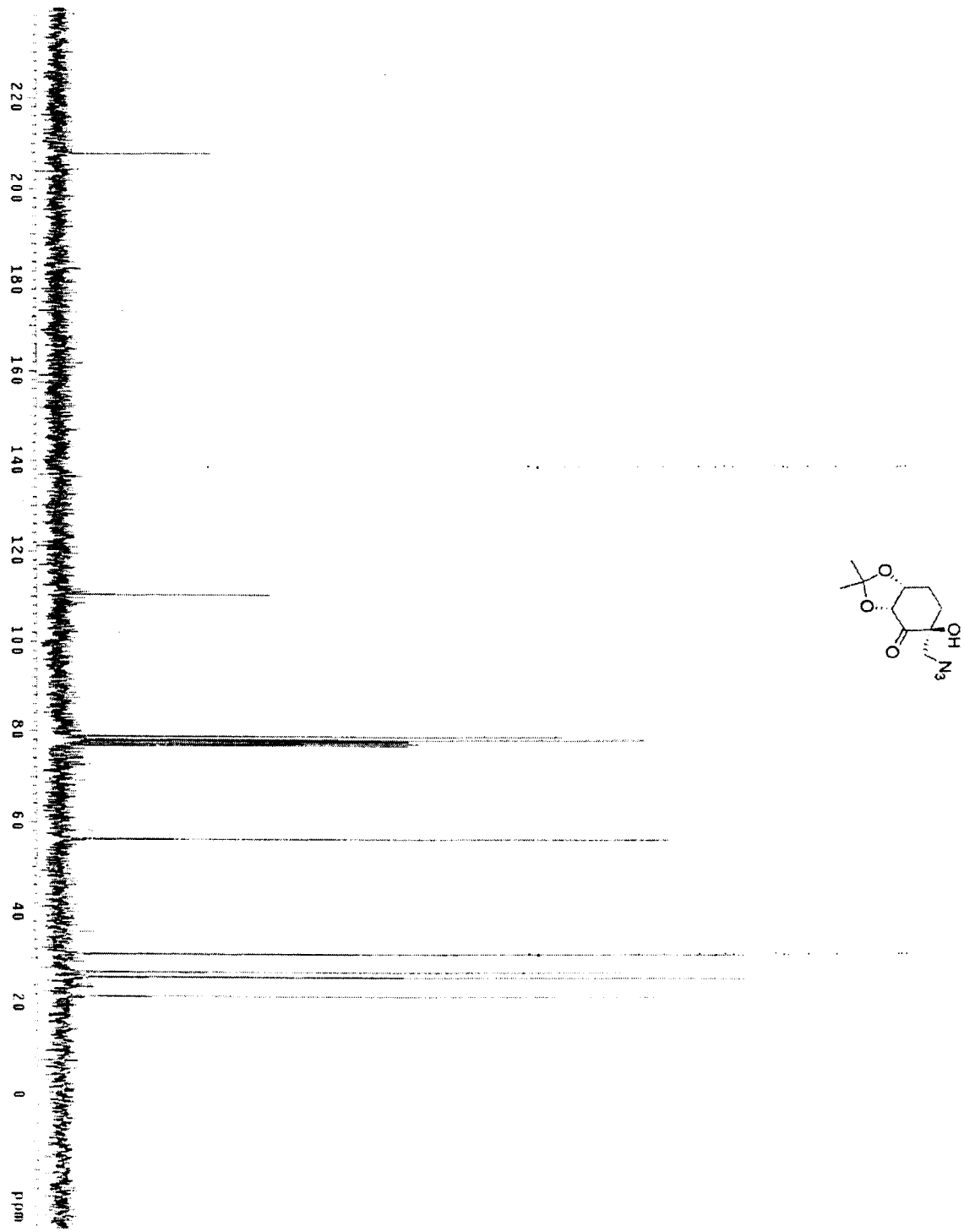

Thu Jan 16 21:17:18 2003
FIND PEAKS:

Spectrum:	DLG-IV-50	
Region:	4000.00	400.00
Absolute threshold:	72.926	
Sensitivity:	26	
Peak list:		

Position:	2106.96	Intensity:	48.165
Position:	1043.77	Intensity:	60.609
Position:	1222.29	Intensity:	60.931
Position:	1734.41	Intensity:	64.373
Position:	1382.61	Intensity:	67.016
Position:	3437.84	Intensity:	69.025
Position:	2936.84	Intensity:	70.541

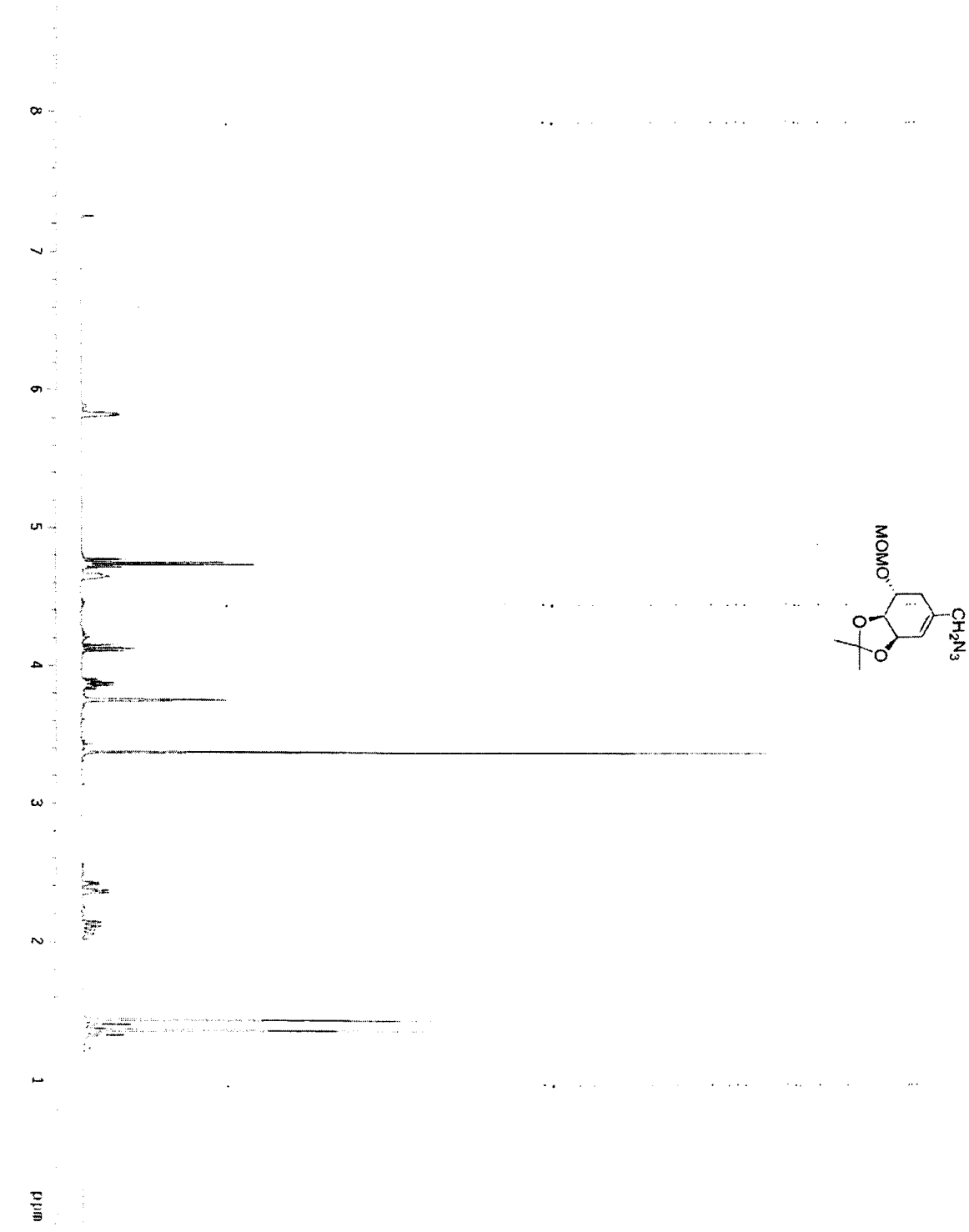

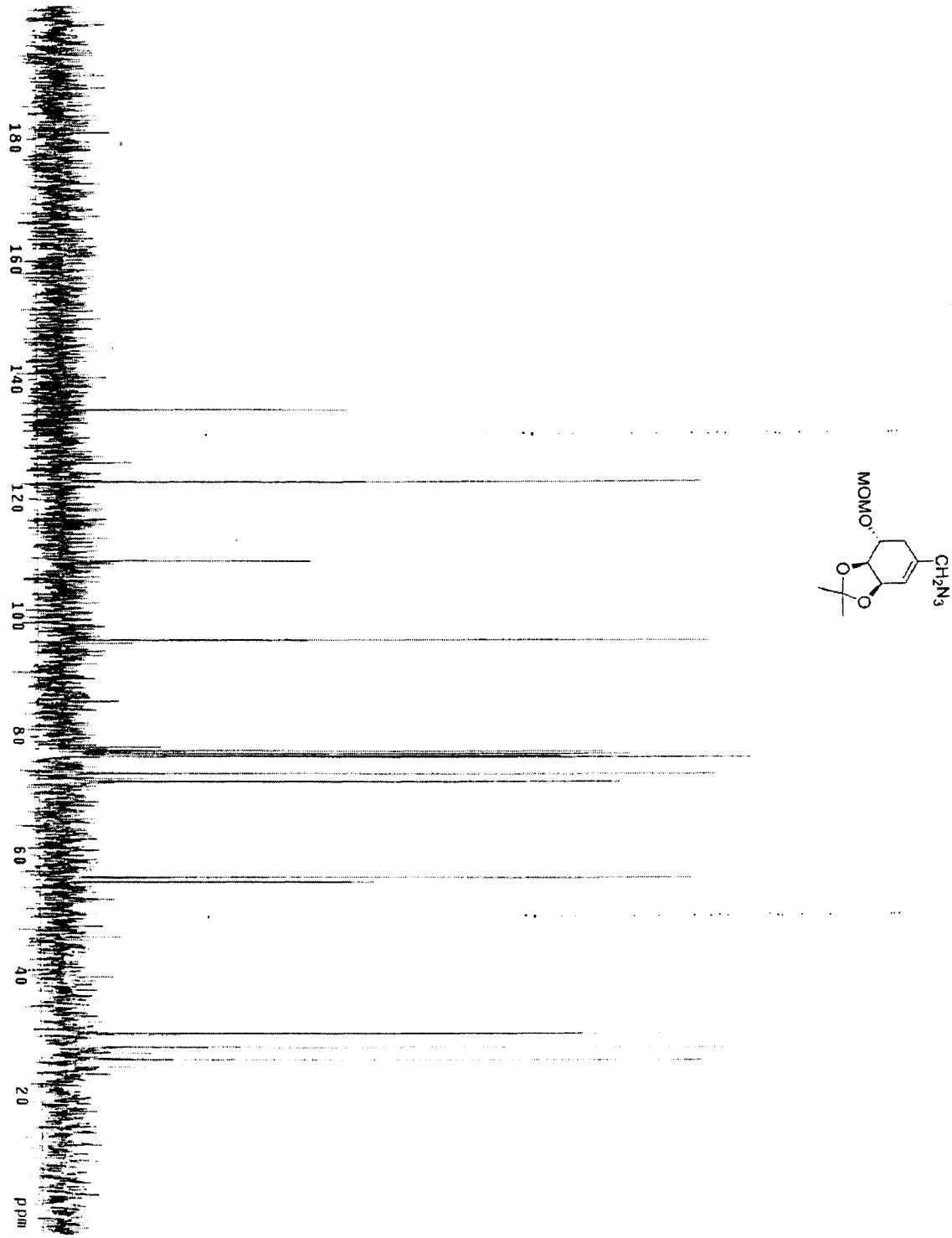

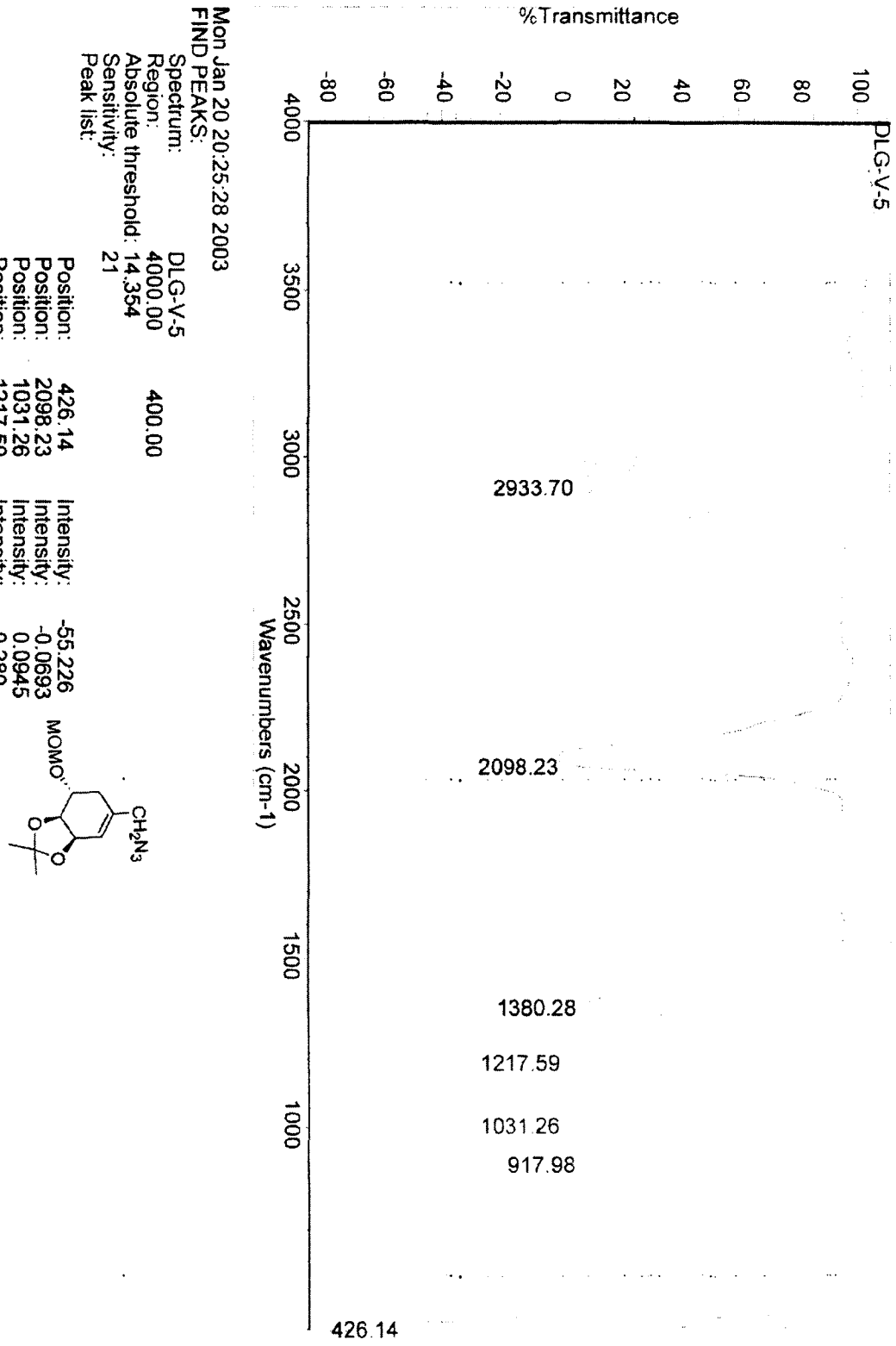

Mon Jan 20 20:25:28 2003
FIND PEAKS:
Spectrum: DLG-V-5
Region: 4000.00 400.00
Absolute threshold: 14.354
Sensitivity: 21
Peak list:

Position:	426.14	Intensity:	-55.226
Position:	2098.23	Intensity:	-0.0693
Position:	1031.26	Intensity:	0.0945
Position:	1217.59	Intensity:	0.280
Position:	2933.70	Intensity:	5.077
Position:	917.98	Intensity:	5.342
Position:	1380.28	Intensity:	5.801

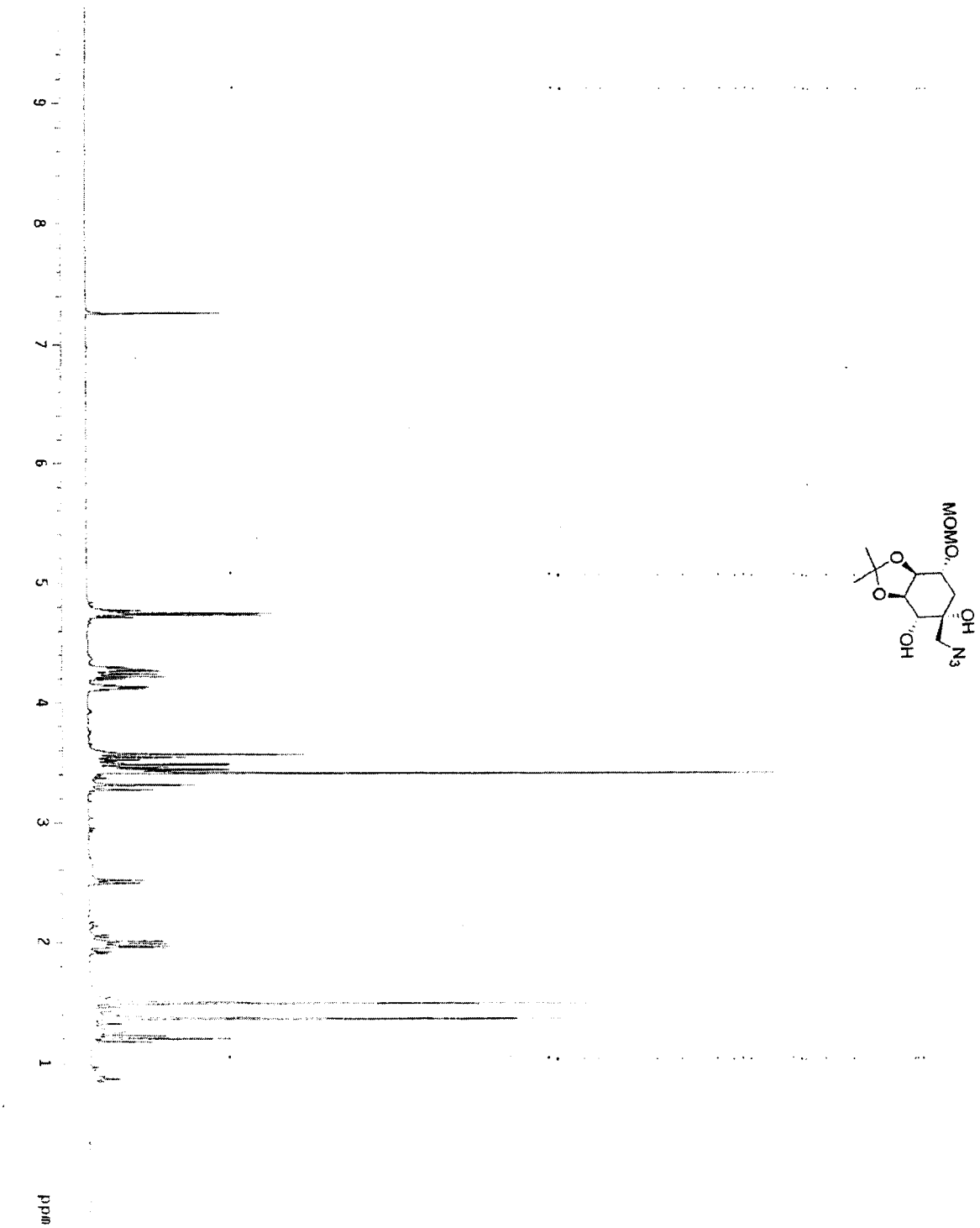

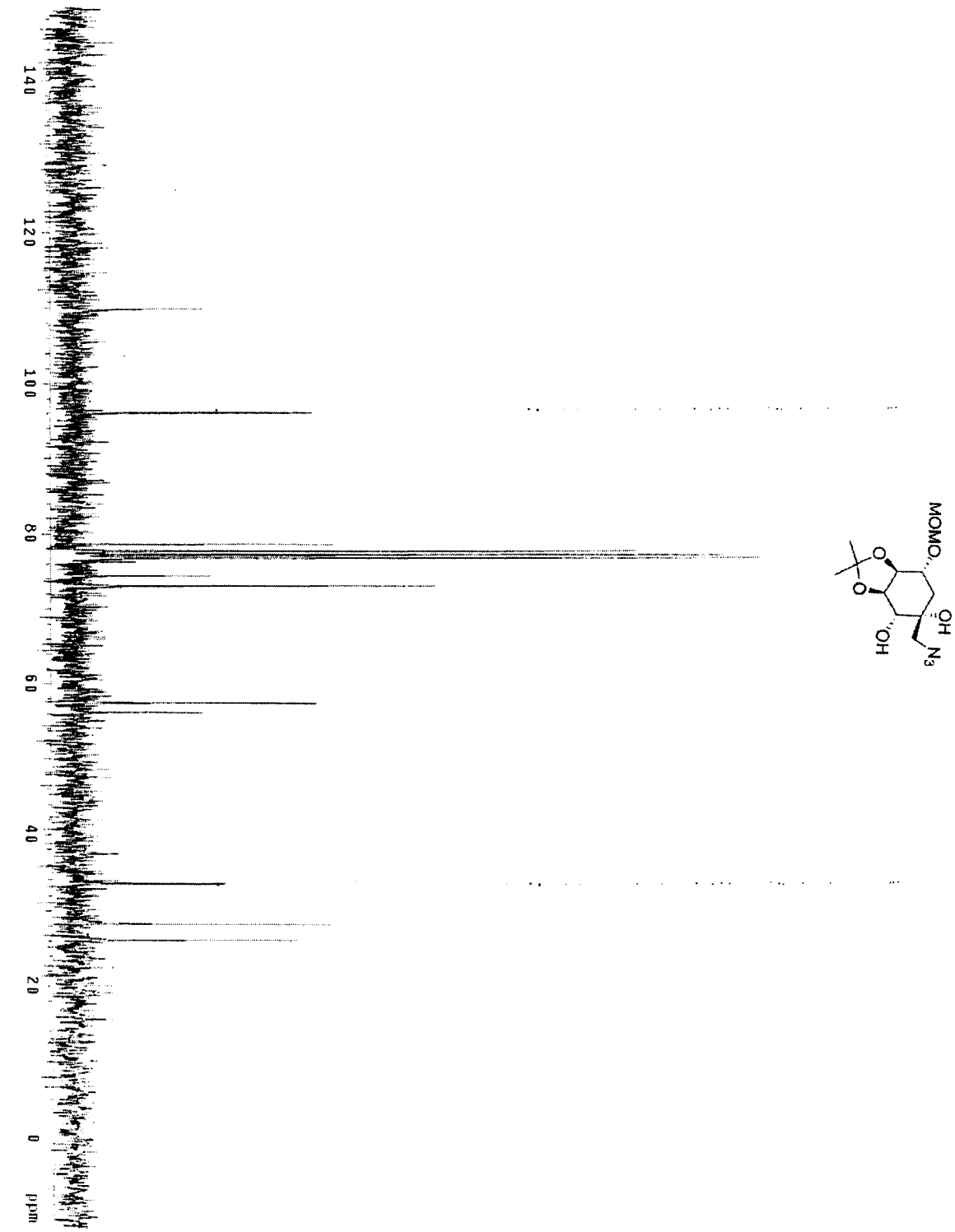

Thu Jan 23 22:23:44 2003
FIND PEAKS:

Spectrum: DLG-V-9diol
Region: 4000.00 400.00
Absolute threshold: 92.671
Sensitivity: 39
Peak list:

Position:	2105.00	Intensity:	56.598
Position:	1031.44	Intensity:	62.814
Position:	410.55	Intensity:	64.684
Position:	1217.66	Intensity:	75.792
Position:	1154.19	Intensity:	79.792
Position:	1382.35	Intensity:	84.015
Position:	432.41	Intensity:	84.276
Position:	915.75	Intensity:	85.787

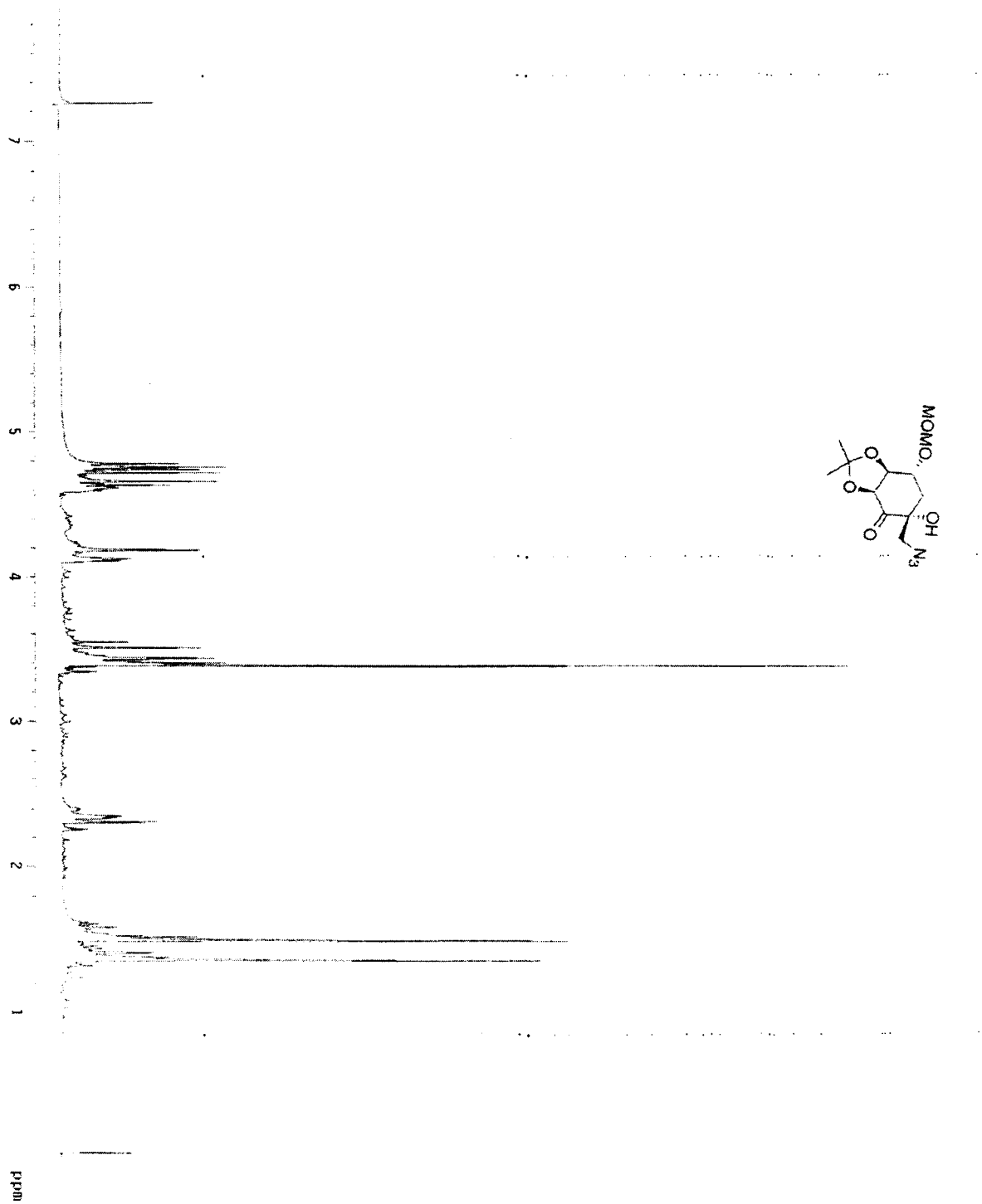

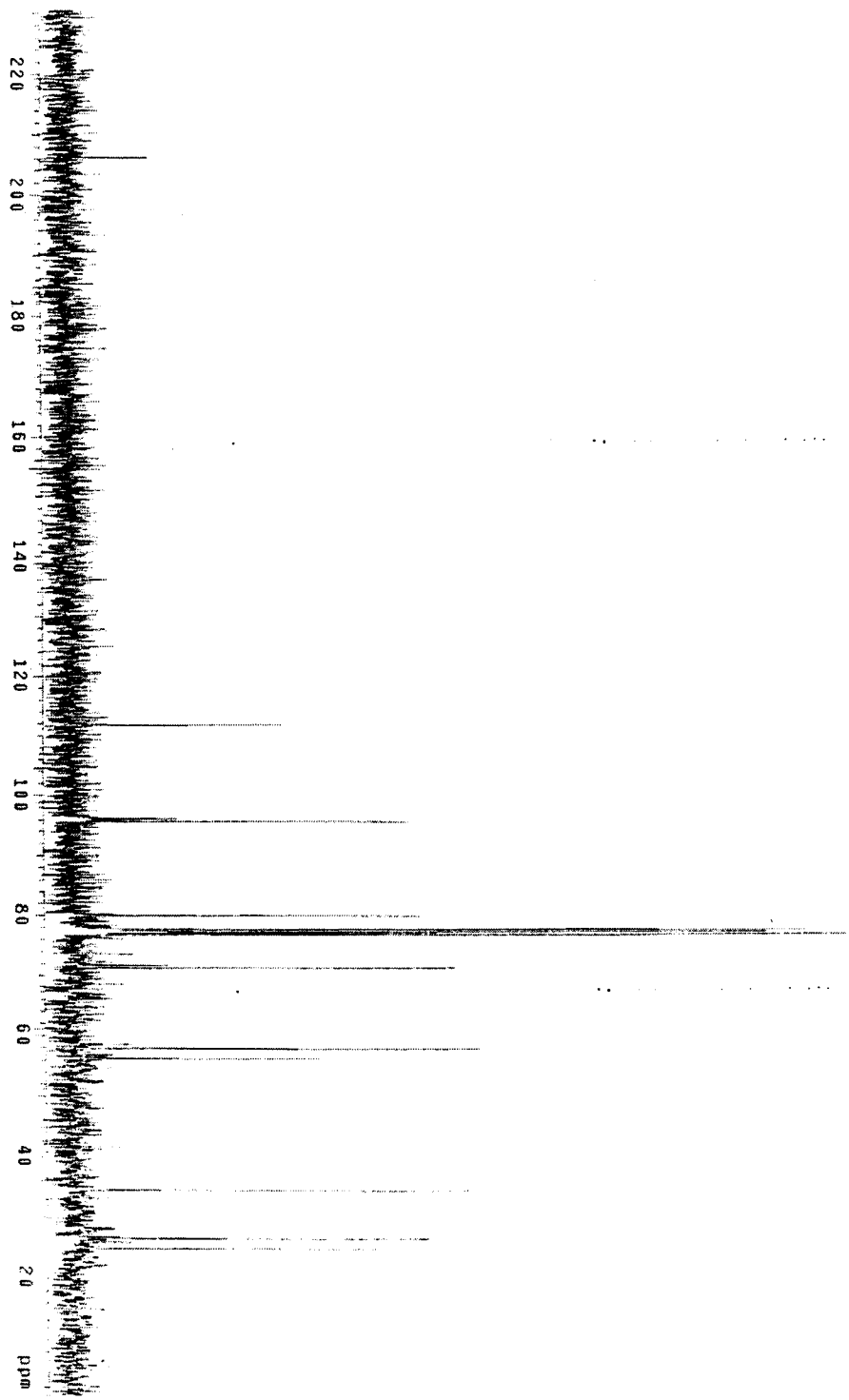

Thu Jan 23 21:43:29 2003
FIND PEAKS:

Spectrum: DLG-V-9ketone
Region: 4000.00 400.00
Absolute threshold: 101.879
Sensitivity: 24
Peak list:

Position:	2105.51	Intensity:	65.217
Position:	1031.35	Intensity:	69.325
Position:	407.15	Intensity:	69.863
Position:	403.50	Intensity:	69.381
Position:	437.10	Intensity:	78.632
Position:	1154.66	Intensity:	80.185
Position:	1212.06	Intensity:	80.614
Position:	420.48	Intensity:	84.029

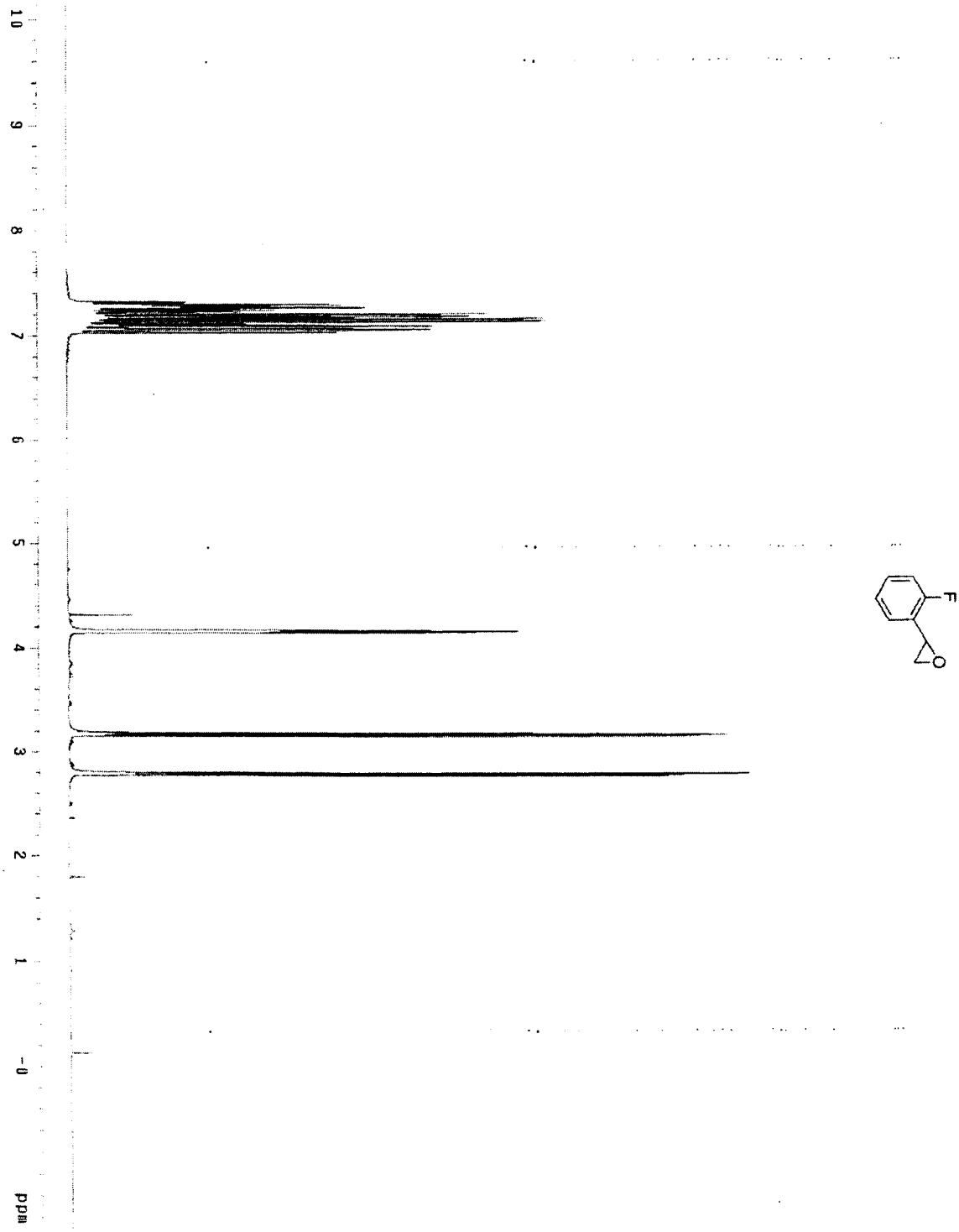

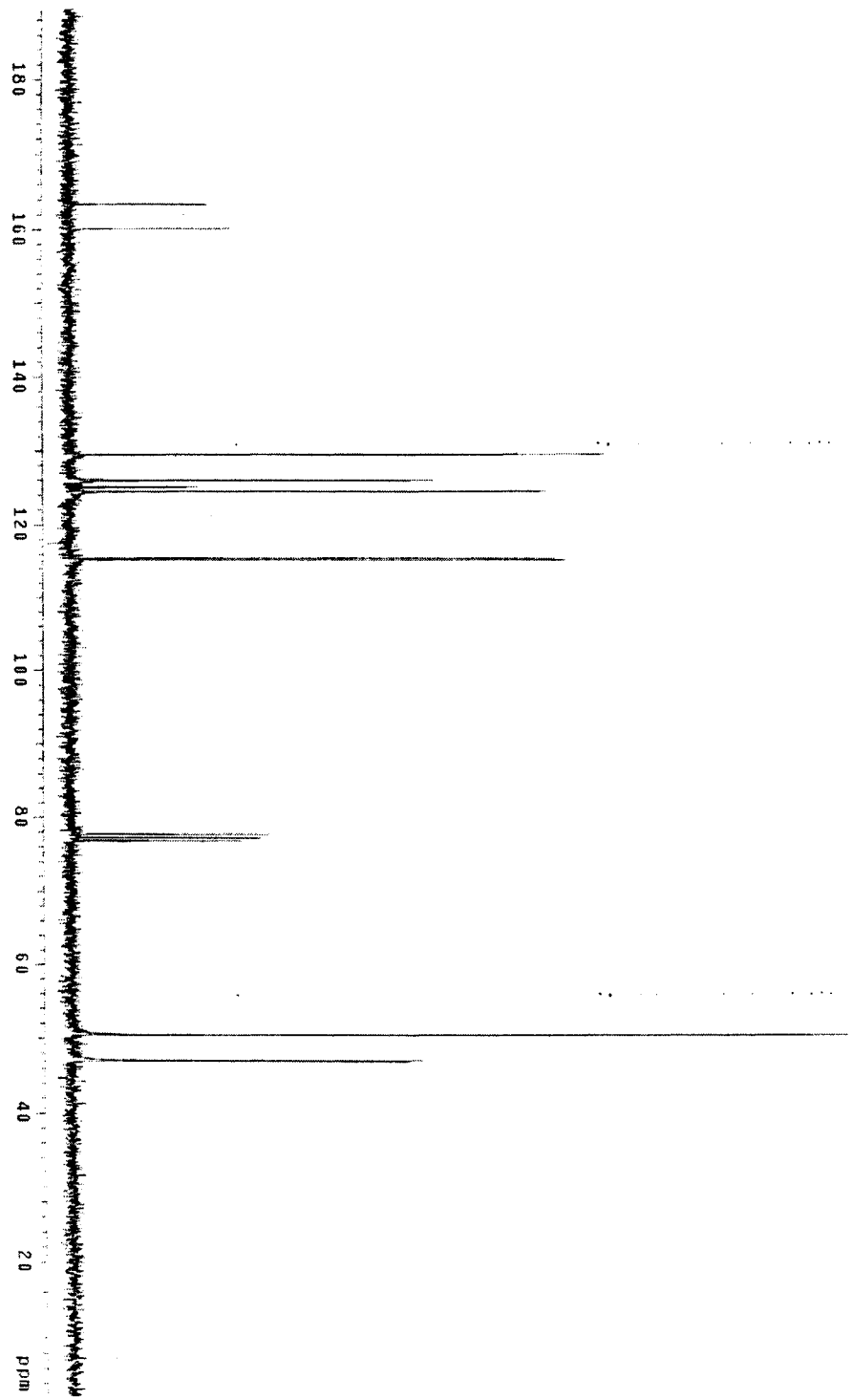

Tue Mar 04 20:23:14 2003
FIND PEAKS:
Spectrum: DLG-V-29
Region: 4000.00 400.00
Absolute threshold: 84.928
Sensitivity: 17
Peak list:

Position:	758.60	Intensity:	24.339
Position:	1495.18	Intensity:	26.275
Position:	1257.46	Intensity:	43.864
Position:	880.63	Intensity:	44.192
Position:	1222.47	Intensity:	48.906
Position:	1454.87	Intensity:	51.118
Position:	1179.95	Intensity:	65.193
Position:	811.15	Intensity:	68.110

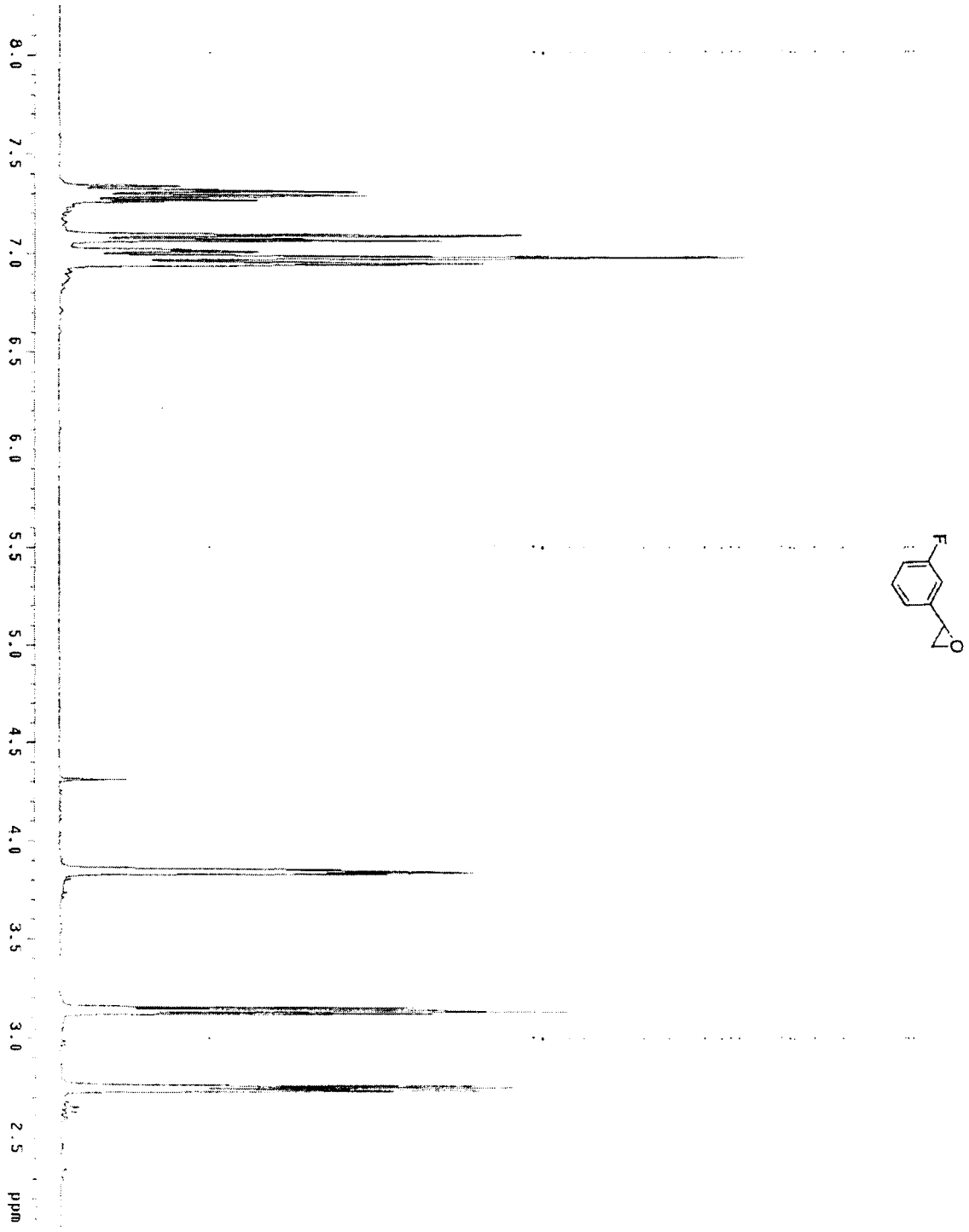

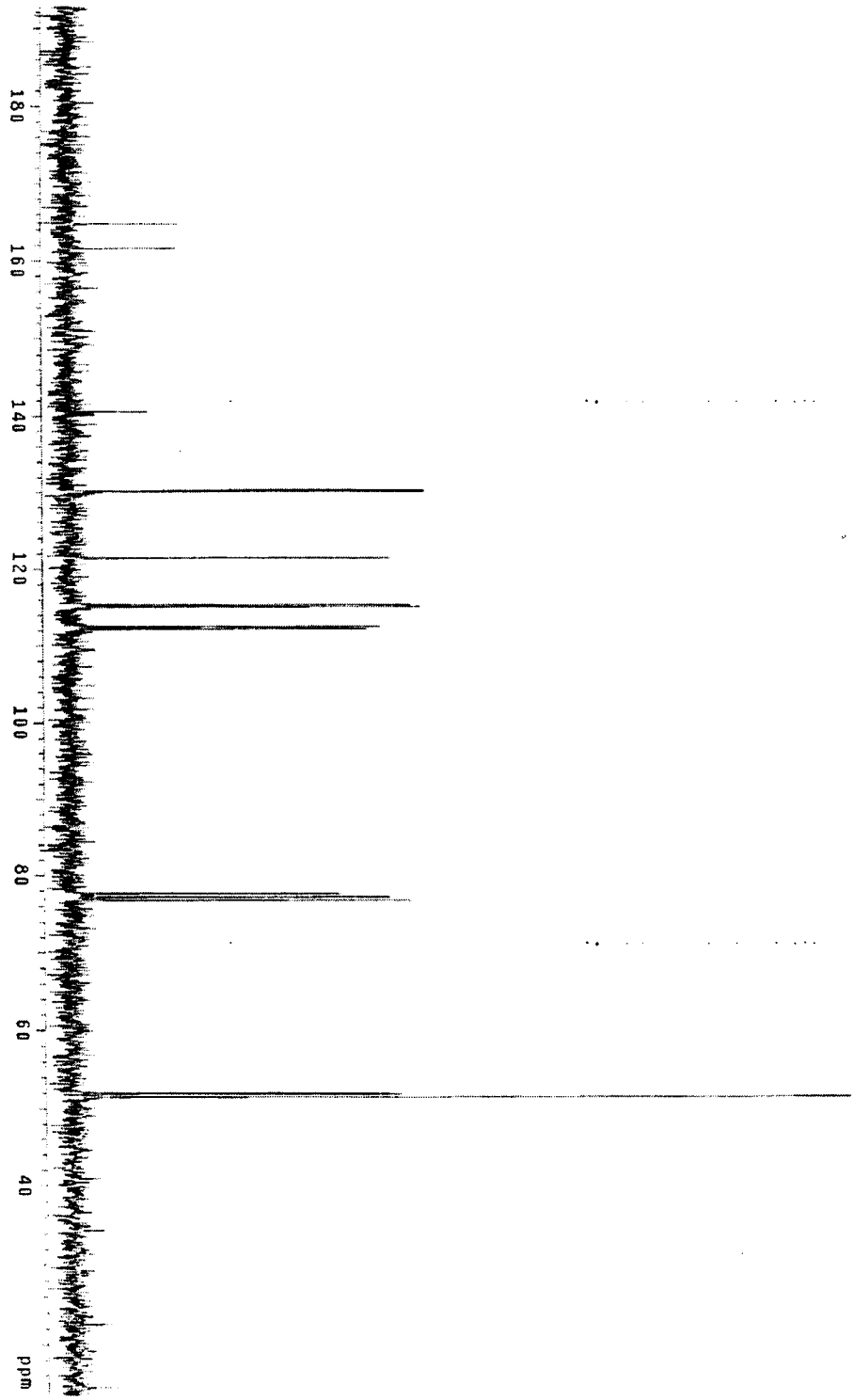

Sun Mar 30 20:40:19 2003
FIND PEAKS:

Spectrum: DLG-V-46
Region: 4000.00 400.00
Absolute threshold: 98.889
Sensitivity: 20
Peak list:

Position:	850.46	Intensity:	50.486
Position:	785.13	Intensity:	50.721
Position:	691.18	Intensity:	54.886
Position:	1592.73	Intensity:	60.603
Position:	927.35	Intensity:	63.920
Position:	1453.52	Intensity:	65.754
Position:	1232.25	Intensity:	68.078
Position:	1617.83	Intensity:	72.531

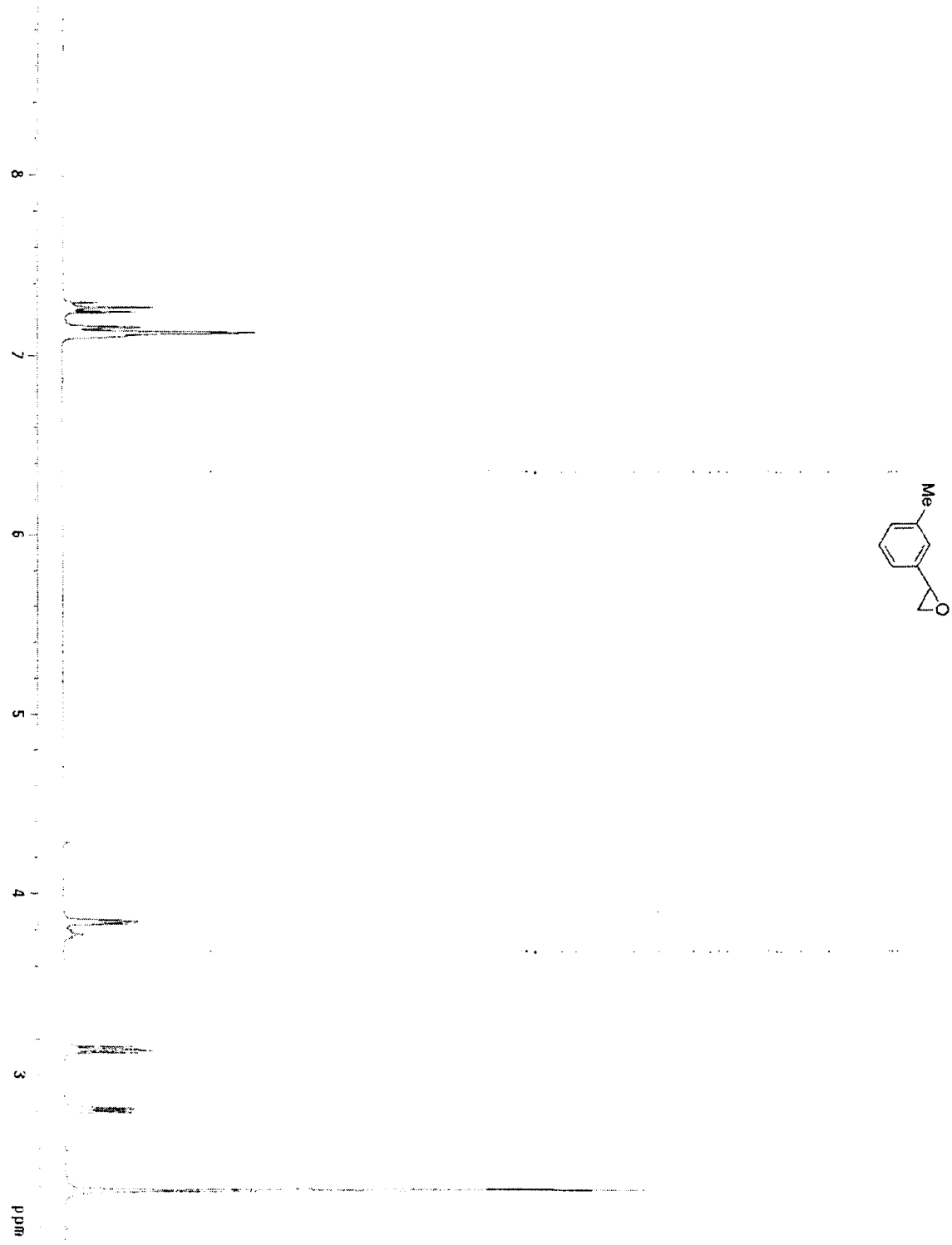

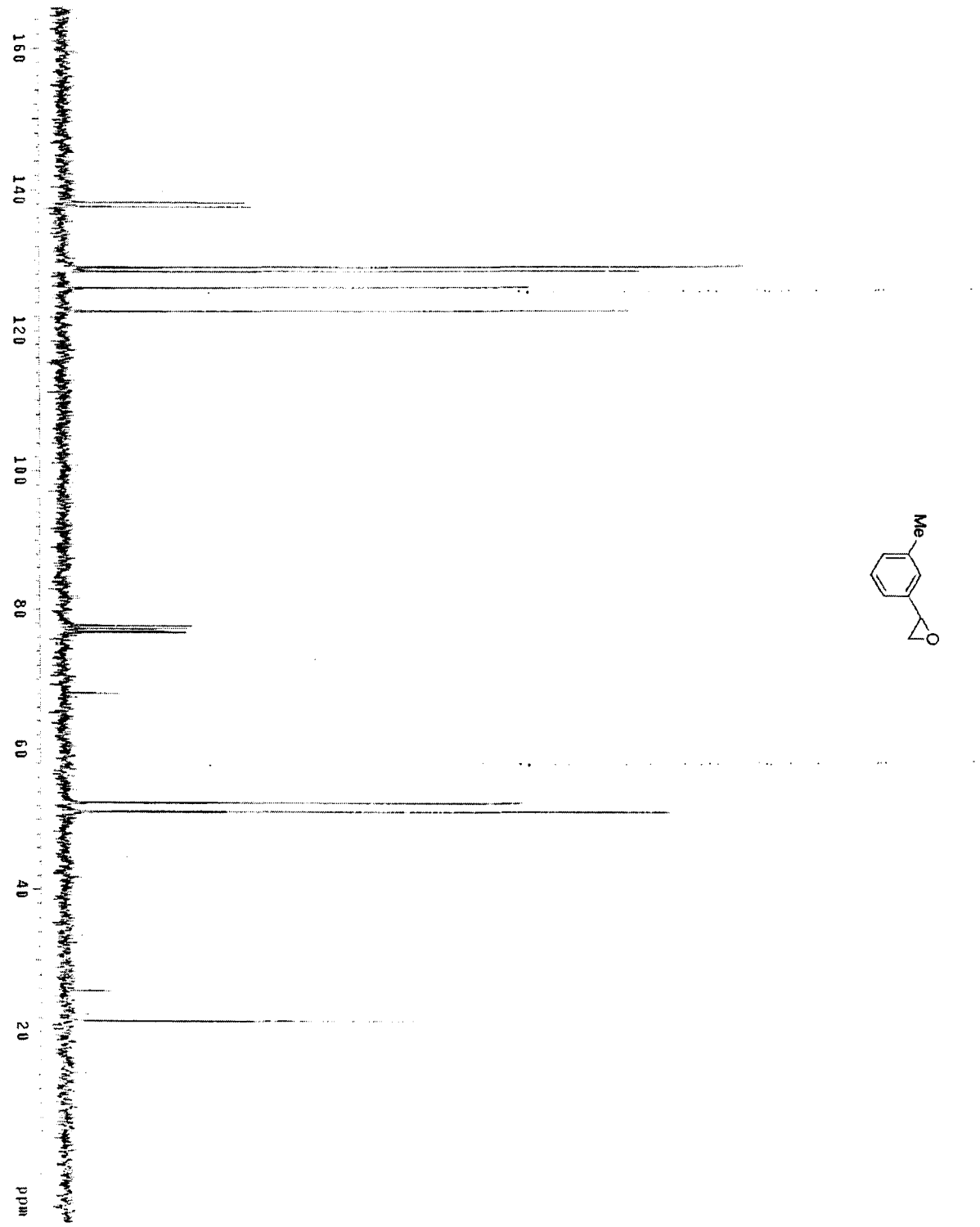

Wed Mar 05 09:43:21 2003
FIND PEAKS:

Spectrum: DLG-V-28
Region: 4000.00 400.00
Absolute threshold: 60.109
Sensitivity: 50
Peak list:

Position:	699.51	Intensity:	11.294
Position:	782.85	Intensity:	12.037
Position:	845.63	Intensity:	17.015
Position:	914.93	Intensity:	42.559
Position:	1490.34	Intensity:	47.723
Position:	2989.66	Intensity:	52.990
Position:	1610.57	Intensity:	57.147
Position:	3048.44	Intensity:	58.338

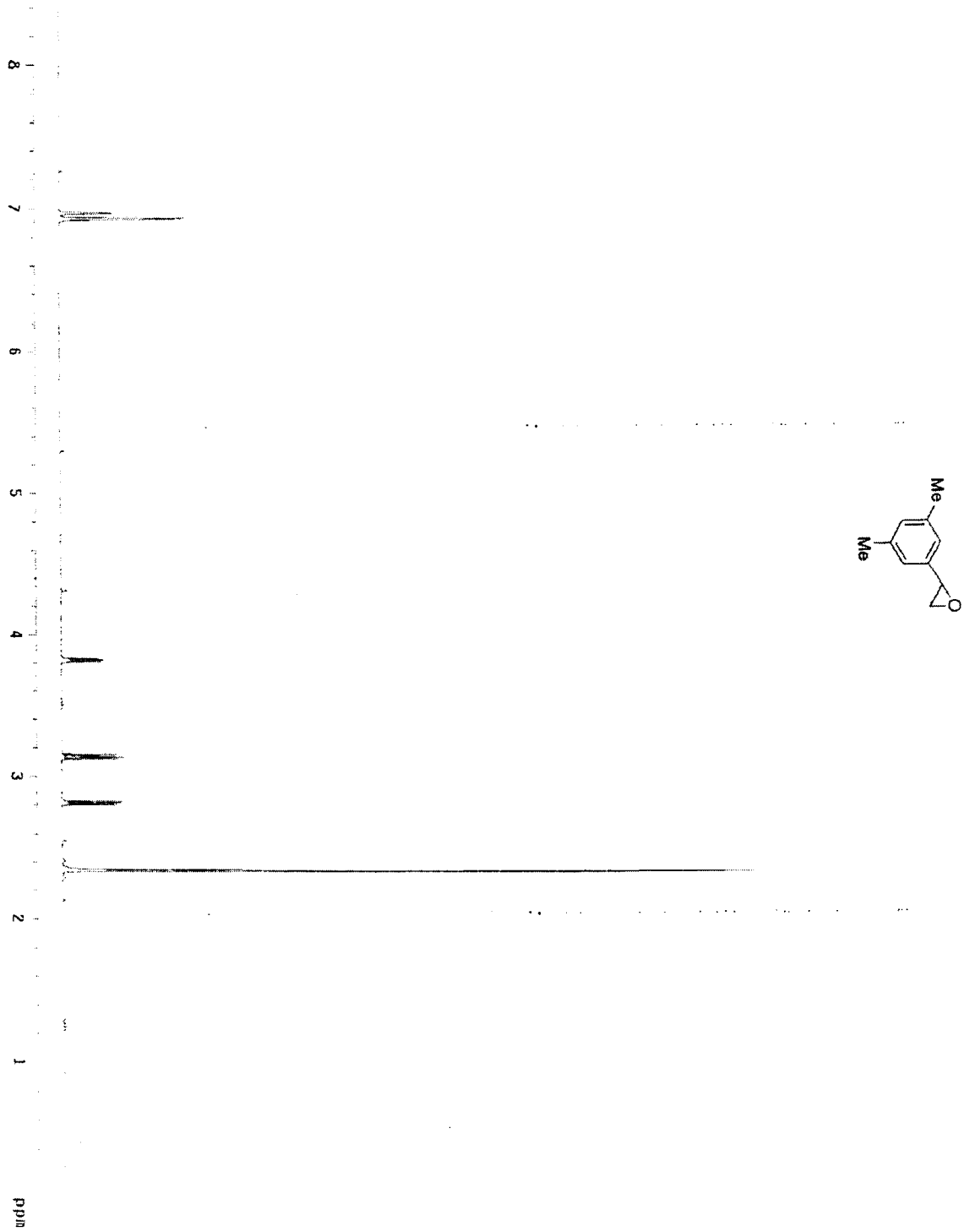

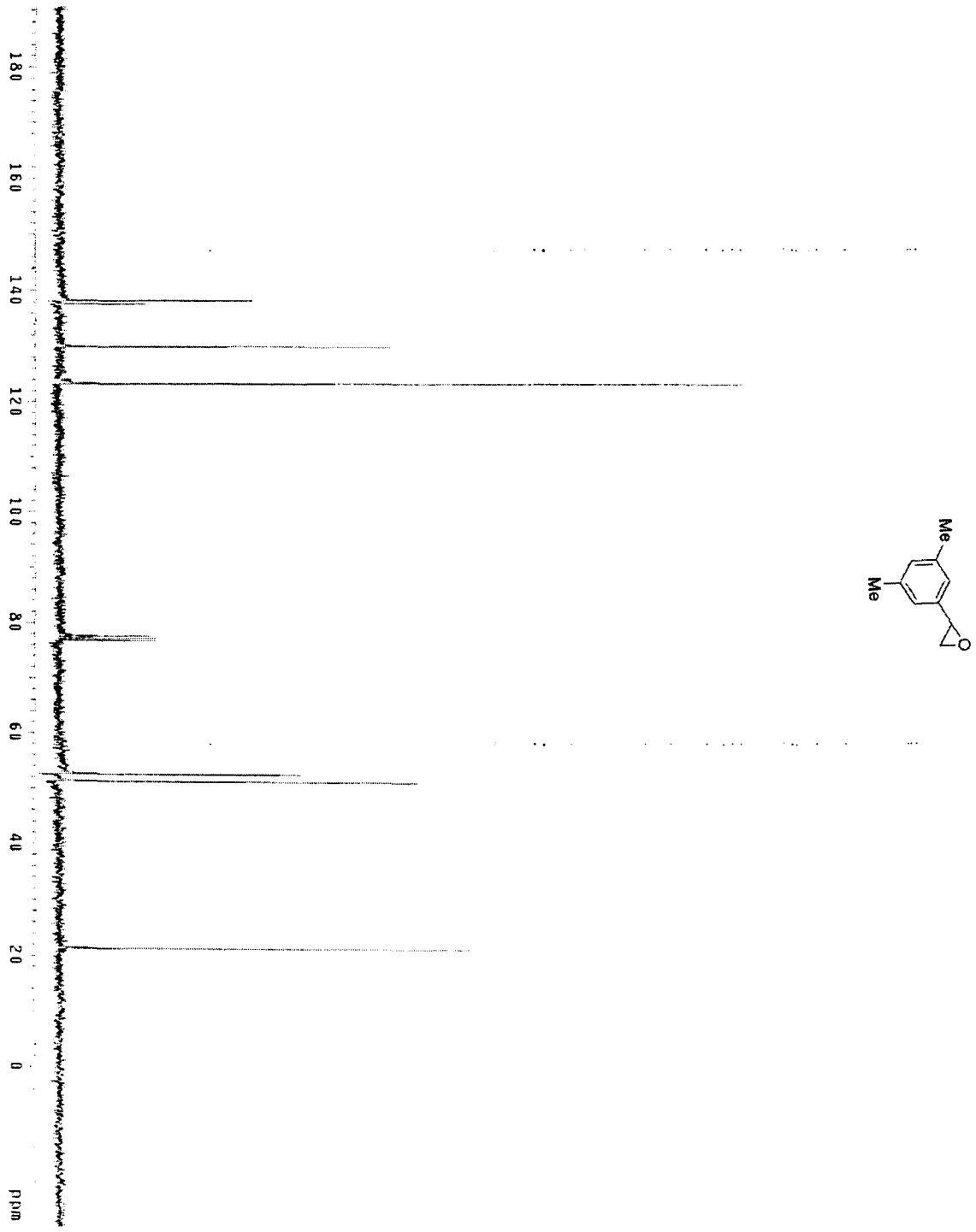

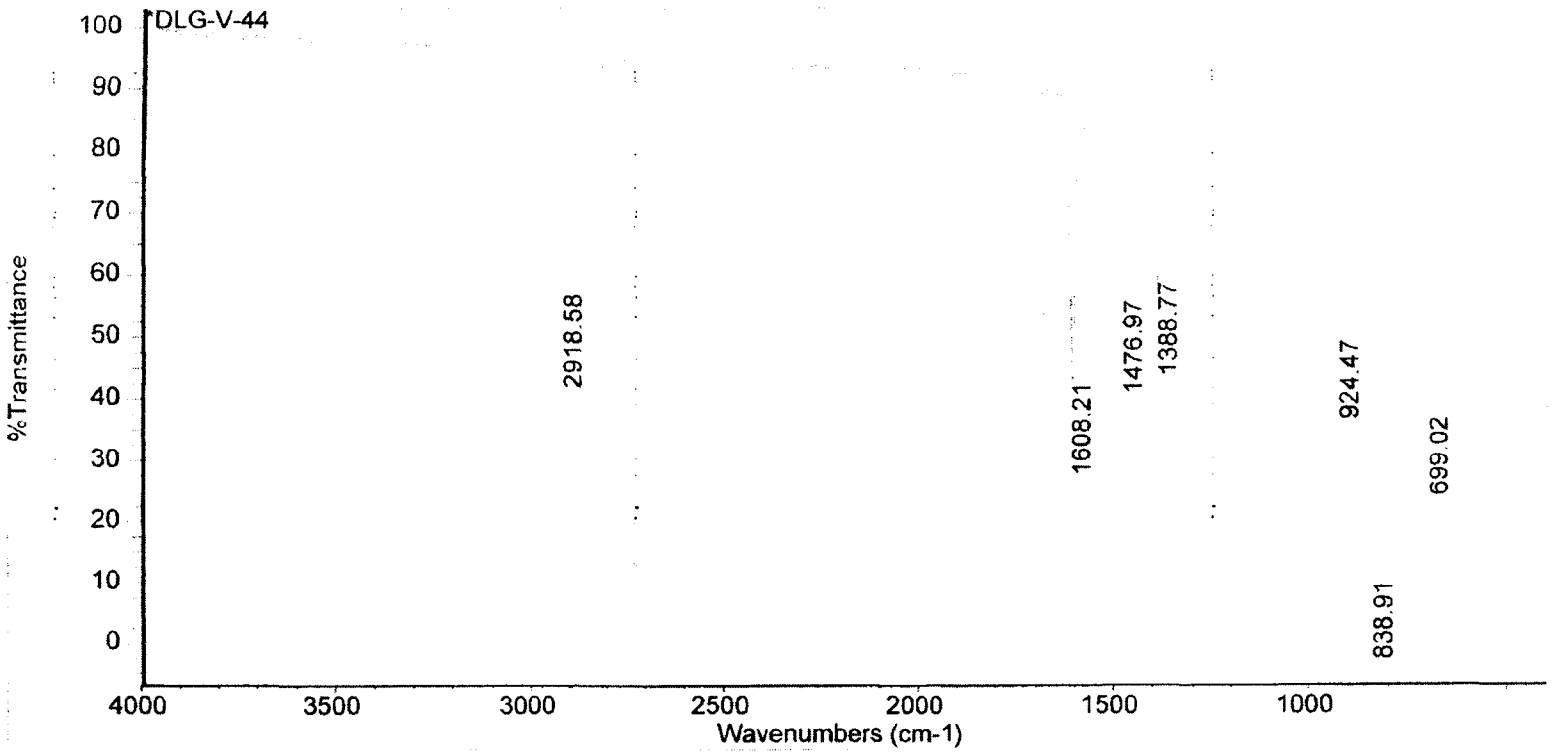

Sun Mar 30 18:25:11 2003
FIND PEAKS:

Spectrum: *DLG-V-44
Region: 4000.00 400.00
Absolute threshold: 60.025
Sensitivity: 50
Peak list:

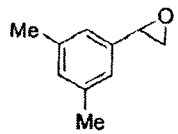

Position:	838.91	Intensity:	10.000
Position:	699.02	Intensity:	36.906
Position:	1608.21	Intensity:	42.658
Position:	924.47	Intensity:	49.404
Position:	1476.97	Intensity:	55.908
Position:	2918.58	Intensity:	57.071
Position:	1388.77	Intensity:	58.772

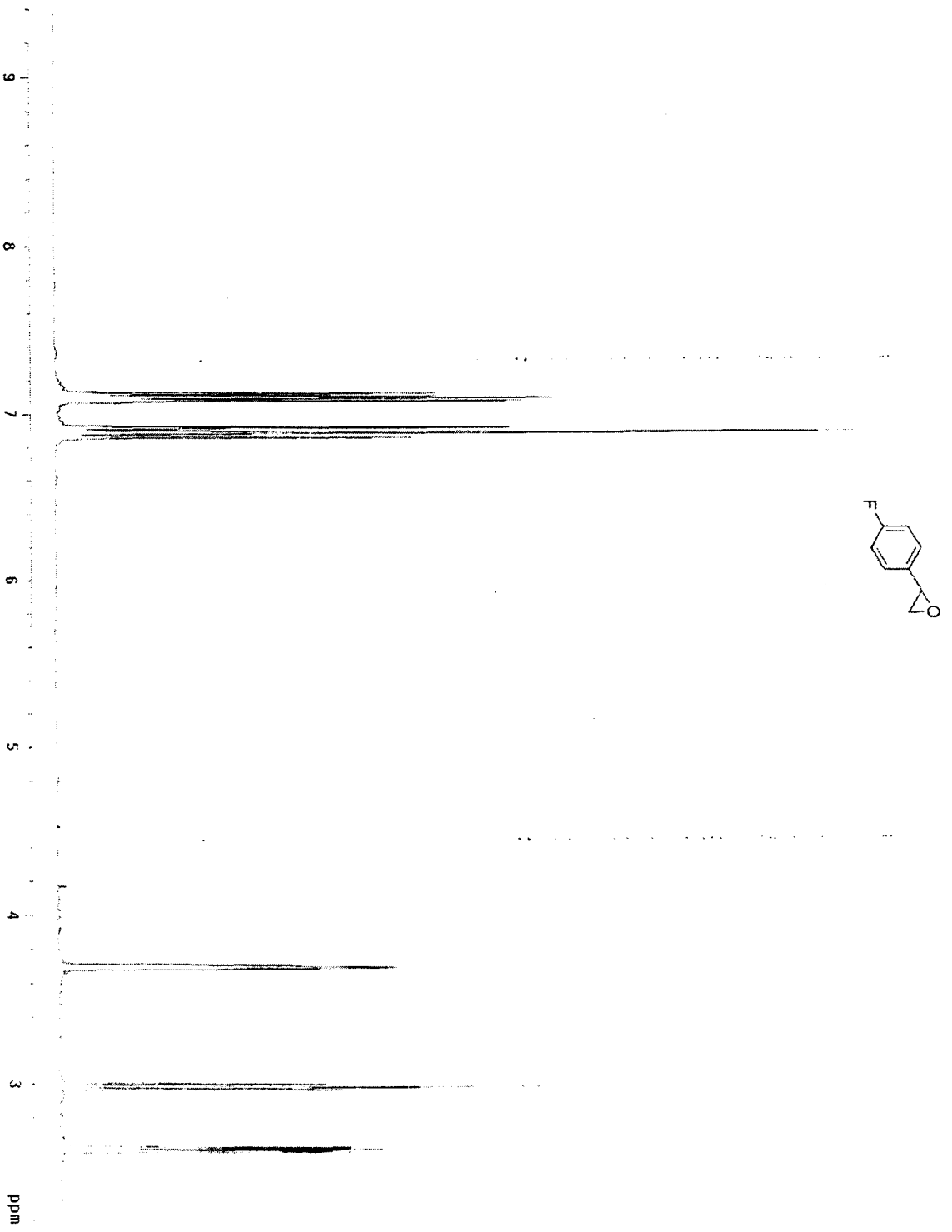

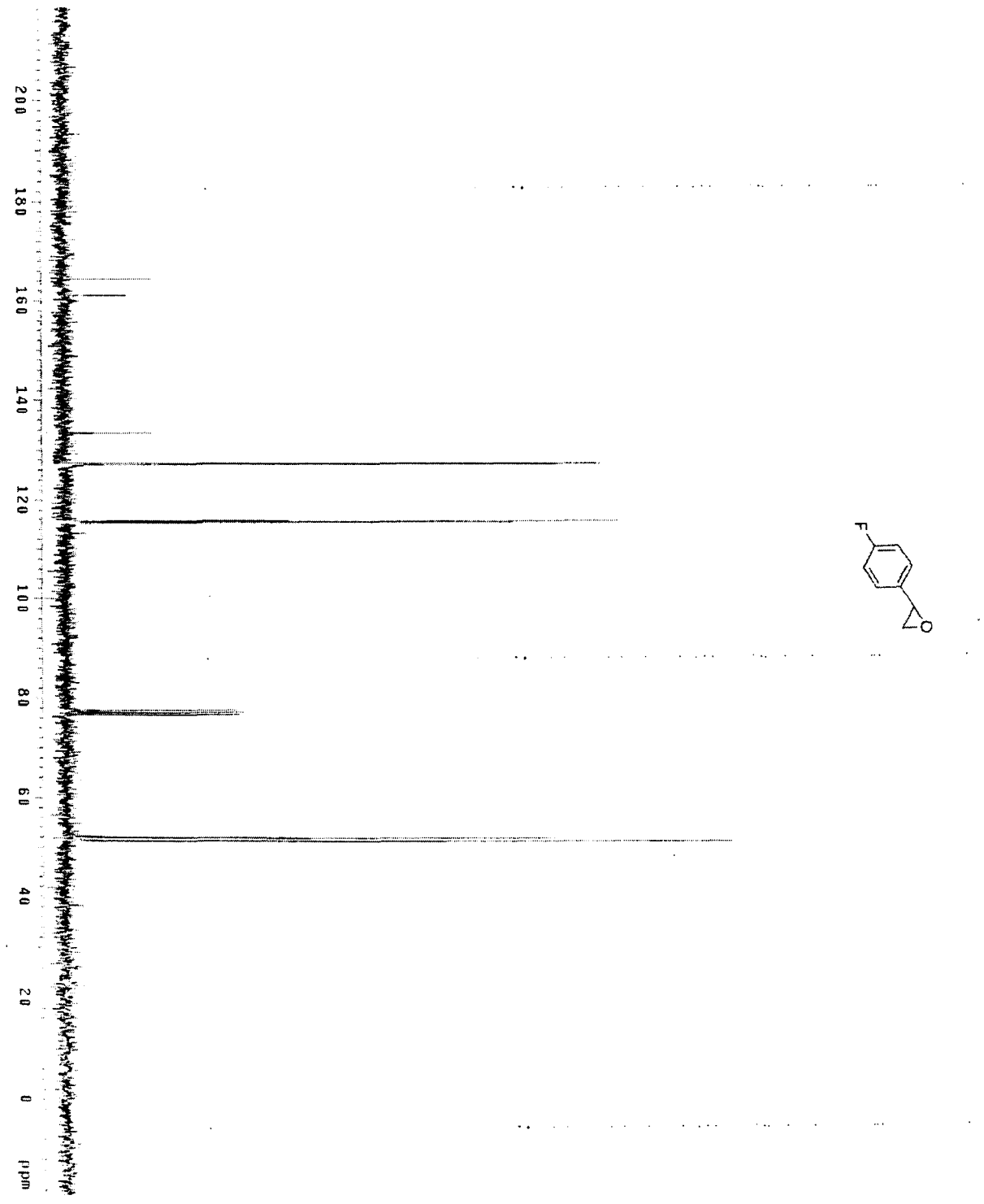

Sat Mar 22 10:27:51 2003
FIND PEAKS:

Spectrum:	DLG-V-27	
Region:	4000.00	400.00
Absolute threshold:	79.781	
Sensitivity:	17	
Peak list:		

Position:	1513.73	Intensity:	1.743
Position:	835.92	Intensity:	7.467
Position:	1221.34	Intensity:	9.195
Position:	1607.47	Intensity:	37.702
Position:	881.32	Intensity:	38.994
Position:	1156.97	Intensity:	42.917
Position:	1382.51	Intensity:	58.950
Position:	987.92	Intensity:	62.645

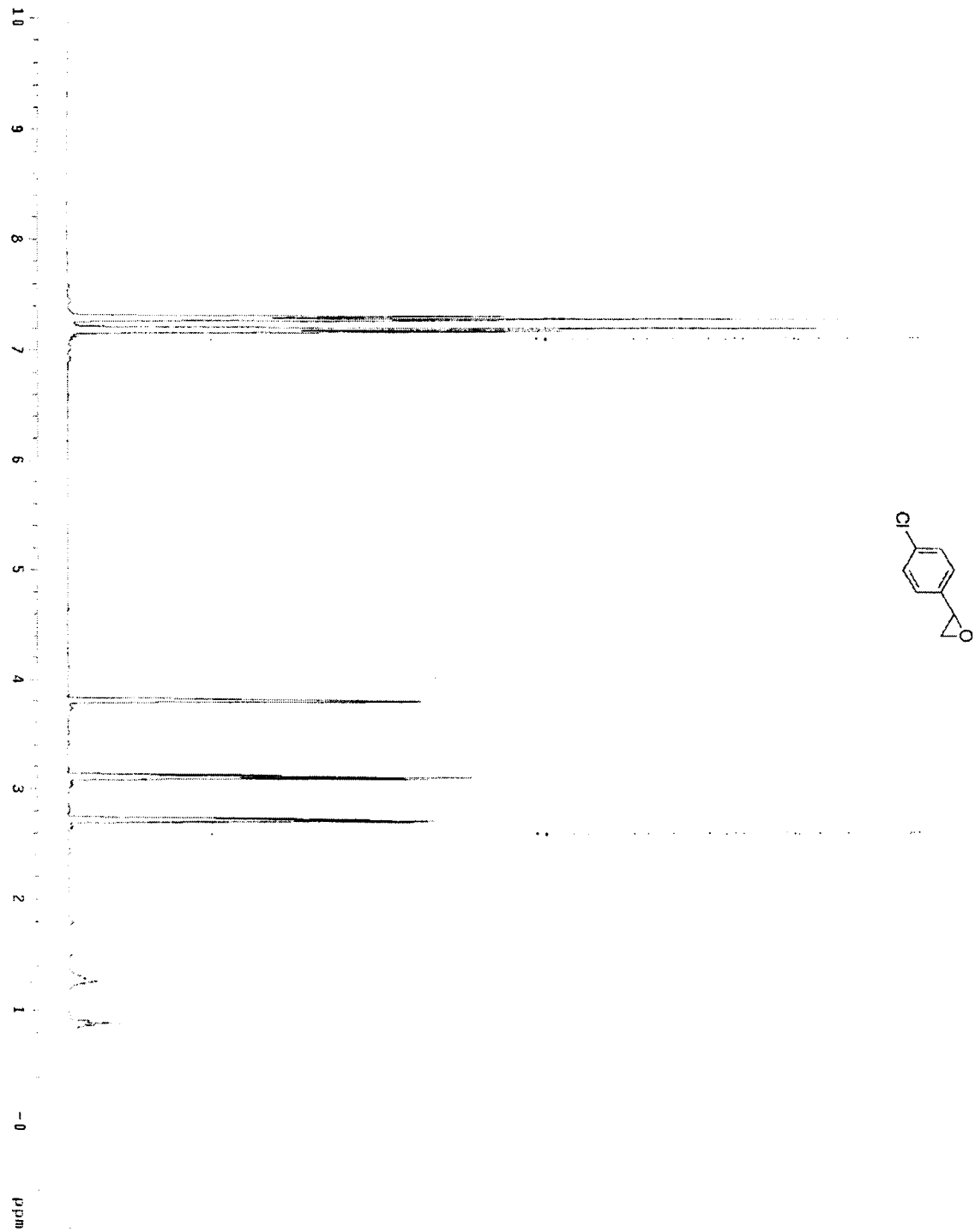

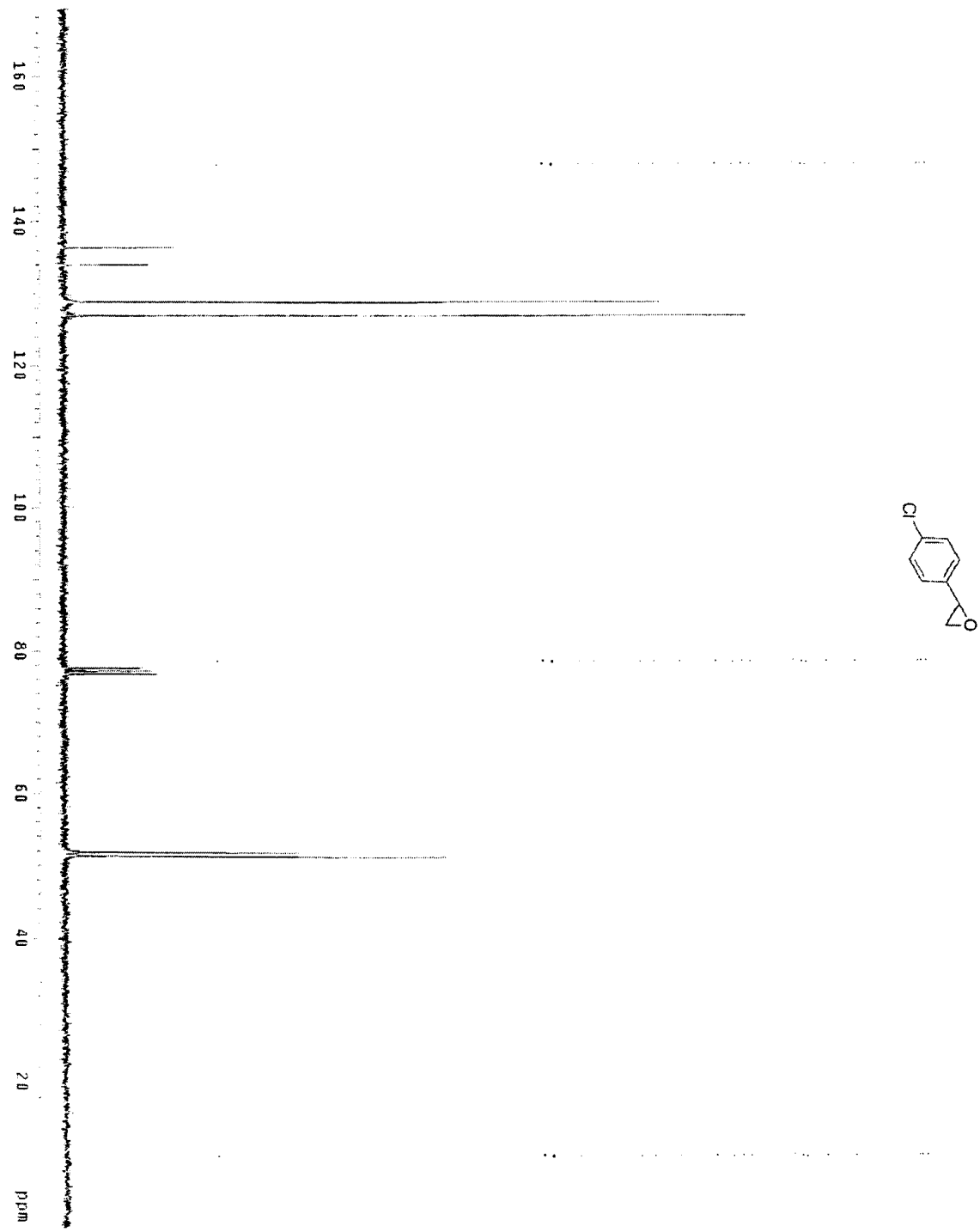

Sat Mar 22 09:50:45 2003
FIND PEAKS:

Spectrum:	DLG-V-36	
Region:	4000.00	400.00
Absolute threshold:	64.906	
Sensitivity:	50	
Peak list:		

Position:	831.39	Intensity:	4.235
Position:	1089.40	Intensity:	7.452
Position:	1495.63	Intensity:	6.382
Position:	878.32	Intensity:	20.565
Position:	1014.53	Intensity:	24.715
Position:	986.69	Intensity:	33.455
Position:	1477.57	Intensity:	39.400
Position:	768.75	Intensity:	41.453

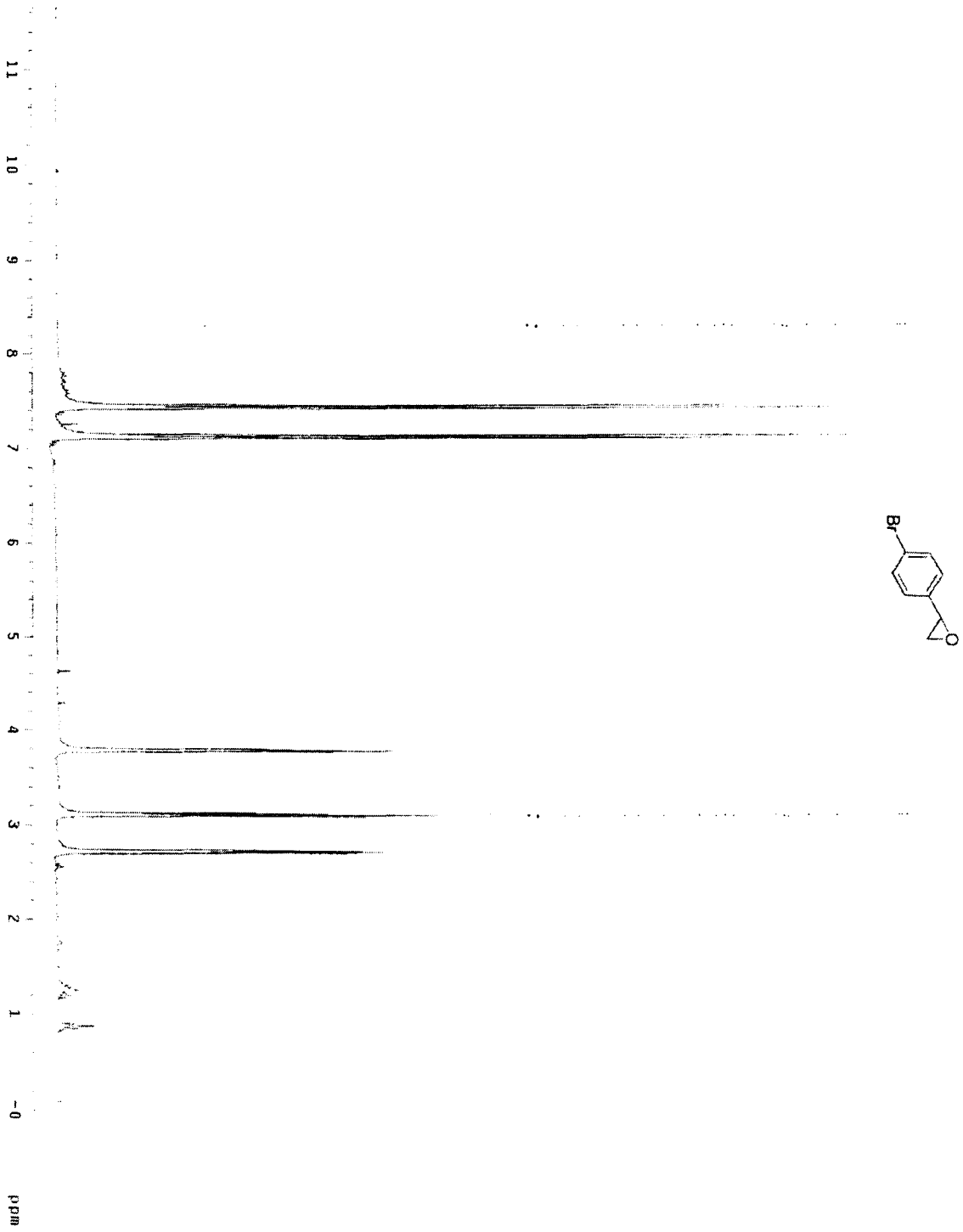

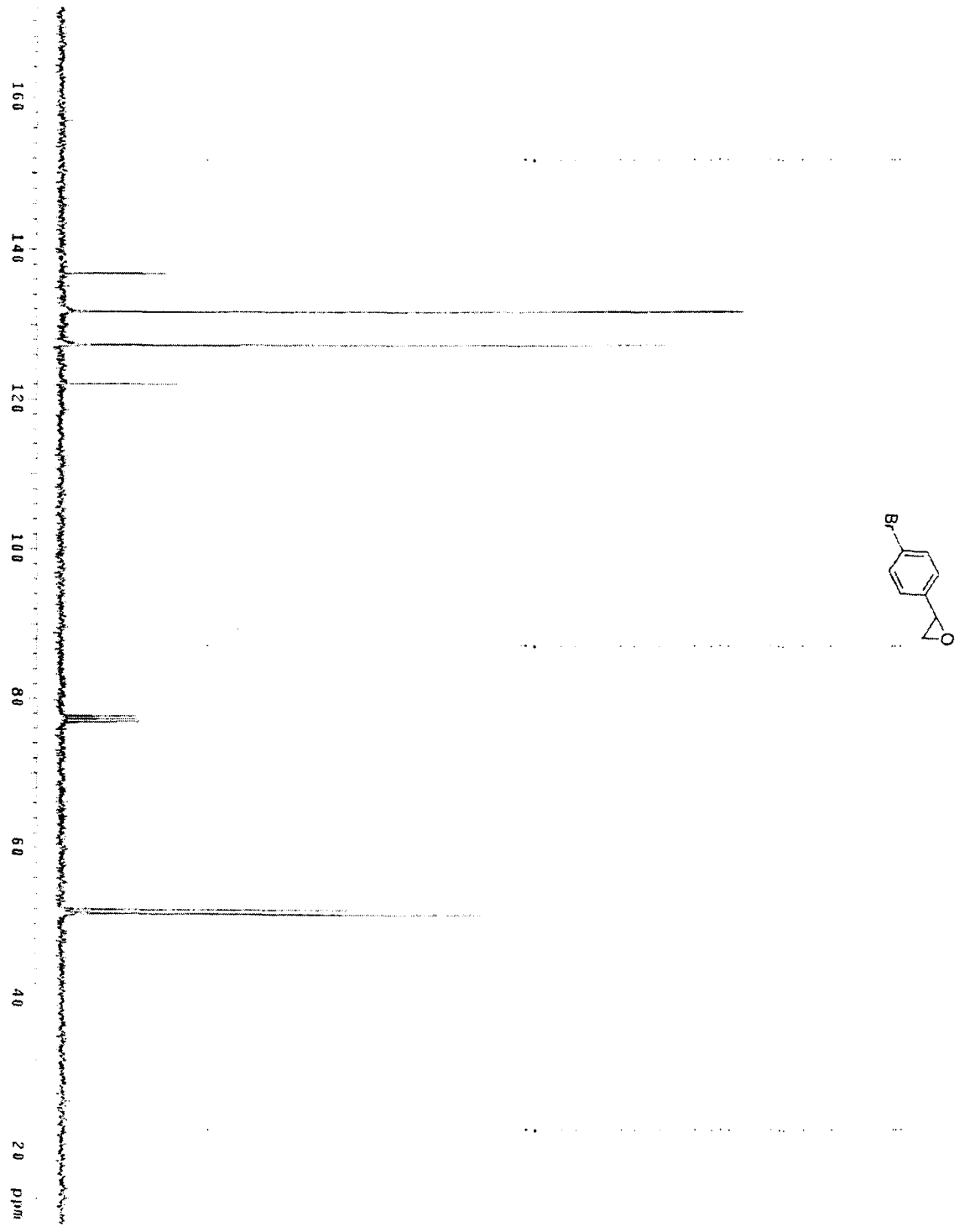

Thu Apr 03 15:25:51 2003
FIND PEAKS:

Spectrum: DLG-V-38
Region: 4000.00 400.00
Absolute threshold: 90.351
Sensitivity: 50
Peak list:

Position:	827.47	Intensity:	78.858
Position:	1010.52	Intensity:	80.358
Position:	1489.94	Intensity:	80.680
Position:	877.68	Intensity:	81.768
Position:	1073.05	Intensity:	81.692
Position:	985.95	Intensity:	83.125
Position:	1475.63	Intensity:	84.891
Position:	761.84	Intensity:	85.610

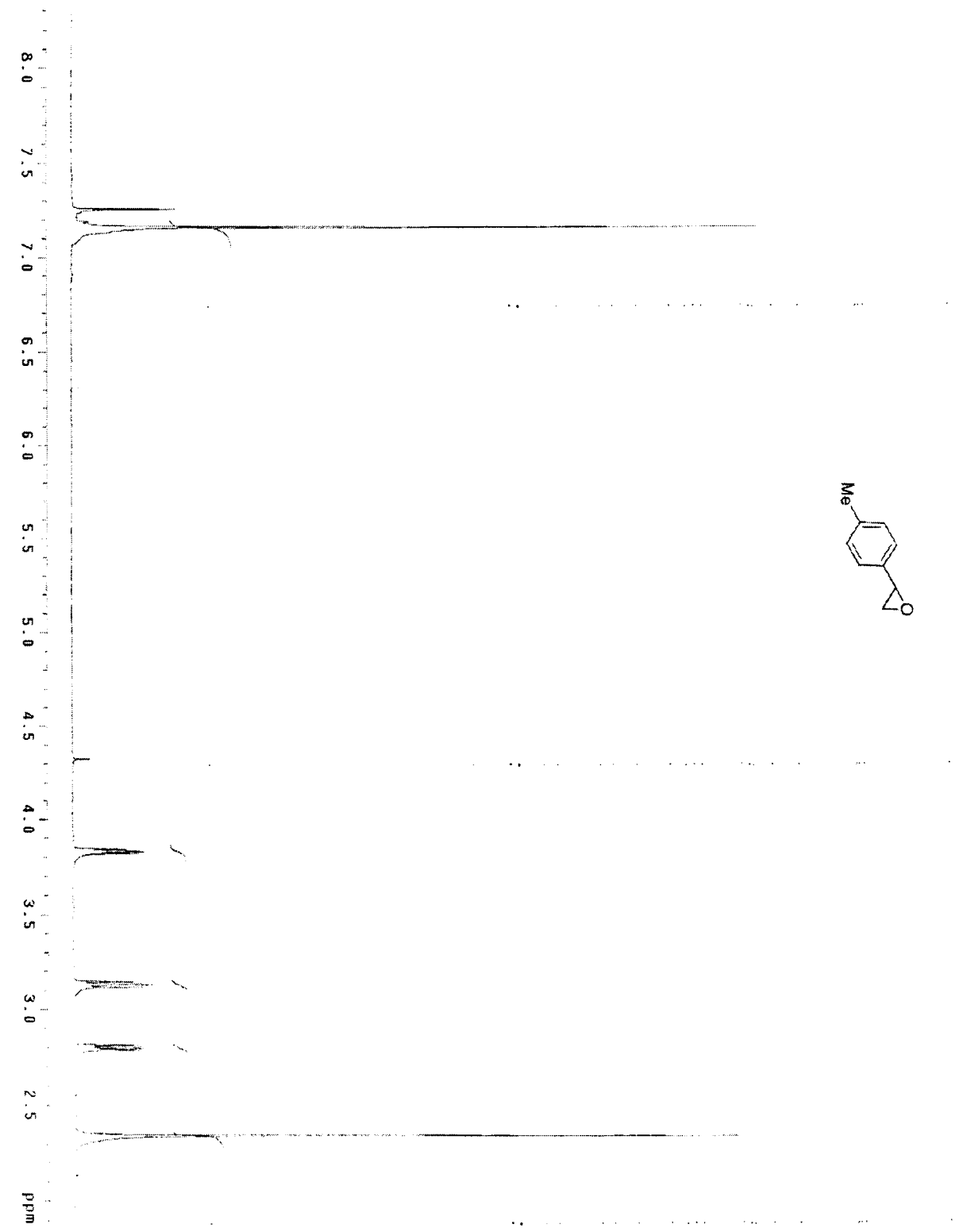

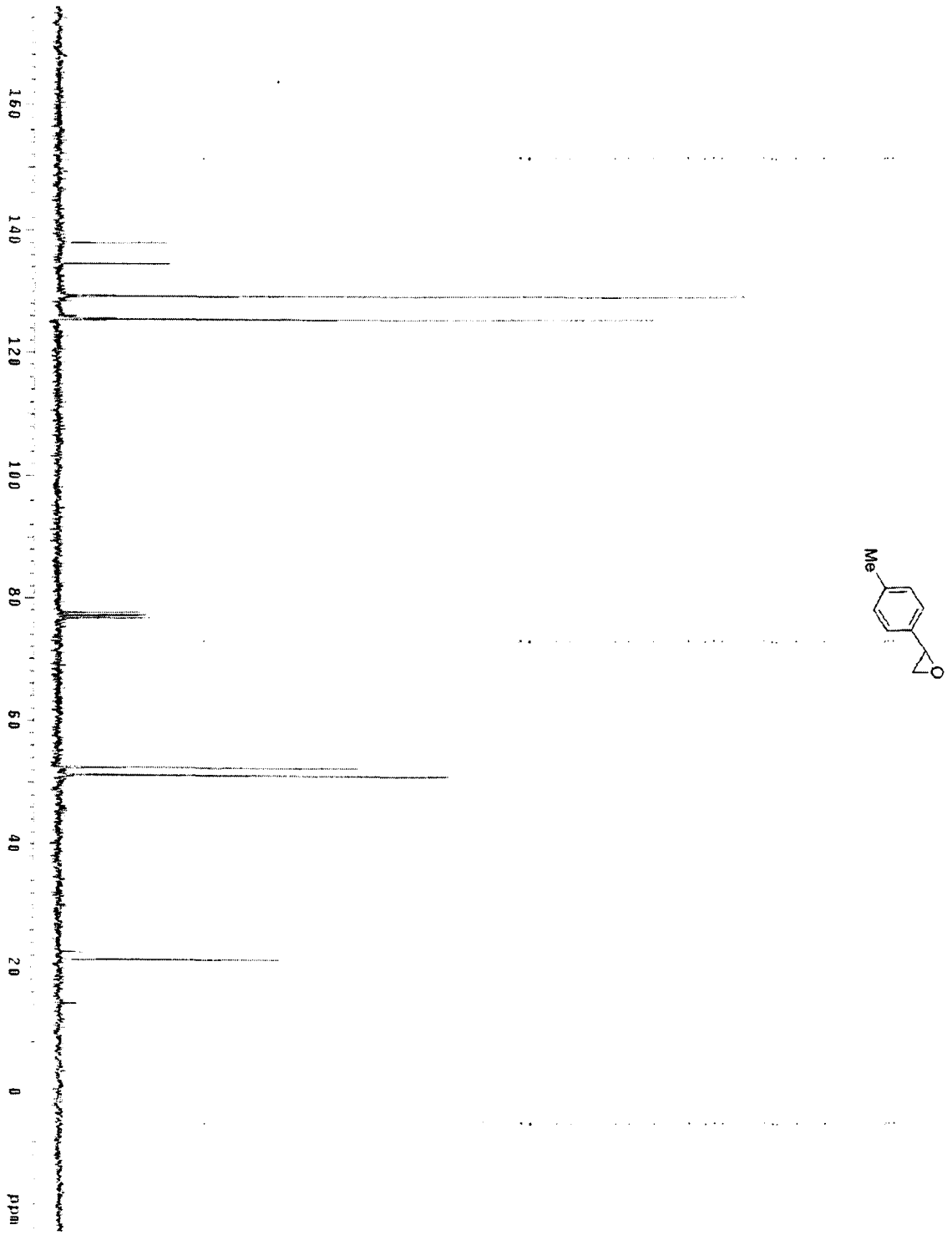

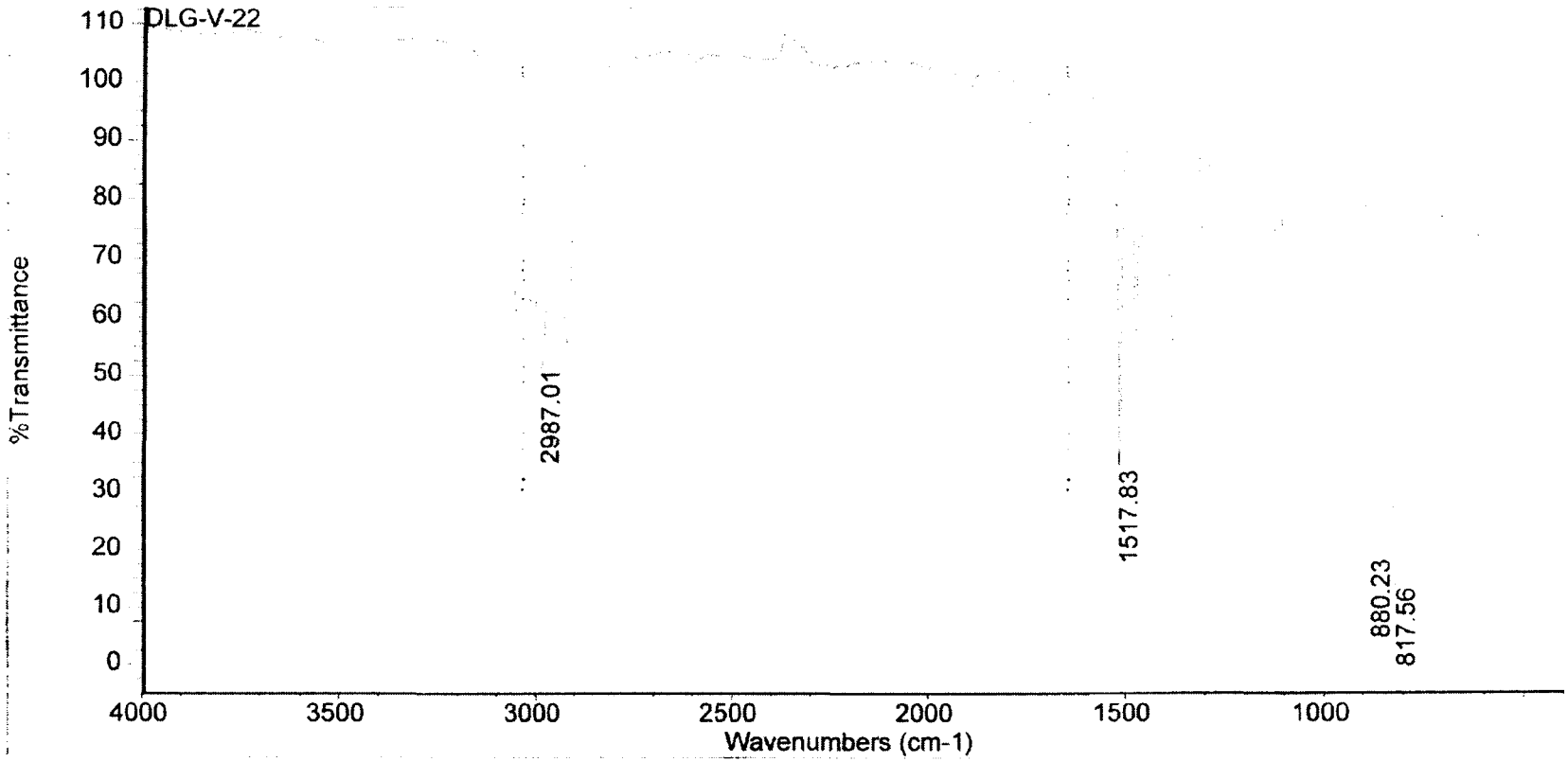

Fri Feb 28 13:36:10 2003
FIND PEAKS:

Spectrum:	DLG-V-22	
Region:	4000.00	400.00
Absolute threshold:	55.265	
Sensitivity:	50	

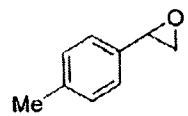

Peak list:

Position:	817.56	Intensity:	13.272
Position:	880.23	Intensity:	18.230
Position:	1517.83	Intensity:	33.767
Position:	2987.01	Intensity:	51.242

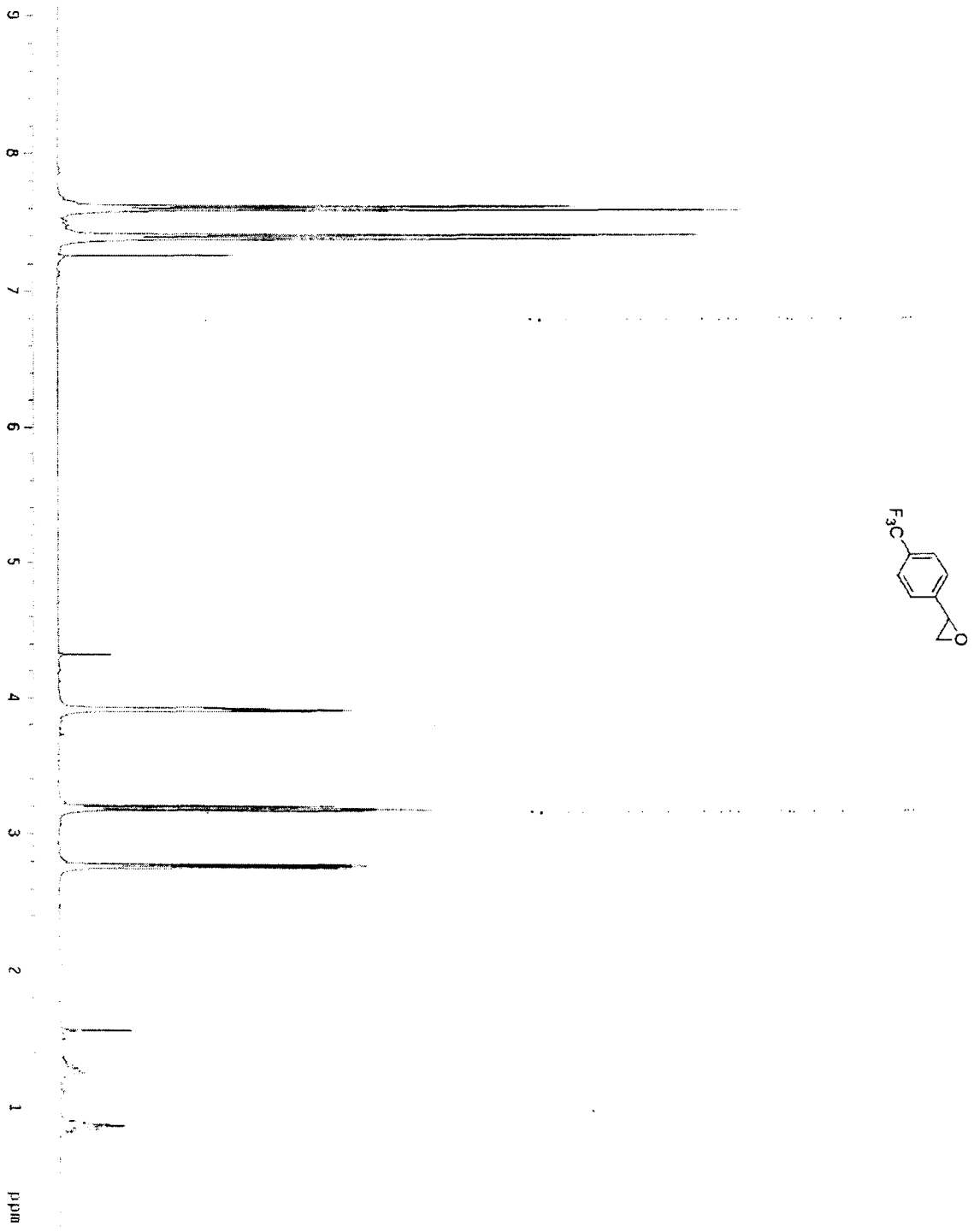

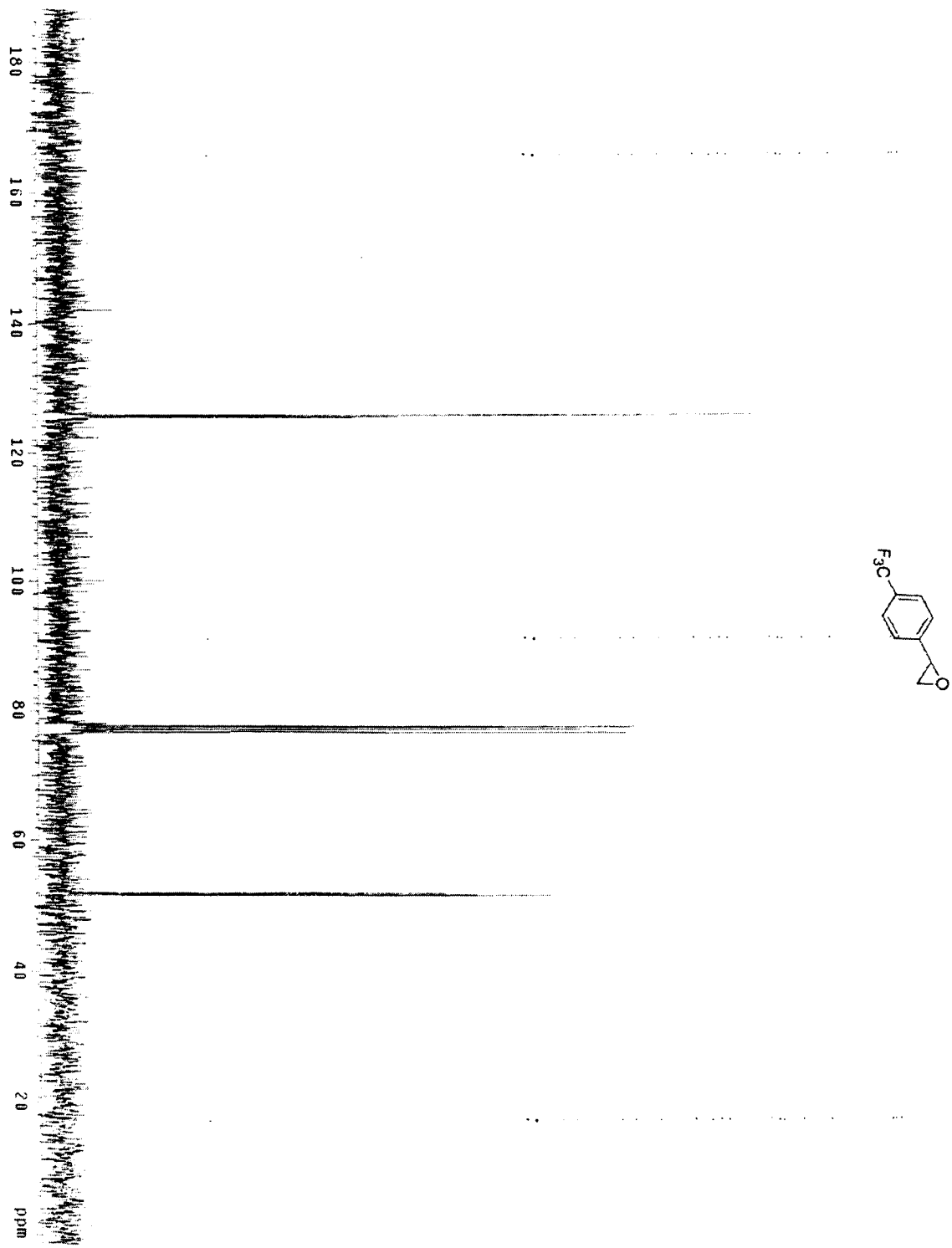

Mon Mar 03 21:12:30 2003
FIND PEAKS:
Spectrum: DLG-V_24
Region: 4000.00 400.00
Absolute threshold: 75.951
Sensitivity: 11
Peak list:

Position:	1325.68	Intensity:	0.0194
Position:	1125.25	Intensity:	0.914
Position:	1068.36	Intensity:	2.005
Position:	842.29	Intensity:	5.263
Position:	1016.54	Intensity:	26.508
Position:	879.92	Intensity:	33.101
Position:	1622.48	Intensity:	32.689
Position:	1425.61	Intensity:	42.776

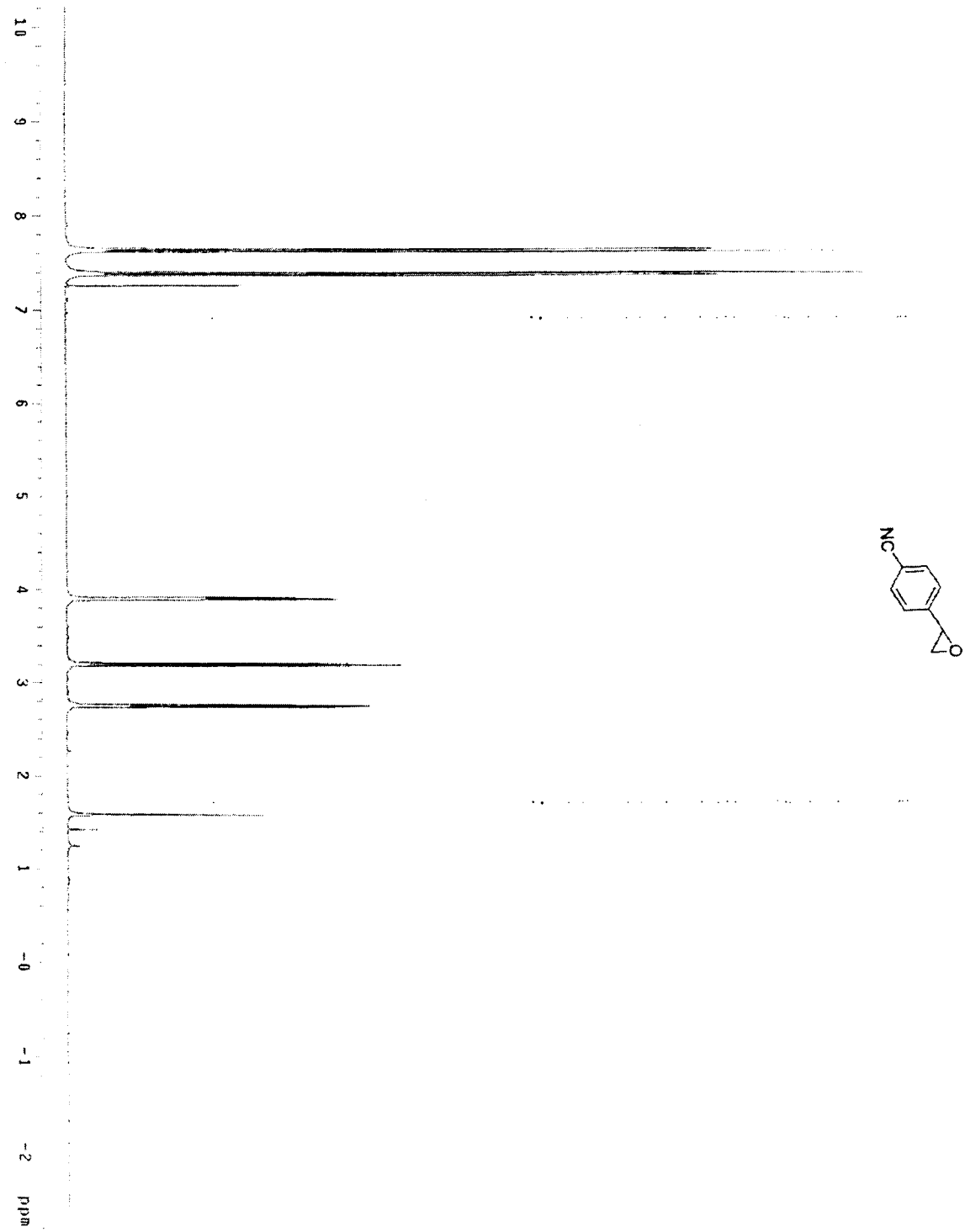

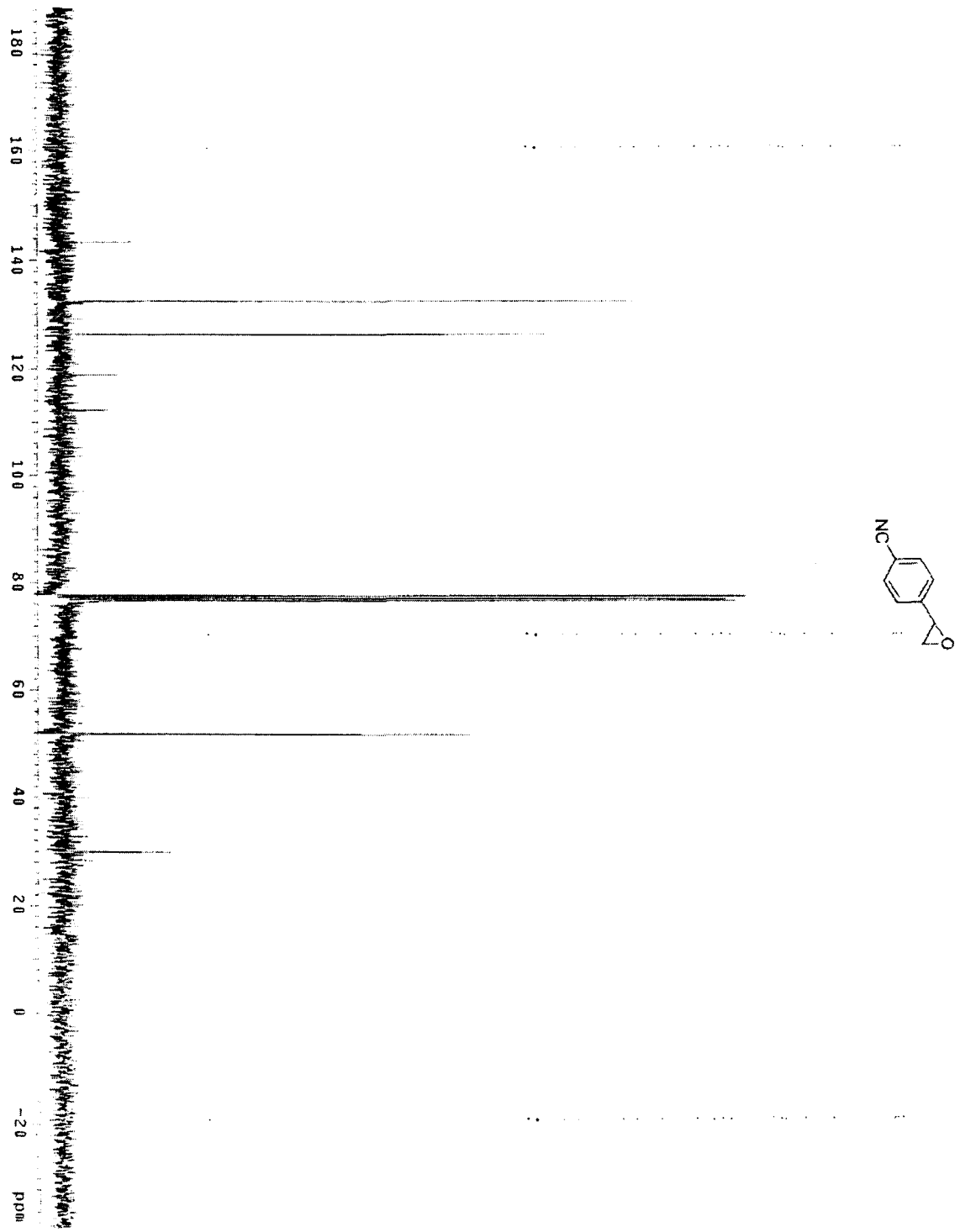

Wed Jul 02 14:46:34 2003
FIND PEAKS:
Spectrum: DLG-4cnstyoxrac
Region: 4000.00 400.00
Absolute threshold: 64.567
Sensitivity: 50
Peak list:

Position:	2228.47	Intensity:	59.680
Position:	838.22	Intensity:	60.005
Position:	1506.36	Intensity:	60.873
Position:	877.01	Intensity:	61.666
Position:	1611.24	Intensity:	61.603
Position:	1418.04	Intensity:	62.288
Position:	986.42	Intensity:	62.371
Position:	1382.65	Intensity:	62.816

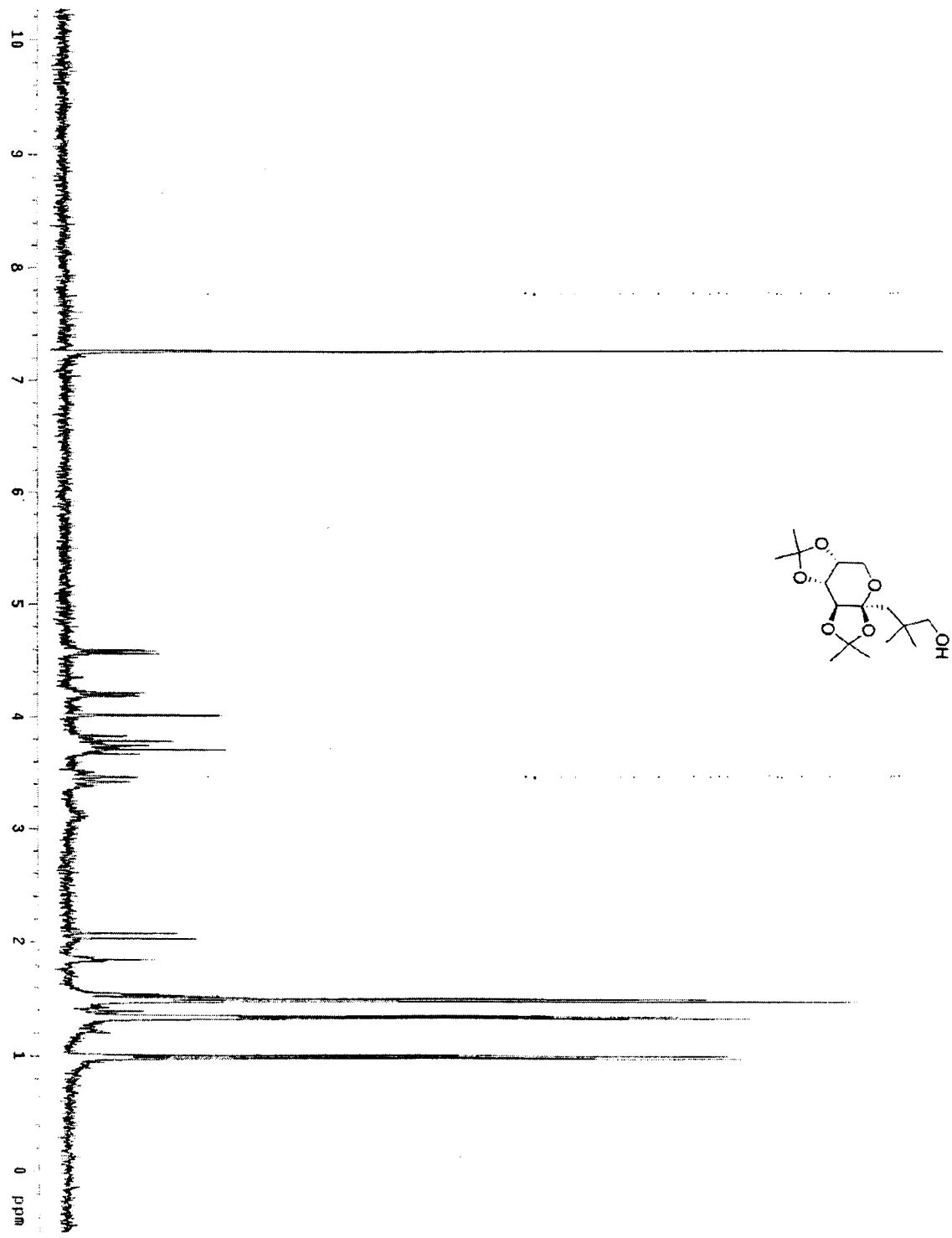

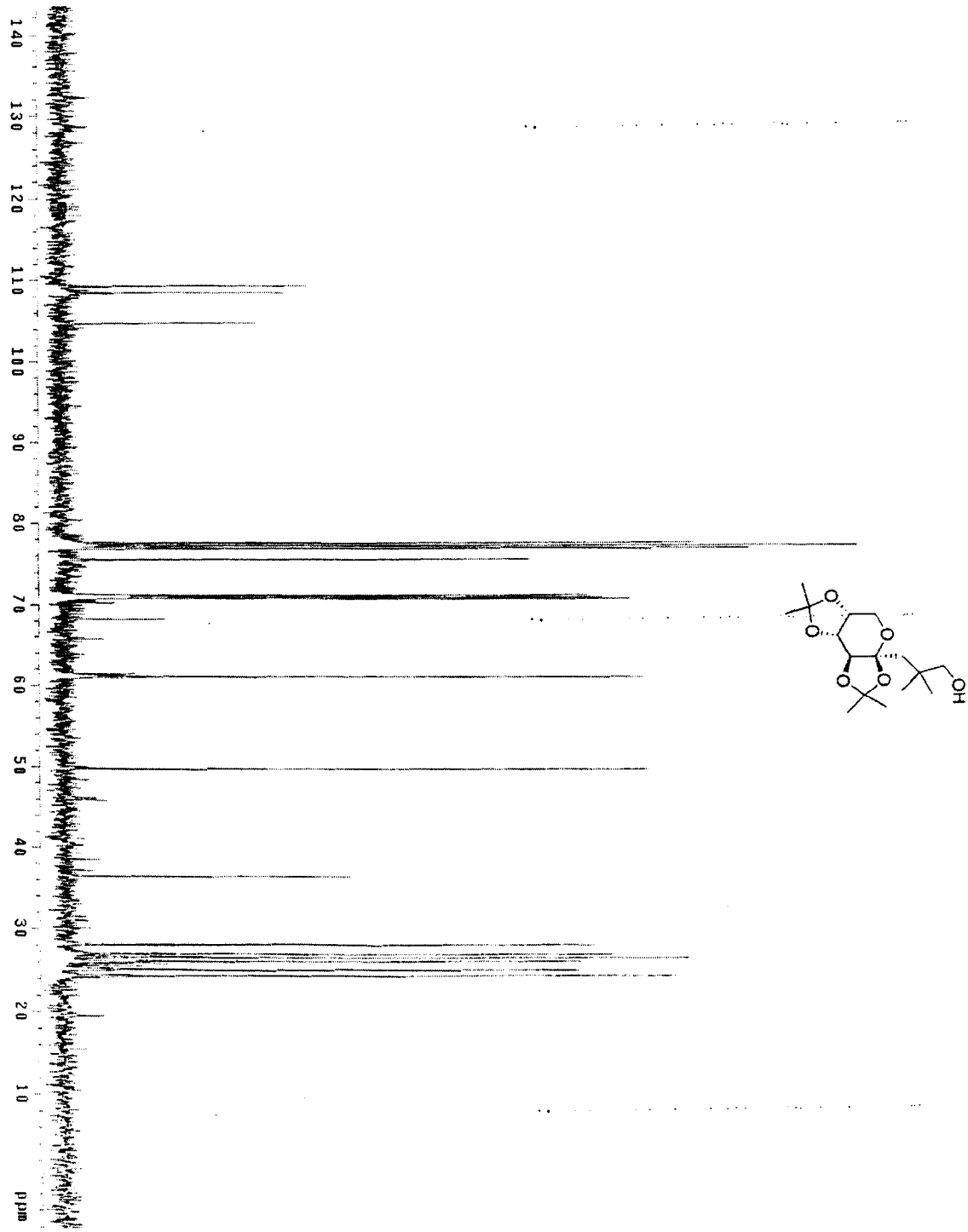

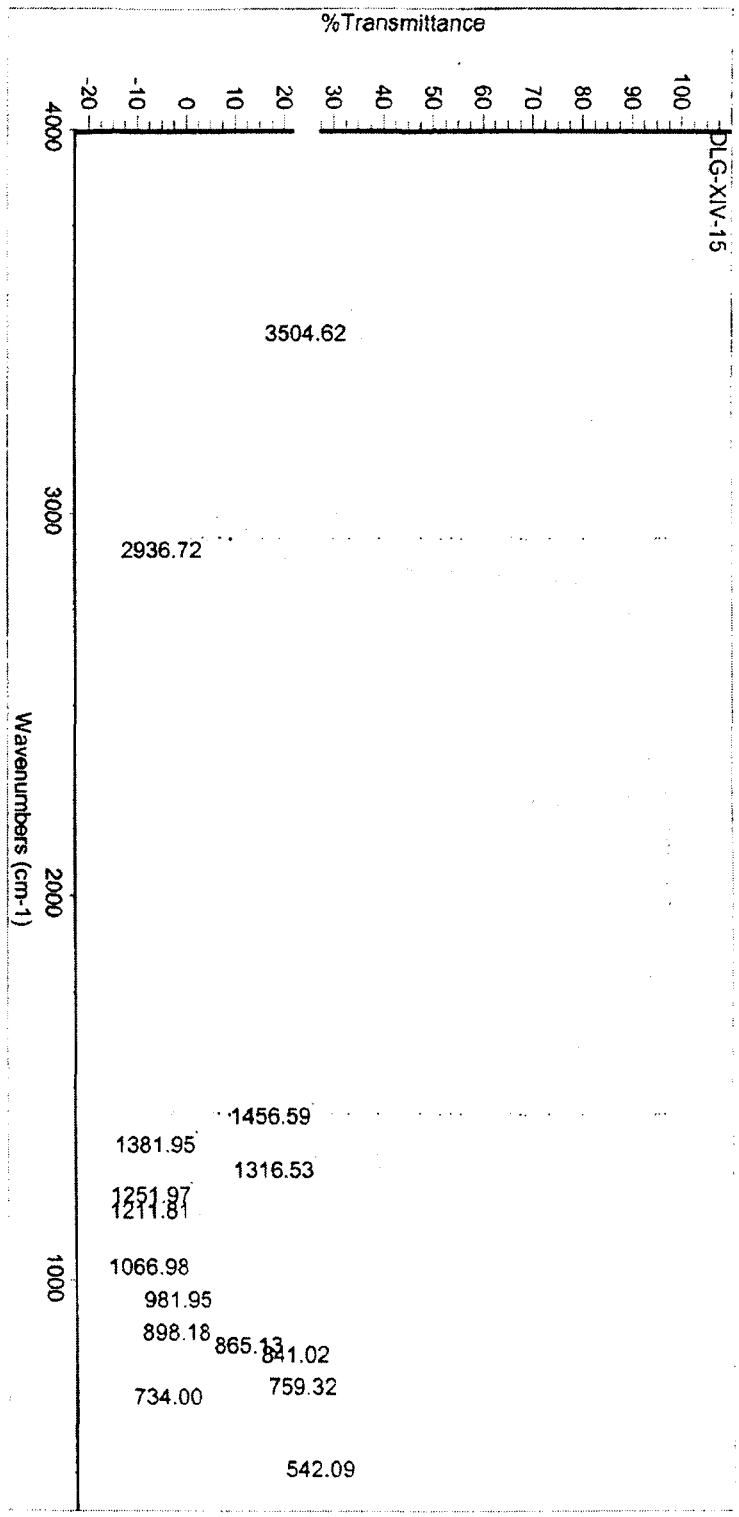

Thu Jun 02 13:14:48 2005
FIND PEAKS:
Spectrum: DLG-XIV-15
Region: 4000.00 400.00
Absolute threshold: 40.581
Sensitivity: 31
Peak list:

Position:	1066.98	Intensity:	0.177
Position:	1211.81	Intensity:	0.449
Position:	1251.97	Intensity:	0.689
Position:	1381.95	Intensity:	1.586
Position:	734.00	Intensity:	2.632
Position:	2936.72	Intensity:	3.090
Position:	898.18	Intensity:	4.480
Position:	981.95	Intensity:	4.858

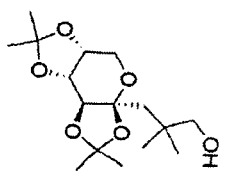

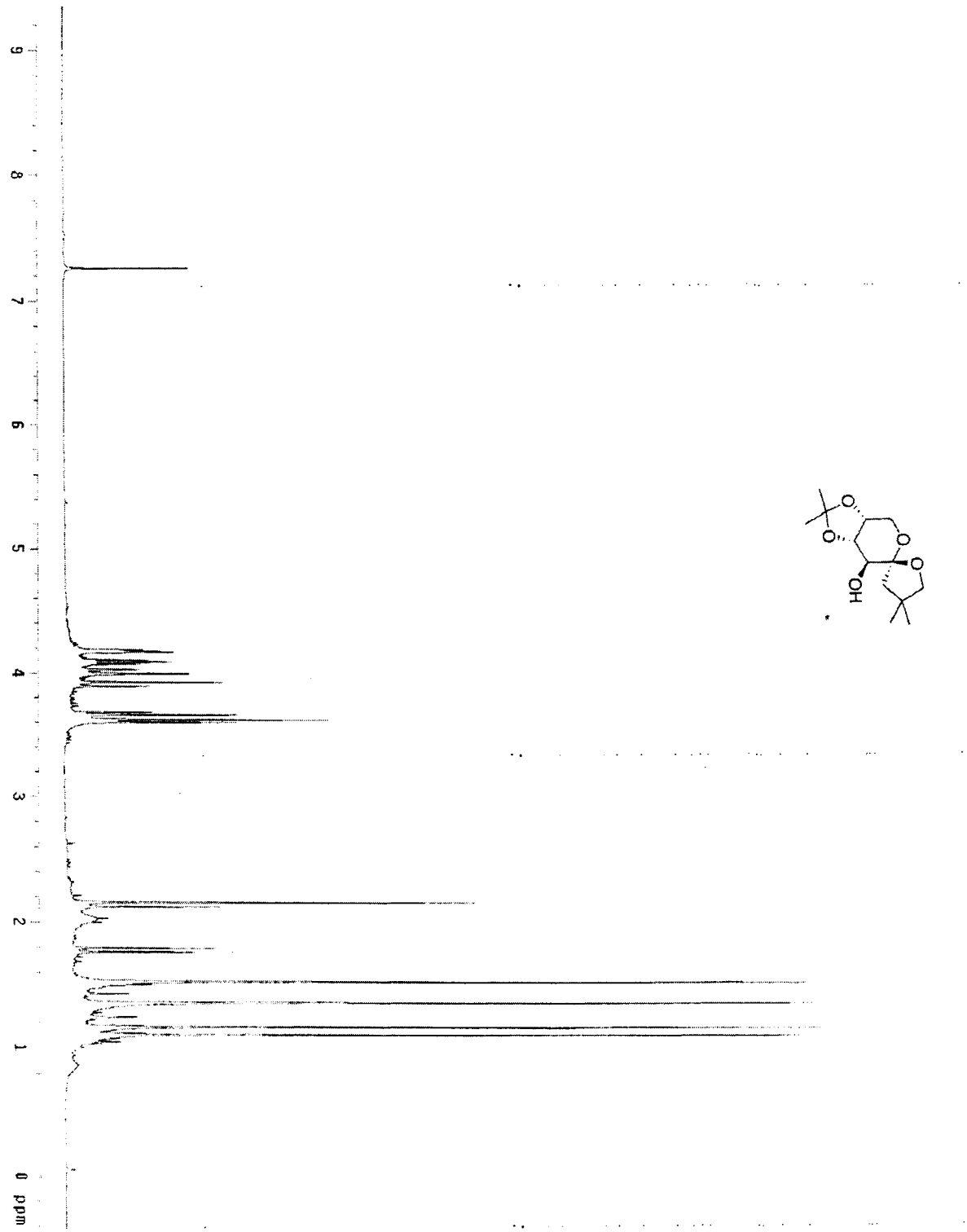

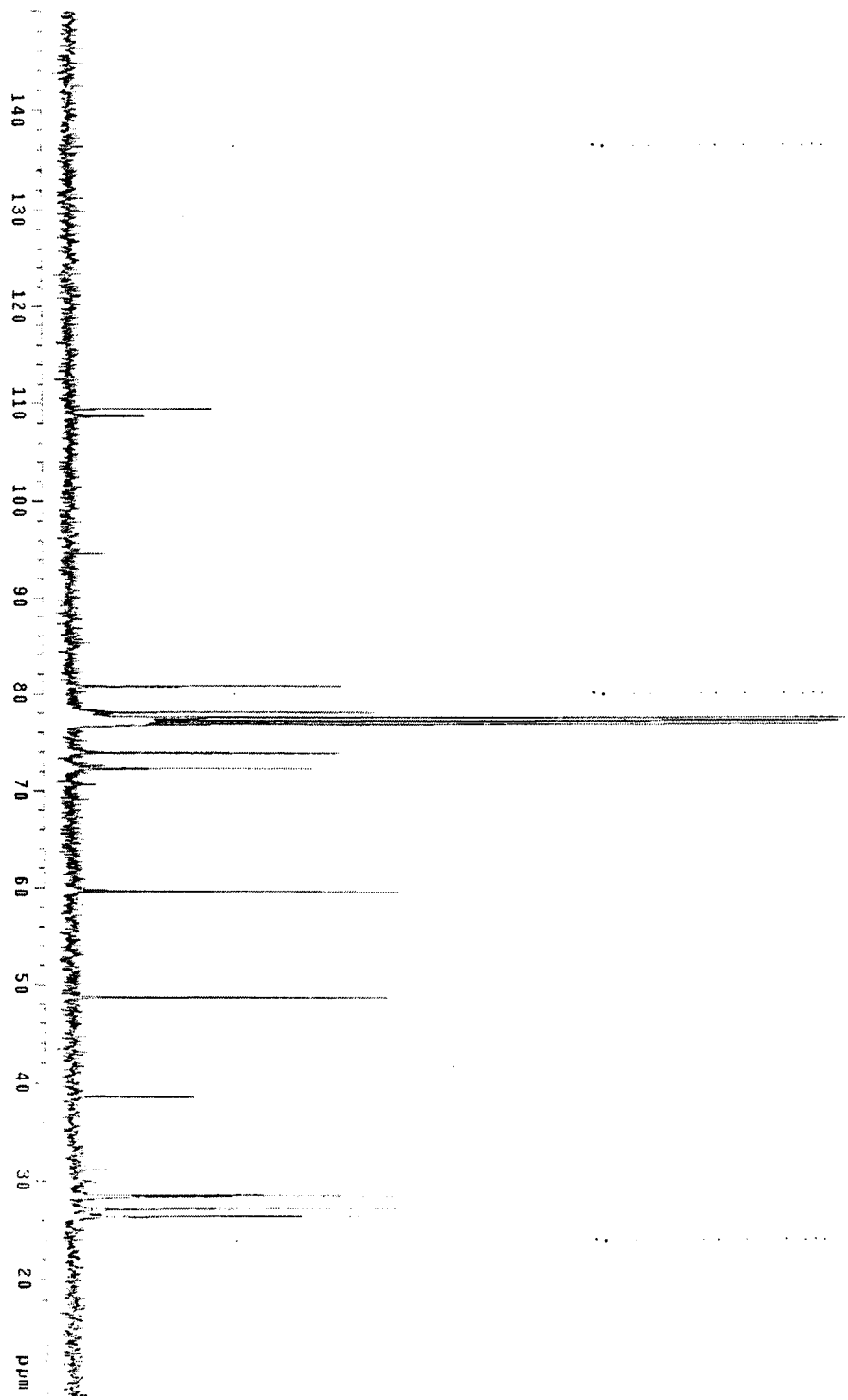

Fri Jun 10 13:44:10 2005
FIND PEAKS:

Spectrum: DLG-XIV-23
Region: 4000.00 400.00
Absolute threshold: 34.667
Sensitivity: 50
Peak list:

Position:	1078.30	Intensity:	28.475
Position:	1012.50	Intensity:	28.484
Position:	2955.42	Intensity:	29.913
Position:	1111.25	Intensity:	30.175
Position:	3453.92	Intensity:	30.502
Position:	1217.87	Intensity:	30.534
Position:	2871.13	Intensity:	30.976
Position:	978.28	Intensity:	31.133

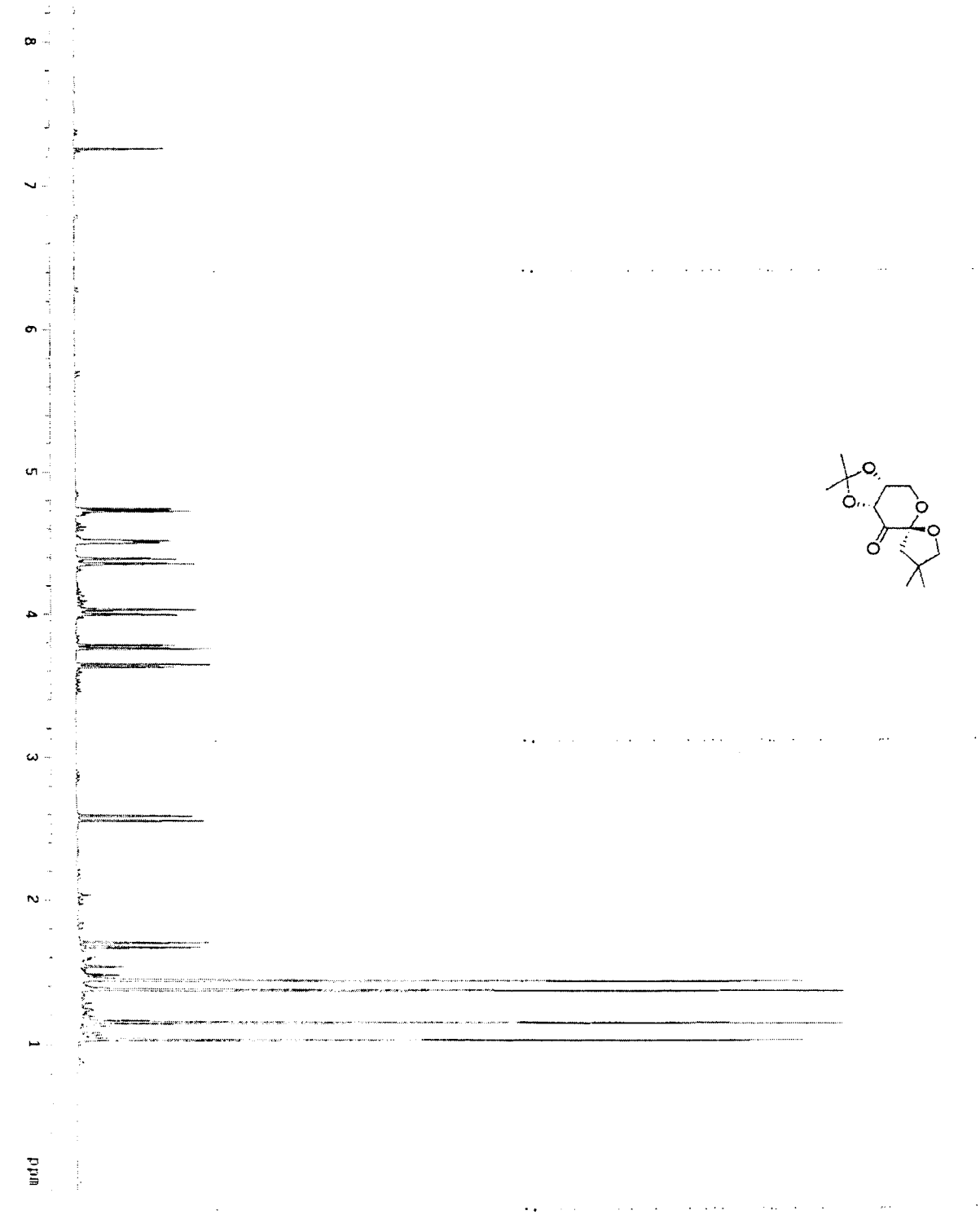

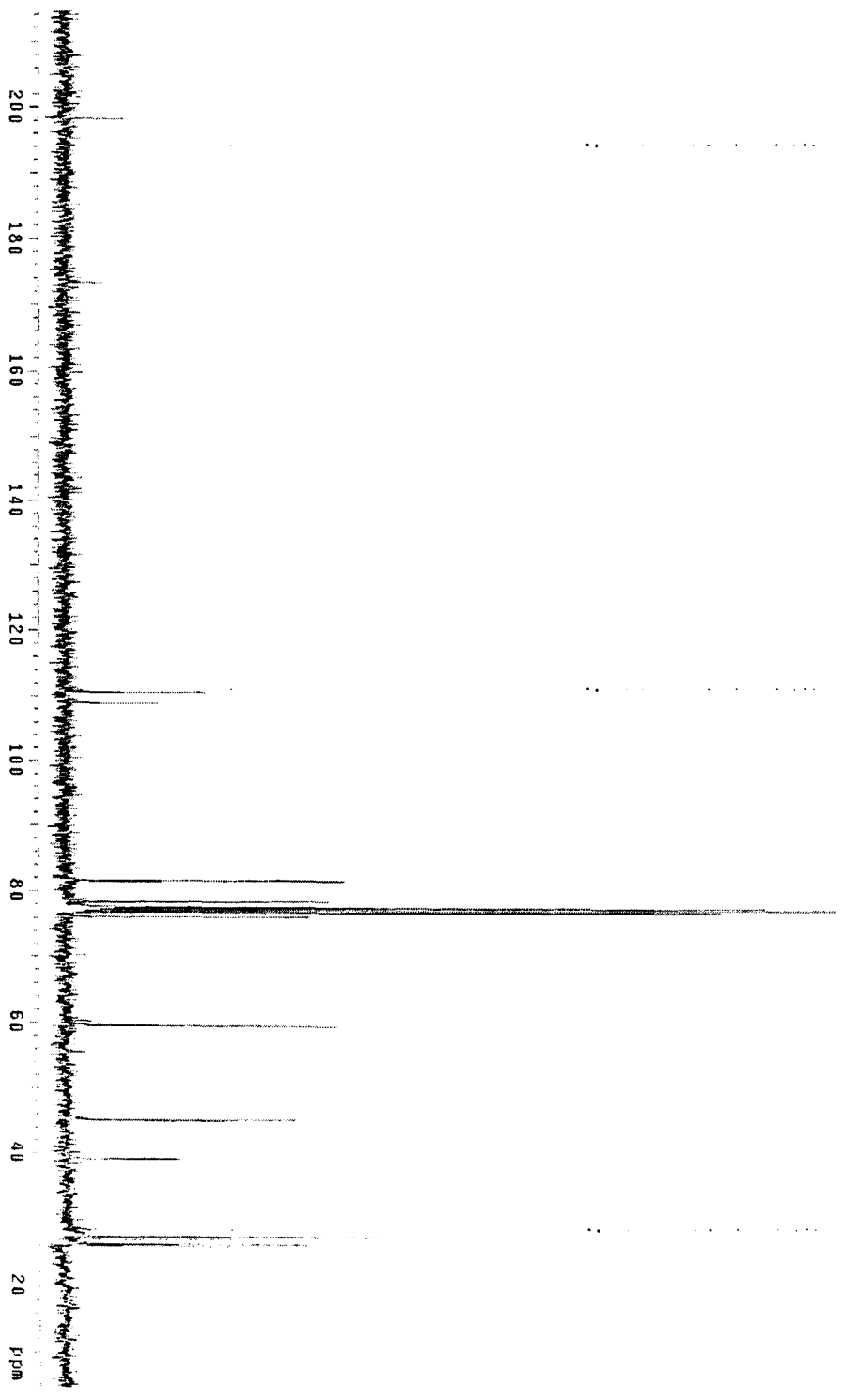

Thu Jun 02 13:25:27 2005
FIND PEAKS:
Spectrum: DLG-XIV-25
Region: 4000.00 400.00
Absolute threshold: 76.494
Sensitivity: 50
Peak list:

Position:	999.16	Intensity:	47.808
Position:	1098.76	Intensity:	50.676
Position:	1747.15	Intensity:	59.291
Position:	1172.83	Intensity:	66.011
Position:	1223.91	Intensity:	67.930
Position:	976.36	Intensity:	68.127
Position:	846.96	Intensity:	71.603
Position:	1239.45	Intensity:	71.686

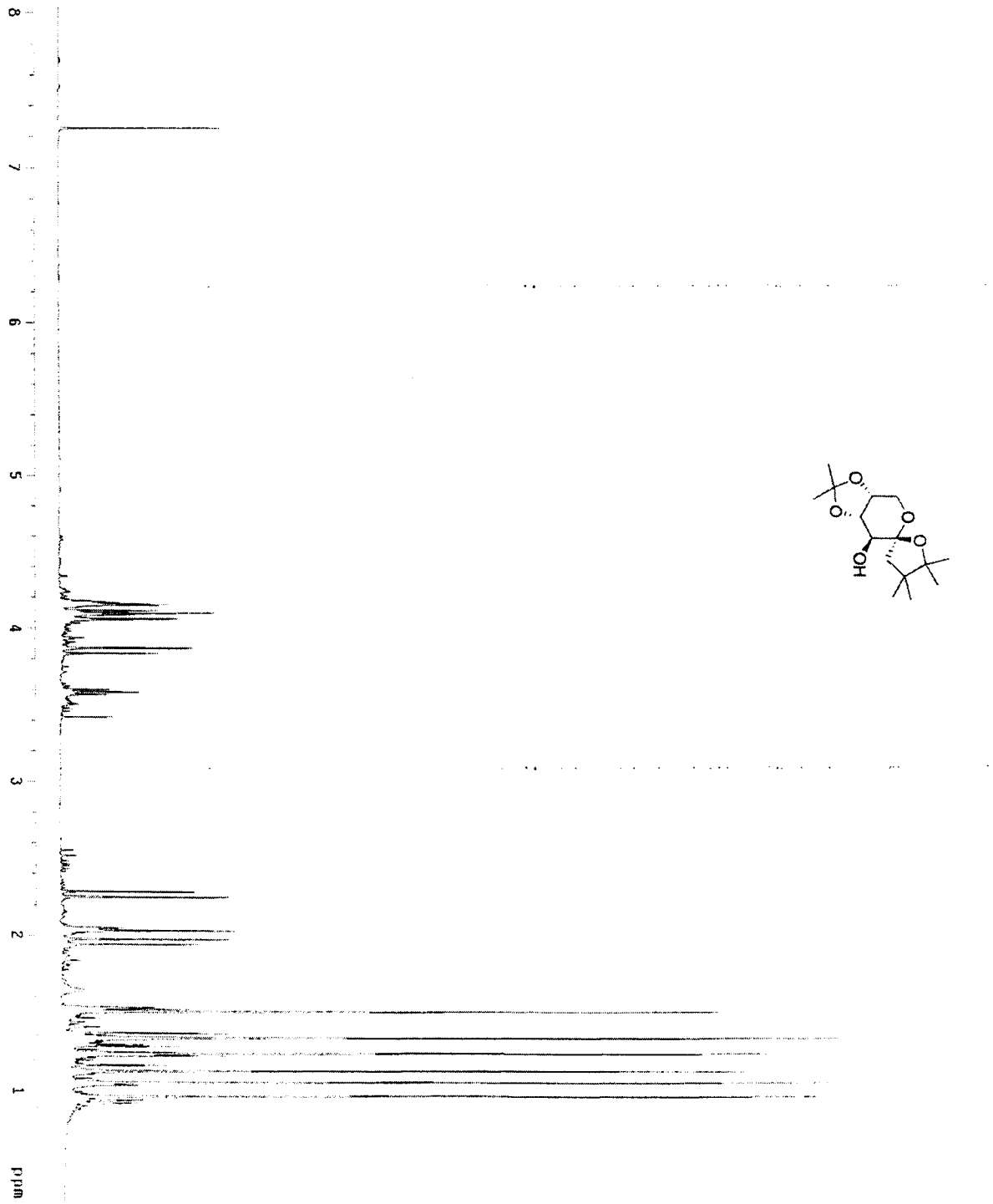

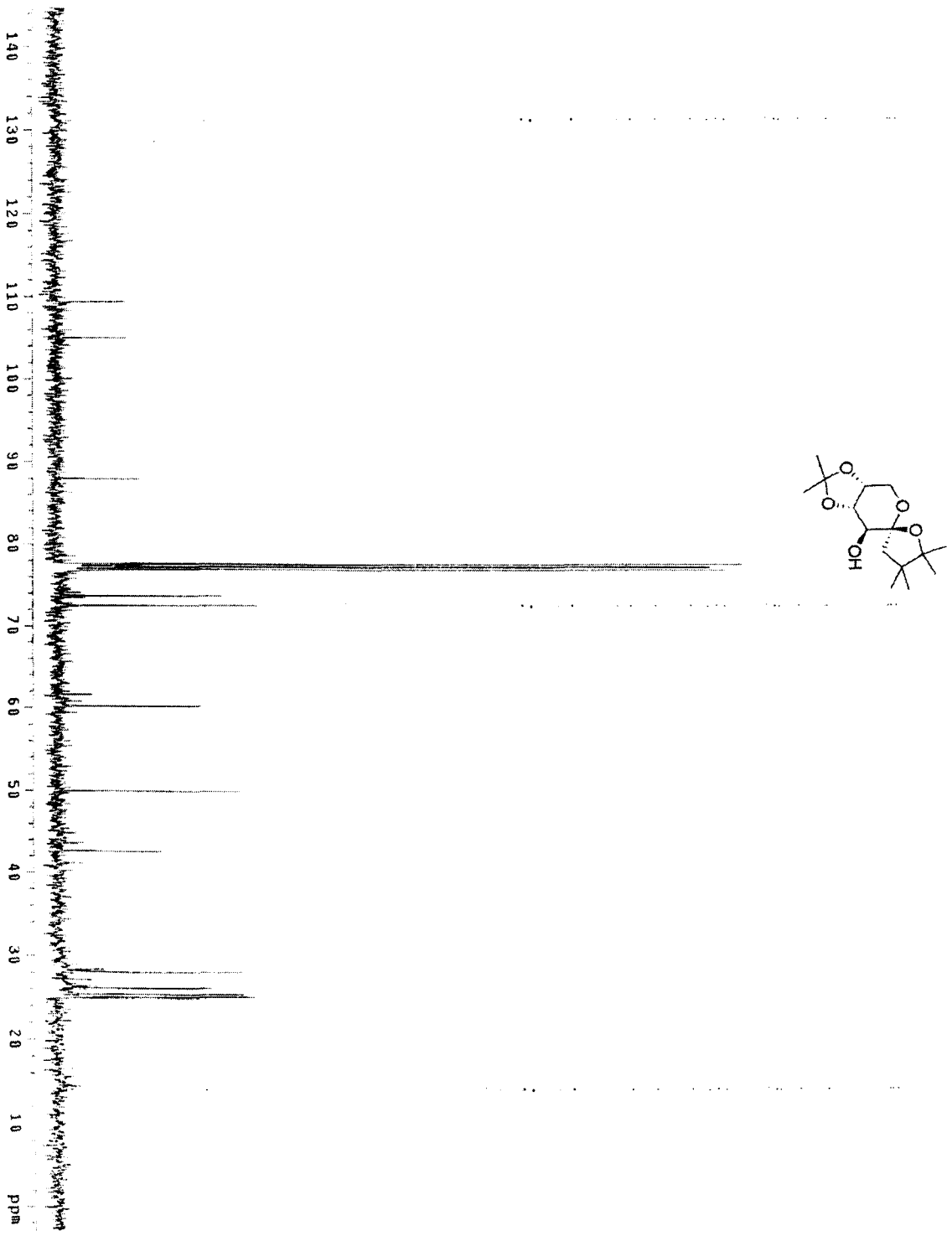

Thu Jun 02 13:30:33 2005
FIND PEAKS:

Spectrum:	DLG-XIV-27	
Region:	4000.00	400.00
Absolute threshold:	95.626	
Sensitivity:	28	
Peak list:		

Position:	1077.06	Intensity:	81.739
Position:	1104.25	Intensity:	85.346
Position:	1218.41	Intensity:	86.241
Position:	1025.61	Intensity:	88.284
Position:	1166.09	Intensity:	89.039
Position:	1379.11	Intensity:	89.445
Position:	985.95	Intensity:	90.681
Position:	2974.44	Intensity:	90.749

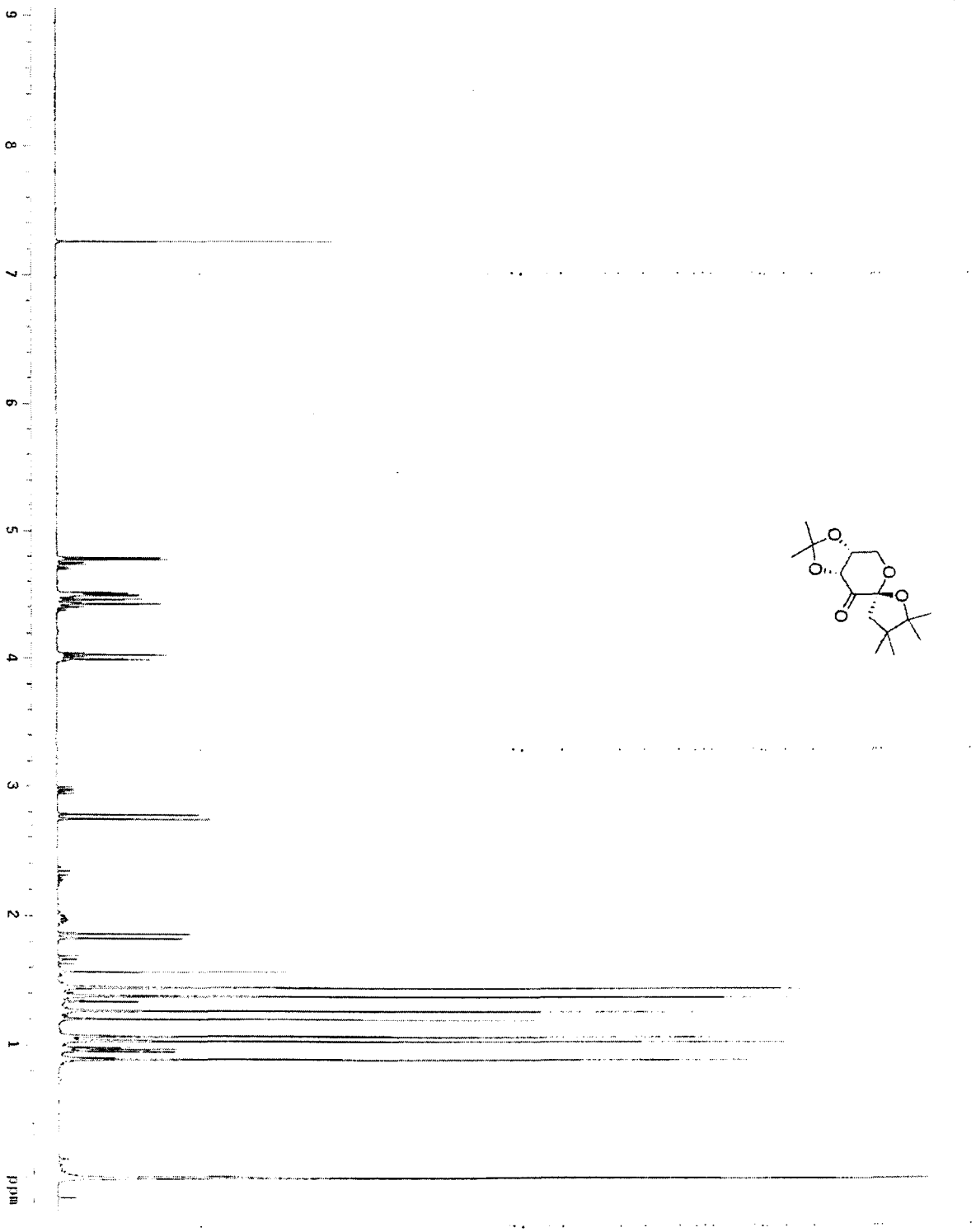

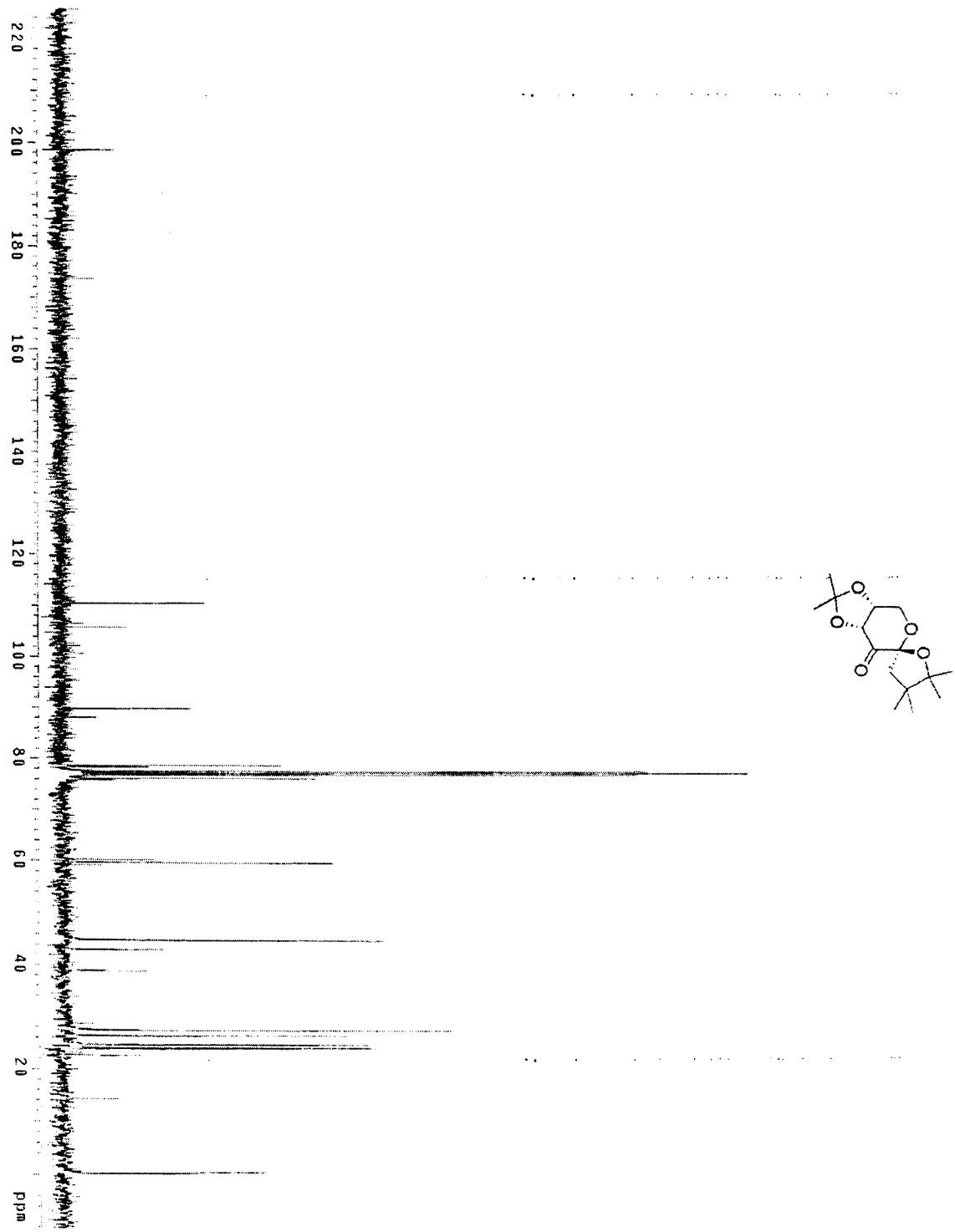

Tue Dec 27 10:26:14 2005
FIND PEAKS:

Spectrum: DLG-XIV-29
Region: 4000.00 400.00
Absolute threshold: 95.842
Sensitivity: 50
Peak list:

Position:	989.94	Intensity:	61.456
Position:	1098.61	Intensity:	71.886
Position:	1225.57	Intensity:	80.297
Position:	1748.96	Intensity:	83.756
Position:	1163.96	Intensity:	85.702
Position:	1121.02	Intensity:	85.622
Position:	1380.84	Intensity:	86.136
Position:	1371.27	Intensity:	87.129

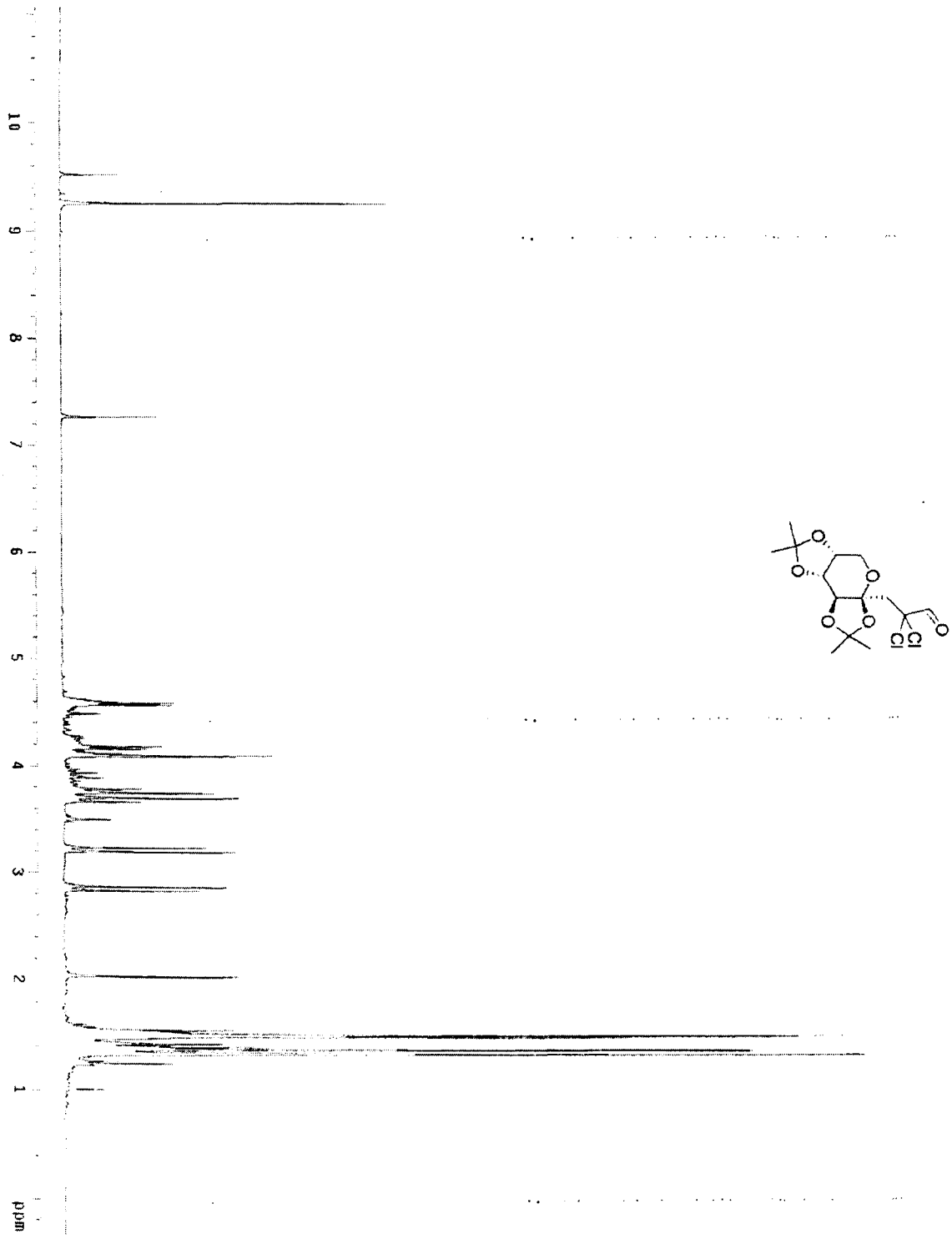

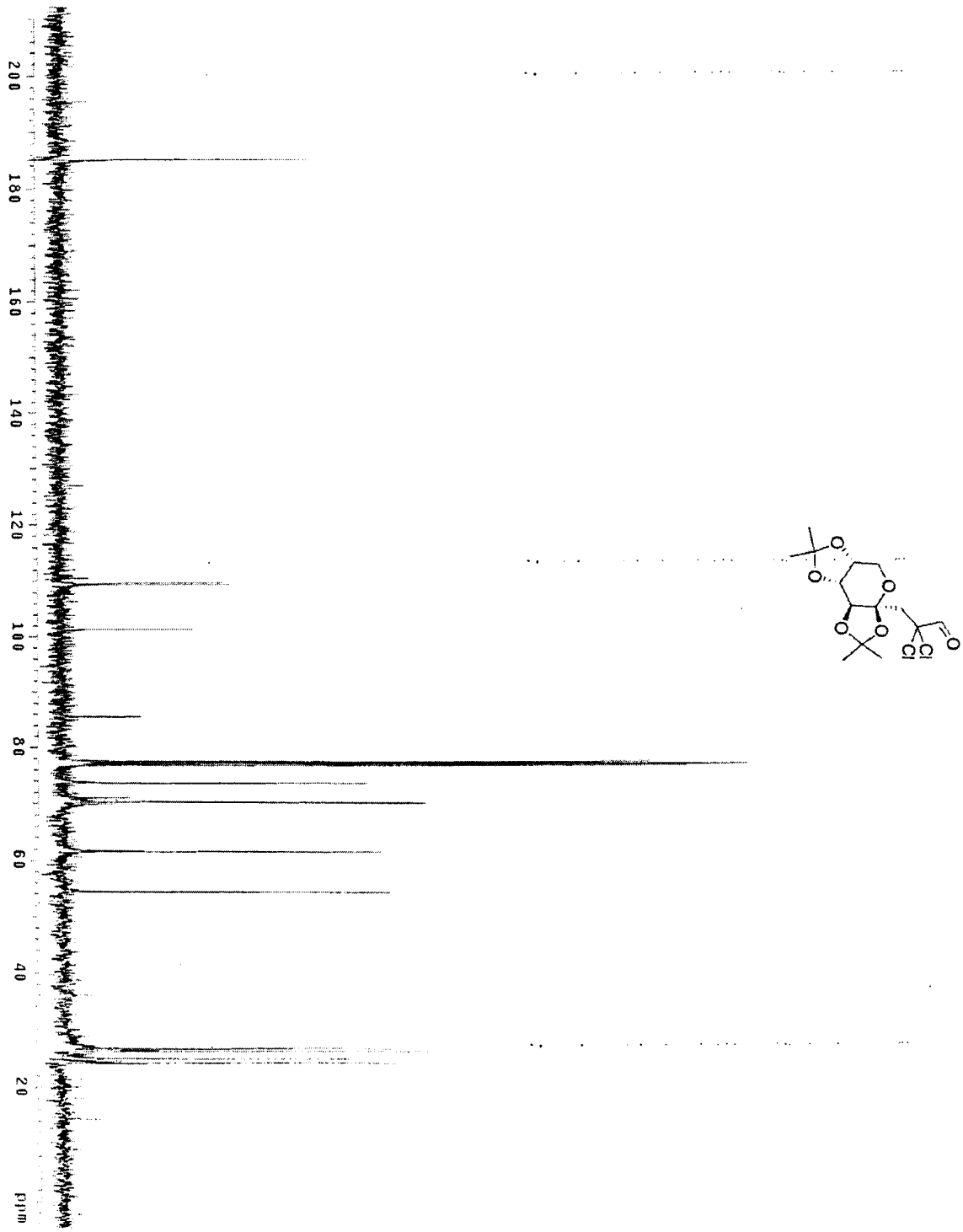

Wed Oct 19 16:25:58 2005
FIND PEAKS:
Spectrum: DLG-XV-48
Region: 4000.00 400.00
Absolute threshold: 78.055
Sensitivity: 50
Peak list:

Position:	1071.26	Intensity:	40.670
Position:	1211.92	Intensity:	48.552
Position:	1252.82	Intensity:	53.977
Position:	1102.93	Intensity:	54.154
Position:	1177.79	Intensity:	58.763
Position:	1383.03	Intensity:	62.349
Position:	1373.74	Intensity:	63.001
Position:	989.63	Intensity:	68.143

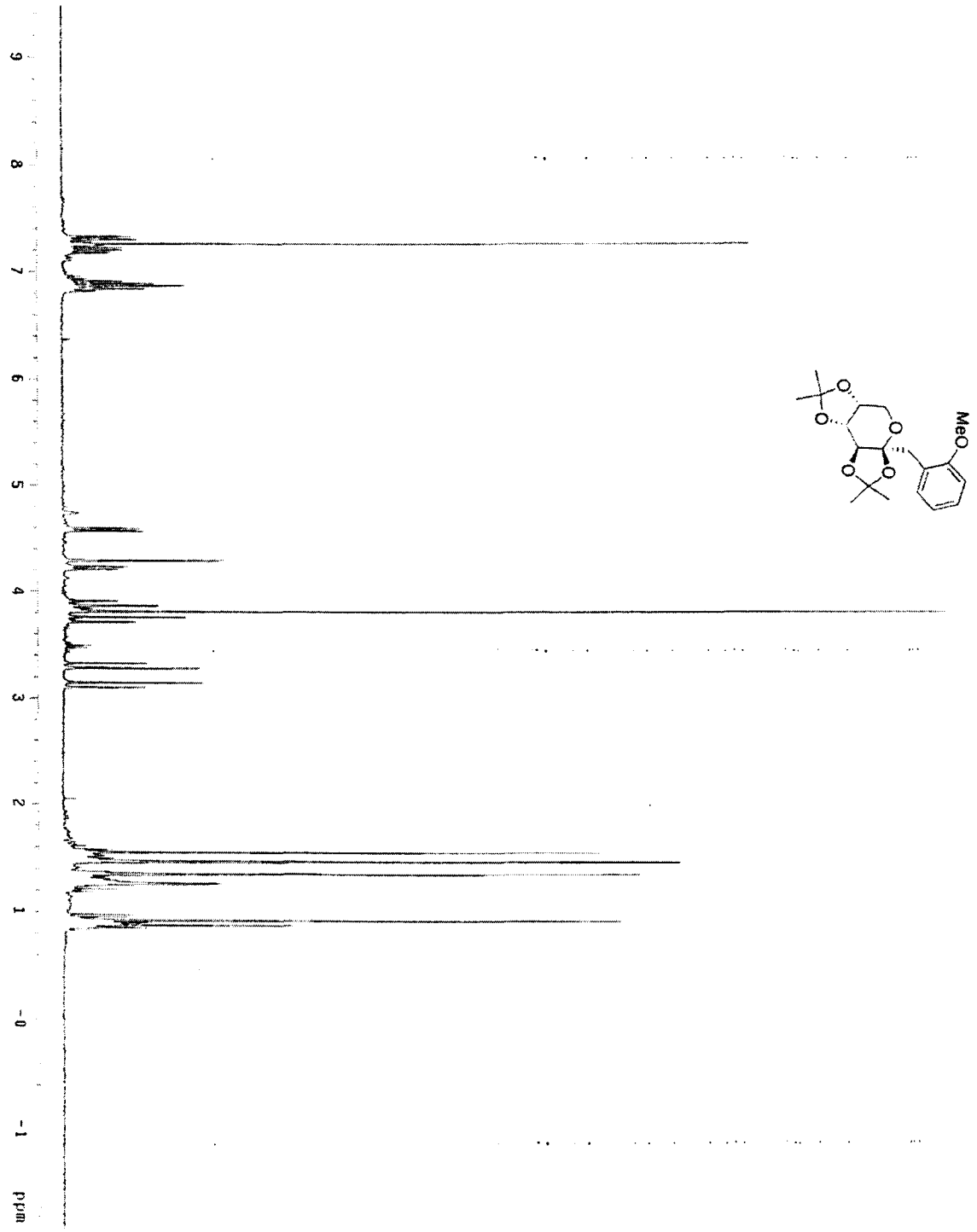

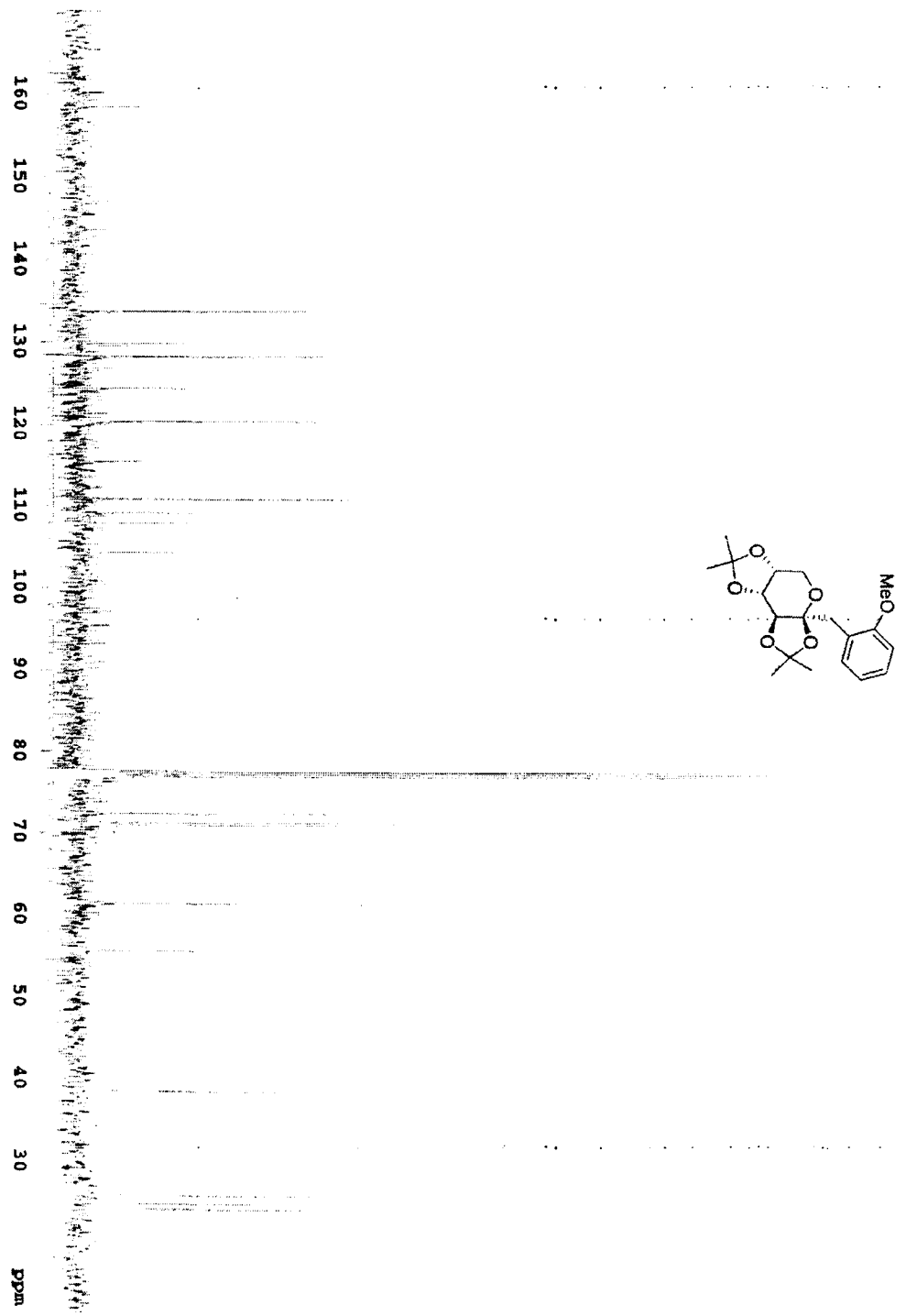

Fri Dec 30 09:52:07 2005
FIND PEAKS:

Spectrum: DLG-XV-19
Region: 4000.00 400.00
Absolute threshold: 48.995
Sensitivity: 50
Peak list:

Position:	1250.15	Intensity:	8.953
Position:	1067.80	Intensity:	14.979
Position:	1211.24	Intensity:	17.761
Position:	1167.08	Intensity:	25.514
Position:	754.63	Intensity:	31.226
Position:	996.03	Intensity:	32.321
Position:	1104.46	Intensity:	32.449
Position:	1495.77	Intensity:	34.645

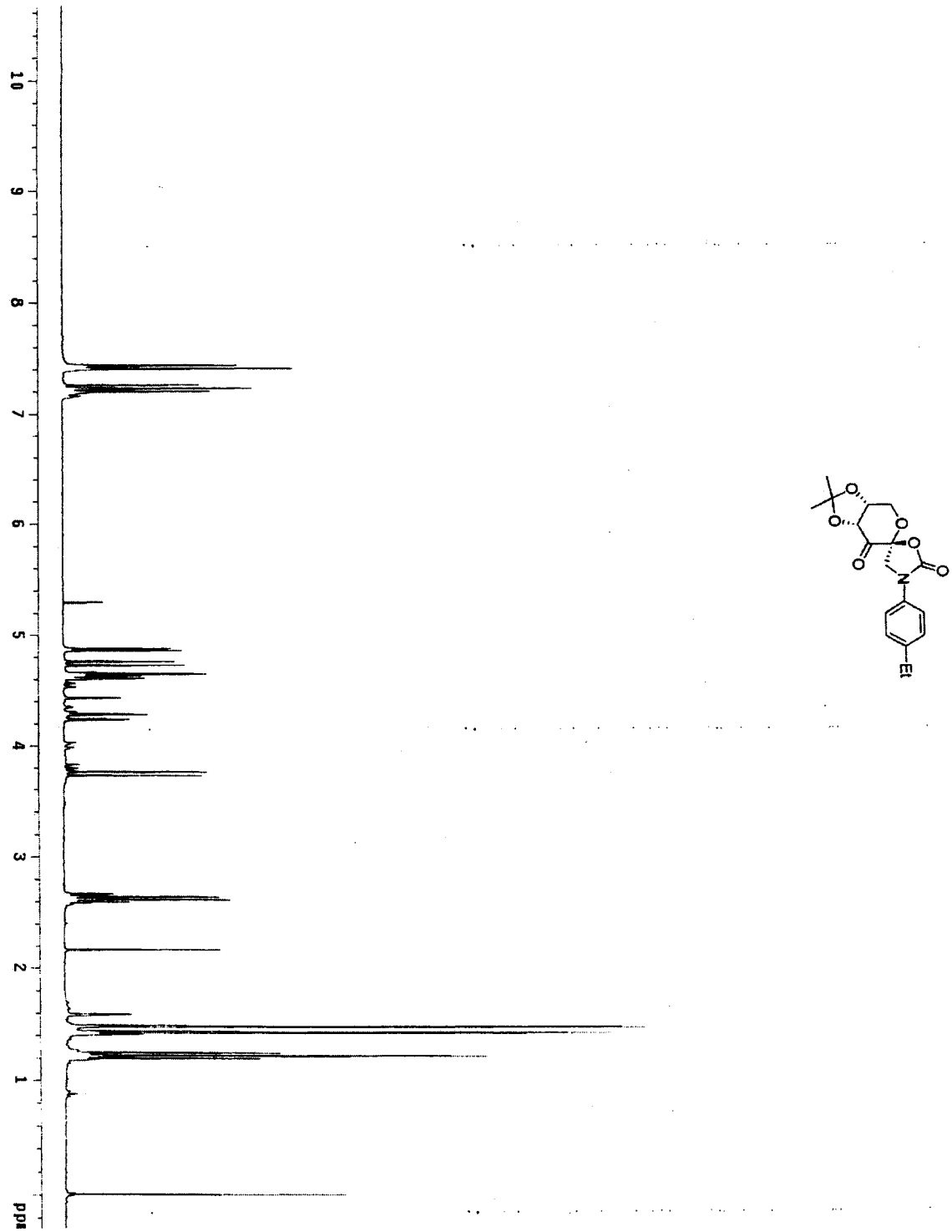

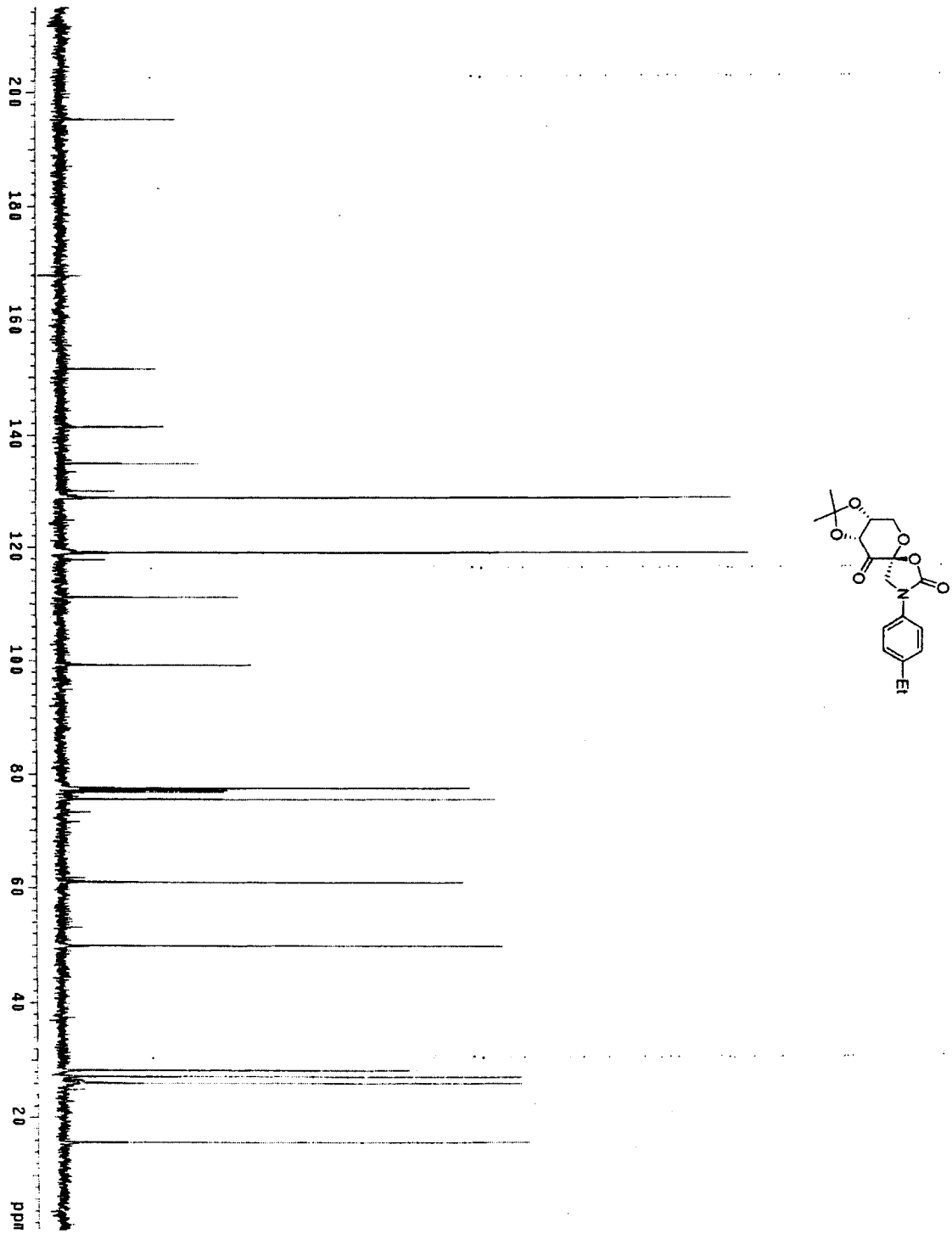

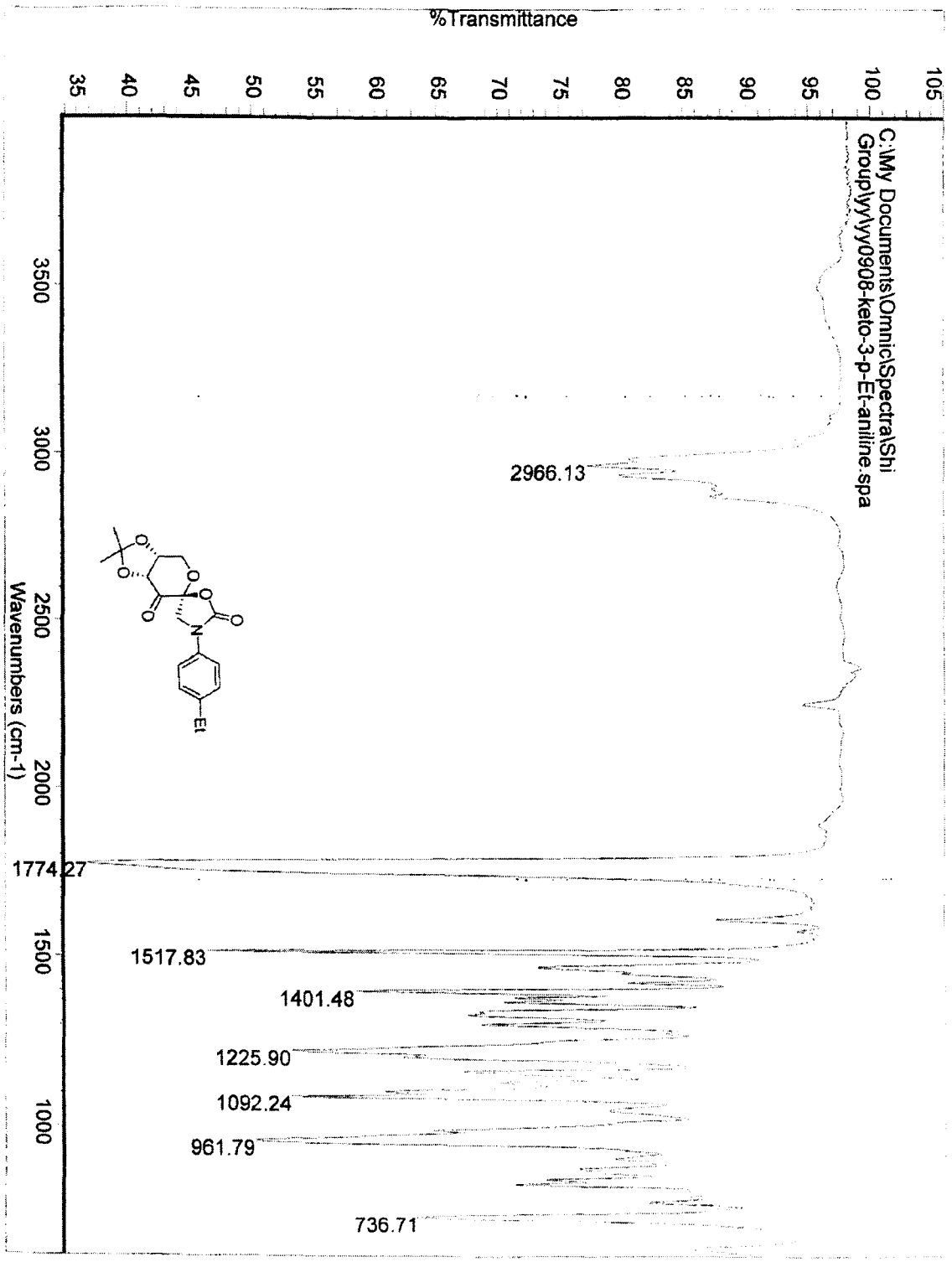

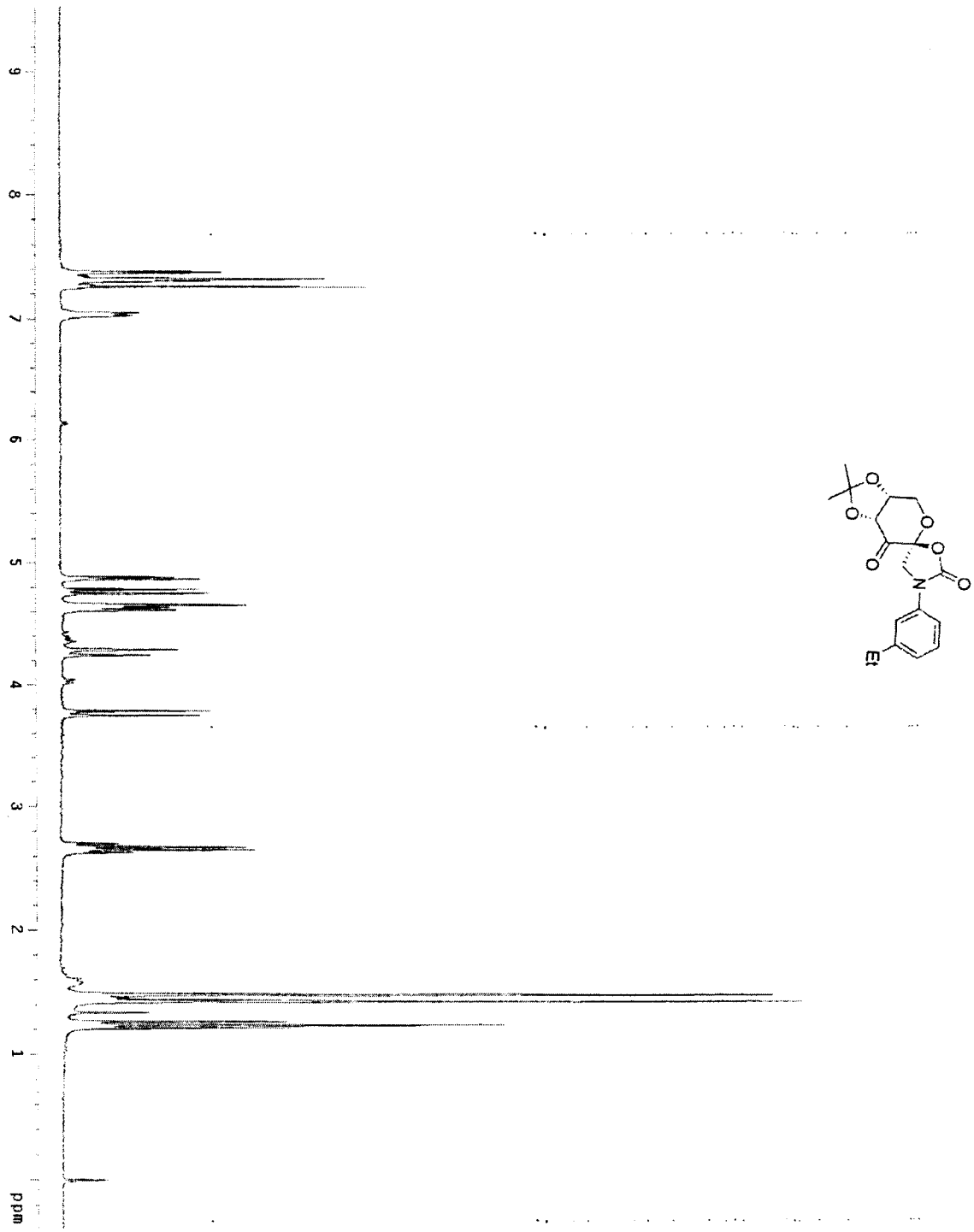

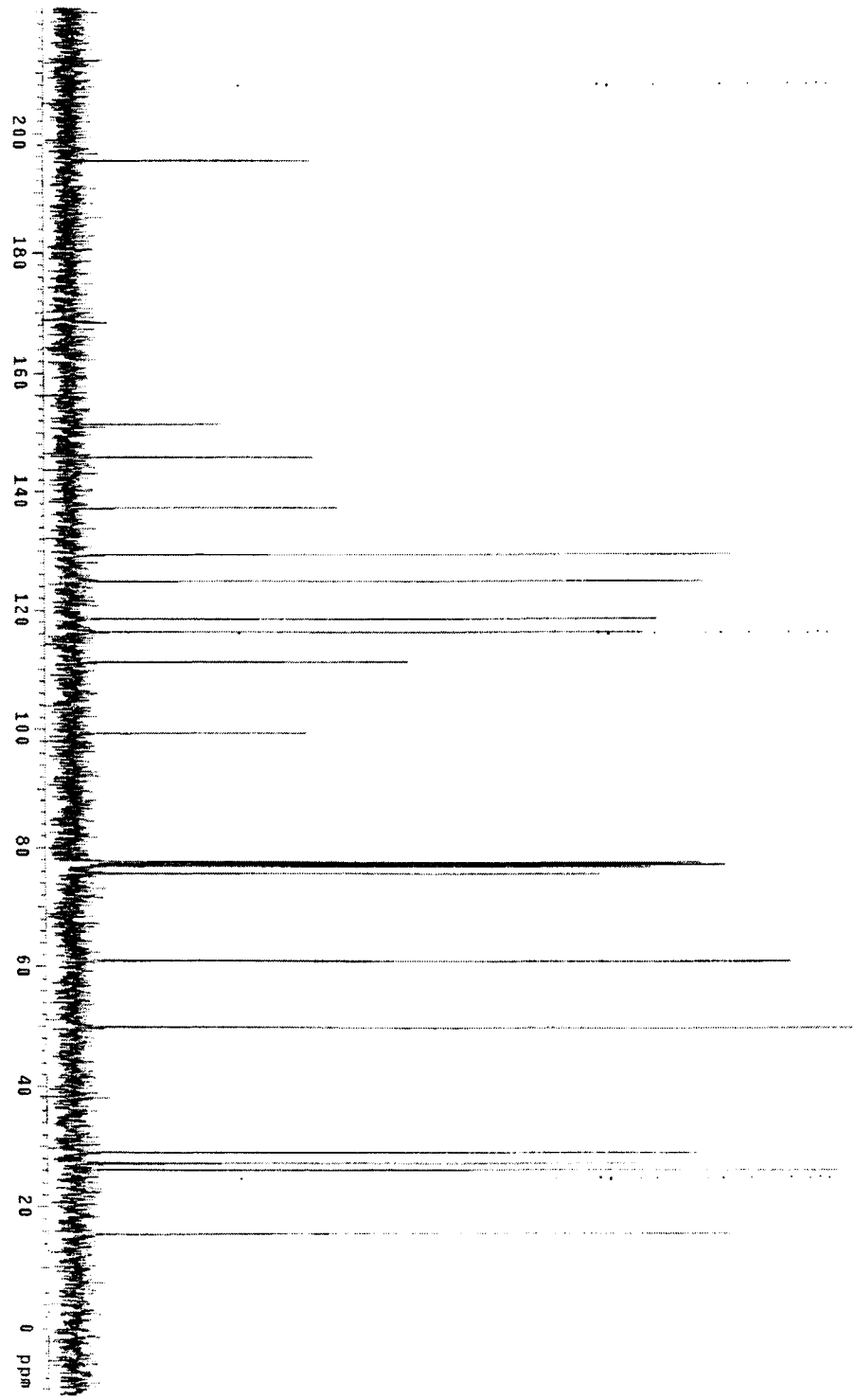

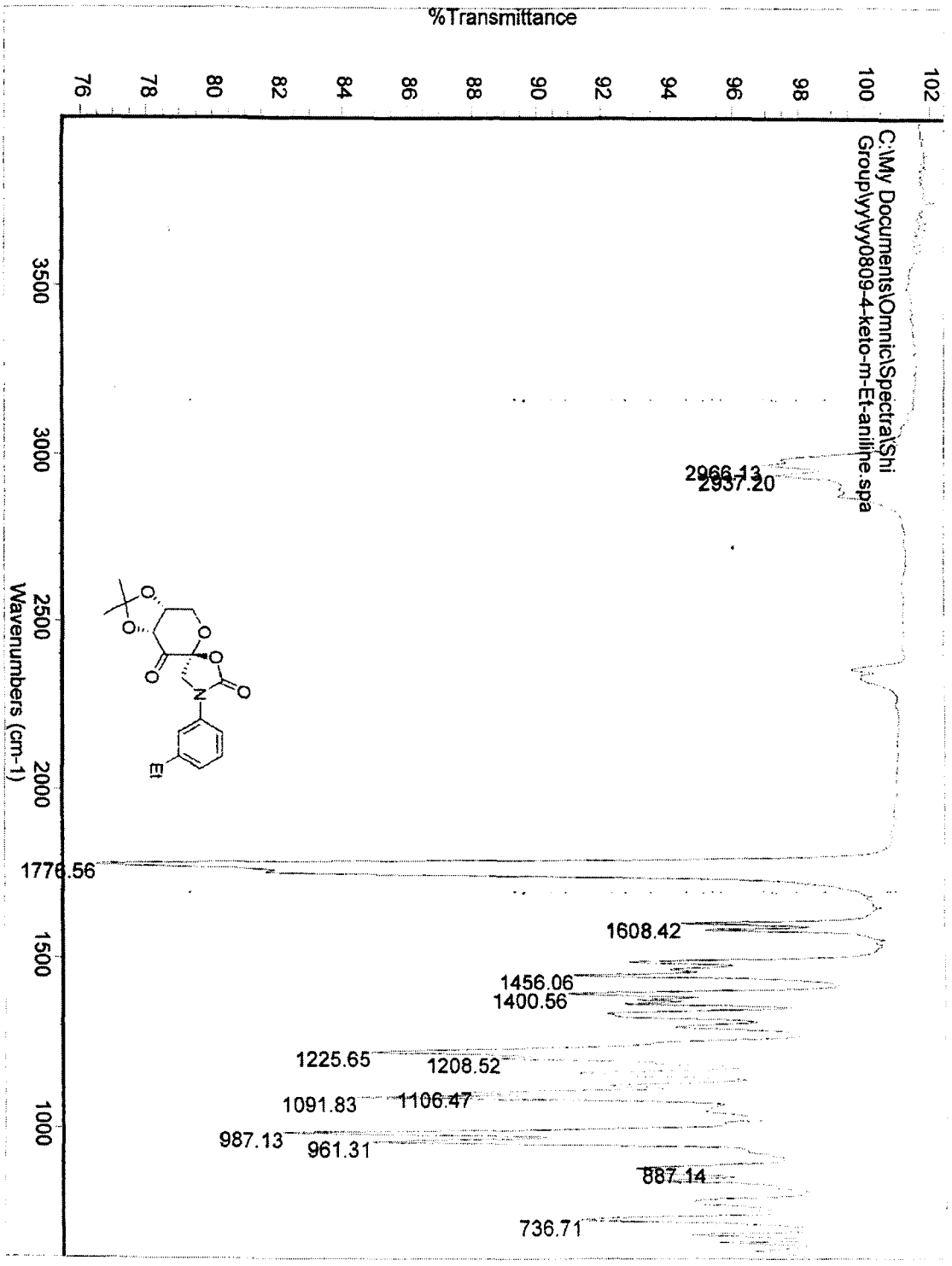

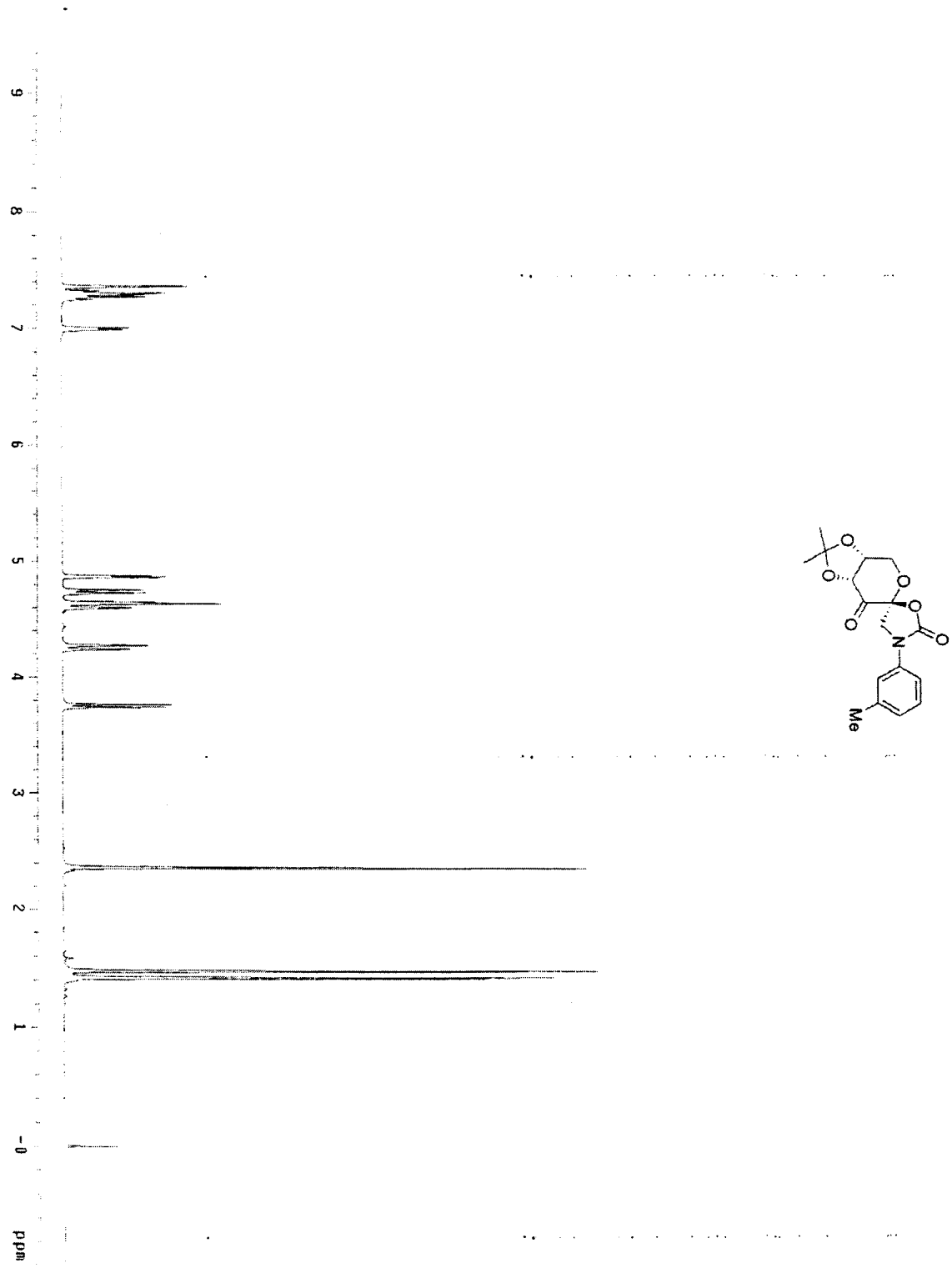

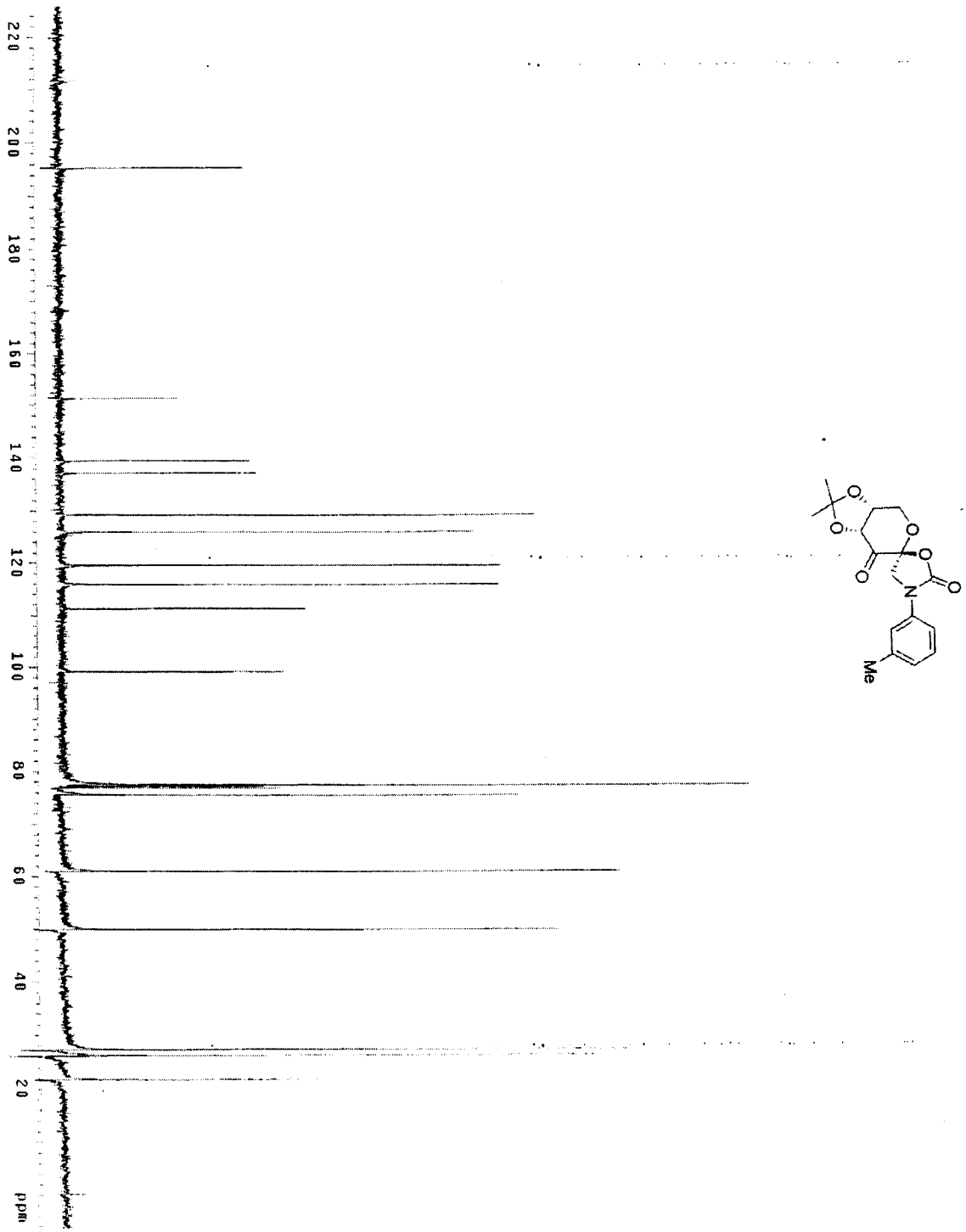

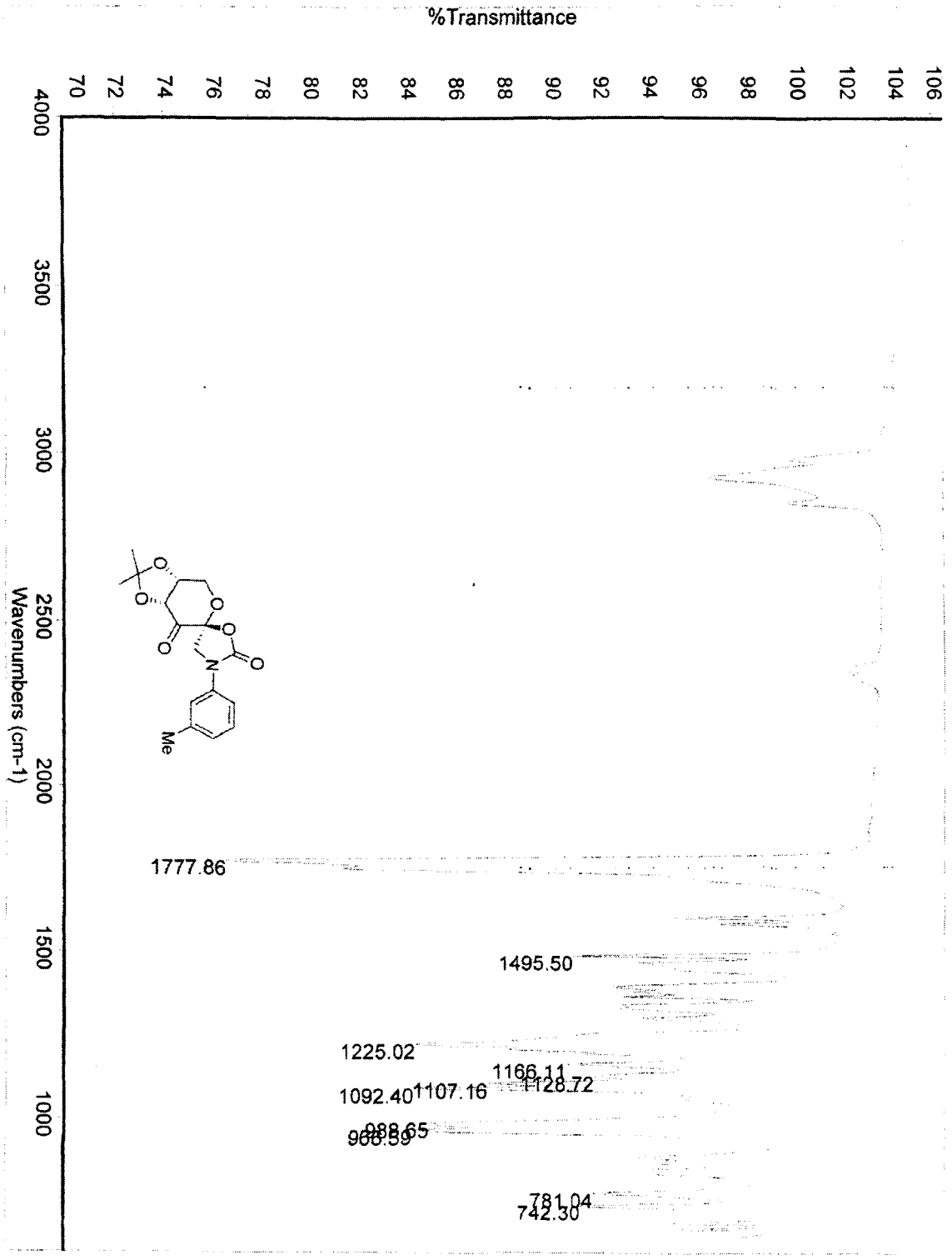

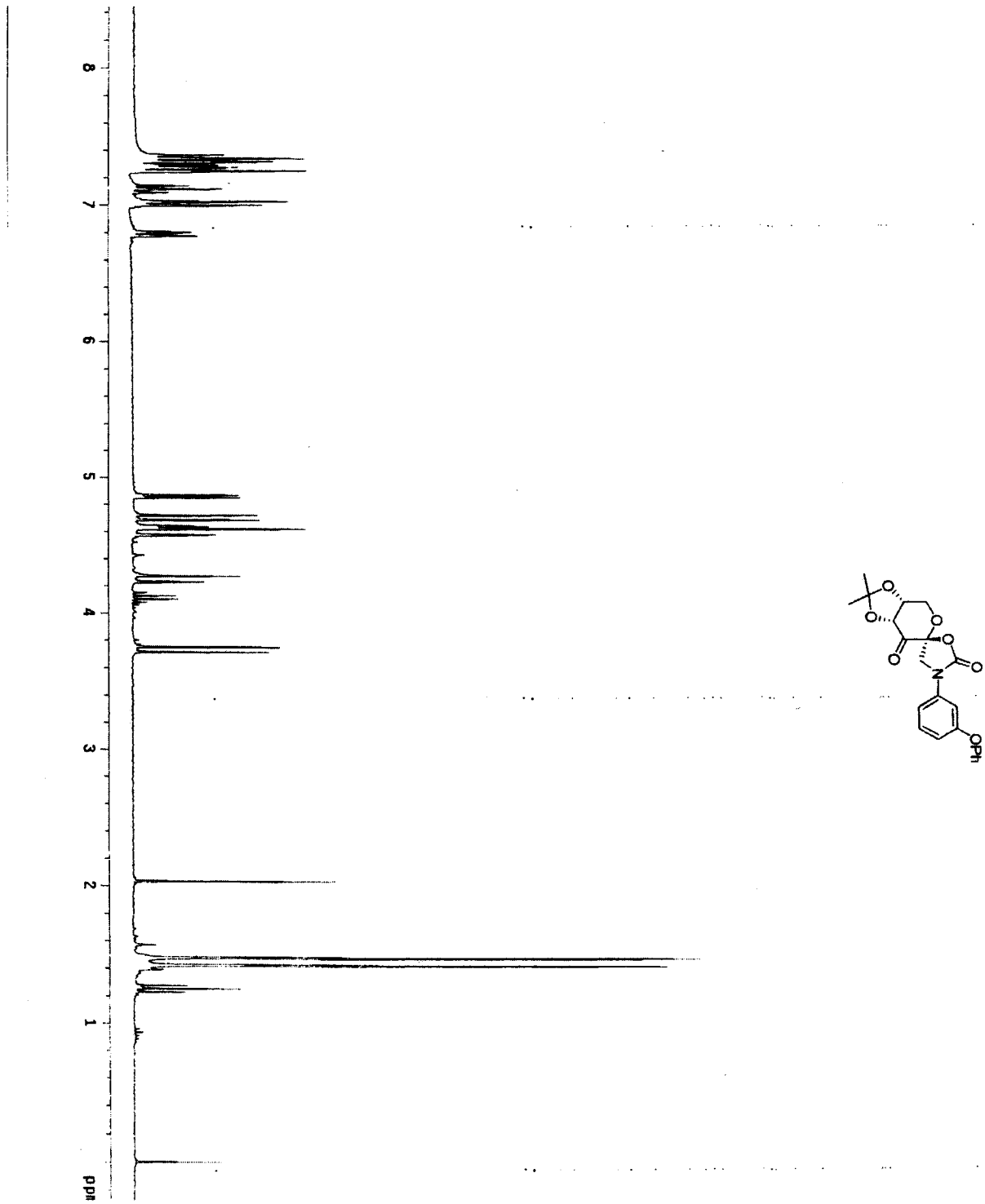

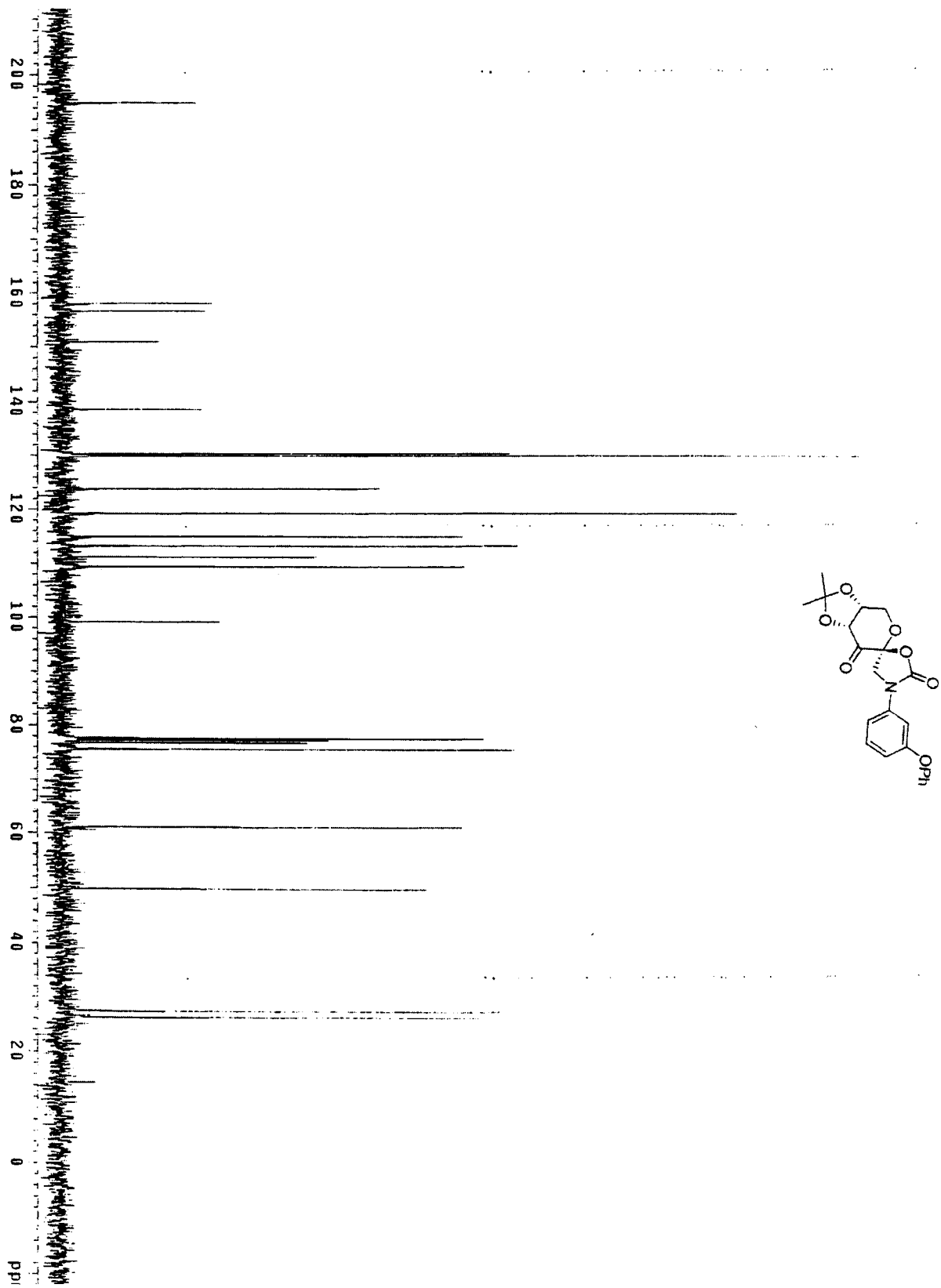

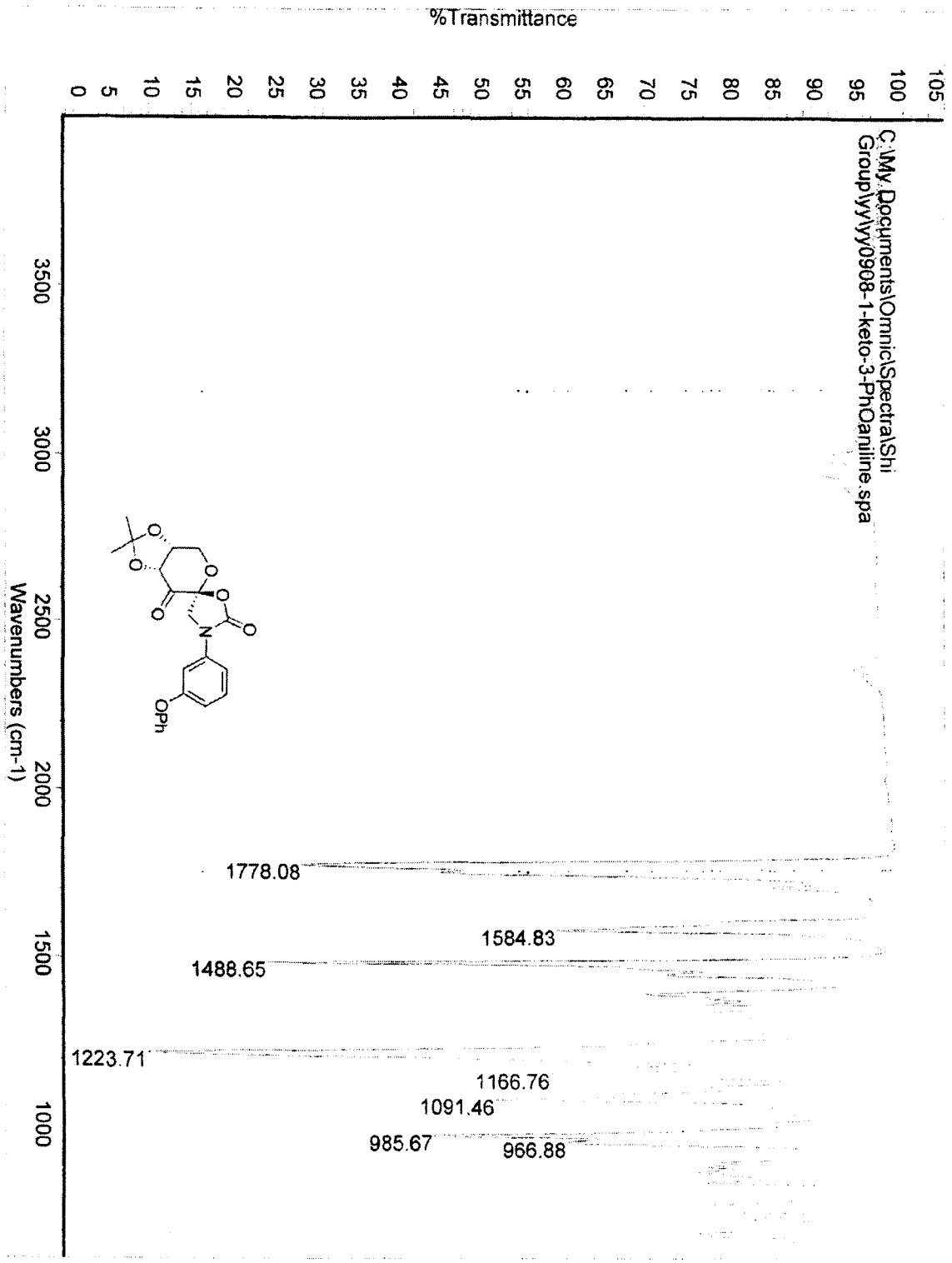

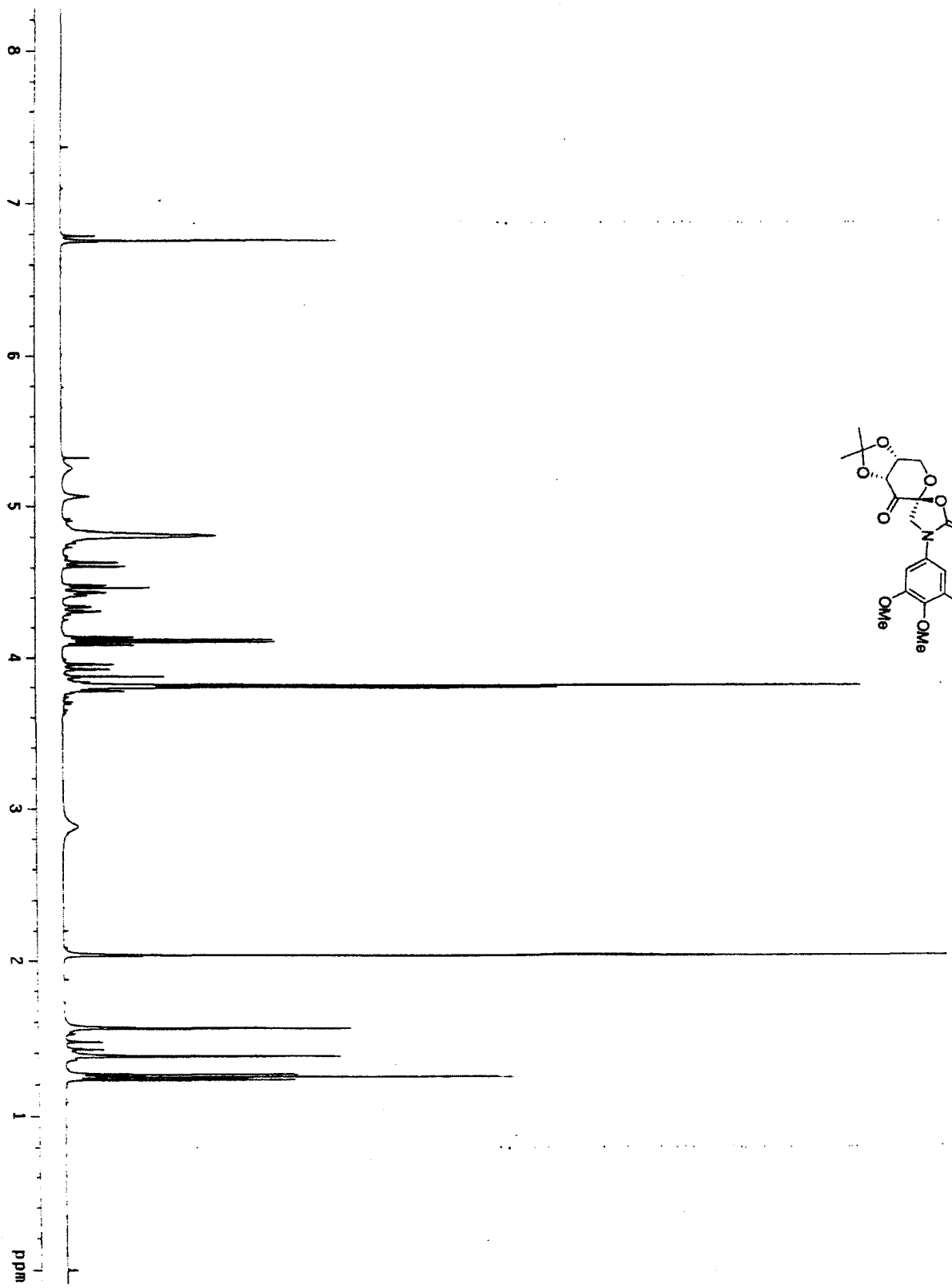

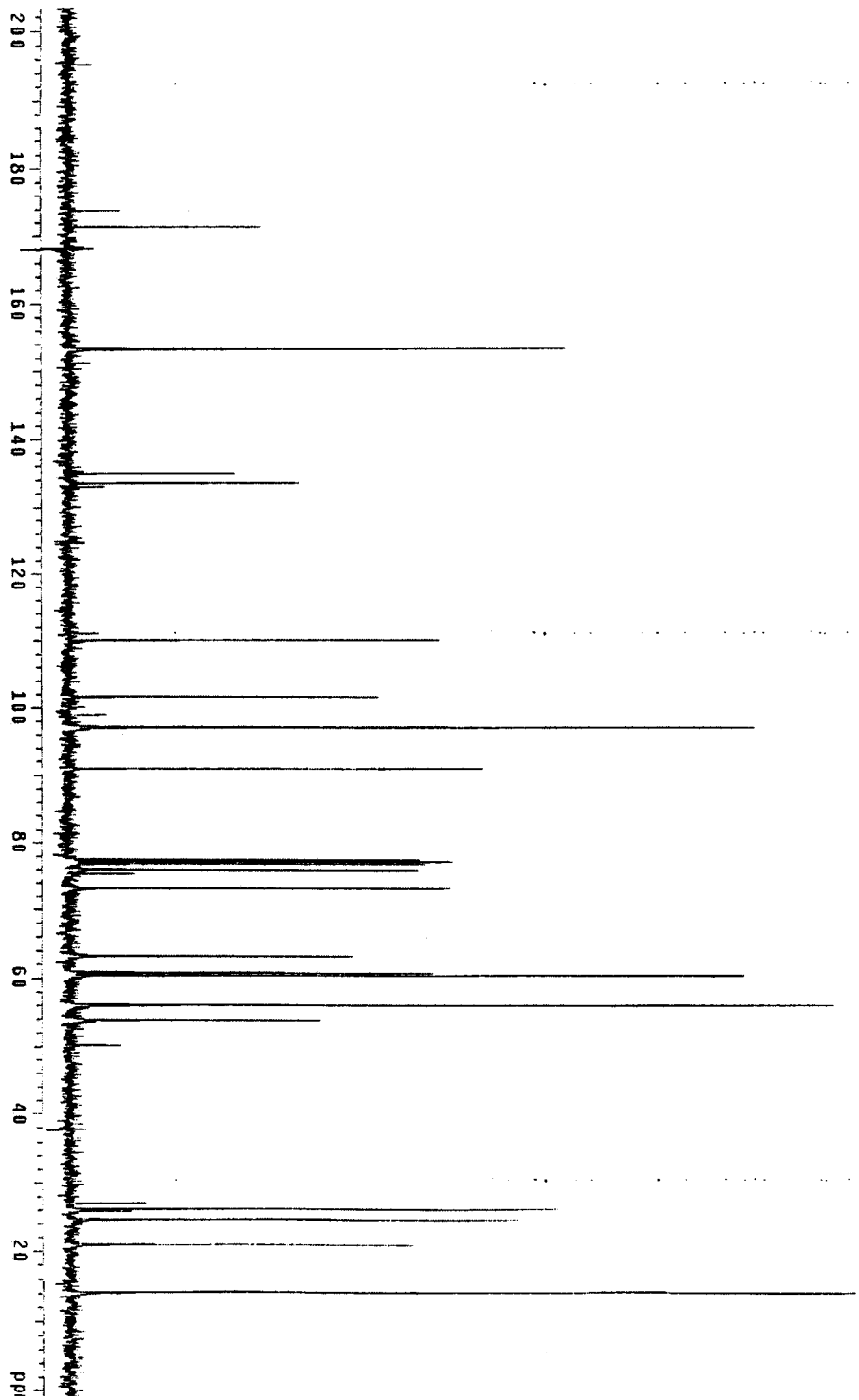

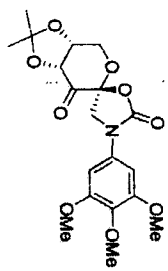

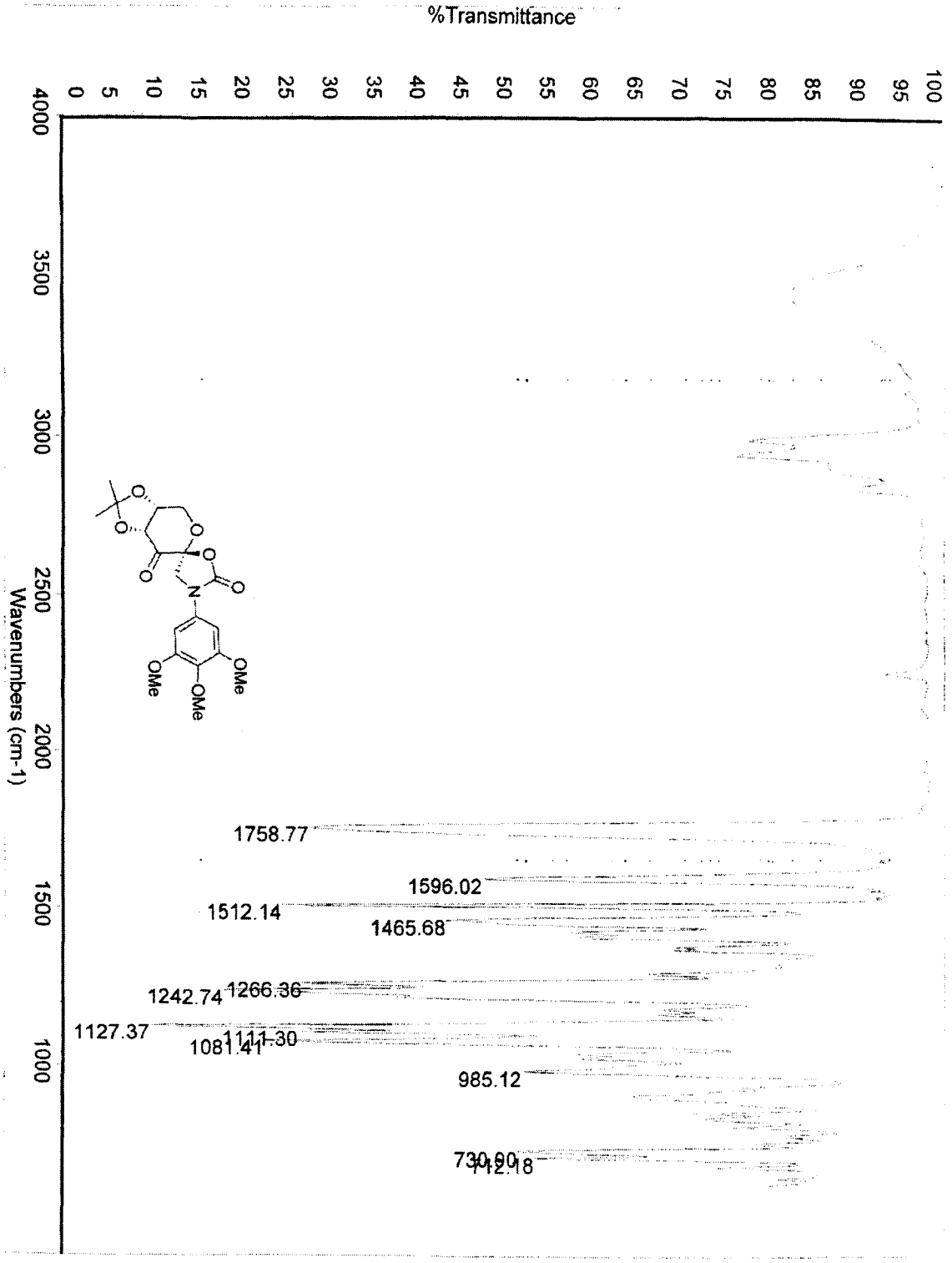

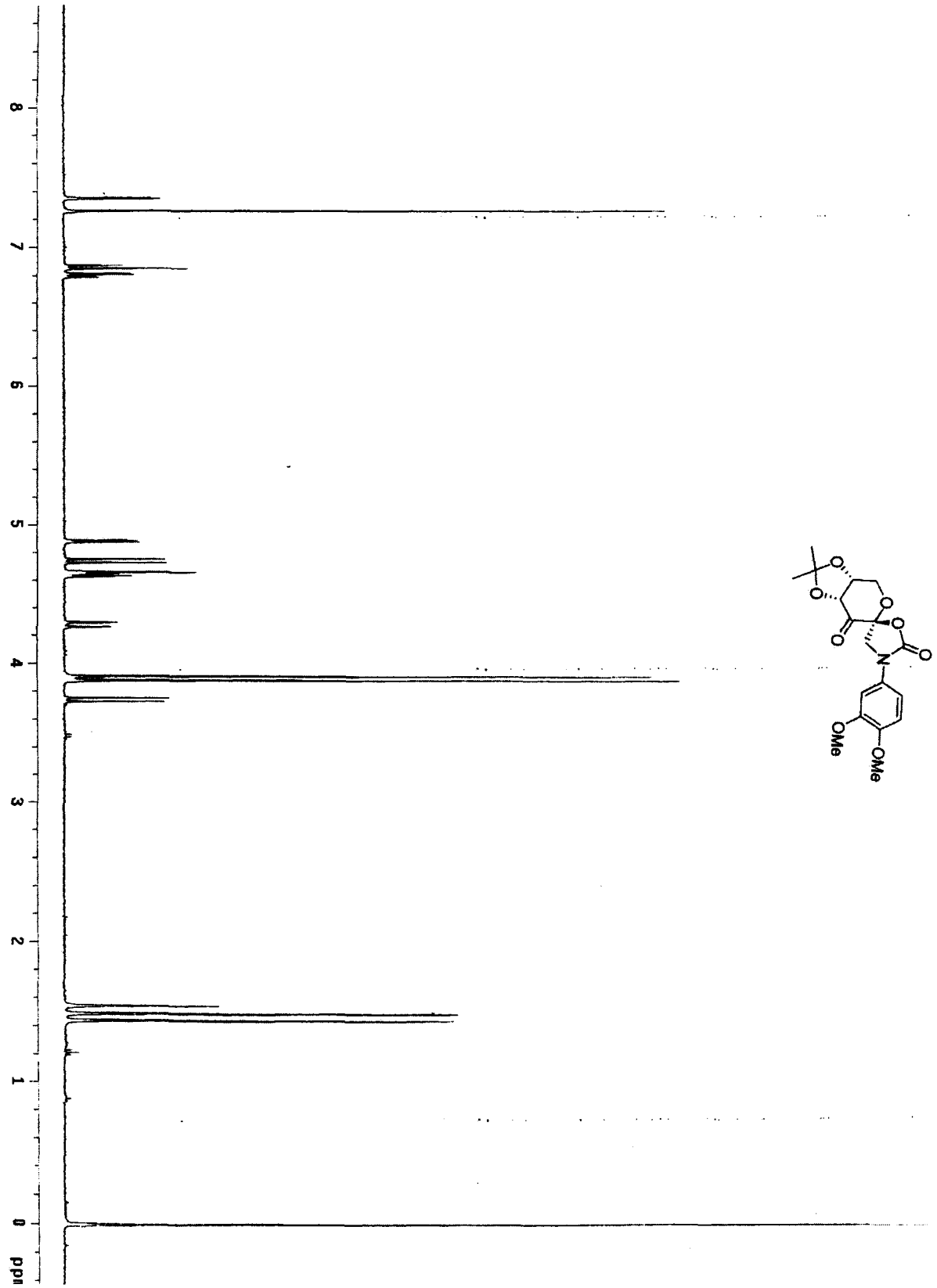

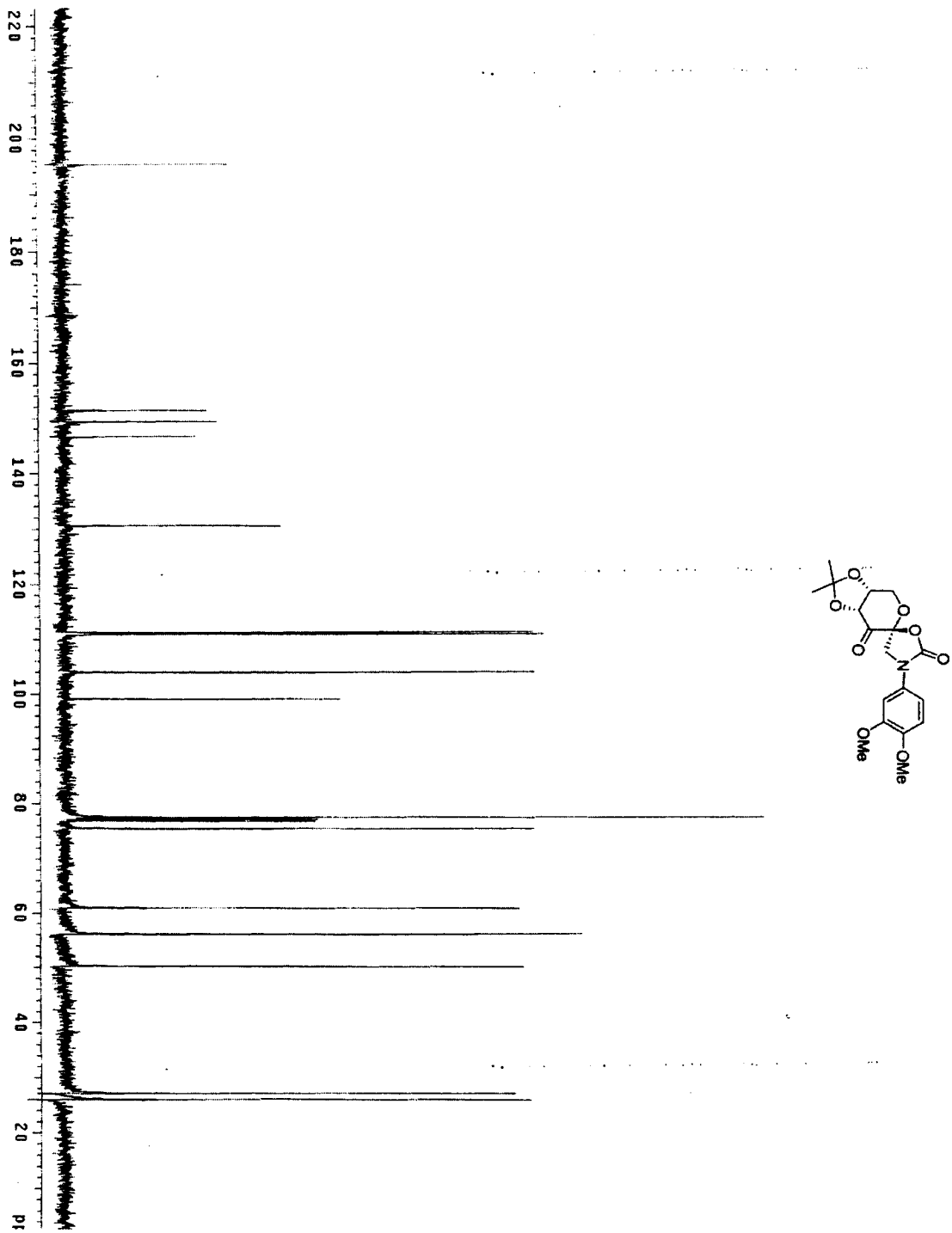

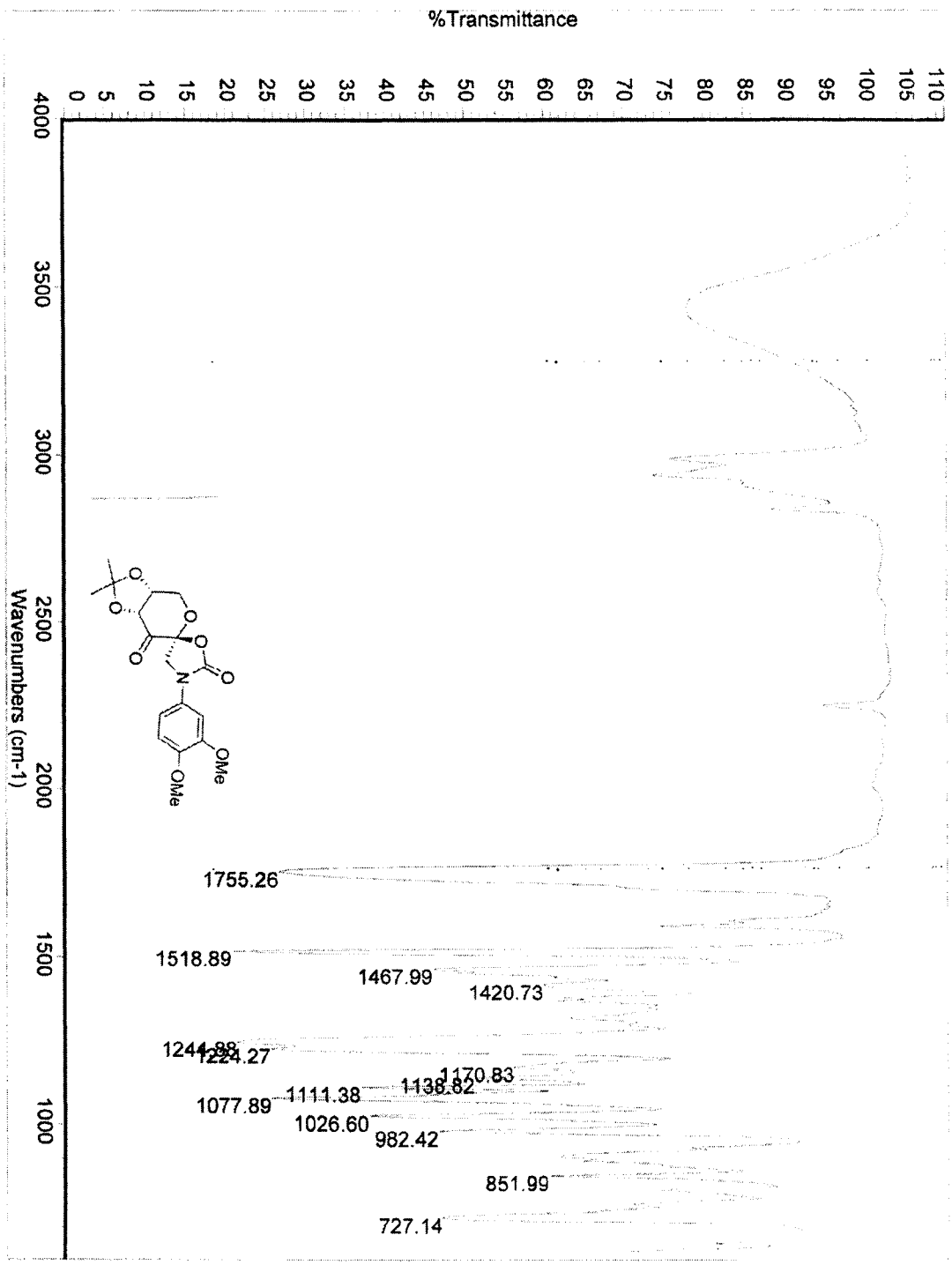

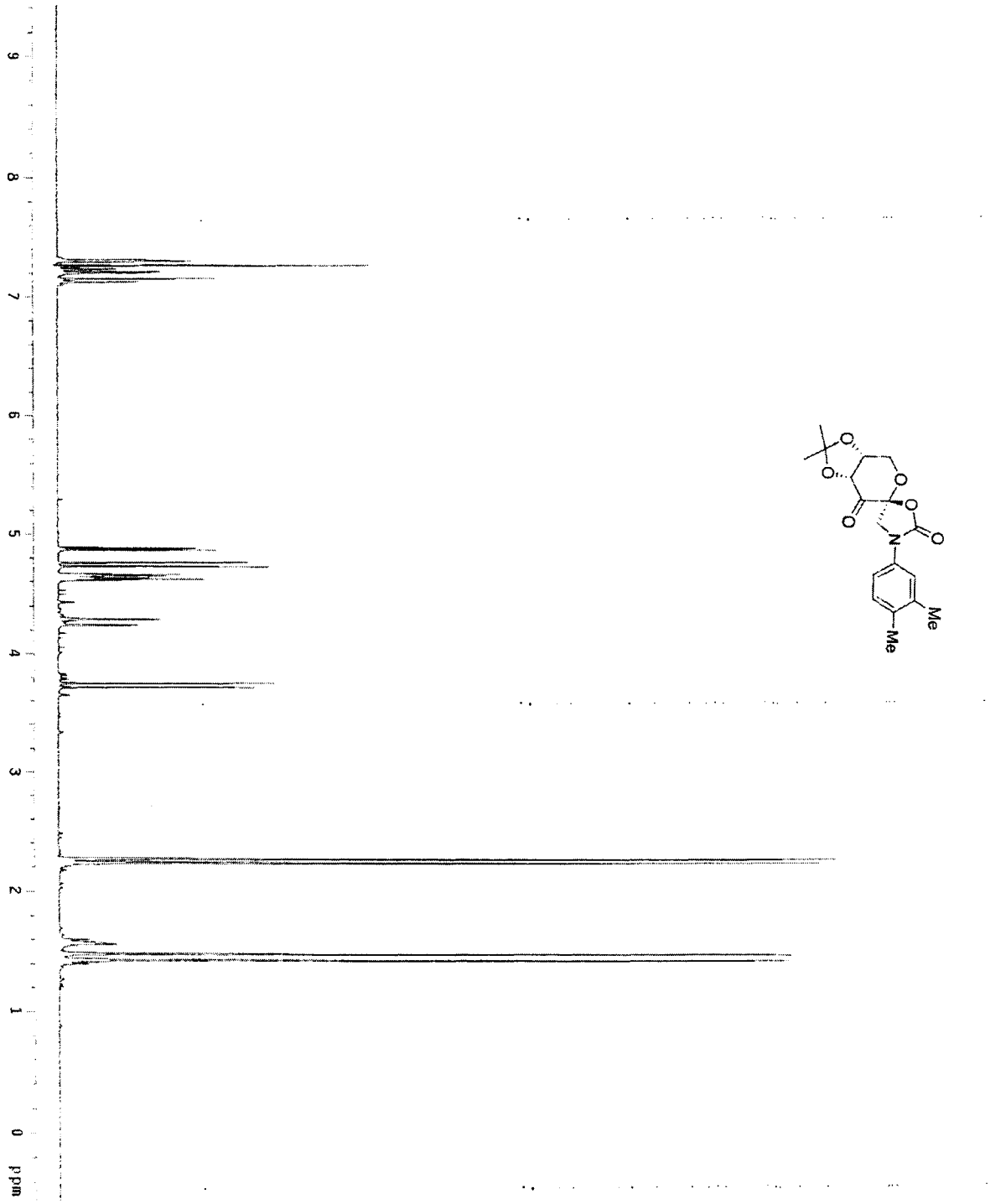

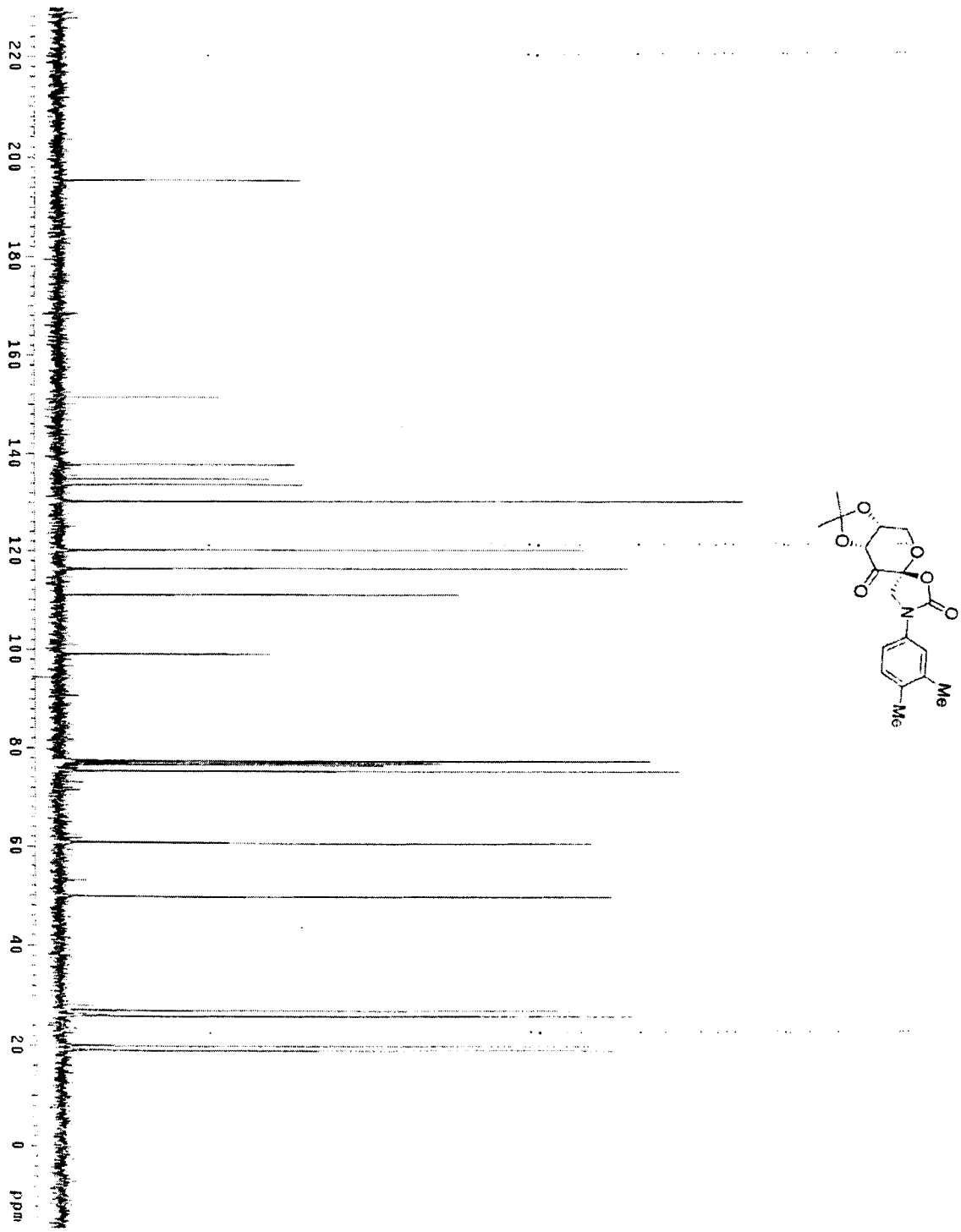

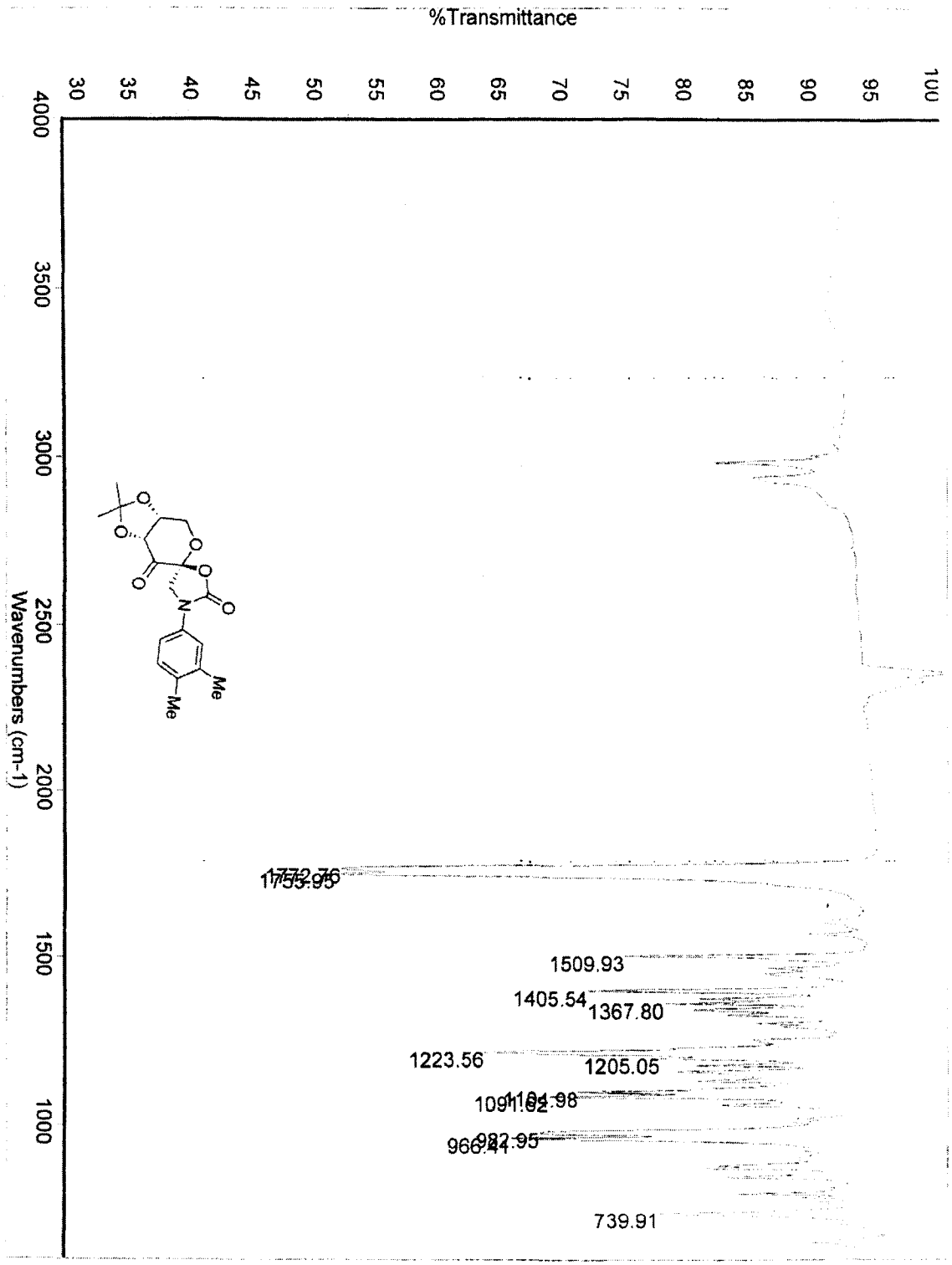

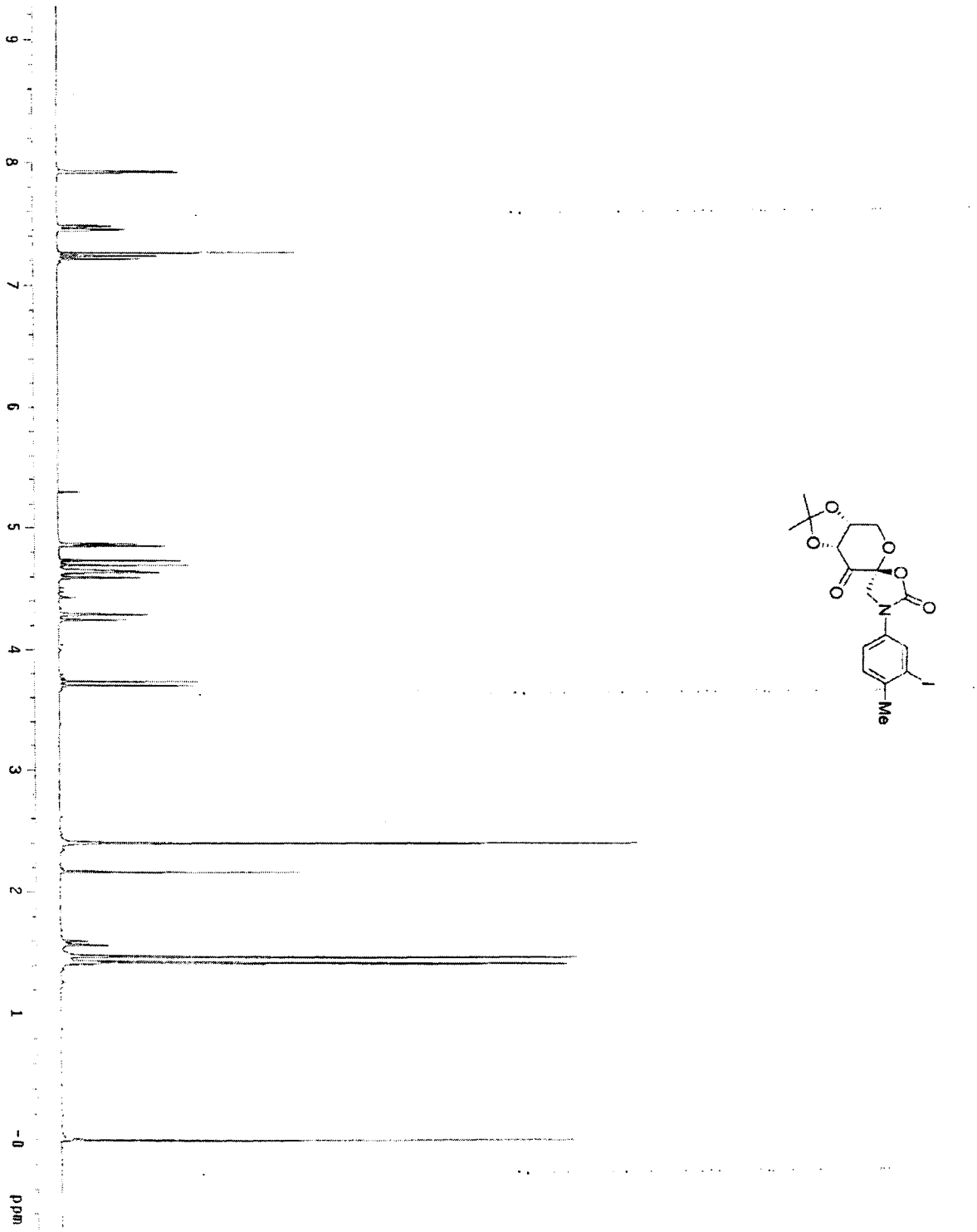

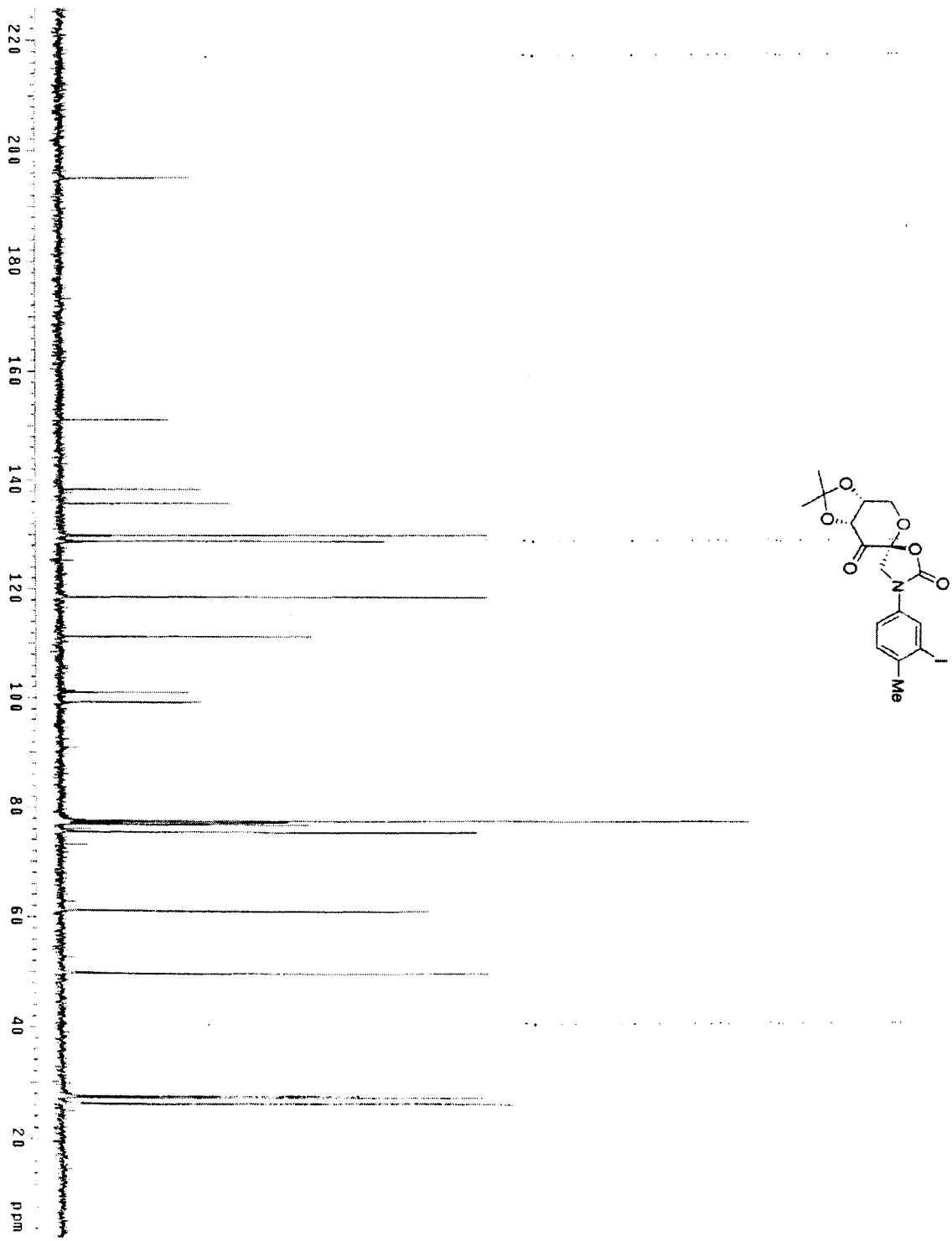

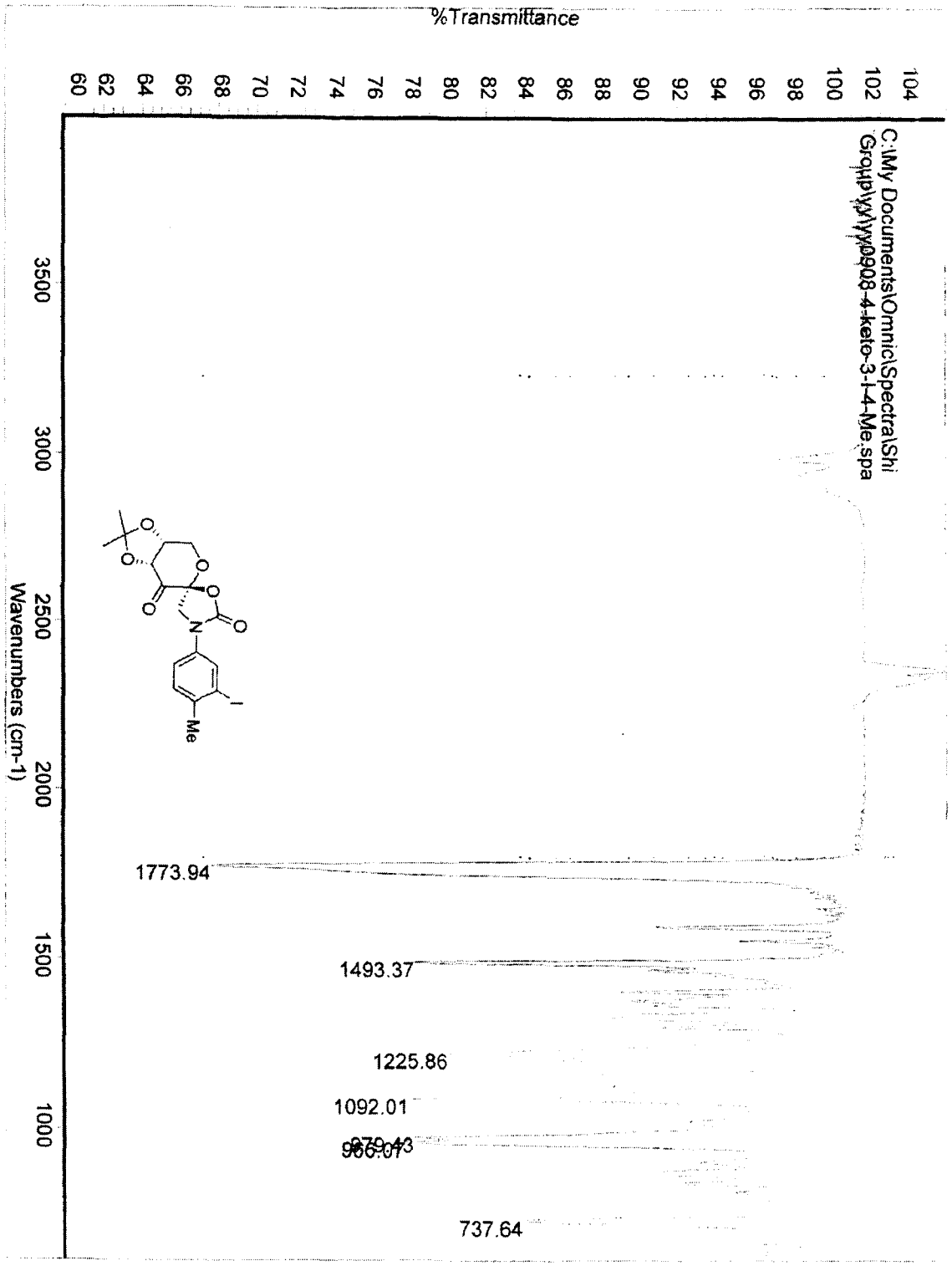

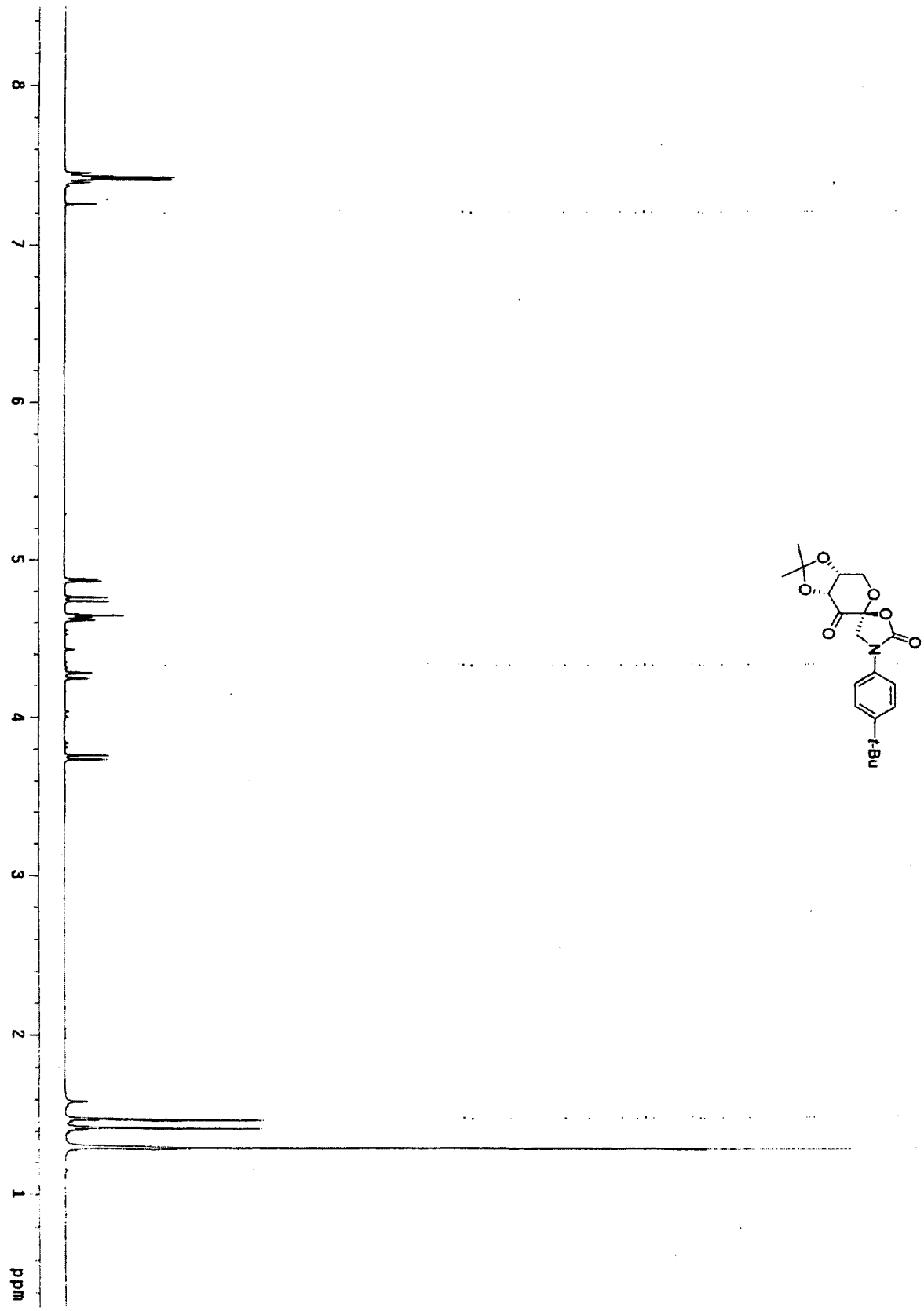

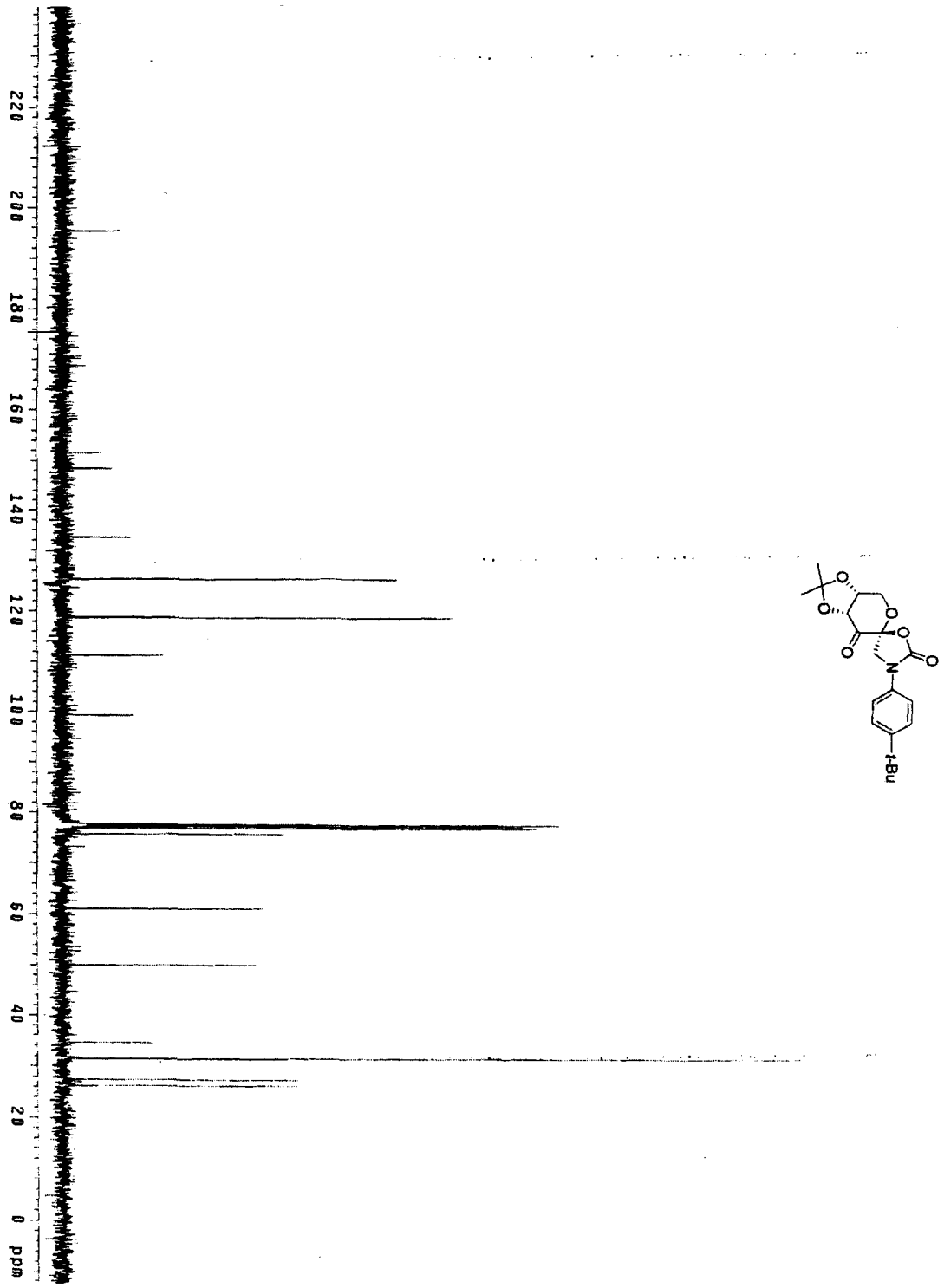

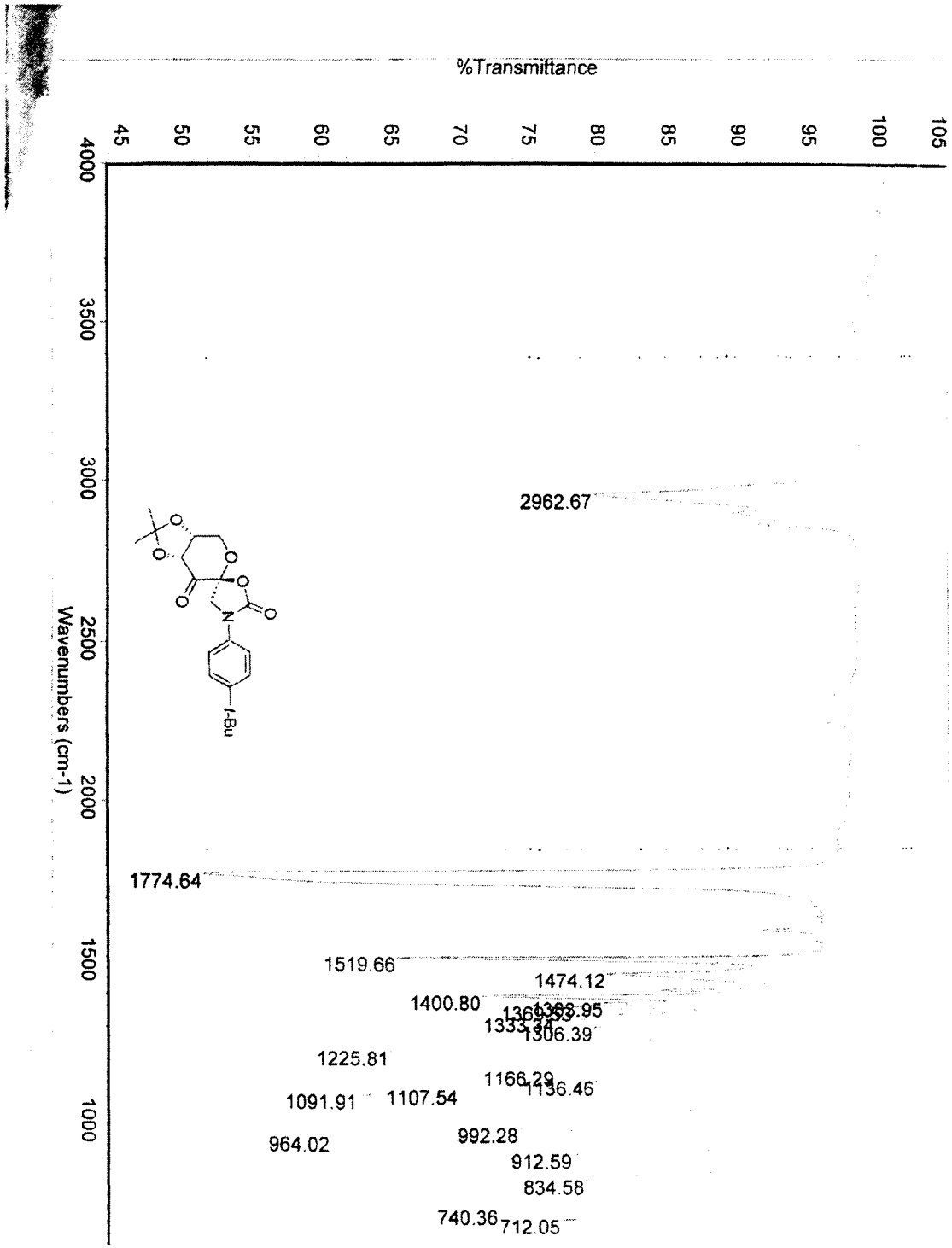

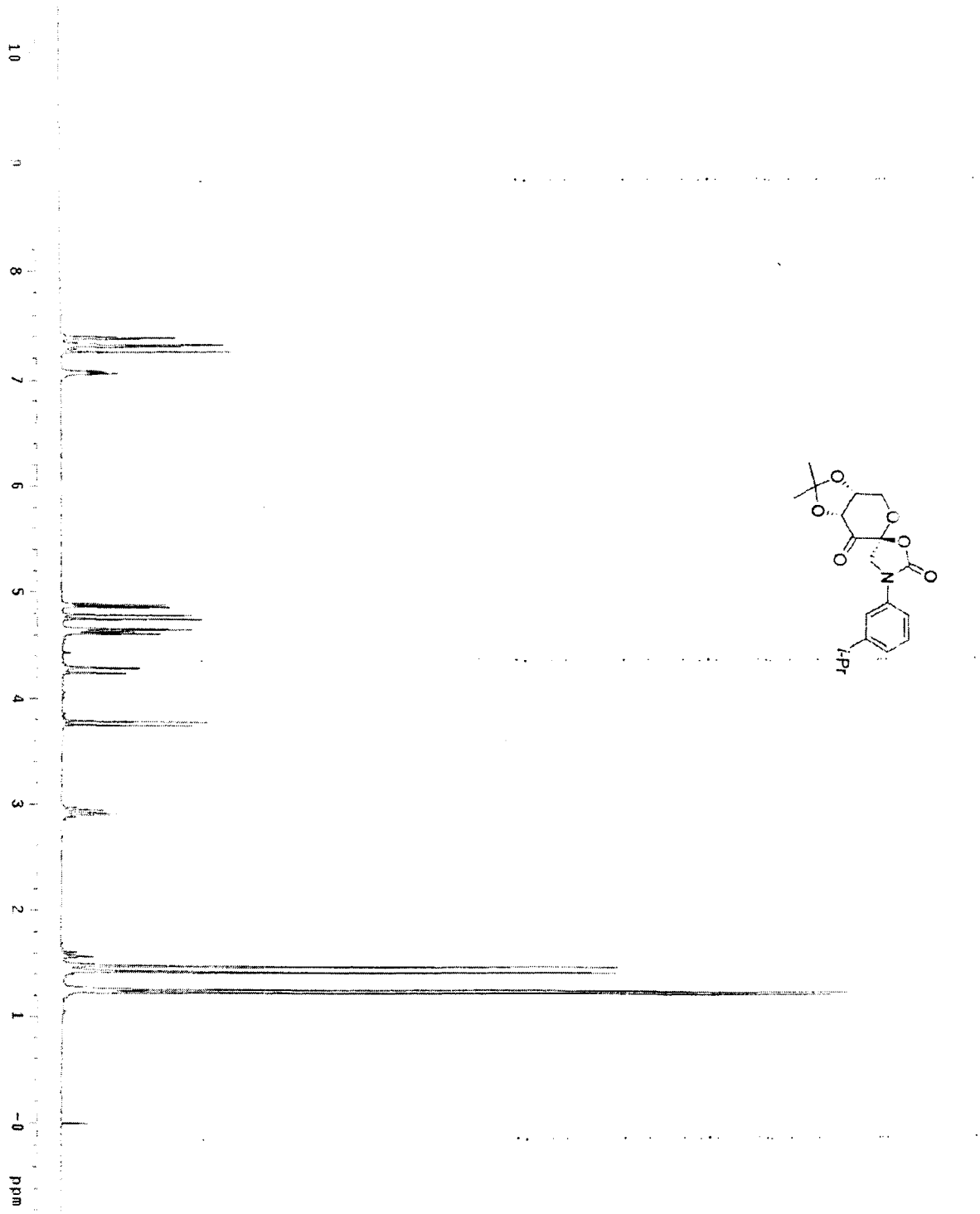

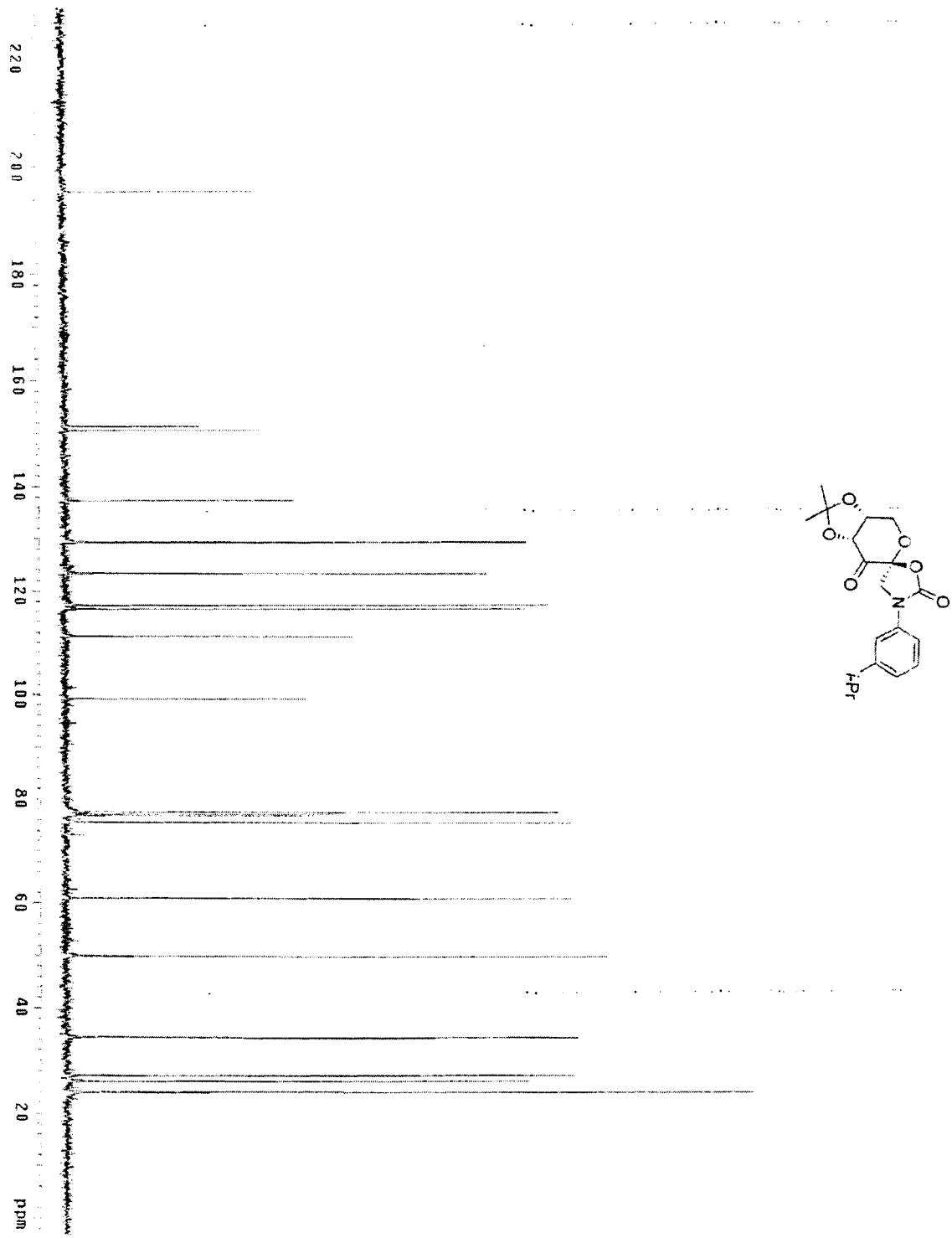

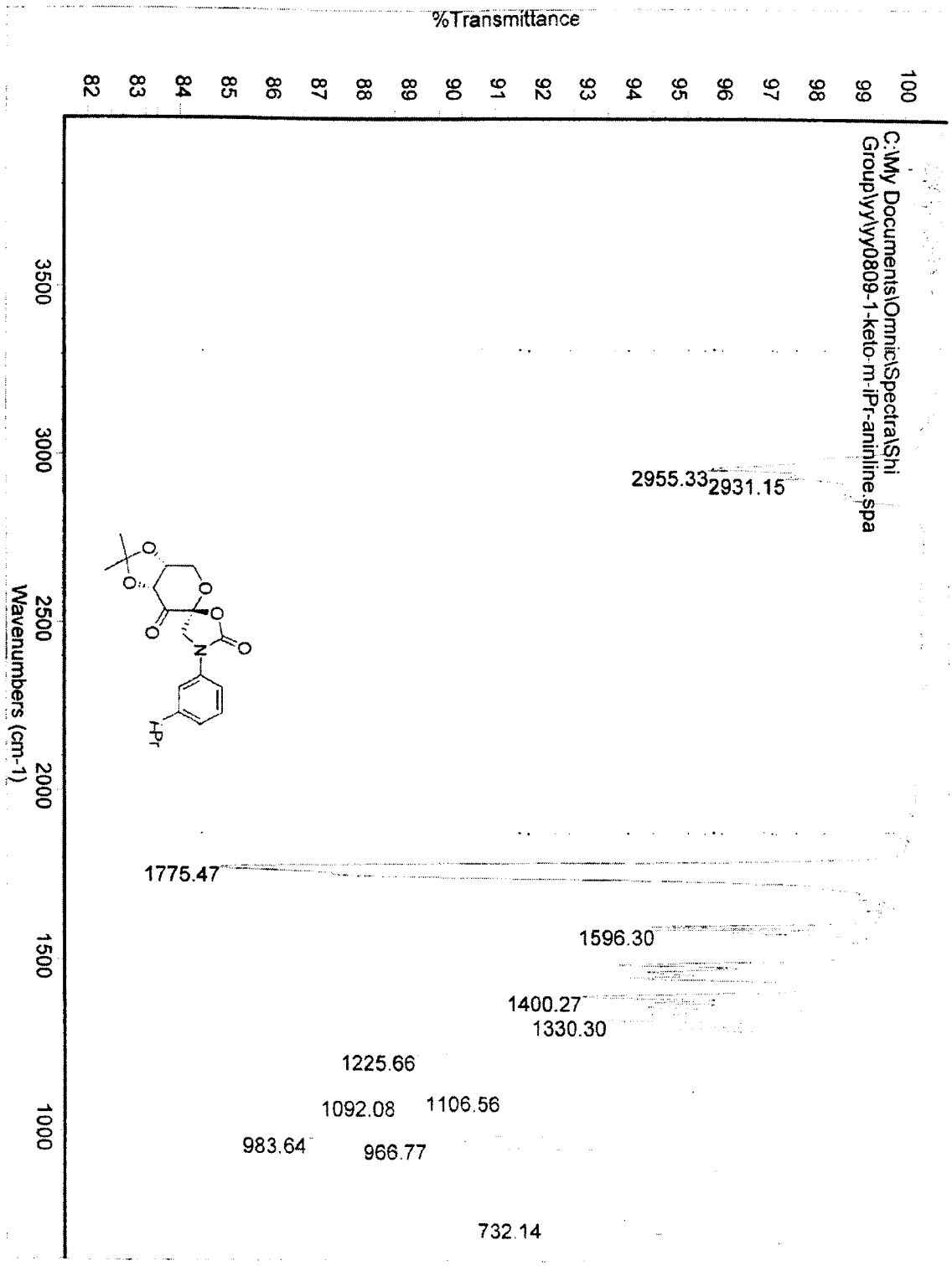

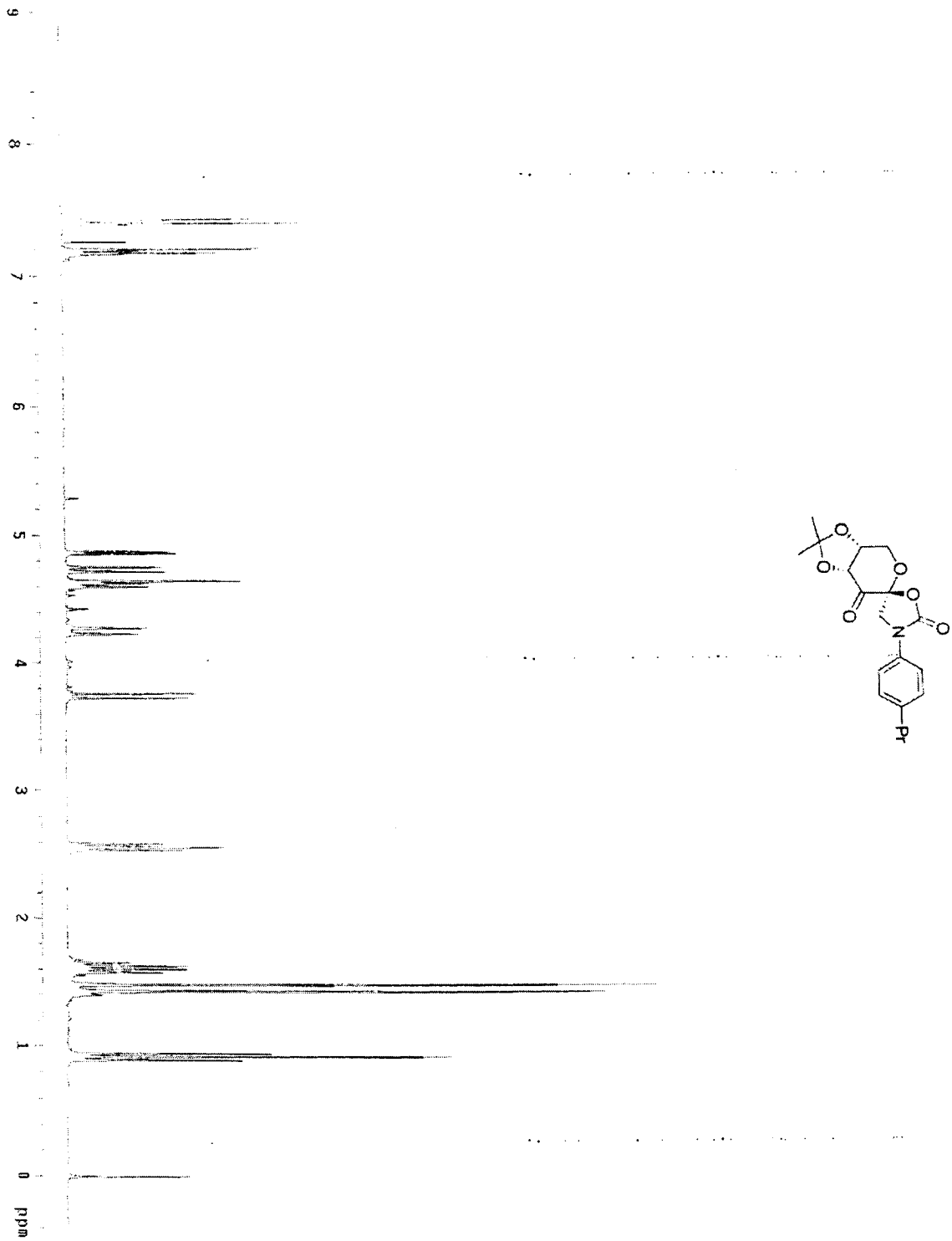

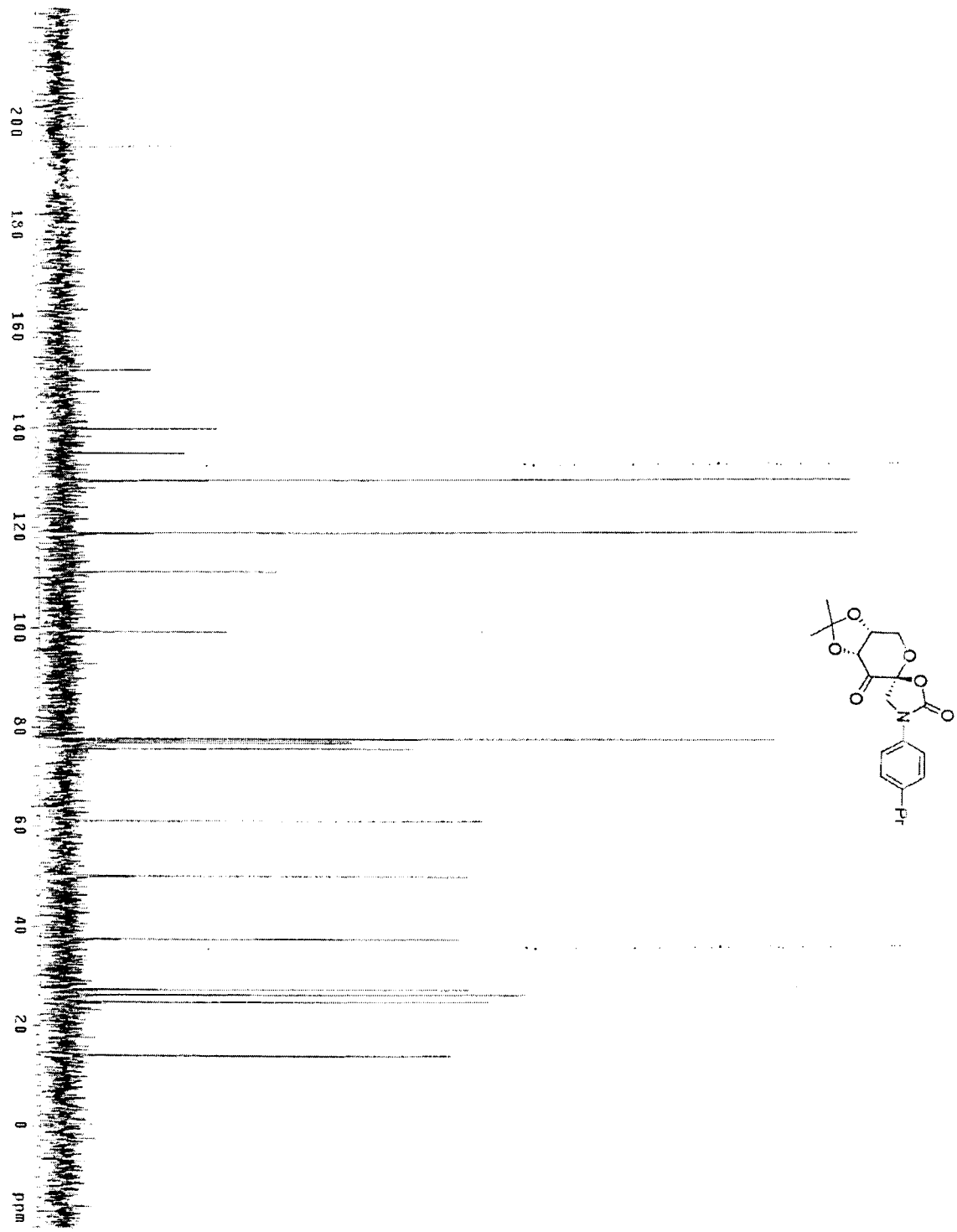

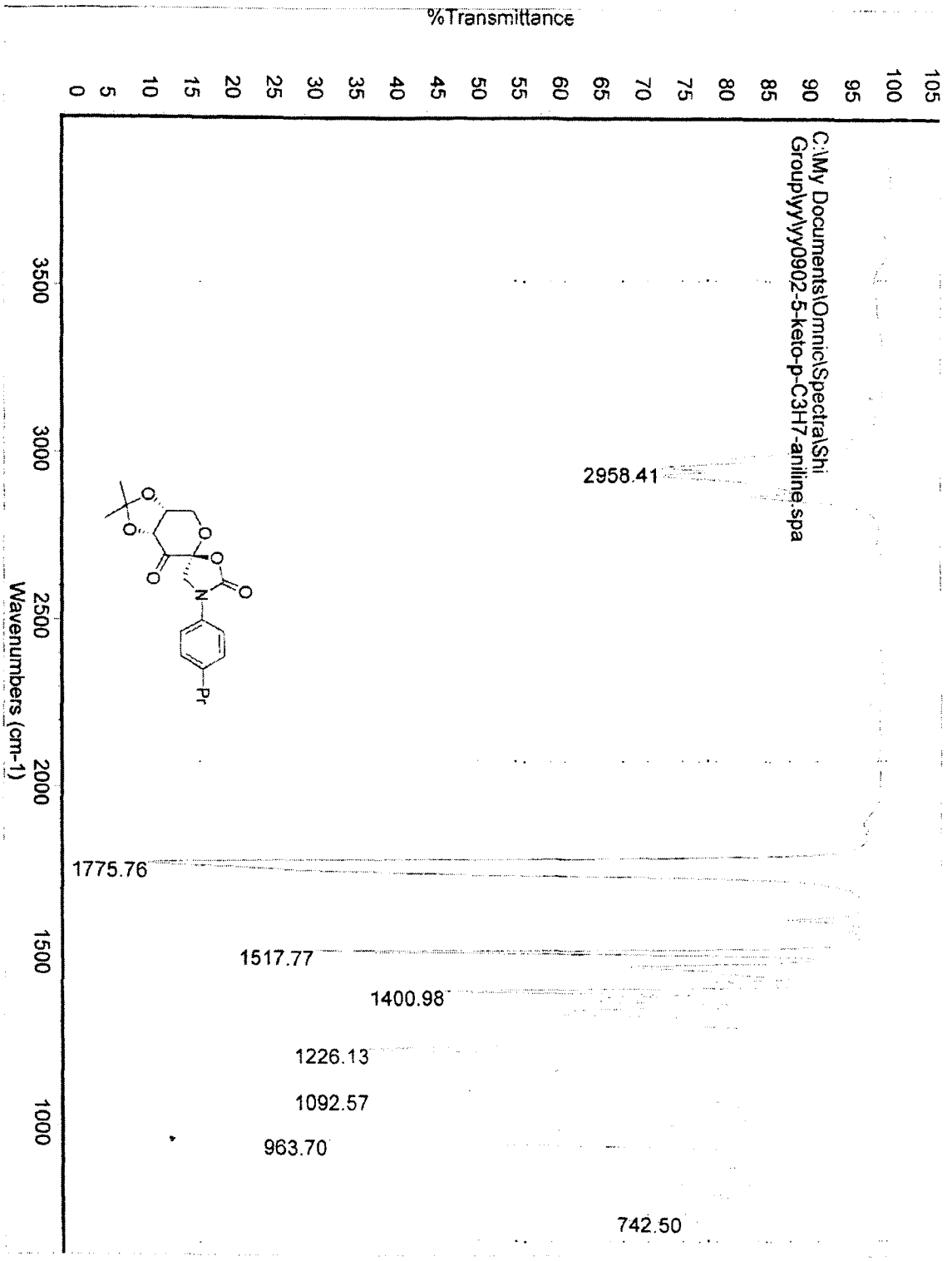

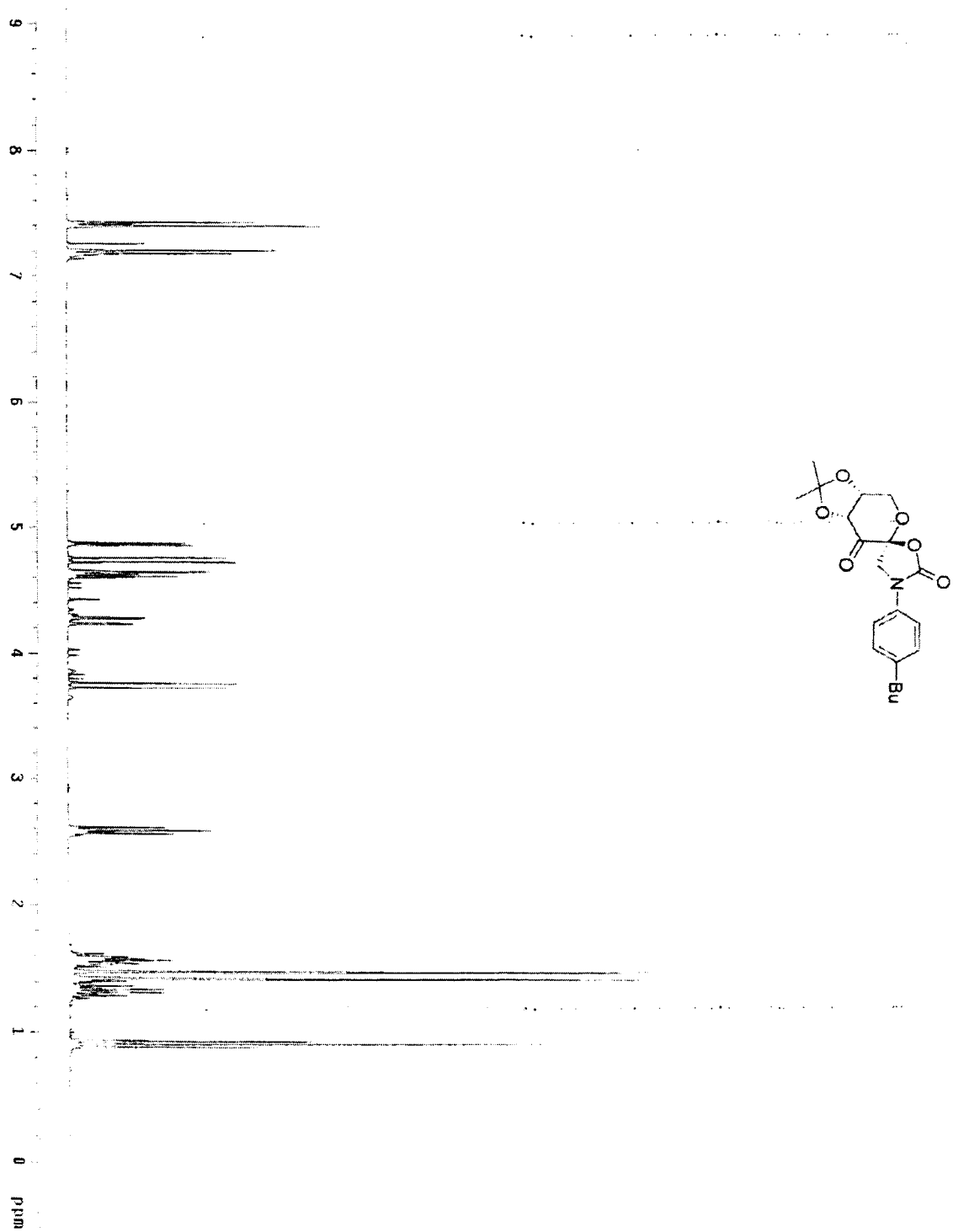

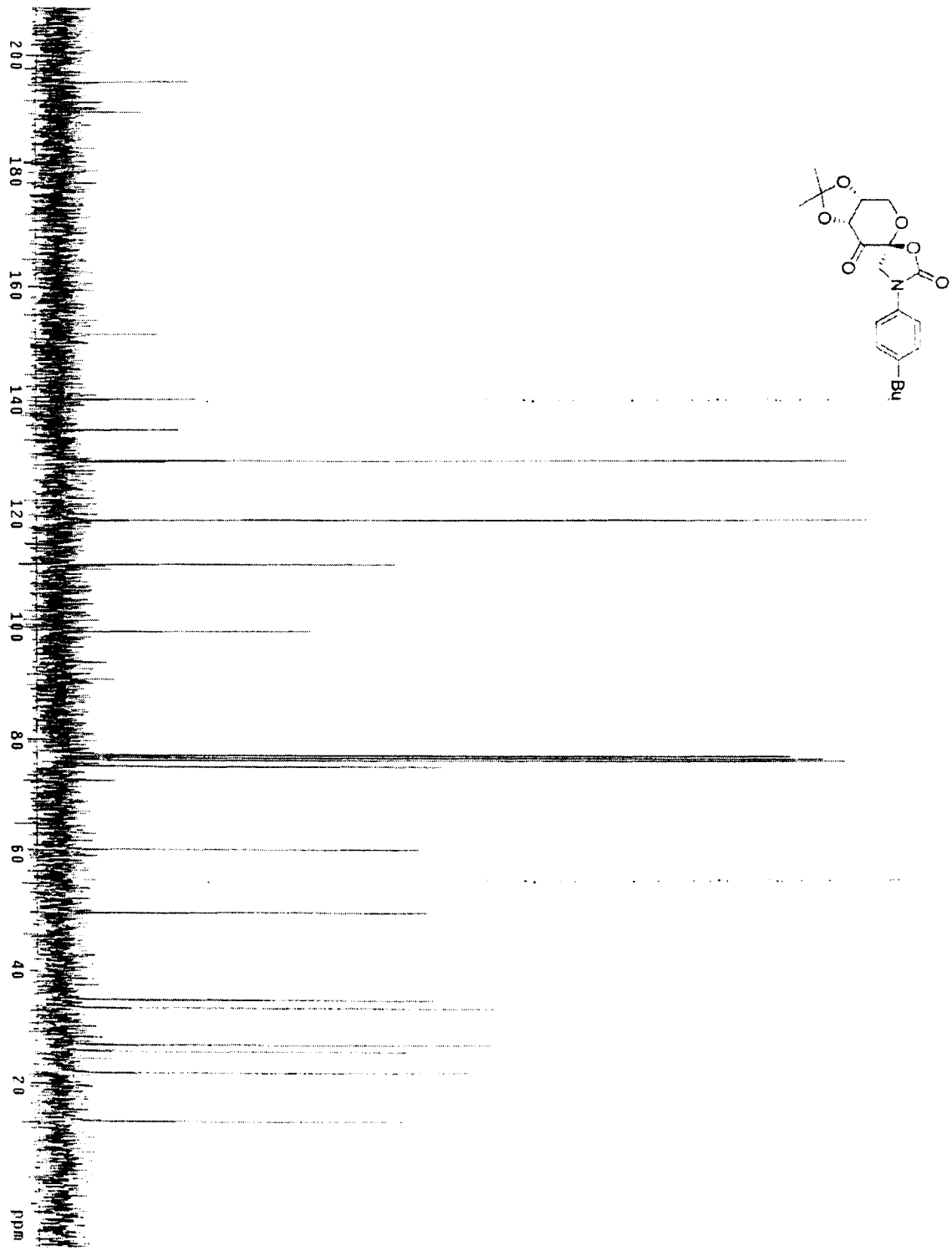

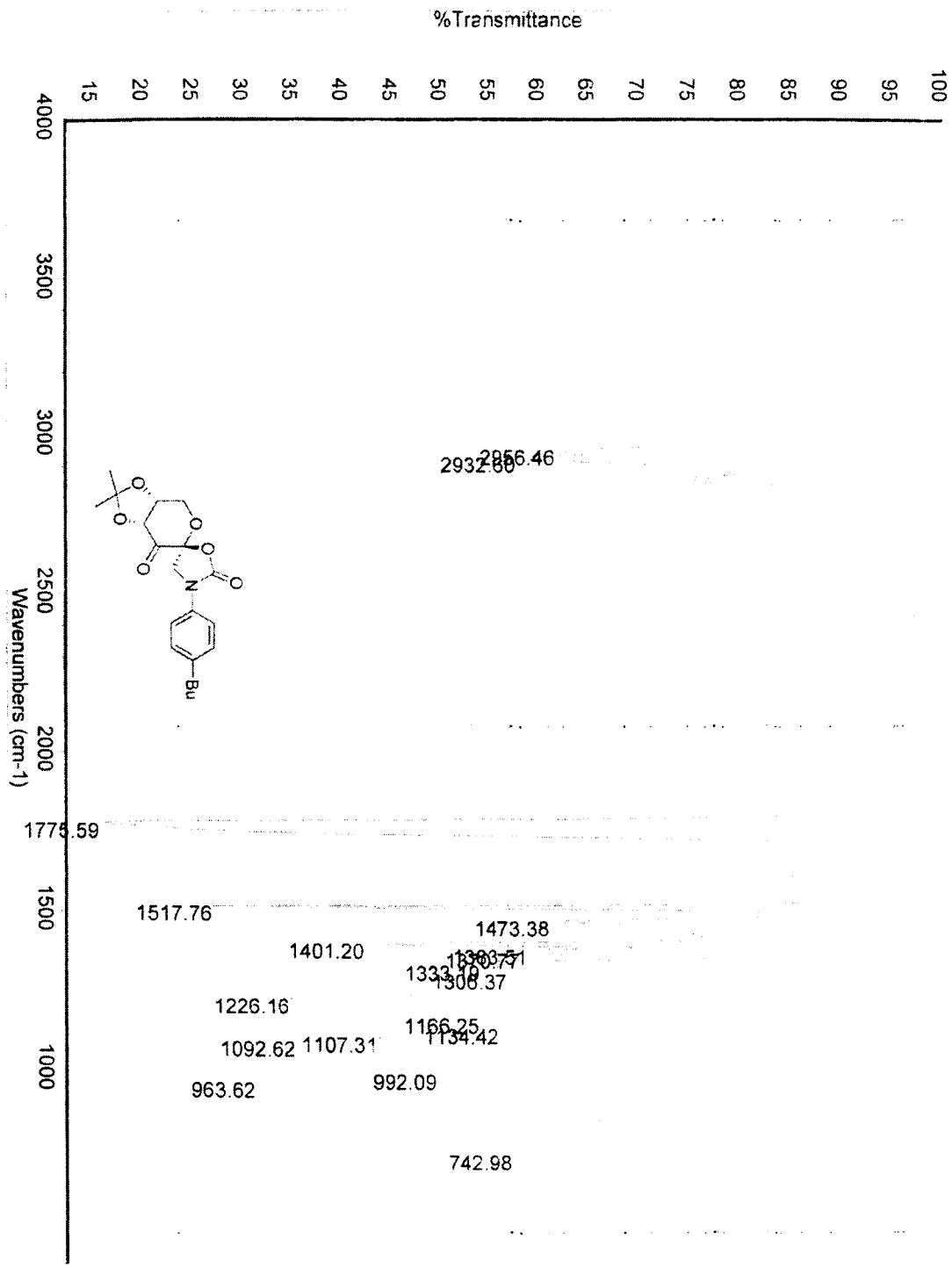

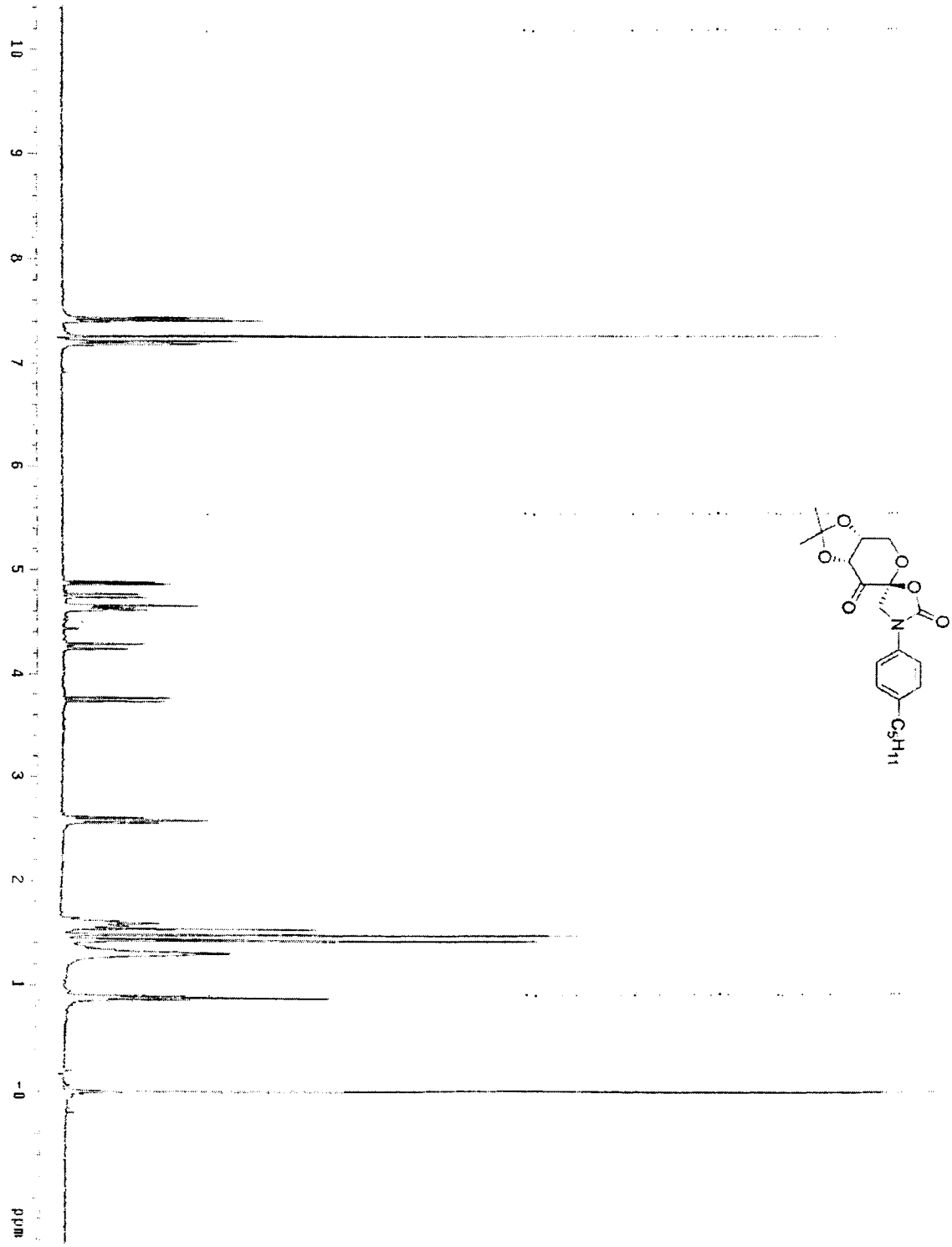

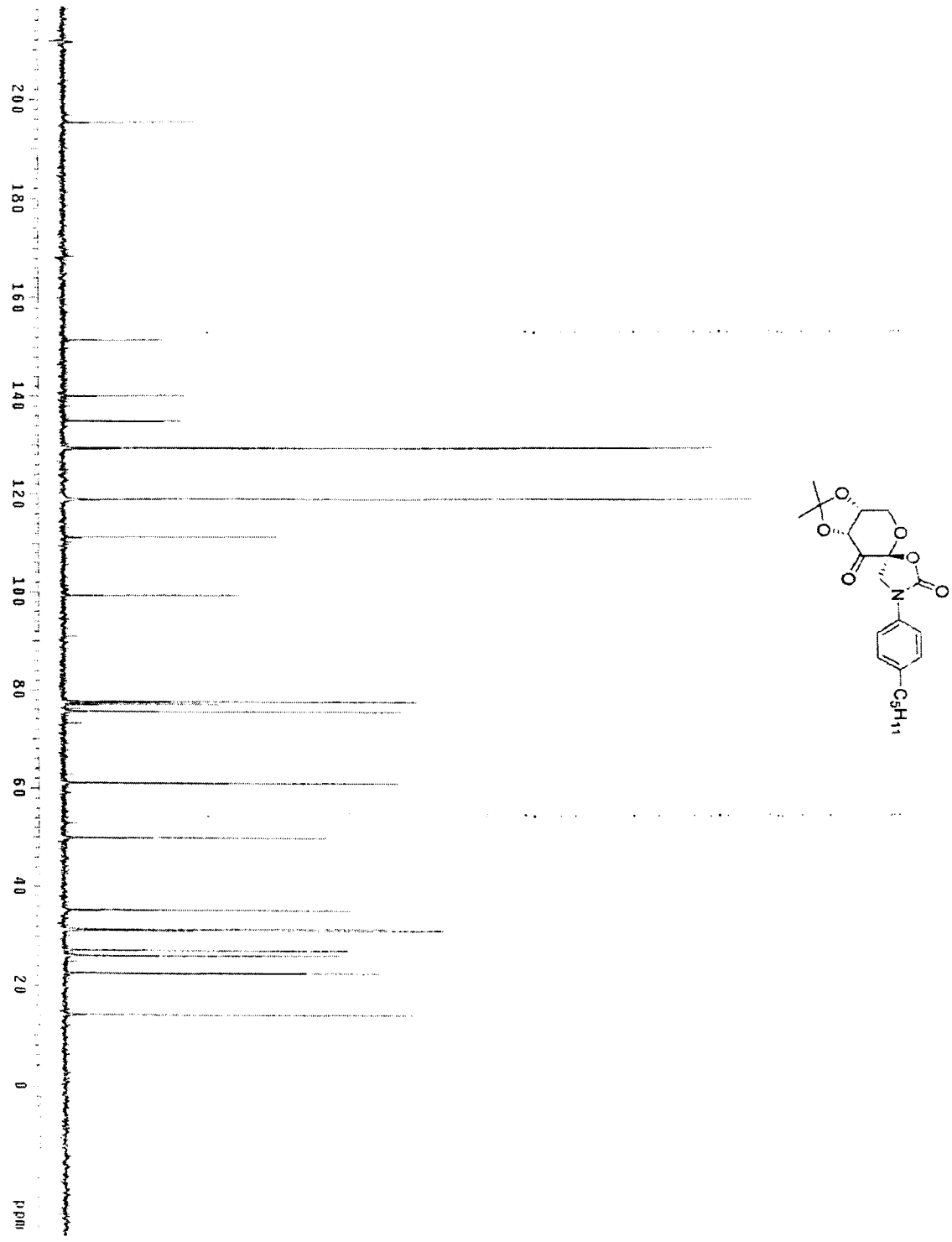

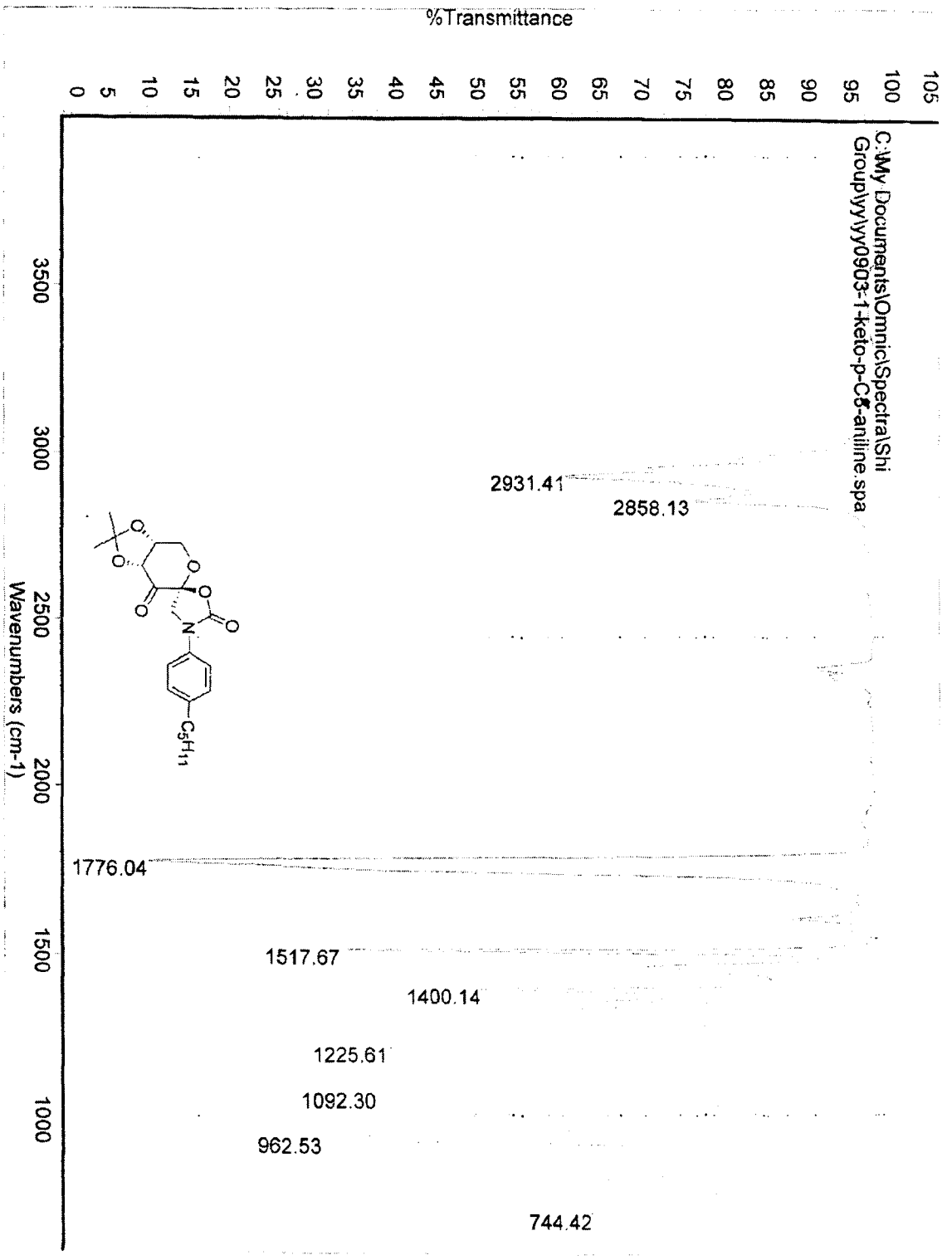

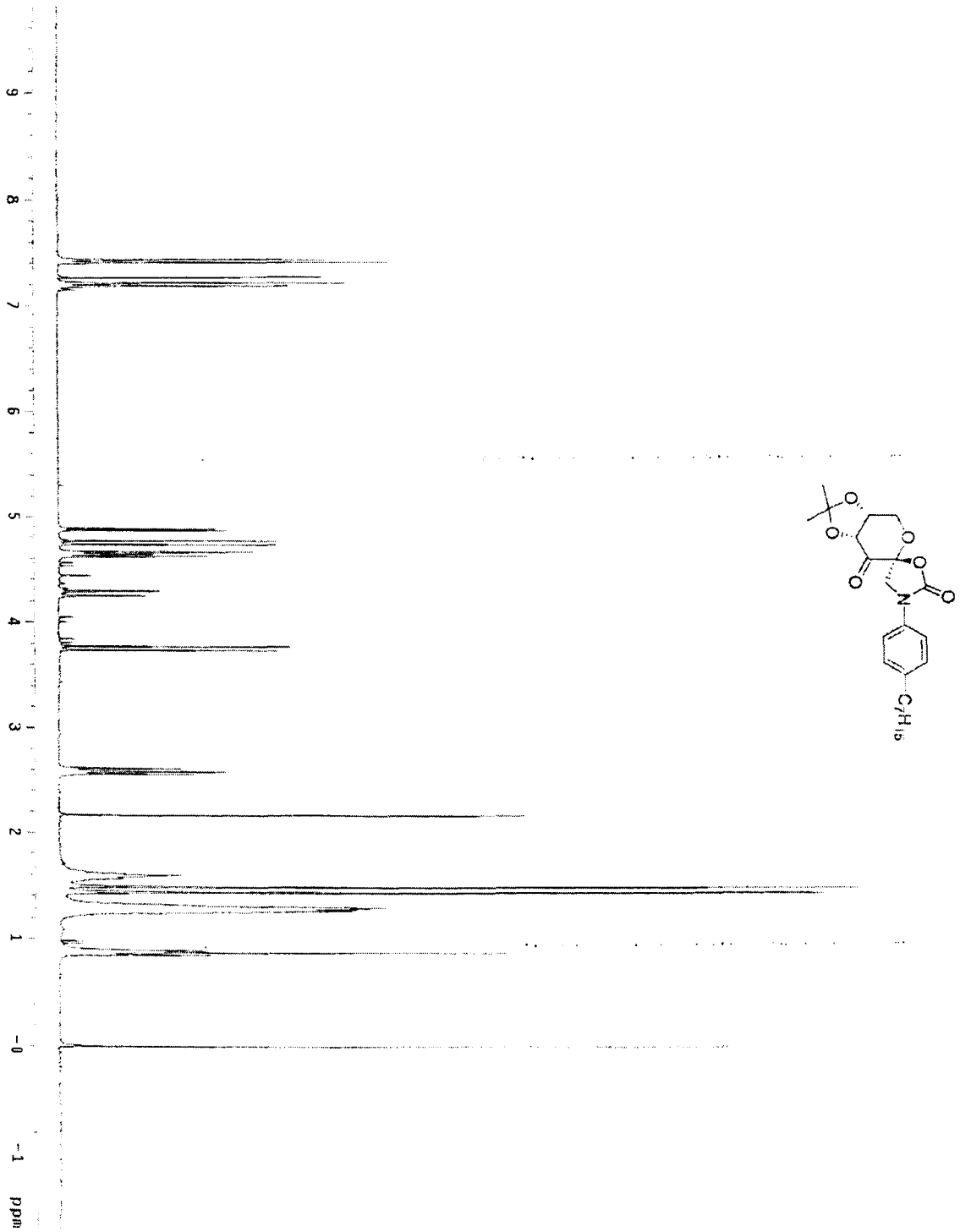

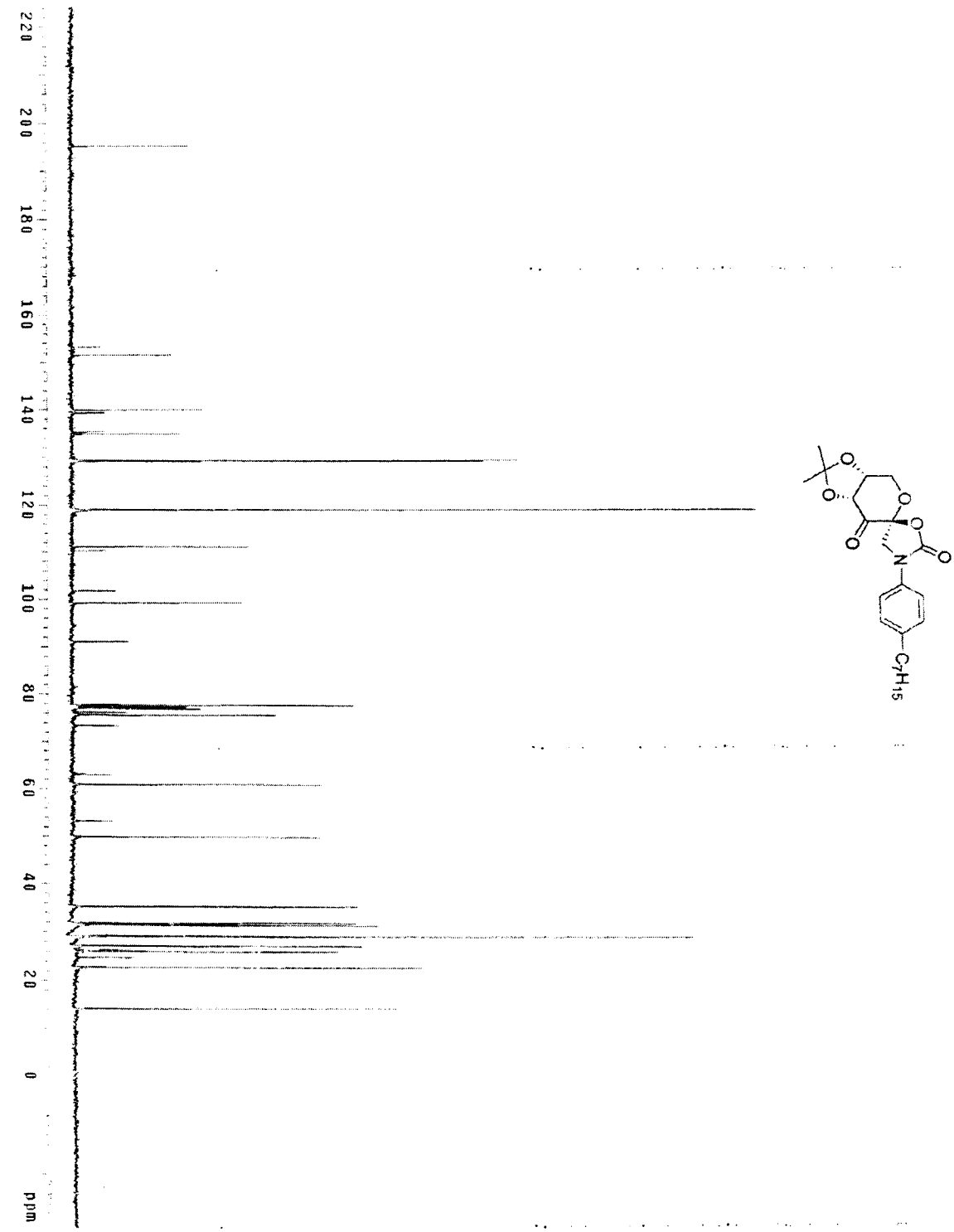

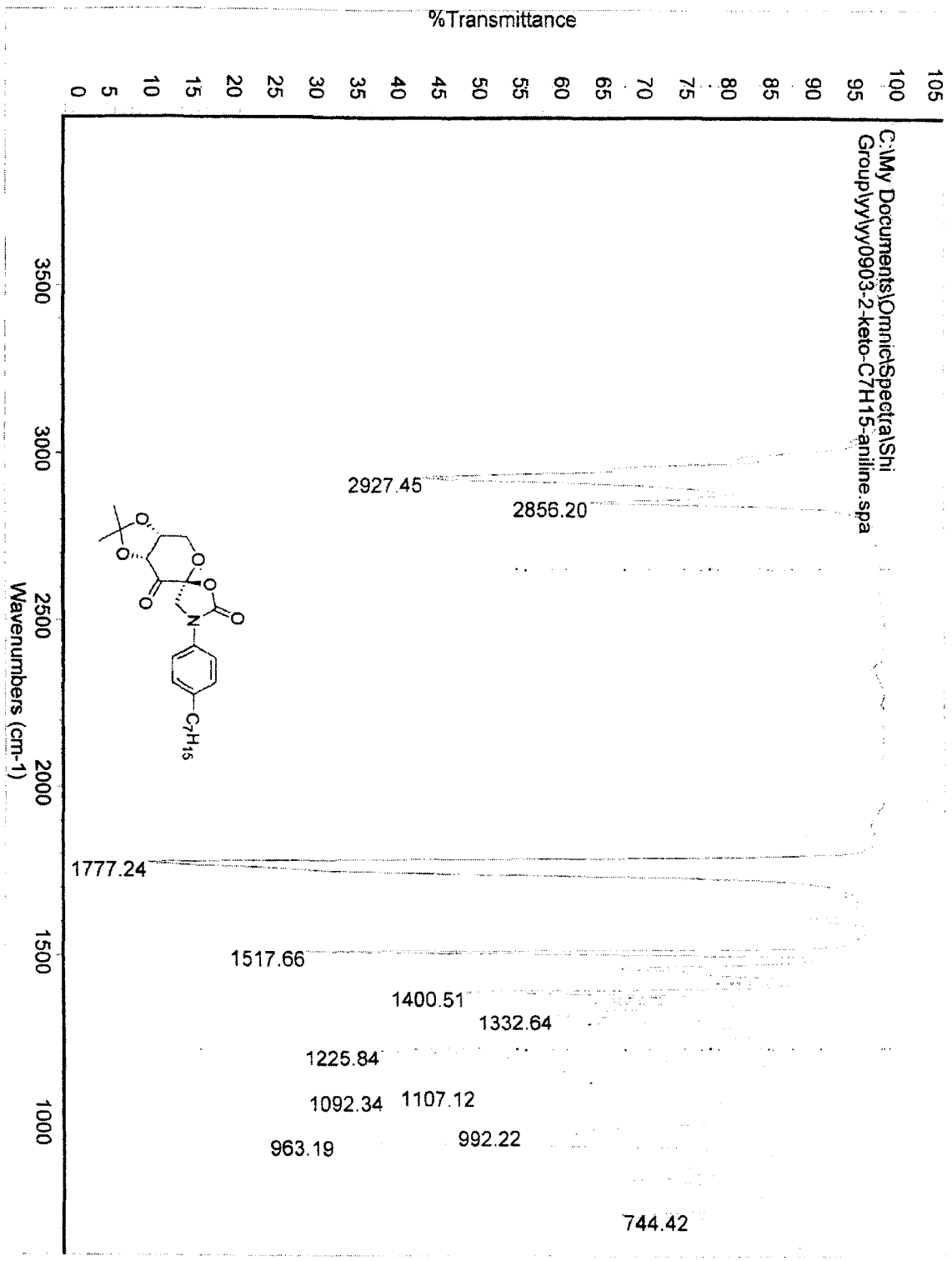

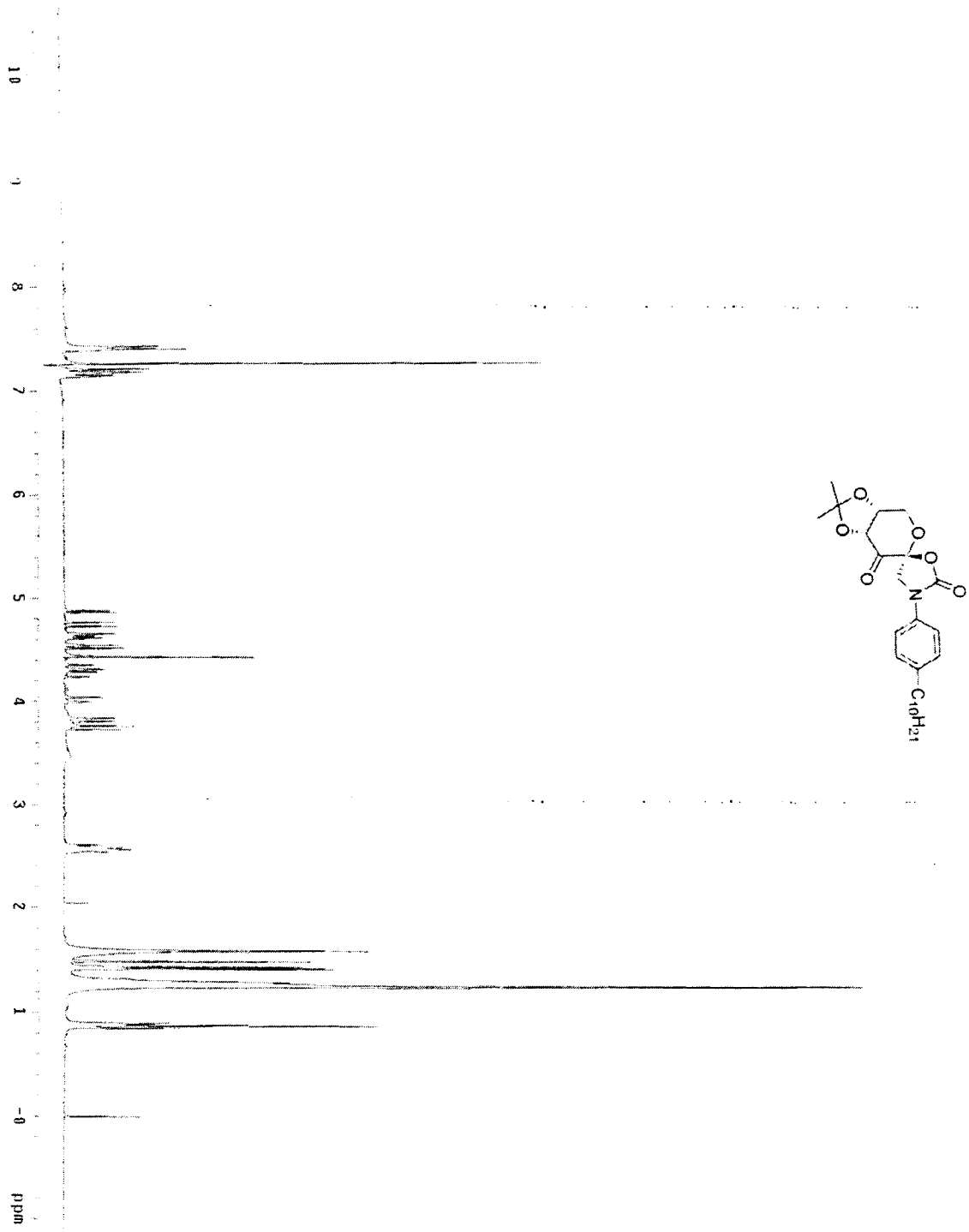

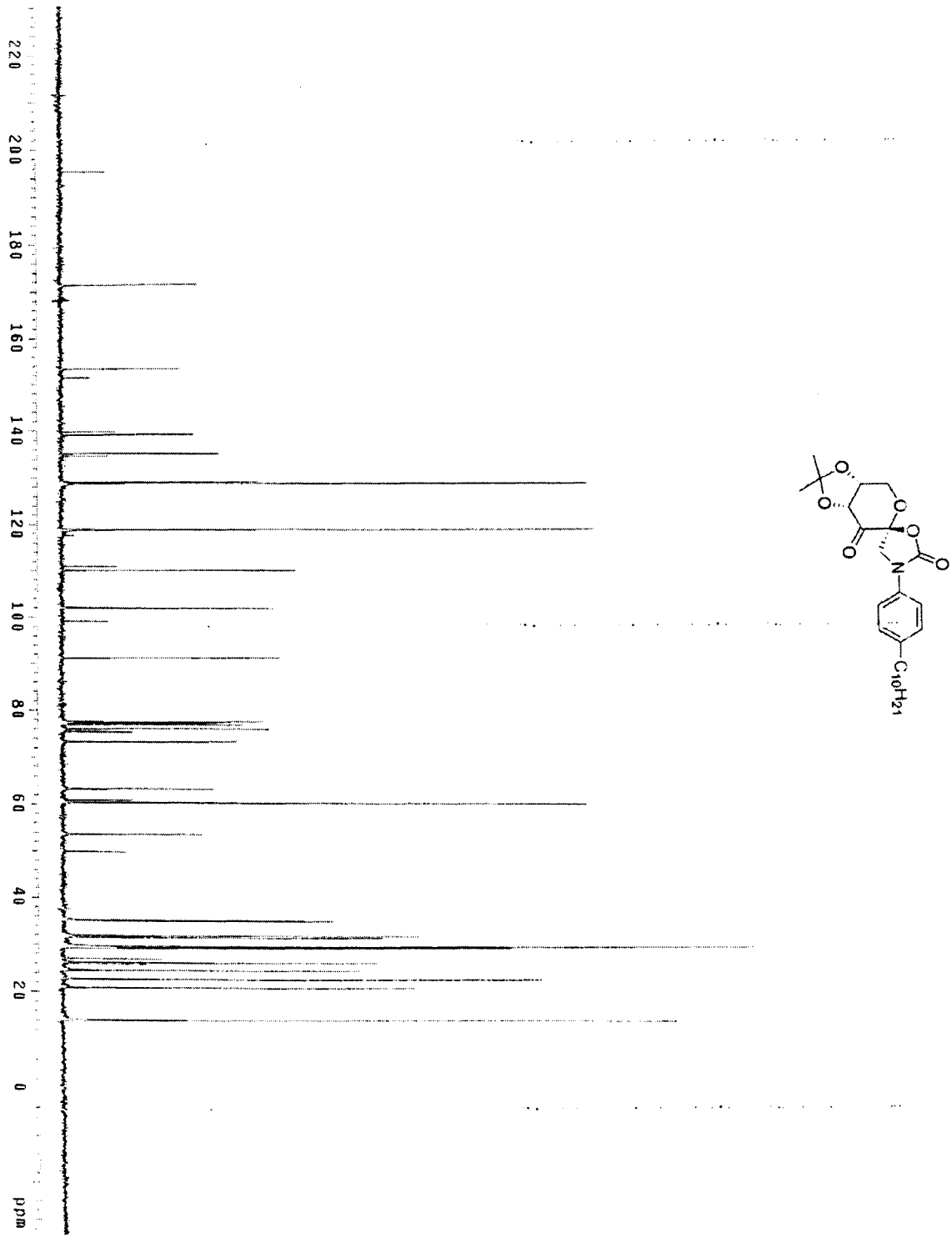

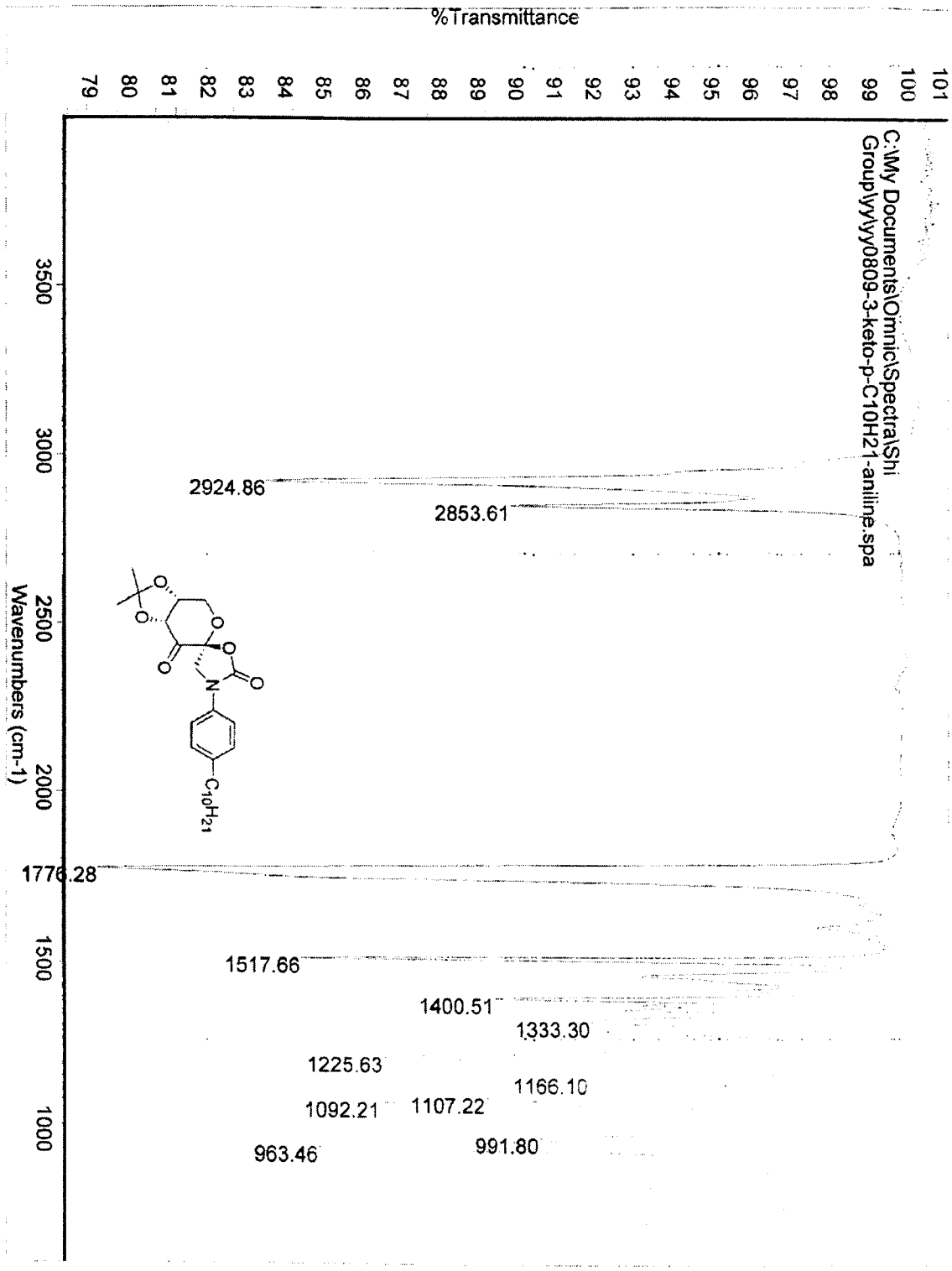

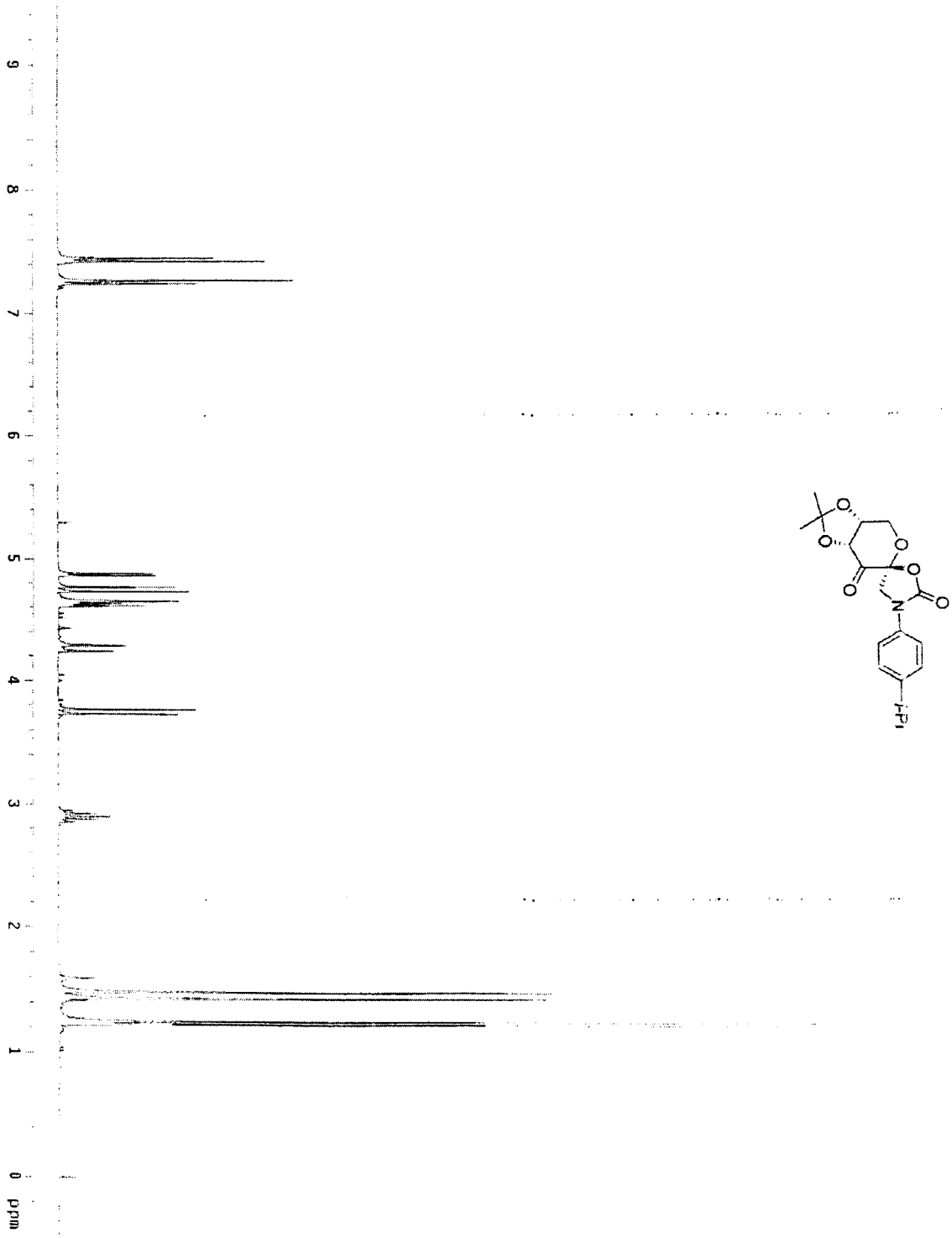

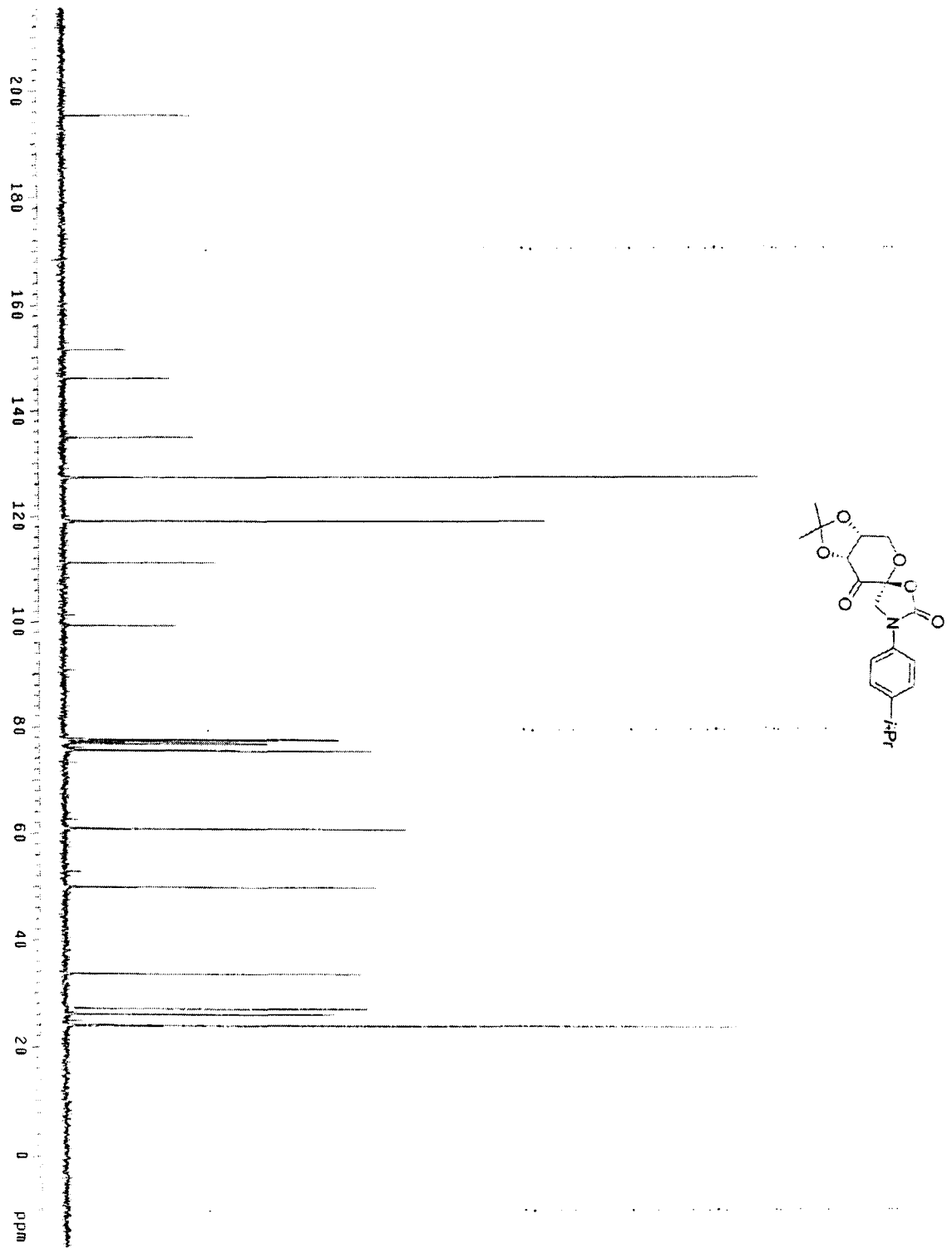

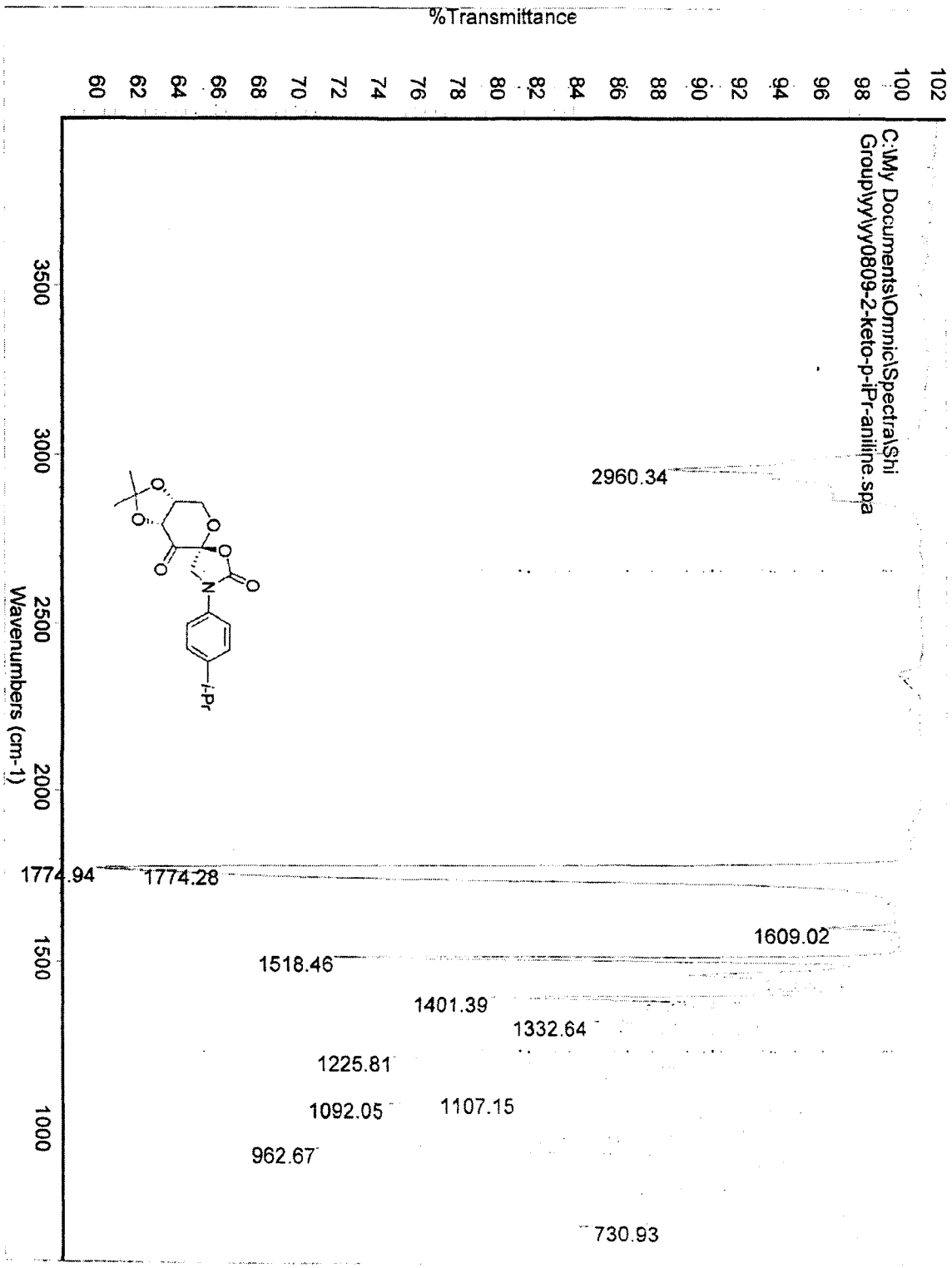

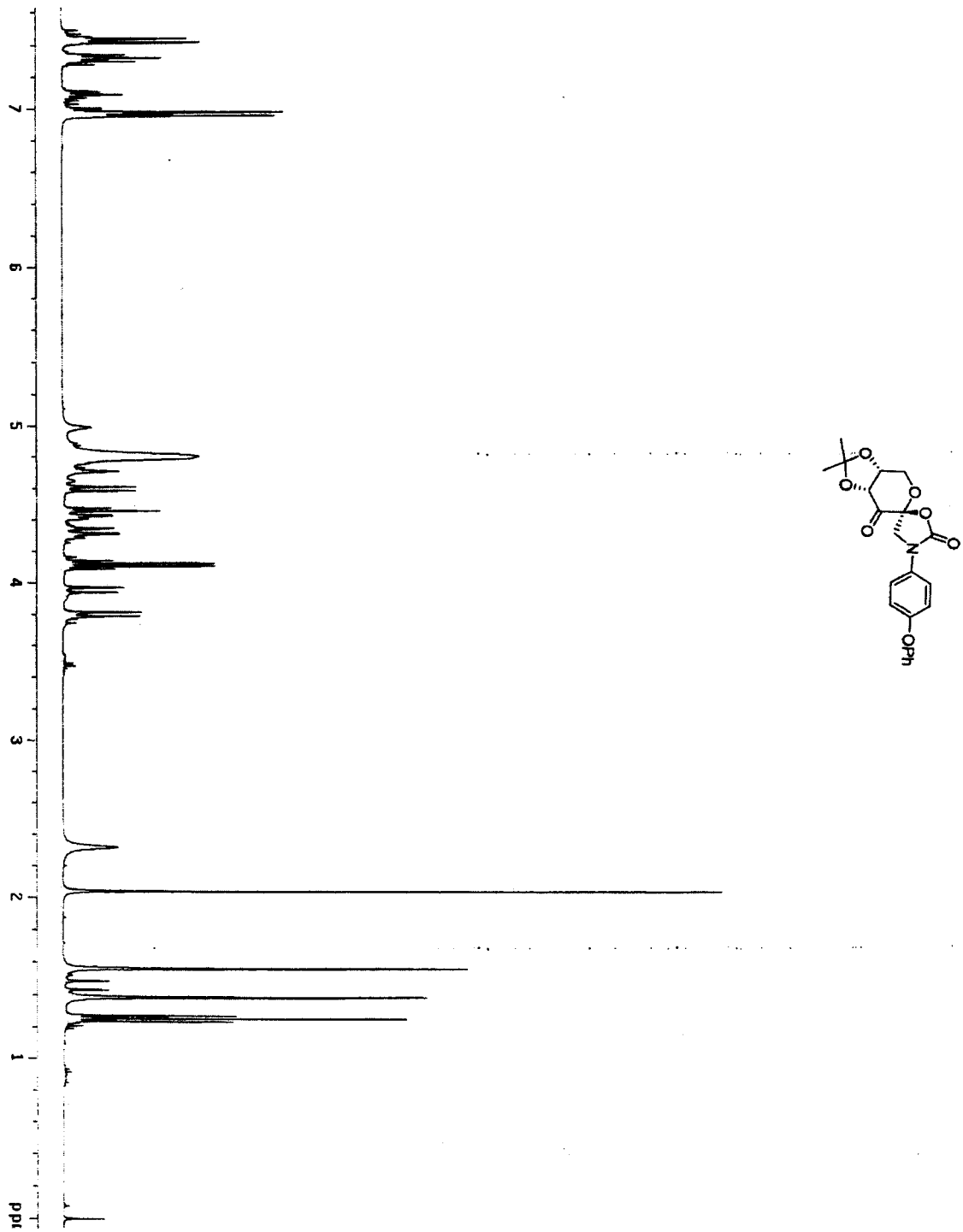

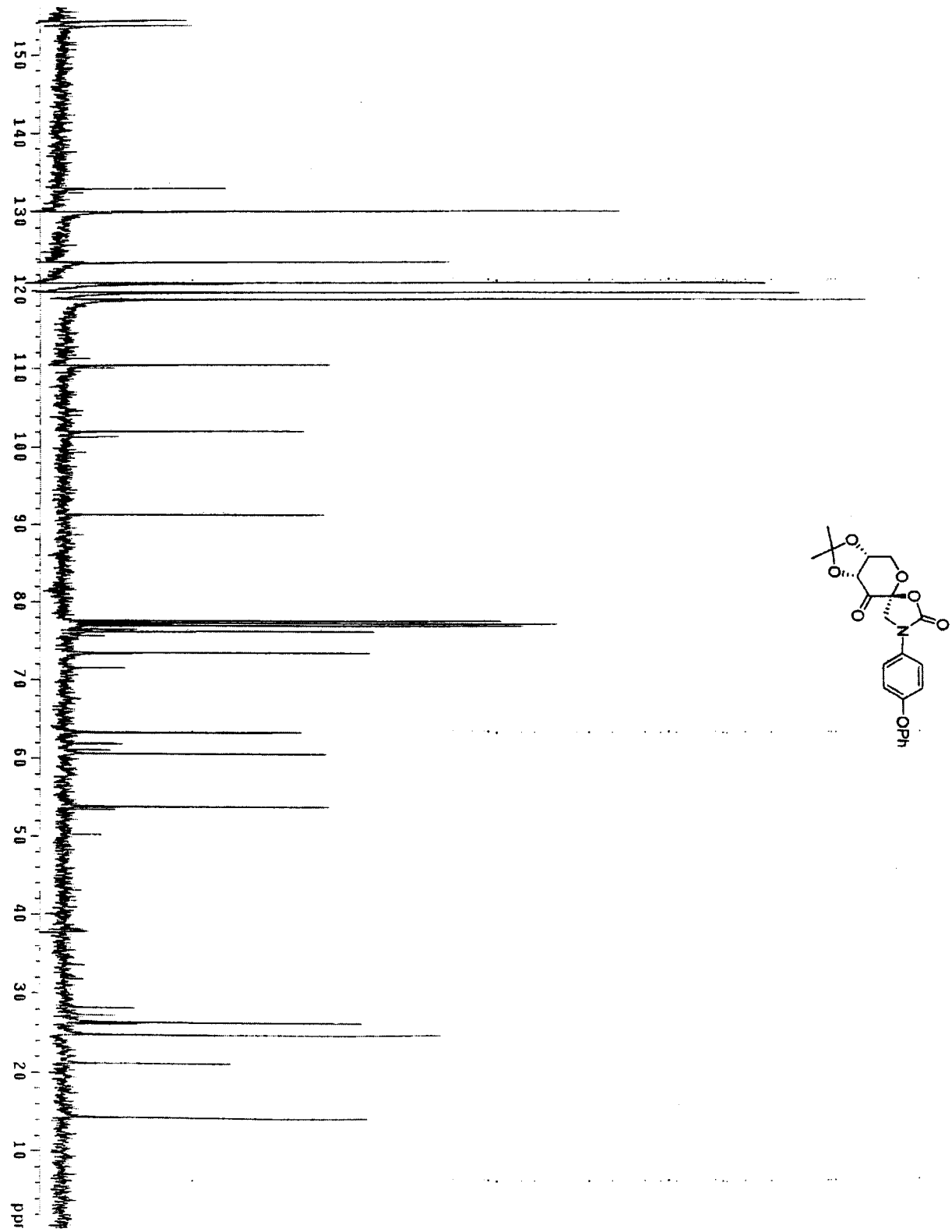

Thu Sep 02 16:07:34 2004
FIND PEAKS:

Spectrum:	DLG-4oph	
Region:	4000.00	400.00
Absolute threshold:	76.075	
Sensitivity:	40	
Peak list:		

Position:	1509.49	Intensity:	61.459
Position:	1237.22	Intensity:	62.702
Position:	1489.23	Intensity:	72.606
Position:	1751.61	Intensity:	73.736

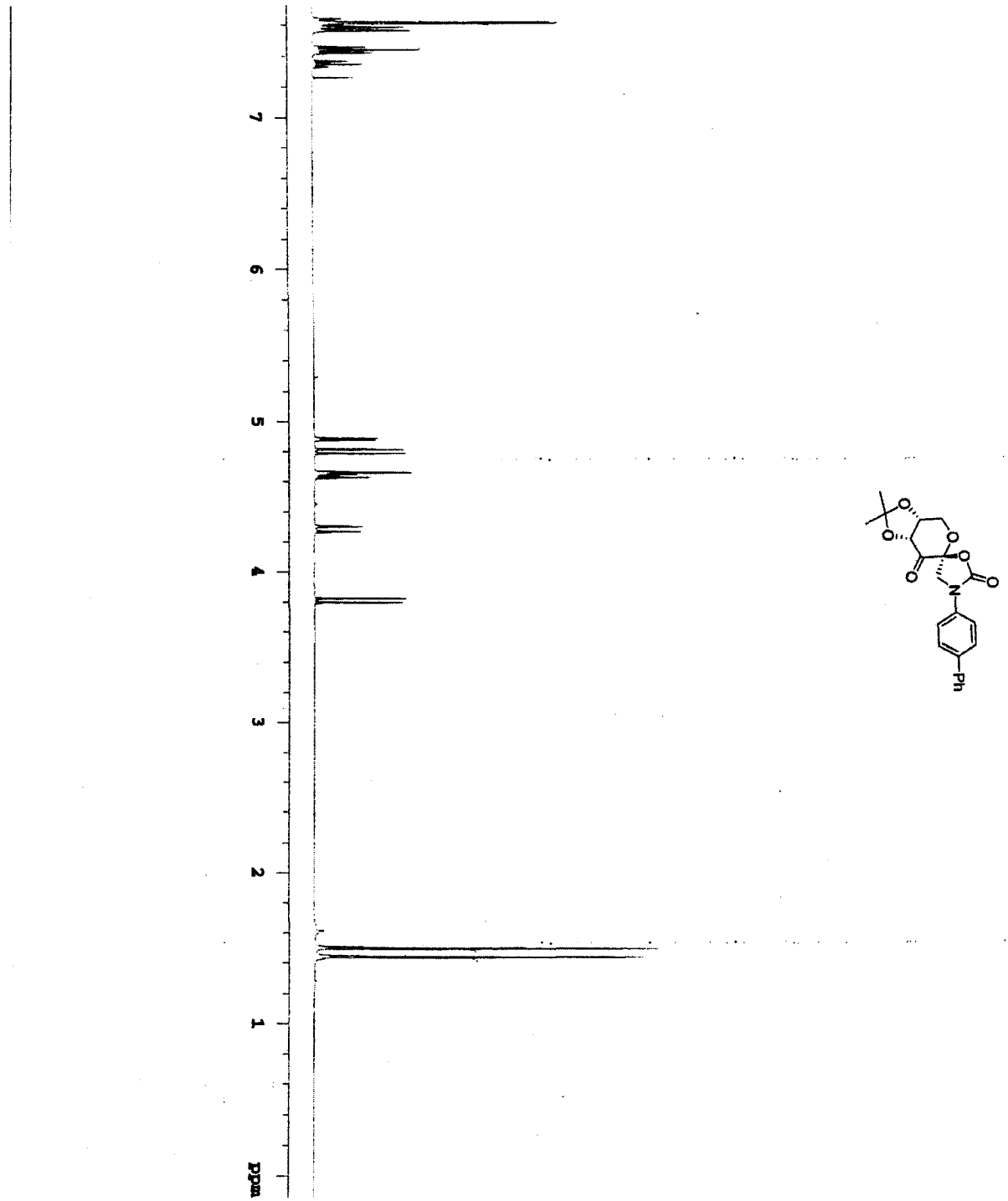

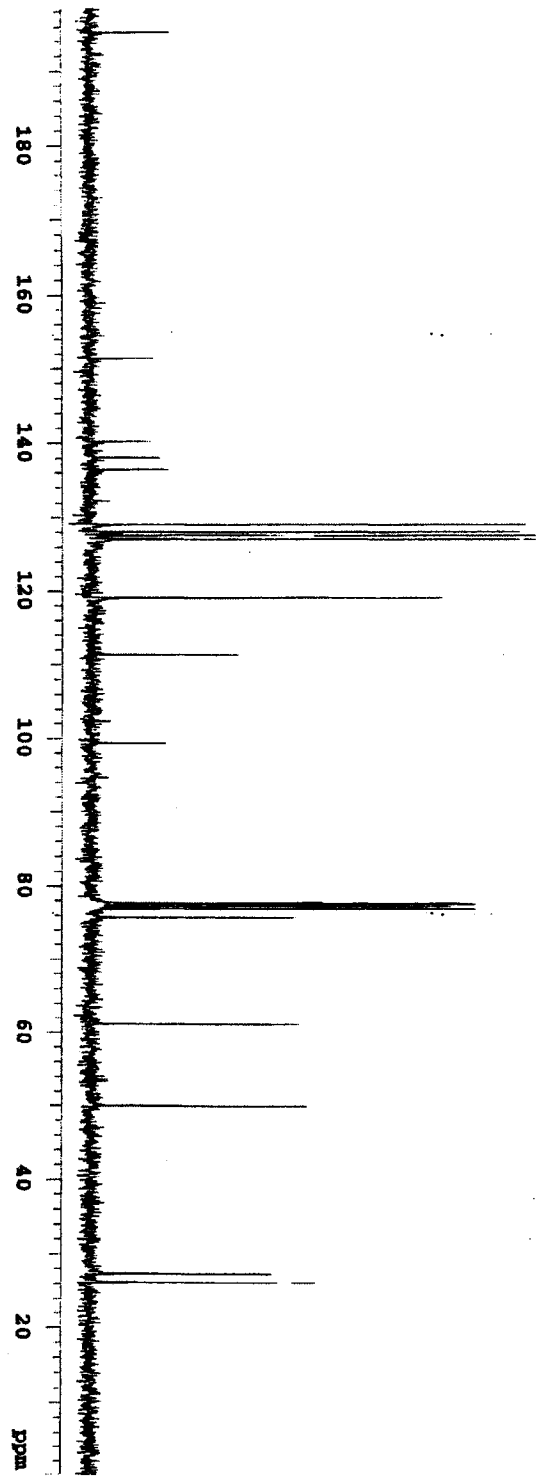

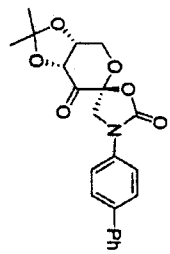

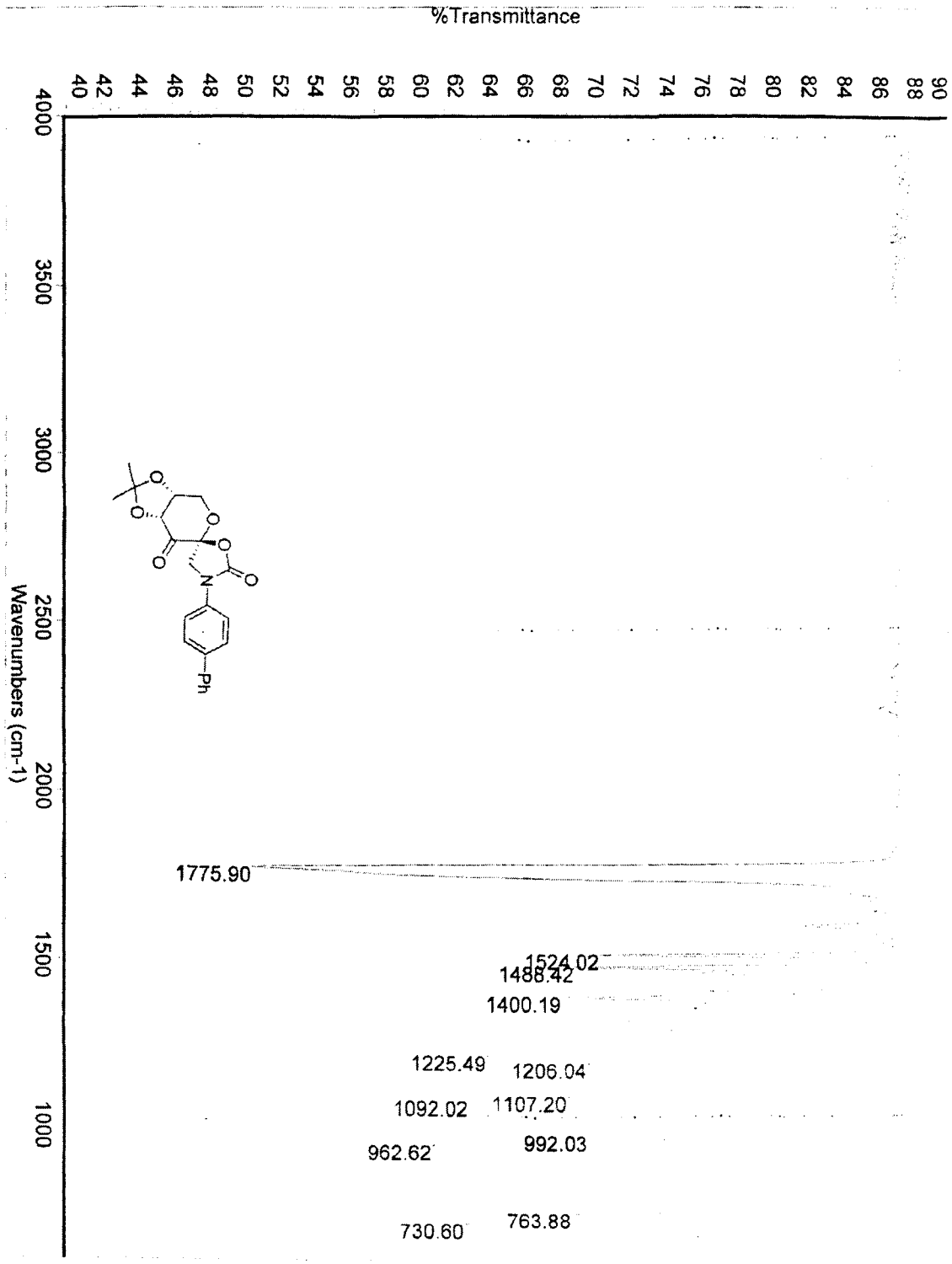

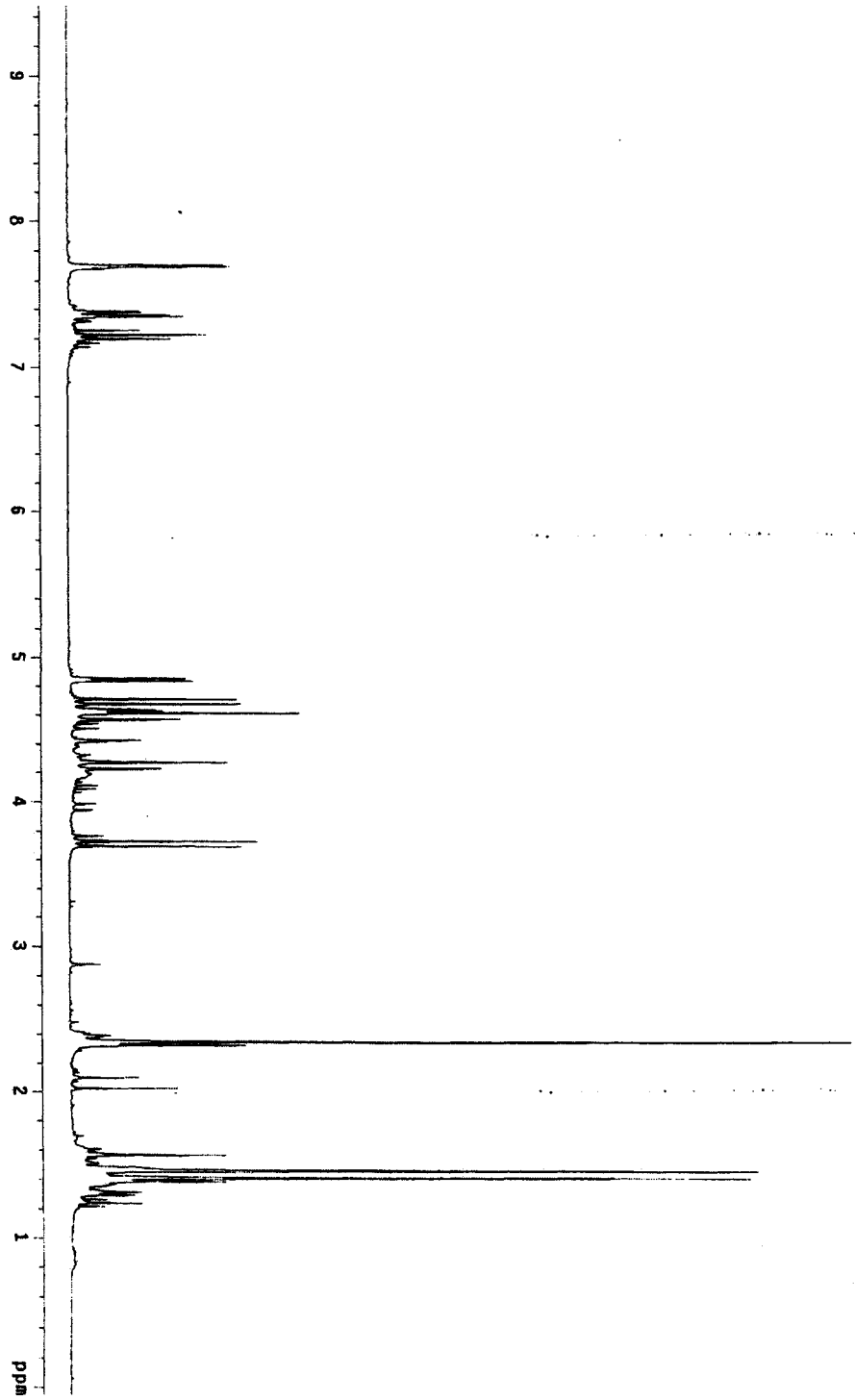

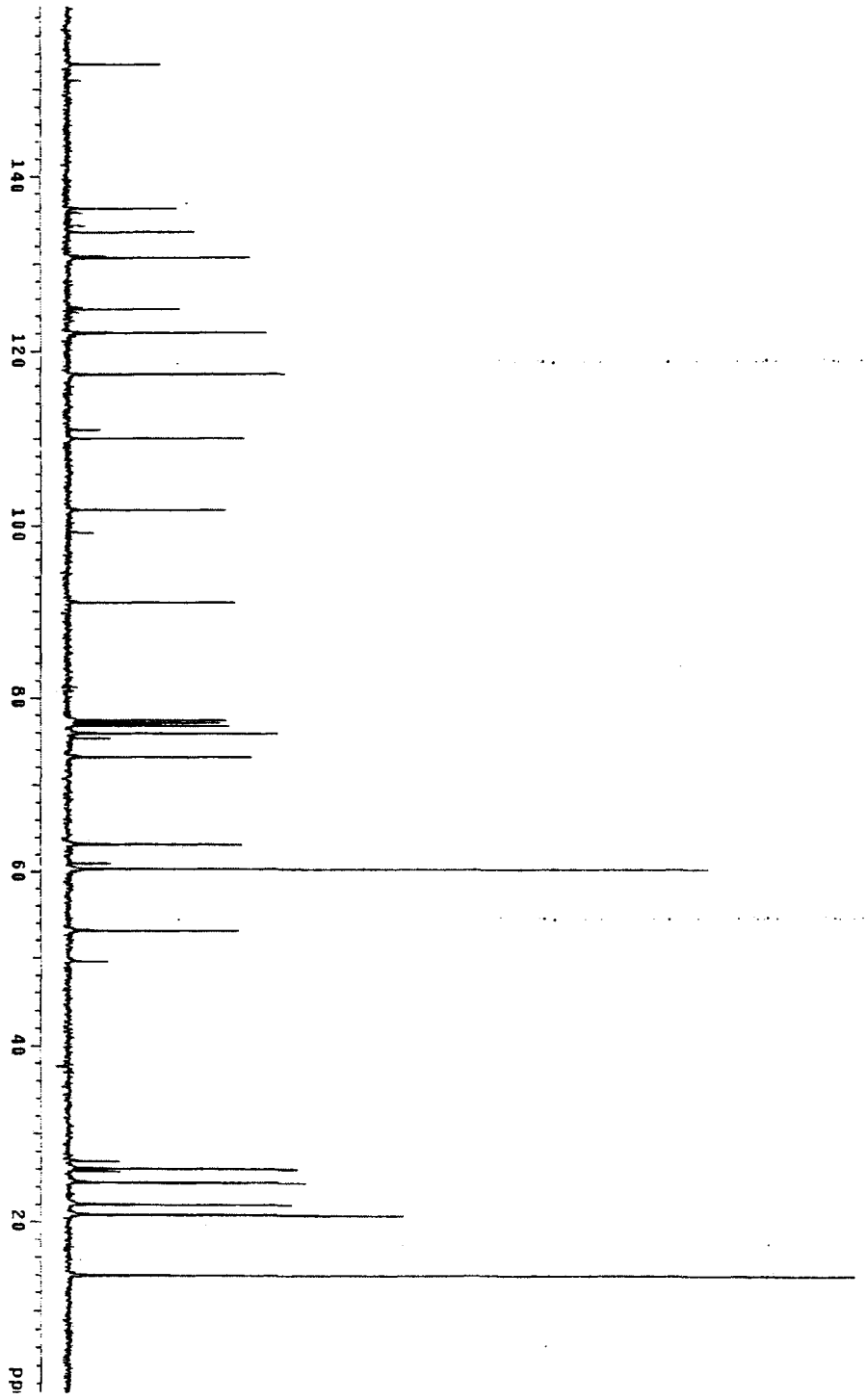

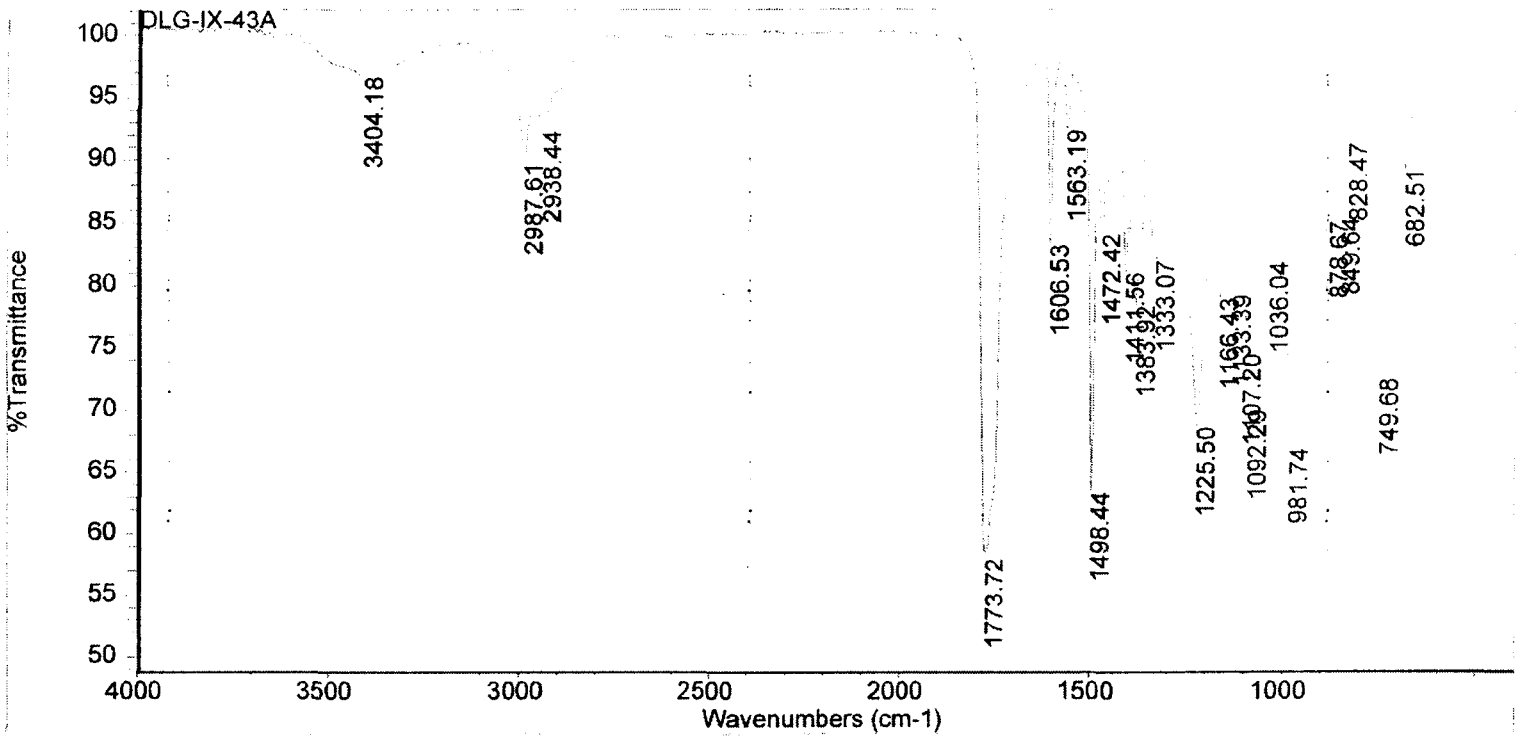

Wed Feb 25 14:57:40 2004
FIND PEAKS:

Spectrum: DLG-IX-43A
Region: 4000.00 400.00
Absolute threshold: 96.901
Sensitivity: 46
Peak list:

Position:	1773.72	Intensity:	58.028
Position:	1498.44	Intensity:	63.459
Position:	981.74	Intensity:	66.982
Position:	1225.50	Intensity:	68.722
Position:	1092.29	Intensity:	70.086
Position:	749.68	Intensity:	72.565
Position:	1107.20	Intensity:	74.562
Position:	1383.92	Intensity:	78.439

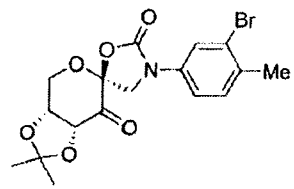

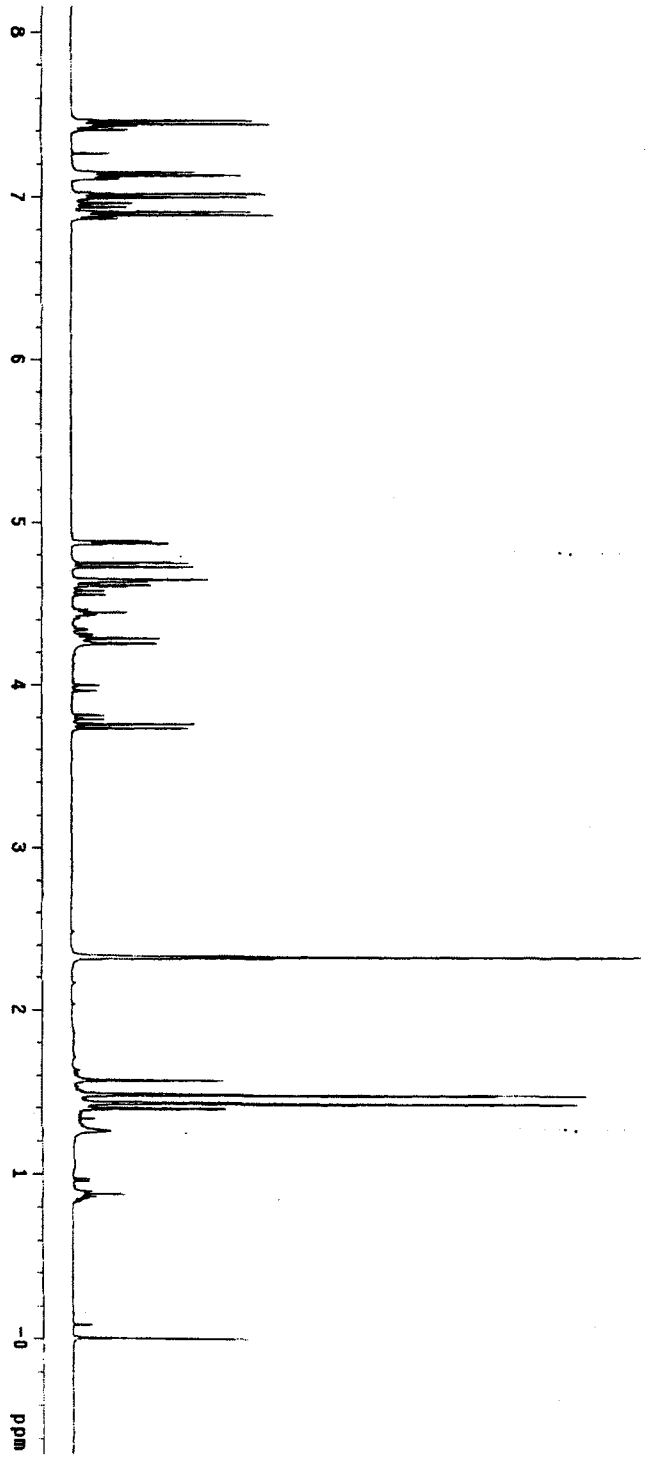

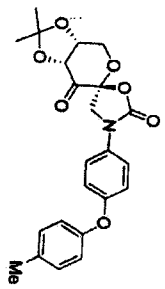

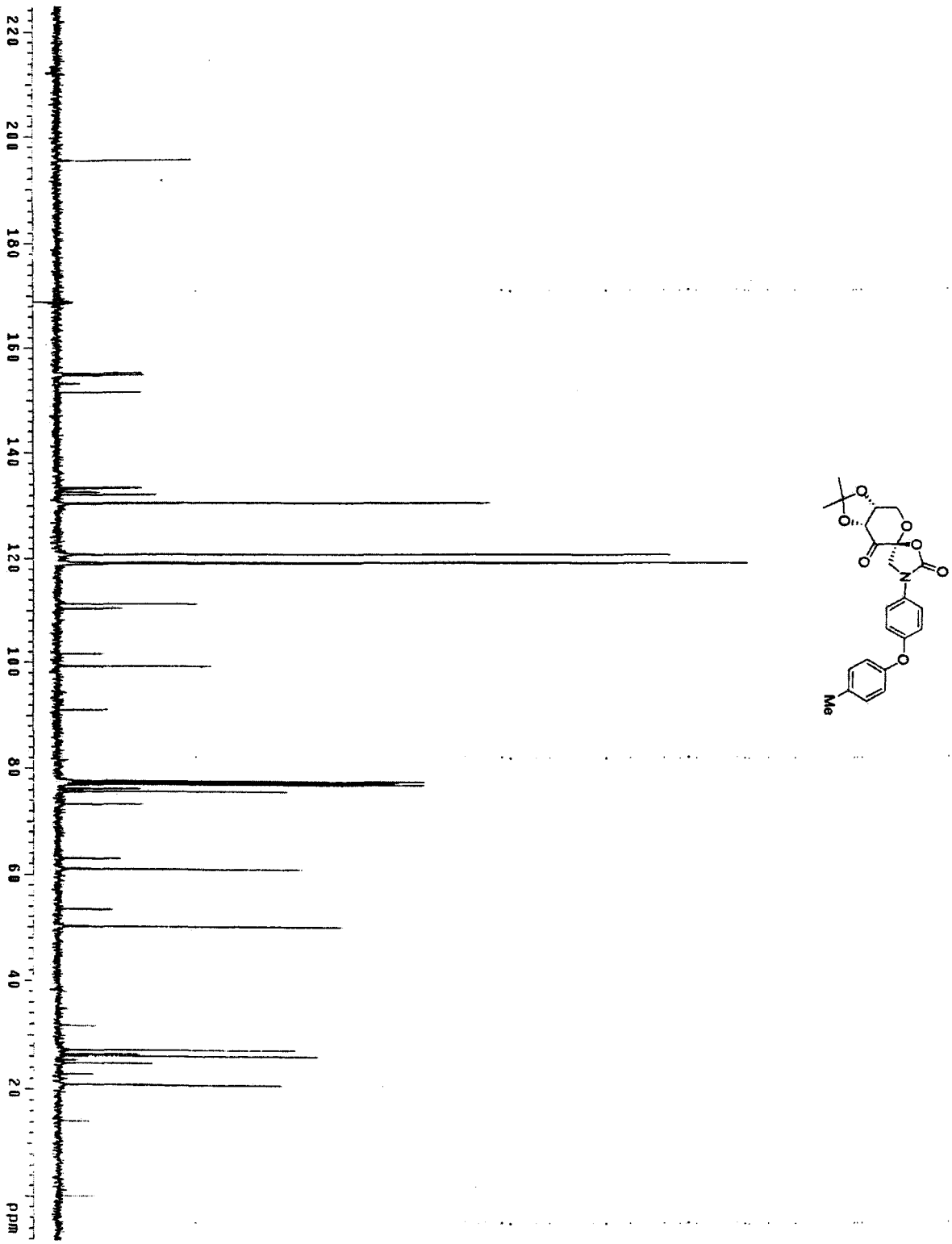

Wed Feb 25 14:27:21 2004
FIND PEAKS:

Spectrum: DLG-X-17A
Region: 4000.00 400.00
Absolute threshold: 83.266
Sensitivity: 24
Peak list:

Position:	1502.34	Intensity:	20.651
Position:	1239.17	Intensity:	28.022
Position:	1760.22	Intensity:	38.167
Position:	965.32	Intensity:	49.712
Position:	753.59	Intensity:	50.533
Position:	1106.72	Intensity:	50.847
Position:	873.85	Intensity:	58.932
Position:	848.43	Intensity:	60.509

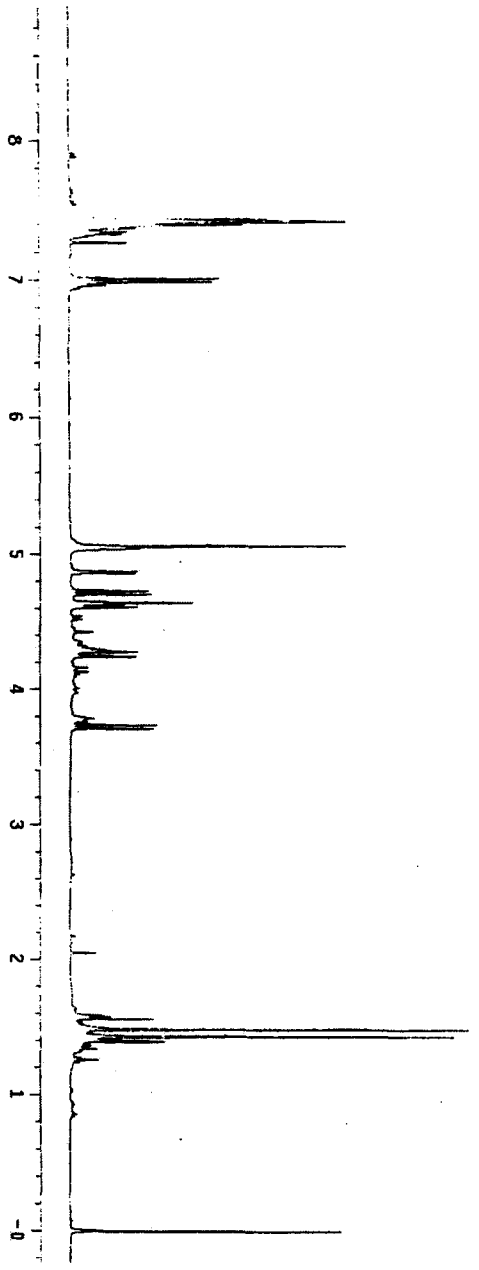

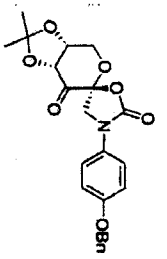

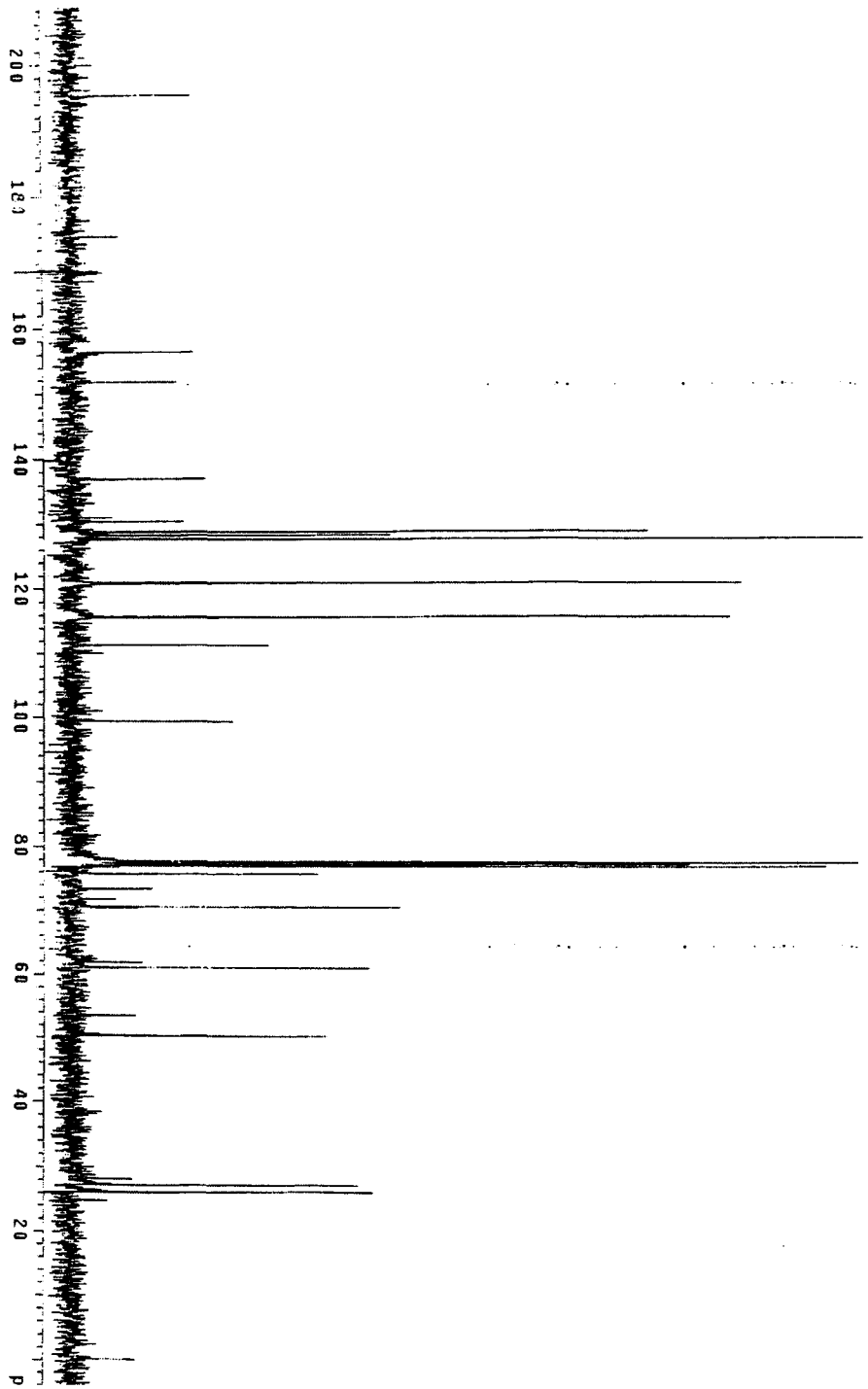

Thu Sep 02 16:12:29 2004
FIND PEAKS:

Spectrum:	DLG-4-obn	
Region:	4000.00	400.00
Absolute threshold:	96.933	
Sensitivity:	40	
Peak list:		

Position:	1513.43	Intensity:	87.069
Position:	1224.90	Intensity:	91.113
Position:	1764.20	Intensity:	92.596
Position:	963.39	Intensity:	92.910
Position:	1091.33	Intensity:	93.692
Position:	743.42	Intensity:	93.983
Position:	828.84	Intensity:	96.190
Position:	1165.56	Intensity:	96.336

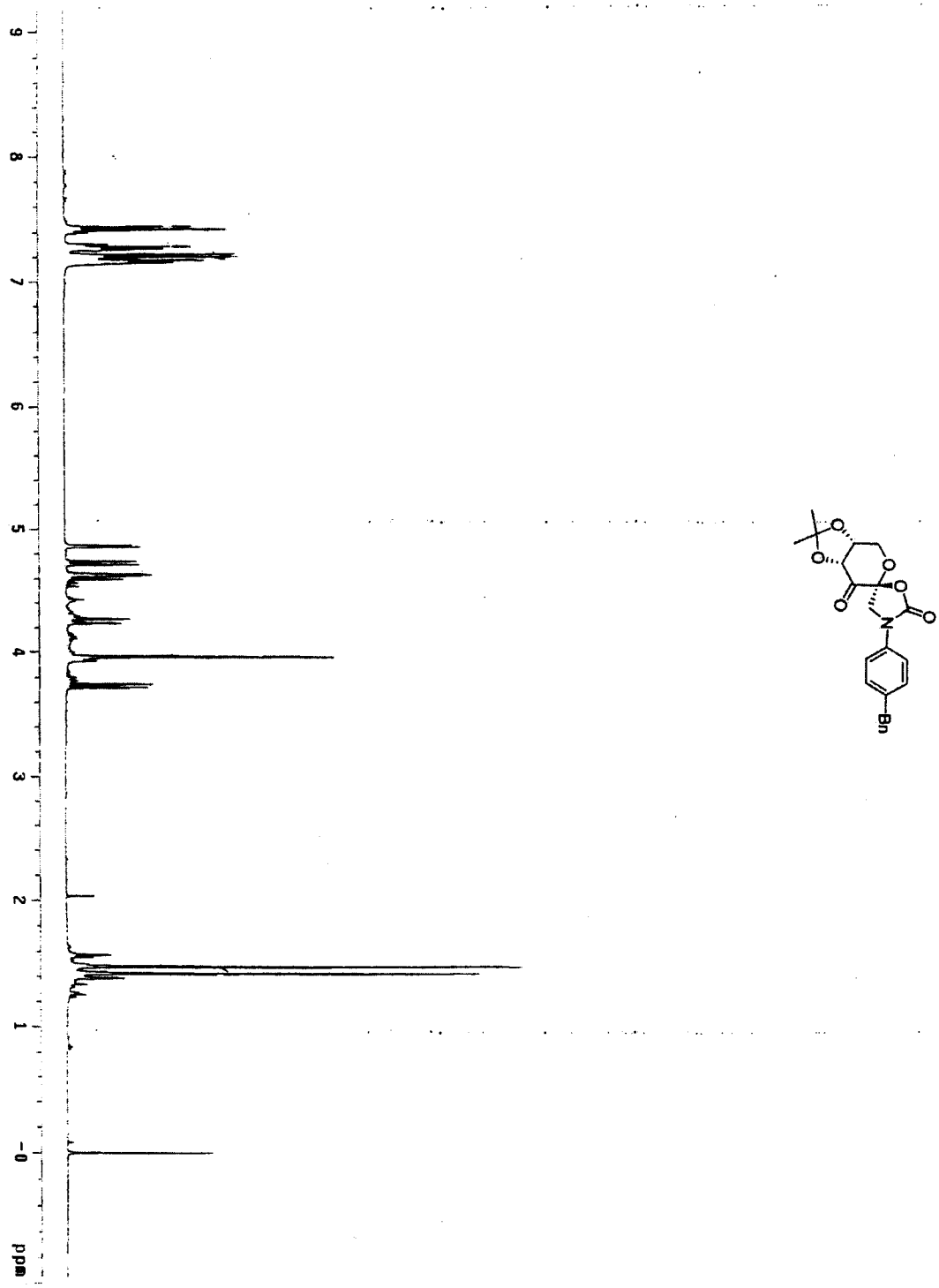

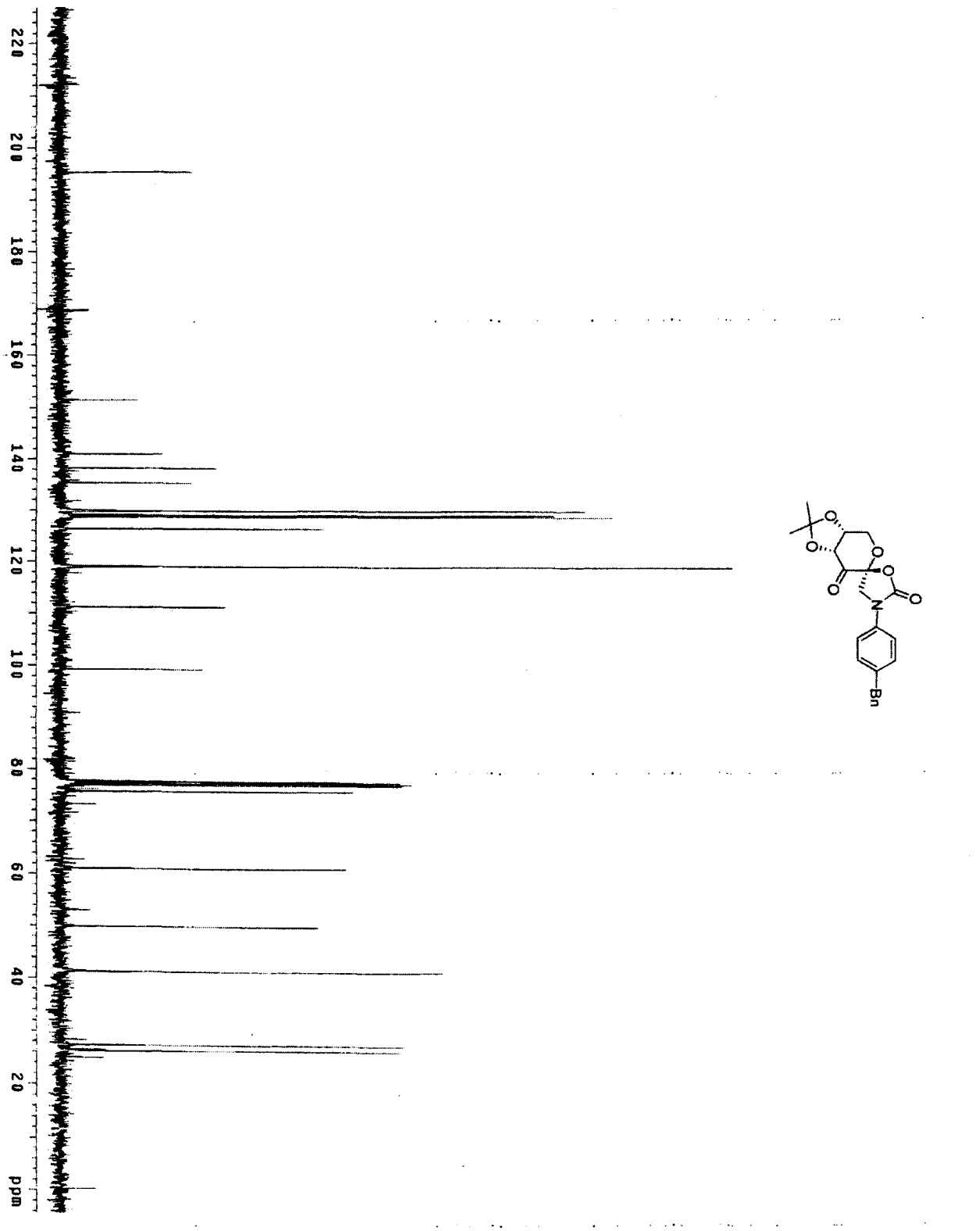

Tue Feb 24 15:51:13 2004
FIND PEAKS:
Spectrum: DLG-IX-17B1
Region: 4000.00 400.00
Absolute threshold: 84.768
Sensitivity: 27
Peak list:

Position:	1762.49	Intensity:	59.971
Position:	1516.30	Intensity:	63.844
Position:	964.98	Intensity:	68.305
Position:	1223.88	Intensity:	68.950
Position:	735.53	Intensity:	69.517
Position:	1091.69	Intensity:	69.655
Position:	1402.00	Intensity:	70.779
Position:	1314.08	Intensity:	72.617

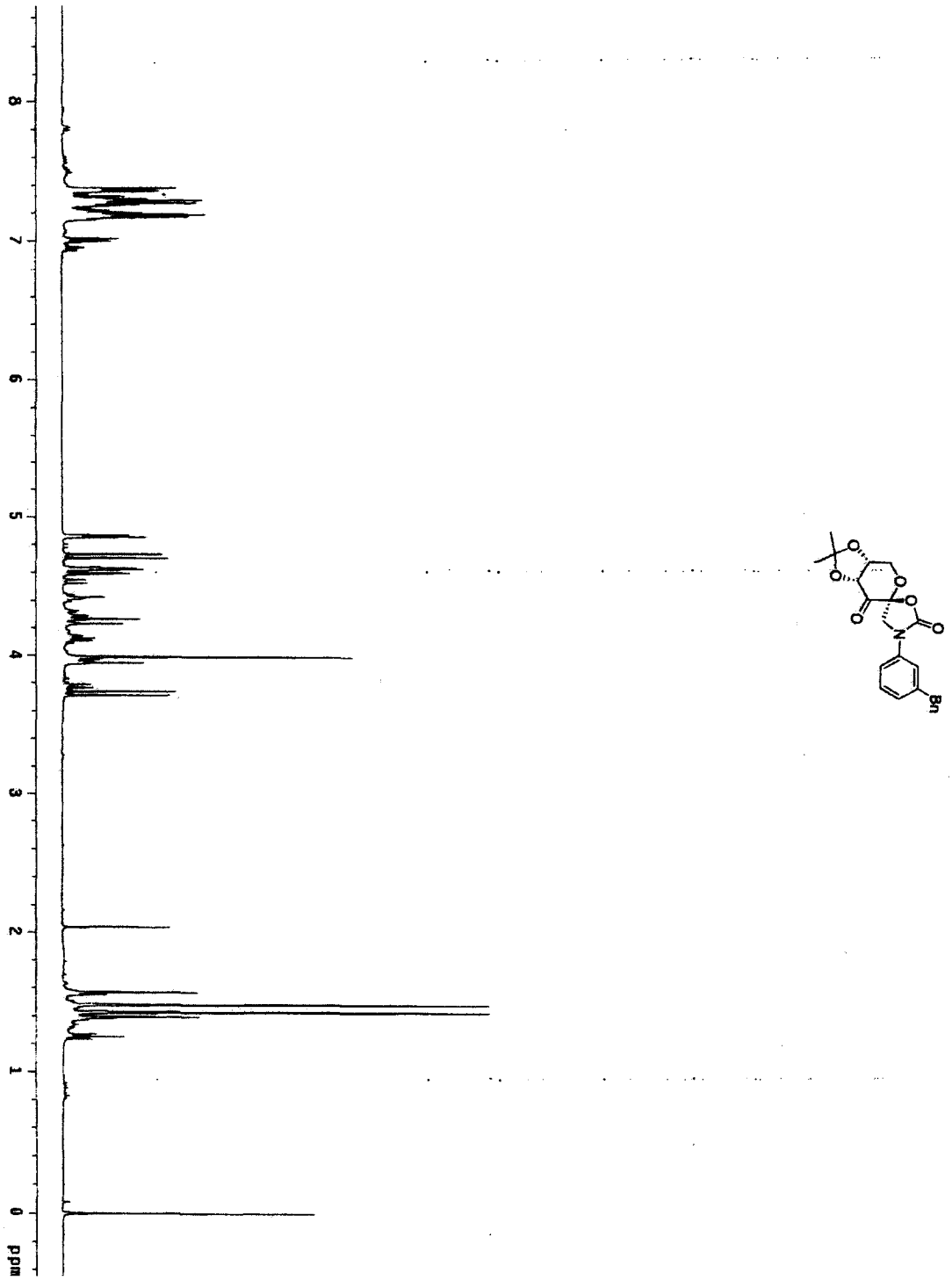

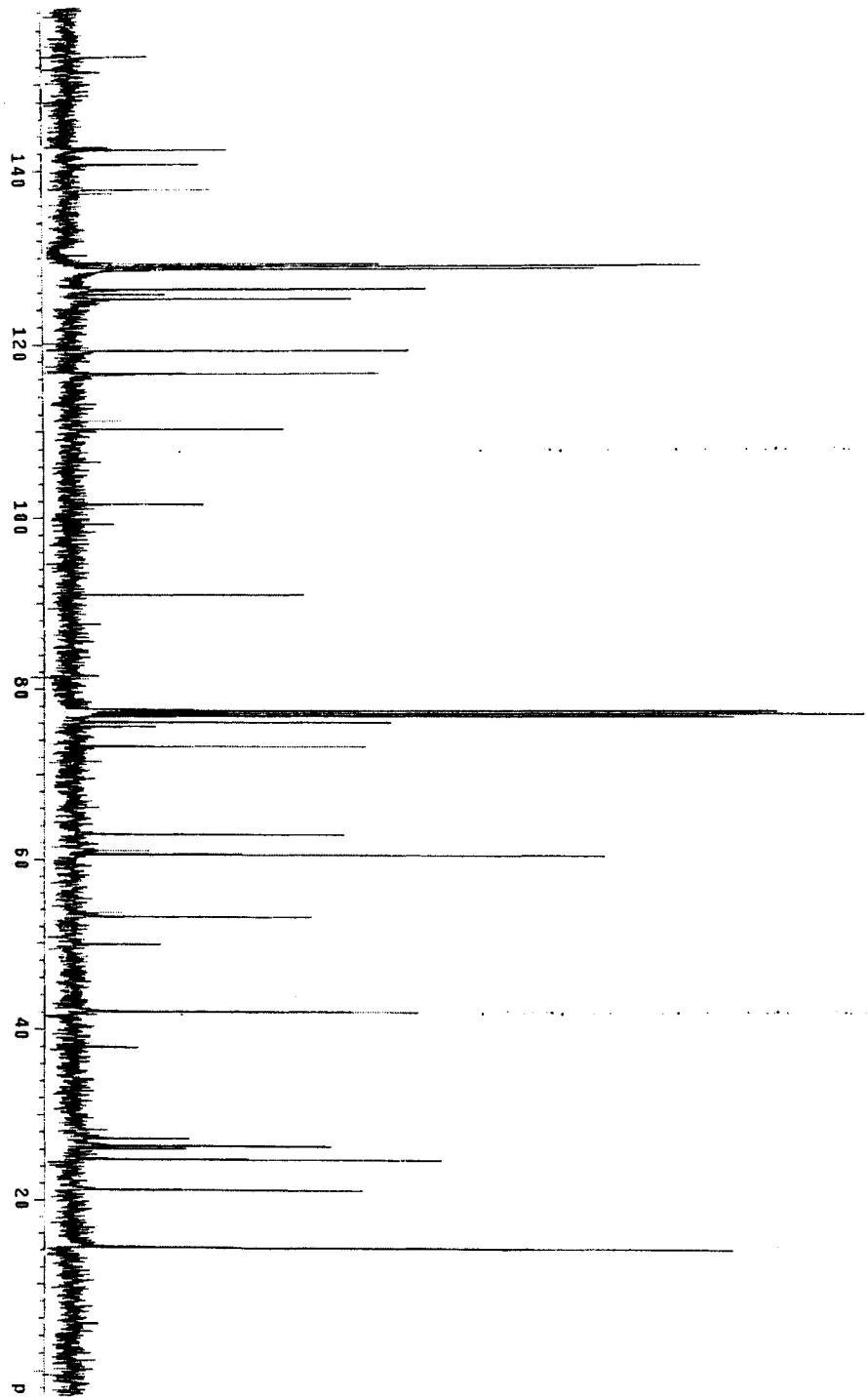

Tue Feb 24 16:00:13 2004
FIND PEAKS:
Spectrum: DLG-IX-50
Region: 4000.00 400.00
Absolute threshold: 92.095
Sensitivity: 26
Peak list:

Position:	1758.92	Intensity:	46.563
Position:	986.24	Intensity:	54.728
Position:	1224.02	Intensity:	60.491
Position:	1493.33	Intensity:	60.960
Position:	1091.81	Intensity:	62.167
Position:	752.75	Intensity:	62.356
Position:	1452.20	Intensity:	67.448
Position:	1401.84	Intensity:	69.124

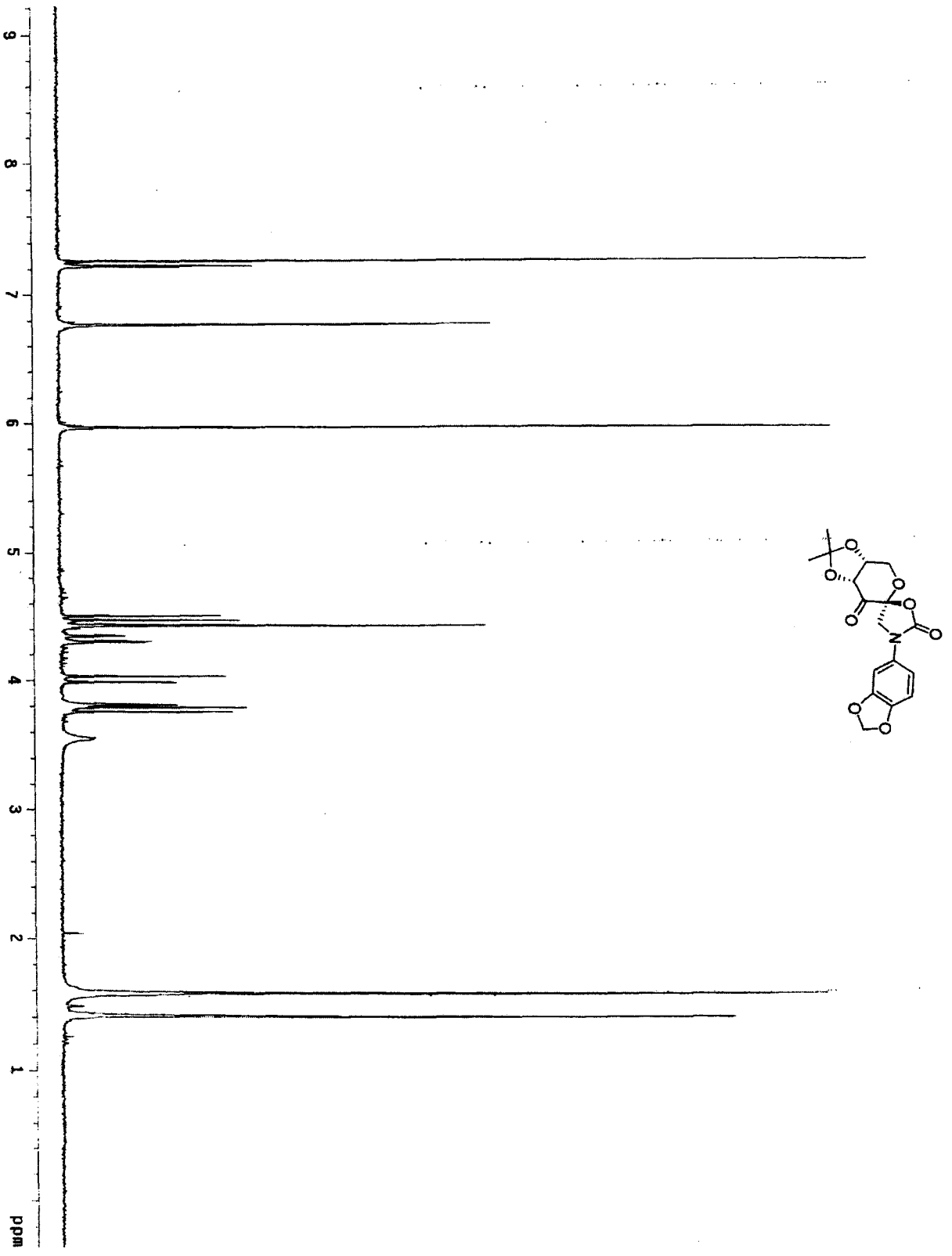

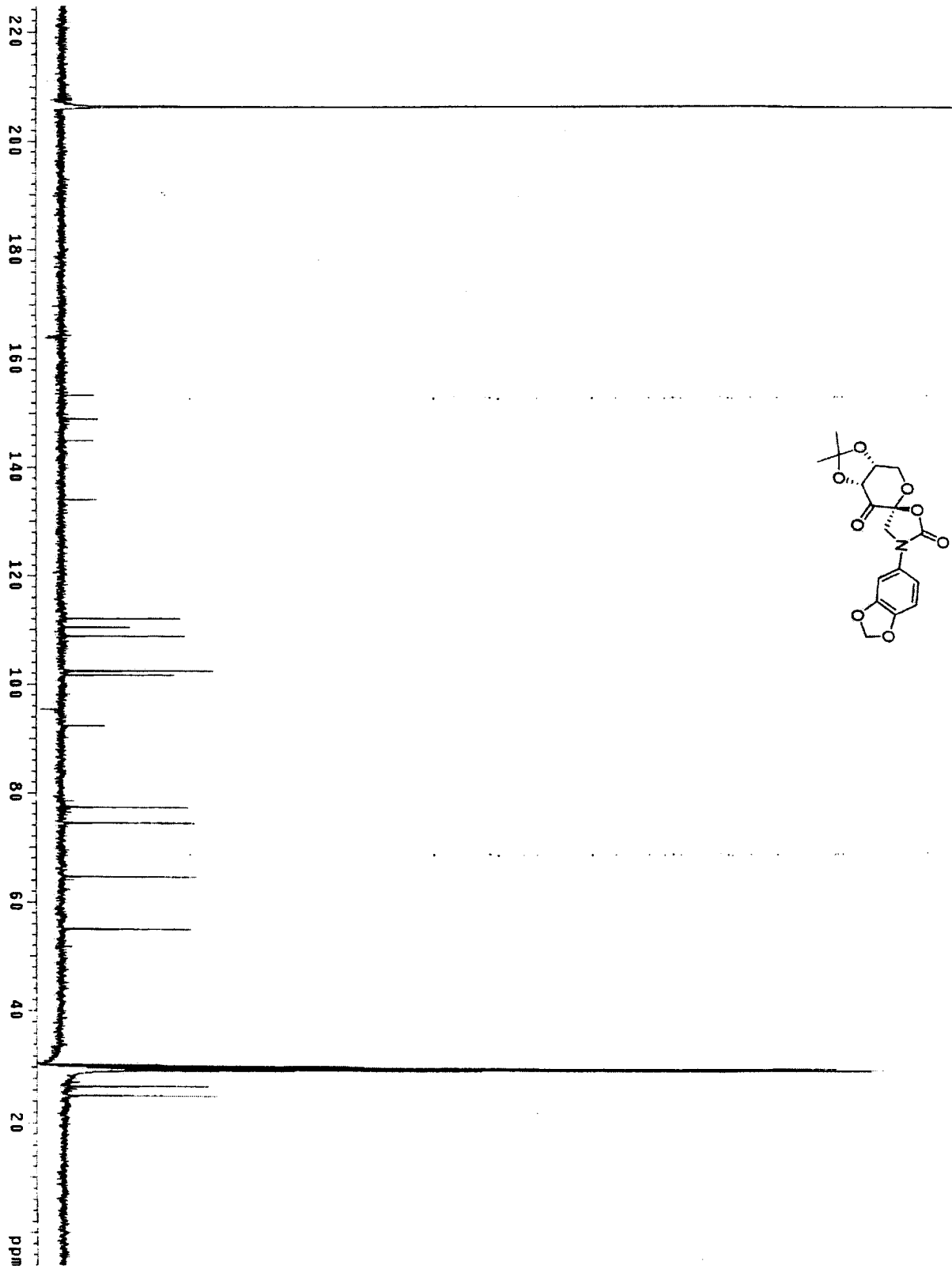

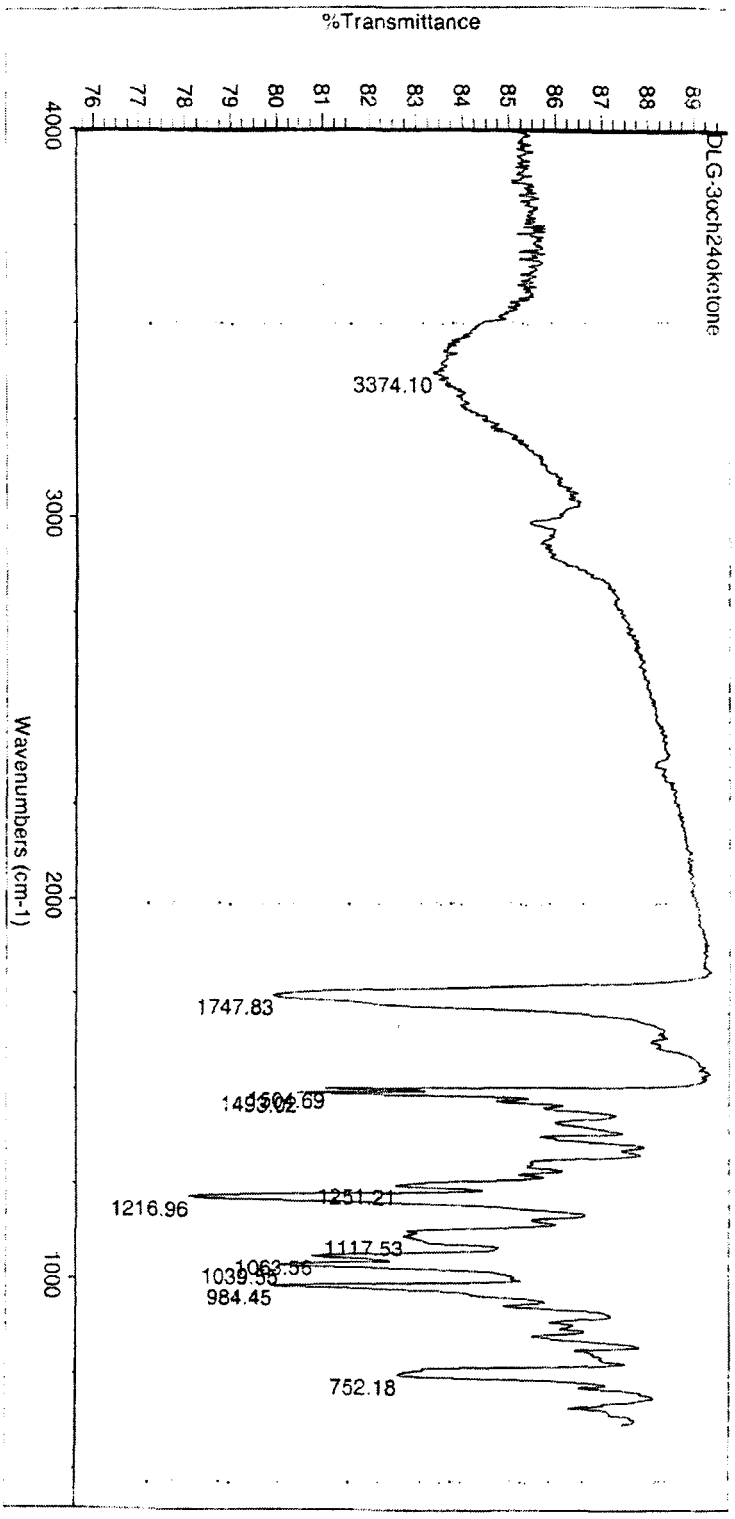

Thu Sep 02 15:43:20 2004
FIND PEAKS:
Spectrum: DLG-3och24oketone
Region: 4000.00 400.00
Absolute threshold: 83.712
Sensitivity: 40
Peak list:

Position:	1216.96	Intensity:	78.075
Position:	1747.83	Intensity:	79.932
Position:	984.45	Intensity:	79.909
Position:	1039.55	Intensity:	80.052
Position:	1493.02	Intensity:	80.470
Position:	1063.56	Intensity:	80.801
Position:	1504.69	Intensity:	81.064
Position:	1251.21	Intensity:	82.587

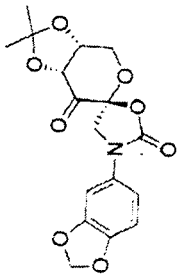

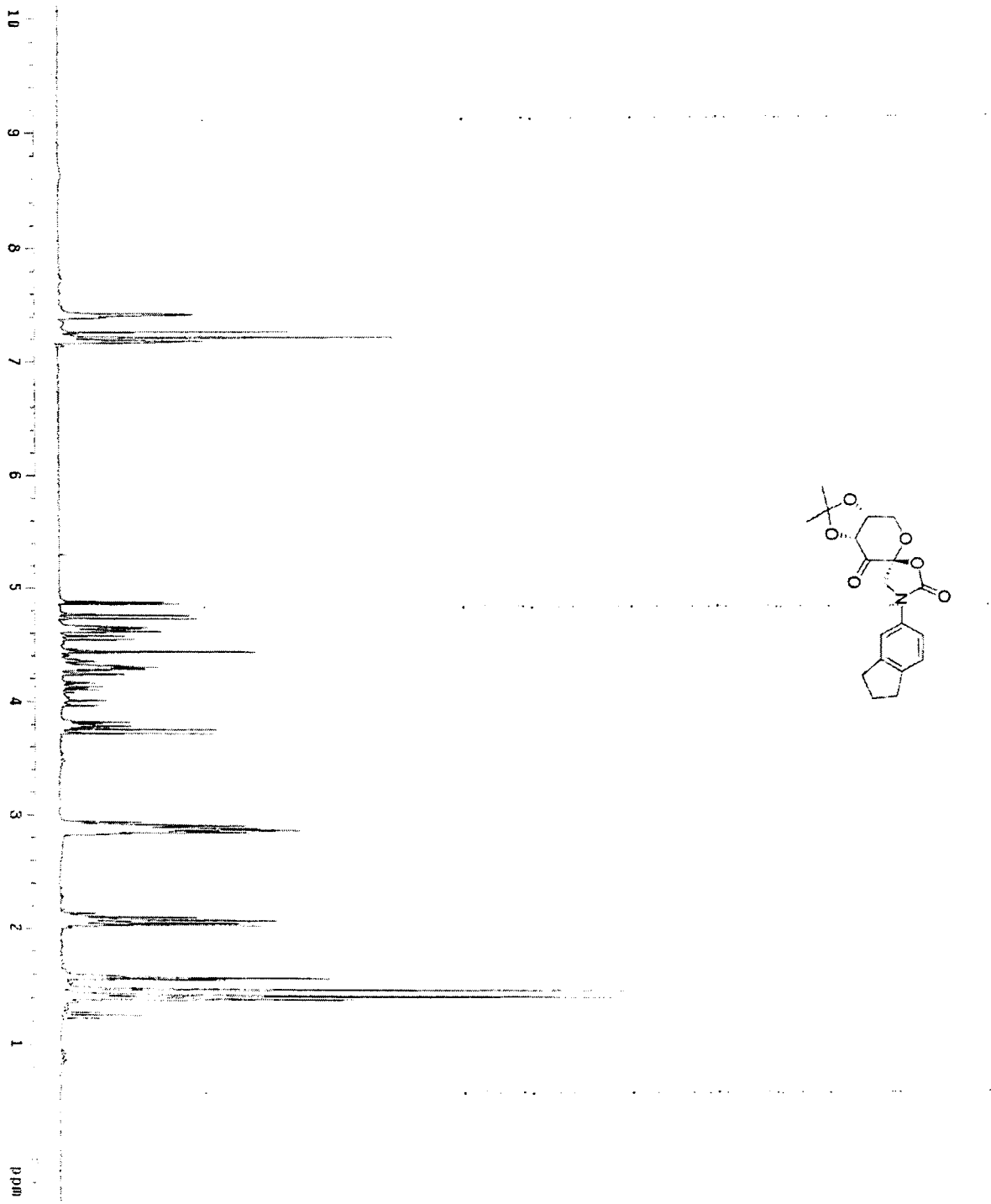

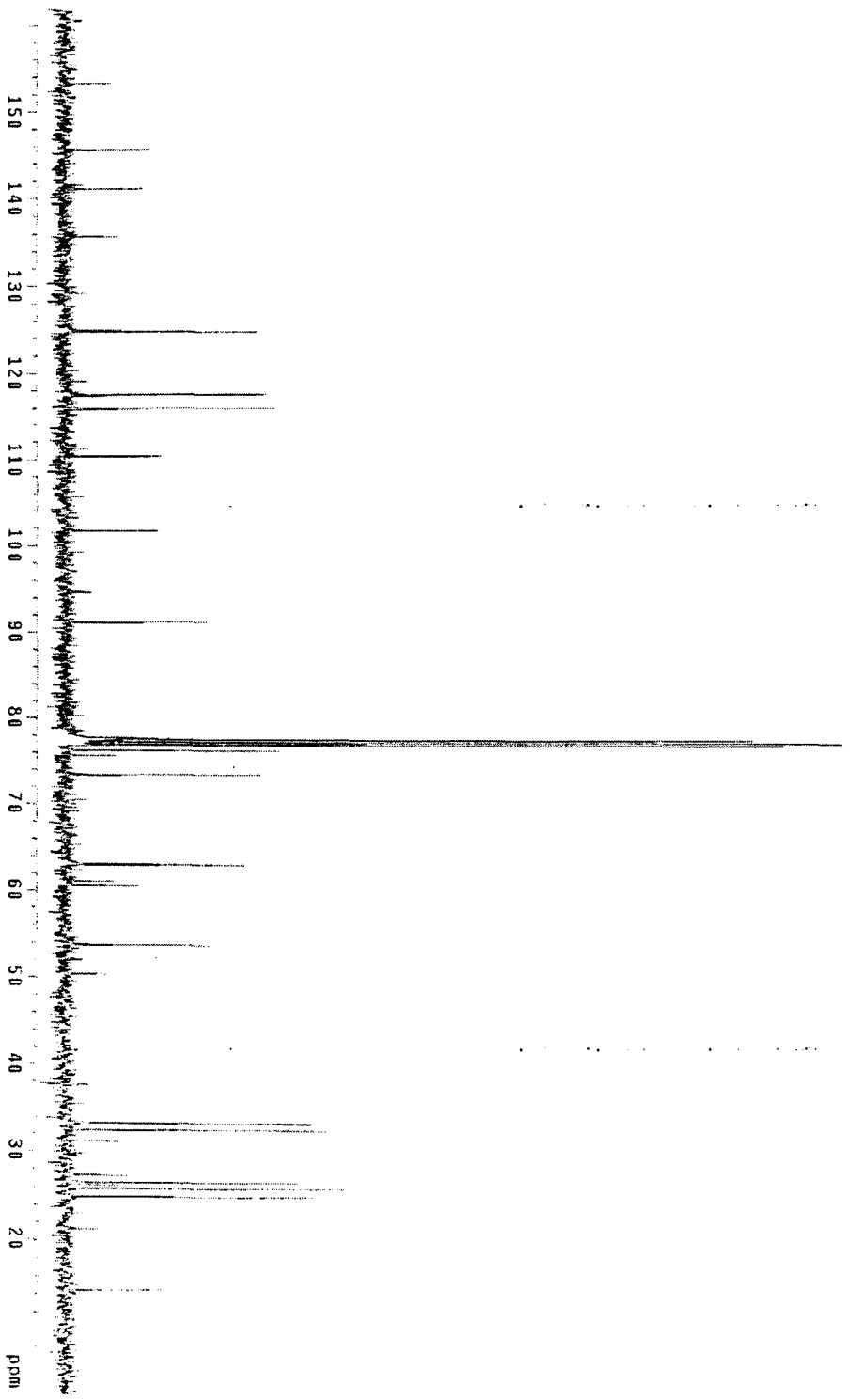

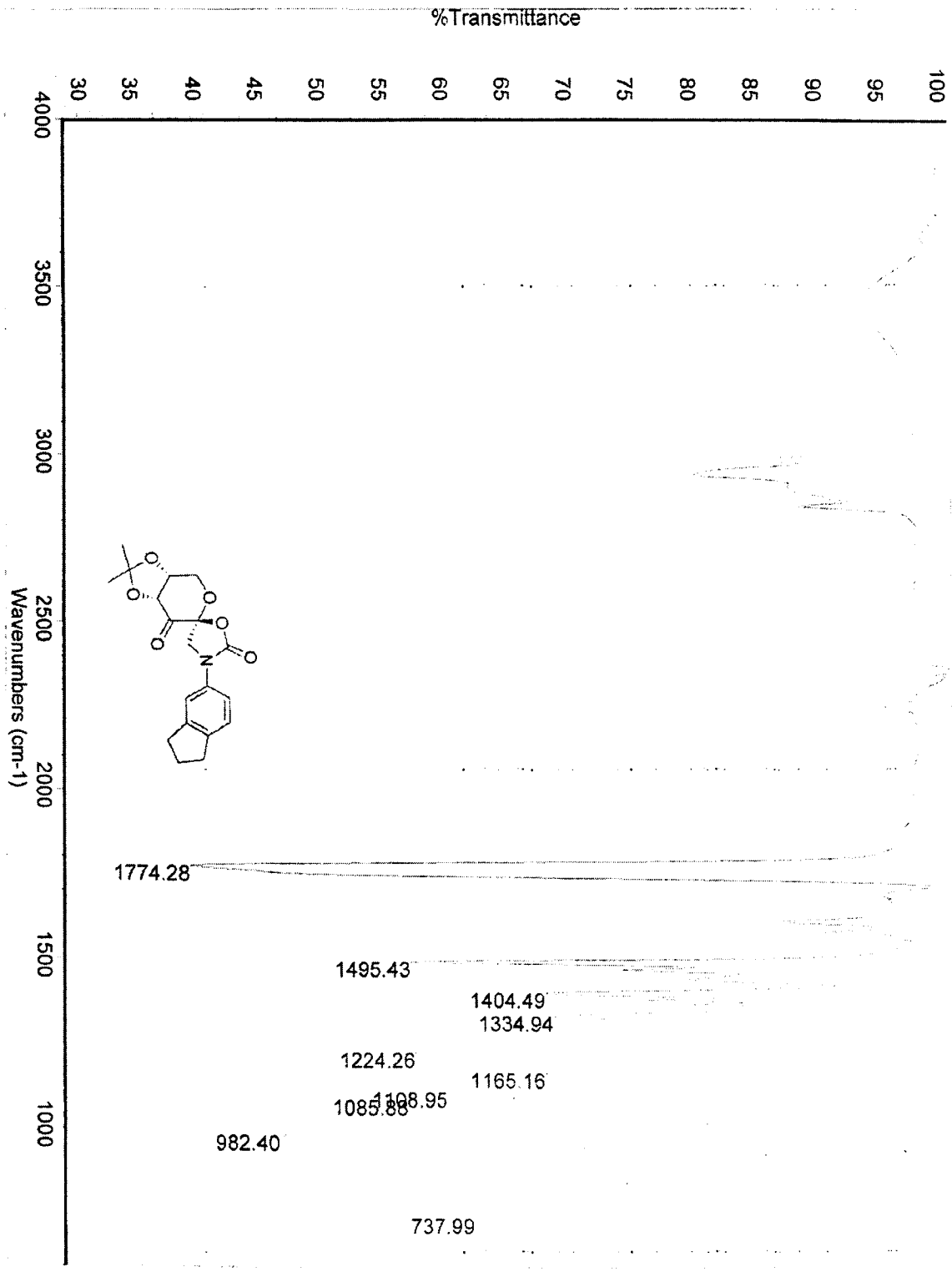

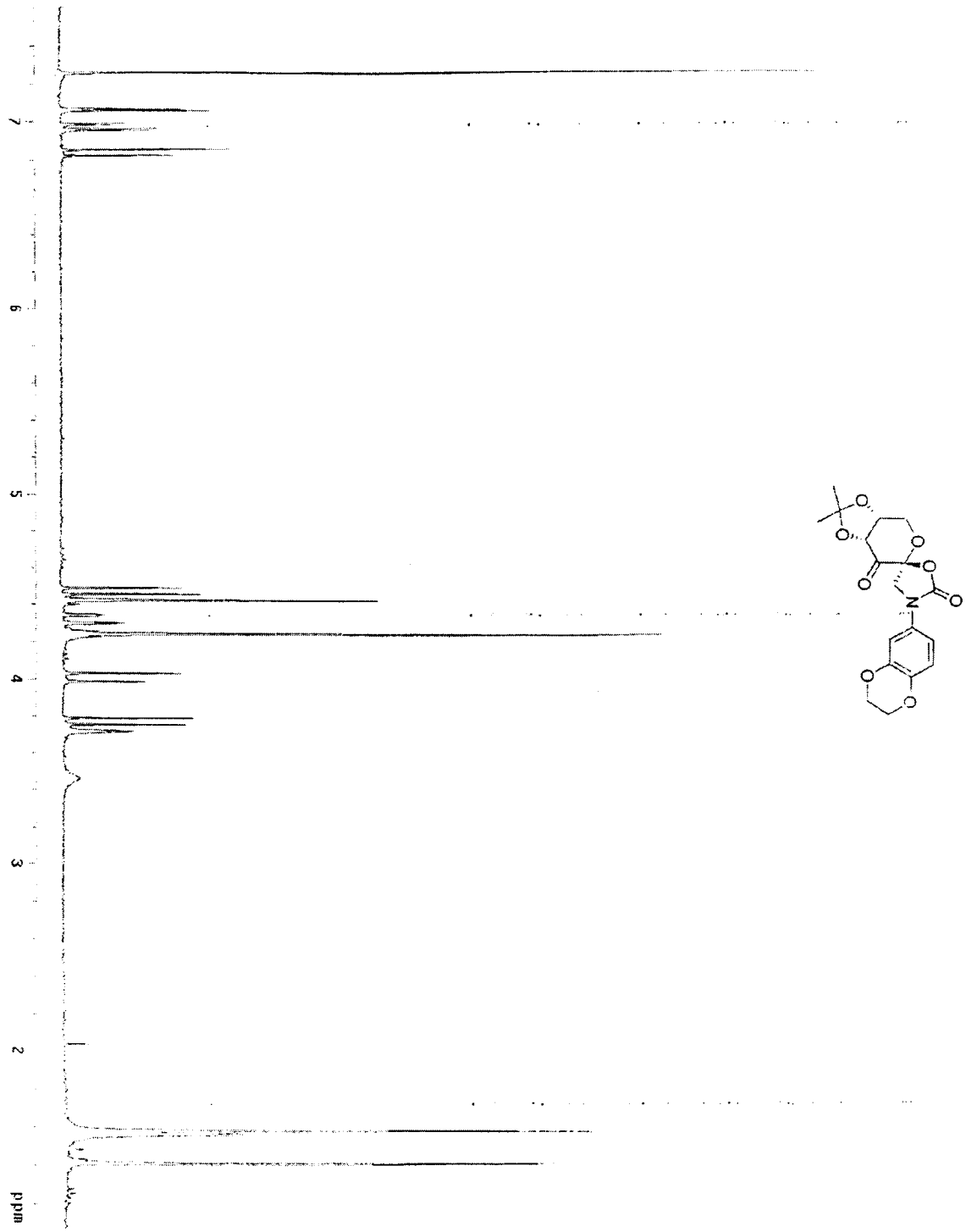

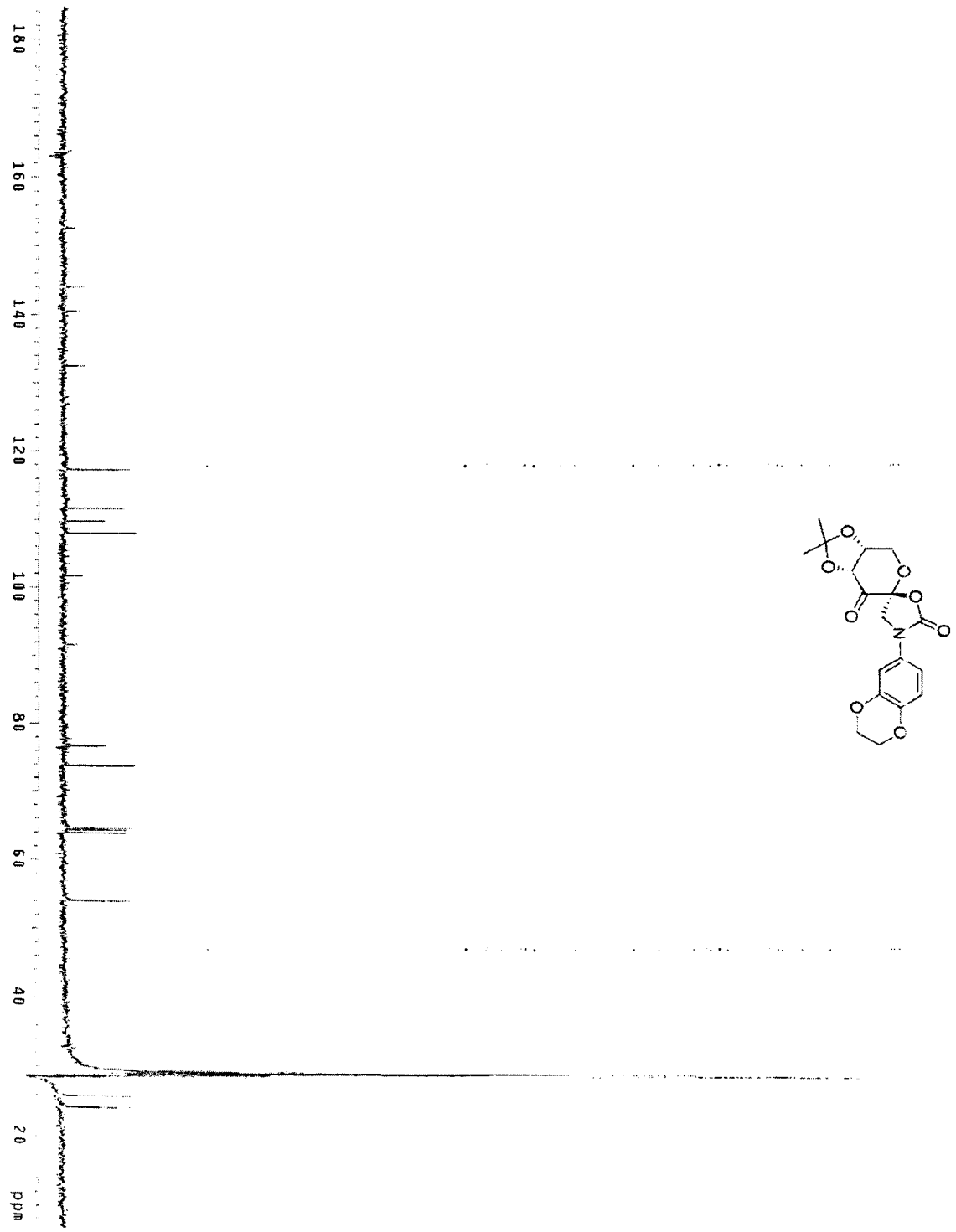

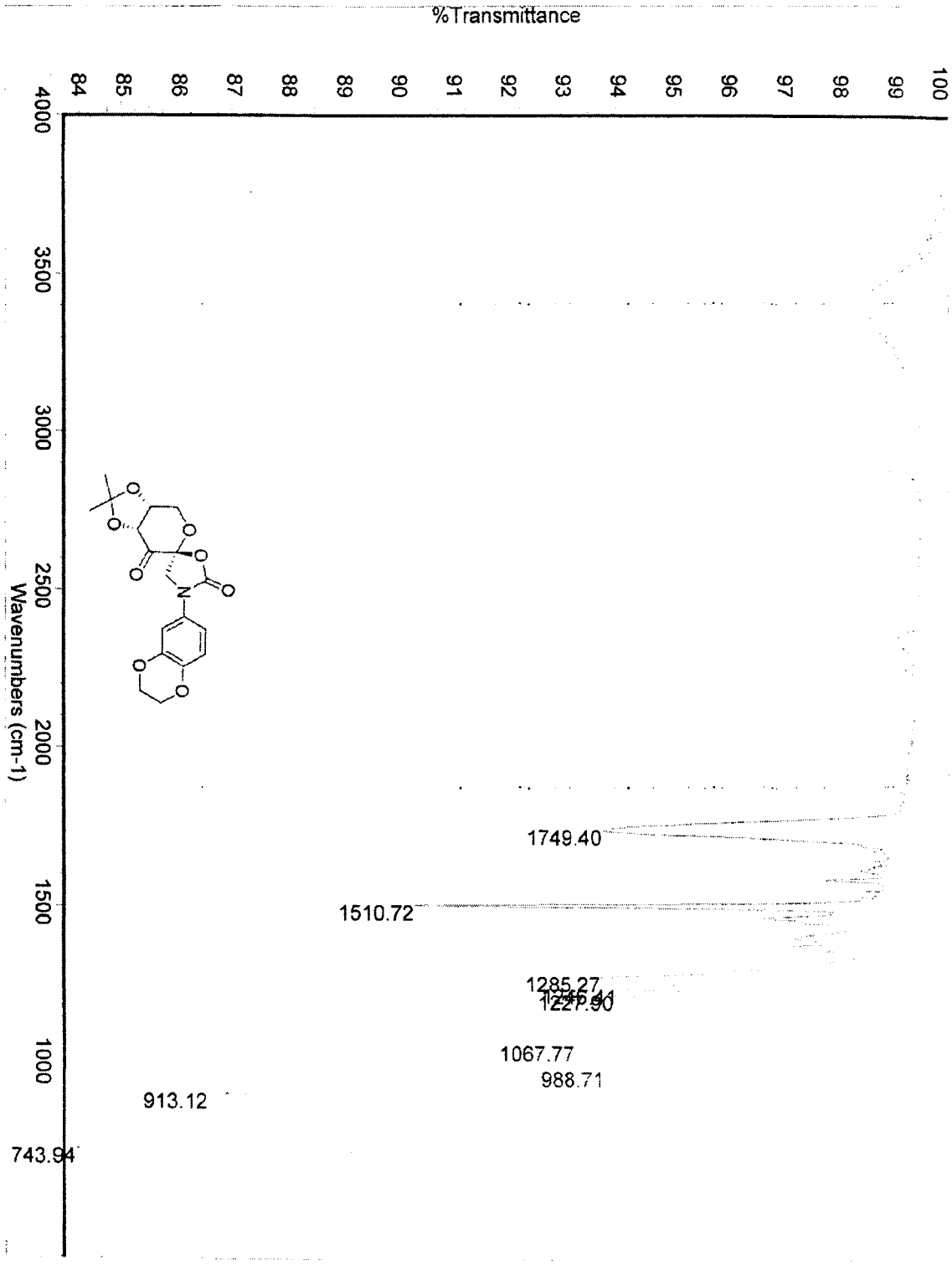

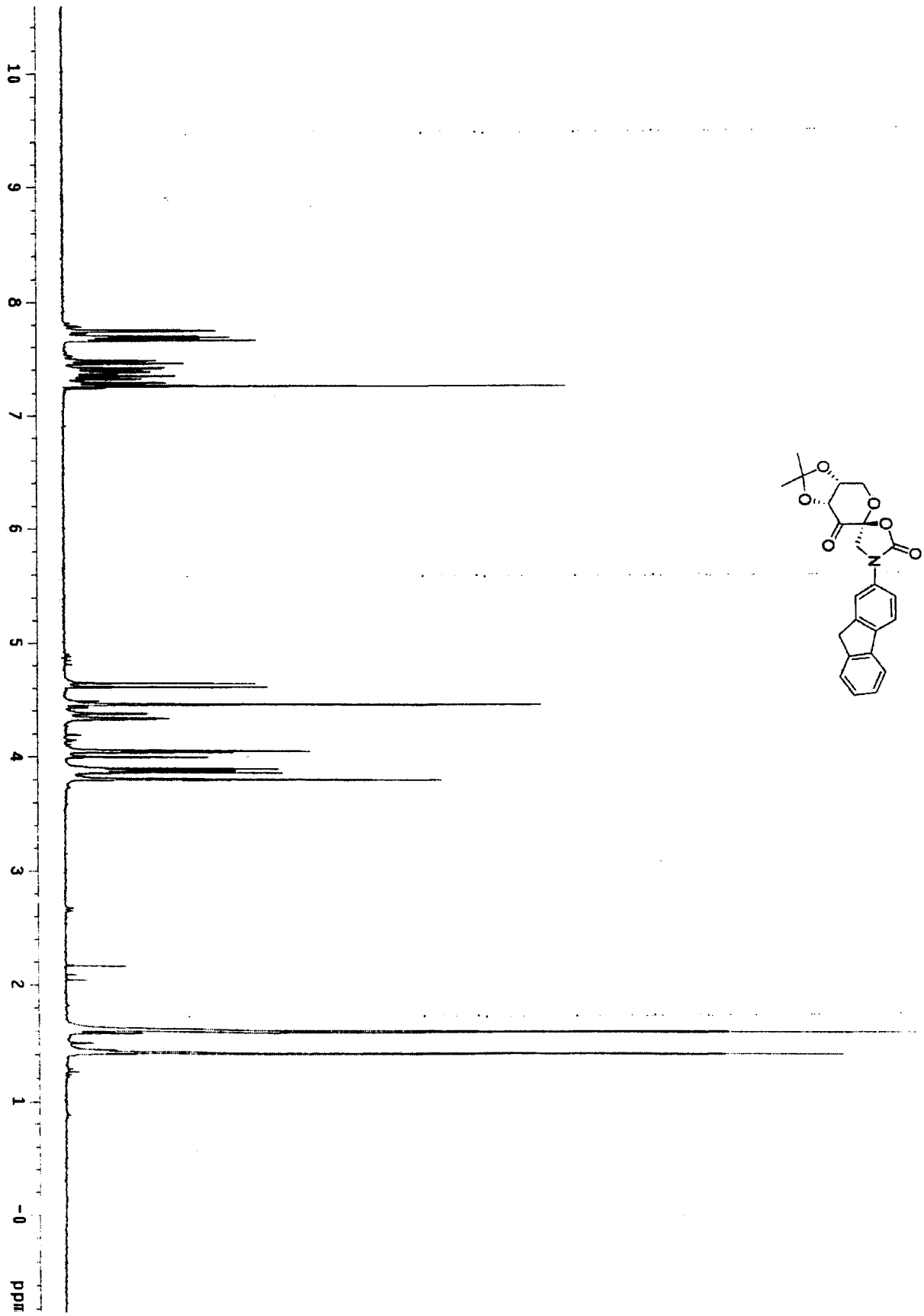

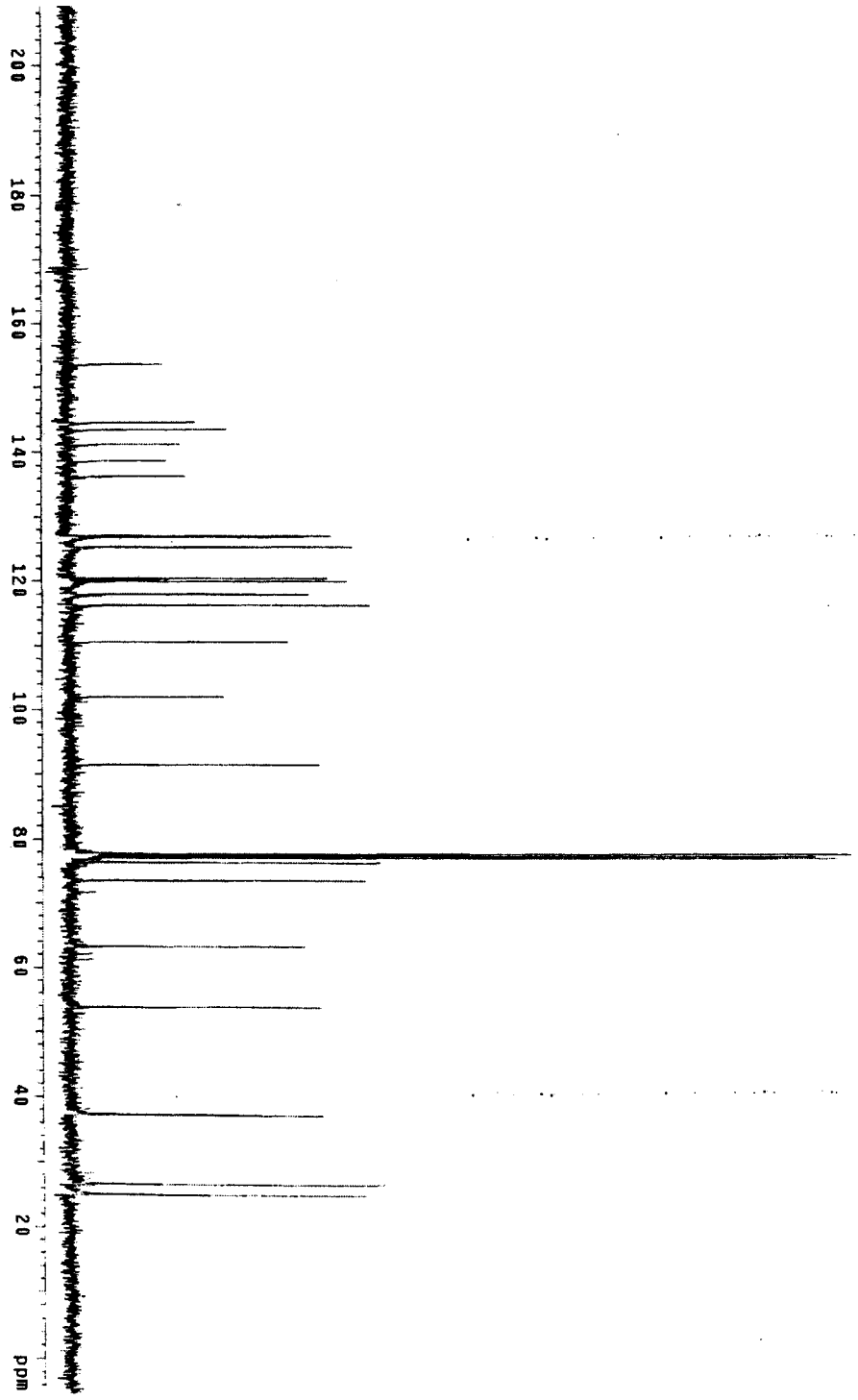

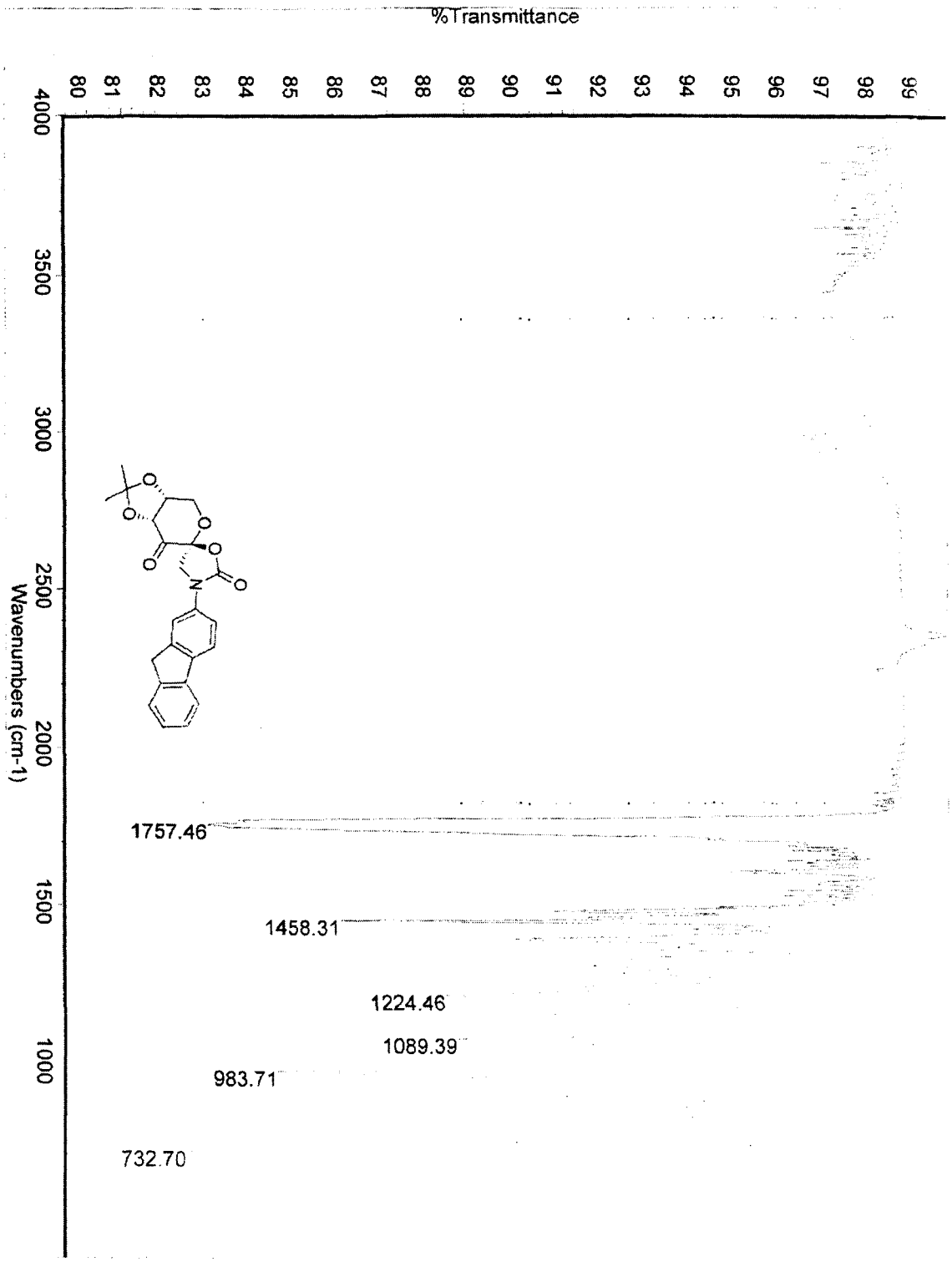

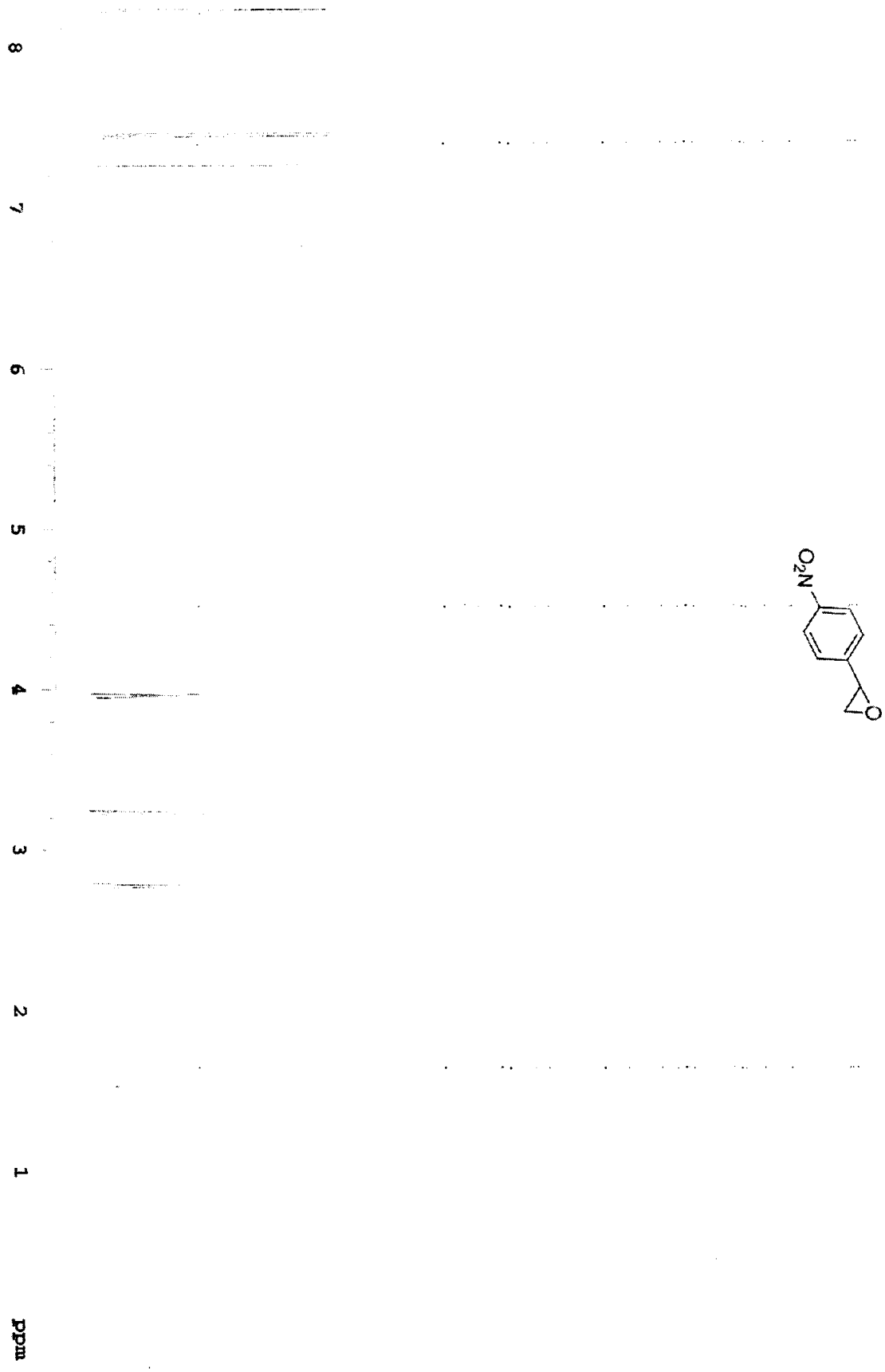

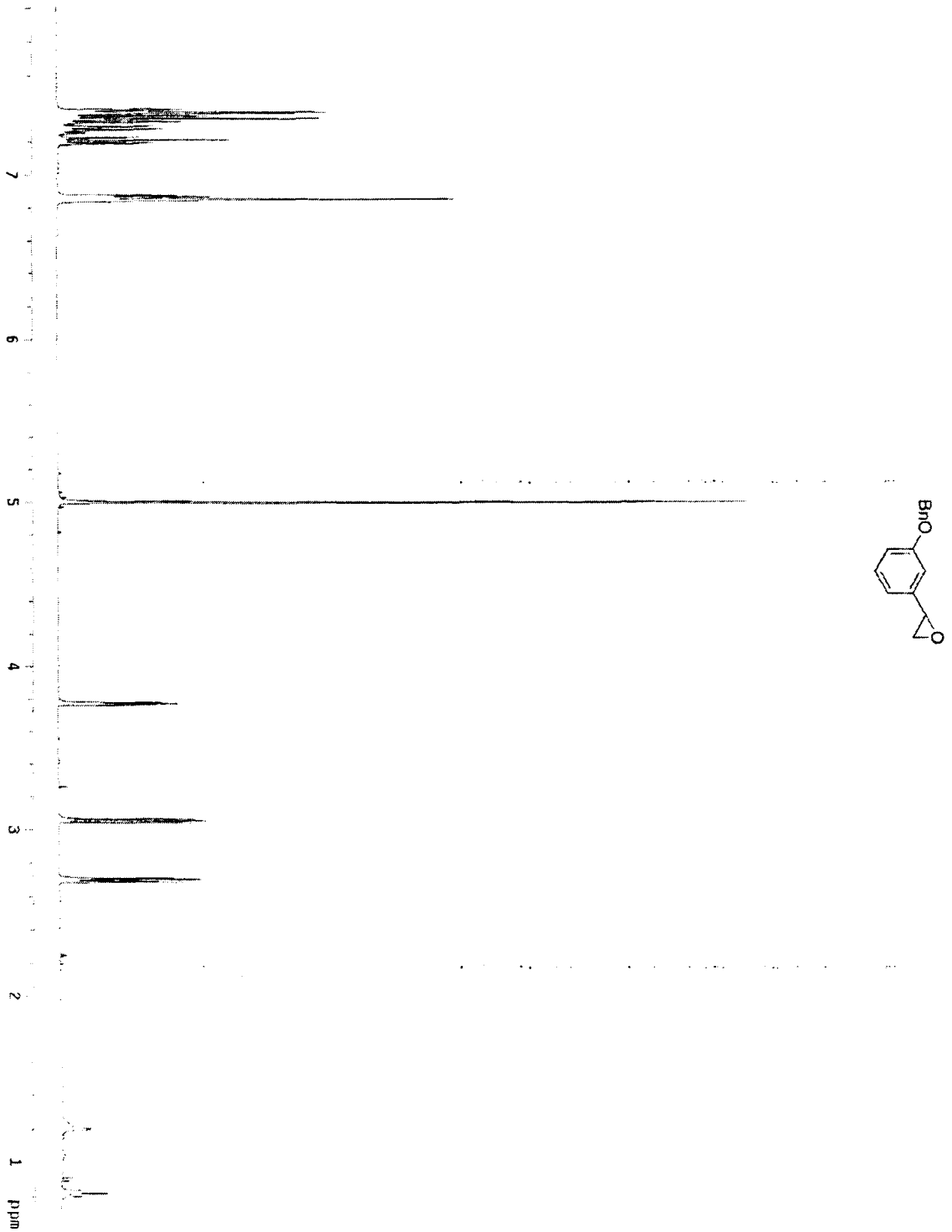

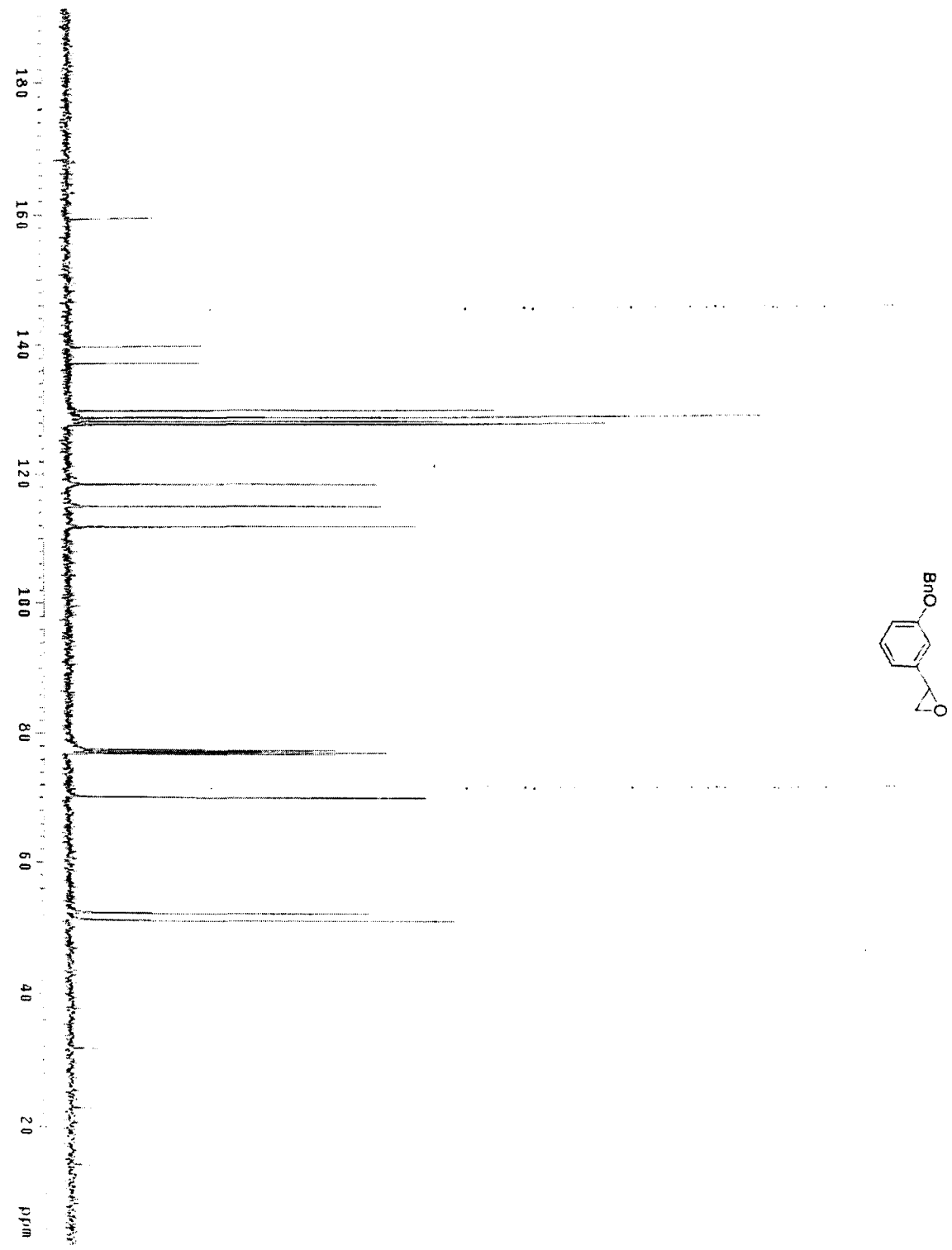

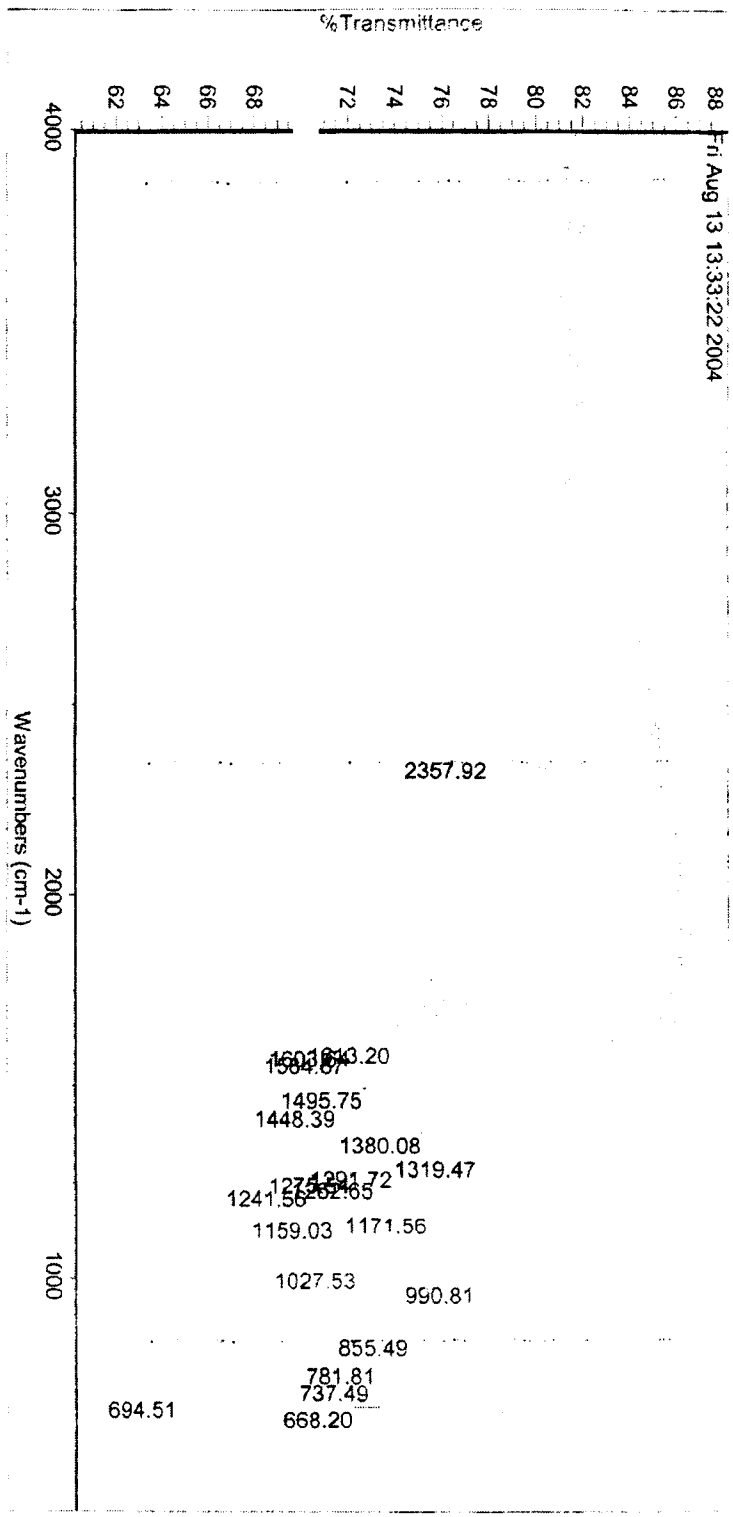

Fri Aug 13 13:36:44 2004
FIND PEAKS:
Spectrum: Fri Aug 13 13:33:22 2004
Region: 4000.00 400.00
Absolute threshold: 78.674
Sensitivity: 50
Peak list:

Position:	694.51	Intensity:	64.549
Position:	1241.56	Intensity:	70.228
Position:	1159.03	Intensity:	71.330
Position:	1448.39	Intensity:	71.485
Position:	1584.87	Intensity:	71.887
Position:	1275.54	Intensity:	72.066
Position:	1603.64	Intensity:	72.107
Position:	668.20	Intensity:	72.160

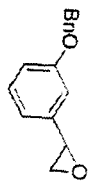

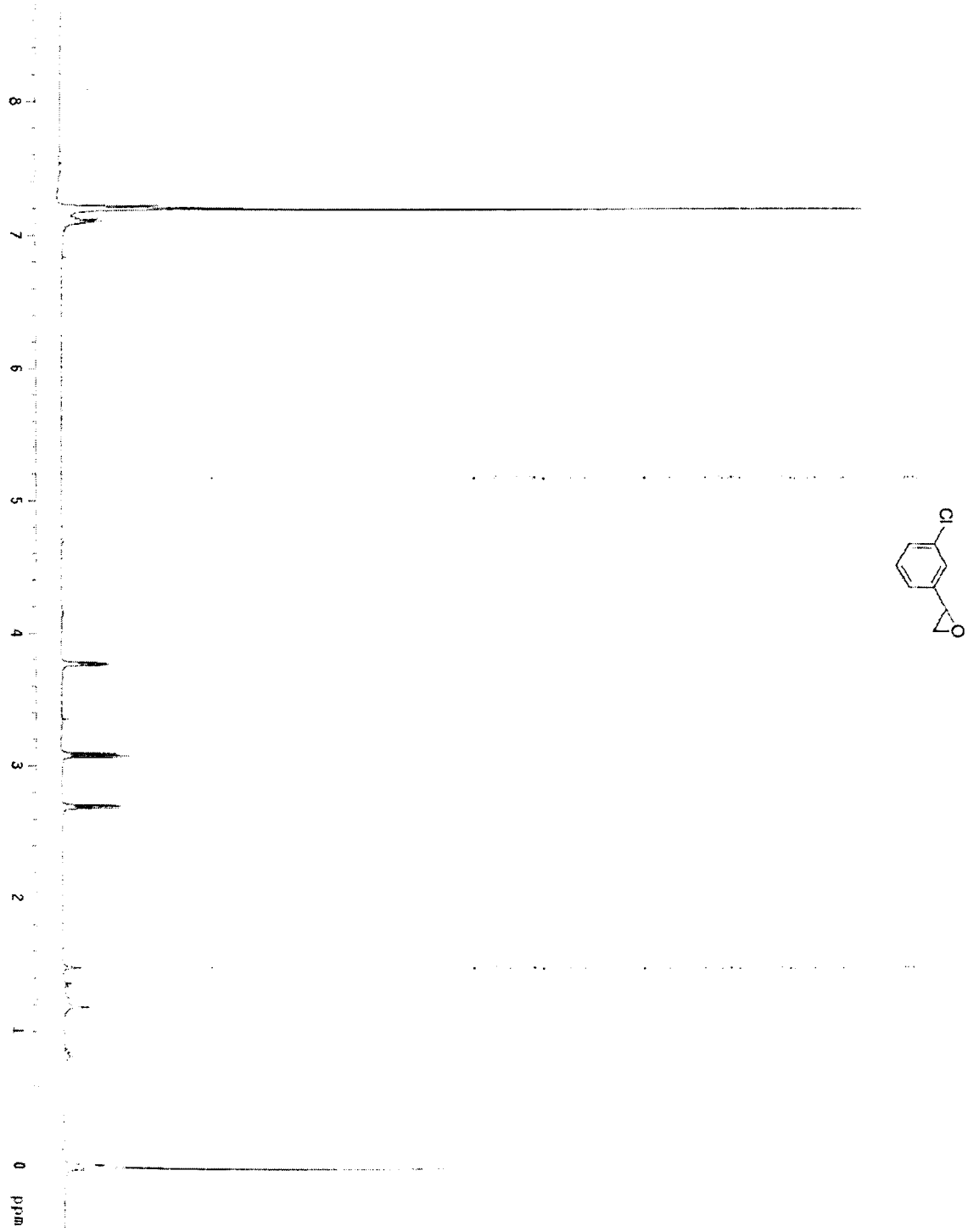

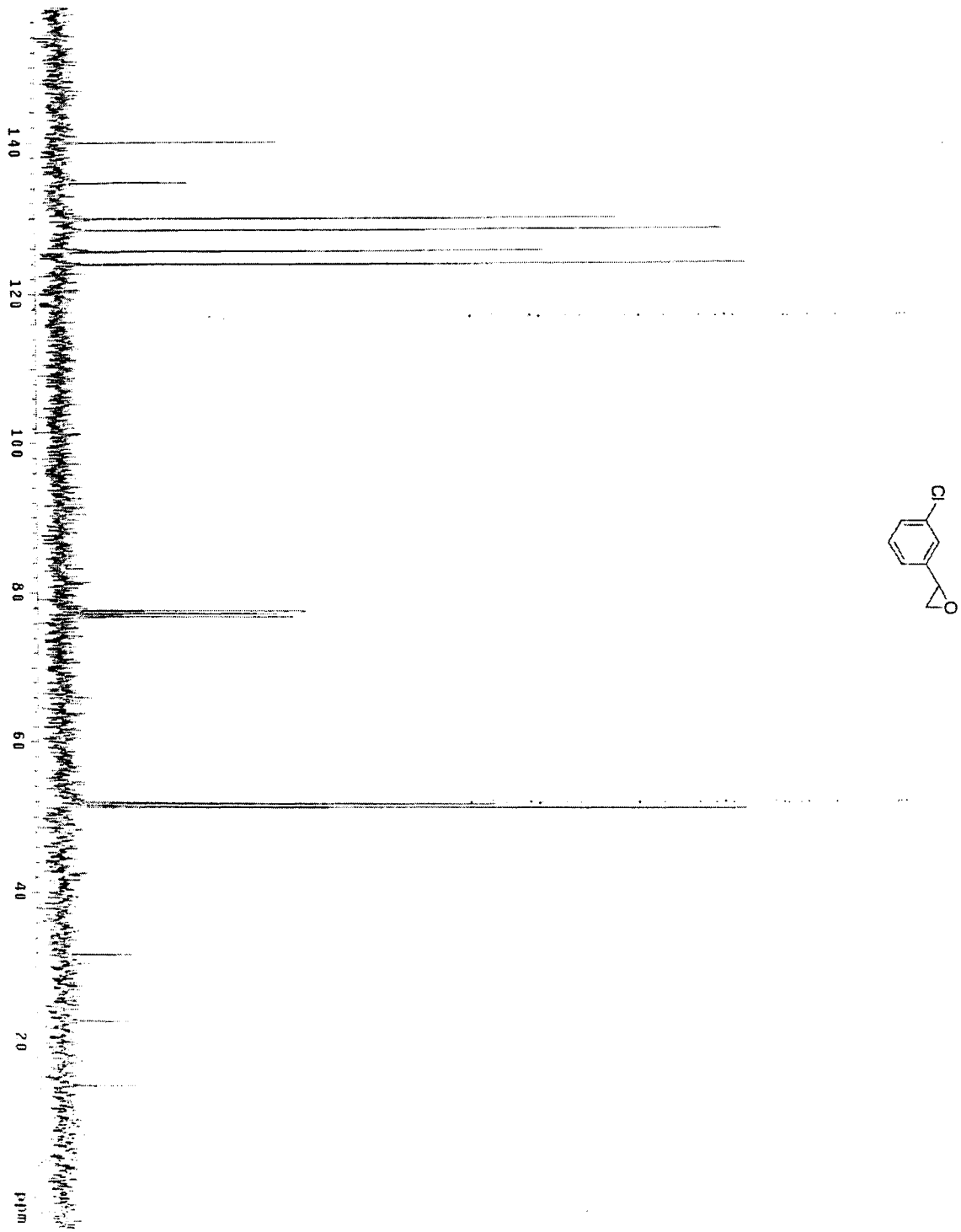

Tue Mar 04 19:35:51 2003
FIND PEAKS:

Spectrum: DLG-V-32
Region: 4000.00 400.00
Absolute threshold: 60.824
Sensitivity: 6
Peak list:

Position:	785.28	Intensity:	5.206
Position:	691.48	Intensity:	7.402
Position:	880.10	Intensity:	12.127
Position:	1434.77	Intensity:	25.549
Position:	1602.19	Intensity:	32.063
Position:	1481.93	Intensity:	32.755
Position:	1200.09	Intensity:	34.023
Position:	1079.40	Intensity:	39.490

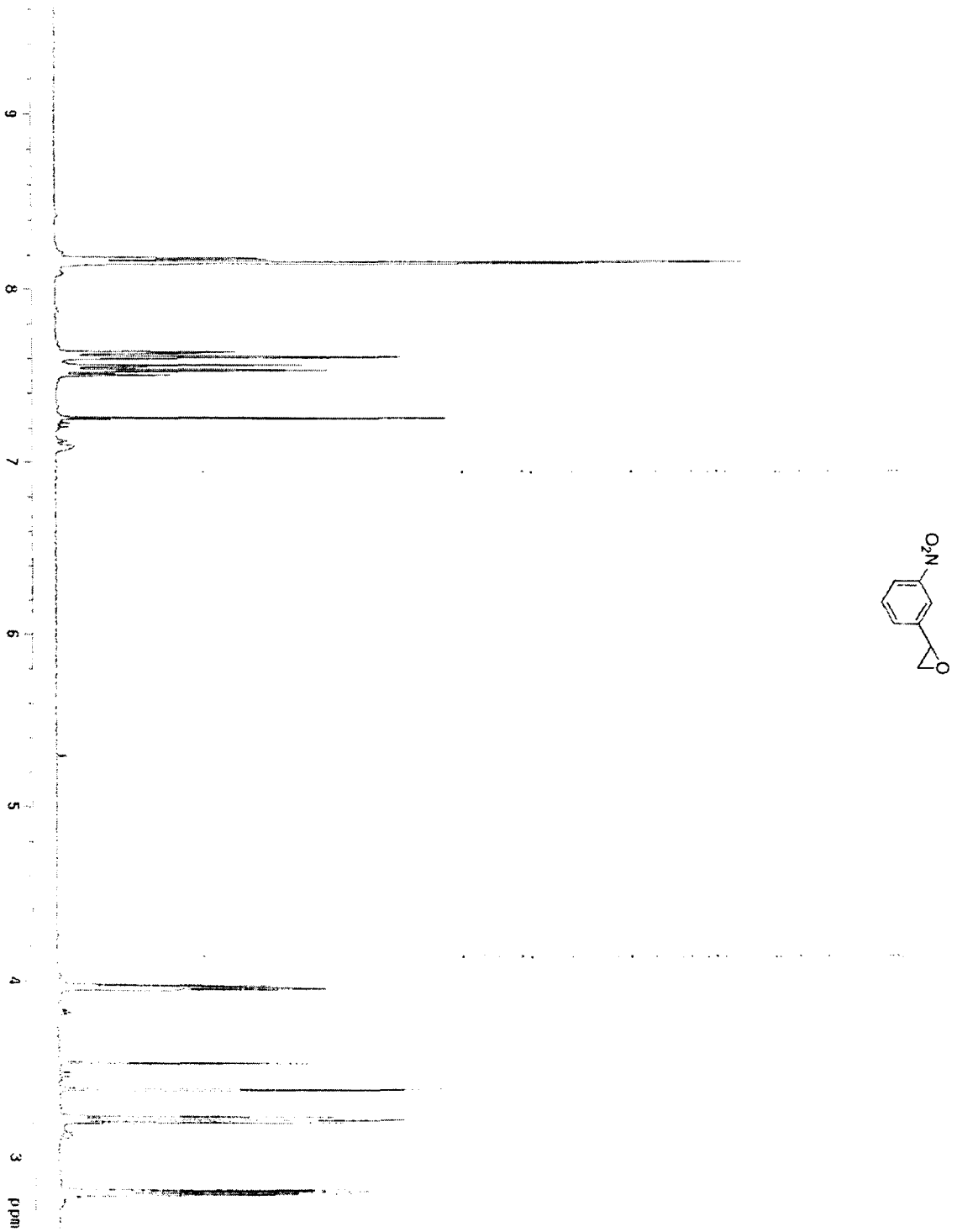

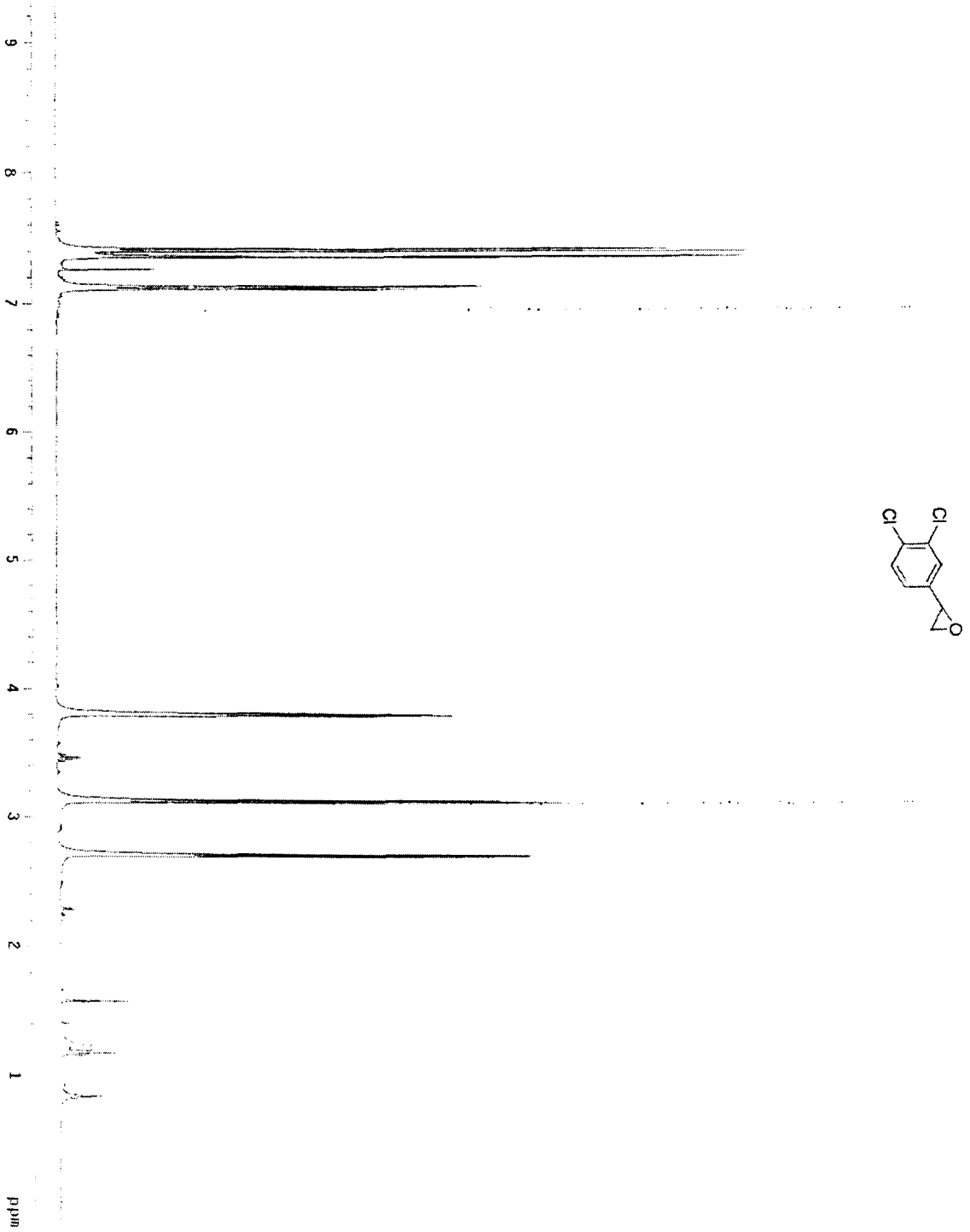

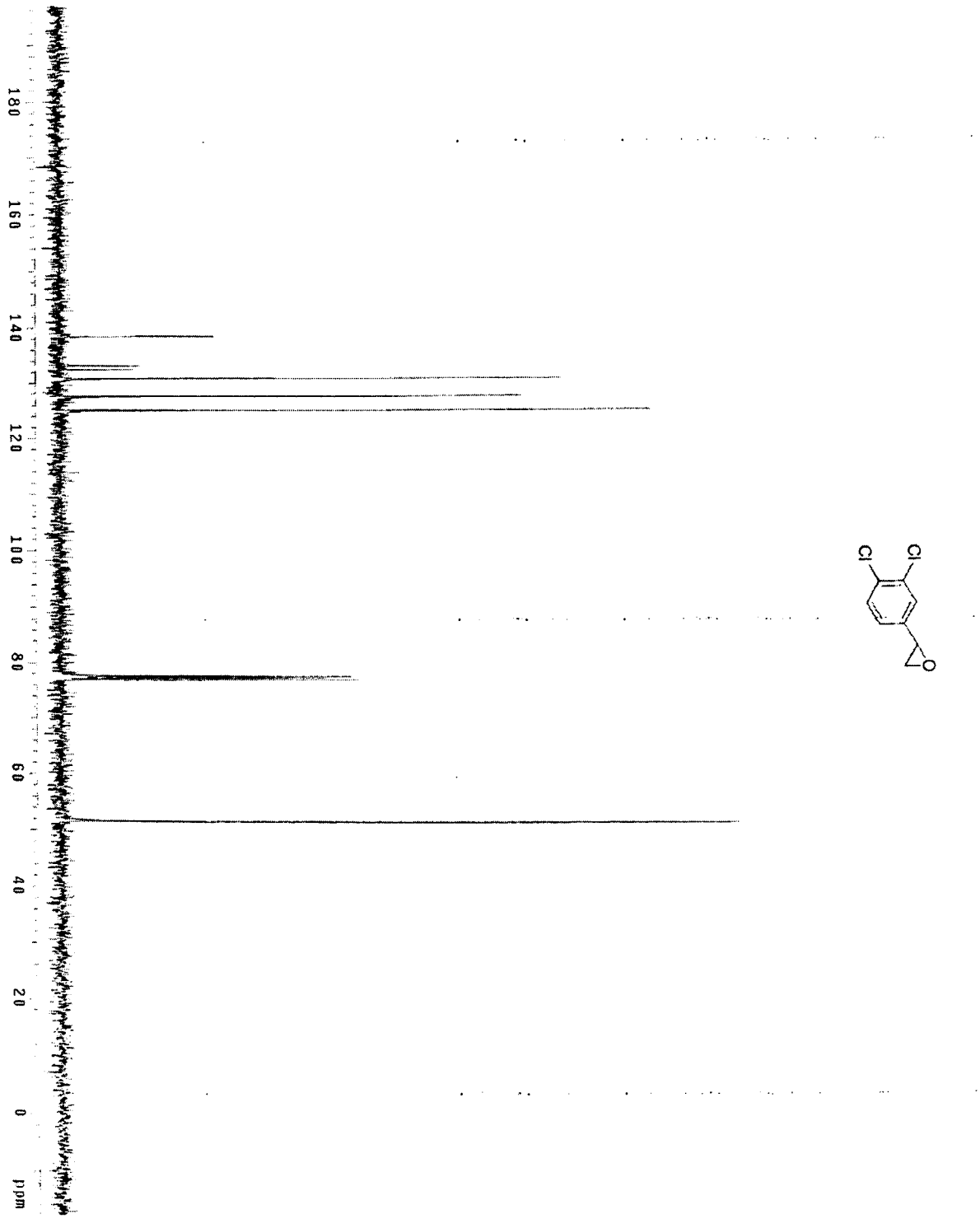

Tue Jul 06 13:49:56 2004 (GMT-06:00)
FIND PEAKS:
Spectrum: Tue Jul 06 13:42:29 2004 (GMT-06:00)
Region: 4000.00 400.00
Absolute threshold: 61.507
Sensitivity: 50
Peak list:

Position:	820.12	Intensity:	54.092
Position:	676.51	Intensity:	55.286
Position:	690.30	Intensity:	56.126
Position:	1030.34	Intensity:	56.528
Position:	1472.36	Intensity:	56.727
Position:	880.86	Intensity:	58.415
Position:	1131.94	Intensity:	58.806

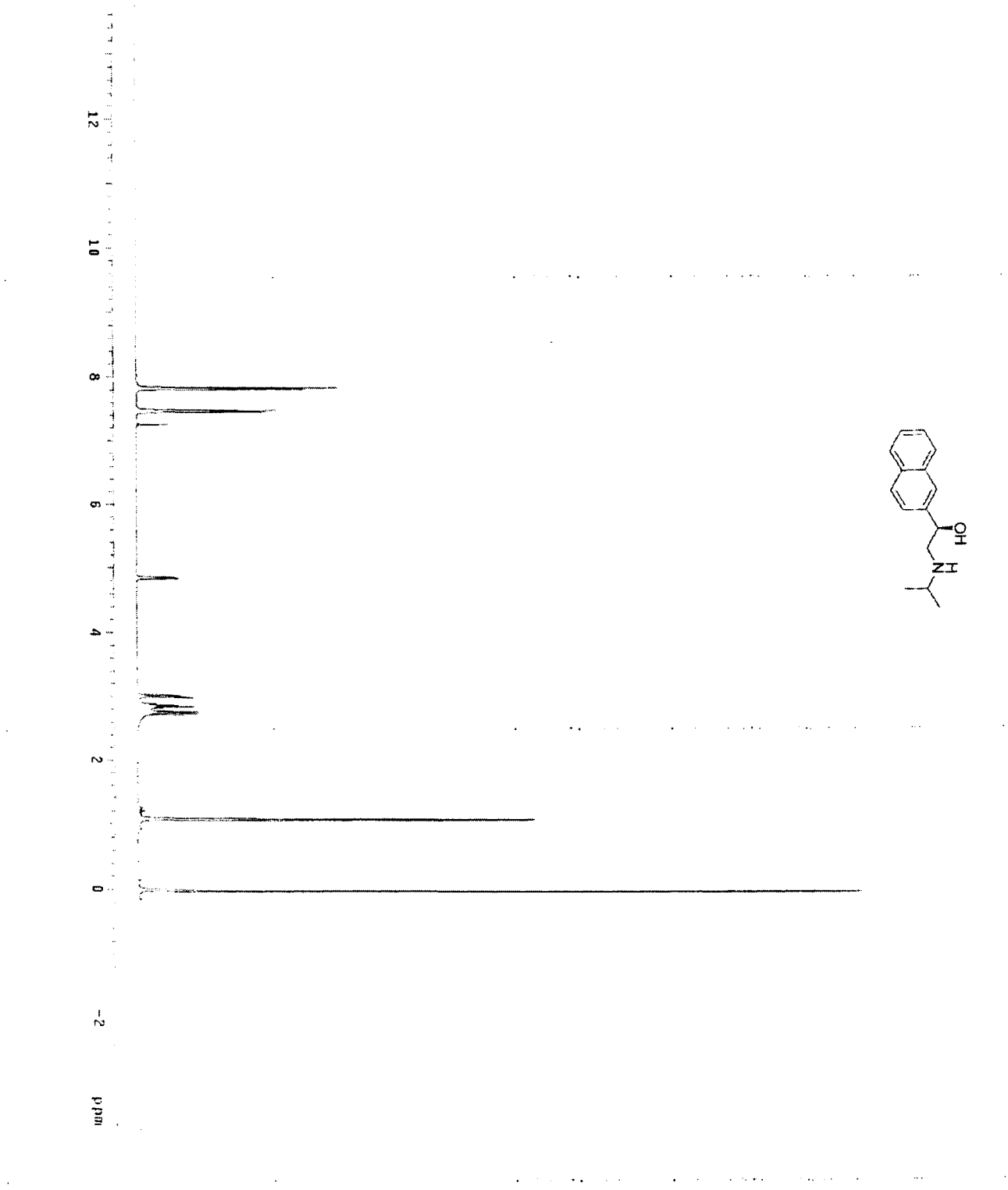

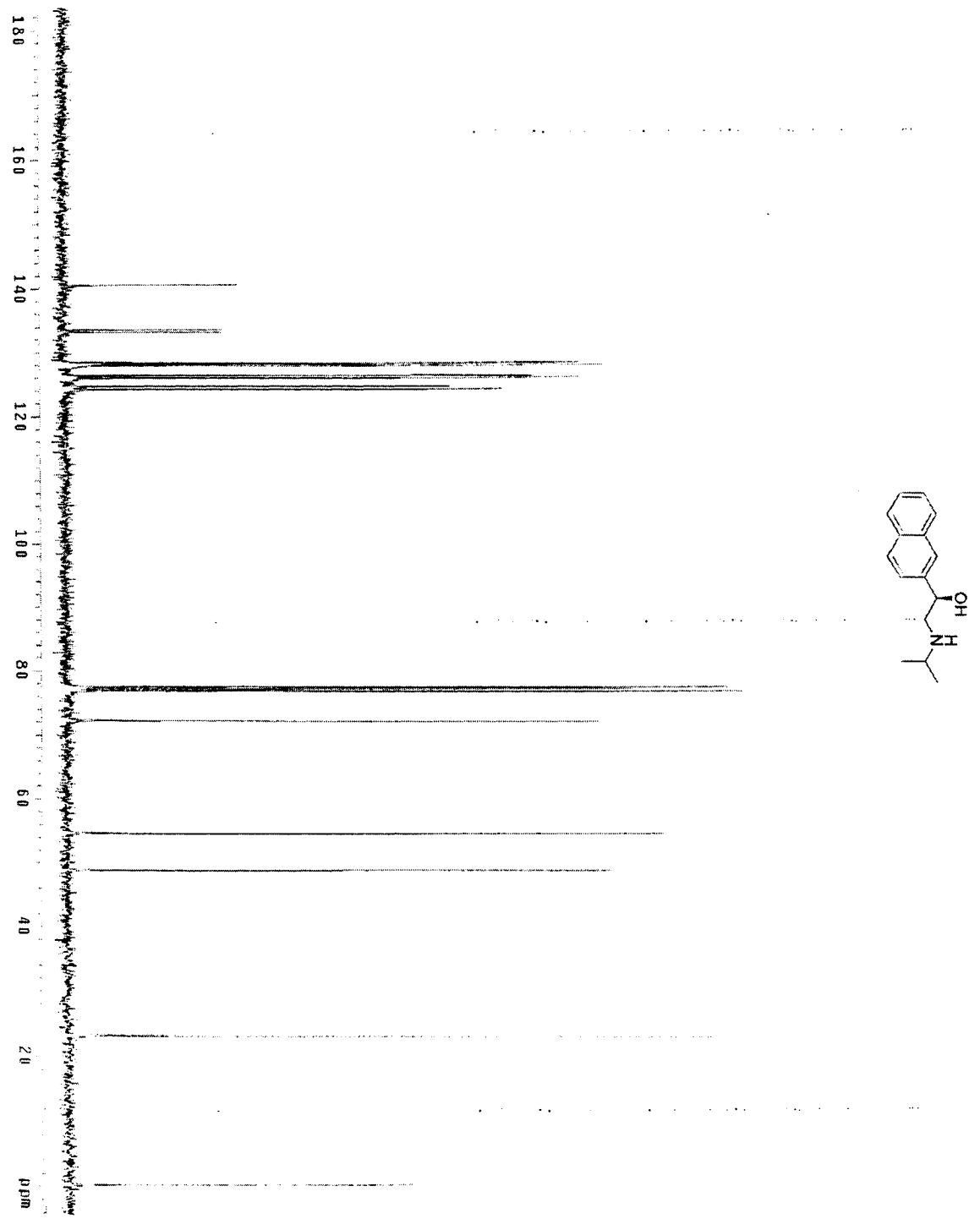

Wed Mar 02 09:29:35 2005
FIND PEAKS:

Spectrum: DLG-pronethalol
Region: 4000.00 400.00
Absolute threshold: 79.140
Sensitivity: 50
Peak list:

Position:	1069.75	Intensity:	65.558
Position:	740.40	Intensity:	65.851
Position:	746.34	Intensity:	66.039
Position:	1084.77	Intensity:	66.693
Position:	822.74	Intensity:	70.319
Position:	2964.10	Intensity:	71.820
Position:	2832.74	Intensity:	72.580
Position:	3054.37	Intensity:	77.161

BIOGRAPHY

David Lee Goeddel was born on September 26, 1978, in Wheeling, West Virginia. He was a 1996 graduate of Central Catholic High School in Wheeling, West Virginia. He then studied the stepwise assembly of rigid rods under the direction of Dr. Debra L. Mohler at West Virginia University, resulting in him being awarded a BS Chemistry in 2000. He later joined the research group of Dr. Yian Shi at Colorado State University and developed a practical catalyst system for the asymmetric epoxidation of olefins. After completing his graduate work in 2006, he accepted a position in the chemical development department at Albany Molecular.